

General Disclaimer

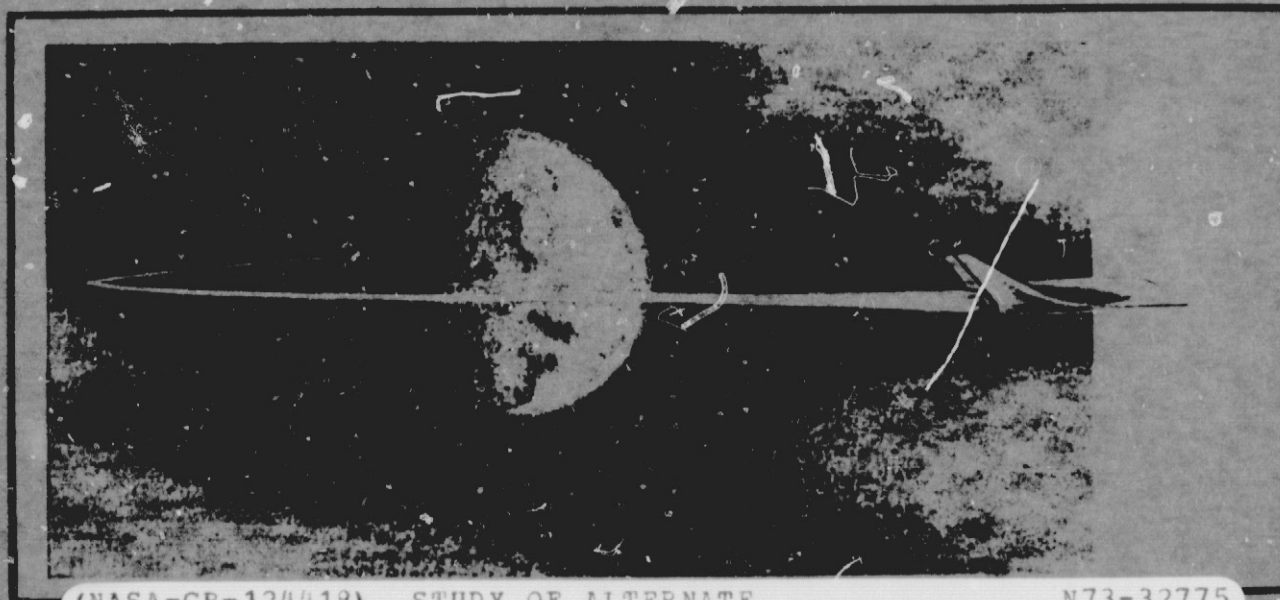
One or more of the Following Statements may affect this Document

- This document has been reproduced from the best copy furnished by the organizational source. It is being released in the interest of making available as much information as possible.
- This document may contain data, which exceeds the sheet parameters. It was furnished in this condition by the organizational source and is the best copy available.
- This document may contain tone-on-tone or color graphs, charts and/or pictures, which have been reproduced in black and white.
- This document is paginated as submitted by the original source.
- Portions of this document are not fully legible due to the historical nature of some of the material. However, it is the best reproduction available from the original submission.

28 JUNE 1971

LMSC-A990949

ACS-136



(NASA-CR-124418) STUDY OF ALTERNATE
SPACE SHUTTLE CONCEPTS, APPENDIX Final
Report (Lockheed Missiles and Space Co.)
437 p HC \$24.00

CSCL 22B

N73-32775

Unclas

G3/31 18188

STUDY OF ALTERNATE SPACE SHUTTLE CONCEPTS

TASK IV FINAL REPORT APPENDIX



Prepared for George C. Marshall Space Flight Center by
Manned Space Programs, Space Systems Division

LOCKHEED MISSILES & SPACE COMPANY

A GROUP DIVISION OF LOCKHEED AIRCRAFT CORPORATION
SUNNYVALE, CALIFORNIA

MSFC DRL No. 216
Line Item No. 7

IMSC-A990949
ACS-136
28 Jun 1971

STUDY OF ALTERNATE
SPACE SHUTTLE CONCEPTS

APPENDIX TO
TASK IV FINAL REPORT

Prepared for George C. Marshall Space Flight Center
by Manned Space Programs, Space Systems Division

LOCKHEED MISSILES & SPACE COMPANY

CONTENTS

EM NO.	TITLE
<u>For Section 2</u>	
I2-12-01-M1-1	Normal Force Distributions and Axial Force Characteristics for the External Droptanks
I2-12-01-M1-2	LH ₂ Tank/Orbiter Ascent Drag Reduction
I2-02-05-M1-6	External Droptank Orbiter System Ascent Trajectories For 50 x 100 NM Orbit Injection
I2-02-05-M1-7	Effects of Earth Oblateness Atmospheric Drag on a Space Shuttle Vehicle in Low Perigee Orbits
<u>For Section 3</u>	
I2-12-M1-2	Orbiter External LH ₂ Tank Fineness Ratio Optimization
I2-12-01-M1-9	LH ₂ External Tanks - Aerodynamic Effects of Tank Fairing and Position
<u>For Section 4</u>	
I2-12-02-M1-1	Gas Generator-Piston Separation Analysis for the Orbiter External LH ₂ Tank
<u>For Section 5</u>	
I2-12-M1-1	Mass Property Estimates for Orbiter External LH ₂ Tank
I2-12-01-M1-11	Retro Rocket Parametrics for the Orbiter External LH ₂ Tank
I2-12-05-M1-8	Separation and Entry Analysis of an External LH ₂ Droptank
<u>For Section 6</u>	
I2-12-M1-3	Performance and Design Requirements for the External Liquid Hydrogen Droptank

CONTENTS (Cont)

EM NO.	TITLE
<u>For Section 8</u>	
✓ I2-12-01-M1-18	Material Selection for Liquid Hydrogen Droptank
<u>For Section 10</u>	
I2-12-01-M1-12	Baseline Droptank Loads
✓ I2-12-01-M1-13	Baseline Droptank Structural Analysis
✓ I2-12-01-M1-14	Strength and Stability Analysis of the Baseline Droptank Thrust Cone (Eng Dwg SKT 100704)
I2-12-01-M1-15	Nonlinear Stress Analysis of Longitudinal Strap Joints in Weldbond LH ₂ Droptank
<u>For Section 11</u>	
✓ I2-12-01-M1-7	G.A.C. External Droptank Orbiter Thermal Evaluation
✓ I2-12-01-M1-10	GAC Droptank Stable Reentry Ablator Requirements
<u>For Section 12</u>	
I2-12-02-M1-2	Droptank Pressurization Study With Ascent TPS
<u>For Section 13</u>	
✓ I2-12-03-M1-1	Orbiter External LH ₂ Droptank Functional Schematic, Controls and Instrumentation
I2-12-03-M1-2	Orbiter External LH ₂ Droptank Event Timing Concept
<u>For Section 14</u>	
I2-12-01-M1-8	Thermodynamic Analysis of Droptank Surface Irregularities.

ENGINEERING MEMORANDUM

TITLE: NORMAL FORCE DISTRIBUTIONS AND AXIAL FORCE CHARACTERISTICS FOR THE EXTERNAL DROPTANKS	EM NO: L2-12-01-M1-1 REF: L2-12-01-P1 DATE: 29 April 1971
AUTHORS: G. Morris <i>G. Morris</i>	APPROVAL: <i>James L. Alberty</i> ENGINEERING SYSTEM ENGRG <i>R.A. Byers</i>

PROBLEM STATEMENT

In support of the NASA LH₂ Droptank Study Contract, NAS 8-26362, aerodynamic characteristics of the tanks are required. Effects of tank fineness ratio on drag are needed for determining effects on ascent performance and normal force distribution for performing loads analysis. This EM presents analytical estimates of these characteristics and compares results with NASA (Ames) Wind Tunnel test results.

RESULTS

Figure 1 shows a sketch of the Shuttle orbiter vehicle with two LH₂ tanks mounted on the body. The actual tank currently has a single 15 deg blunted conical nose, a nominal overall length of 86.6 ft and diameter of 14 ft. Ames test results indicate that interference effects from the tanks are large, constant with angle of attack, and act on the orbiter wing surface. It is concluded that forces and moments on the tanks (in presence of the orbiter) are essentially the same as the isolated tanks.

Normal Force Distribution

Distribution of the normal force curve slope, C_{N_α}' over the LH₂ droptank at Mach 1.2 is presented in Figure 2. This force distribution is based on empirical results presented in References 1 and 2.

Total tank normal force is obtained by integrating this distribution, W.R.T. (X/D) as follows:

$$N_T = \alpha \bar{q} S_{ref} \int_0^T C_{N_\alpha}' d\left(\frac{X}{D}\right)$$

where $C_{N_\alpha}' = \frac{\partial C_{N_\alpha}}{\partial (X/D)}$, $\frac{1/\text{Rad}}{\text{Caliber}}$

Reference area, S_{Ref} is the tank maximum cross sectional area $\pi D^2/4$, $D = 168$ in.

Interference Effects

Force and moment test results obtained from NASA Ames (Ref. 3) were reviewed to determine normal force, axial force, and pitching moment characteristics of these tanks including interference effects in the presence of the orbiter. The variation of (tank + interference) normal force coefficient with angle of attack is shown in Figure 3, as obtained from Reference 3. These static aerodynamic characteristics show a large increment in C_N due to the tanks and a slight variation with angle of attack. The normal force variation with angle of attack

EM NO: L2-12-01-M1-1

DATE: 29 April 1971

$$\left(\frac{\partial C_{N_T} + I}{\partial \alpha} \right) \quad (\text{at } M = 1.2)$$

corresponds to the value of C_{N_α} obtained by integration of the distribution in Figure 2.

The conclusion reached is that the normal force of the LH₂ tank in presence of the orbiter is approximately equal to the isolated tank normal force with a large normal force induced by the tank acting over the orbiter wing. This induced (wing) normal force is approximately constant acting over the wing aft of the tank base, and gives a negative pitching moment increment.

Figure 3 also shows pitching moment coefficient for the tank + interference. The value of $-C_m$ at $\alpha = 0$ represents the constant increment due to tank interference effects acting on the wing.

Summarizing:

$$C_{N_{\text{Tank} + \text{Intf}}} = \Delta C_{N_{\text{Intf}}} + (C_{N_\alpha})_{\text{Tank}} \alpha$$

$$C_{m_{\text{Tank} + \text{Intf}}} = \Delta C_{m_{\text{Intf}}} + (C_{m_\alpha})_{\text{Tank}} \alpha$$

where $\Delta C_{N_{\text{Intf}}}$ and $\Delta C_{m_{\text{Intf}}}$ act on orbiter wing surface and are constants at a given Mach number.

Axial Force

The estimated axial force coefficient of the isolated LH₂ tank is presented in Figure 4 as a function of tank "overall" fineness ratio and Mach number. Results from the Ames test (Reference 3) show the axial force of the tanks plus interference effects are ≈ 3.0 times the value of the isolated tanks.

Axial force coefficients for the isolated tanks were obtained using Reference 4 for forebody wave drag (15 deg blunted cone), skin friction drag using the reference temperature method, and base drag from a correlation of experimental results. The slope of C_{A_0} vs $(L/D)_{\text{Tanks}}$, Figure 4, yields the drag partial for performance effects.

REFERENCES

1. "Linear Aerodynamic Loads on Cone-Cylinders At Mach Numbers From 0.7 to 2.0," HREC/11289-I, IMSC/HREC A710463, by Roger Lee Hamner, Alan D. Leff, dated 10 March 1965.
2. "OGO-E Launch Vehicle Estimated Transonic-Supersonic Aerodynamic Characteristics and Aerodynamic Coefficient Distributions," IMSC-806993, TM 55-21-110, by A. B. Ward, April 1967.

Lockheed Missiles & Space Company

Space Shuttle Project

EM NO: 12-12-01-M1-1

DATE: 29 April 1971

3. "Transmittal of Tabulated Force and Moment Data of the Grumman-Boeing Orbiter/Launch Configurations Tested in the NASA-Ames 8-By-6Ft Supersonic Wind Tunnel (Test No. 546), March 8-13, 1971," NASA Ames Letter STH: 229-1, by Jack A. Mellenthin, 7 April 1971.
4. "Aerodynamic Characteristics of Spherically Blunted Cones At Mach Numbers From 0.5 to 5.0," NASA TN D-3088

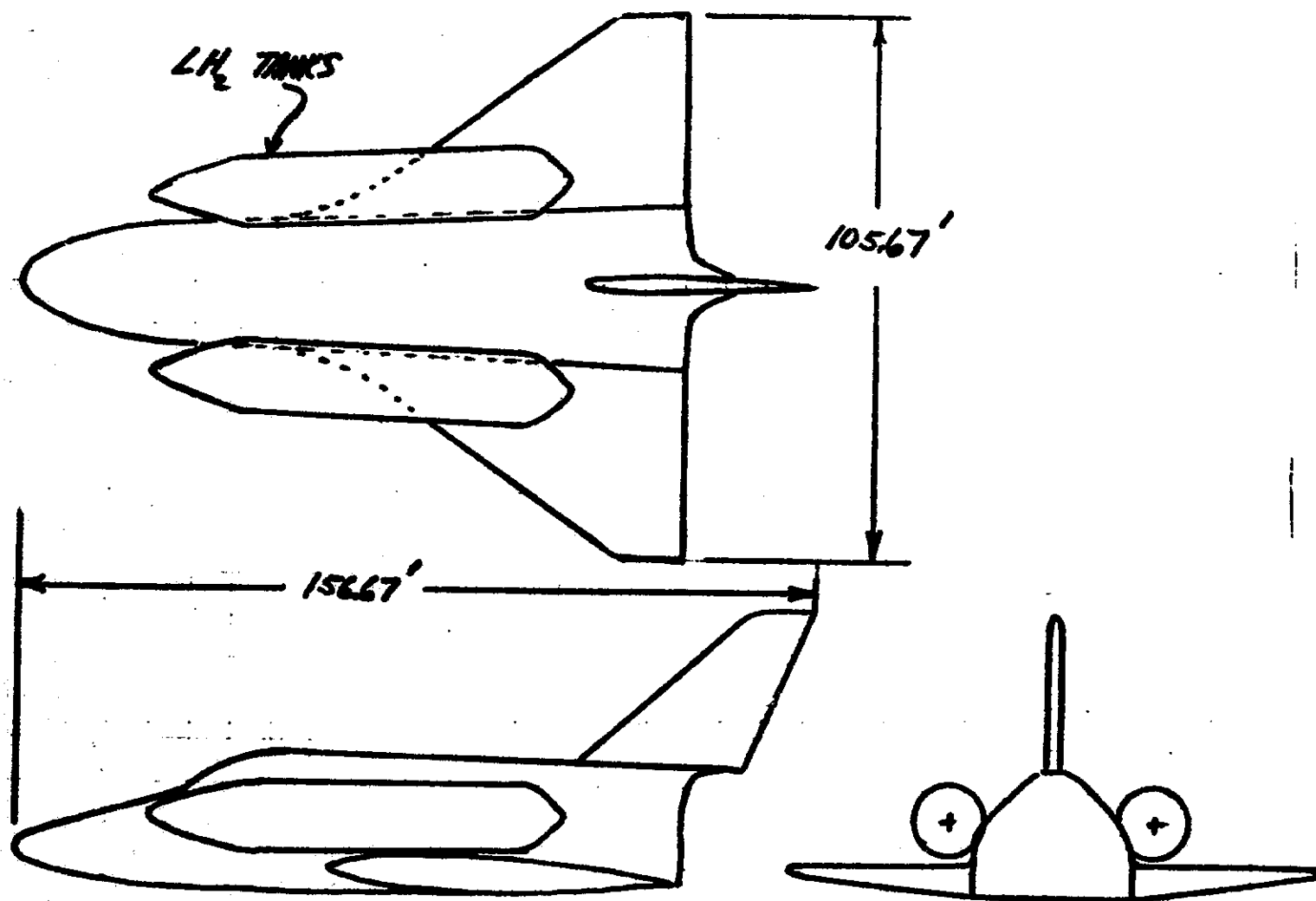


Fig. 1 External Tank Orbiter

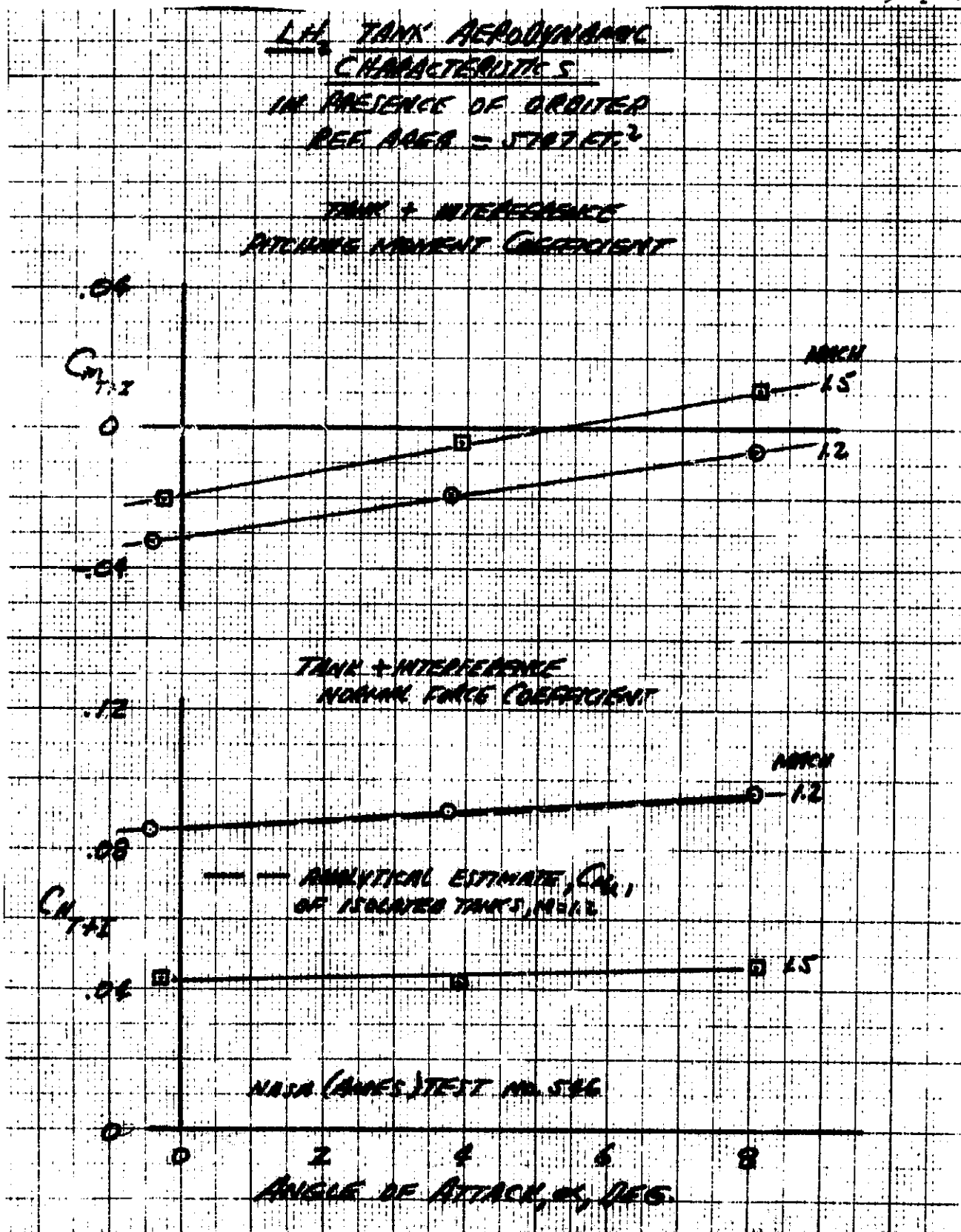


Fig. 3 External Tank Orbiter

MACH 1.2

TANK DIAMETER = 168 IN.

$$\text{REF. AREA} = \frac{\pi D^2}{4}$$

$$D = 168 \text{ IN.}$$

$$C_{L'} = \frac{2C_{N_L}}{2(x/D)}$$

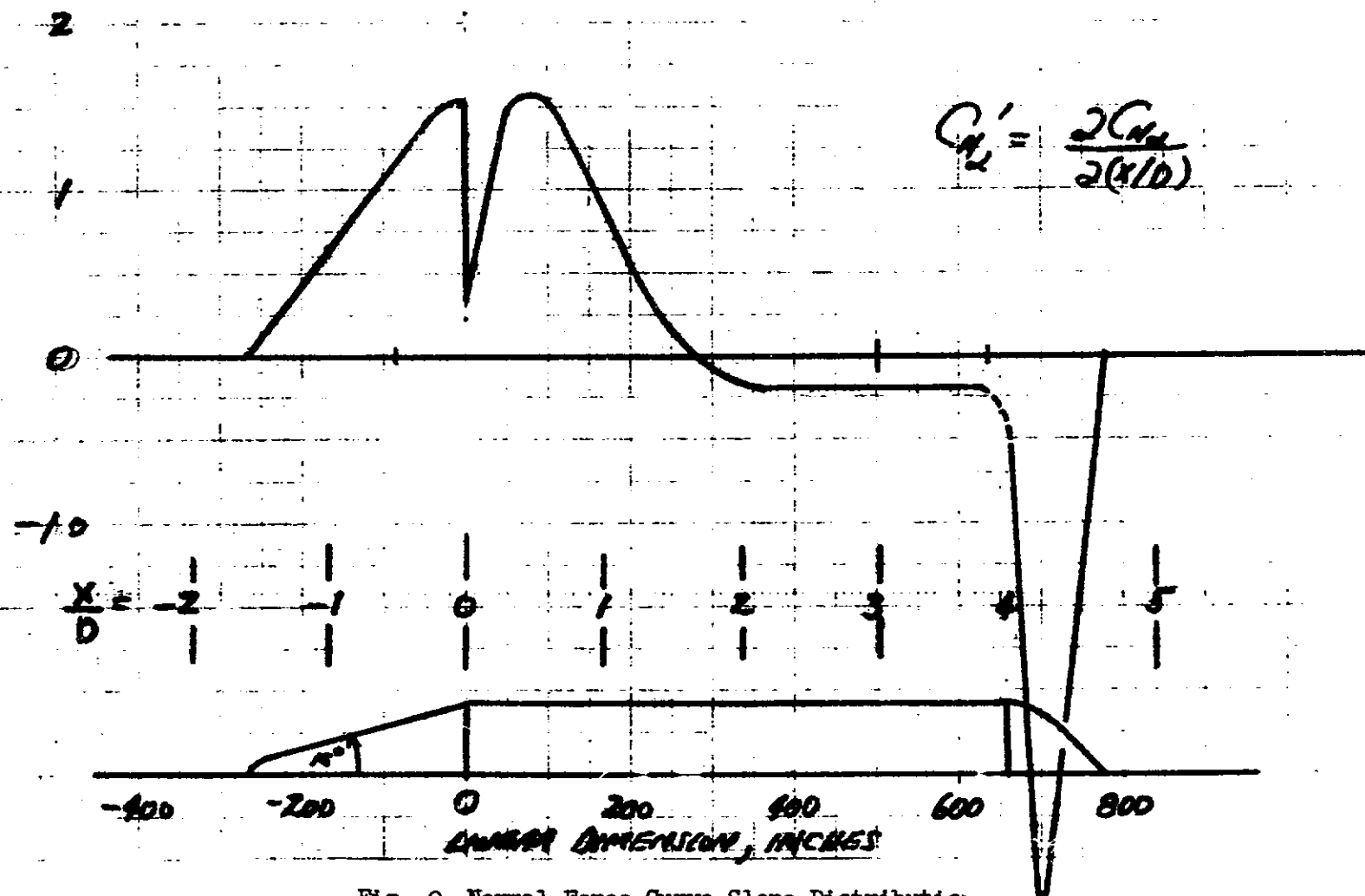


Fig. 2 Normal Force Curve Slope Distribution

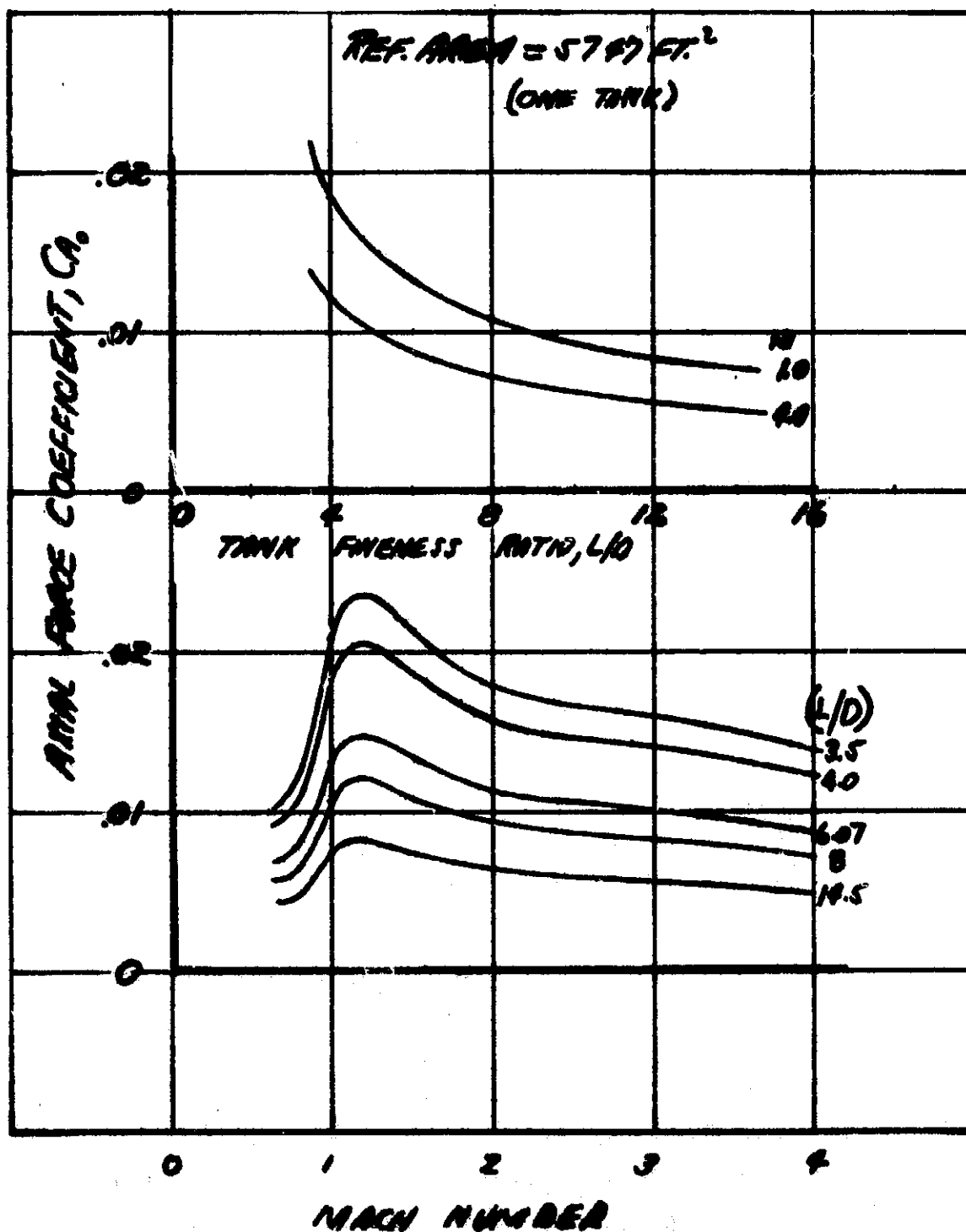


Fig. 4 Effect of Fineness Ratio on Tank Drag

ENGINEERING MEMORANDUM

TITLE: LH ₂ TANK/ORBITER ASCENT DRAG REDUCTION	EM NO: 12-12-01-M1-2 REF: 12-12-01-P1 DATE: 29 April 1971
AUTHORS: G. W. Morris, <i>G. W. Morris</i>	APPROVAL: ENGINEERING <i>Thomas L. Alexander</i> SYSTEM ENGRG <i>R. A. Byers</i>

PROBLEM

During ascent flight of the two-and-one-half stage shuttle vehicle, external tanks placed on the sides of the orbiter are a source of significant drag. These external tanks, in addition to their own drag, create an interference drag acting on the orbiter which is of the order of 3 times the drag of the isolated tanks. Tanks shaping/location and fuselage-tank fairings are possible solutions to drag reduction and are discussed qualitatively herein.

RESULTS

Wind tunnel test results (NASA AMES TEST 66-546) are presented in Fig. 1 showing drag of the two external LH₂ tanks plus their interference drag. Also shown on Fig. 1 is the estimated drag of two isolated (free body) tanks. The interference drag can be seen in this figure to vary from 2.5 to > 3 times the isolated tank drag. This is not unusual and has been experimentally verified many times for externally mounted stores. The greatest problem area is in the transonic region up to 2 or 2.5 Mach number, with interference effects dissipating on either side. The source of the problem is located in the region behind the blunt base of the tanks over the surface of the orbiter wings. Reference 1 which reviewed the NASA AMES test results (Test 66-546) shows a large positive increment in normal force due to these tanks at zero degrees angle-of-attack and a negative pitching moment increment. Since the tank base is less than one tank diameter from the center of gravity, this pinpoints the interference effects as acting over the wing surface aft of the tank base.

Since the primary interference effects are in the transonic-supersonic region, it would appear that an attempt at area ruling through fuselage-tank fairings on tank shaping would provide a smoother cross-sectional area distribution of the orbiter-tank combination. Fig. 2 presents a plot of drag impulse, ($C_D \bar{q}$) versus time, for the tanks + interference. A second curve shows the potential reduction in ascent drag due to reduction of interference effects.

Figs. 3 and 4 show possible solutions to reduce interference ascent drag due to these tanks. In Fig. 3, a higher fineness ratio tank is shown schematically with a higher fineness ratio boattail terminating at the wing trailing edge. Interference areas on the wing are reduced with the tank base located aft and the more gradual tank boattail will provide smoother flow characteristics. Also shown in Fig. 3 is the existing tank/orbiter configuration.

Fig. 4 shows two additional concepts -

- Same tank diameter and location as original tank but with the tank boattail fineness ratio increased for area ruling effect yielding smoother air flow.
- A dropable fairing, contouring the existing tank base into the fuselage - also an area ruling effects.

These potential solutions can easily be checked in a brief wind tunnel test. The final solution must be one compatible with structural, mechanical, and weight design considerations.

REFERENCE

1. "Normal Force Distributions and Axial Force Characteristics for the LH₂ Droptanks On the Grumman/Boeing Orbiter, EM No. 12-12-01-M1-1, G. Morris, 29 April 1971.

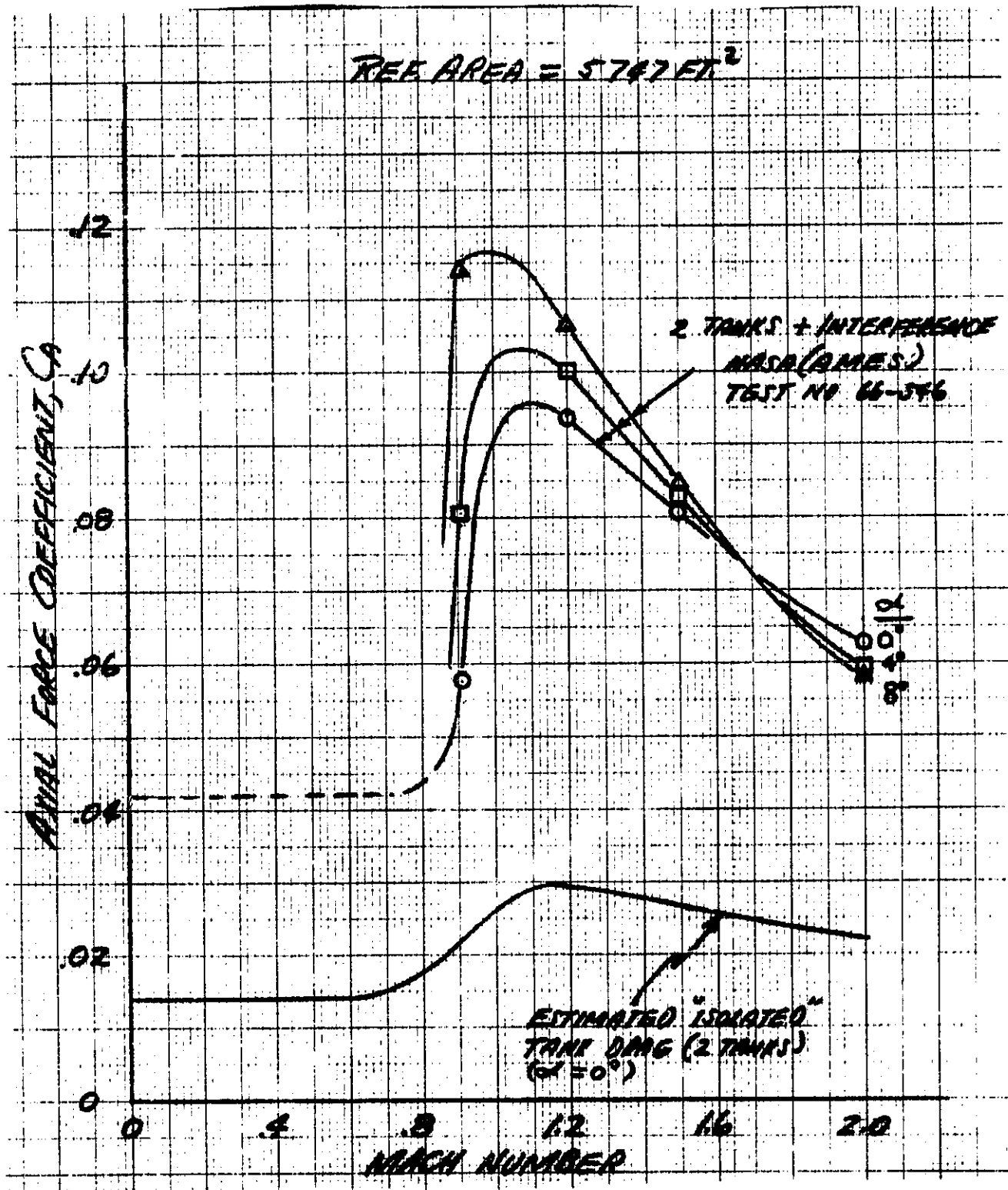


Fig. 1 LH₂ Tank Axial Force

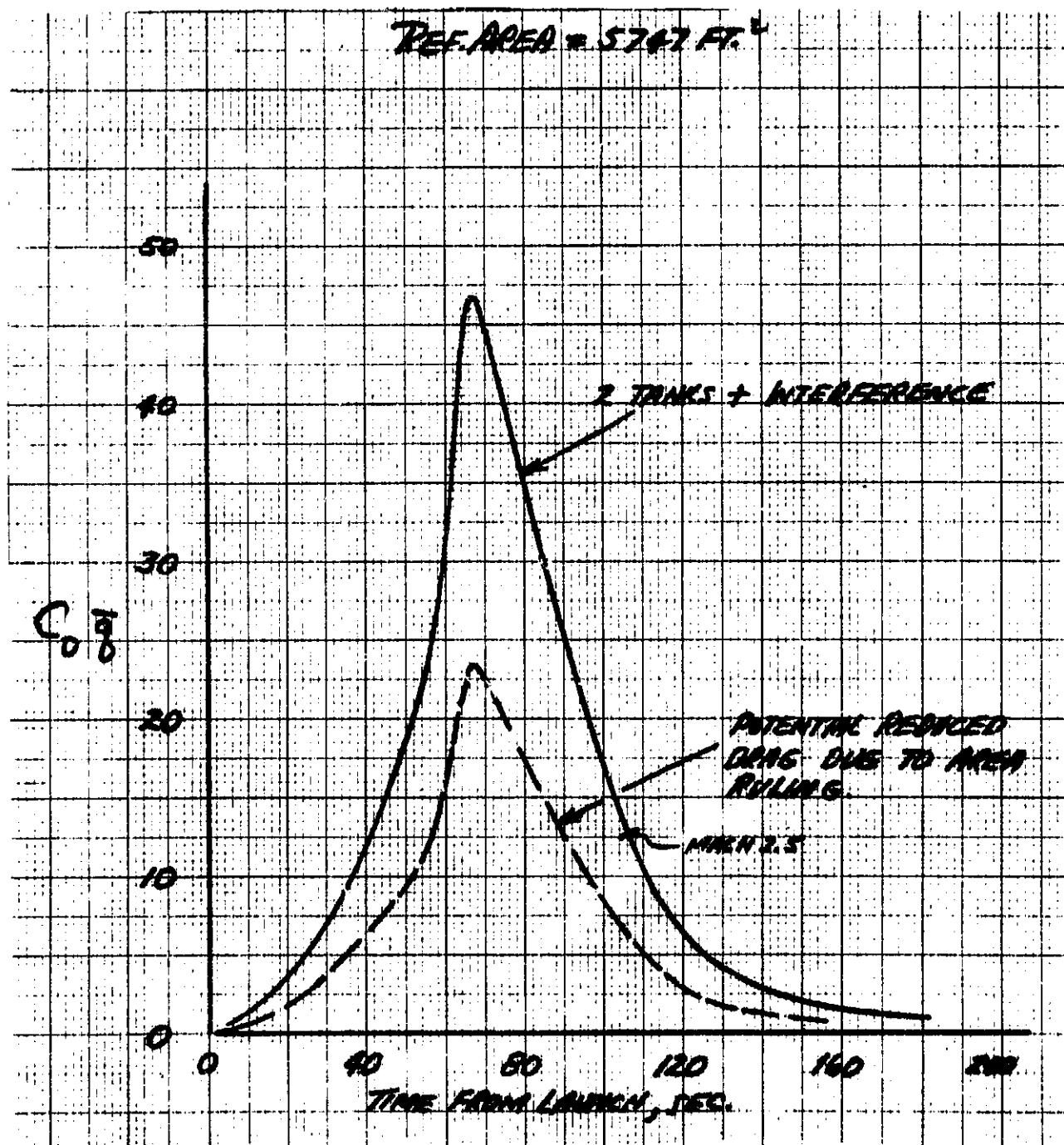


Fig. 2 LH₂ Tank Ascent Drag Impulse

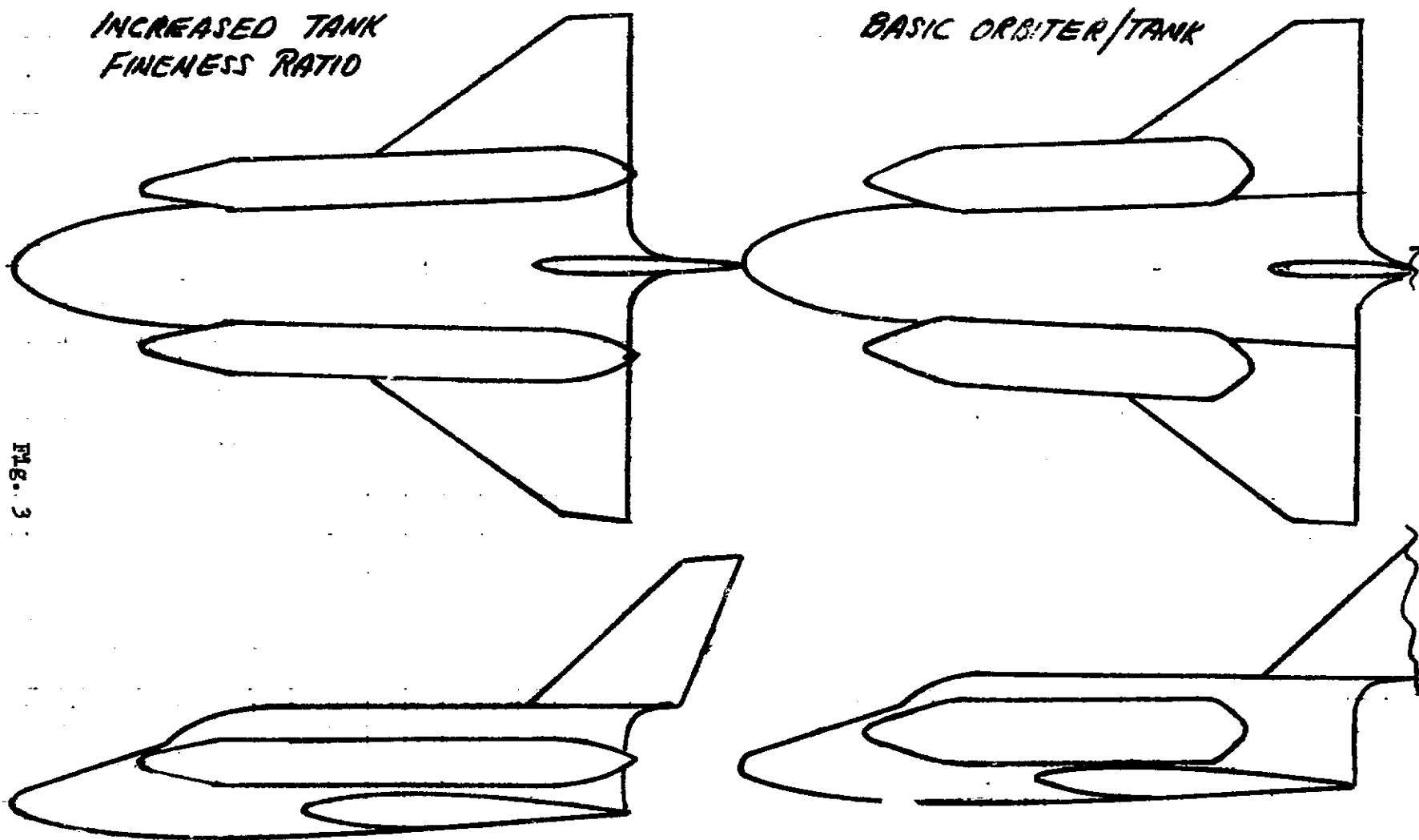


Fig. 3 LH₂ Tank - Ascent Drag Reduction Concepts

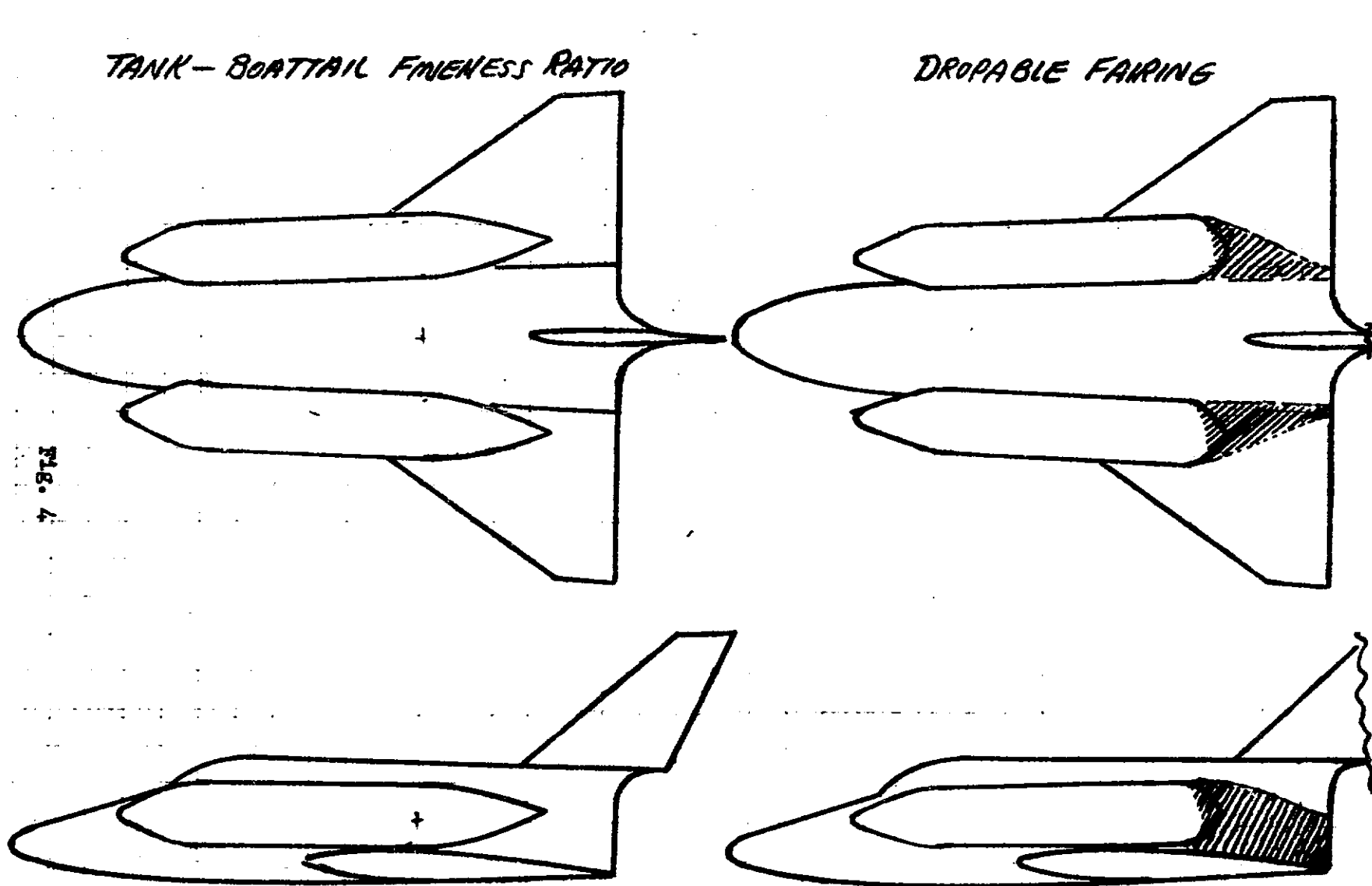


Fig. 4 LH₂ Tank - Ascent Drag Reduction Concepts

ENGINEERING MEMORANDUM

TITLE: EXTERNAL DROPTANK ORBITER SYSTEM ASCENT TRAJECTORIES FOR 50 x 100 NM ORBIT INJECTION	EM NO: I2-02-05-M1-6 REF: I2-02-05-P1 DATE: 7 June 1971
AUTHORS: E. T. Fitzgerald <i>E. T. Fitzgerald</i>	APPROVAL: ENGINEERING SYSTEM ENGRG <i>W. A. Byrd</i>

PROBLEM STATEMENT

Pertinent to this study is the identification of ascent-trajectory profiles and Orbiter-injection conditions from which reentry trajectories emanate. The analysis presented herein establishes nominal ascent-trajectory profiles for injection at the perigee of 50 x 100 nm orbits with inclinations of 28.5, 55, and 90 deg. Also included are alternate trajectories simulating drag variations resulting from alternative droptank geometry.

RESULTS

Four nominal ascent trajectories were generated representing launches from ETR (inclination, $I = 28.5, 55, \text{ and } 90 \text{ deg}$) and WTR ($I = 90 \text{ deg}$). A summary of injection conditions for each trajectory is presented in Table 1 for a nominal tank configuration designated by a fineness ratio, $l/d = 6.07$. Also shown are summary data for tank geometry changes to evaluate tank configuration (drag) effects on ascent and injection conditions.

AFFECTED WORK BREAKDOWN STRUCTURE ELEMENTS

The following study areas are affected by the results of this analysis:

- Droptank thermal and structural design
- Orbit ephemeris generation
- Range safety

Given-and-Assumed Conditions

The Booster/Orbiter/Droptank configuration used in the study was furnished by NASA under the External Liquid Hydrogen Droptank System Design Study Contract. Launch weight was assumed at 4.25M lb for all cases with a corresponding 1.35 thrust-to-weight ratio (T/W) at launch. A weight summary for a typical launch configuration is in Table 2. Maximum thrust (vacuum) propulsion characteristics are described in Table 3 for both the orbiter and booster, and assumed drag data are shown in Fig. 1.

Trajectory constraints assumed in the analysis included flight path optimization and lateral loading limitations ($\alpha \bar{q} = 1000 \text{ deg-psf}$)*, both accomplished with pitch attitude control throughout ascent and a 3g longitudinal acceleration limit. The acceleration limit was accomplished by throttling the booster and orbiter engines, as needed, to maintain 3g.

Droptank geometry variations assumed, l/d changes for d given (constant) volume. Nominal tank $l/d = 6.07$; assumed variations were $l/d = 14.5$ for the minimum drag configuration and $l/d = 3.5$ for the maximum drag configuration.

* α is angle-of-attack, \bar{q} is the dynamic pressure

EM NO: 12-02-05-M1-6
DATE: 7 June 1971Table 1
ORBIT INJECTION SUMMARY

Tank Configuration	Orbit Inclination (deg)	Launch Site	Altitude (nm)	Inertial Velocity (fps)	Injection Conditions		
					Inertial Flight Path (deg)	Latitude (deg)	Longitude (deg)
$L/a = 6.07$ (Nominal)	28.5	ETR	50.01	25856.1	0.01	27.76N	68.27W
	55.0	ETR	50.01	25856.1	0.01	36.92N	71.83W
	90.0	ETR	50.02	25856.1	0.01	16.65N	81.19W
	90.0	WTR	50.02	25856.1	0.01	22.83N	121.25W
$L/a = 3.5$ (Maximum Drag)	28.5	ETR	50.01	25856.1	0.01	27.69N	68.31W
	55.0	ETR	50.02	25856.1	0.01	36.90N	71.83W
	90.0	ETR	50.01	25856.1	0.00	16.68N	81.19W
	90.0	WTR	50.03	25856.1	0.02	22.85N	121.23W
$L/a = 14.5$ (Minimum Drag)	28.5	ETR	50.01	25856.1	0.00	27.78N	68.25W
	55.0	ETR	50.02	25856.1	0.01	36.94N	71.81W
	90.0	ETR	50.02	25856.1	0.01	16.64N	81.20W
	90.0	WTR	50.02	25856.1	0.01	22.81N	121.24W

Lockheed Missiles & Space Company

Space Shuttle Project

EM NO: 12-02-05-M1-6
DATE: 7 June 1971

Table 2

WEIGHT SUMMARY -- TYPICAL TWO-AND-ONE-HALF STAGE CONFIGURATION

● Launch Weight	4,254,970 lb
-Booster Propellant Expended to 3g Point	<u>-2,135,967</u>
● Weight at 3g Point	2,119,003 lb
-Remaining Booster Propellant	<u>-466,600</u>
● Weight at Booster Burnout	1,652,403 lb
-Booster Jettison Weight	<u>-674,033</u>
● Orbiter Ignition Weight	978,370 lb
-Orbiter Propellant Expended to 3g Point	<u>-539,035</u>
● Orbiter Weight at 3g	439,335 lb
-Remaining Propellant	<u>-122,131</u>
● Orbiter Burnout (Injection) Weight	317,204 lb

Table 3

PROPULSION SUMMARY AT MAXIMUM THRUST

● Booster	
Vacuum Thrust (Total)	6,358,000 lb
Vacuum I_{sp}	443 sec
Flow Rate (Total)	14,350 lb/sec
● Orbiter	
Vacuum Thrust (Total)	1,318,000 lb
Vacuum I_{sp}	445 sec
Flow Rate (Total)	2961.8 lb/sec

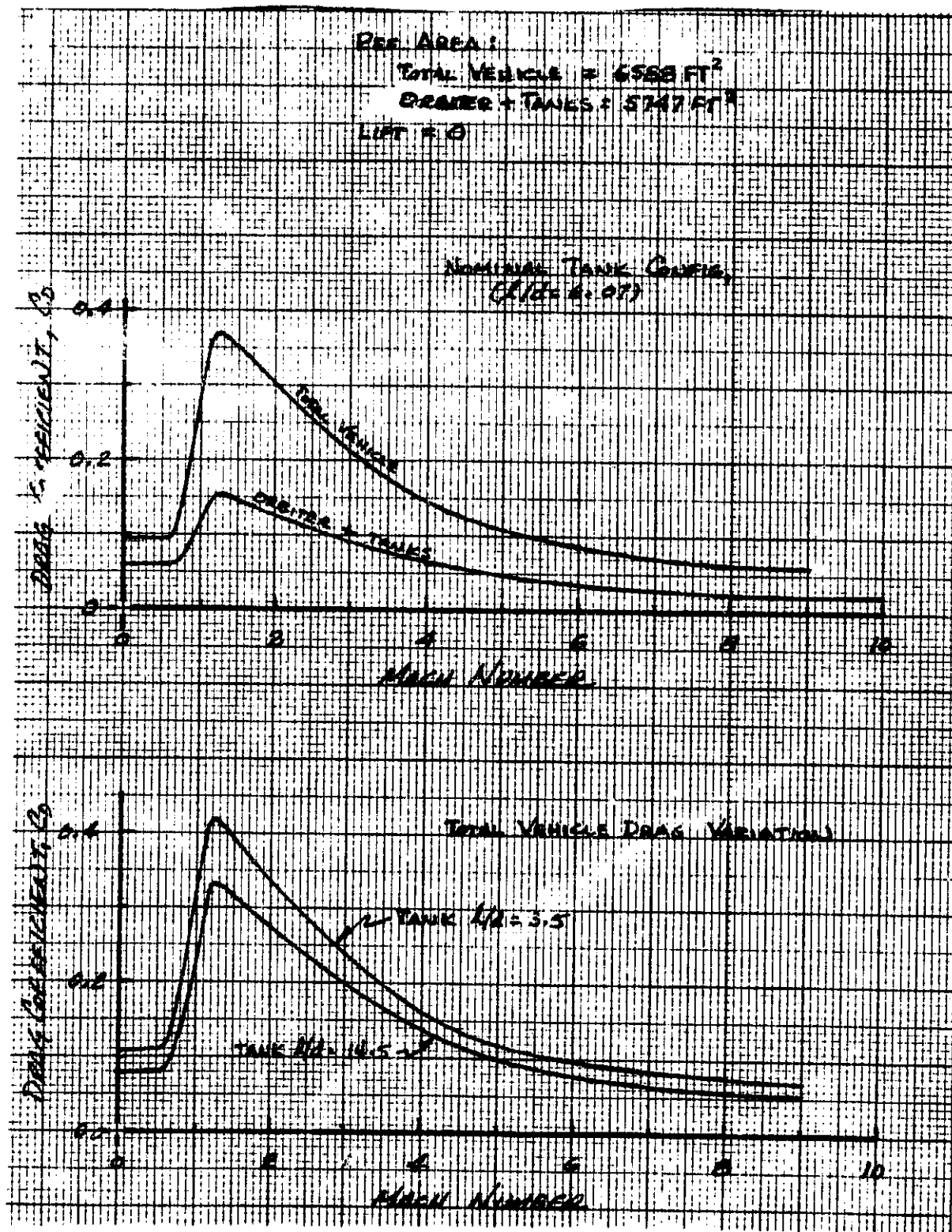


Fig. 1 Assumed Two-and-One-Half Stage Vehicle Drag Characteristics (Power Off)

The sequence of events for all trajectories is shown in Table 4 with representative time points. The indicated sequencing was assumed in lieu of a more detailed event history for a specific system.

Table 4

TYPICAL FLIGHT SEQUENCE FOR LAUNCH TO PERIGEE INJECTION (50 x 100 NM ORBIT)

<u>Time (sec)</u>	<u>Event</u>
0.0	Launch
17.0	Begin pitch maneuver
148.5	Maximum g point - begin booster engine throttling
185.56	Booster burnout/separation - orbiter ignition
367.55	Maximum g point - begin orbiter engine throttling
415.0 to 433.0	Orbit injection/burnout

DISCUSSION

The launch trajectory simulations were generated using the PRESTO program (Ref. 1), which optimizes total injection weight for given orbit conditions by minimizing ascent propellant requirements of a given system configuration. The program assumes a spherical earth. The effect of oblateness on perigee (injection) velocity requirements is discussed in Ref. 2. The related effects on booster propellant requirements are shown in Fig. 2.

All trajectories were optimized for injection at a perigee of a 50 x 100 nm orbit with inclinations and launch sites varying as indicated in Table 1. Highlights of all trajectories are presented in Table 5, and a complete trajectory parameter history listing is included in Appendix A for one of the nominal ascent-flight profiles.

A comparison of nominal ascent trajectories for the four assumed orbits show that increased orbit-inclination angles (I) require increased total energy for injection at a given orbit altitude. This comparative effect is indicated by the lower injection weights for high inclinations reflecting greater propellant usage. The primary cause of the increased energy requirement is the lessening effects of earth rotation on inertial velocity as I approaches 90 deg.

ORBIT ~ 50x100 NM

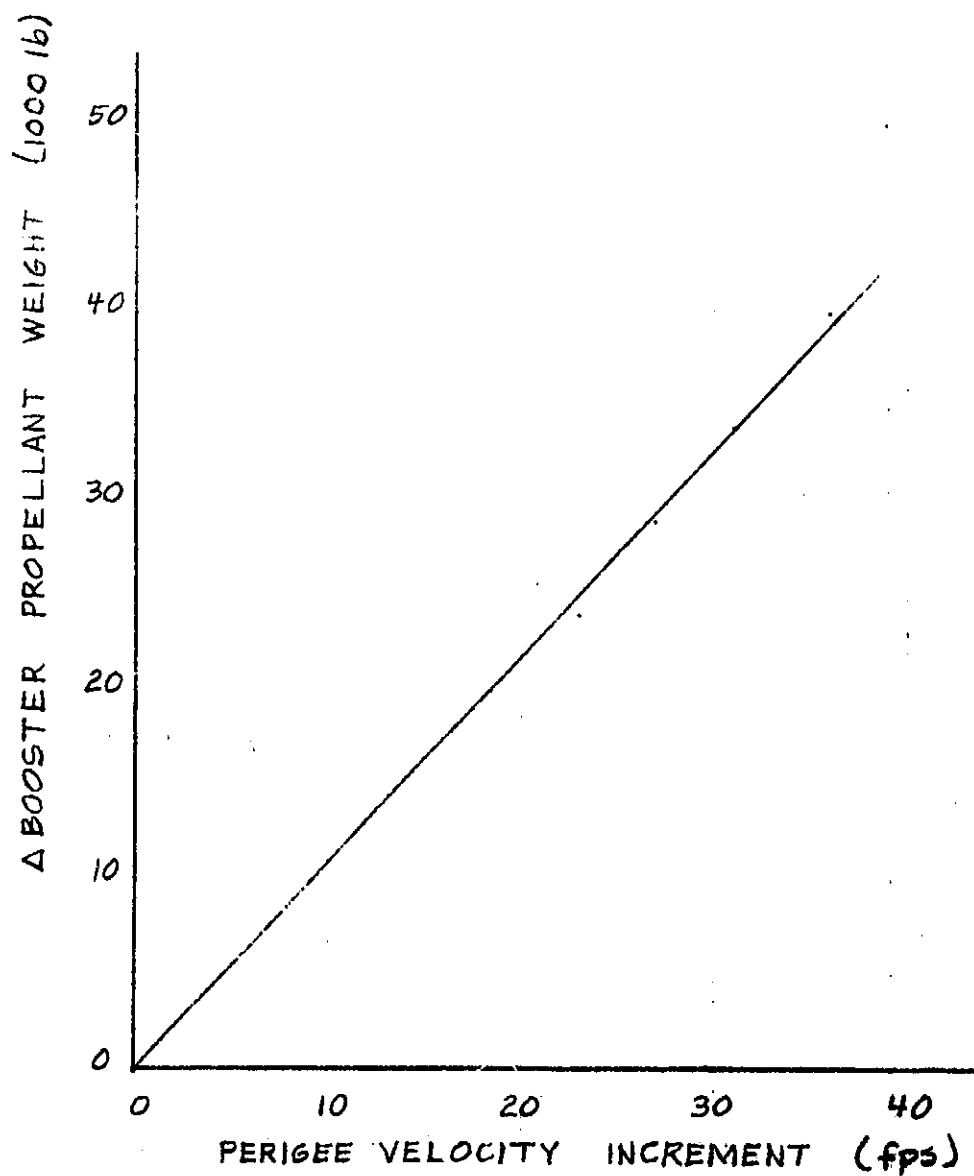


FIG 2 EFFECT OF PERIGEE VELOCITY ON BOOSTER PROPELLANT REQUIREMENTS

EM NO: 12-02-05-M1-6

DATE: 7 June 1971

Table 5

ASCENT TRAJECTORY HIGHLIGHTS

TARE COND.	ORBIT DECL. (deg)	LAUNCH SITE	EVENT	TIME FROM LAUNCH (sec.)	ALTITUDE H (ft.)	DYN PRESS q (psf)	VELOCITY V (ft/s)	RELATIVE VEL. V _r (ft/s)	RELATIVE FLIE FARE V _r (deg)
8/4-6.07 (nominal)	28.5	HTH	MAX Q	69.74	34762	369	3094.213	1833	53.9
			Booster 30 Ft.	148.85	133308	119	2119.003	9609	14.8
			Booster Separ.	185.56	189773	31	1652.403	8837	10.6
			Max Altitude	356.64	306878	1	471.677	18834	-0.0
			Orbiter 30 Ft.	367.55	305669	1	439.335	19846	-0.09
			Orbit Injunct.	415.05	303898	1	317.804	24498	-0.01
8/4-6.07 (nominal)	55	HTH	MAX Q	69.74	34799	366	3094.213	1833	54.3
			Booster 30 Ft.	148.85	134798	111	2119.003	9990	15.8
			Booster Separ.	185.56	190815	28	1652.403	8819	10.8
			Max Altitude	349.36	307590	0	493.238	18166	0.0
			Orbiter 30 Ft.	367.55	307012	1	439.334	19813	-0.16
			Orbit Injunct.	421.89	303888	1	309.770	24984	-0.01
8/4-6.07 (nominal)	90	HTH	MAX Q	69.74	34815	368	3094.213	1833	54.3
			Booster 30 Ft.	148.85	134815	112	2119.003	9990	15.1
			Booster Separ.	185.56	190872	28	1652.404	8825	10.9
			Max Altitude	349.36	310148	0	493.238	18193	0.0
			Orbiter 30 Ft.	367.55	309427	0	439.335	19799	-0.20
			Orbit Injunct.	430.92	303888	1	288.552	25099	-0.01
8/4-6.07 (nominal)	90	HTH	MAX Q	69.74	34840	365	3094.213	1833	54.5
			Booster 30 Ft.	148.85	135668	107	2119.003	9990	15.4
			Booster Separ.	185.56	190854	26	1652.403	8817	11.0
			Max Altitude	345.72	308894	0	504.019	17649	0.0
			Orbiter 30 Ft.	367.55	308887	0	439.335	19801	-0.23
			Orbit Injunct.	430.88	303814	1	286.600	25099	-0.01
8/4-5.5 (max. drag)	28.5	HTH	MAX Q	65.34	34878	536	3317.281	1108	58.9
			Booster 30 Ft.	148.85	133024	120	2119.003	9669	15.1
			Booster Separ.	185.56	188448	31	1652.401	8706	10.8
			Max Altitude	356.64	306869	1	471.677	18650	-0.08
			Orbiter 30 Ft.	367.55	306997	1	439.335	19703	-0.12
			Orbit Injunct.	417.34	303887	1	314.822	24498	-0.01
8/4-5.5 (max. drag)	55	HTH	MAX Q	69.74	34846	538	3094.213	1834	55.1
			Booster 30 Ft.	148.85	131116	123	2119.005	9669	15.9
			Booster Separ.	185.56	187880	38	1652.399	8697	13.9
			Max Altitude	356.64	306823	1	471.677	18698	-0.0
			Orbiter 30 Ft.	367.55	306888	1	439.335	19669	-0.09
			Orbit Injunct.	422.81	303896	1	302.647	24984	-0.01
8/4-5.5 (max. drag)	90	HTH	MAX Q	65.34	34834	531	3317.281	1098	59.7
			Booster 30 Ft.	148.85	131329	112	2119.003	9663	15.4
			Booster Separ.	185.56	190832	29	1652.404	8697	10.9
			Max Altitude	353.00	308898	0	482.457	18321	0.0
			Orbiter 30 Ft.	367.55	308849	0	439.334	19658	-0.14
			Orbit Injunct.	432.45	303880	1	283.994	25099	0.00
8/4-5.5 (max. drag)	90	HTH	MAX Q	65.34	34819	532	3317.281	1099	59.4
			Booster 30 Ft.	148.85	131106	116	2119.003	9666	15.2
			Booster Separ.	185.56	190111	29	1652.403	8698	11.1
			Max Altitude	349.36	307841	0	493.238	18009	0.0
			Orbiter 30 Ft.	367.55	307401	0	439.335	19655	-0.19
			Orbit Injunct.	432.40	303888	1	283.478	25099	-0.02
8/4-14.5 (min. drag)	28.5	HTH	MAX Q	69.74	34871	576	3094.213	1846	53.4
			Booster 30 Ft.	148.85	133,713	120	2119.003	9662	14.5
			Booster Separ.	185.56	190,113	31	1652.404	8908	10.6
			Max Altitude	360.34	305,596	1	460.896	19839	0.0
			Orbiter 30 Ft.	367.55	305,489	1	439.335	19928	-0.07
			Orbit Injunct.	415.05	303,857	1	318.910	24498	0.0
8/4-14.5 (min. drag)	55	HTH	MAX Q	69.74	34,862	577	3094.213	1847	53.4
			Booster 30 Ft.	148.85	133,321	122	2119.003	9663	14.4
			Booster Separ.	185.56	189,562	31	1652.403	8908	10.6
			Max Altitude	356.64	306,603	1	471.677	18879	0.0
			Orbiter 30 Ft.	367.55	306,366	1	439.335	19890	-0.10
			Orbit Injunct.	420.48	303,937	1	307.441	24984	-0.01
8/4-14.5 (min. drag)	90	HTH	MAX Q	69.74	34,921	575	3094.213	1846	53.8
			Booster 30 Ft.	148.85	134,769	114	2119.003	9668	14.8
			Booster Separ.	185.56	192,811	28	1652.407	8890	11.0
			Max Altitude	345.72	309,583	0	504.019	17983	0.0
			Orbiter 30 Ft.	367.55	309,335	1	439.335	19875	-0.28
			Orbit Injunct.	430.15	303,938	1	288.032	25099	-0.01
8/4-14.5 (min. drag)	90	HTH	MAX Q	69.74	34,882	577	3094.213	1847	53.5
			Booster 30 Ft.	148.85	133,274	122	2119.003	9670	14.8
			Booster Separ.	185.56	189,290	32	1652.402	8903	10.7
			Max Altitude	353.00	309,403	0	482.457	18941	0.0
			Orbiter 30 Ft.	367.55	308,892	0	439.335	19874	-0.10
			Orbit Injunct.	430.10	303,906	1	288.125	25099	-0.01

The effects of drag are obvious. Decreasing the vehicle frontal area to reduce drag (as exemplified by the $L/A = 14.5$ tank data) decreases comparative ascent times and propellant requirements for injection which in turn affect system gross lift-off weight (GLOW). Figure 3 shows this effect for the $I = 28.5$ deg mission.

Expansion capabilities of the system were investigated by varying booster size. The preliminary analysis shows the obvious, i.e., increased orbit injection weight is available by increasing booster size. However, the results show that the ratio of booster weight increase per pound of injected weight or payload weight is large (Fig. 4) and more detailed analysis is required for conclusive design results.

The effect of booster size increase on ideal (impulsive) velocity capabilities for ascent is shown in Fig. 5.

A change in launch site has little effect on ascent requirements. Variations in injection weight are $\ll 1$ percent and flight times vary less than 1 sec.

REFERENCES

1. "Program for Rapid Earth-to-Space Trajectory Optimization, PRESTO," LMSC 4-36-65-1, Lockheed Missiles & Space Company, Sunnyvale, California, 18 May 1964.
2. "Effects of Earth Oblateness and Atmospheric Drag on A Space Shuttle Vehicle in Low Perigee Orbits," L. A. Bleich, EM L2-02-05-M1-7, Lockheed Missiles & Space Company, Sunnyvale, California, May 1971.

- 9 -

FIGURE 3

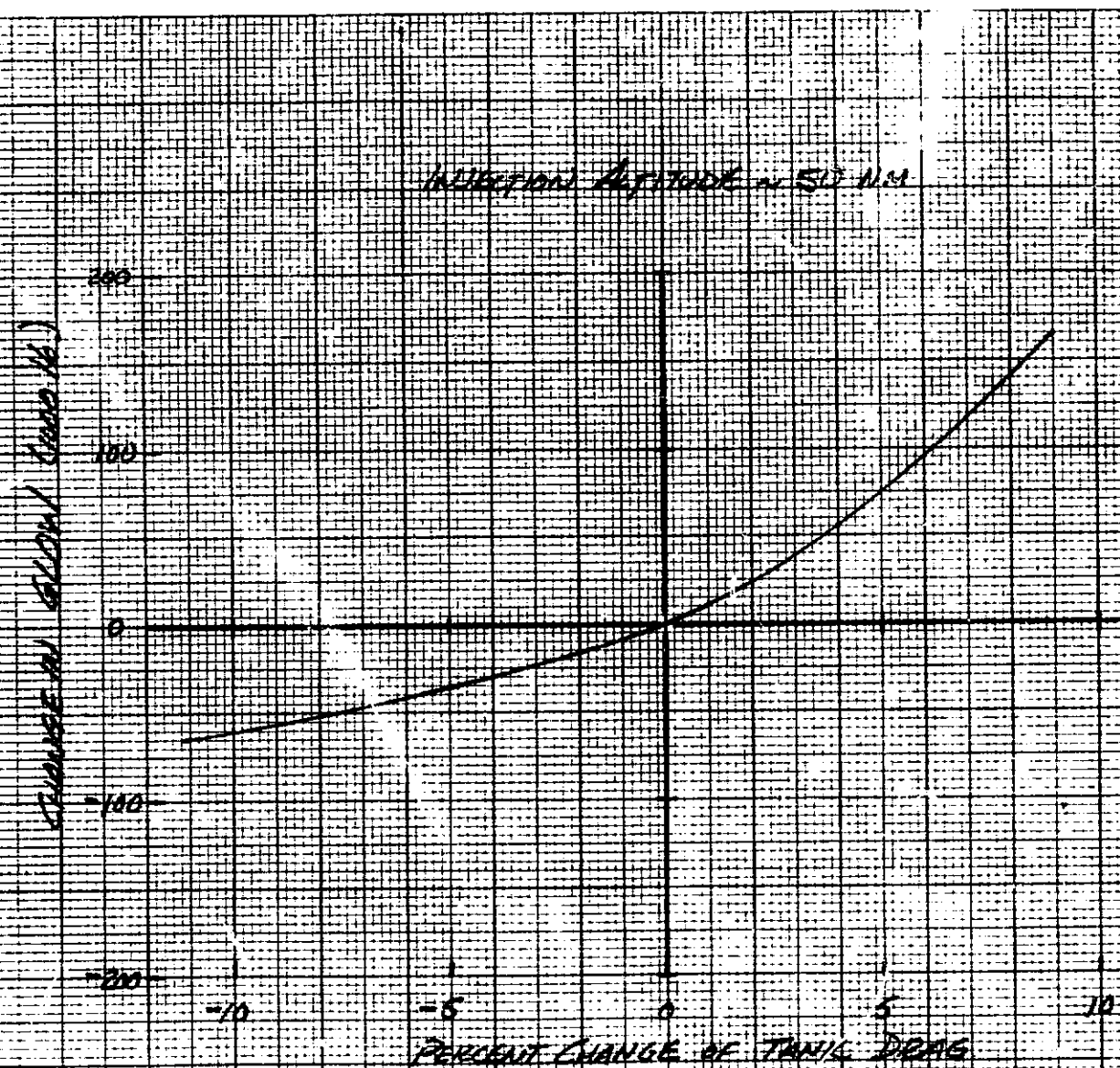


FIG. 3 EFFECT OF TANK CONFIGURATION ON GROSS LAUNCH WEIGHT

DATE: 7 June 1971

INJECTION ALTITUDE ~ 50 NM

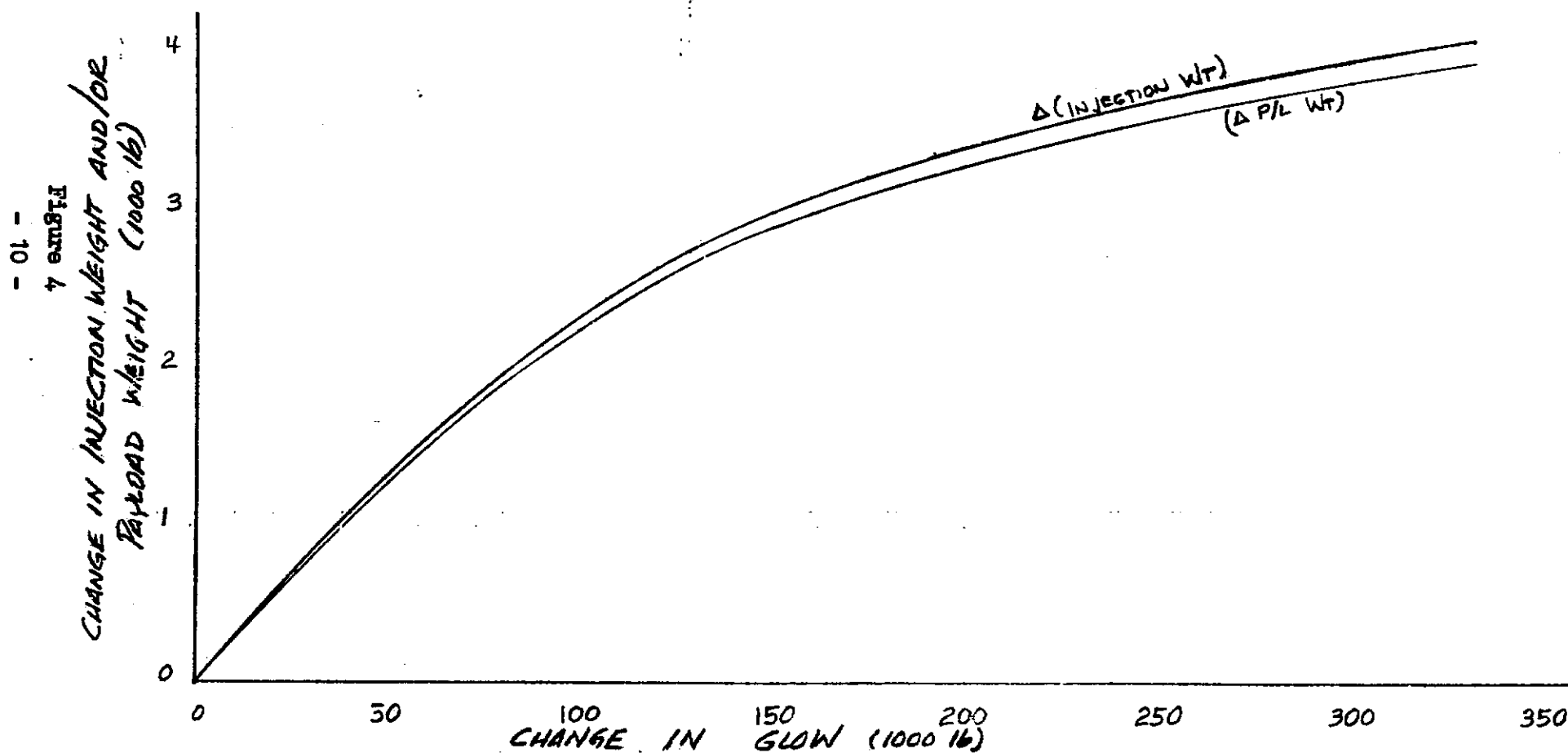


FIG 4 EFFECT OF INJECTION WEIGHT AND PAYLOAD INCREMENT ON GLOW

EM NO: 12-02-05-M1-6
DATE: 7 June 1971

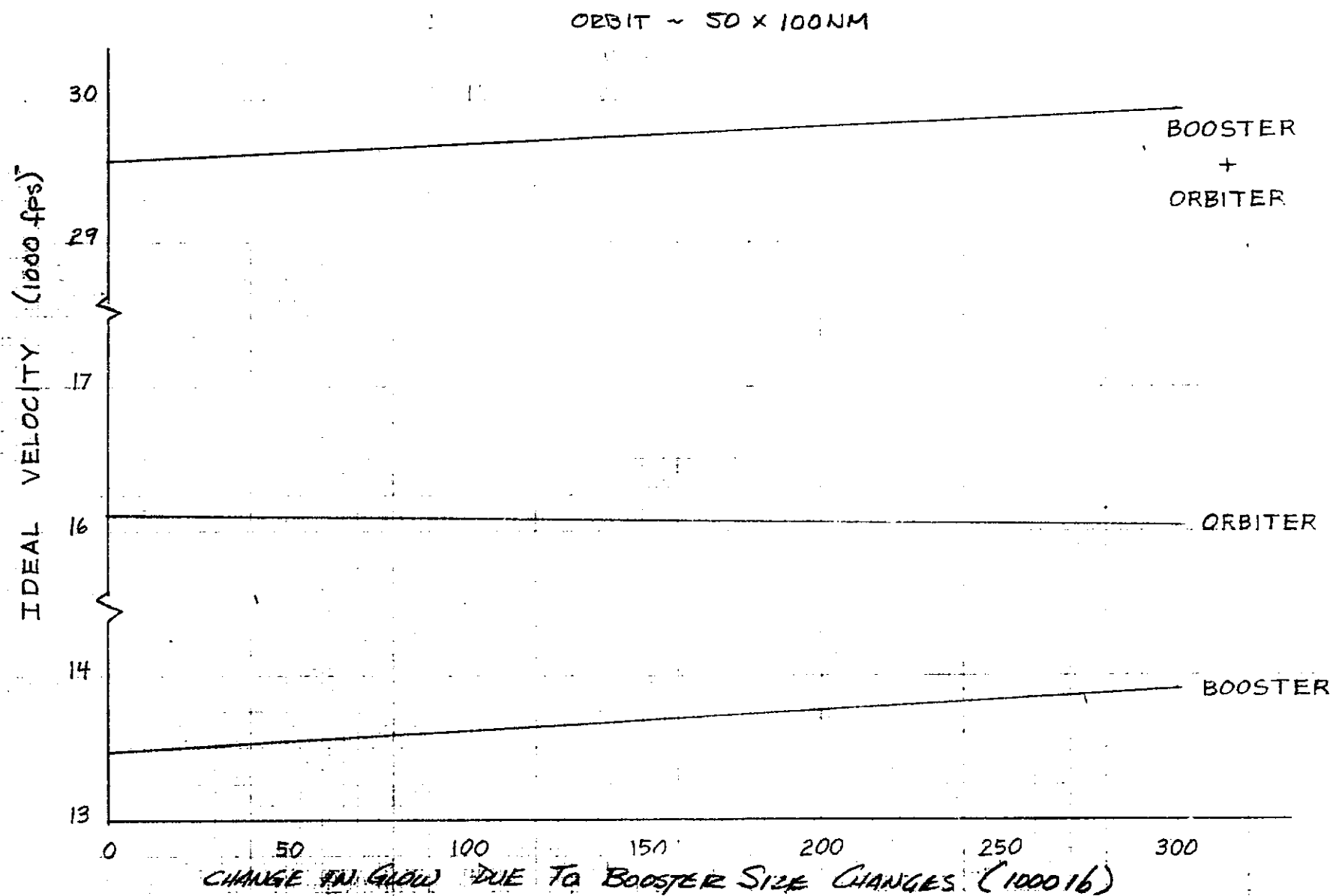


FIG 5 EFFECT OF IDEAL VELOCITY REQUIREMENTS ON GROSS LIFT OFF WEIGHT

Figure 5

EM NO: I2-02-05-M1-6

DATE: 7 June 1971

Appendix A

The listing of trajectory parameter histories on the subsequent pages is for launch to a perigee injection of a 50 x 100 nm orbit with a 55-deg inclination. A launch weight of 4.25 lb is assumed with a thrust-to-weight ratio of 1.35.

Although the two-and-one-half stage system has only two ascent boost stages - booster and orbiter, four stages are indicated in the computer listings. The discrepancy is necessary for purposes of programming and is related to actual conditions as follows:

<u>Computer Stage</u>	<u>Vehicle Stage</u>	<u>Event</u>
1	Booster	Maximum thrust to 3g limit
2	Booster	Engines throttled for 3g to burnout
3	Orbiter	Maximum thrust to 3g limit
4	Orbiter	Engines throttled for 3g to injection

GRUMMAN 2.5 STAGE THROTTLED TO 3.6

FINAL GUIDANCE 7

ETR 50 X 101 28.5 DEG. INCL

CASE 1-M-2

TIME SEC	VEL FT/SEC	GAMMA DEG	PSI DEG	ALTITUDE FT	LAN DEG	TAU DEG	QBAR PSF	THRUST LB	WEIGHT LB	THETA DEG	CHI DEG	ETA DEG	DCHI DEG	DETA DEG
TIME SEC	VI FT/SEC	GAM1 DEG	PS1 DEG	MACH	ALPHA DEG	DRAG LB	LIFT LB	Q ALPHA PSF-DEG	PSIBAR DEG	LONG ACCEL G	JET T	JETFUEL		
LAUNCH TIME = 0.000000														
STAGE = 1														
.00	.0	89.90	89.87	0.	28.47	-80.53	0.	57.2000.	4254970.	90.00	.00	.00	.00	.00
.00	1339.9	9.07	96.00	.00	.00	0.	0.	0.	.00	.000				
DTAU =	0.000	0.000	0.000	0.000	0.000	0.000	0.000	0.000	0.000	0.000	-9.750-05	0.000		
17.00	214.0	89.90	89.82	1819.	28.47	-80.53	52.	5775102.	4011020.	89.11	.00	-.79	.00	.00
17.50	1357.4	9.07	96.00	.19	-.79	28405.	0.	-41.	89.82	1.433	0.	0.		
21.39	276.9	88.97	89.82	2894.	28.47	-80.53	84.	5795893.	3947953.	86.94	.00	-2.03	.00	-.00
21.39	1373.3	11.43	96.00	.25	-2.03	44871.	0.	-170.	89.82	1.456	0.	0.		
25.79	343.2	86.67	89.82	4256.	28.47	-80.53	123.	5822146.	3884886.	84.13	.00	-2.54	.00	-.00
25.79	1402.0	14.14	96.00	.31	-2.54	69134.	0.	-314.	89.82	1.481	0.	0.		
30.18	413.5	83.45	89.82	5911.	28.47	-80.53	170.	5854082.	3821818.	81.86	.00	-1.59	.00	-.00
30.18	1447.0	16.49	86.99	.36	-1.59	95427.	0.	-270.	89.82	1.507	0.	0.		
34.58	488.6	80.18	89.82	7871.	28.47	-80.53	224.	5891905.	3758751.	79.67	.00	-.51	.00	-.00
34.58	1503.0	18.68	89.99	.45	-.51	125451.	0.	-113.	89.82	1.534	0.	0.		
38.97	569.1	76.98	89.82	10144.	28.47	-80.53	283.	5935062.	3695684.	77.46	.00	.48	.00	-.00
38.97	1570.0	20.68	89.98	.53	.48	155558.	0.	135.	89.82	1.563	0.	0.		
43.37	655.4	73.87	89.82	12748.	28.47	-80.52	346.	5971743.	3632617.	74.68	.00	.81	.00	-.00
43.37	1647.0	22.46	87.98	.61	.81	193627.	0.	280.	89.82	1.591	0.	0.		
47.76	747.3	70.68	89.88	15491.	28.47	-80.52	409.	6013106.	3569550.	71.87	-.10	1.19	-.00	-.00
47.76	1737.7	23.94	89.98	.71	1.20	285592.	0.	489.	89.85	1.605	0.	0.		
52.16	842.3	67.44	89.86	18941.	28.47	-80.52	466.	6059075.	3506482.	69.01	-.08	1.56	-.00	-.00
52.16	1837.0	25.05	89.97	.81	1.57	436544.	0.	730.	89.83	1.603	0.	0.		
56.55	939.6	64.21	89.86	22512.	28.47	-80.51	519.	6099120.	3443415.	65.62	-.06	1.47	-.00	-.00
56.55	1944.0	25.80	89.97	.92	1.42	616428.	0.	730.	89.83	1.592	0.	0.		
60.95	1037.7	60.84	89.87	26365.	28.47	-80.51	547.	6137655.	3380348.	62.20	-.05	1.35	-.00	-.00
60.95	2057.5	26.13	87.96	1.03	1.35	846607.	0.	742.	89.84	1.565	0.	0.		
65.34	1135.9	57.39	89.89	30463.	28.47	-80.50	565.	6177241.	3317281.	58.75	-.05	1.36	-.00	-.00
65.34	2175.7	26.09	87.96	1.14	1.36	1079905.	0.	768.	89.86	1.537	0.	0.		
69.74	1234.9	53.90	89.91	34762.	28.47	-80.49	569.	6207332.	3254213.	55.30	-.04	1.40	-.00	-.00
69.74	2277.7	25.74	87.97	1.27	1.40	126248.	0.	796.	89.88	1.518	0.	0.		

EM No.: 12-02-05-M-6
Date: 7 June 1971

GRUMMAN 2.5 STAGE THROTTLED TO 3 G

FINAL GUIDANCE 7

ETA 50 X 10n 28.5 DEG. INCL

CASE 1-H-2

TIME SEC	VEL FT/SEC	GAMMA DEG	PSI DEG	ALTITUDE FT	LAM DEG	TAU DEG	WBAR PSF	THRUST LB	WEIGHT LB	THETA DEG	CHI DEG	ETA DEG	OCHI DEG	DETA DEG
TIME SEC	VI FT/SEC	GAMI DEG	PSII DEG	MACH	ALPHA DEG	DRAG LB	LIFT LB	Q ALPHA PSF-DEG	PSIBAR DEG	LONG ACCEL G	JET T	JETFUEL		
74.13	1342.6	50.40	89.93	39228.	28.47	-80.48	550.	6238594.	3191146.	51.88	-0.04	1.48	-0.00	-0.00
74.13	2429.5	25.20	89.97	1.39	1.48	1188134.	0.	815.	89.91	1.583	0.	0.		
78.53	1465.4	46.94	89.96	43854.	28.47	-80.47	525.	6260572.	3128079.	48.79	-0.03	1.84	-0.00	-0.00
78.53	2576.3	24.56	89.98	1.51	1.84	1096390.	0.	967.	89.93	1.651	0.	0.		
82.92	1603.6	43.63	89.98	46639.	28.47	-80.45	500.	6281148.	3065012.	45.57	-0.03	1.94	-0.00	-0.00
82.92	2737.3	23.84	89.99	1.66	1.94	1003632.	0.	967.	89.96	1.722	0.	0.		
87.32	1757.8	40.46	90.01	53578.	28.47	-80.43	474.	6296661.	3001945.	42.51	-0.03	2.05	-0.00	-0.00
87.32	2913.5	23.05	90.01	1.82	2.05	909192.	0.	973.	89.99	1.795	0.	0.		
91.71	1928.3	37.44	90.04	50461.	28.47	-80.42	448.	6310356.	2938877.	39.64	-0.03	2.19	-0.00	-0.01
91.71	3109.6	22.19	90.02	1.96	2.19	813145.	0.	983.	90.02	1.871	0.	0.		
96.11	2115.4	34.60	90.07	63879.	28.47	-80.39	420.	6320594.	2875810.	36.97	-0.03	2.37	-0.00	-0.01
96.11	3310.8	21.28	90.04	2.19	2.37	717269.	0.	995.	90.05	1.948	0.	0.		
100.50	2319.2	31.96	90.10	69217.	28.47	-80.37	388.	6329670.	2812743.	34.28	-0.03	2.31	-0.00	-0.01
100.50	3532.2	20.34	90.06	2.31	2.31	618694.	0.	697.	90.08	2.030	0.	0.		
104.90	2540.1	29.48	90.13	74563.	28.47	-80.34	355.	6335663.	2749676.	32.28	-0.02	2.80	-0.00	-0.01
104.90	3769.3	19.37	90.08	2.59	2.80	525086.	0.	995.	90.11	2.113	0.	0.		
109.29	2777.8	27.23	90.17	80204.	28.47	-80.31	324.	6341102.	2686608.	30.30	-0.02	3.07	-0.00	-0.01
109.29	4021.2	18.42	90.11	2.81	3.07	433818.	0.	995.	90.15	2.197	0.	0.		
113.69	3031.8	25.16	90.20	85830.	28.47	-80.27	294.	6343915.	2623541.	28.54	-0.02	3.38	-0.00	-0.01
113.69	4287.9	17.50	90.14	3.05	3.38	363100.	0.	994.	90.18	2.280	0.	0.		
118.08	3301.6	23.29	90.24	91533.	28.47	-80.23	266.	6346766.	2560474.	27.02	-0.02	3.73	-0.00	-0.01
118.08	4568.8	16.60	90.17	3.29	3.73	305703.	0.	994.	90.22	2.359	0.	0.		
122.48	3586.6	21.59	90.28	97302.	28.47	-80.19	240.	6349651.	2497407.	25.73	-0.02	4.14	-0.00	-0.02
122.48	4863.6	15.74	90.20	3.55	4.14	253998.	0.	993.	90.26	2.441	0.	0.		
126.87	3886.7	20.06	90.32	103133.	28.47	-80.14	216.	6351626.	2434339.	24.67	-0.02	4.61	-0.00	-0.02
126.87	5172.2	14.94	90.24	3.82	4.61	207934.	0.	993.	90.31	2.524	0.	0.		
131.27	4201.7	18.69	90.37	109022.	28.47	-80.09	193.	6352804.	2371272.	23.84	-0.02	5.15	-0.00	-0.02
131.27	5494.6	14.19	90.27	4.10	5.15	170784.	0.	993.	90.35	2.607	0.	0.		
135.66	4531.1	17.48	90.41	114973.	28.47	-80.03	172.	6353995.	2308205.	23.25	-0.01	5.77	-0.00	-0.02
135.66	5830.2	13.50	90.31	4.39	5.77	143805.	0.	993.	90.40	2.690	0.	0.		

 EM No.: 12-02-05-MI-6
 Date: 7 June 1971

GRUMMAN 2.5 STAGE THROTTLED TO 3 G

FINAL GUIDANCE 7

FT= 50 x 10m 28.4 DEG. INCL

CASE 1-H-2

TIME SEC	VEL FT/SEC	GAMMA DEG	PSI DEG	ALTITUDE FT	LAM DEG	TAU DEG	WBAR PSF	THRUST LB	WEIGHT LB	THETA DEG	CHI DEG	ETA DEG	DCHI DEG	DETA DEG
TIME SEC	VI FT/SEC	GAMI DEG	PSII DEG	MACH	ALPHA DEG	DRAO LB	LIFT LB	Q ALPHA PSF-DEG	PSIBAR DEG	LONG ACCEL G	JET T	JETFUEL		
140.06	4874.7	16.42	90.46	120994.	28.47	-79.97	153.	6355199.	2245138.	22.92	-0.01	6.49	-0.00	-0.02
140.06	6179.1	12.89	90.36	4.69	6.49	119959.	0.	993.	90.45	2.777	0.	0.	0.	0.
144.45	5232.5	15.51	90.51	127098.	28.47	-79.91	135.	6356056.	2182071.	22.85	-0.00	7.33	-0.00	-0.02
144.45	6541.4	12.35	90.40	5.07	7.33	99018.	0.	992.	90.51	2.867	0.	0.	0.	0.
148.85	5604.5	14.75	90.57	131308.	28.47	-79.83	119.	6356221.	2119003.	22.08	-0.00	7.33	-0.00	-0.02
148.85	6917.1	11.90	90.45	5.31	7.33	80740.	0.	942.	90.56	2.962	0.	0.	0.	0.
STAGE 2														
148.85	5604.5	14.75	90.57	131308.	28.47	-79.83	119.	6357009.	211900	22.66	-0.00	7.91	-0.00	-0.02
148.85	6917.1	11.90	90.45	5.31	7.91	80740.	0.	942.	90.56	2.962	0.	0.	0.	0.
150.89	5780.7	14.44	90.59	136233.	28.47	-79.80	112.	6269779.	2089933.	22.42	-0.00	7.98	-0.00	-0.03
150.89	7094.8	11.72	90.48	5.46	7.98	73091.	0.	895.	90.59	2.965	0.	0.	0.	0.
152.93	5957.4	14.14	90.62	139186.	28.47	-79.76	105.	6183781.	2061263.	22.19	-0.00	8.05	-0.00	-0.03
152.93	7272.8	11.54	90.50	5.61	8.05	65944.	0.	847.	90.61	2.968	0.	0.	0.	0.
154.97	6134.6	13.85	90.64	142167.	28.47	-79.73	99.	6098938.	2032979.	21.96	-0.01	8.11	-0.00	-0.03
154.97	7451.4	11.37	90.53	5.76	8.11	59298.	0.	799.	90.64	2.971	0.	0.	0.	0.
157.01	6312.2	13.58	90.67	145176.	28.47	-79.69	92.	6015255.	2005085.	21.74	-0.01	8.17	-0.00	-0.03
157.01	7630.3	11.20	90.55	5.90	8.17	53144.	0.	753.	90.67	2.973	0.	0.	0.	0.
159.05	6490.3	13.31	90.70	148211.	28.47	-79.65	86.	5932715.	1977572.	21.53	-0.01	8.22	-0.00	-0.03
159.05	7809.6	11.03	90.58	6.06	8.22	47841.	0.	707.	90.69	2.976	0.	0.	0.	0.
161.08	6668.7	13.06	90.73	151272.	28.46	-79.61	80.	5851304.	1950436.	21.32	-0.01	8.25	-0.00	-0.03
161.08	7989.2	10.87	90.60	6.19	8.25	43641.	0.	662.	90.72	2.978	0.	0.	0.	0.
163.12	6847.5	12.82	90.76	154359.	28.46	-79.57	75.	5771006.	1923669.	21.08	-0.01	8.26	-0.00	-0.03
163.12	8169.2	10.72	90.63	6.34	8.26	39736.	0.	617.	90.75	2.979	0.	0.	0.	0.
165.16	7026.8	12.59	90.78	157469.	28.46	-79.52	63.	5691806.	1897269.	20.92	-0.01	8.33	-0.00	-0.03
165.16	8349.6	10.57	90.66	6.49	8.33	32783.	0.	526.	90.77	2.983	0.	0.	0.	0.
167.20	7206.5	12.36	90.81	160634.	28.46	-79.48	59.	5613688.	1871229.	20.69	-0.01	8.33	-0.00	-0.03
167.20	8530.3	10.42	90.68	6.64	8.33	29814.	0.	491.	90.80	2.984	0.	0.	0.	0.
169.24	7386.4	12.14	90.84	163761.	28.46	-79.44	55.	5536635.	1845545.	20.47	-0.01	8.32	-0.00	-0.03
169.24	8711.3	10.29	90.71	6.83	8.32	27040.	0.	458.	90.83	2.985	0.	0.	0.	0.
171.28	7566.7	11.93	90.87	166942.	28.46	-79.39	51.	5460634.	1826211.	20.25	-0.01	8.31	-0.00	-0.03
171.28	8892.5	10.13	90.74	6.99	8.32	24456.	0.	425.	90.86	2.987	0.	0.	0.	0.

LM No.: 12-02-05-M-4
Date: 7 June 1971

GRUMMAN 2.5 STAGE THROTTLED TO 3 G

FINAL GUIDANCE 7

ETA 50 X 10H 25.5 DEG INCL

CASE 1-H-2

TIME SEC	VEL FT/SEC	GAMMA DEG	PSI DEG	ALTITUDE FT	LAM DEG	TAU DEG	MBAR PSF	THRUST LB	WEIGHT LB	THETA DEG	CHI DEG	ETA DEG	DCHI DEG	DETA DEG
-------------	---------------	--------------	------------	----------------	------------	------------	-------------	--------------	--------------	--------------	------------	------------	-------------	-------------

TIME SEC	VI FT/SEC	GAMI DEG	PSII DEG	MACH	ALPHA DEG	DRAG LB	LIFT LB	Q ALPHA PSF-DEG	PSIBAR DEG	LONG ACCEL G	JET T	JETFUEL
-------------	--------------	-------------	-------------	------	--------------	------------	------------	--------------------	---------------	-----------------	-------	---------

173.32	7747.3	11.73	90.91	170144.	28.46	-79.34	47.	5385670.	1795223.	20.03	-.02	8.30	-.00	-.03
173.32	9074.1	10.00	90.77	7.16	8.30	22059.	0.	394.	90.89	2.988	0.	0.		
175.36	7928.3	11.54	90.94	173367.	28.46	-79.29	44.	5311730.	1770577.	19.82	-.02	8.29	-.00	-.03
175.36	9255.9	9.86	90.80	7.35	8.29	19867.	0.	367.	90.92	2.989	0.	0.		
177.40	8139.5	11.34	90.97	174610.	28.46	-79.24	41.	5238800.	1746267.	19.61	-.02	8.27	-.00	-.03
177.40	9438.0	9.73	90.83	7.56	8.27	17857.	0.	342.	90.95	2.990	0.	0.		
179.44	8290.9	11.16	91.00	179873.	28.46	-79.19	39.	5166932.	1722311.	19.40	-.02	8.24	-.00	-.03
179.44	9620.4	9.60	90.86	7.74	8.24	15965.	0.	318.	90.99	2.991	0.	0.		
181.48	8472.7	10.98	91.04	183156.	28.46	-79.14	36.	5096080.	1698687.	19.20	-.02	8.22	-.00	-.04
181.48	9803.0	9.48	90.89	8.00	8.22	14194.	0.	295.	91.02	2.992	0.	0.		
183.52	8654.7	10.81	91.07	184457.	28.46	-79.09	33.	5026157.	1675386.	18.93	-.02	8.12	-.00	-.04
183.52	9905.8	9.35	90.92	8.22	8.12	13153.	0.	270.	91.05	2.992	0.	0.		
185.56	8837.0	10.64	91.10	189775.	28.46	-79.03	31.	4957209.	1652403.	18.76	-.02	8.12	-.00	-.04
185.56	10168.9	9.23	90.95	8.45	8.12	12158.	0.	250.	91.09	2.993	0.	0.		

STAGE = 1

185.56	8837.0	10.64	91.10	189775.	28.46	-79.03	31.	1317762.	978370.	18.68	-.01	8.04	-.00	-.02
185.56	10168.9	9.23	90.95	8.45	8.04	4620.	0.	247.	91.09	1.342	0.	0.		
189.20	8972.3	10.17	91.17	195627.	28.46	-78.94	26.	1317784.	967589.	17.98	-.01	7.81	-.00	-.02
189.20	10306.7	8.84	91.01	8.68	7.81	3748.	0.	200.	91.16	1.358	0.	0.		
192.84	9111.4	9.70	91.23	201305.	28.45	-78.84	21.	1317802.	956809.	17.30	-.01	7.59	-.00	-.02
192.84	10447.3	8.45	91.07	8.92	7.57	3042.	0.	161.	91.22	1.374	0.	0.		
196.48	9252.8	9.25	91.29	205897.	28.45	-78.73	18.	1317809.	946028.	17.07	-.01	7.82	-.00	-.02
196.48	10590.6	8.07	91.13	9.16	7.82	2471.	0.	139.	91.28	1.390	0.	0.		
200.12	9397.8	8.81	91.36	212132.	28.45	-78.63	15.	1317816.	935247.	16.84	-.01	8.03	-.00	-.02
200.12	10736.5	7.70	91.18	9.41	8.03	2009.	0.	119.	91.35	1.407	0.	0.		
203.76	9543.9	8.38	91.42	217283.	28.45	-78.53	12.	1317823.	924466.	16.61	-.01	8.23	-.00	-.02
203.76	10885.0	7.34	91.24	9.66	8.23	1635.	0.	102.	91.41	1.424	0.	0.		
207.40	9693.5	7.97	91.49	222261.	28.44	-78.42	10.	1317830.	913686.	16.38	-.01	8.41	-.00	-.02
207.40	11036.2	7.00	91.31	9.92	8.41	1332.	0.	89.	91.48	1.441	0.	0.		
211.04	9845.9	7.57	91.56	227068.	28.44	-78.31	9.	1317836.	902905.	16.14	-.01	8.57	-.00	-.02
211.04	11189.9	6.66	91.37	10.17	8.57	1112.	0.	75.	91.54	1.458	0.	0.		

EM No. 12-02-05-M1-6
Date: 7 June 1971

GRUMMAN 2-5 STAGE

THROTTLED TO 3 G

FINAL GUIDANCE 7

ETA 50 X 100 28.5 DEG. INCL

CASE 1-H-2

TIME	VEL	GAMMA	PSI	ALTITUDE	LAN	TAU	WBAR	THRUST	HEIGHT	THETA	CHI	ETA	DCHI	DETA
SEC	FT/SEC	DEG	DEG	FT	DEG	DEG	PSF	LB	LB	DEG	DEG	DEG	DEG	DEG
TIME	VI	GAMI	PSII	HACH	ALPHA	DRA	LIFT	Q ALPHA	PSIBAR	LONG ACCEL	JET T	JETFUEL		
SEC	FT/SEC	DEG	DEG	--	DEG	LB	LB	PSF-DEG	DEG	G				
214.68	10001.0	7.19	91.62	231707.	28.44	-78.20	7.	1317842.	892124.	15.90	-.02	8.71	-.00	-.03
214.68	11346.3	6.33	91.43	10.44	8.71	937.	0.	65.	91.61	1.474	0.	0.		
218.32	10158.9	6.82	91.69	234180.	28.44	-78.09	6.	1317848.	881344.	15.66	-.02	8.84	-.00	-.03
218.32	11505.4	6.02	91.49	10.74	8.84	796.	0.	56.	91.68	1.494	0.	0.		
221.96	10319.6	6.46	91.76	240487.	28.43	-77.97	5.	1317854.	870563.	15.42	-.02	8.95	-.00	-.03
221.96	11667.2	5.71	91.56	11.02	8.95	677.	0.	48.	91.75	1.513	0.	0.		
225.60	10483.1	6.12	91.83	244636.	28.43	-77.86	5.	1317859.	859782.	15.17	-.02	9.05	-.00	-.03
225.60	11831.8	5.42	91.62	11.31	9.05	578.	0.	41.	91.82	1.532	0.	0.		
229.24	11649.5	5.79	91.90	248424.	28.43	-77.74	4.	1317865.	849001.	14.92	-.02	9.14	-.00	-.03
229.24	11999.1	5.13	91.69	11.61	9.14	495.	0.	36.	91.89	1.552	0.	0.		
232.88	10818.7	5.47	91.98	252453.	28.42	-77.62	3.	1317870.	838221.	14.67	-.02	9.20	-.00	-.03
232.88	12169.2	4.86	91.76	11.91	9.20	426.	0.	31.	91.96	1.572	0.	0.		
236.52	10990.9	5.16	92.05	256127.	28.42	-77.50	3.	1317875.	827440.	14.39	-.02	9.23	-.00	-.03
236.52	12342.3	4.59	91.82	12.21	9.23	368.	0.	27.	92.03	1.592	0.	0.		
240.16	11166.1	4.86	92.12	259644.	28.42	-77.37	3.	1317880.	816659.	14.11	-.02	9.25	-.00	-.04
240.16	12518.2	4.34	91.89	12.53	9.25	319.	0.	23.	92.10	1.613	0.	0.		
243.80	11344.4	4.58	92.20	263018.	28.41	-77.25	2.	1317884.	805879.	13.84	-.02	9.26	-.00	-.04
243.80	12697.2	4.09	91.96	12.83	9.26	306.	0.	22.	92.18	1.635	0.	0.		
247.44	11525.7	4.30	92.27	266238.	28.41	-77.12	2.	1317888.	795099.	13.56	-.02	9.26	-.00	-.04
247.44	12879.1	3.85	92.03	13.04	9.26	264.	0.	19.	92.25	1.657	0.	0.		
251.08	11710.2	4.04	92.35	269311.	28.40	-76.99	2.	1317892.	784317.	13.28	-.02	9.24	-.00	-.04
251.08	13064.2	3.62	92.11	13.25	9.24	229.	0.	17.	92.33	1.680	0.	0.		
254.72	11897.8	3.78	92.43	272238.	28.40	-76.86	2.	1317896.	773537.	13.00	-.02	9.22	-.00	-.04
254.72	13252.4	3.39	92.18	13.44	9.22	201.	0.	15.	92.40	1.703	0.	0.		
258.36	12088.8	3.54	92.51	275023.	28.39	-76.73	1.	1317900.	762756.	12.72	-.03	9.18	-.00	-.04
258.36	13443.6	3.18	92.25	13.68	9.18	177.	0.	13.	92.48	1.728	0.	0.		
262.00	12283.0	3.30	92.59	277667.	28.39	-76.59	1.	1317904.	751975.	12.44	-.03	9.14	-.00	-.04
262.00	13636.5	2.97	92.33	13.97	9.14	158.	0.	11.	92.56	1.752	0.	0.		
265.64	12480.6	3.07	92.67	280172.	28.38	-76.45	1.	1317907.	741194.	12.16	-.03	9.09	-.00	-.05
265.64	13836.6	2.77	92.40	14.12	9.09	141.	0.	10.	92.64	1.778	0.	0.		

 241 No. 12-02-05-MI-6
 Date: 7 June 1971

GRUMMAN 2.5 STAGE THROTTLED TO 3 G											FINAL GUIDANCE 7			
ETA 50 X 100 28.5 DEG. INCL CASE 1-M-2														
TIME	VEL	GAMMA	PSI	ALTITUDE	LAM	TAU	UBAR	THRUST	WEIGHT	THETA	CHI	ETA	DCHI	DETA
SEC	FT/SEC	DEG	DEG	FT	DEG	DEG	PSF	LB	LB	DEG	DEG	DEG	DEG	DEG
TIME	VI	GAMI	PSII	MACH	ALPHA	DRAW	LIFT	Q ALPHA	PSIBAR	LONG ACCEL	JET T	JETFUEL		
SEC	FT/SEC	DEG	DEG	-	DEG	LB	LB	PSF-DEG	DEG	G				
269.28	12681.7	2.86	92.75	28254.0	28.38	-76.31	1.	1317910.	730414.	11.88	-0.03	9.02	-0.00	-0.05
269.78	14038.1	2.58	92.48	14.35	9.02	128.	0.	9.	92.72	1.804	0.	0.		
272.92	12886.4	2.65	92.83	284776.	28.37	-76.17	1.	1317913.	719633.	11.60	-0.03	8.95	-0.00	-0.05
272.92	14243.0	2.40	92.56	14.55	8.95	116.	0.	8.	92.80	1.831	0.	0.		
276.56	13094.7	2.45	92.91	286980.	28.36	-76.02	1.	1317916.	708852.	11.32	-0.03	8.87	-0.00	-0.05
276.56	14451.6	2.22	92.64	14.81	8.87	107.	0.	7.	92.88	1.859	0.	0.		
280.20	13306.6	2.26	93.00	288855.	28.36	-75.88	1.	1317918.	698072.	11.04	-0.03	8.78	-0.00	-0.05
280.20	14663.9	2.05	92.72	15.05	8.78	99.	0.	7.	92.97	1.889	0.	0.		
283.84	13522.4	2.08	93.09	290703.	28.35	-75.73	1.	1317921.	687291.	10.76	-0.03	8.68	-0.00	-0.05
283.84	14879.9	1.89	92.80	15.30	8.68	92.	0.	6.	93.05	1.917	0.	0.		
287.48	13742.0	1.91	93.17	292427.	28.34	-75.57	1.	1317923.	676510.	10.48	-0.03	8.57	-0.00	-0.06
287.48	15099.8	1.73	92.89	15.55	8.57	86.	0.	6.	93.14	1.948	0.	0.		
291.12	13965.7	1.74	93.26	294031.	28.33	-75.42	1.	1317925.	665729.	10.20	-0.03	8.46	-0.00	-0.06
291.12	15323.6	1.59	92.97	15.80	8.46	81.	0.	5.	93.23	1.980	0.	0.		
294.76	14193.5	1.58	93.35	295516.	28.33	-75.26	1.	1317927.	654949.	9.92	-0.04	8.34	-0.00	-0.06
294.76	15551.6	1.44	93.06	16.00	8.34	77.	0.	5.	93.31	2.012	0.	0.		
298.40	14425.4	1.43	93.44	296886.	28.32	-75.10	1.	1317929.	644168.	9.64	-0.04	8.21	-0.00	-0.06
298.40	15783.7	1.31	93.14	16.09	8.21	72.	0.	5.	93.40	2.046	0.	0.		
302.04	14661.7	1.29	93.53	298144.	28.31	-74.94	1.	1317931.	633387.	9.36	-0.04	8.07	-0.00	-0.06
302.04	16020.2	1.18	93.23	16.19	8.07	68.	0.	4.	93.49	2.081	0.	0.		
305.68	14902.5	1.16	93.62	299792.	28.30	-74.78	1.	1317932.	622607.	9.08	-0.04	7.92	-0.00	-0.07
305.68	16261.1	1.06	93.32	16.31	7.92	65.	0.	4.	93.59	2.117	0.	0.		
309.32	15147.9	1.03	93.72	300333.	28.29	-74.61	0.	1317934.	611826.	8.79	-0.04	7.77	-0.00	-0.07
309.32	16506.5	.94	93.41	16.44	7.77	63.	0.	4.	93.68	2.154	0.	0.		
312.96	15398.0	.91	93.81	301272.	28.28	-74.44	0.	1317935.	601045.	8.52	-0.04	7.61	-0.00	-0.07
312.96	16756.7	.83	93.50	16.60	7.61	61.	0.	4.	93.77	2.193	0.	0.		
316.60	15653.0	.80	93.91	302111.	28.27	-74.27	0.	1317936.	590264.	8.24	-0.04	7.45	-0.00	-0.07
316.60	17011.8	.73	93.60	16.77	7.45	59.	0.	4.	93.87	2.233	0.	0.		
320.24	15913.0	.69	94.01	302854.	28.26	-74.09	0.	1317937.	579484.	7.97	-0.04	7.28	-0.00	-0.07
320.24	17271.9	.63	93.69	16.95	7.28	59.	0.	3.	93.96	2.274	0.	0.		

LHM NO. 1
 Date: 7 June 1971
 LHM-47-M1-B

GRIMMAN 2.5 STAGE THROTTLED TO 3 G

FINAL GUIDANCE 7

ETA 50 X 10h 20.5 DEG. INCL

CASE 1-H-2

TIME SEC	VEL FT/SEC	GAMMA DEG	PSI DEG	ALTITUDE FT	LAM DEG	TAU DEG	WBAR PSF	THRUST LB	WEIGHT LB	THETA DEG	CHI DEG	ETA DEG	DCHI DEG	DETA DEG
TIME SEC	VI FT/SEC	RAMI DEG	PSII DEG	MACH -	ALPHA DEG	DRAO LB	LIFT LB	Q ALPHA PSF-DEG	PSIBAR DEG	LONG ACCEL G	JET T	JETFUEL		
323.08	16178.3	.59	94.11	303504.	28.25	-73.91	0.	1317938.	568703.	7.70	-.04	7.11	-.00	-.08
323.58	17537.2	.54	94.79	17.16	7.11	58.	0.	3.	94.06	2.317	0.	0.		
327.52	16449.0	.50	94.21	304065.	28.24	-73.73	0.	1317939.	557922.	7.44	-.04	6.94	-.00	-.08
327.52	17807.9	.46	93.88	17.37	6.94	58.	0.	3.	94.16	2.362	0.	0.		
331.16	16725.2	.41	94.31	304542.	28.23	-73.55	0.	1317939.	547142.	7.17	-.05	6.76	-.00	-.08
331.16	18029.2	.38	93.98	17.60	6.76	58.	0.	3.	94.26	2.409	0.	0.		
334.80	17007.2	.33	94.41	304937.	28.21	-73.36	0.	1317940.	536361.	6.91	-.05	6.58	-.00	-.08
334.80	18366.3	.31	94.08	17.85	6.58	59.	0.	3.	94.36	2.457	0.	0.		
338.44	17295.3	.26	94.51	305257.	28.20	-73.17	0.	1317940.	525580.	6.66	-.05	6.40	-.00	-.09
338.44	18654.3	.24	94.19	18.11	6.40	59.	0.	3.	94.47	2.507	0.	0.		
342.08	17589.5	.19	94.62	305505.	28.19	-72.97	0.	1317941.	514800.	6.40	-.05	6.21	-.00	-.09
342.08	18948.5	.18	94.29	18.36	6.21	61.	0.	3.	94.57	2.560	0.	0.		
345.72	17890.2	.13	94.73	305685.	28.17	-72.78	0.	1317941.	504019.	6.16	-.05	6.03	-.00	-.09
345.72	19249.3	.12	94.39	18.66	6.03	62.	0.	3.	94.68	2.615	0.	0.		
349.36	18197.7	.08	94.84	305804.	28.16	-72.57	1.	1317941.	493238.	5.91	-.05	5.84	-.00	-.09
349.36	19556.7	.07	94.50	18.92	5.84	64.	0.	3.	94.79	2.672	0.	0.		
353.00	18512.1	.03	94.95	305866.	28.14	-72.37	1.	1317941.	482457.	5.68	-.05	5.65	-.00	-.10
353.00	19871.2	.03	94.61	19.30	5.65	66.	0.	3.	94.90	2.732	0.	0.		
356.64	18833.9	-.01	95.06	305879.	28.13	-72.16	1.	1317941.	471677.	5.45	-.05	5.46	-.00	-.10
356.64	20192.9	-.01	94.72	19.64	5.46	68.	0.	3.	95.01	2.794	0.	0.		
360.28	19163.3	-.04	95.17	305845.	28.11	-71.95	1.	1317941.	460896.	5.23	-.05	5.27	-.00	-.10
360.28	20522.3	-.04	94.83	19.99	5.27	70.	0.	3.	95.12	2.857	0.	0.		
DTAU = 0.000 0.000 0.000 0.000 0.000 0.000 0.000 0.000 -9.750-05 0.000														
363.92	19500.6	-.07	95.29	305773.	28.09	-71.74	1.	1317941.	450115.	5.01	-.05	5.08	-.00	-.11
363.92	20859.6	-.07	94.94	20.35	5.08	73.	0.	3.	95.23	2.928	0.	0.		
367.55	18846.3	-.09	95.40	305669.	28.07	-71.52	1.	1317941.	439335.	4.99	-.05	5.08	-.00	-.11
367.55	21205.2	-.09	95.06	20.72	5.08	76.	0.	3.	95.35	3.000	0.	0.		
STAGE = 4														
LAST BUR:														
367.55	19846.3	-.09	95.40	305460.	28.07	-71.52	1.	1318002.	439334.	4.80	-.05	4.90	-.00	-.11
367.55	21205.2	-.09	95.06	20.72	4.90	76.	0.	3.	95.35	3.000	0.	0.		

EM No.: 12-02-05-M1-6
Date: 7 June 1971

GRUMMAN 2-5 STAGE THROTTLED TO 3 6

FINAL GUIDANCE 7

ETA 50 X 100 28.5 DEG. INCL

CASE 1-H-2

TIME	VEL	GAMMA	PSI	ALTITUDE	LAM	TAU	QBAR	THRUST	WEIGHT	THETA	CHI	ETA	DCHI	DETA
SEC	FT/SEC	DEG	DEG	FT	DEG	DEG	PSF	LB	LB	DEG	DEG	DEG	DEG	DEG

TIME	VI	GAMI	PSII	MACH	ALPHA	DRAG	LIFT	Q ALPHA	PSIBAR	LONG ACCEL	JET T	JETFUEL
SEC	FT/SEC	DEG	DEG	-	DEG	LB	LB	PSF-DEG	DEG	G		

370.89	20166.8	-0.1	95.51	30555.0	28.06	-71.32	1.	1288711.	429570.	4.63	-0.06	4.73	-0.00	-0.11
--------	---------	------	-------	---------	-------	--------	----	----------	---------	------	-------	------	-------	-------

370.89	21525.7	-0.10	95.16	21.08	4.73	79.	0.	3.	95.46	3.000	0.	0.		
--------	---------	-------	-------	-------	------	-----	----	----	-------	-------	----	----	--	--

374.22	20487.5	-0.12	95.62	30541.0	28.04	-71.11	1.	1260069.	420023.	4.46	-0.06	4.57	-0.00	-0.12
--------	---------	-------	-------	---------	-------	--------	----	----------	---------	------	-------	------	-------	-------

374.22	21846.4	-0.11	95.27	21.43	4.57	83.	0.	3.	95.57	3.000	0.	0.		
--------	---------	-------	-------	-------	------	-----	----	----	-------	-------	----	----	--	--

377.55	20808.2	-0.13	95.73	30527.1	28.02	-70.90	1.	1232059.	410686.	4.24	-0.06	4.36	-0.00	-0.12
--------	---------	-------	-------	---------	-------	--------	----	----------	---------	------	-------	------	-------	-------

377.55	22167.1	-0.12	95.38	21.79	4.36	86.	0.	3.	95.68	3.000	0.	0.		
--------	---------	-------	-------	-------	------	-----	----	----	-------	-------	----	----	--	--

380.89	21129.1	-0.13	95.85	30511.5	28.00	-70.69	1.	1204670.	401557.	4.02	-0.06	4.15	-0.00	-0.12
--------	---------	-------	-------	---------	-------	--------	----	----------	---------	------	-------	------	-------	-------

380.89	22487.9	-0.12	95.49	22.15	4.15	90.	0.	3.	95.79	3.000	0.	0.		
--------	---------	-------	-------	-------	------	-----	----	----	-------	-------	----	----	--	--

384.22	21450.0	-0.13	95.96	30495.3	27.98	-70.47	1.	1177887.	392629.	3.80	-0.06	3.93	-0.00	-0.13
--------	---------	-------	-------	---------	-------	--------	----	----------	---------	------	-------	------	-------	-------

384.22	22808.8	-0.12	95.60	22.51	3.93	93.	0.	3.	95.90	3.000	0.	0.		
--------	---------	-------	-------	-------	------	-----	----	----	-------	-------	----	----	--	--

387.55	21771.0	-0.13	96.07	30479.9	27.96	-70.25	1.	1151695.	383898.	3.59	-0.06	3.72	-0.00	-0.13
--------	---------	-------	-------	---------	-------	--------	----	----------	---------	------	-------	------	-------	-------

387.55	23129.8	-0.12	95.72	22.88	3.72	97.	0.	3.	96.01	3.000	0.	0.		
--------	---------	-------	-------	-------	------	-----	----	----	-------	-------	----	----	--	--

390.89	22092.1	-0.12	96.19	30462.6	27.94	-70.03	1.	1126082.	375361.	3.38	-0.06	3.51	-0.00	-0.13
--------	---------	-------	-------	---------	-------	--------	----	----------	---------	------	-------	------	-------	-------

390.89	23450.8	-0.12	95.83	23.24	3.51	101.	0.	3.	96.13	3.000	0.	0.		
--------	---------	-------	-------	-------	------	------	----	----	-------	-------	----	----	--	--

394.22	22413.3	-0.12	96.31	30447.0	27.92	-69.80	1.	1101035.	367012.	3.18	-0.06	3.30	-0.00	-0.14
--------	---------	-------	-------	---------	-------	--------	----	----------	---------	------	-------	------	-------	-------

394.22	23772.0	-0.11	95.95	23.60	3.30	105.	0.	3.	96.25	3.000	0.	0.		
--------	---------	-------	-------	-------	------	------	----	----	-------	-------	----	----	--	--

397.55	22734.5	-0.11	96.43	30432.3	27.90	-69.58	1.	1076546.	358849.	2.98	-0.06	3.09	-0.00	-0.14
--------	---------	-------	-------	---------	-------	--------	----	----------	---------	------	-------	------	-------	-------

397.55	24093.1	-0.10	96.07	23.97	3.09	109.	0.	3.	96.37	3.000	0.	0.		
--------	---------	-------	-------	-------	------	------	----	----	-------	-------	----	----	--	--

400.89	23055.7	-0.09	96.55	30419.0	27.87	-69.34	1.	1052622.	350874.	2.79	-0.06	2.88	-0.00	-0.15
--------	---------	-------	-------	---------	-------	--------	----	----------	---------	------	-------	------	-------	-------

400.89	24414.3	-0.09	96.18	24.33	2.88	113.	0.	3.	96.49	3.000	0.	0.		
--------	---------	-------	-------	-------	------	------	----	----	-------	-------	----	----	--	--

404.22	23377.0	-0.08	96.67	30407.5	27.85	-69.11	1.	1029226.	343075.	2.60	-0.06	2.68	-0.00	-0.15
--------	---------	-------	-------	---------	-------	--------	----	----------	---------	------	-------	------	-------	-------

404.22	24735.6	-0.07	96.30	24.69	2.68	117.	0.	2.	96.61	3.000	0.	0.		
--------	---------	-------	-------	-------	------	------	----	----	-------	-------	----	----	--	--

407.55	23678.3	-0.06	96.80	30398.4	27.82	-68.87	1.	1006349.	335450.	2.42	-0.06	2.48	-0.00	-0.15
--------	---------	-------	-------	---------	-------	--------	----	----------	---------	------	-------	------	-------	-------

407.55	25056.9	-0.05	96.43	25.04	2.48	121.	0.	2.	96.73	3.000	0.	0.		
--------	---------	-------	-------	-------	------	------	----	----	-------	-------	----	----	--	--

410.89	24019.6	-0.03	96.92	30392.1	27.80	-68.63	1.	983978.	327993.	2.25	-0.06	2.28	-0.00	-0.16
--------	---------	-------	-------	---------	-------	--------	----	---------	---------	------	-------	------	-------	-------

410.89	25378.1	-0.03	96.55	25.39	2.28	125.	0.	2.	96.86	3.000	0.	0.		
--------	---------	-------	-------	-------	------	------	----	----	-------	-------	----	----	--	--

414.22	24340.9	-0.01	97.05	30389.2	27.77	-68.39	1.	962102.	320701.	2.07	-0.06	2.08	-0.00	-0.16
--------	---------	-------	-------	---------	-------	--------	----	---------	---------	------	-------	------	-------	-------

414.22	25699.4	-0.01	96.67	25.74	2.08	128.	0.	2.	96.98	3.000	0.	0.		
--------	---------	-------	-------	-------	------	------	----	----	-------	-------	----	----	--	--

415.85	24497.6	0.01	97.11	30389.2	27.76	-68.27	1.	951611.	317204.	2.09	-0.06	2.08	-0.00	-0.16
--------	---------	------	-------	---------	-------	--------	----	---------	---------	------	-------	------	-------	-------

415.85	25856.1	0.01	96.73	25.91	2.08	130.	0.	2.	97.04	3.000	0.	0.		
--------	---------	------	-------	-------	------	------	----	----	-------	-------	----	----	--	--

THOE = -0.6590429+09 EM = .54039507+12 RP = .21206797+08 EYE = 28.50 BETAP = 101.74 OMEGAE = 288.91

EM No.: 12-02-05-MI-6
Date: 7 June 1971

GRUMMAN 2.5 STAGE

THROTTLED TO 3 G

FINAL GUIDANCE

ETR 50 X 100 28.5 DEG. INCL

CASE 1-H-2

VELOCITY LOSS COMPUTATIONS DURING FINAL GUIDANCE

SOURCE OF VELOCITY LOSS (FT/SEC)

STAGE 1

GAIN DUE TO EARTH ROTATION	7.5855+00
GRAVITY LOSS	-3.3734+03
DRAG LOSS	-6.6205+02
THRUST ATMOSPHERIC PRESSURE LOSS	-2.8326+02
THRUST ATTITUDE LOSS	-1.6333+01
GAIN DUE TO THRUST FORCE	9.9320+03

STAGE 2

GAIN DUE TO EARTH ROTATION	7.1014+01
GRAVITY LOSS	-2.5150+02
DRAG LOSS	-2.1789+01
THRUST ATMOSPHERIC PRESSURE LOSS	0.0000
THRUST ATTITUDE LOSS	-3.6259+01
GAIN DUE TO THRUST FORCE	3.5413+03

STAGE 3

GAIN DUE TO EARTH ROTATION	1.3813+00
GRAVITY LOSS	-3.3678+02
DRAG LOSS	-3.4189+00
THRUST ATMOSPHERIC PRESSURE LOSS	-8.0114-01
THRUST ATTITUDE LOSS	-1.0720+02
GAIN DUE TO THRUST FORCE	1.1456+04

STAGE 4

GAIN DUE TO EARTH ROTATION	2.3740-01
GRAVITY LOSS	2.5578+00
DRAG LOSS	-4.3411-01
THRUST ATMOSPHERIC PRESSURE LOSS	0.0000
THRUST ATTITUDE LOSS	-9.5244+00
GAIN DUE TO THRUST FORCE	4.6585+03

SUM FOR ALL STAGES

VACUUM THRUST

GAIN DUE TO EARTH ROTATION	9.9144+00
GRAVITY LOSS	-3.9591+03
DRAG LOSS	-6.8769+02
THRUST ATMOSPHERIC PRESSURE LOSS	-2.8406+02
THRUST ATTITUDE LOSS	-1.6932+02
GAIN DUE TO THRUST FORCE	2.9588+04

SUM OF ALL VELOCITY LOSSES = 2.4477615+04

6.3580000+06 6.3580000+06 1.3180000+06 1.3180000+06 0.0000000

 EMI No. 12-02-05-M-16
 Date: 7 June 1971

ENGINEERING MEMORANDUM

TITLE: EFFECTS OF EARTH OBLATENESS ATMOSPHERIC DRAG ON A SPACE SHUTTLE VEHICLE IN LOW PERIGEE ORBITS	EM NO: L2-02-05-M1-7 REF: DATE: 1 June 1971
AUTHORS: L.A. Bleich <i>L.A. Bleich</i>	APPROVAL: ENGINEERING SYSTEM ENGRG <i>E.C. Payne</i>

PROBLEM STATEMENT

Establish the velocity requirements for the orbiter vehicle to obtain the four specified low perigee orbits.

RESULTS

The velocity requirements for the orbiter vehicle to attain the desired 50 x 100 nm elliptical orbits are shown in Fig. 1. Results show that both orbiter-inclination and injection-latitude have an effect on perigee-injection velocities, when considering both vehicle drag and earth oblateness in performance analyses.

AFFECTED WORK STRUCTURE BREAKDOWN ELEMENTS

Ascent performance requirements.

ASSUMED CONDITIONS

The vehicle assumed in this study is the orbiter stage of a two-stage (with external droptank on orbiter) space shuttle configuration. Figure 2 shows ballistic zero-lift-to-drag data for the vehicle based on a planform area of 5,747 ft². At altitudes below 40 nm, the vehicle is assumed to be in the continuum flow regime with a (constant) hypersonic drag coefficient of 0.022. Above 80 nm, a free-molecule drag coefficient of 0.5 is assumed. Between 40 and 80 nm, the vehicle is in a transition drag region with drag coefficient varying from the hypersonic value of free-molecule conditions. The transition drag curve is based on an expansion obtained from Ref. 1.

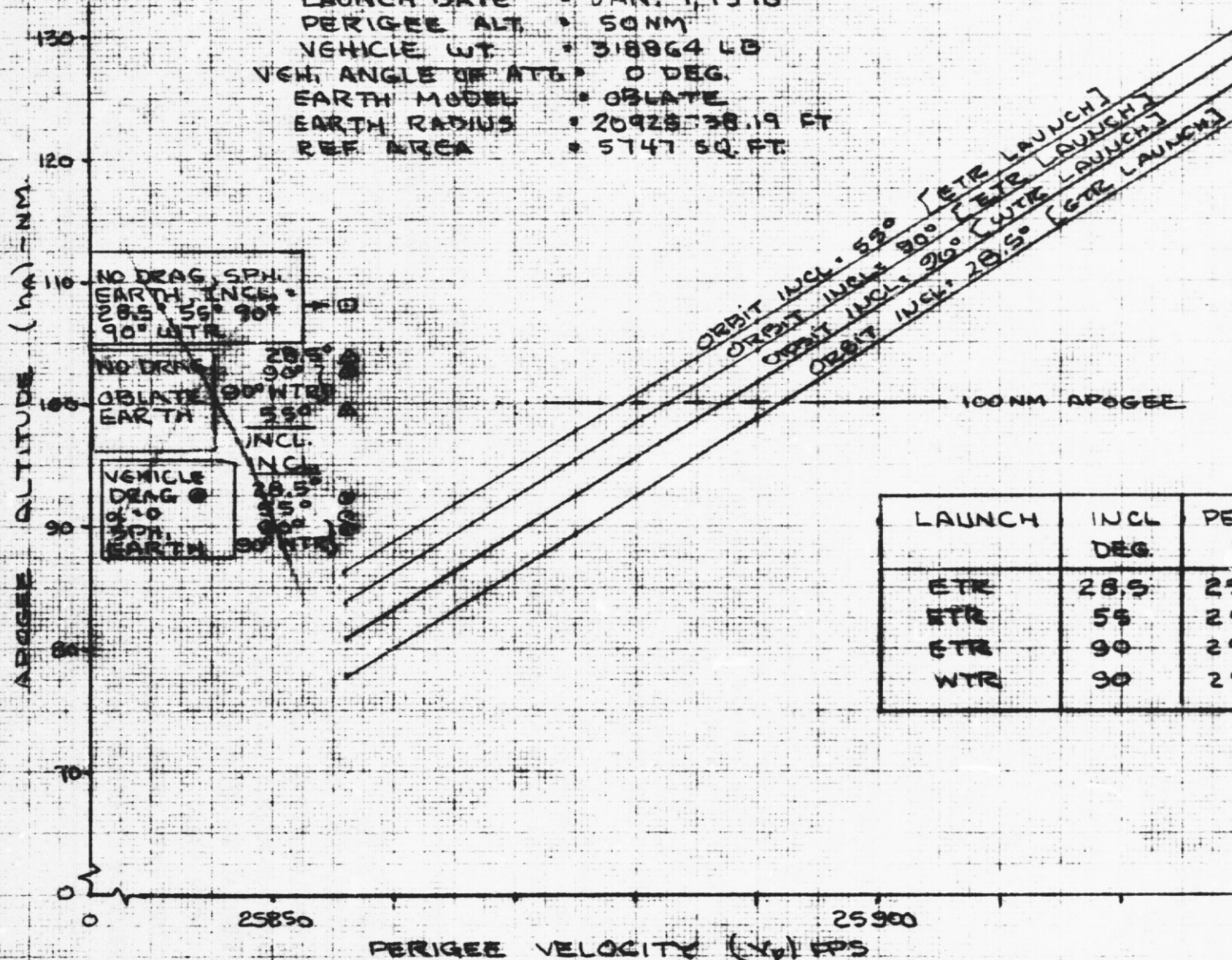
Four nominal orbits, with injective conditions as listed in Table 1, were used in the study. Perturbations about these orbits included changes in vehicle weight, injection velocity, earth oblateness, and vehicle drag.

Table 1
ASSUMED NOMINAL ORBIT CONDITIONS

	ORBIT CASE			
	1	2	3	4
LAUNCH SITE	ETR	ETR	ETR	WTR
PERIGEE ALTITUDE (nm)	50	50	50	50
EARTH LONGITUDE (deg)	68.27W	71.83W	81.19W	121.25W
EARTH GEOMETRIC LATITUDE (deg)	27.75N	36.92N	16.65N	22.83N
INERTIAL VELOCITY (fps)	25,856.1	25,856.1	25,856.1	25,856.1
AZIMUTH (deg)	96.73	45.85	180	180
FLIGHT PATH ANGLE (deg)	0	0	0	0
ORBIT INCLINATION (deg)	28.5	55	90	90

APOGEE ALTITUDE VS PERIGEE VELOCITY ORBITER VEHICLE

LAUNCH DATE • JAN. 1, 1978
 PERIGEE ALT • 50NM
 VEHICLE WT • 318864 LB
 VEH. ANGLE OF ATG • 0 DEG.
 EARTH MODEL • OBLATE
 EARTH RADIUS • 20925-38.19 FT
 REF AREA • 5747 SQ. FT.



PREPARED BY LAF
 DATE 5/17/71
 CHECKED BY

LOCKHEED MISSILES & SPACE COMPANY
 A GROUP DIVISION OF LOCKHEED AIRCRAFT CORPORATION

LOCK-07-1-1
 1 June 1971
 PAGE
 MODEL
 REPORT NO.

DRAG COEFFICIENT VS ALTITUDE ORBITER VEHICLE

DRAG COEFFICIENT C_D

REF AREA = 5747 SQ FT
ANGLE OF ATTACK = 0 DEG

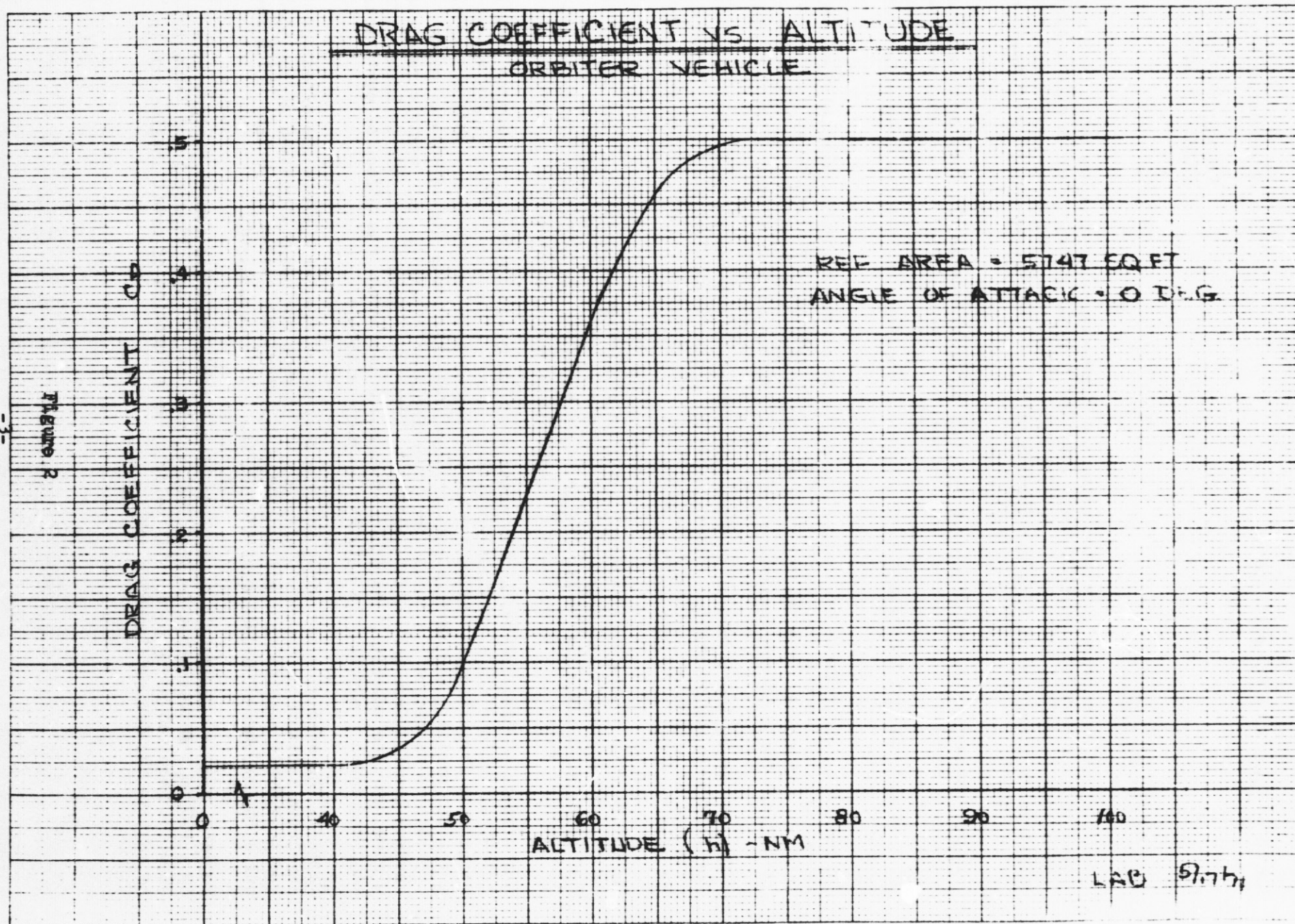
ALTITUDE (H) - NM

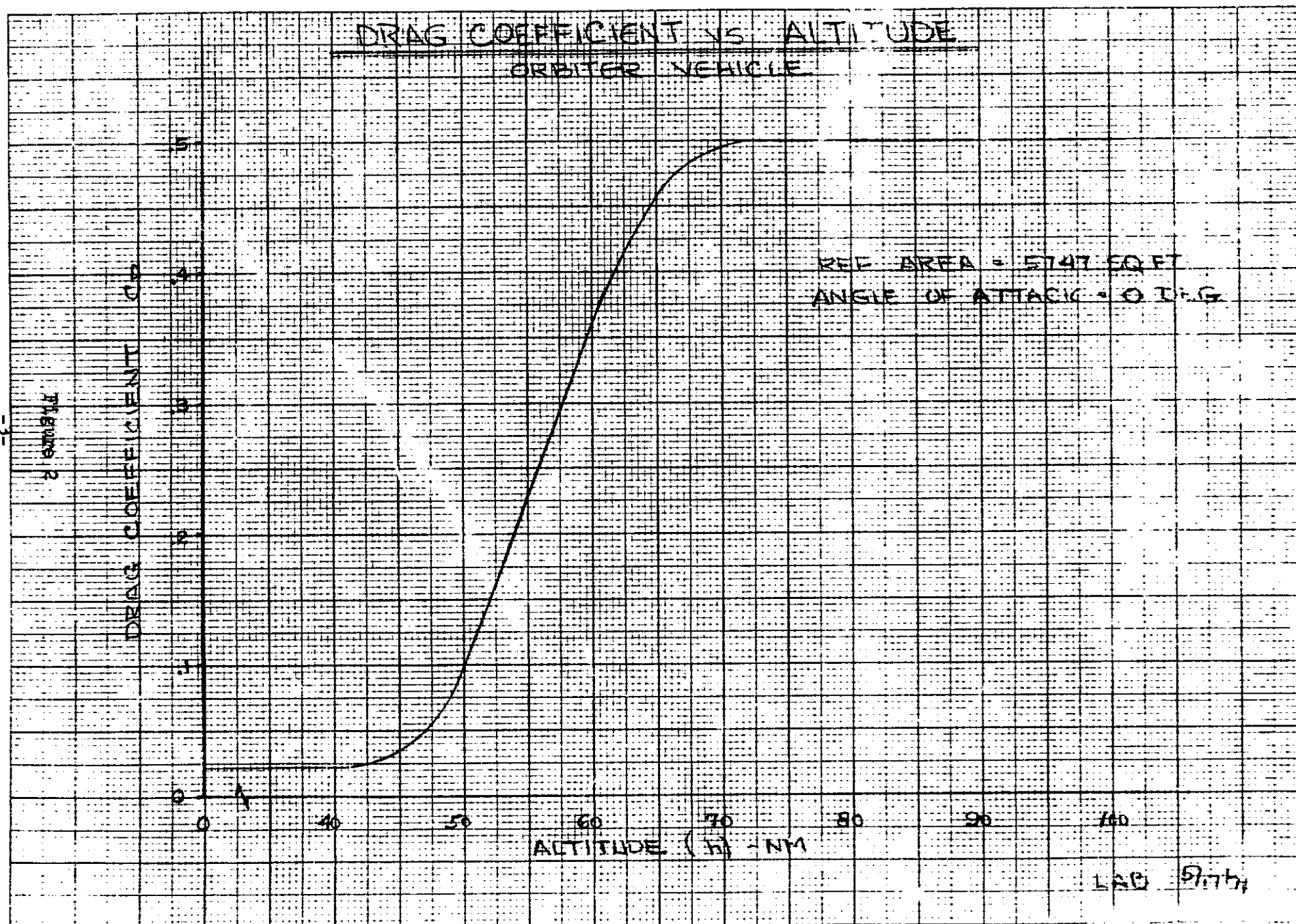
-3-

Figure 2

L2-02-05-M1-7
1 June 1971

LAB 51771





DISCUSSION OF RESULTS

Orbit trajectories were generated using the three-degree-of-freedom point mass computer program developed by LMSC (Ref. 2). The program incorporates an oblate earth and a time-dependent atmospheric density model (Ref. 3). The drag coefficient versus altitude is presented in Fig. 2. Results of this study are presented in Figs. 1 and 3.

Figure 3 shows variations of apogee altitude with vehicle weight for three orbit conditions - namely: ETR-launched trajectories with orbit inclinations of 28.5 and 55-deg and a 90-deg inclined-orbit launched from WTR. Note that apogee altitude increases with vehicle weight indicating a corresponding decrease in relative drag effects for heavier vehicles.

In reviewing the effects of inclination angle on apogee altitude, the added effects of earth rotation and specific orbit injection locations relative to an oblate earth must be considered. For the unique cases considered herein, orbit injection perigee conditions for a 55-deg inclined orbit result in the highest apogee altitudes (Fig. 3).

Figure 1 shows the effect of perigee (injection) velocities on apogee altitude for the four 50 x 100 nm orbits. The data assume a constant-weight vehicle (318,864 lb) oriented at a constant-zero angle-of-attack. The perigee velocity range considered is from 25,856.1 to 25,930 fps.

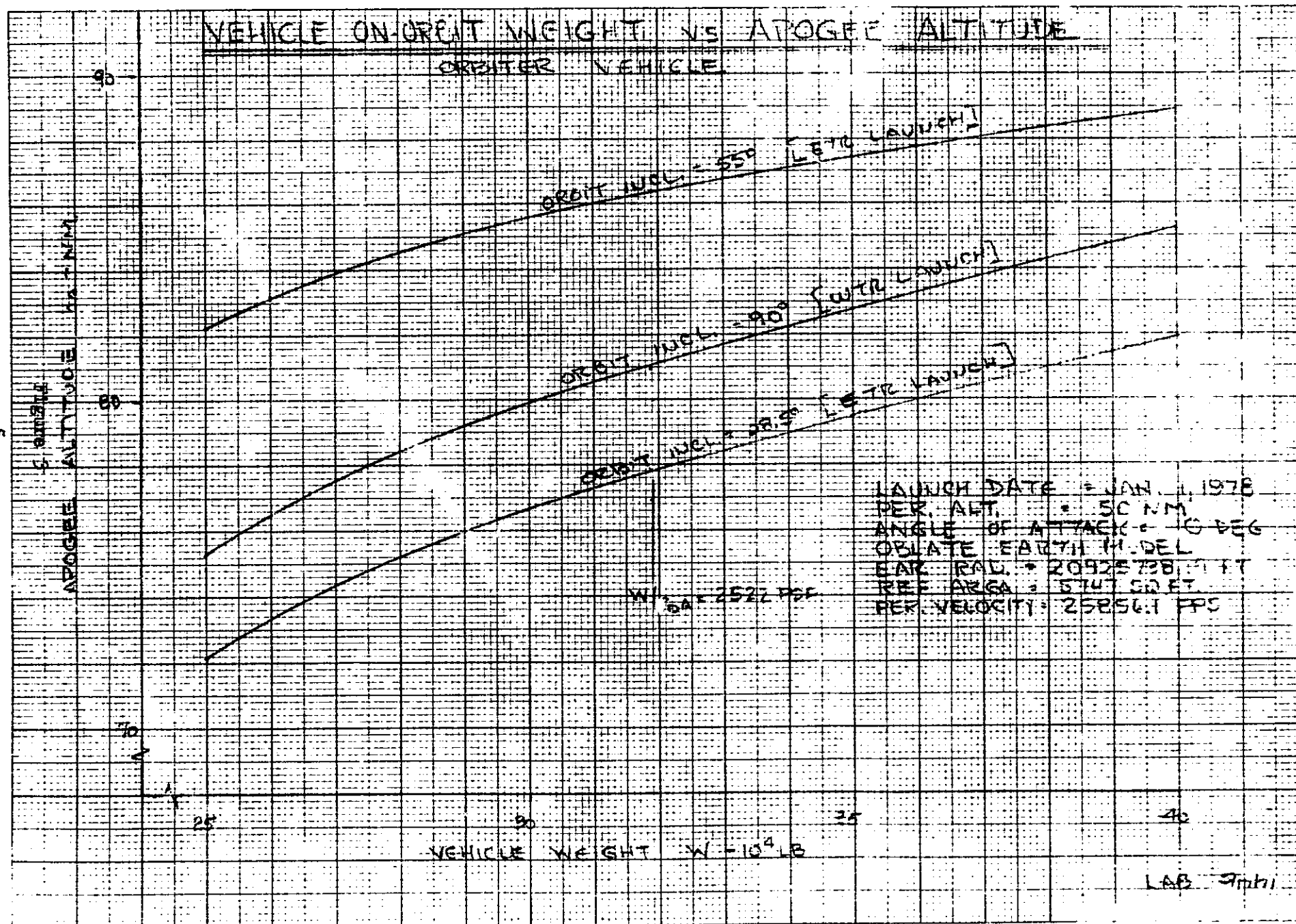
As before, the 55-deg inclined-orbit attains higher apogee altitudes than either the 28.5 or 90 deg orbits at corresponding perigee velocities. The apogee altitude differential between the 90-deg inclined orbits is due to differences in orbit-injection latitudes (16.65 deg N for ETR launch and 22.83 deg N for WTR launch).

The effects of drag and earth oblateness are also shown in Fig. 1. Assuming both a zero-drag vehicle and a spherical-rotating earth, an apogee altitude of 108 nm is attainable for all cases indicating an independence to inclination. Adding drag to a vehicle orbiting a spherical-rotating earth clearly shows the effects of orbit inclination on apogee altitude. For lower inclination angles, the vehicle receives maximum benefit from the earth's rotation vector, and apogee altitude is highest for a given perigee velocity. As inclination angle increases, the effect of earth rotation decreases, reducing the attainable apogee altitude.

Finally, the case of a zero-drag vehicle over an oblate earth shows the effect of injection latitude on the orbit altitude. The more northerly injection of the 55-deg inclined-orbit results in a radius vector-velocity combination at perigee which results in the lowest apogee altitudes of the orbits considered.

To date, most space shuttle operations have considered injection at perigee of a 50 x 100 nm transfer orbit before circularizing at 100 nm. Figure 1 and Table 2 show the required perigee inertial velocity as a function of orbit inclination to achieve the desired transfer orbit.

- 5 -



LA-02-05-M1-7
1 June 1971

EM NO: L2-02-05-M1-7

DATE: 1 June 1971

Table 2

PERIGEE VELOCITY REQUIREMENTS FOR 50 x 100 NM ORBITS

LAUNCH SITE	ORBIT INCLINATION (deg)	PERIGEE VELOCITY (fps)
ETR	28.5	25,892
ETR	55.0	25,879
ETR	90.0	25,883
WTR	90.0	25,887

REFERENCES

1. "Experimental Sphere Drag Results in a Near-Free Molecule Regime," William H. Sims, LMSC/HREC Report, Huntsville, Ala, June 1967.
2. "Programming of Three-Degree-Of-Freedom Equations of Motion For a Point Mass Including A Rotating Oblate Earth, Thrust and Drag," V. P. Peline et al, LMSC IDC AXA/128, Sunnyvale, Cal., 26 October 1959.
3. "Atmospheric Density Between 70 and 200 Nautical Miles From Satellite Observations," H. W. Small, LMSC Tracking Note N23, LMSC/A376332, Sunnyvale, Cal., 25 July 1964.

ENGINEERING MEMORANDUM

TITLE: ORBITER EXTERNAL LH ₂ TANK FINENESS RATIO OPTIMIZATION	EM NO: L2-12-M1-2 REF: DATE: 20 May 1971
AUTHORS: R. A. Byers <i>R. A. Byers</i>	APPROVAL: ENGINEERING SYSTEM ENGRG

PROBLEM STATEMENT

It is desired to know what external LH₂ tank fineness ratio provides the best performance potential based on the configuration presented in Reference (1).

RESULTS

The analysis shows that if the tank fineness ratio could be increased from the value of six as indicated in Reference (1), the system performance would improve. For example, a tank fineness ratio of about 8:1 would result in a payload increase at perigee injection of about 500 to 600 pounds. A 1-1/2 to 2 percent reduction in composite drag coefficient is also derived by reducing the forward cone half angle from 24° to 15°, but this effect is not included in the above payload increase.

AFFECTED WORK BREAKDOWN STRUCTURE

Orbiter
Orbiter External LH₂ Tank

ASSUMPTIONS

The following assumptions apply:

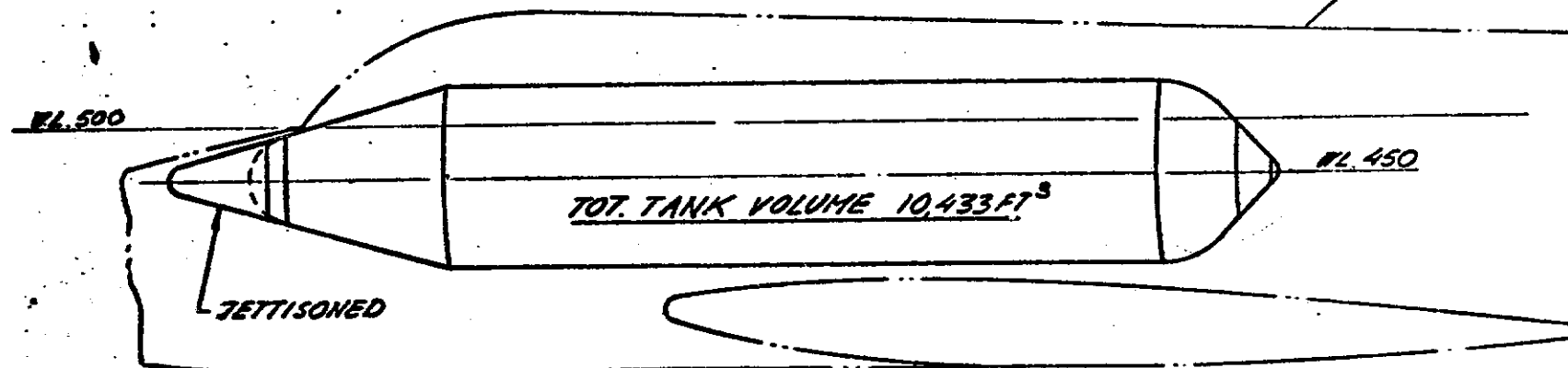
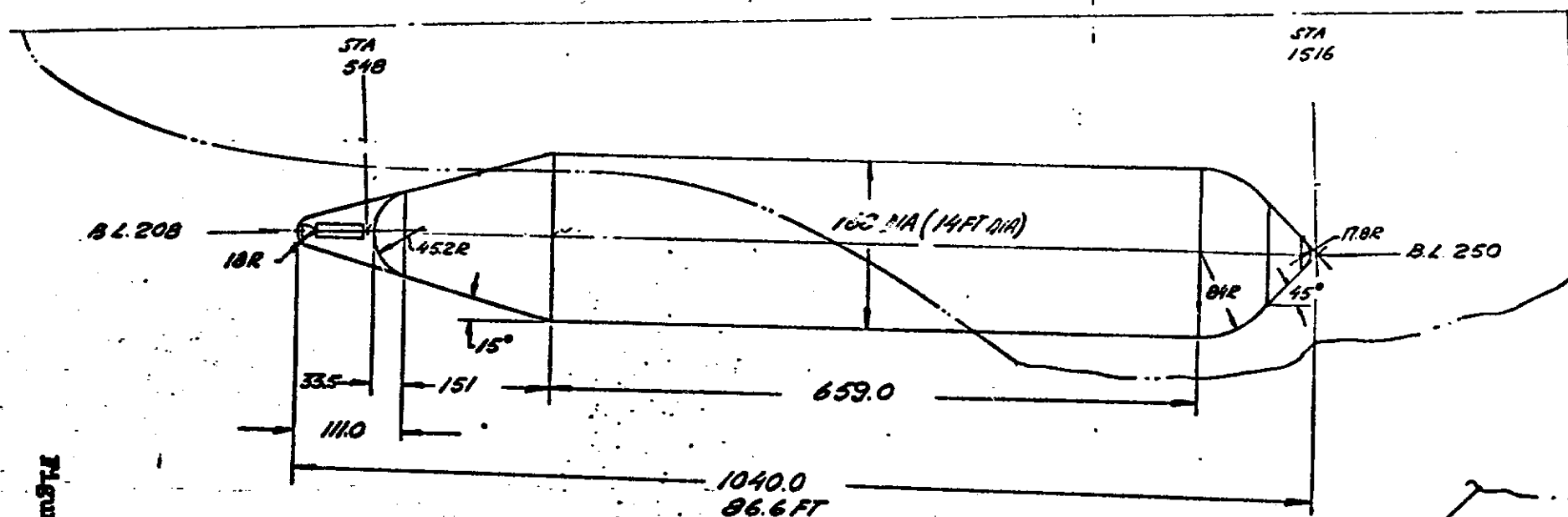
1. The tank configuration is shown in Figure 1 and the dimensions vary as shown in the curves.
2. The volume is constant at 10,300 cubic feet.
3. The composite vehicle drag coefficient varies according to the curves in Figure 2.
4. 55° orbit inclination
5. Internal pressure designs the tank wall with a maximum pressure of 33 psig

DISCUSSION

The weight effects of varying tank fineness ratio were analyzed for four primary weight (performance) contributors: (1) The tank weight, (2) the insulation and T.P.S. weight, (3) the tank/orbiter support structure weight, and (4) the effect of composite drag coefficient. These four contributors were then combined to show the effect on injected payload.

The tank system weight variation is shown in Figure 3. The weight variation is slight and reduces as the tank diameter increases. The variation of the associated tank support structure is presented in Figure 4. The support structure variation has the least effect of any of the contributors.

The insulation and T.P.S. weight variations are presented in Figure 5. The chart presents weights for two conditions; for ascent protection only and also for intact entry protection. The bottom curve on the graph shows the variation of orbiter T.P.S. weight with tank fineness ratio.

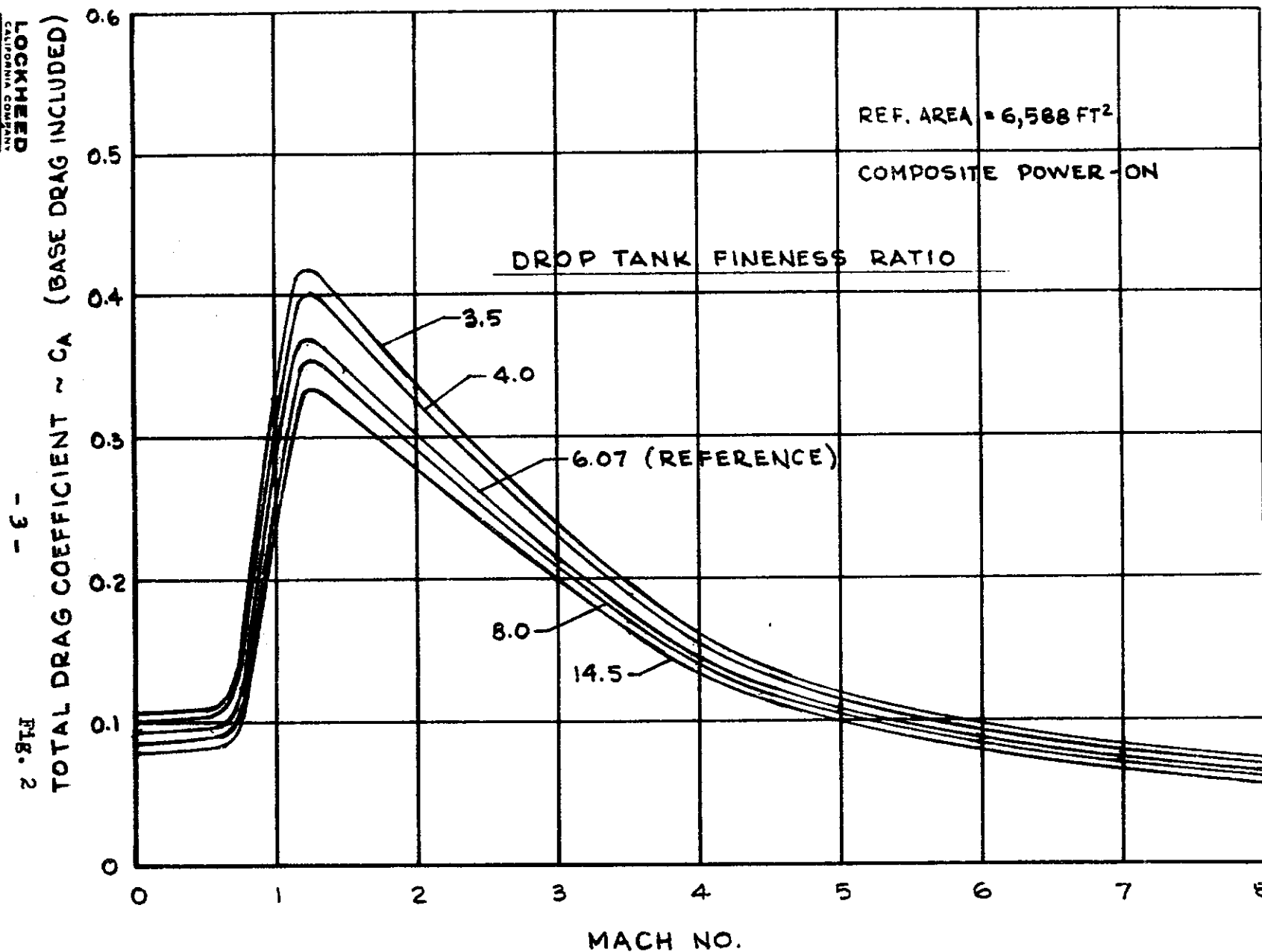


4-21-71 ST.

INSTALLATION AND TANK GEOMETRY
GRUMMAN DROP TANK. SKT 100703

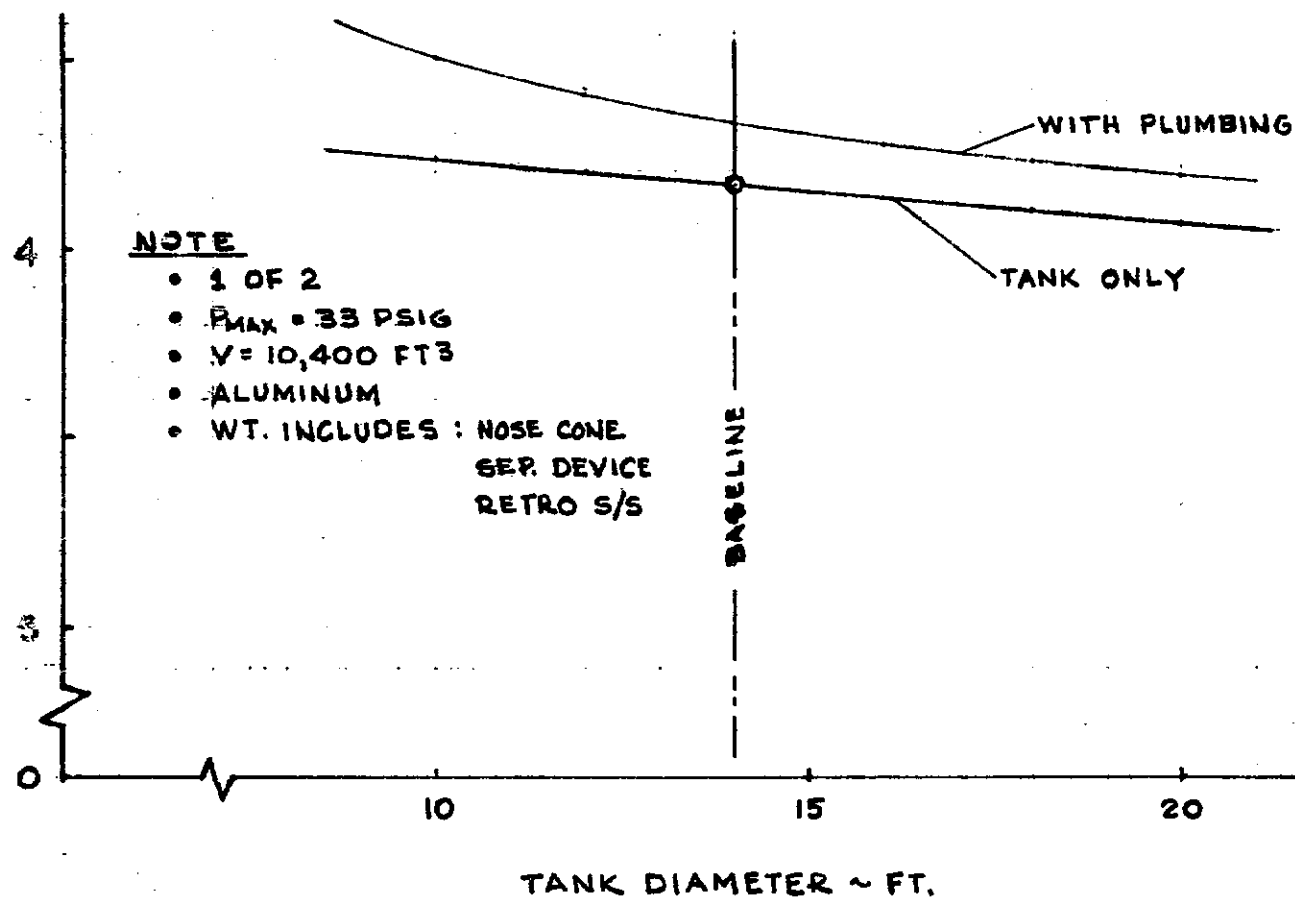
12-12-M1-1
20 May 1971

DRAG COEFFICIENT FOR DROPTANK GEOMETRY STUDY



12-12-M1-2
20 May 1971

EXTERNAL DROPTANK WEIGHT/DIAMETER VARIATION



LC-14-M1-2
20 May 1971

SUPPORT STRUCTURE WEIGHT VARIATION

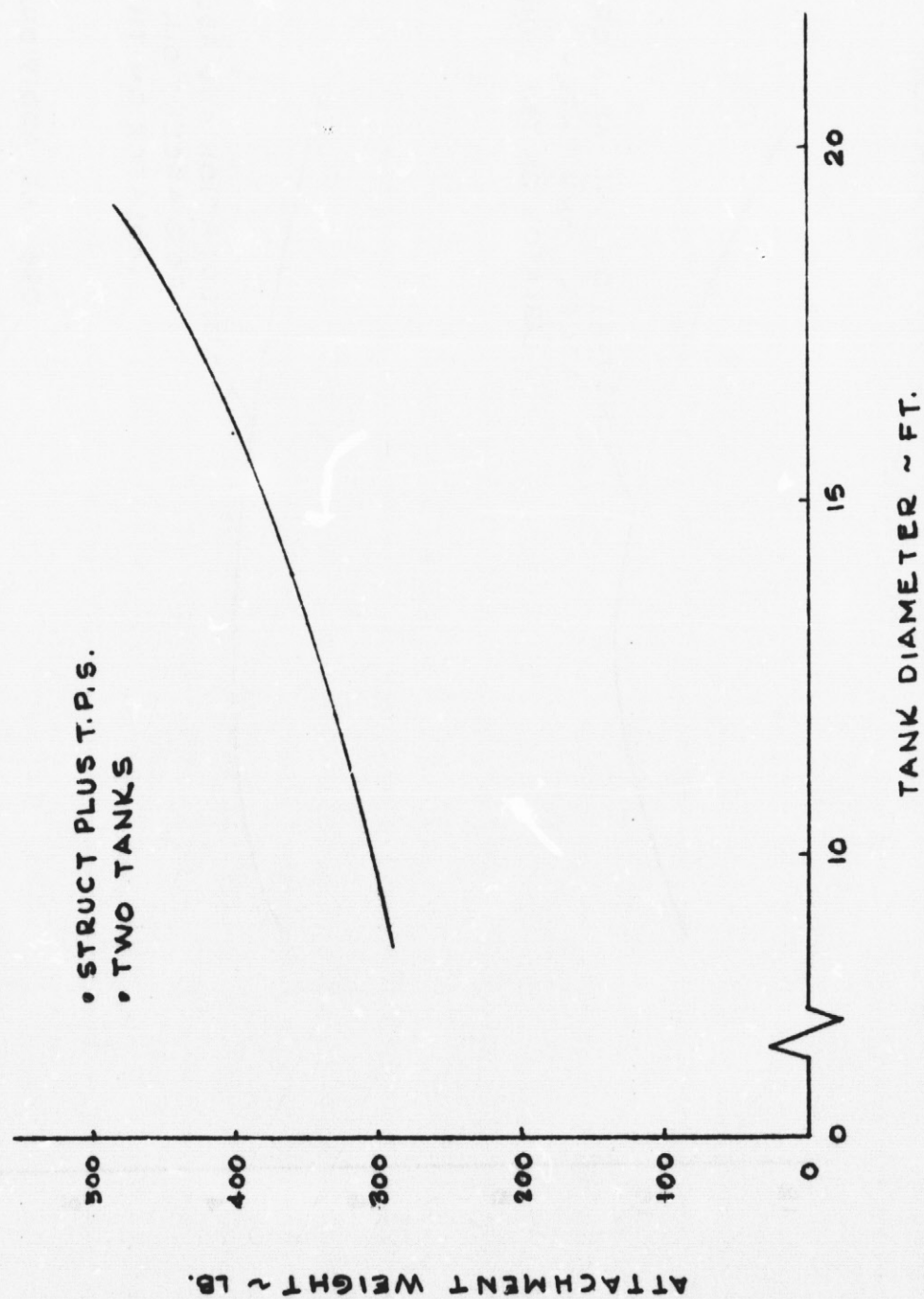
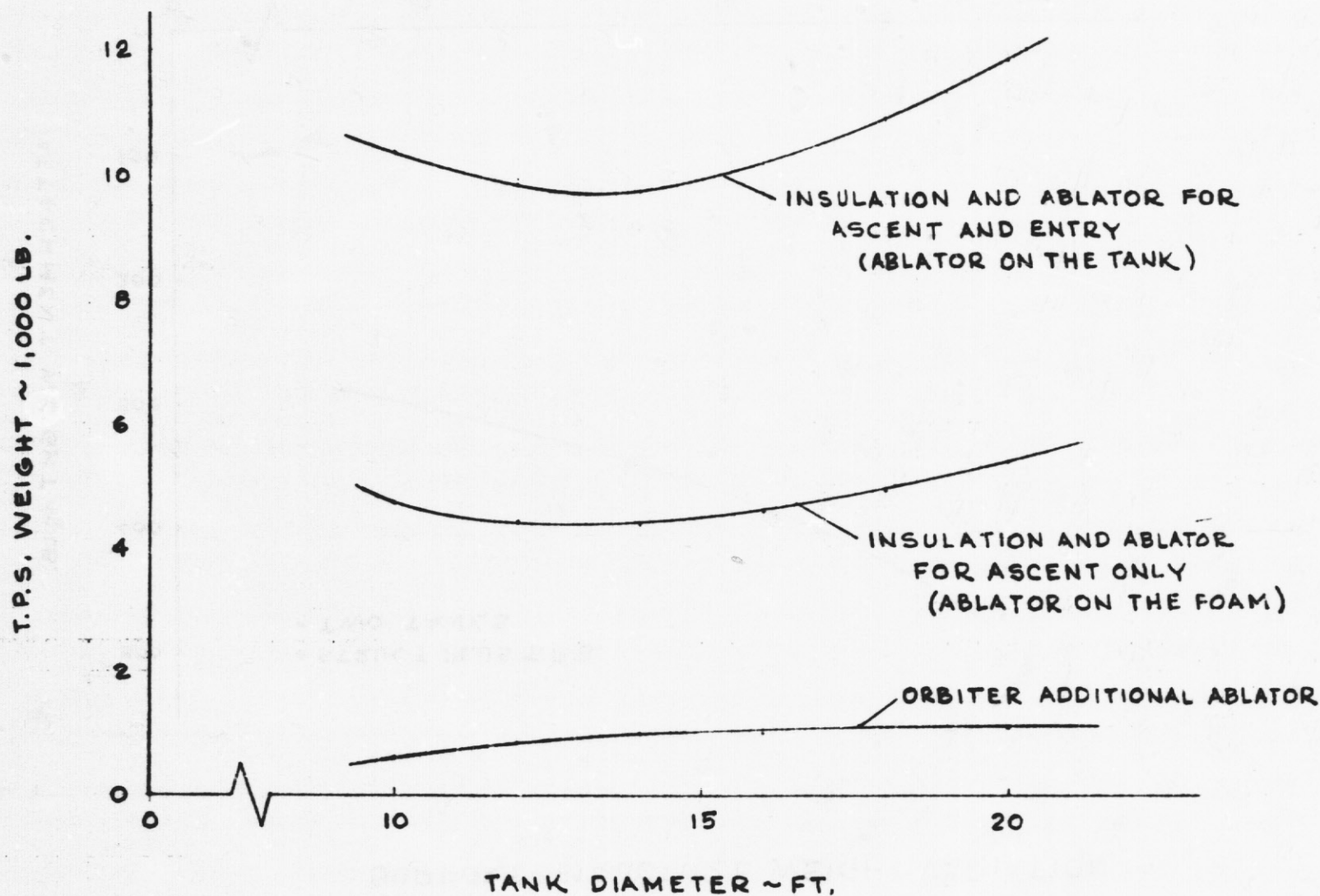


Fig. 4

ORBITER/DROPTANK T.P.S. WEIGHT VARIATION TWO TANKS



L2-12-M1-2
20 May 1971

Fig. 5

EM NO: L2-12-M1-2
DATE: 20 May 1971

Figure 6 shows the relationship between tank diameter and fineness ratio for the fixed volume.

The composite effect of the foregoing weight variations is shown in Figure 7. The dashed line shows the effect on payload of the tank fineness ratio when only the ascent insulation and T.P.S. is considered. The solid line indicates the variations when the tanks are protected for intact entry. The boundary at a fineness ratio of eleven is approximately where a transition occurs from design for internal pressure to design for in-flight bending loads. At this tank volume, however, a ratio of about 12.5 is physically practicable with regard to the Orbiter interface. By reducing the cone half and to 15 degrees, a reduction in composite drag coefficient of about 1-1/2 percent is realized. This amounts to payload increase of about 250 pounds.

CONCLUSION

Two basic conclusions are derived from this analysis: (1) the fineness ratio for the Orbiter external tank should be as high as possible, and (2) secondary benefits are derived from shallow forward cone angles.

REFERENCES

1. "Alternate Space Shuttle Contract Study - External Hydrogen Tank Orbiter - Heat Sink Booster," March 1971 Review
2. EM L2-12-05-M1-6 "External Droptank Orbiter System Ascent Trajectories for 50 X 100 NM Orbit Injection," E. T. Fitzgerald, 7 June 1971
3. EM L2-12-01-M1-7, "GAC External Droptank Orbiter Thermal Evaluation," K. W. McGee, 11 May 1971
4. EM L2-12-01-M1-1 "Normal Force Distributions and Axial Force Characteristics for the External Droptanks," G. Morris, 29 April 1971
5. Unpublished data from S. A. Carter and J. J. Baserga

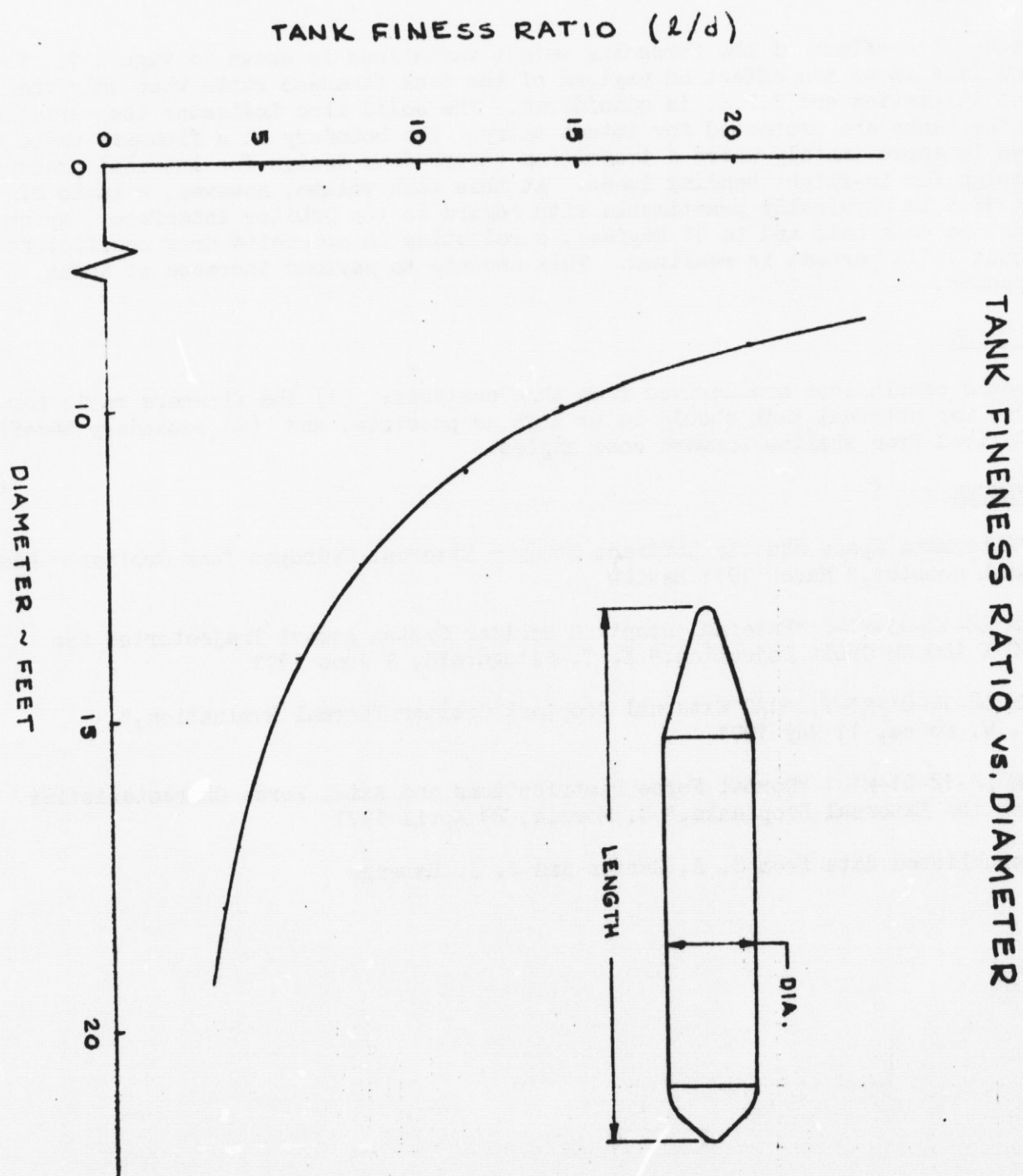


Fig. 6

L2-12-M1-2
20 May 1971

EFFECT OF TANK DIAMETER ON PAYLOAD

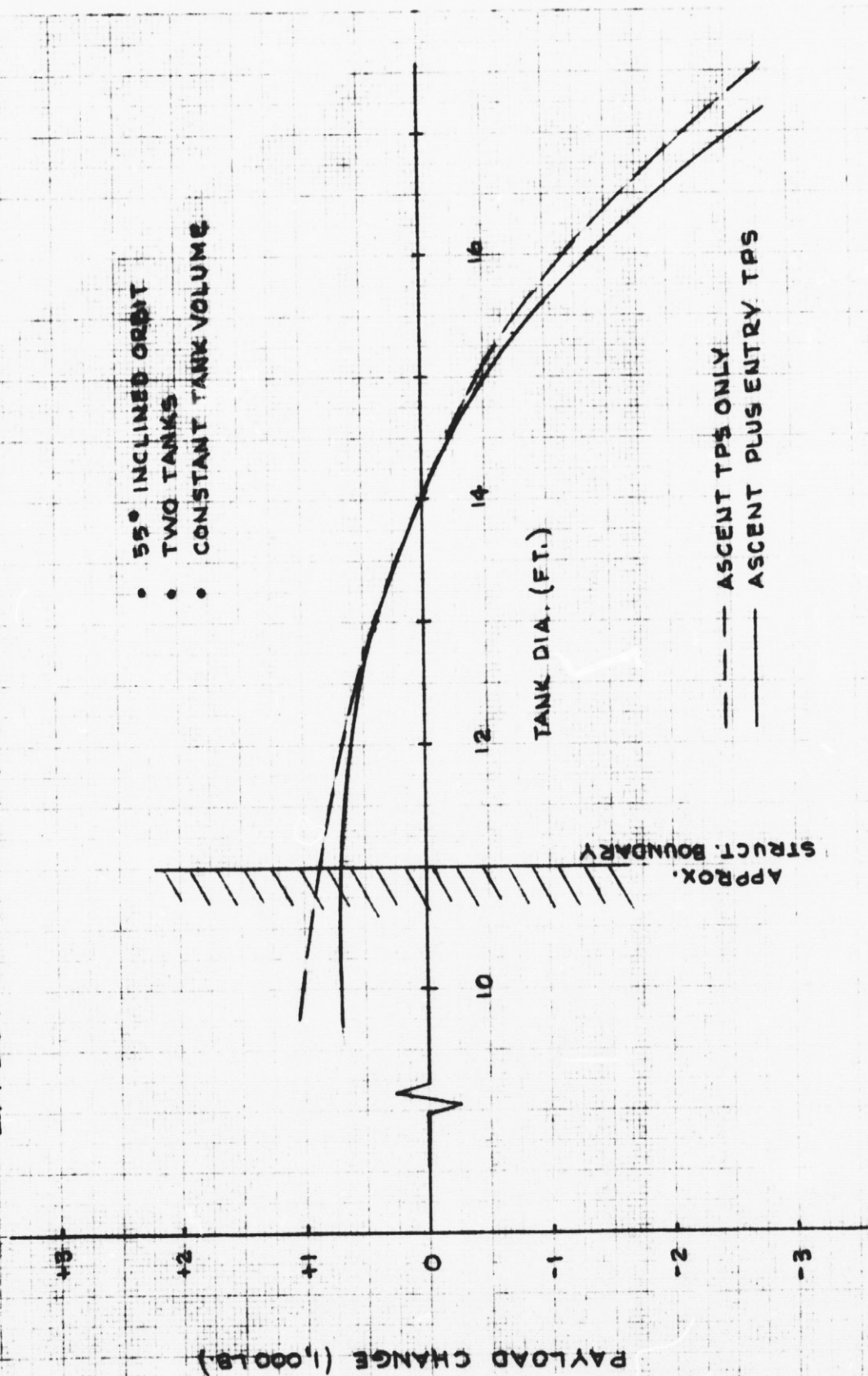


Fig. 7

ENGINEERING MEMORANDUM

TITLE: LH ₂ EXTERNAL TANKS - AERODYNAMIC EFFECTS OF TANK FAIRING AND POSITION	EM NO 12-12-01-M1-9 REF: DATE: 8 June 1971
AUTHORS: G. W. Morris <i>G. W. Morris</i>	APPROVAL: ENGINEERING SYSTEM ENGRG <i>P. A. Byers</i>

PROBLEM STATEMENT

Interference forces/moments due to adding LH₂ external droptanks to the orbiter vehicle are of the same order or greater than forces of the isolated tanks themselves. Alleviation of these interference forces through tank positioning, geometry changes, and tank-orbiter fairings, can reduce these characteristics significantly. Wind tunnel tests have been conducted by NASA in the Ames 6 ft x 6 ft test facility to measure these characteristics and to determine effects of tank position and fairings. These Ames test results (Ames Tests 66-551, 66-546, and 66-561), have been briefly analyzed and the results summarized herein.

DISCUSSION

LH₂ external droptanks tested on the ascent configuration in the Ames 6 ft x 6 ft facility are shown in Fig. 1. In addition to tank fairing, the effect of moving the T₂ conical tank to an aft fuselage position was also determined.

Figure 2 shows drag contribution of the composite ascent vehicle (including tanks), drag of orbiter plus tanks (in presence of booster), and drag of orbiter without tanks in presence of booster. This figure gives a feeling for the relative magnitude of the drag of major components of ascent vehicle. Figure 2 also shows percent reduction in composite vehicle drag due to moving the bi-conic LH₂ tank to an aft fuselage position and also due to fairing the tank nose when in the forward fuselage position. These results are all based on NASA Ames tests 66-551, 66-546, and 66-561. It can be seen the drag of the tanks plus mutual interference is of the same magnitude (or greater) than the orbiter itself.

Figure 3 gives a breakdown of the drag of, and due to, the bi-conic (forward mounted) tanks. The total axial force increment due to adding the tanks of the orbiter is designated as:

$$(T + T_{BW} + B_T + W_T)$$

where:

- T → Contribution of isolated tank (free body) (no interference effects)
- T_{BW} → Axial force acting on tank due to presence of orbiter
- B_T → Axial force acting on orbiter body due to presence of tanks
- W_T → Axial force acting on orbiter wings due to presence of tanks

Forces on the tank in presence of the orbiter (T + T_{BW}), were measured by a separate balance in the tank, with the tank supported entirely by a separate sting. Tanks plus total interference effects (T + T_{BW} + B_T + W_T) were obtained by subtracting the axial force of the composite vehicle without tanks from the composite vehicle with tanks.

$$(BOT - BO) = (T + T_{BW} + B_T + W_T)$$

Isolated tank axial forces were analytically estimated (See Reference 1). At Mach 1.2 it is seen that the total installed tank drag is 3.2 times the drag of the isolated tanks.

Figure 4 shows the effect on installed tank axial force due to a fairing over the biconic nose and due to locating the tanks farther aft. The interference effects of the tanks on the orbiter, i.e., $(B_T + W_T)$, are seen to be of the same magnitude as the forces on the tanks, $T + T_{BW}$. The effects of the nose fairing have the major influence on reducing the drag of the tank, $T + T_{BW}$, and a smaller effect on reducing the interference drag of the tanks on the orbiter, $B_T + W_T$. Moving the biconic tanks to an aft fuselage position reduces tank drag ($T + T_{BW}$) by 23 percent at Mach 1.2. This is most probably caused by movement of the tank nose away from the influence of the high pressure field of the orbiter nose. The fairing over the conical nose reduces drag of the tank ($T + T_{BW}$) by 42 percent at $M=1.2$.

Figure 5 presents estimated axial force characteristics of the isolated tanks as a function of tank fineness ratio and Mach number. The analytical approach for obtaining these results is described in Ref. 1. Also shown in Fig. 5 is a bar graph indicating the drag reduction potential of the composite ascent vehicle due to LH_2 tank position, geometry, and fairing. A combination of:

- Aft fuselage position
- Tank nose fairing
- Increased tank fineness ratio

could potentially reduce ascent vehicle drag by more than 11 percent.

Figure 6 presents test results showing the pitching moments and normal force contributions of, and due to the LH_2 tanks. The tanks themselves ($T + T_{BW}$) do not have a large effect, however, the interference effects on the orbiter ($B_T + W_T$) are seen to be significant. Because of the positive normal force increment and the negative pitching moment increment these interference effects apparently are acting over the orbiter wing in the region of the tank base. Movement of the tank to an aft position would possibly reduce or eliminate this effect. It should be pointed out that on the composite ascent vehicle, this interference effect is destabilizing since the orbiter is mounted forward of the booster cg position.

Effects of drag increment on a payload are shown in Figure 7 as a function of orbit inclination. The variation $\frac{\partial PL}{\partial \Delta C_D}$ is seen to be fairly linear, showing

approximately 250 lb payload loss per percent drag increase. The 5 percent drag reduction due to a fairing over the tank nose (see Fig. 5) would thus give a 1250 lb payload increase. The added weight from the fairing would of course subtract from this payload benefit. These results were obtained by relating the change in orbit injection weight as a function of tank fineness ratio (Ref. 2) to the change in ascent drag as a function of tank fineness ratio, Ref. 1.

Lockheed Missiles & Space Company

Space Shuttle Project

EM NO: L2-02-01 M1-9

DATE: 8 June 1971

REFERENCES:

1. EM L2-12-01-M1-1, "Normal Force Distributions and Axial Force Characteristics For the External Droptanks," G.W. Morris, dated 29 April 1971.
2. EM L2-02-05-M1-6, "External Droptank Orbiter System Ascent Trajectories for 50 x 100 nm Orbit Injection," E. T. Fitzgerald, 7 June 1971.

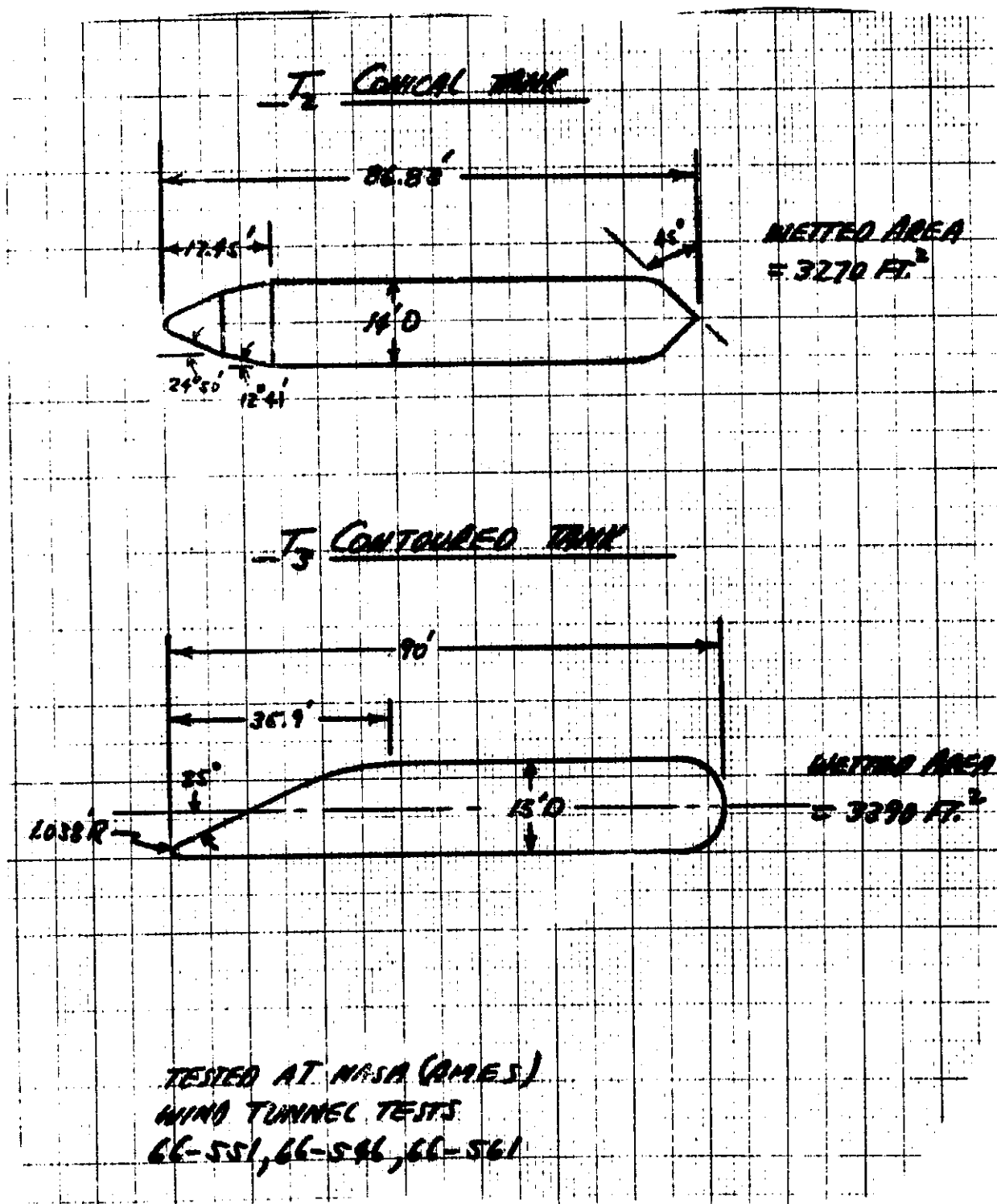


Fig. 1 LH₂ DROPTANKS

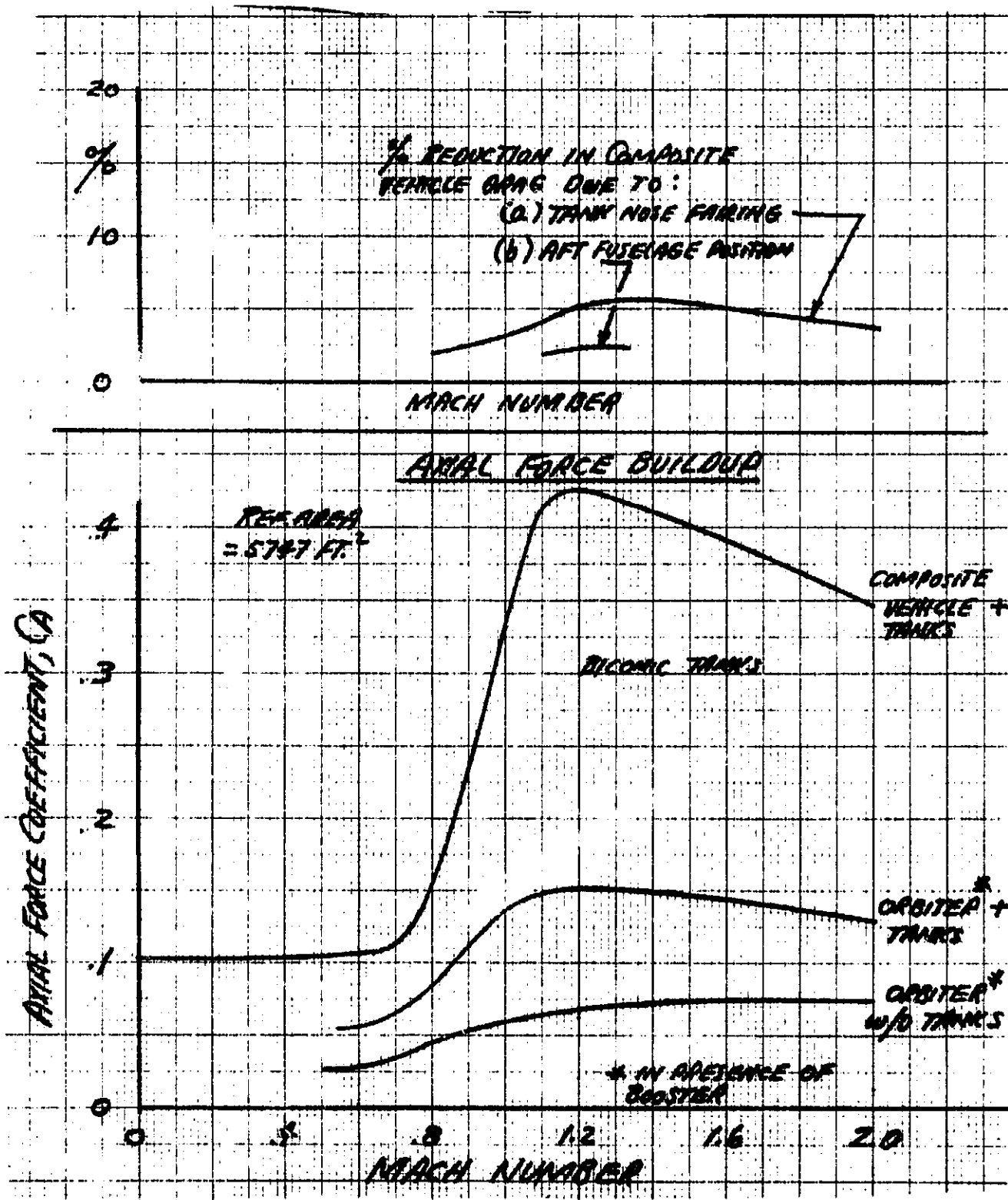


Fig. 2 AXIAL FORCE CHARACTERISTICS-ASCENT VEHICLE

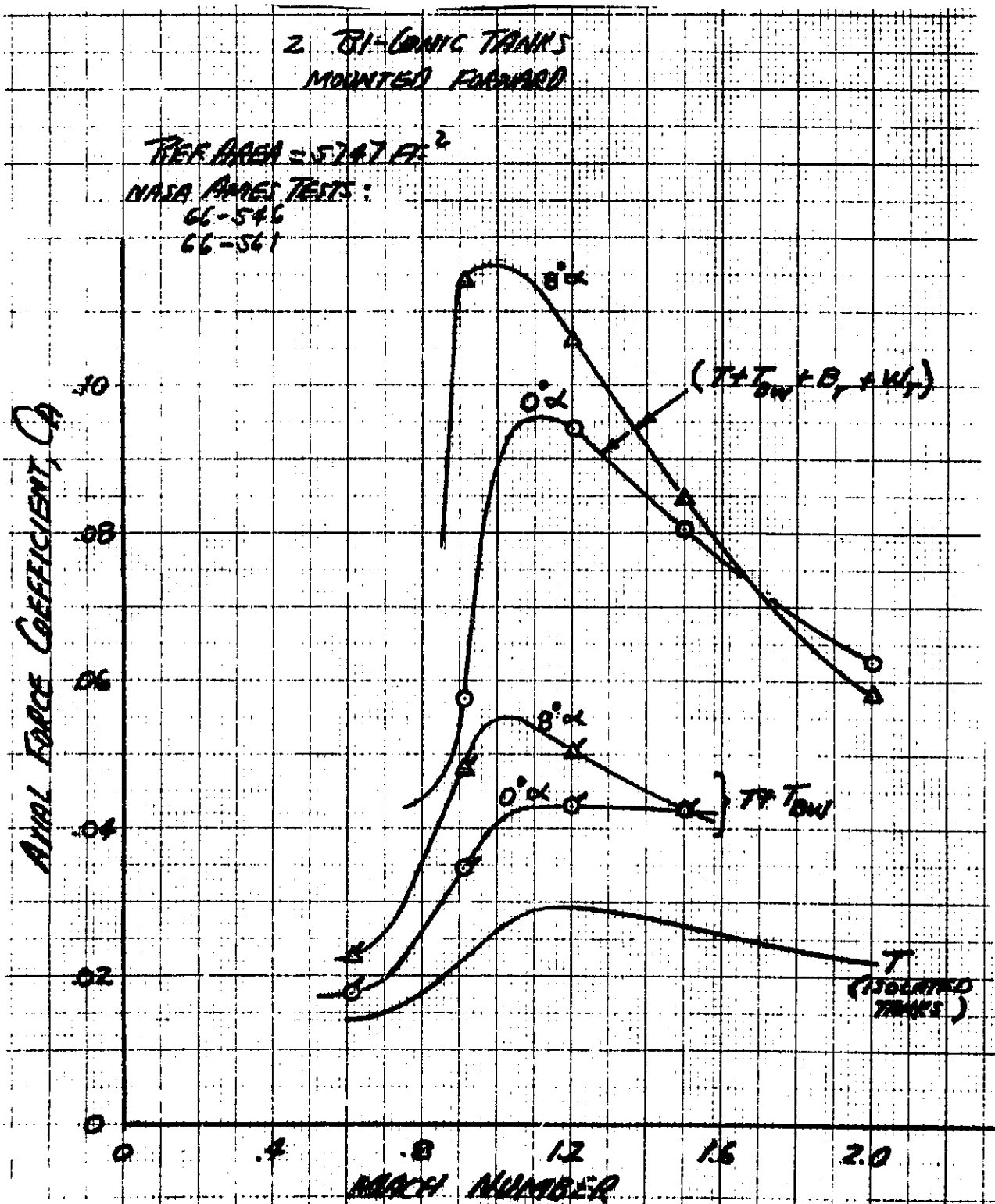


Fig. 3 AXIAL FORCE OF, AND DUE TO LH₂ TANKS

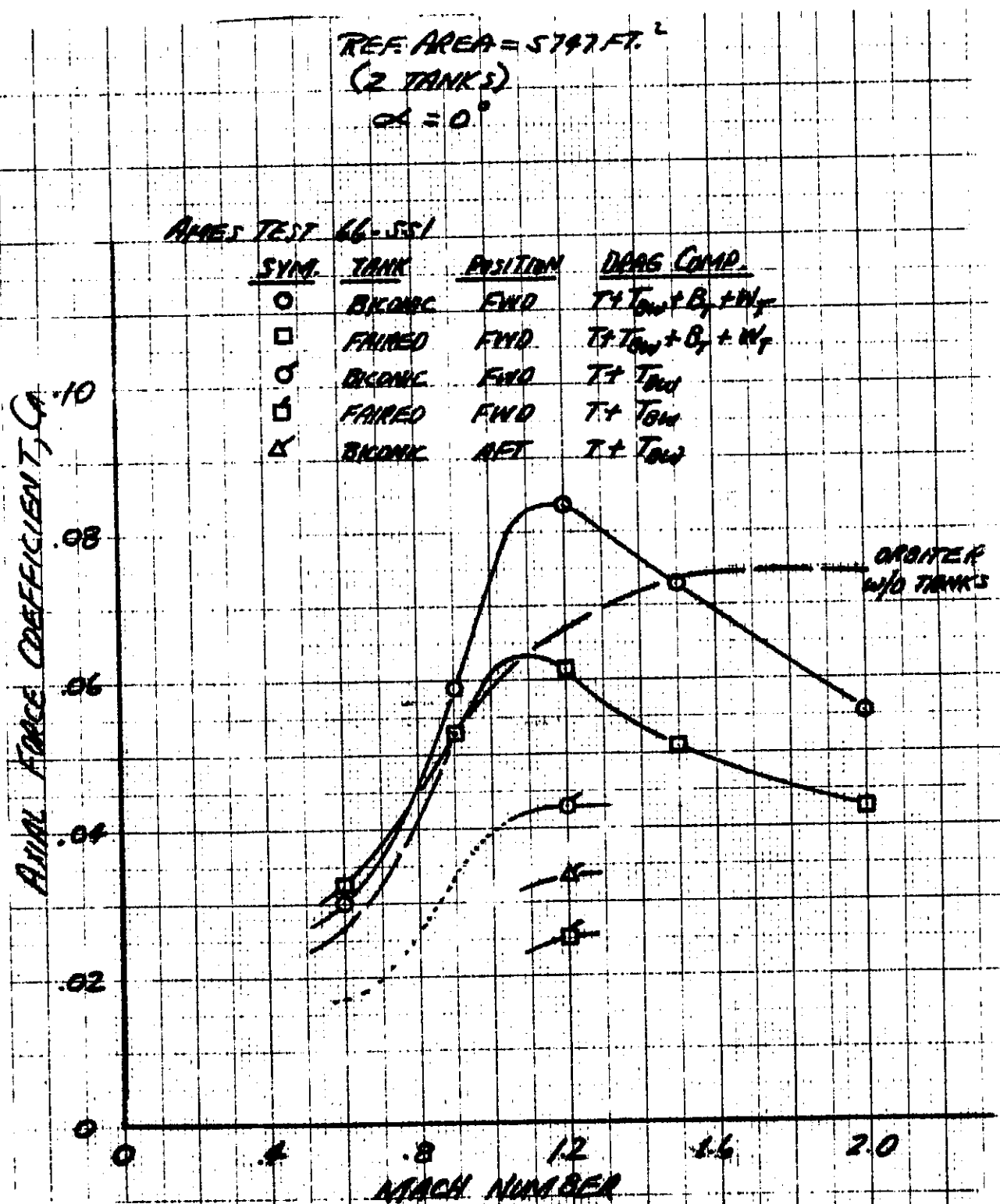


Fig. 4 LH₂ TANKS AXIAL FORCE - EFFECTS OF AXIAL LOCATION AND FAIRINGS

EM NO: L2-12-01-M-9
DATE: 8 June 1971

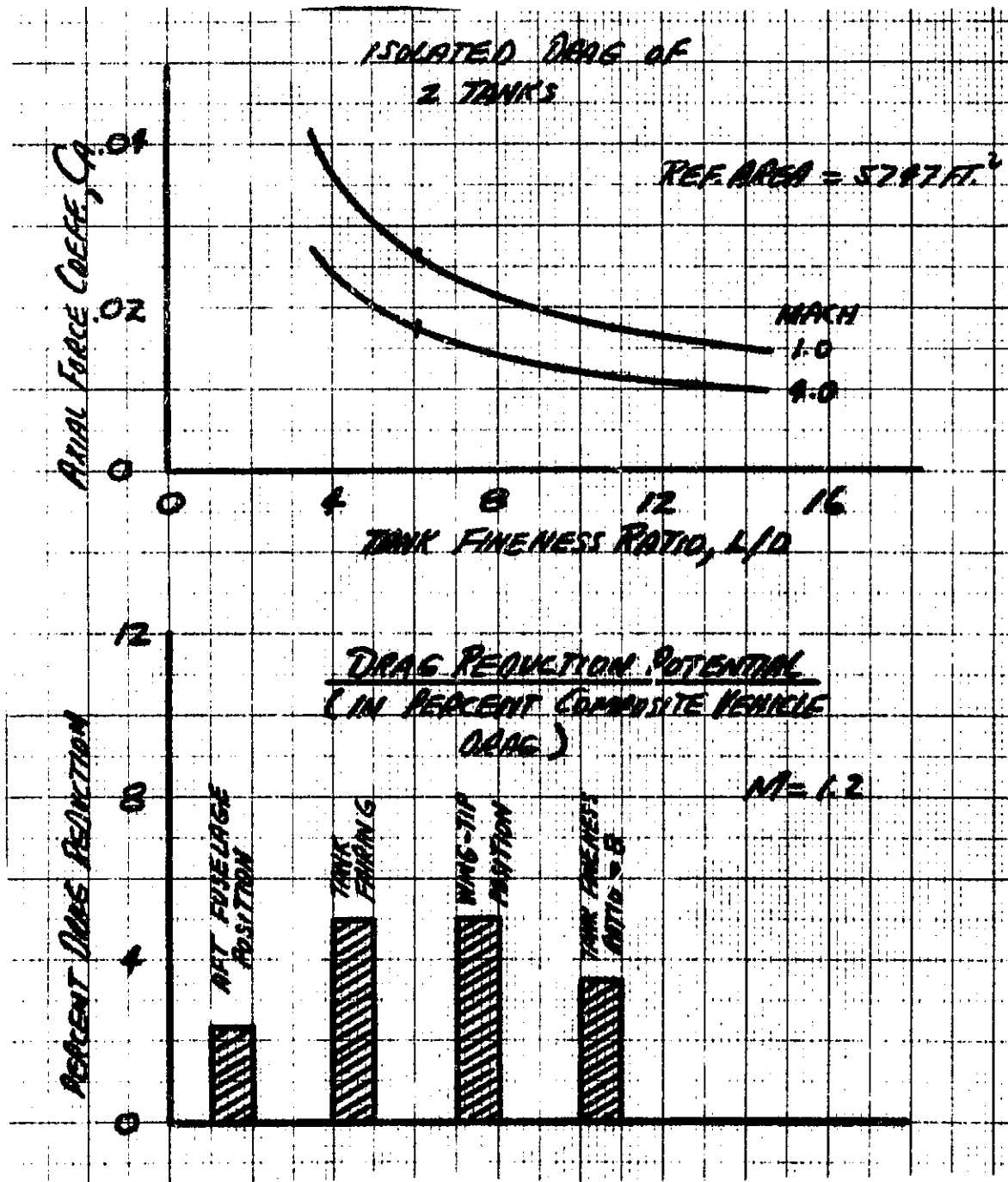


Fig. 5 ISOLATED TANK DRAG AND DRAG REDUCTION POTENTIAL

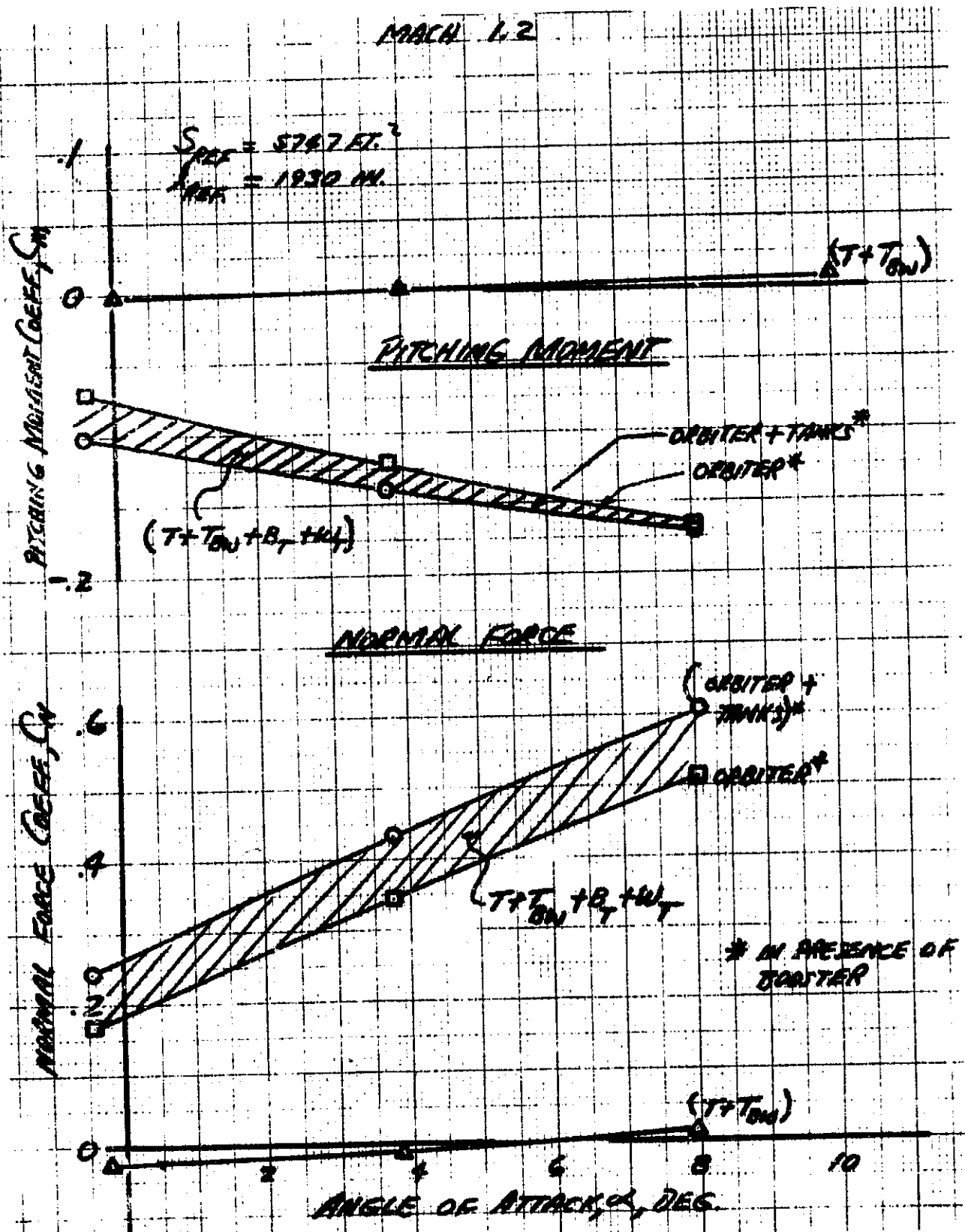


Fig. 6 ORBITER/LH₂ TANKS LONGITUDINAL CHARACTERISTICS

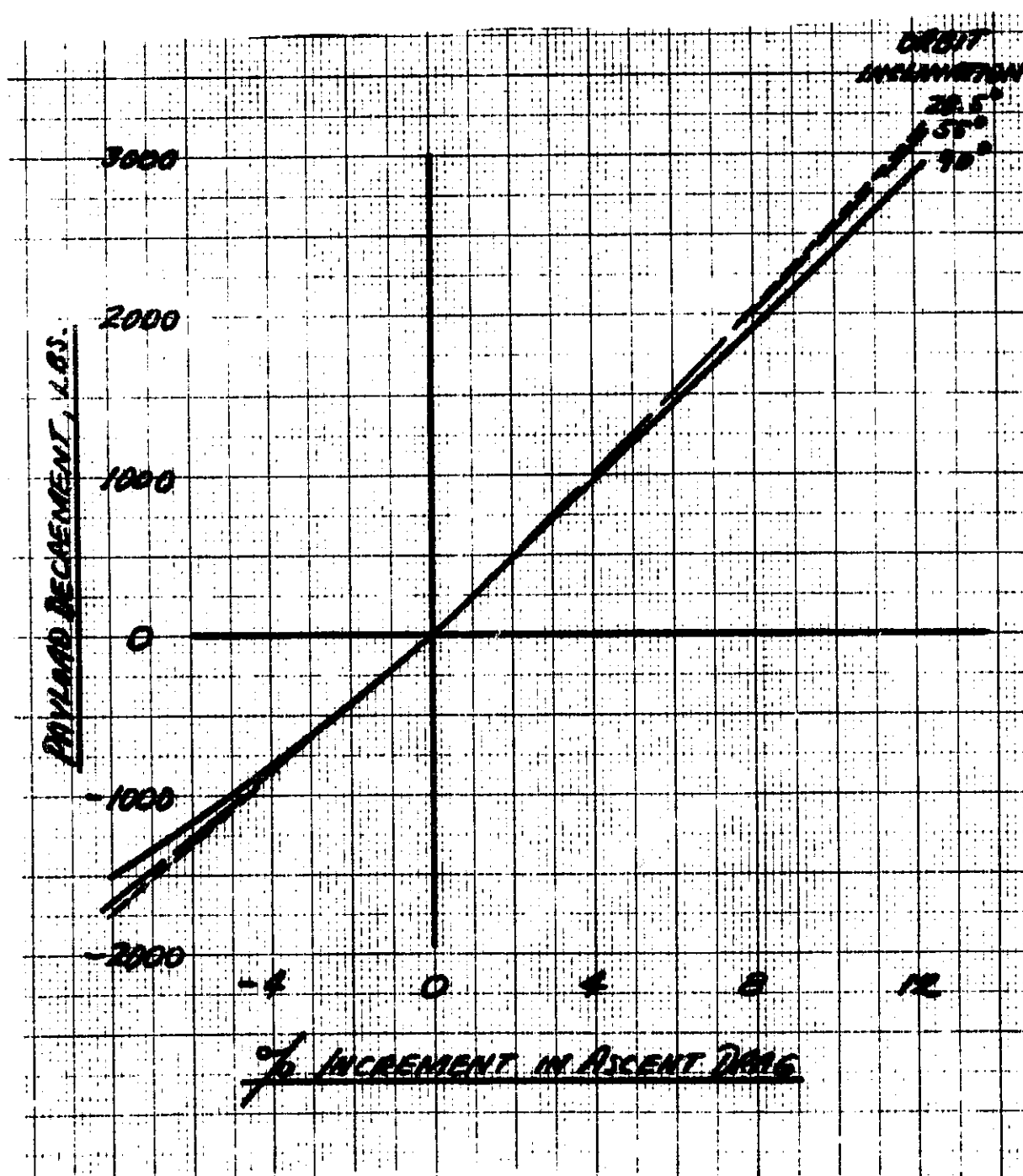


Figure 7 - Payload Increment As a Function of Ascent Vehicle Drag Increment

ENGINEERING MEMORANDUM

TITLE: GAS GENERATOR-PISTON SEPARATION ANALYSIS FOR THE ORBITER EXTERNAL LH ₂ TANK	EM NO: 12-12-02-M1-1 REF: DATE: 12 May 1971
AUTHORS: R. A. Byers <i>R. A. Byers</i>	APPROVAL: ENGINEERING SYSTEM ENGRG

PROBLEM STATEMENT

It is necessary to provide parametrics for a gas generator separation device with an estimate of the probable deviations at separation.

RESULTS

Parametric data are presented for separation time, piston size, gas generator pressure, translation distance and angular deviations.

AFFECTED WORK BREAKDOWN STRUCTURES

Orbiter
Orbiter External LH₂ Tank

ASSUMPTIONS

The following assumptions apply:

1. Tank weight = 10,390 lb
2. Two separation devices per tank (fore and aft) in the attach struts
3. Effective working pressure = 1,000 psia.

DISCUSSION

The baseline mechanical separation system consists of two gas generators which operate separate pistons in the forward and aft attachment struts. The struts are physically separated from the Orbiter, after which the gas generators are simultaneously ignited. The gas pressure forces the tanks away from the Orbiter at the desired acceleration level. After physical separation is completed, the tanks are allowed to translate away from the Orbiter to a predetermined distance at which time the tank retro rocket is fired to expedite tank entry.

The separation load factor as a function of piston diameter for a constant pressure of 1,000 psia is presented in Figure 1. The piston diameter is for one of two pistons but the acceleration is for two devices operating concurrently. A piston diameter of about six inches appears to be near the maximum to be compatible with the separation struts. Two six-inch pistons will accelerate the tanks at about 5-1/2 g's. With the residual ullage pressure, the tank can sustain a lateral acceleration of about 8 g's.

The time to achieve separation versus the piston stroke with the piston diameter as a parameter, is presented in Figure 2. An arbitrary lower boundary for a piston l/d of 3 is indicated on the graph. This shows that separation can be completed in 0.2 second for six inch piston 42 inches long. This was used in subsequent analyses.

The separation velocity-time relationship for various piston diameters is shown in Figure 3. The chart indicates a separation velocity of 35 F.P.S. for a six inch piston at 0.2 second.

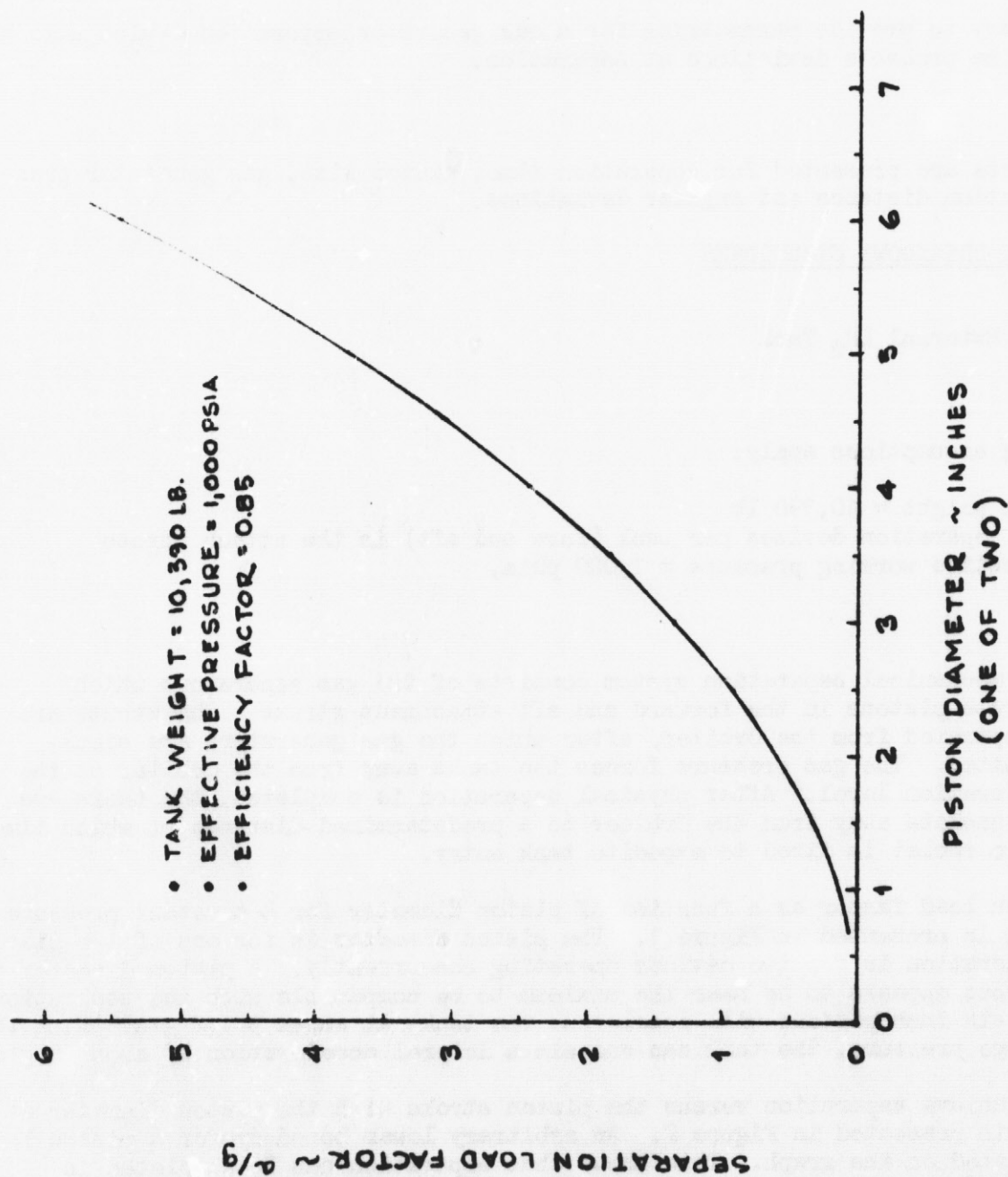


Figure 1 Separation Load Factor Vs. Piston Diameter (Two Pistons)

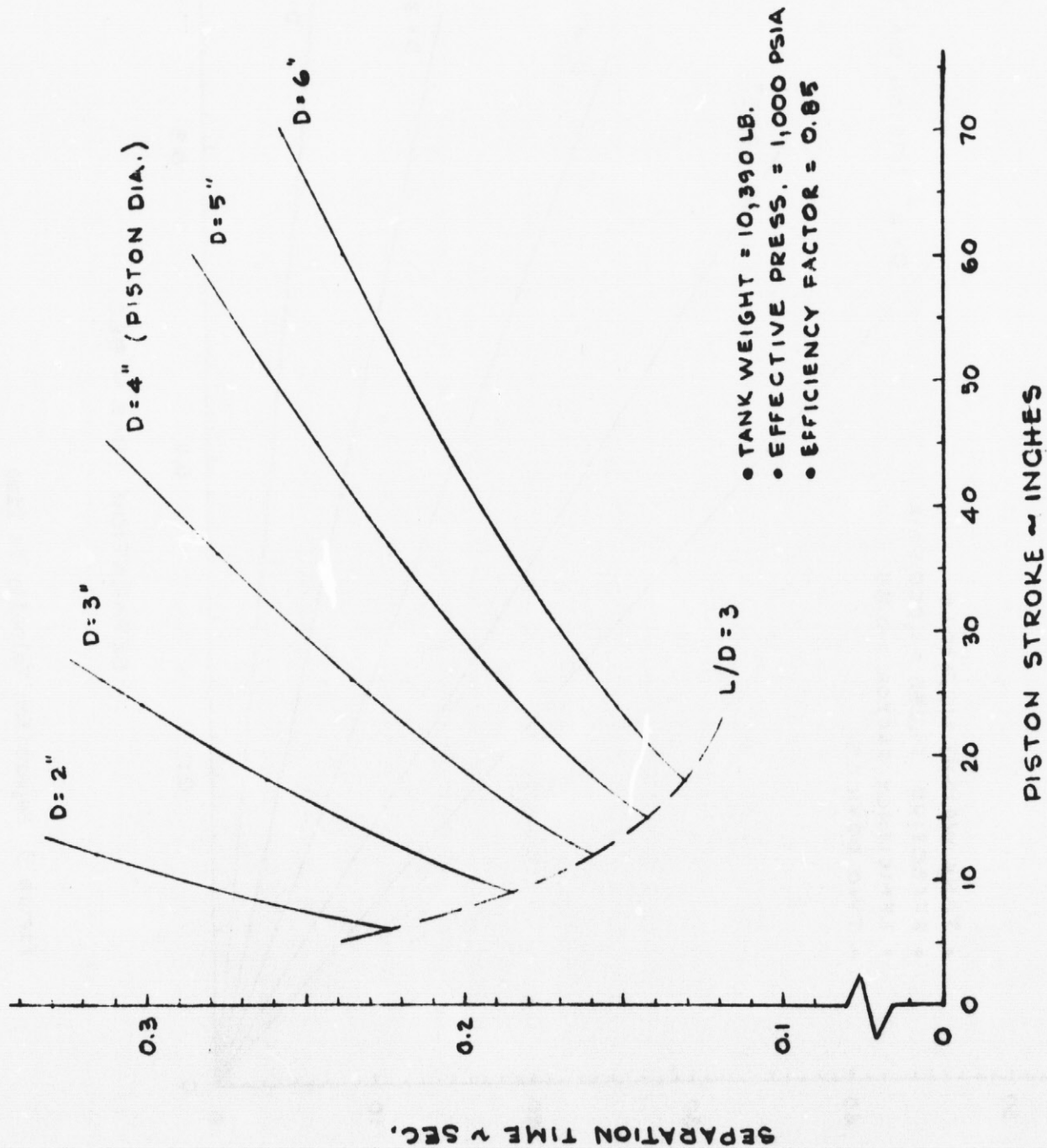


Figure 2 Separation Time Vs Piston Length (1 of 2)

Figure 2

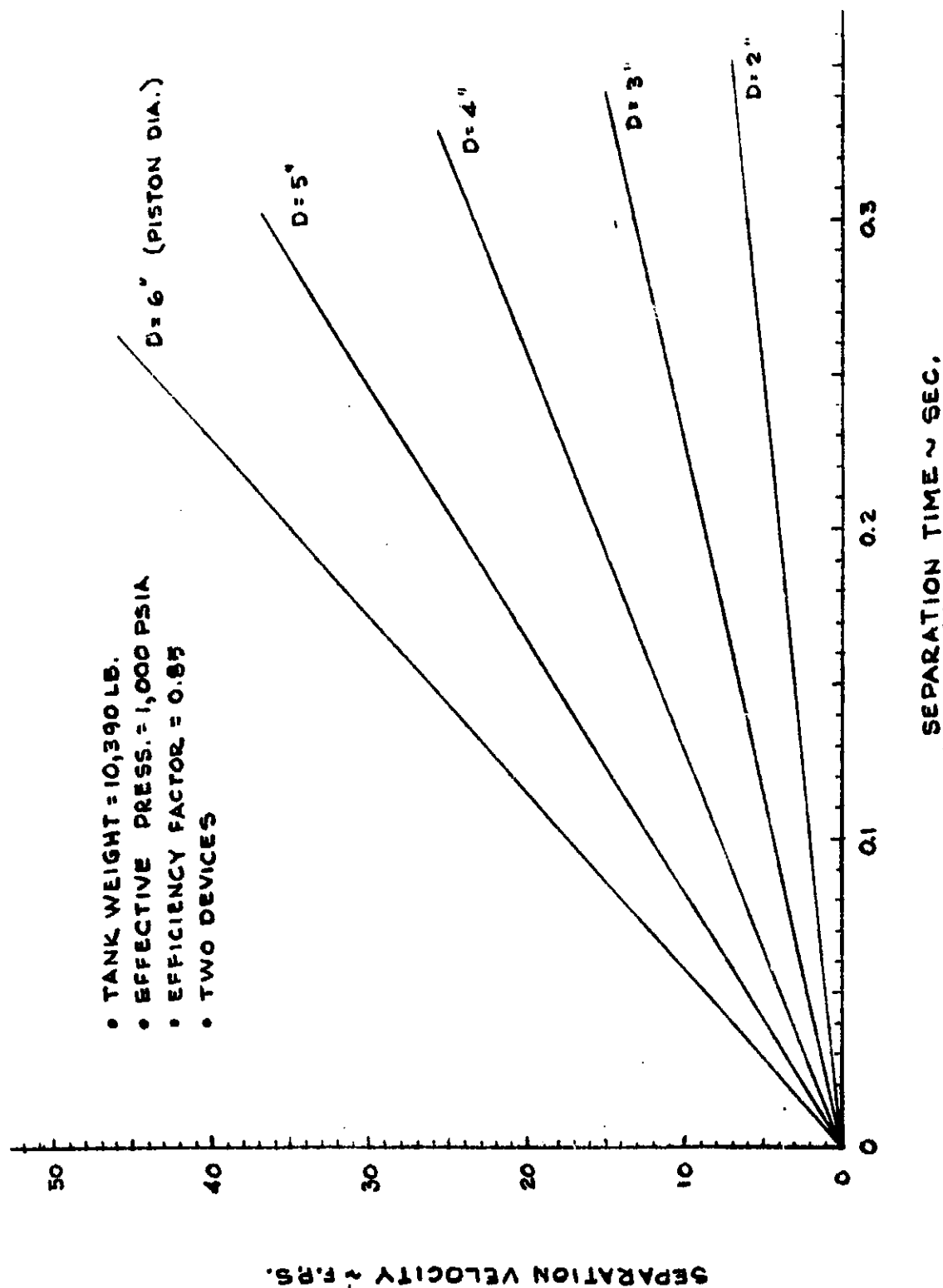


Figure 3 Separation Velocity Vs Time

The translation distance is a function of the energy imparted to the tanks and the time involved. Figure 4 shows that the tanks will translate radially away from the Orbiter to a distance of 70 feet in two seconds for an imparted energy of 2.38 million pound-inches.

The angular deviations of the tank at the instant of separation were also analyzed. For the specified gas generator-piston arrangement and a separation interval of 0.2 second, Figure 5 shows the variation of tank rotation angle and rate as a function of gas generator pressure deviation. The indicated angle and rate at zero ΔP results from deviations of the tank C.G. and piston area. Figure 6 shows the RSS pressure deviation as a function of RSS grain temperature deviation for several combustion pressure variations. Included in the RSS pressure deviation are the effects of grain variations and piston efficiency. The previous two figures are combined to generate Figure 7 which shows the rotation angle and rate deviations as a function of differential grain temperatures for various pressure deviations. This graph indicates that the angular rate may present a problem with regard to retro attitude. Lower separation forces would result in lower angular deviations, but the corresponding translation times would be greater. If the angular rate at separation proves to be a problem, further optimization analyses are in order.

REFERENCES

1. "Alternate Space Shuttle Contract Study - External Hydrogen Tank Orbiter - Heat Sink Booster," March 1971 Review.
2. "Rocketdyne Solid Propellant Gas Generators," BC 60-32, Rocketdyne, a division of NAR.

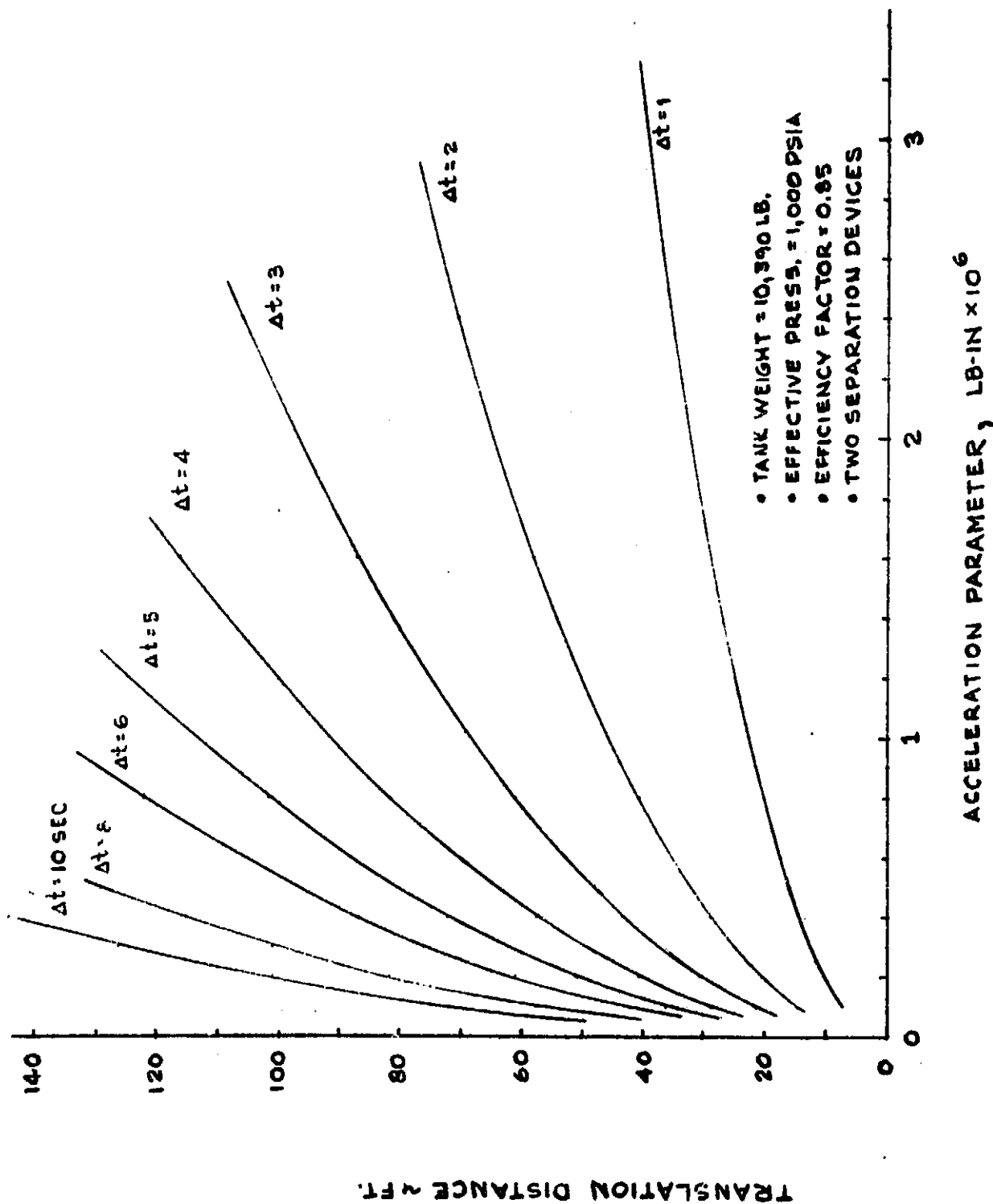


Figure 4 Droptank Translation Distance

Figure 4

EM NO: 12-12-M1-1
DATE: 12 May 1971

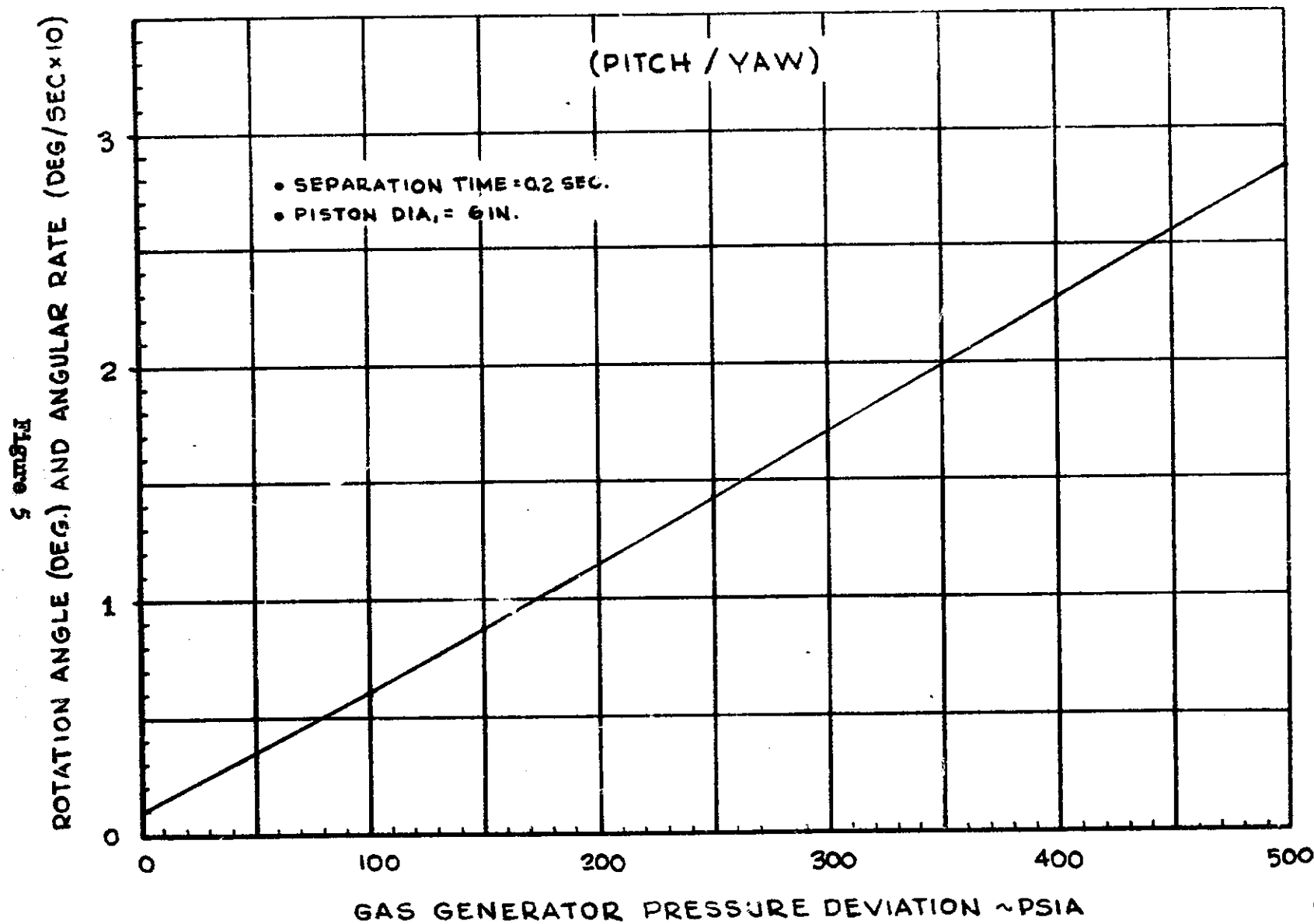


Figure 5 Droptank Separation Angular Errors (Pitch/Yaw)

EM NO: 12-12-M1-1
DATE: 12 May 1971

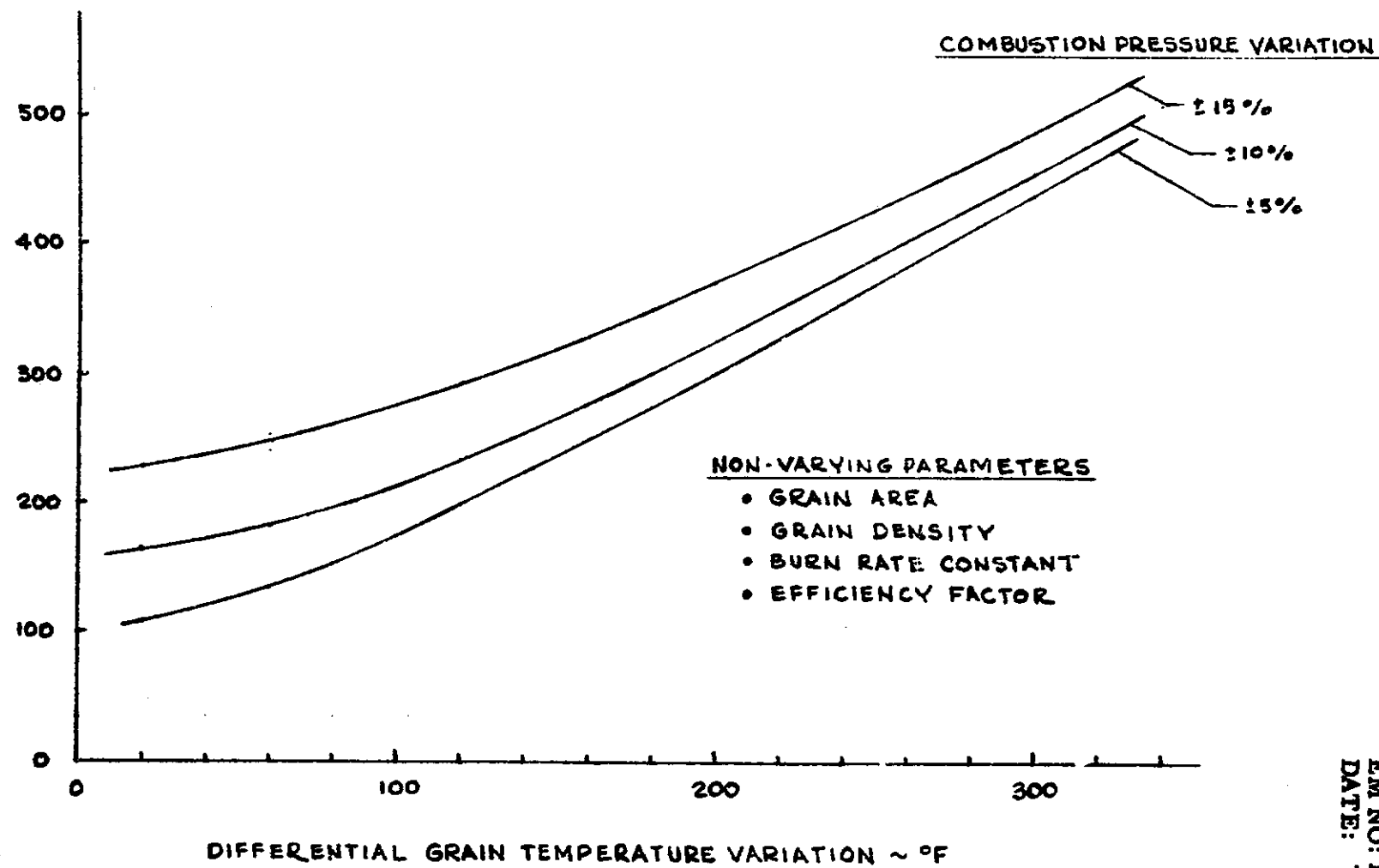


Figure 6 Separation Pressure Deviations (Two Devices)

Figure 6
RSS PRESSURE DEVIATION ~ PSIA

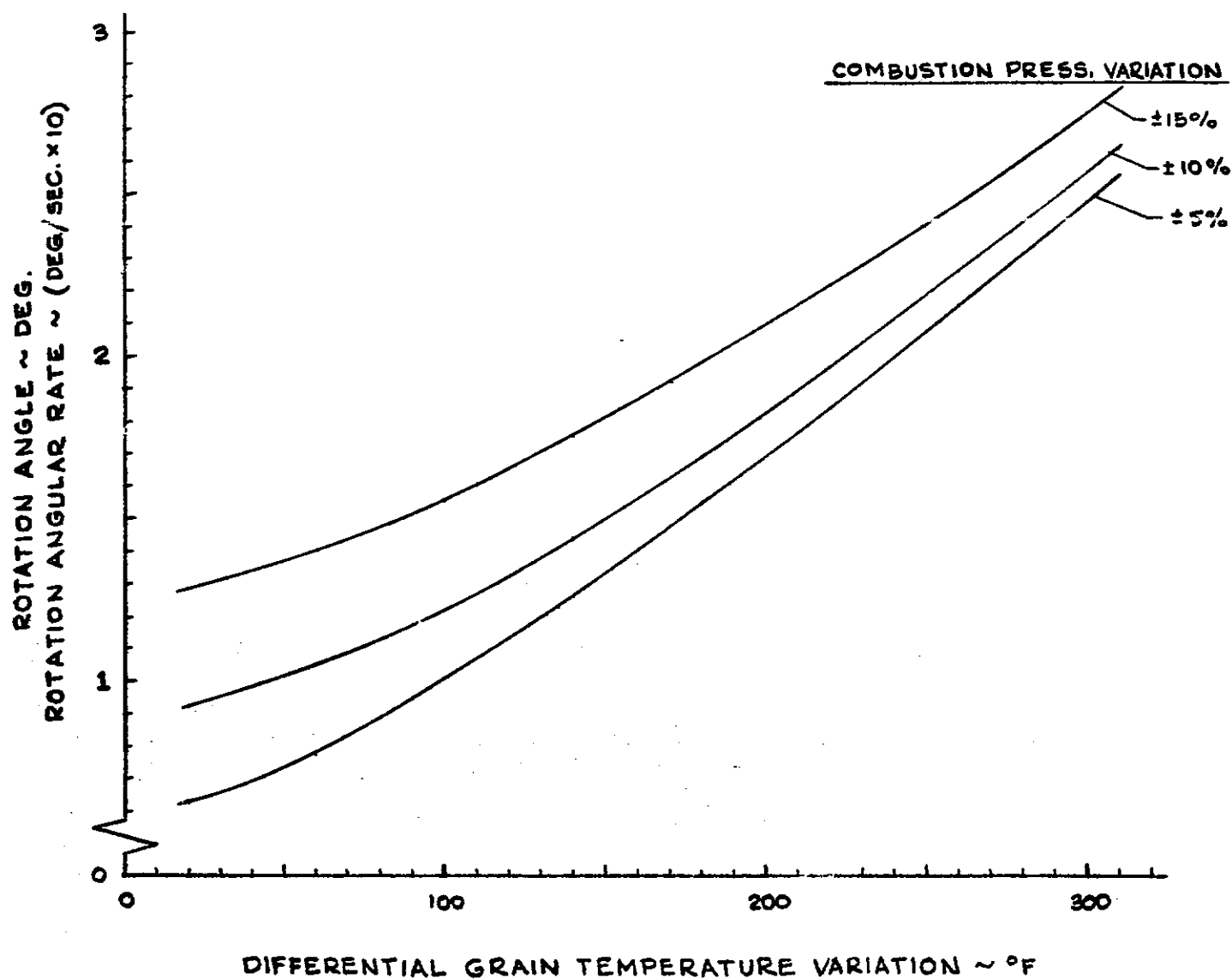


Figure 7 Droptank Separation Parametrics (Pitch/Yaw)

ENGINEERING MEMORANDUM

TITLE: MASS PROPERTY ESTIMATES FOR ORBITER EXTERNAL LH ₂ TANK	EM NO: L2-12-M1-1 REF: DATE: 3 May 1971
AUTHORS: R. A. Byers <i>R. A. Byers</i>	APPROVAL: ENGINEERING SYSTEM ENGRG

PROBLEM STATEMENT

To provide mass property data for the Orbiter external tank intact entry analyses.

RESULTS

Weight data, centers-of-gravity and mass moments-of-inertia are provided, including estimated mean values and RSS deviations.

AFFECTED WORK BREAKDOWN STRUCTURE

Orbiter
Orbiter ascent LH₂ tank

ASSUMPTIONS

The following assumptions apply:

1. LH₂ tank volume is 10,300 ft³ (each)
2. Tank would be tumbling during entry
3. T.P.S. shall be sufficient to sustain intact entry
4. Dry weight growth is 10 percent
5. Ancillary hardware may be jettisoned, as necessary.
6. The tank is 2219 aluminum
7. The cryogenic insulation is spray-on foam (2 lb/ft³)
8. The ablator for interference heating and intact entry is 30 lb/ft³ cork

DISCUSSION

The estimated weight summary for a liquid hydrogen tank protected for tumbling intact entry is presented in Table I. The tank configuration is shown in Figure 1.

The longitudinal and lateral centers-of-gravity for various conditions of tank separation and retro are presented in Table II. Figure 2 shows the lateral C.G. coordinate arrangement, estimated mean values and RSS deviations based on probable variations of the position and weight of the tanks system elements.

Mass moments-of-inertia for various separation and retro conditions are presented in Table III. The values shown are estimated means with RSS deviations based on probable system weight and position variations. The product-of-inertia is negligible because the lateral C.G. displacement is small.

L2-12-M1-1
3 May 1971

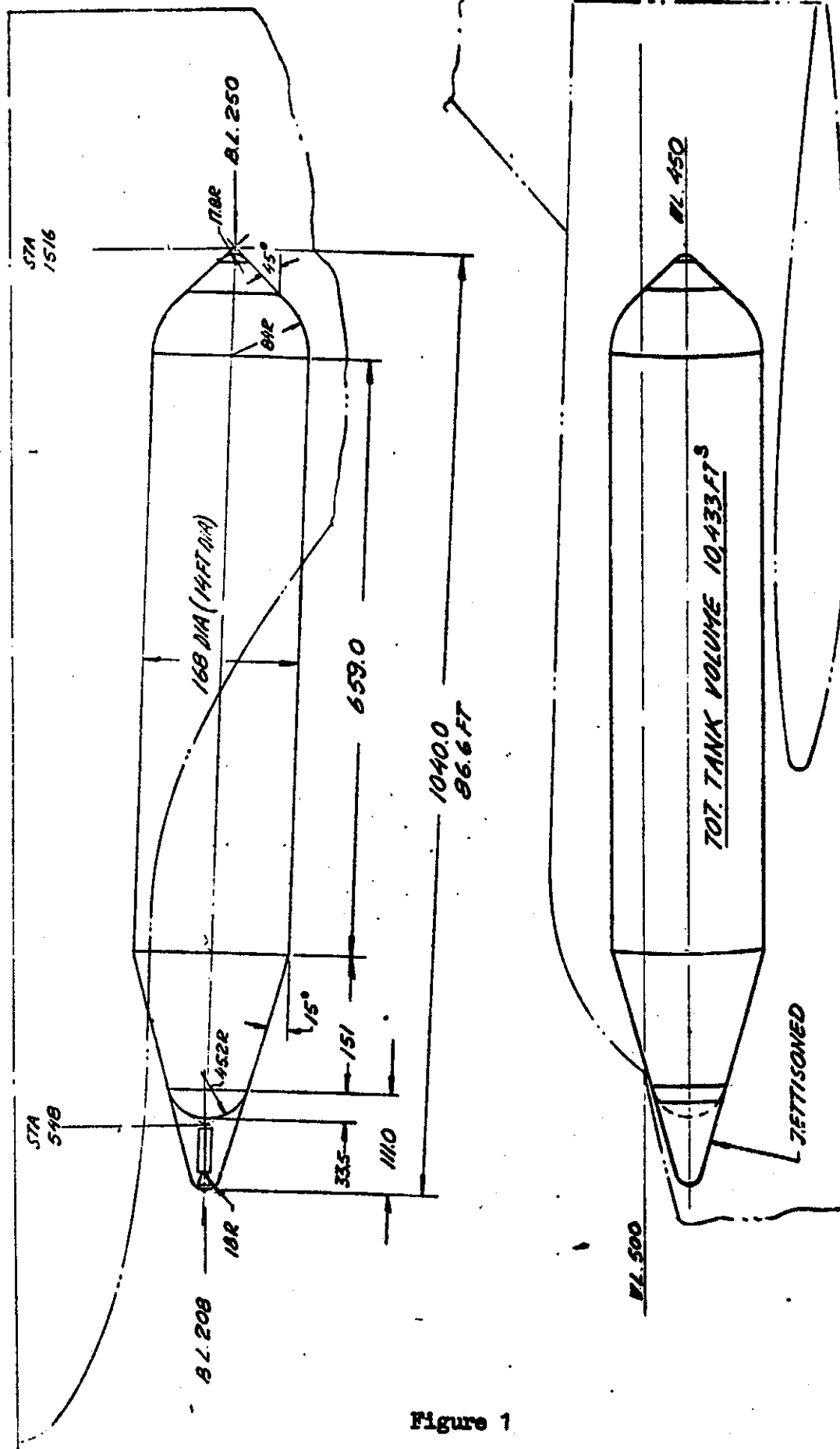


Figure 1

INSTALLATION AND TANK GEOMETRY
GRUHMANN DEEP TANK. SKT 100703

4-21-71 ST

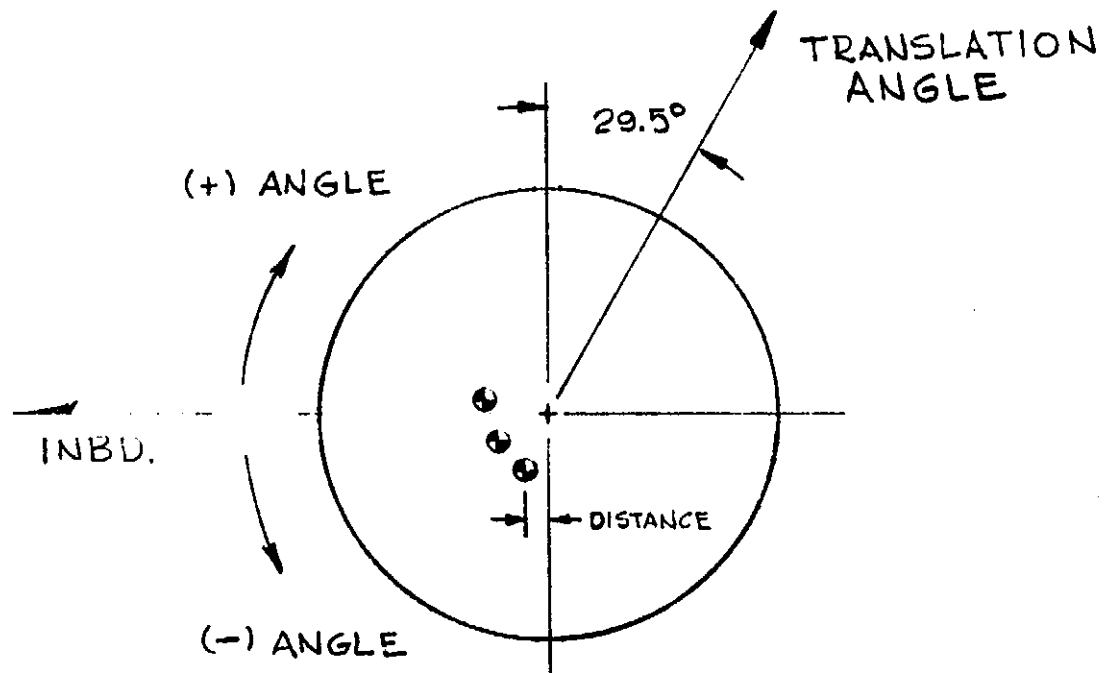
Lockheed Missiles & Space Company

Space Shuttle Project

EM NO: L2-12-M1-1

DATE: 3 May 1971

TANK C.G. CONVENTION



VIEW LOOKING FWD

Figure 2

EM NO: L2-12-M1-1

DATE: 3 May 1971

Table I
TANK WEIGHT SUMMARY*
(Intact Entry)

1. STRUCTURE - TANK			3,920
1.1 FWD H/S DOME	600		
1.2 FWD CONE	40		
1.3 CYLINDER	2,960		
1.4 AFT DOME	320		
2. STRUCTURE - ATTACHMENTS			640
2.1 FWD	180		
2.2 AFT	460		
3. INSULATION AND T.P.S.			2,600
3.1 FWD H/S DOME	30		
3.2 FWD CONE	1,050		
3.3 CYLINDER	1,350		
3.3.1 CRYO. INSUL.	260		
3.3.2 ABLATOR	900		
3.3.3 INSUL. SUPPORT	190		
3.4 AFT DOME		170	
3.4.1 CRYO. INSUL.	70		
3.4.2 CORK FOR ENTRY	100		
4. SEPARATION DEVICES (45# EA.)			90
5. DEORBIT			420
5.1 RETRO ROCKET		290	
5.1.1 INERTS	40		
5.1.2 PROPELLANT	250		
5.2 SUPPORT		130	
6. PROPULSION			980
6.1 PLUMBING		170	
6.2 FWD DISCONNECTS, VALVES, ETC.		200	
6.3 AFT DISCONNECTS, VALVES, ETC.		610	
7. CONTINGENCY (10%)			<u>860</u>
EMPTY WEIGHT			(9,510)
8. FLUIDS			880
8.1 LH ₂ RESERVE (NOMINAL)		480	
8.2 RESIDUALS (NOMINAL)		400	
8.2.1 LH ₂	260		
8.2.2 GH ₂	140		
SEPARATION WEIGHT			<u>(10,390)</u>

*Single tank

Table II

DROPTANK CENTER-OF-GRAVITY

(Ref. Dwg. SKT 100703)

AXIAL (X-AXIS)

	C.G. STATION		
	MEAN	+ DEVIATION	- DEVIATION
<u>SEPARATION</u>			
1. Including attaching hardware, plumbing and retro-rocket	1030	1019	1040
<u>RETRO</u>			
1. Pre-ignition - before hardware jettison with LH ₂ forward	1003	983	1023
2. Post retro - before hardware jettison with LH ₂ forward	1012	992	1032
3. Post retro - spent rocket, attach, plumbing jettisoned	974	955	994

LATERAL

	MEAN		+ DEVIATION		- DEVIATION	
	DISTANCE	ANGLE	DISTANCE	ANGLE	DISTANCE	ANGLE
RETRO	10.8"	+21.6°	12.2"	+23.2°	9.5"	+19.5°
ENTRY	4.6" (INBD)	- 1.5°	6.1" (INBD)	+ 3.2°	3.4" (INBD)	-11.2°

Table III

DROPTANK M.O.I. SUMMARY

(Ref. Dwg. SKT 100703)

SEPARATION

PITCH/YAW (LH ₂ not oriented)	238,000 slug ft ² (± 7,500)
ROLL	10,500 slug ft ² (± 500)

RETRO/ENTRY

PITCH/YAW

PRE-IGNITION (With Hardware and LH ₂ Fwd)	243,500 slug ft ² (± 11,000)
POST RETRO (With hardware and LH ₂ Fwd)	230,000 slug ft ² (± 11,000)
ENTRY (Hardware Jettisoned)	138,500 slug ft ² (10,500)
<u>ROLL</u> (Hardware Jettisoned)	8,400 slug ft ² (400)

REFERENCES

1. "Alternate Space Shuttle Contract Study - External Hydrogen Tank Orbiter - Heat Sink Booster," March 1971 Review.

ENGINEERING MEMORANDUM

TITLE: RETRO ROCKET PARAMETRICS FOR THE ORBITER EXTERNAL LH ₂ TANK	EM NO: L2-12-01-M1-11 REF: DATE: 18 May 1971
AUTHORS: R. A. Byers <i>R.A. Byers</i>	APPROVAL: ENGINEERING SYSTEM ENGRG

PROBLEM STATEMENT

It is desired to provide parametric data which may be used in the sizing and establishment of requirements for the LH₂ tank retro rocket.

RESULTS

Retrorocket parametric data are provided for velocity requirements ranging from zero to 300 f.p.s. based on a tank weighing 10,300 pounds. Tanks of different weight can be accommodated by proportioning the ΔV requirement and the weight. Parametric curves which relate propellant to ΔV ; thrust to throat diameter; rocket length to throat diameter; and impulse deviation to ΔV are provided.

AFFECTED WORK BREAKDOWN STRUCTURE ELEMENTS

Orbiter External LH₂ Tank

ASSUMPTIONS

The following assumptions apply:

1. Retro rocket is solid propellant with a sea level standard specific impulse of 245 seconds at optimum expansion ratio.
2. Chamber pressure is 1,000 psia.
3. Burn time is 5 seconds.
4. Rocket efficiency is 0.95.
5. Grain temperature coefficient for pressure and burn time is 0.1% per °F.
6. Tank weight is 10,300 pounds.
7. Port-to-throat area ratio is 1.44.
8. Burn rate is one inch per second at 1,000 psia.
9. Propellant density is 0.0625 lb per cubic inch.
10. Volumetric efficiency is 90 percent.
11. The nozzle is contoured and case ends are $\sqrt{2}$ ellipsoids.
12. The case diameter and the nozzle exit diameter are equal.

DISCUSSION

Figure 1 shows the variation of propellant weight required to achieve desired velocities for selected nozzle expansion ratios. The corresponding delivered thrust is presented in Figure 2 as a function of throat diameter with the expansion ratio as a parameter and selected velocities indicated.

In order to determine a rocket size which is consistent with the above parameters, it may be necessary to iterate through the curves to achieve the desired results. The curves were derived on the premise that the case diameter and the exit diameter are equal. For example, if the required velocity is 230 f.p.s., it will be observed that

Lockheed Missiles & Space Company

Space Shuttle Project

EM NO: L2-12-01-M1-11

DATE: 18 May 1971

a rocket with either a 25:1 or 16:1 expansion ratio is not consistent but an interim expansion ratio of about 18:1 is acceptable for sizing purposes. This would have a diameter of 14.2 inches, as indicated in Figure 3a.

The case length between the intersection of the ellipsoidal contours and the rocket centerline is shown in Figure 3b with the propellant weight as a parameter. It is assumed that the plane of the nozzle throat is coincident with the aft intersecting point. The overall rocket length parametrics (including the nozzle) are presented in Figure 3c.

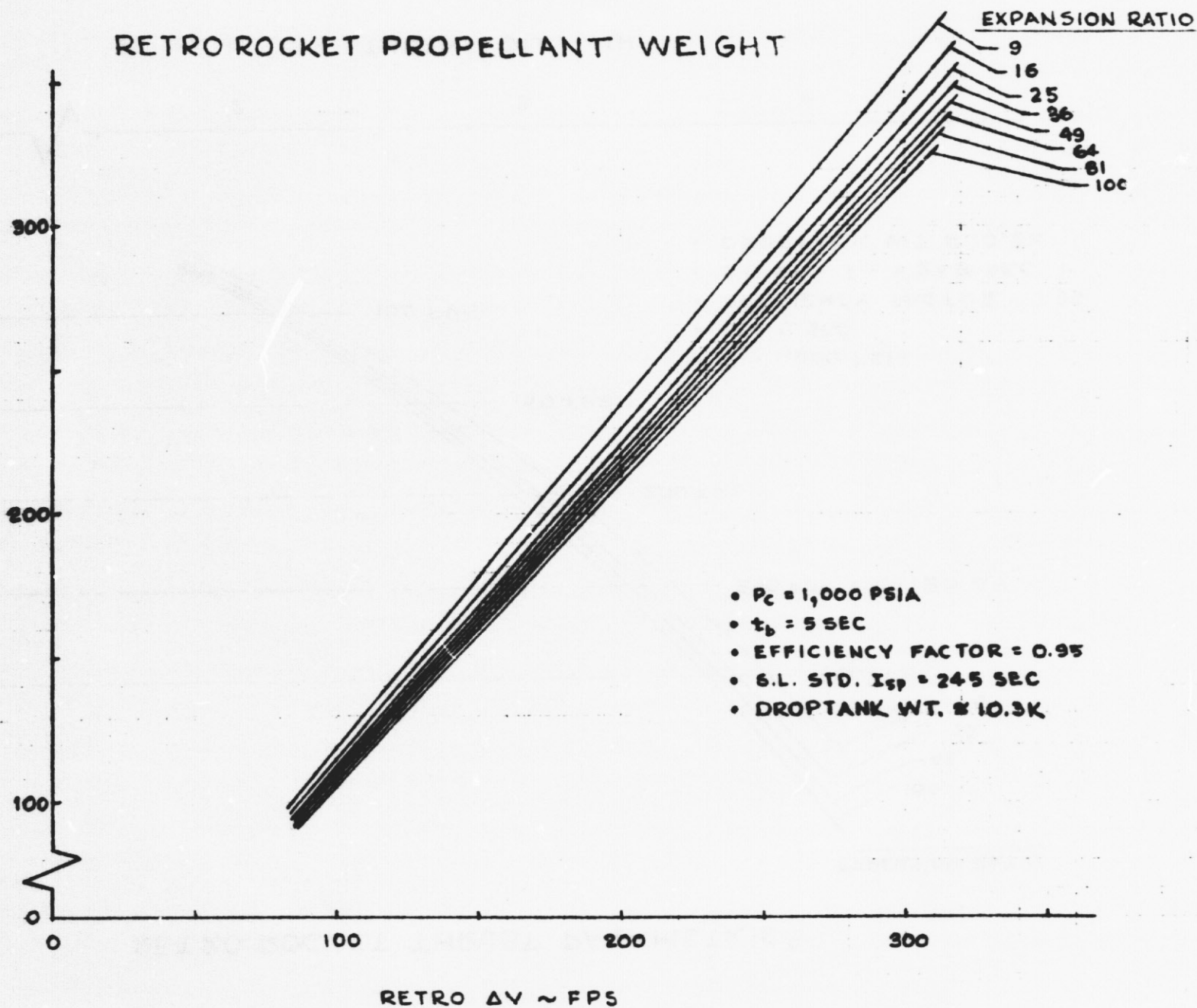
The deviation of the retro impulse as a function of retro ΔV is shown in Figure 4 with the grain temperature deviation as a parameter. The grain temperature deviations are root-sum-square values in combination with chamber pressure deviations of five and ten percent.

REFERENCES

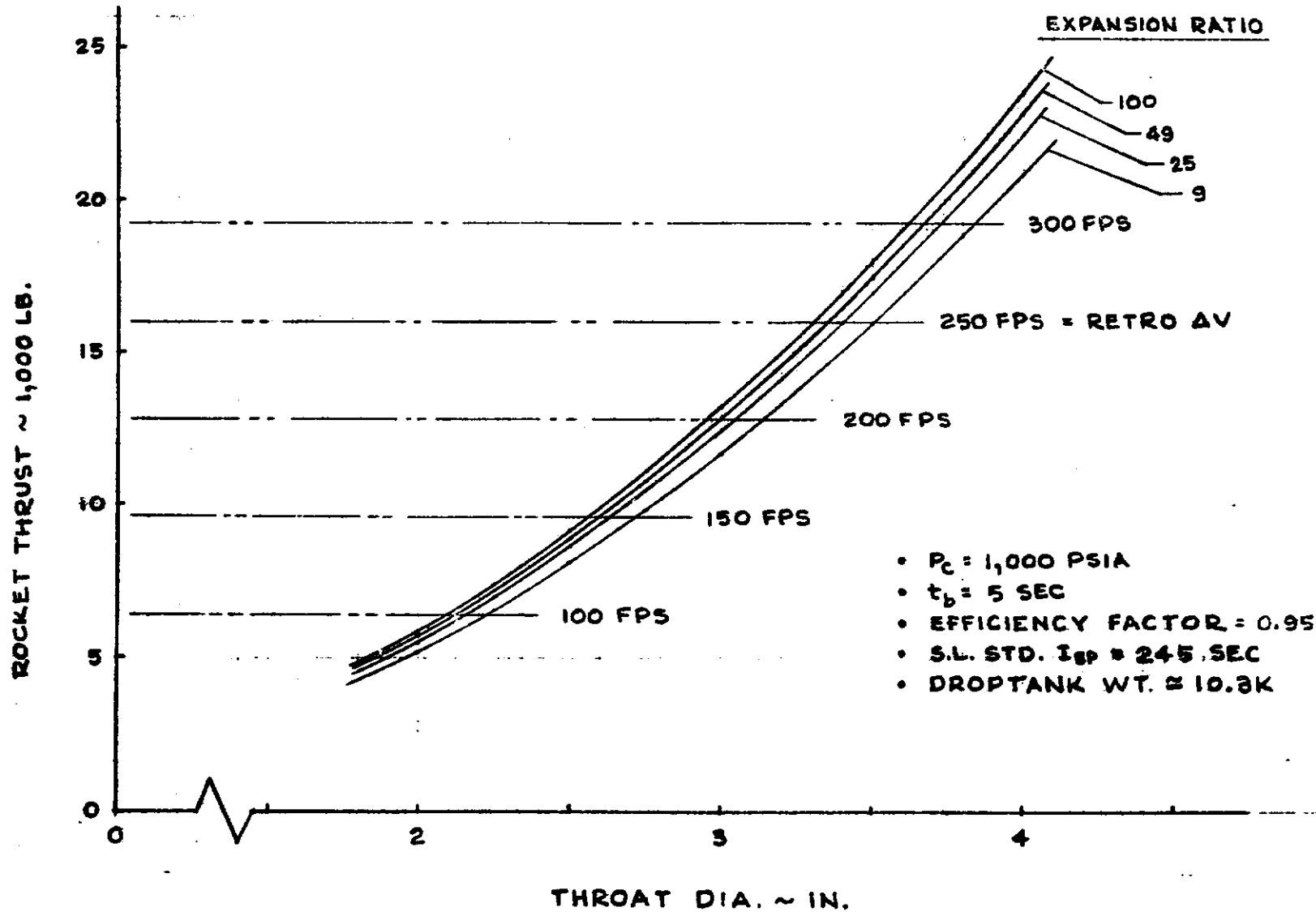
1. "Rocket Propulsion Elements," G. P. Sutton, John Wiley & Sons, Inc., 1956.

Figure 1

ROCKET PROPELLANT WEIGHT ~ LB.

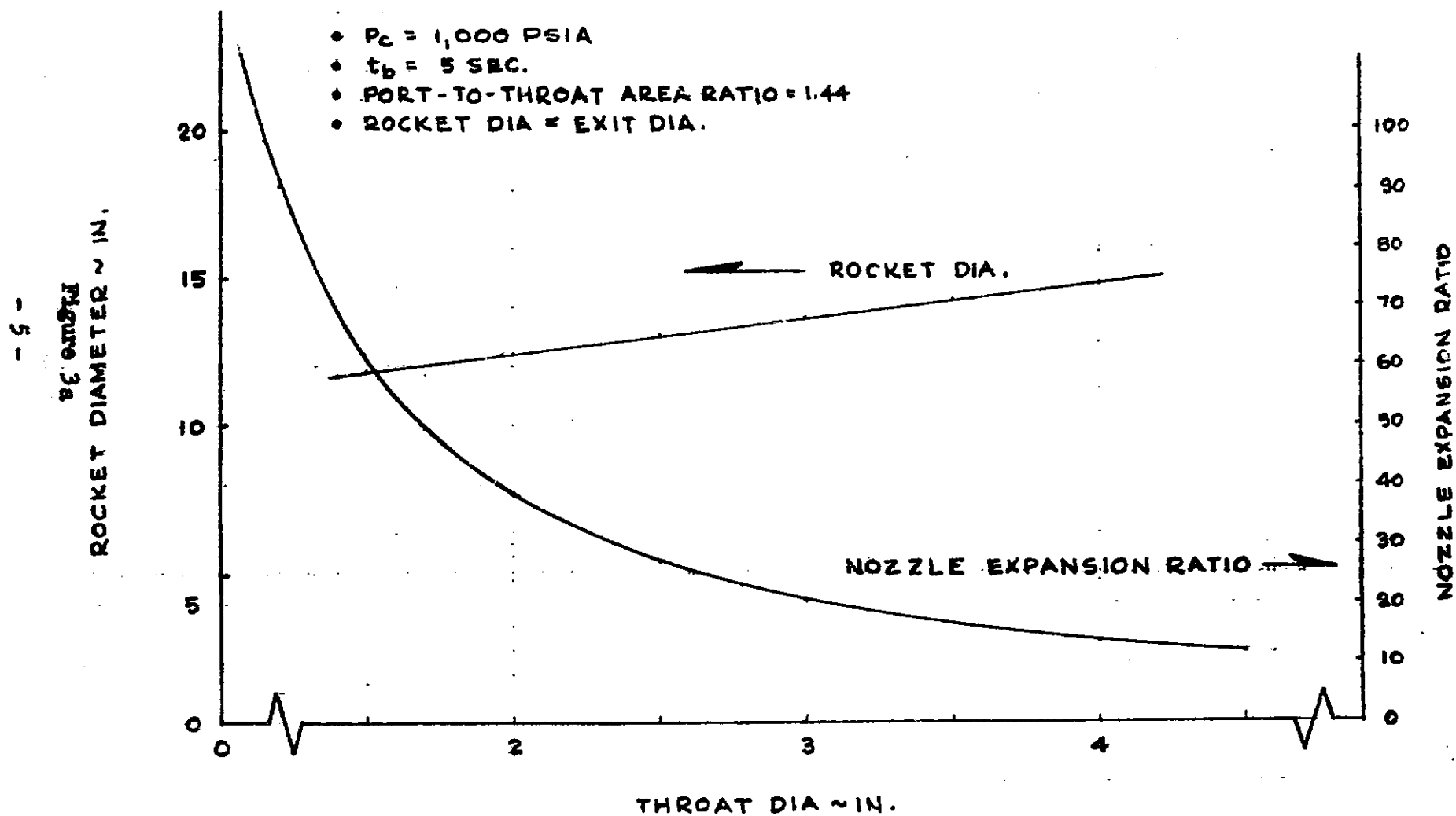


RETRO ROCKET THRUST PARAMETRICS



12-12-01-M1-11
18 May 1971

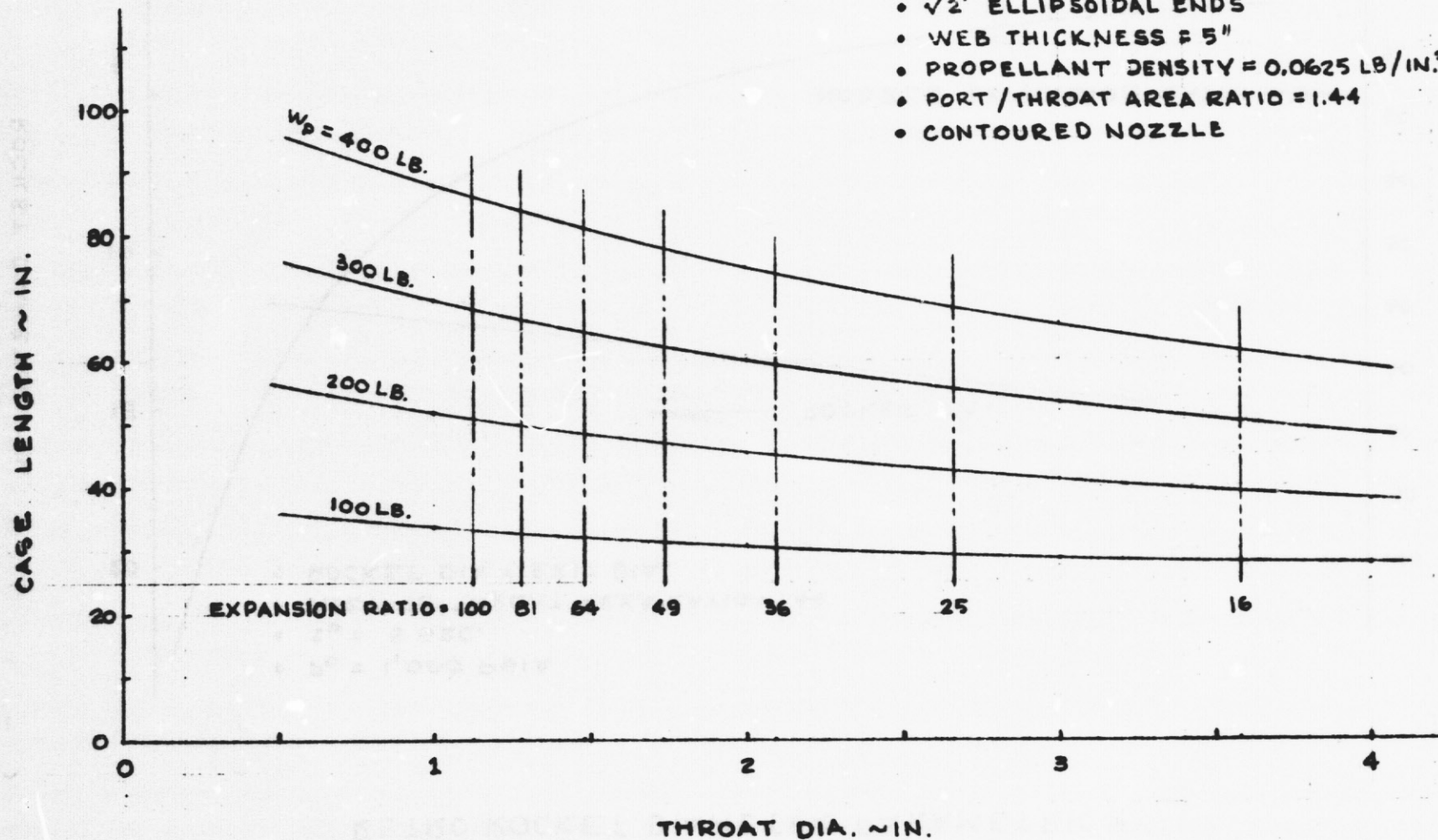
RETRO ROCKET DIAMETER PARAMETRICS



12-12-01-M1-11
18 MAY 1971

RETRO ROCKET CASE LENGTH PARAMETRICS

- VOLUMETRIC EFFICIENCY = 0.9
- $\sqrt{2}$ ELLIPSOIDAL ENDS
- WEB THICKNESS = 5"
- PROPELLANT DENSITY = 0.0625 LB/IN.³
- PORT / THROAT AREA RATIO = 1.44
- CONTOURED NOZZLE



12-12-01-M-11
18 May 1971

RETRO ROCKET CASE LENGTH PARAMETRICS

• NOZZLE EXIT = CASE DIA.

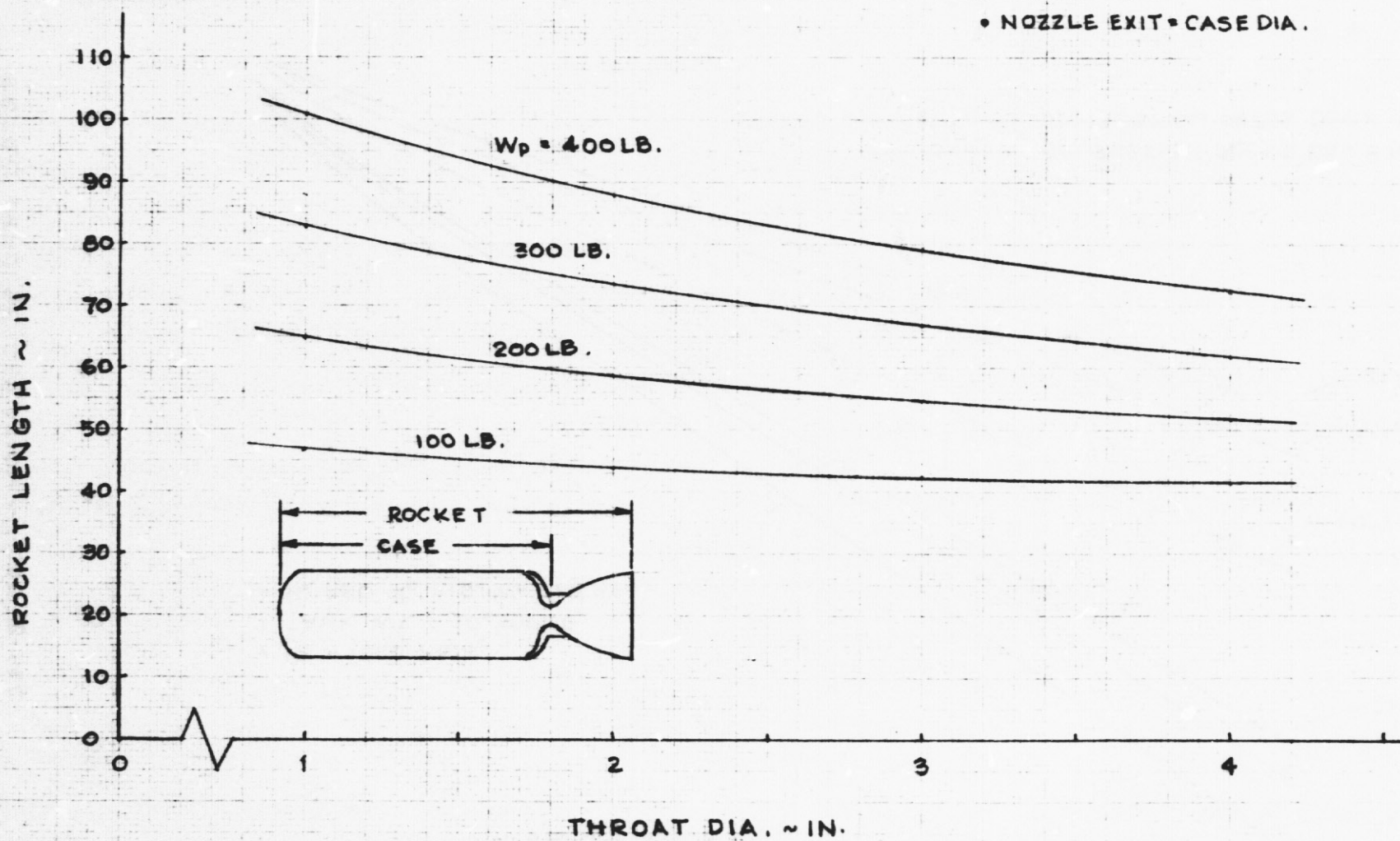


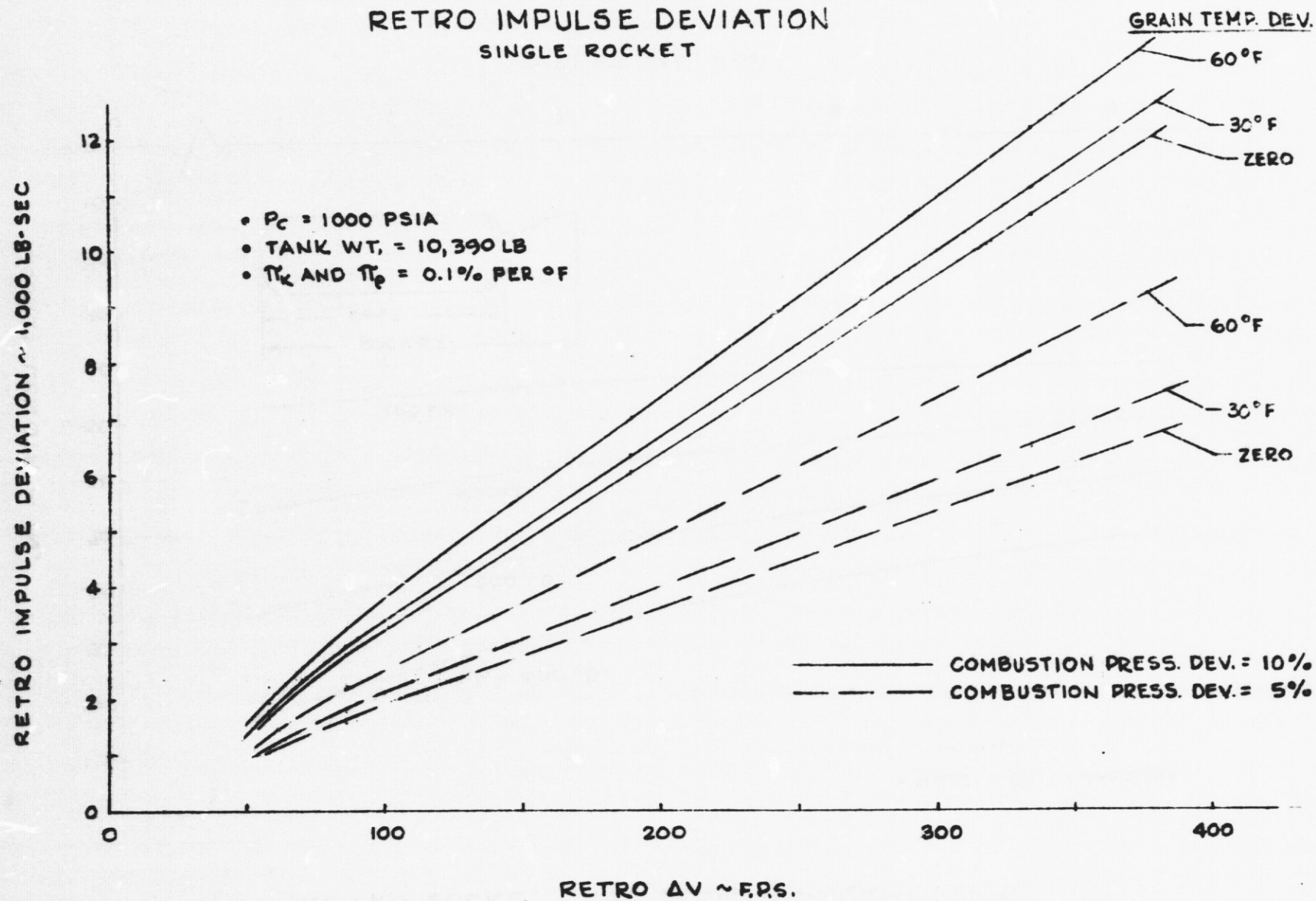
Figure 3c

- 7 -

12-12-01-M1-11
18 May 1971

REPRODUCIBILITY OF THE ORIGINAL PAGE IS POOR.

RETRO IMPULSE DEVIATION SINGLE ROCKET



12-12-01-M1-11
18 May 1971

ENGINEERING MEMORANDUM

TITLE: SEPARATION AND ENTRY ANALYSIS OF AN EXTERNAL LH ₂ DROPTANK	EM NO: L2-12-05-M1-8 REF: DATE: 18 June 1971
AUTHORS: P. J. Douglas, L. A. Reich, E. Hsu <i>P. J. Douglas, L. A. Reich, E. Hsu</i>	APPROVAL: ENGINEERING SYSTEM ENGRG <i>R. A. Byers</i>

PROBLEM STATEMENT

Among the Alternate Concept Study vehicles are orbiter configurations employing external droptanks for storage of liquid hydrogen (LH₂) for use during ascent. The tanks are jettisoned after orbit injection and deboosted to ensure entry and subsequent impact in desired ocean locations. Obviously, overall system design must include a complete analysis of the droptanks to establish requirements for accommodating both ascent and entry environmental conditions while maintaining minimum tank weight for maximum storage volume. Furthermore, tank flight characteristics must be adequately defined to facilitate dependable prediction of tank entry trajectories and expected range dispersions about desired impact locations. In the event of tank breakup during descent, realistic fragment impact patterns must also be identified.

In the analysis reported herein, separation and entry characteristics of a specific droptank configuration are investigated to provide pertinent data for detailed design studies. The analysis includes establishing entry trajectories from various locations on typical space shuttle orbits, investigating separation and deboost characteristics after the tank is jettisoned from the orbiter and identifying dynamic flight characteristics during entry assuming various perturbations to the nominal droptank configuration. Entry range sensitivities to parametric system biases are identified and typical root-sum-square dispersions are calculated. Fragment trajectories following an assumed breakup at various points along the droptank trajectories are also generated for a more definitive impact envelope analysis. Both three degree-of-freedom (3D) point mass trajectories and six degree-of-freedom body motion/trajectory simulation techniques were used in the study to define droptank separation deboost and entry characteristics for analysis.

AFFECTED WORK BREAKDOWN STRUCTURAL ELEMENTS

The following areas are affected by this study:

- Droptank separation system design
- Droptank aerodynamic, structural, and thermodynamic design
- Droptank deboost system design
- Orbiter operational procedures
- Range safety

RESULTS

The separation and entry analysis indicated entry ranges from 1900 nm to 6000 nm with maximum downrange dispersion for a single droptank of +1010 nm, -763 nm for the assumed tank configuration. Crossrange dispersion is +32 nm, -174 nm. The separation study phase indicated a need to optimize tolerable angular rates (caused by separation devices) to separation distance requirements and separation velocities. A nominal pitch rate of 5 deg/sec with a separation velocity of 35 fps were used in the analysis. A study of body dynamic motion during descent revealed the tank will trim to an angle of attack of

EM NO: L2-12-05-M1-8

DATE: 18 June 1971

40 deg following an initial tumble induced by angular rates at separation. Trim conditions are extremely sensitive to center of gravity location, however, and a 2 percent forward shift in center of gravity increases entry downrange by over 600 nm. Effects of other parametric deviations on flight dynamics resulted in individual range errors of no more than 125 nm of an assumed impact point.

GIVEN AND ASSUMED CONDITIONS

Droptank trajectory simulations were generated assuming a rotating, oblate earth (Ref. 1) and the 1962 U.S. Standard Atmosphere modified to include the effects of the 11-year solar cycle on atmospheric volume/density relationships (Ref's. 2 and 3). A launch date of January 1978 was used to align separation and entry simulations with assumed actual launch dates.*

Four shuttle orbits were assumed in the analysis, all 50 x 100 nm orbits but varying in orbit inclination (I) and/or vehicle launch site. The assumed perigee injection conditions shown in Table 1 are based on the preliminary spherical earth ascent analysis reported in Ref. 4 with modifications for oblate earth effects as discussed in Ref. 5. Orbit Numbers 1 through 4 are used for convenient identification in the study.

Ground tracks of the four orbits are shown in Fig. 1. Note the common intersection of orbit planes in the Indian Ocean for Orbits 1, 2 and 3.

The assumed droptank configuration is illustrated in Fig. 2 with corresponding nominal weights and mass properties in Table 2 (Ref. 6).** The ascent configuration assumes a fairing over the retro rocket which is jettisoned immediately following separation. After retro-fire, (deboost), the retro rocket and other supporting hardware (not shown) are also jettisoned resulting in an aerodynamically symmetric entry configuration. Though protuberances such as plumbing, struts, etc., will affect entry simulation details, realistic analysis of generalized configuration flight characteristics are still applicable to droptank design studies.

Also shown in Fig. 2 is the axis convention used in the study and the location of the reference body station (body-ref.) for various longitudinal locating dimensions, i.e., center of gravity longitudinal location, (l_{cg}), and aero-moment center location, (l_{cga}). Detailed definitions of forces, moments, angular rates, and geometric and reference axis systems are included in Appendix A together with a summary of symbols used in this report.

Droptank aerodynamic characteristics are shown in Appendix B as a function of total angle of attack, η , Mach number, and altitude, H. Data were calculated using the arbitrary body aerodynamic computer program of Ref. 7.

*Launch date selection is critical since calendar variations alter solar heating effects on atmospheric density.

**Mass properties are for the left droptank as viewed by the orbiter pilot.

EM NO: 12-12-05-M1-8
DATE: 18 June 1971

TABLE 1
PERIGEE INJECTION CONDITIONS FOR DROPTANK STUDY ORBITS
(50 x 100 NM)

Orbit No.	INCLINATION/ LAUNCH SITE	ALTITUDE (ft)	LONGITUDE (deg)	GEOC. LAT. (deg)	INERTIAL VEL.(fps)	INERTIAL FLT PATH (deg)	INERTIAL AZIM (deg)
1	28.5°/ETR	303806	68.27(W)	27.76(N)	25890	0	96.73
2	55°/ETR	303806	71.83(W)	36.92(N)	25872	0	45.85
3	90°/ETR(S)	303806	81.19(W)	16.65(N)	25890	0	180
4	90°/WTR(S)	303806	121.25(W)	22.83(N)	25890	0	180

EM NO: 12-12-05-M1-8
DATE: 18 June 1971

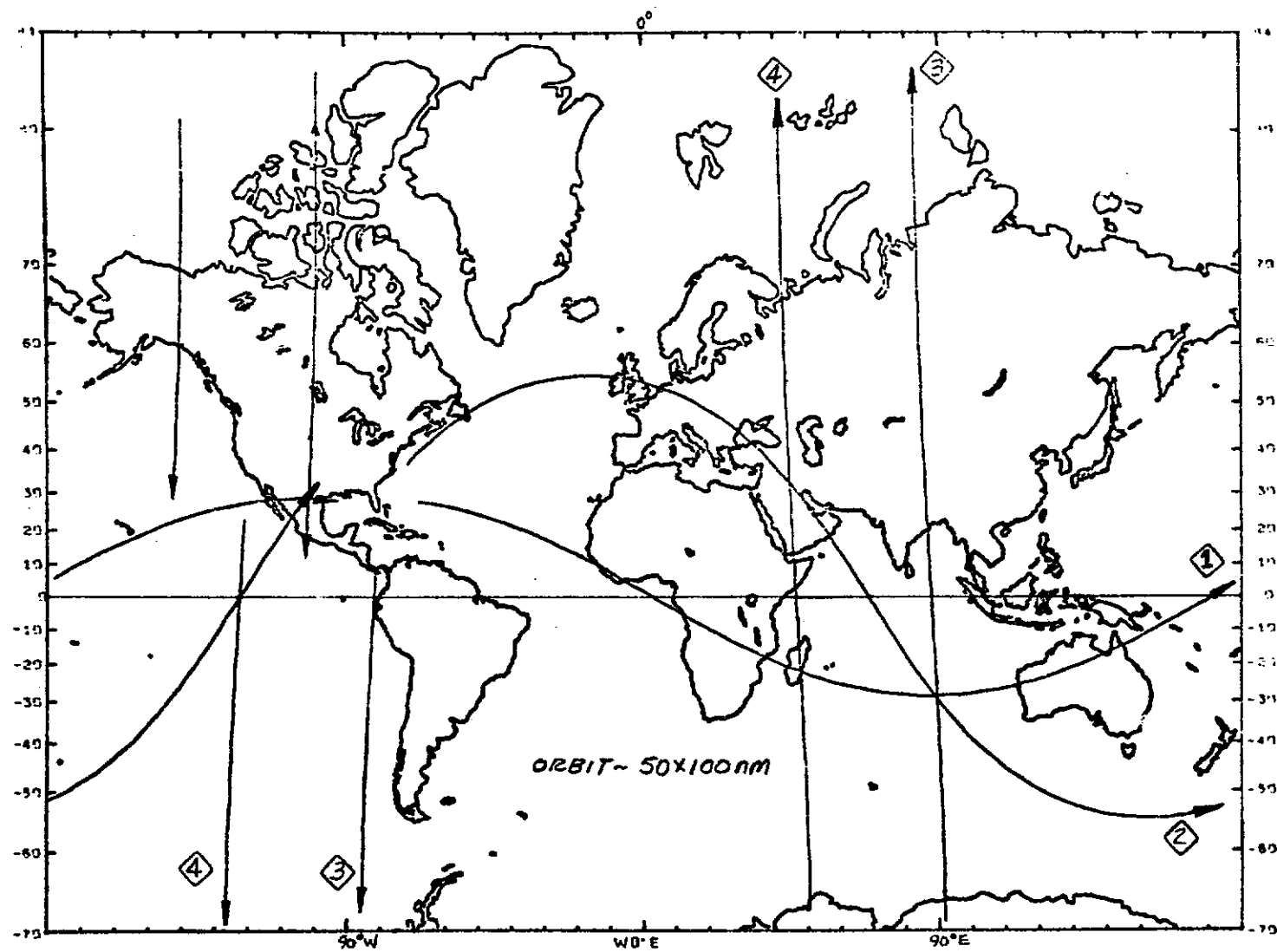


Figure 1 Ground Tracks of Orbits 1, 2, 3 and 4

Figure 1

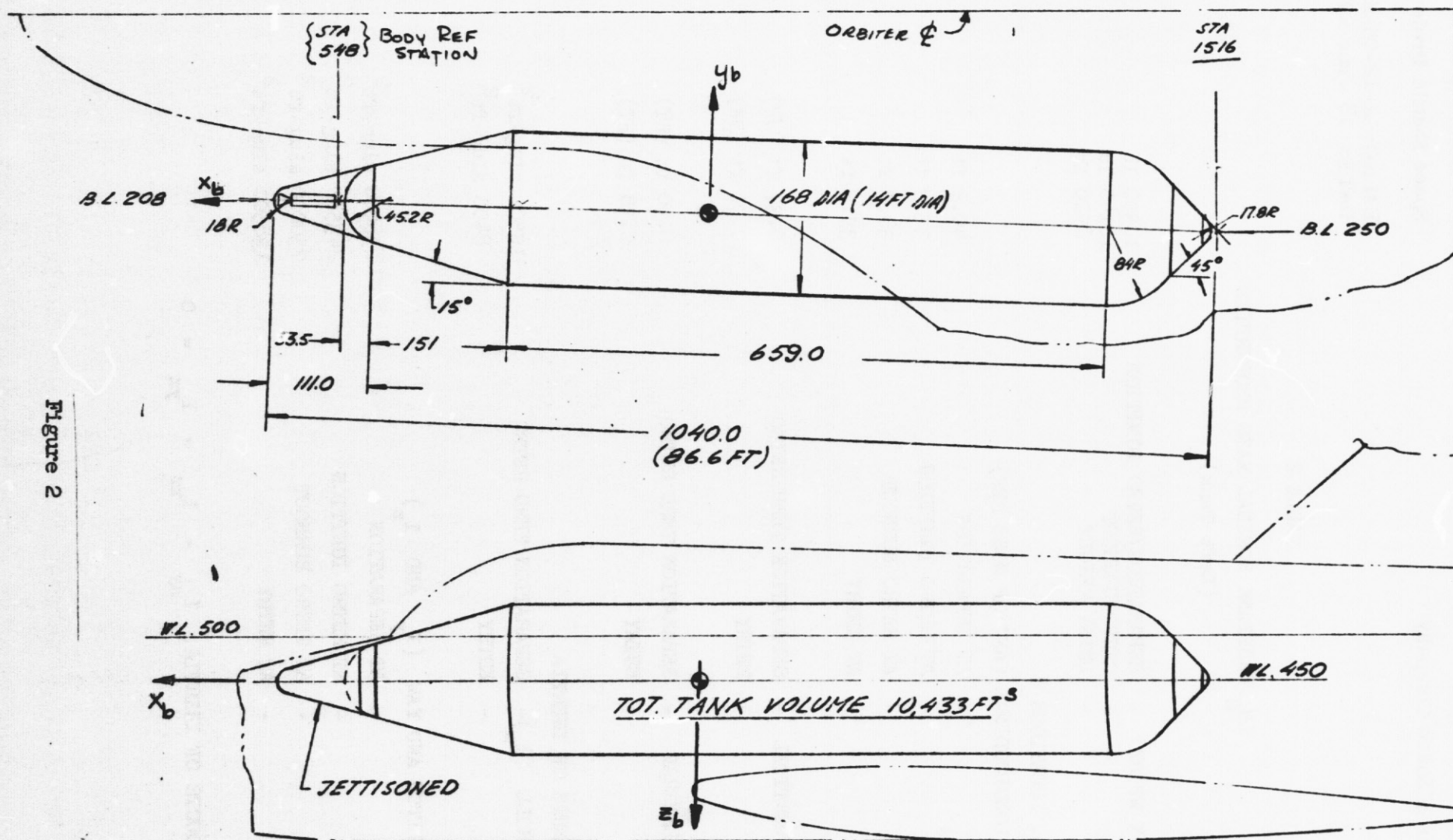


Figure 2 External LH₂ Droptank Geometry and Installation

EM NO: 12-12-05-M1-8
DATE: 18 June 1971

TABLE 2

LH₂ DROPTANK NOMINAL MASS PROPERTIES
(Left Tank)

●	TANK WEIGHT	- SEPARATION/RETRO IGNITION	10390 lb
		- RETRO BURNOUT	10140 lb
		- ENTRY WEIGHT	8520 lb
●	C.G. LOCATIONS		
	LONGITUDINAL (AFT OF NOSE REF)		
		- AT SEPARATION	40.2 ft
		- AT RETRO IGNITION	37.9 ft
		- AT RETRO BURNOUT	38.7 ft
		- AT ENTRY	35.5 ft
	VERTICAL	- SEPARATION THRU RETRO	0.37 ft (UP)
		- ENTRY	0.01 ft (DN)
	LATERAL	- SEPARATION THRU RETRO	0.90 ft (RT)
		- ENTRY	0.38 ft (RT)
●	MOMENTS OF INERTIA		
	ROLL (I_x)-	SEPARATION THRU RETRO	10500 slug-ft ²
		- ENTRY	8400 slug-ft ²
	PITCH AND YAW (I_y AND I_z)		
		- AT SEPARATION	238000 slug-ft ²
		- AT RETRO IGNITION	243500 slug-ft ²
		- AT RETRO BURNOUT	230000 slug-ft ²
		- AT ENTRY	138500 slug-ft ²
●	PRODUCTS OF INERTIA,	$I_{xy} = I_{xz} = I_{yz} = 0$	

Minimum and tumbling drag characteristics are used in 3D point mass simulations* with assumed drag coefficients as follows:

$$C_{D_{\min}} = (C_A)_{\eta=0}$$

$$C_{D_{\text{Tumble}}} = \frac{2}{3} (C_N)_{\eta=90^\circ}$$

where C_A and C_N are defined in Appendix A. Ballistic coefficients ($W/C_D A$) referred to in the study are computed using drag data at Mach number 10 and a reference area, $A_{\text{ref}} = 154 \text{ ft}^2$.

In the CD analysis, aero-force and moment data for $0 \leq |\eta| \leq 180 \text{ deg}$ were used.

Nominal retro rocket characteristics are shown in Table 3 (Ref. 8). When changes in retro velocity (V_R) are required, modified rocket performance and weights are calculated assuming constant thrust and constant specific impulse.

Table 3

ASSUMED NOMINAL RETRO ROCKET CHARACTERISTICS

Total Rocket Weight*	420 lb
Propellant	250 lb
Burnout Weight*	170 lb
Specific Impulse (Vac), I_{sp_v}	290 sec
Vacuum Thrust, T_v	14,500 lb
Burn Time	5 sec
Retro Velocity Increment, V_R	227 fps

*Includes attachment hardware

The generalized flight sequence assumed in the analyses includes inverting the orbiter after perigee injection (relative to the local horizontal or earth's surface) then executing an orbiter pitch-down maneuver (nose up relative to local horizontal) to orient the droptanks for a favorable retro attitude after separation. The inverted position takes advantage of gravitational acceleration components after tank separation. An illustration of orbiter/tank orientation at separation is in Fig. 3. Retro pitch angle (θ_R) and velocity conventions and orbiter/tank reference axis orientations are also indicated.

*It assumed tank entry occurs with a composite of flight conditions, from tumbling to minimum drag trim. By assuming these as extremes, actual entry flight profiles are bounded by 3D Simulations.

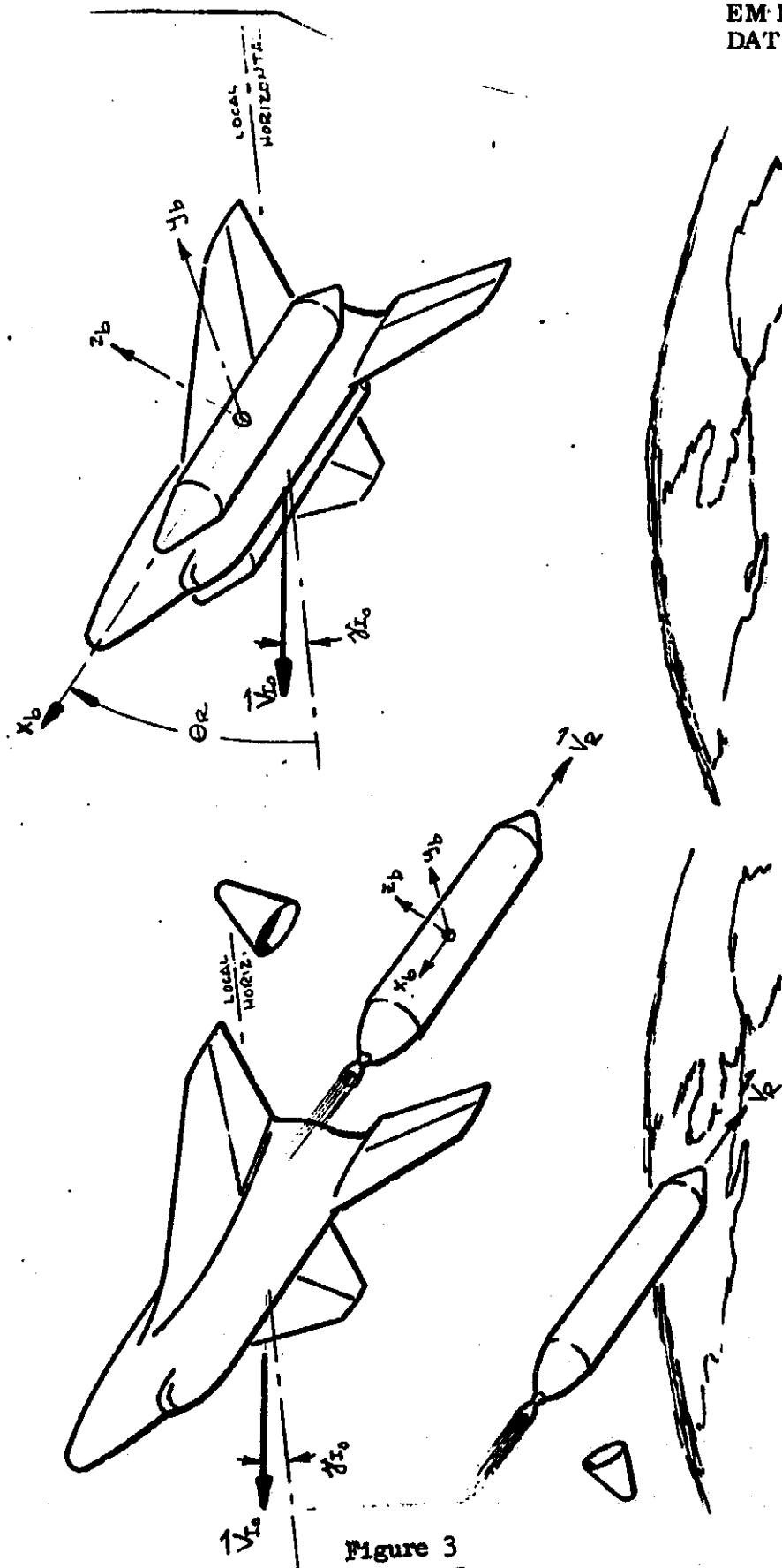


Figure 3

Figure 3 Orbiter/Droptank Orientation at Separation

Droptank jettisoning is accomplished with either pyrotechnic or mechanical devices, and occurs at a post injection time compatible with tank entry to impact at a specific location. A coast period before retro initiation allows a separation distance of at least one tank length from the orbiter. The retro-rocket protective fairing is discarded during the coast period and the retro-rocket together with ancillary and other miscellaneous hardware are jettisoned one second after retro termination.*

DISCUSSION OF RESULTS

Following an initial, but brief survey of potential impact locations, concurrent studies establishing nominal, perturbed and fragment trajectory profiles from orbit to impact, separation dynamic histories, and 6D descent trajectories incorporating tank flight dynamics were performed. Results of these related studies are discussed individually followed by a comparative analysis of point mass and 6D prediction techniques and impact and dispersions predictions for a representative case.

Potential Droptank Impact Locations

Two criteria are primary in the selection of impact locations; relative danger to land masses, and relative danger to shipping. The former is an obvious danger and purposeful dropping of space debris in areas of high land mass concentrations is avoided from human, physical, and political considerations. The later criterion, relative danger to shipping, is not as clear for most situations. The probability of hitting a ship 650 ft long and 85 ft wide moving at speeds anywhere from 5 to 15 Kts is much less than hitting a land mass of equal dimensions fixed in time and position (Ref. 9). Current range procedures associated with launches of rocket vehicles seem to reflect this consideration. "Notices to Mariners" are issued indicating programmed launch dates and times based on information supplied by Range Control facilities at least 10 days prior to the actual launch. It would be fatuous, however, to purposely plan launches which result in debris or tankage falling in areas where there are large concentrations of merchant and fishing fleets. Consequently, in this study, impact locations ensuring no land impact and relatively minimum shipping densities were established.

Figure 4 shows a map of worldwide shipping density forecasts for 1980 (Ref. 10). Numbers on the map indicate number of ships in a square area of 5° longitude x 5° latitude at any given time.

Also shown are nominal droptank impact areas selected for the analysis. The Indian Ocean impact area corresponds to the common intersection of Orbits 1, 2 and 3 (Fig. 1). Note, that shipping density in this area is minimal. Indian Ocean impact is also possible for deboost from Orbit 4, but at a more westerly location (approximately 45° S, 50° E). There is virtually no shipping in this area.

Since Indian Ocean impacts require a delay in tank separation and retro, (after perigee injection), mid-Atlantic impact locations for assumed droptank separation and entry from near perigee were also considered. The area shown is in a fairly low shipping region and in the vicinity of current launch vehicle booster stage impacts.

*In 3D point mass analyses, simulations were initiated at time of retro ignition.

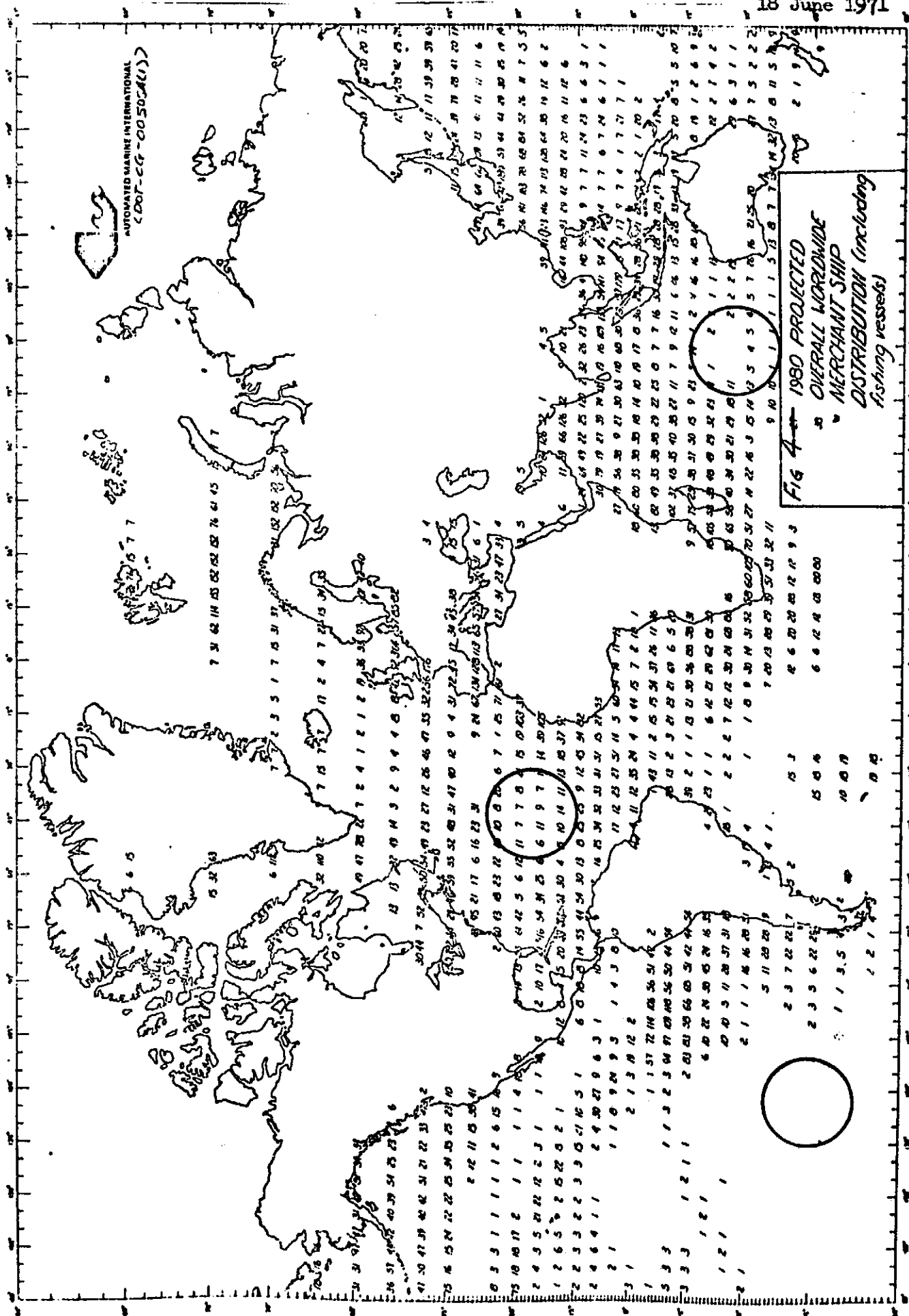


Figure 4

A third area, in the South Pacific Ocean, offers a virtually shipping-free region for impact of launch debris for polar orbit missions from the Western Test Range complex (orbit 4).

Point Mass (3D) Intact Droptank Deboost/Entry Simulations*

Since minimum range generally results in minimum dispersions for ballistic entry trajectories, initial phases of the 3D analysis were concerned with ascertaining relationships of retro pitch angle (θ_R) to entry range for the assumed nominal retro rocket (Table 3). Furthermore, since a specific impact location is desired, (Indian Ocean), the effects on range and impact location of time delays from perigee injection to retrofire are also of importance.

Figures 5 and 6 show variations in range from deboost to impact** from the four reference orbits and for various retro times (from perigee). Tumbling drag conditions are assumed. In all cases range increases with delay time except for the 25 minute delays on orbits 3 and 4. In these two cases, range decreases as delay time exceeds 20 minutes. The reasons are not obvious although combined effects of earth oblateness and relative retro locations may be contributing factors.

Range differences in entry from the different orbits but with retro at the same time from perigee, are due to both inclination differences and earth oblateness. The latter is more clearly discernible when comparing data of orbits 3 and 4 (both have $I = 90^\circ$).

A trace of retro pitch angle for minimum range (θ_R)_{opt} is shown for each of the orbits. For retro near perigee, relatively high pitch angles are required ($\theta_R \sim 75$ deg) indicating that tank drag has a significant effect on tank deceleration and the retro velocity increment is used primarily to lower tank flight path angle, forcing the body into a steep descent trajectory. As time from perigee increases, orbit altitude also increases and the advantageous effects of drag on deboost conditions are reduced. The application of retro velocity becomes more important for reducing orbital velocity and ensuring entry. The result is lower magnitudes of θ_R . Range is correspondingly increased because of the combined effects of increased altitude, decreased drag, and small changes in droptank post-retro flight path angle.

Though not shown, the effect of trim at minimum drag conditions is to increase entry range. The corresponding change in (θ_R)_{opt} is an increase of less than 10 degrees for comparative cases.

Impact locations corresponding with deboost at (θ_R)_{opt} are shown in Fig. 7 as a function of retro time from perigee. (Tumbling drag is again assumed). The common impact location for orbits 1, 2 and 3 is illustrated by the convergence of impact longitudes and the near convergence of impact latitudes. In all cases, retro initiation time is about 20 minutes for the common Indian Ocean impact area.

*Point mass (3D) entry simulations assume initial conditions at retro ignition.

**Impact altitude is assumed at 50,000 ft.

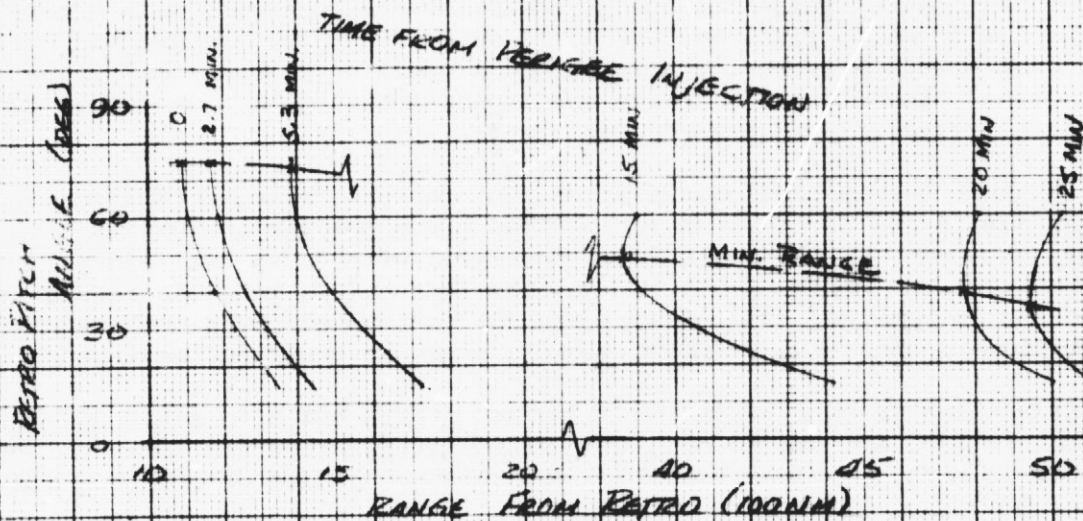
Space Shuttle Project

EM NO: 12-12-05-M1-8

DATE: 18 June 1971

ORBIT 1
RETRO VEL. $V_R = 227 \text{ FPS}$

ORBIT 1
 $I = 28.5^\circ \text{ (ETR)}$



ORBIT 2
 $I = 55^\circ \text{ (ETR)}$

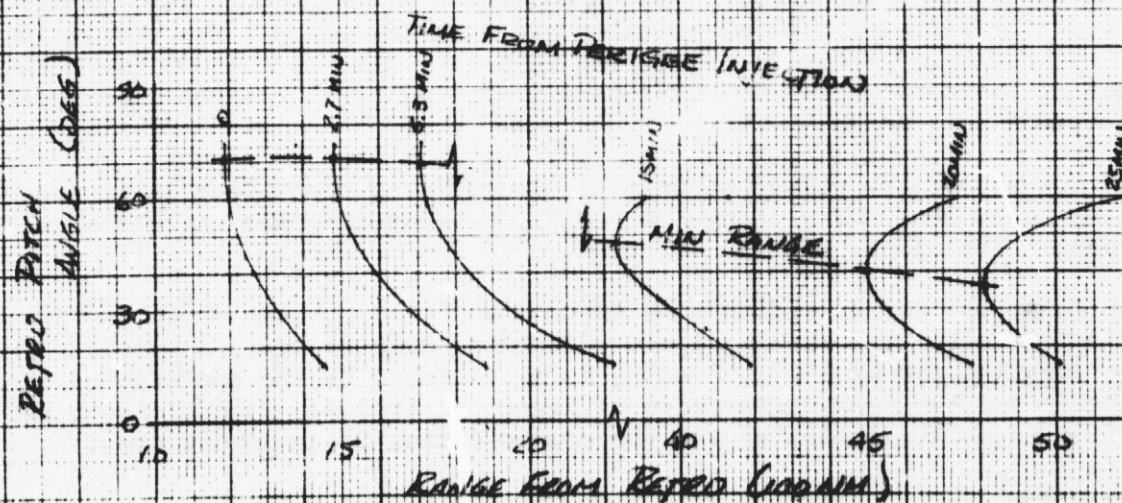
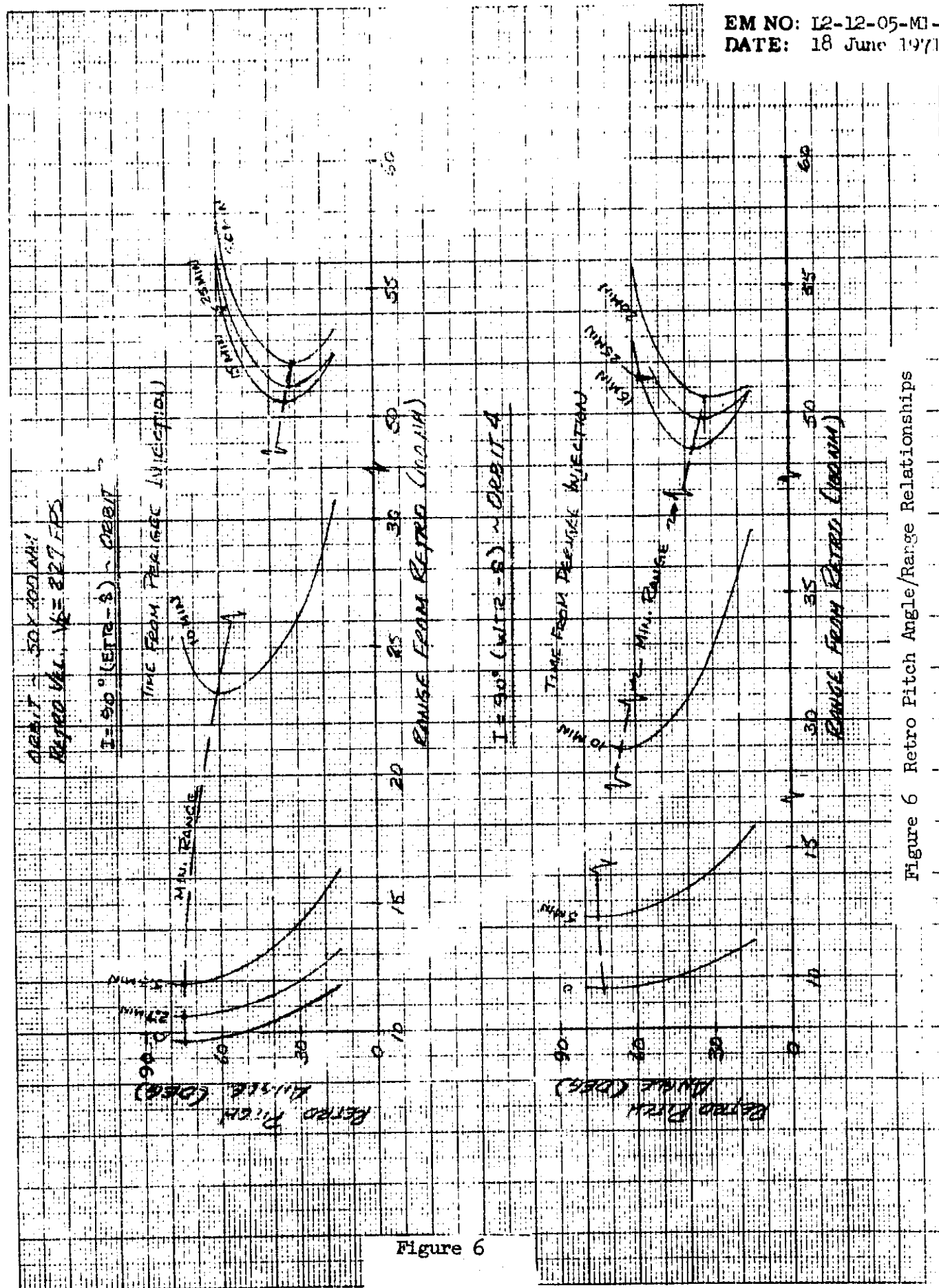


Figure 5 Retro Pitch Angle/Range Relationships



Space Shuttle Project

EM NO: 12-12-05-M1-8

DATE: 18 June 1971

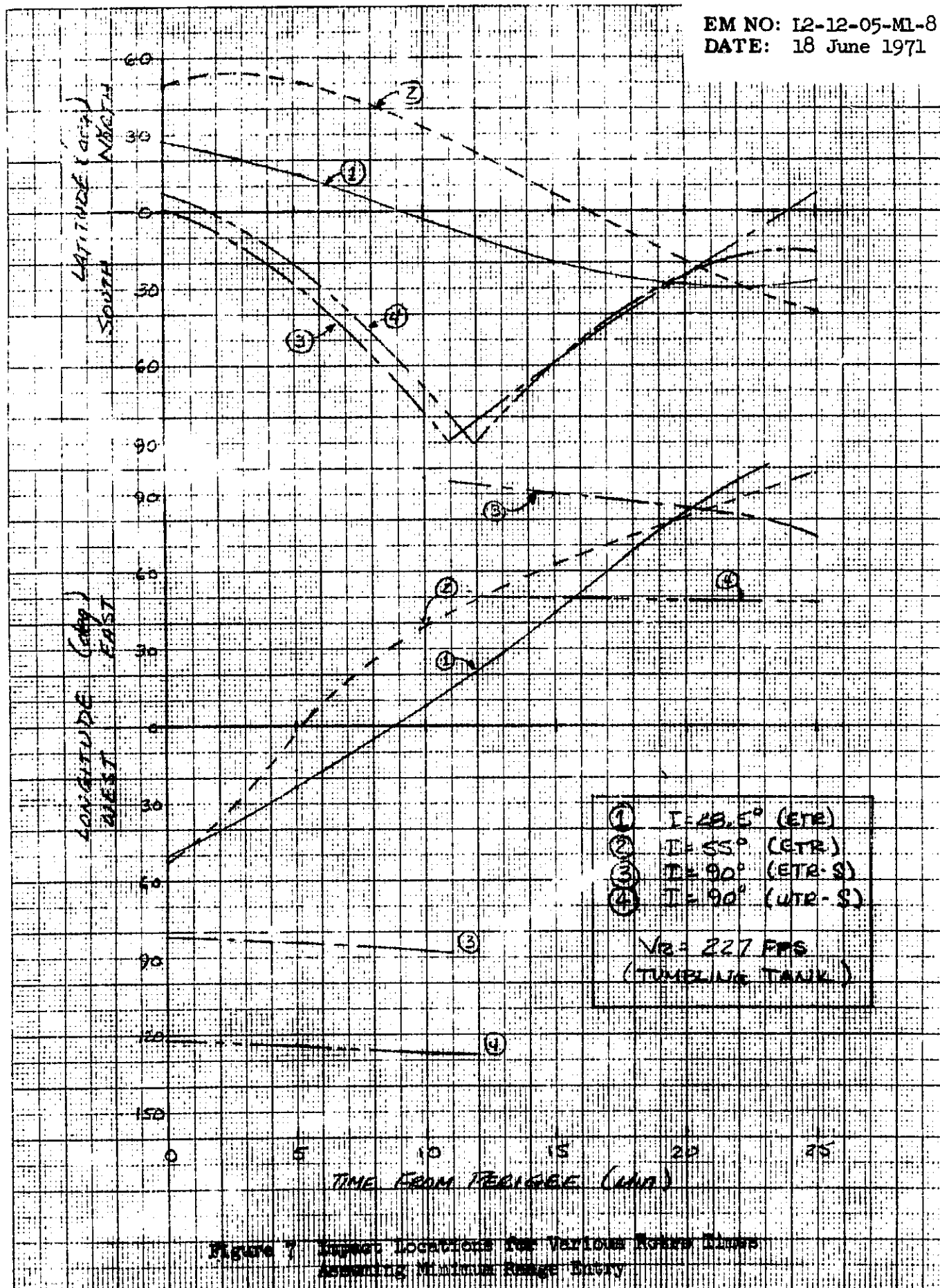


Figure 7 Impact Locations for Various Range Times Assuming Minimum Range Entry

Retro at about 18 minutes from perigee on orbit 4 provides an impact area about 45° S latitude and 49° E longitude.

The effect of minimum drag entry to Indian Ocean impact is to move retro initiation closer to perigee by 1 to 3 minutes.

Retro at perigee is practical only for orbit 1 and 4 with tumbling entry conditions. For orbit 2, droptank impact occurs dangerously near Canada's Newfoundland coastline. Impact coordinates of 10° N and 82° W for tumbling entry with a perigee retro from orbit 3 endangers both Panama and Columbia. Minimum drag entry provides little relief, since orbit 2 impact moves to about 1000 nm from the coast of Ireland and impact for orbit 3 conditions is still along the coast of South America.

Figures 8 and 9 show how changes in retro velocity affect both entry range and time of retro initiation for entry from orbits 1 and 2 to an Indian Ocean impact. The data are summarized in Fig. 10 and 11 for both tumbling and minimum drag conditions. As expected, entry range decreases with both increased V_R and increased drag, moving retro time farther from perigee. Optimum pitch angle is correspondingly increased. Inclination angle and the related effects of injection location and earth oblateness alter entry range about 200 nm and time of retro about 2 minutes.

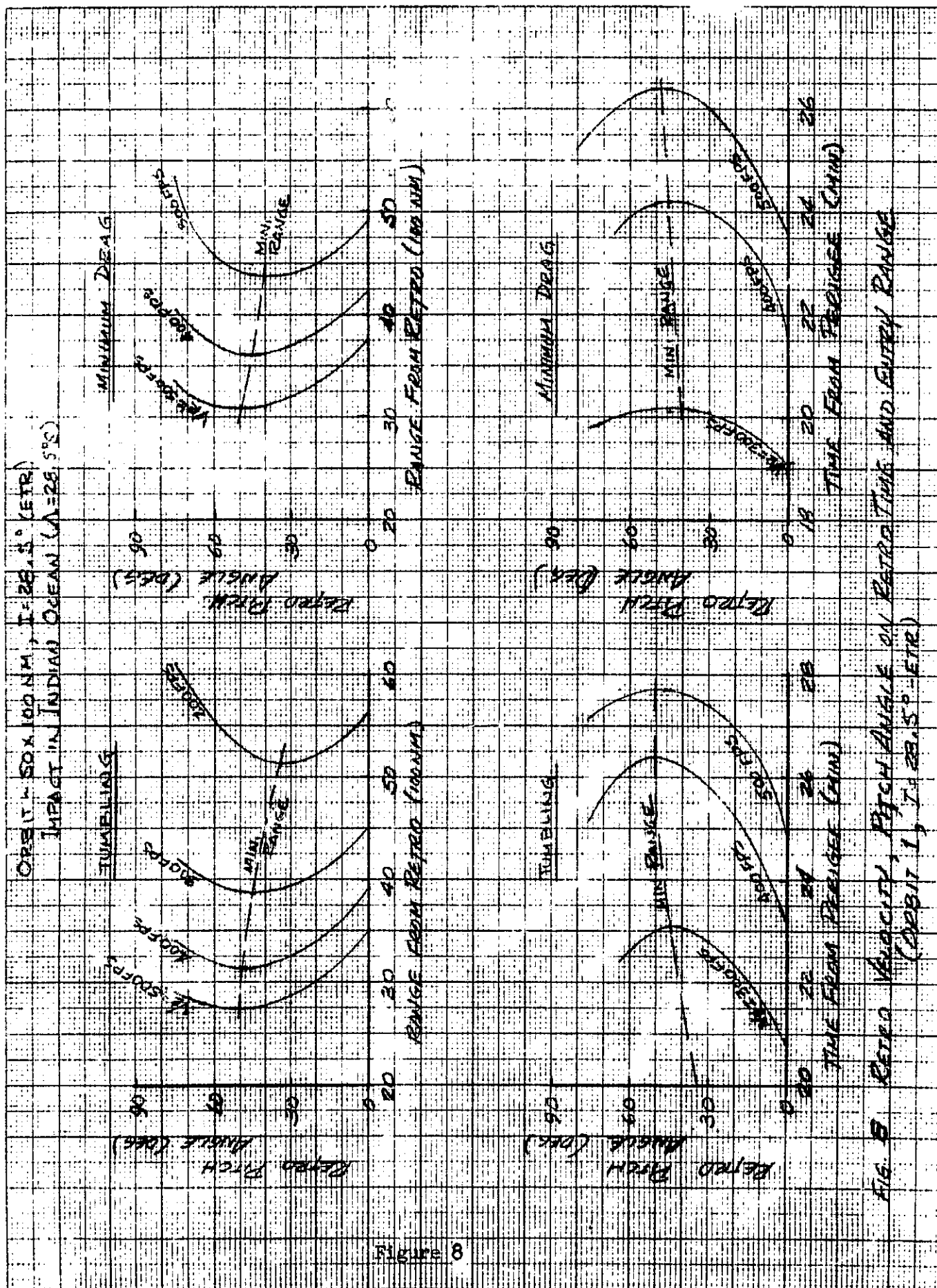
Reducing V_R below 200 fps rapidly increases range, the limiting case being $V_R = 0$ at some time near perigee. Dispersions are also increased because of the longer corresponding flight times.

Definite trends for minimizing entry range and, therefore, impact dispersions, are indicated by the study results in Figs. 5 through 11, i.e., retro at perigee, V_R of the order of 500 fps and $(\theta_R)_{opt}$ around 60 degrees to 75 degrees. There are subtleties which contradict these trends, however, and they must be considered. First, the obvious, impact proximity to land areas for perigee-retro and entry from orbits 2 and 3. Higher V_R moves impact locations for these cases closer to the launch site increasing the danger to either the North or Central America regions. Therefore, perigee retro for these orbits, is eliminated from consideration at this time.

A less obvious subtlety is the effect of θ_R on orbiter performance. As indicated earlier, and based on the results of Ref. 5, vehicle on-orbit drag is critical to minimizing perigee velocity requirements. A low on-orbit drag profile at injection (probably near zero angle of attack) is most desirable. Yet, since the orbiter must assume the tank retro attitude before separation, the overall system would be operating at near maximum drag conditions if pitched to $\theta_R = 60$ deg or 75 deg. The corresponding effect on injection velocity requirements is obvious.

The relative cost of operating a space shuttle system at non-optimal conditions is much more critical than ramifications of tank deorbit at non-optimal retro pitch conditions. Therefore, the requirement of selecting an appropriate $(\theta_R)_{opt}$ (for minimum range entry) for all retro conditions was relaxed. A single retro pitch angle was selected for each orbit which corresponds to $(\theta_R)_{opt}$ for Indian Ocean

DATE: 18 June 1971





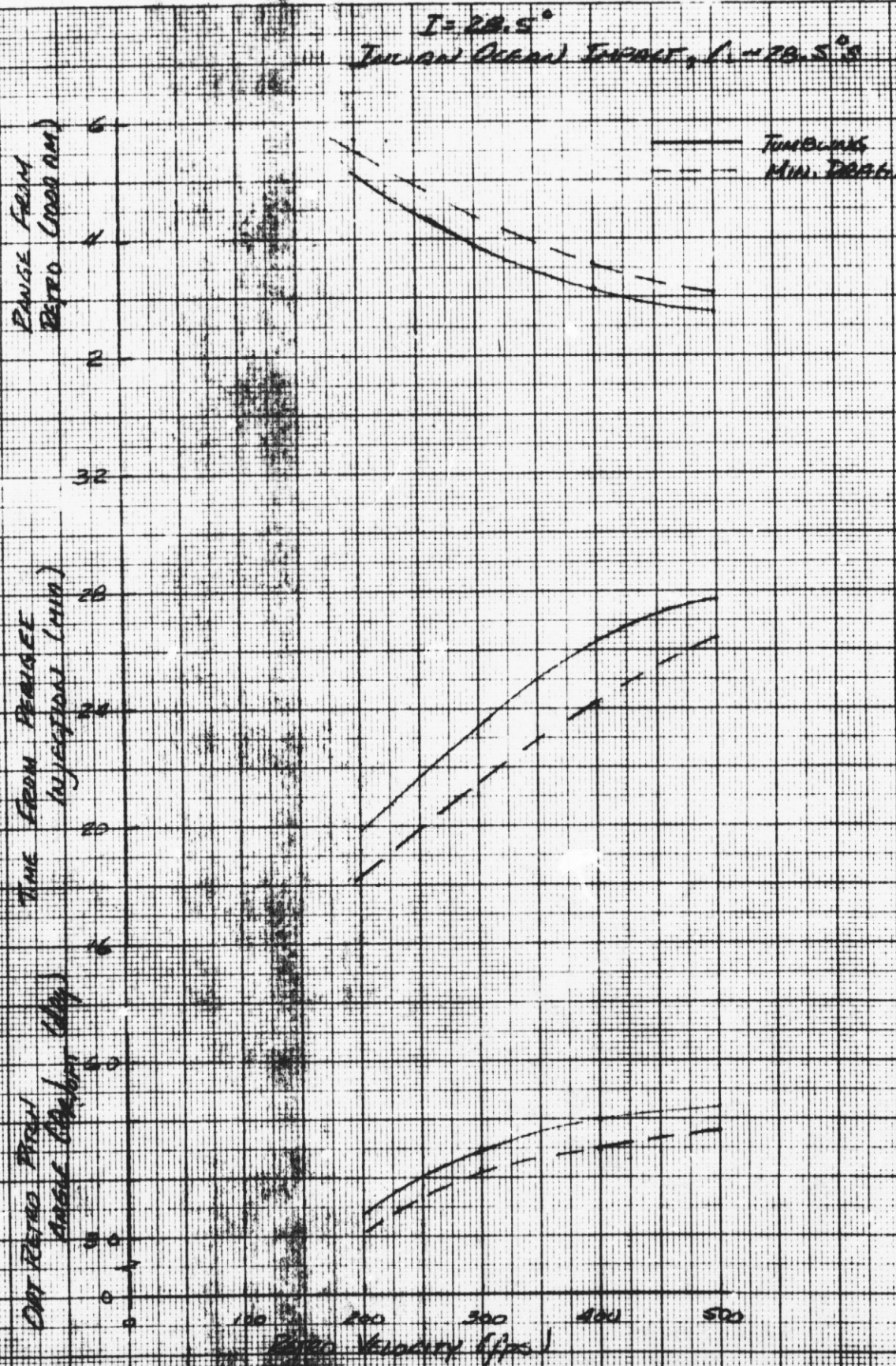
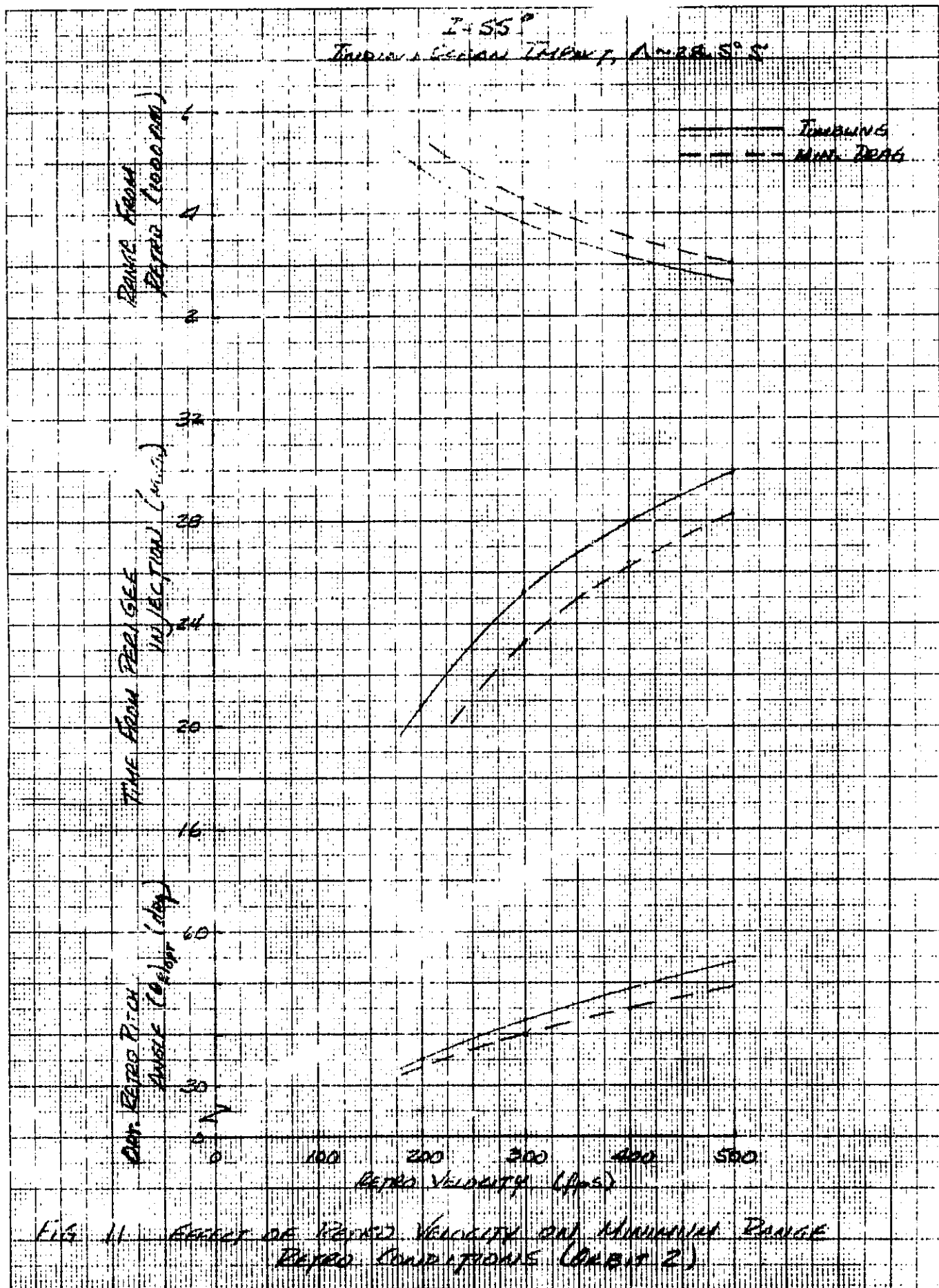


FIG 10. EFFECT OF RETRO VELOCITY ON MINIMUM RANGE
RANGE CONDITIONS (ORBIT 1)



impacts with $V_R = 227$ fps.* These angles, listed in Table 4, are used for all droptank entry simulations emanating from their respective orbits regardless of retro point, drag profile, or retro velocity.**

Table 4

SELECTED RETRO PITCH ANGLES

Orbit 1	θ_R	=	37	deg
Orbit 2	θ_R	=	39.5	deg
Orbit 3	θ_R	=	32.4	deg
Orbit 4	θ_R	=	33.5	deg

Nominal entry trajectories were generated for Indian Ocean impact from orbits 1, 2, 3 and 4. Impact coordinates of orbit 1, 2 and 3 entry trajectories are at a geodetic latitude of about $\Lambda = 28.5^\circ$ S and longitudes between $\tau_E = 80^\circ$ E and 90° E. Impact coordinates for the orbit 4 case are 45° S, 49° E. Initial conditions (at retro) for these nominals were obtained using trajectory iterative techniques employed in LMSC point mass entry trajectory programs. They are shown in Table 5. Also included are conditions for entry trajectories from orbits 1 and 4 with retro at perigee.

Table 6 is a summary of entry parameters for the nominal trajectories. Note the similarity in respective comparisons. For Indian Ocean impact, inclination angle changes alter entry range a maximum of about 300 nm regardless of the comparative entry profiles. Flight times are within 2 minutes for all tumbling drag or all minimum drag profiles and comparisons of peak dynamic pressure, $(\bar{q})_{\max}$ and peak laminar stagnation point heat rate, $(\dot{q}_S)_{\max}$ also show similarities. Comparison of tumbling and minimum drag entry from a given orbit, to an Indian Ocean impact show greater differences, however, (except for flight times). Ranges vary to about 600 nm, $(\bar{q})_{\max}$ changes by an order of magnitude and $(\dot{q}_S)_{\max}$ differs by at least a factor of 3.

The altitude-velocity (H-V) plots in Fig. 12 provide more insight into the differences of tumbling and minimum drag trajectories.

*Nominal V_R is based on rocket characteristics in Table 3. This rocket selection is not the product of a detailed optimization study, but is sufficiently optimum when considering V_R - θ_R relationships for minimum range.

**The θ_R magnitudes in Table 4 were not optimized for orbiter on-orbit performance. They probably do, however, represent near tolerable maximums for the system.

TABLE 5

INITIAL (ORBIT) CONDITIONS FOR NOMINAL ENTRY TRAJECTORIES

 $(V_R = 227 \text{ FPS})$

ORBIT NO.	TIME FROM PERIG. (min)	ALTITUDE (ft)	LONGITUDE (deg)	GEOC. LATIT. (deg)	INERTIAL VEL. (fps)	INERTIAL FLT PATH (deg)	INERTIAL AZIM (deg)	IMPACT AREA*	ENTRY PROFILE
1 (I=28.5°, ETR)	0 20.3 21.0	303806 439698 448333	68.27(W) 8.74(E) 11.34(E)	27.76(N) 3.47(S) 4.97(S)	25890 25638 25673	0 0.40 0.41	96.73 118.34 118.14	AO IO IO	ALL Min. Drag Tumbling
2 (I=55°, ETR)	19.8 22.1	450181 468795	36.72(E) 45.51(E)	39.04(N) 32.27(N)	25667 25650	0.42 0.42	132.39 137.29	IO IO	Min. Drag Tumbling
3 (I=90°, ETR-S)	17.3 19.6	461222 495724	85.53(W) 86.09(W)	55.73(S) 64.88(S)	25691 25657	0.41 0.42	180.0 180.0	IO IO	Min. Drag Tumbling
4 (I=90°, WTR-S)	0 15.6 17.8	303806 419905 453257	121.25(W) 125.14(W) 125.70(W)	22.83(N) 42.16(S) 51.37(S)	25890 25722 25690	0 0.37 0.39	180.0 180.0 180.0	PO IO IO	ALL Min. Drag Tumbling

* AO - Atlantic Ocean
IO - Indian Ocean
PO - Pacific Ocean

Space Shuttle Project
EM NO: 12-12-05-MI-8
DATE: 18 June 1971

Table 6

NOMINAL ENTRY TRAJECTORY PARAMETER SUMMARY

$$(V_R = 227 \text{ FPS})$$

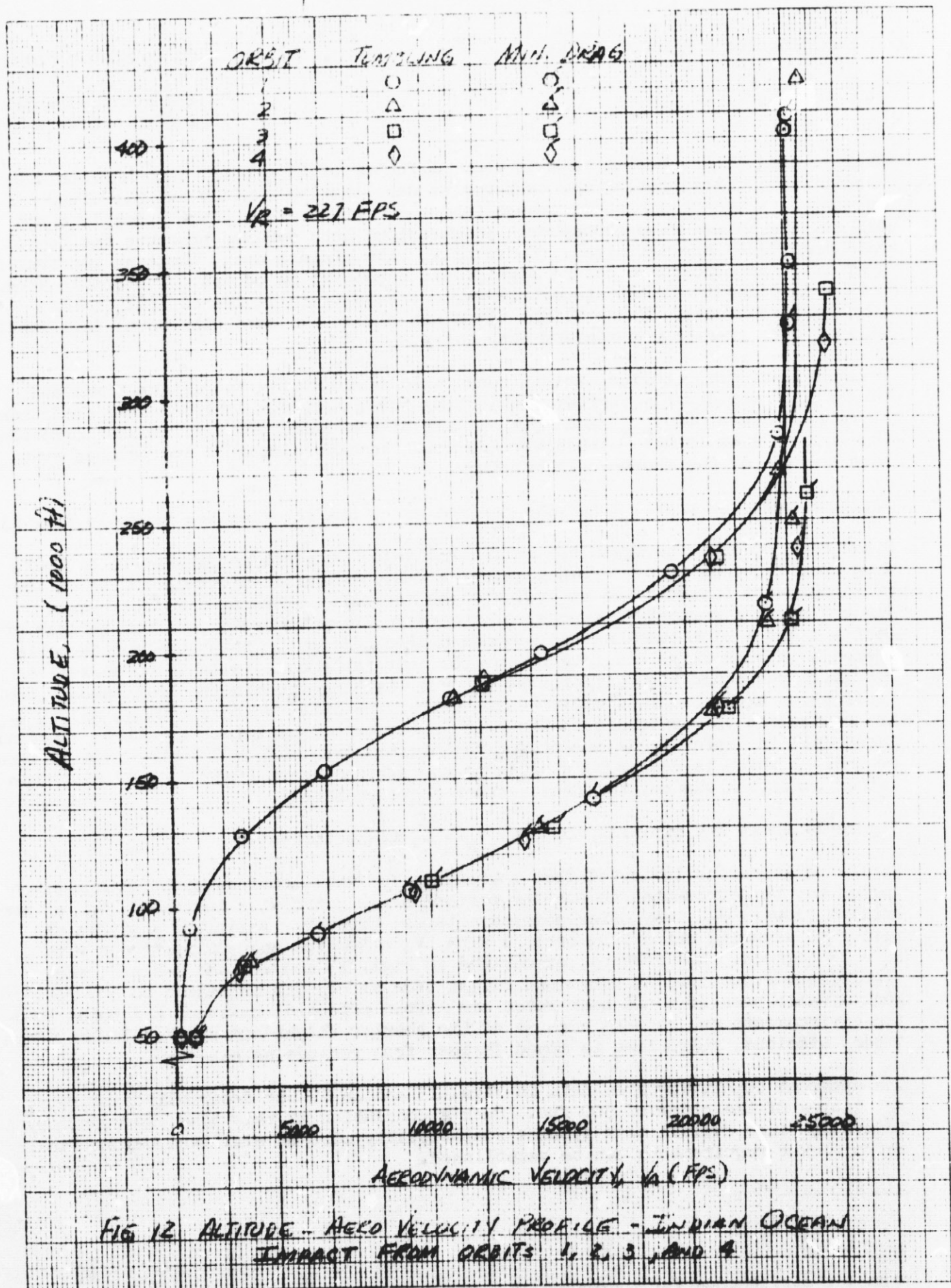
ORBIT No.	RETRO TIME (MIN.)	RETRO PITCH (deg)	FLIGHT TIME (sec)	RANGE (nm)	$(\bar{Q})_{\text{MAX}}$ (psf)	$(\dot{Q}_S)_{\text{MAX}}$ (BTU/ft ^{3/2} -sec)	IMPACT			ENTRY PROFILE
							AREA*	Λ (deg)	τ_E (deg)	
1	20.3	37	1385	5365	975	200	IO	28.5S	94.2E	Min. Drag
	21.0	37	1381	4744	63	60	IO	28.6S	85.8E	Tumbling
2	19.8	39.5	1335	5152	977	209	IO	28.5S	88.3E	Min Drag
	22.1	39.5	1351	4597	65	63	IO	28.5S	89.3E	Tumbling
3	17.3	32.4	1484	5759	1042	233	IO	28.5S	88.6E	Min Drag
	19.6	32.4	1508	5210	68	72	IO	28.5S	88.6E	Tumbling
4	15.6	33.5	1438	5575	1014	230	IO	45.1E	49.2E	Min. Drag
	17.8	33.5	1463	5029	68	48	IO	45.0E	49.2E	Tumbling
1	0	37	575	2030	991	190	AO	19.5N	34.8W	Min. Drag
	0	37	515	1173	63	51	AO	24.2N	49.0W	Tumbling
4	0	33.5	551	1903	1054	220	PO	8.9S	123.1W	Min. Drag
	0	33.5	496	1042	67	63	PO	5.5N	122.3W	Tumbling

* AO - Atlantic Ocean
IO - Indian Ocean
PO - Pacific Ocean

Lockheed Missiles & Space Company

Space Shuttle Project

EM NO: 12-12-05-M-8
DATE: 18 June 1971



EM NO: 12-12-05-M1-8

DATE: 18 June 1971

Average drag of a tumbling tank is about a factor of 10 greater than minimum drag conditions. Consequently, the tank begins decelerating rapidly shortly after encountering the sensible atmosphere (about 300,000 feet). Since velocity drops off quickly before deep atmospheric penetration, both dynamic pressure and heat rate magnitudes are minimized. Conversely, with minimum drag, the tank penetrates deep into the atmosphere before significant deceleration occurs. The combination of high velocities in denser atmosphere regions results in increased $(\dot{Q})_{\max}$ and $(\dot{Q}_s)_{\max}$ magnitudes. Since flight times are almost the same, the total heat impulse* will also be greater for minimum drag entry.

Perigee-retro trajectories exhibit comparable similarities but flight times and ranges are considerably shorter, reflecting lower altitude - higher drag conditions at retro. Since $(\dot{Q})_{\max}$ and $(\dot{Q}_s)_{\max}$ are of the order of magnitude as corresponding Indian Ocean impact trajectories, total loading histories are reduced even more because of the shorter flight times.

Altitude-velocity profiles for the perigee-retro trajectories are shown in Fig. 13.

Since mission orbit perigees are sufficiently low to merit consideration of body drag contributions to performance calculations, natural decay trajectories of the droptanks were investigated to evaluate the necessity of using a retro rocket. Table 7 shows a parametric summary of non-retro entry trajectories from perigee of orbits 1 and 4 with tumbling and minimum drag conditions. Note, the considerable increase in both range and flight time for comparable data in Table 6, as well as the large range and time differences between tumbling and minimum drag cases. Orbit inclination angle has less effect than in previous data, whereas $(\dot{Q})_{\max}$ and $(\dot{Q}_s)_{\max}$ are equivalent to magnitudes in Table 6. A review of the impact locations shows all cases fall in "safe" areas except for the minimum drag, $V_R = 0$ entry from perigee of orbit 1 which is dangerously close to the African coast (0.5° N, 1.9° E). This latter condition was omitted from further consideration.

Figure 14 shows H-V profiles for the $V_R = 0$ trajectories.

Earlier discussions indicated that increased V_R when combined with optimum pitch angles may be detrimental to orbiter performance. Retro with increased V_R at non-optimum (lower) θ_R may offer some advantages, however. A limited analysis was performed assuming retro from orbit 1 with $V_R = 300$ fps and 500 fps** and with $\theta_R = 37$ degrees. The results, summarized in Figs. 15 and 16, and Table 8, show significant reductions in range and flight time as V_R is increased to 500 fps. Peak dynamic pressures and heat rates are little affected, however, and total loading environments are reduced because of the shorter flight times. For Indian Ocean impact missions, retro time is moved farther from perigee as expected.

The apparent conclusion from data in Figs. 15 and 16 is the desirability of retro velocities of the order of 500 fps. Such a conclusion at this time, however, may be myopic since overall tank systems compatibility must be evaluated before final retro rocket requirements can be established.

$$* \quad Q_s = \int_0^t \dot{Q}_s \, dt$$

**Rocket performance for increased V_R was modified by assuming constant nominal values of I_{sp} and T_V . Resulting burntimes a 6.6 sec for $V_R = 300$ fps and 11.2 sec for $V_R = 500$ fps.

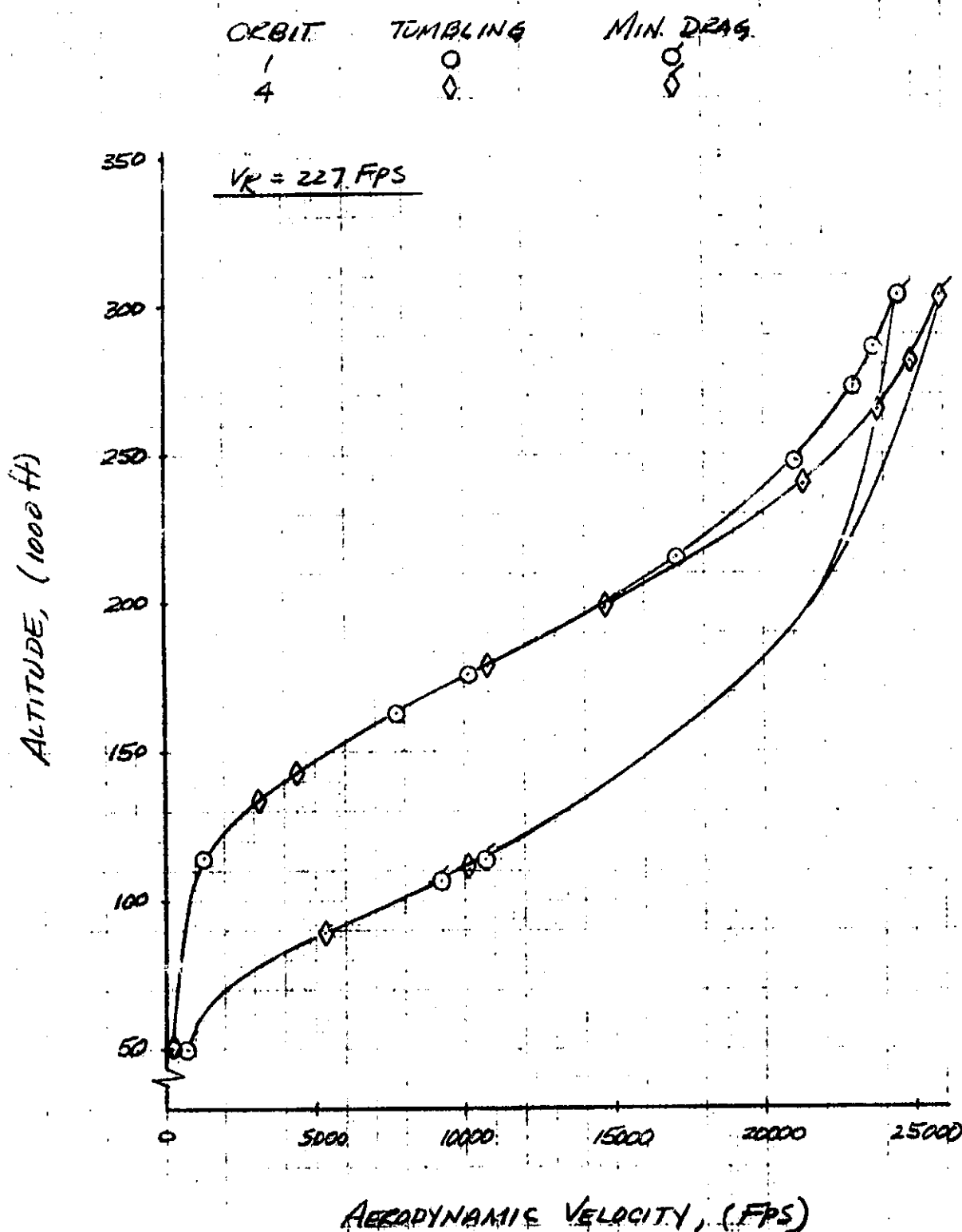


FIG. 13 ALTITUDE - AERD VELOCITY PROFILE FOR PERIGEE RETRO ENTRY FROM ORBIT 1 AND 4.

TABLE 7

ENTRY TRAJECTORY PARAMETER SUMMARY

- NON-RETRO ($V_R=0$) DESCENT FROM PERIGEE -

ORBIT	FLIGHT TIME (sec)	RANGE (nm)	$(\bar{Q})_{MAX}$ (psi)	$(\dot{Q}_S)_{MAX}$ BTU/ft ^{3/2} -sec	IMPACT			ENTRY PROFILE
					AREA *	Λ (deg)	τ_E (deg)	
1	1194	4599	991	134	AO	0.5N	1.9E	Min. Drag
	632	1652	63	55	AO	21.8N	41.3W	Tumbling
4	1098	4170	1022	194	PO	46.9S	125.4W	Min. Drag
	588	1415	67	63	PO	0.7S	122.7W	Tumbling

* AO - Atlantic Ocean

PO - Pacific Ocean

Space Shuttle Project

EM NO: 12-12-05-M1-8
DATE: 18 June 1971

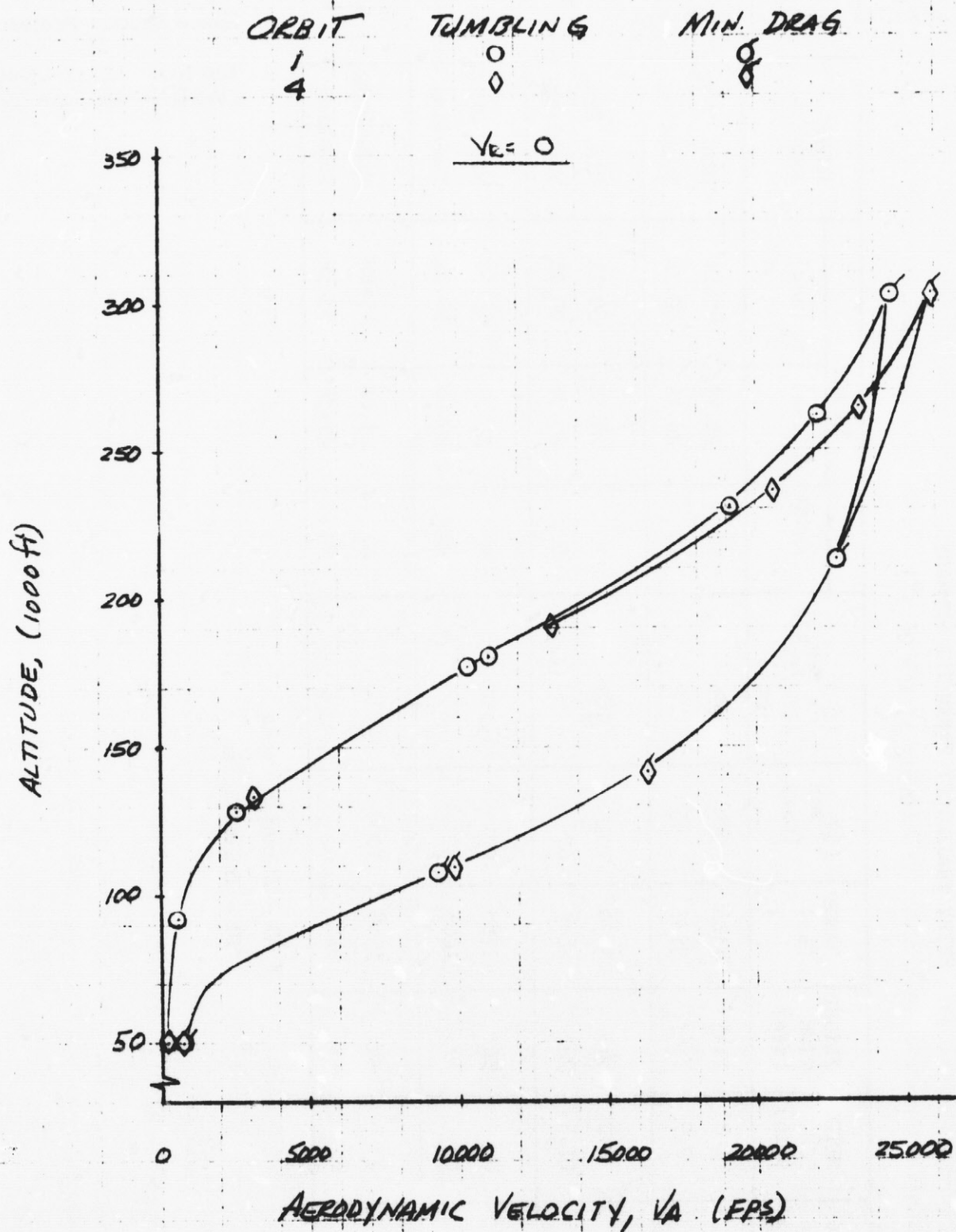


FIG. 14 ALTITUDE - AERO VELOCITY PROFILE FOR NON-RETRO ENTRY FROM PERIGEE

TABLE 8
ENTRY TRAJECTORY PARAMETER SUMMARY
(Orbit 1, $I = 28.5^\circ$)

RETRO VEL (fps)	RETRO PITCH (deg)	RETRO TIME (min)	FLIGHT TIME (sec)	RANGE (nm)	$(\bar{q})_{\max}$ (psf)	$(\dot{q}_s)_{\max}$ (BTU/ft ^{3/2} -sec)	IMPACT			ENTRY PROFILE
							AREA*	Λ (deg)	τ_E (deg)	
300	37	21.2	1143	4366	979	205	IO	28.4S	80.1E	Min. Drag
	37	22.9	1187	3939	63	62	IO	28.4S	80.1E	Tumbling
500	37	26.2	845	3130	1016	182	IO	28.5S	80.1E	Min. Drag
	37	27.5	921	2845	67	68	IO	28.5S	80.1E	Tumbling
300	37	0	517	1788	991	~180	AO	20.9N	38.6W	Min. Drag
	37	0	493	1085	62	~65	AO	24.6N	50.5W	Tumbling
500	37	0	419	1388	1000	~180	AO	23.0N	45.0W	Min. Drag
	37	0	450	915	63	~65	AO	25.3N	53.3W	Tumbling

* AO - Atlantic Ocean

IO - Indian Ocean

Space Shuttle Project

EM NO: 12-12-05-M-8
DATE: 18 June 1971

Table 8



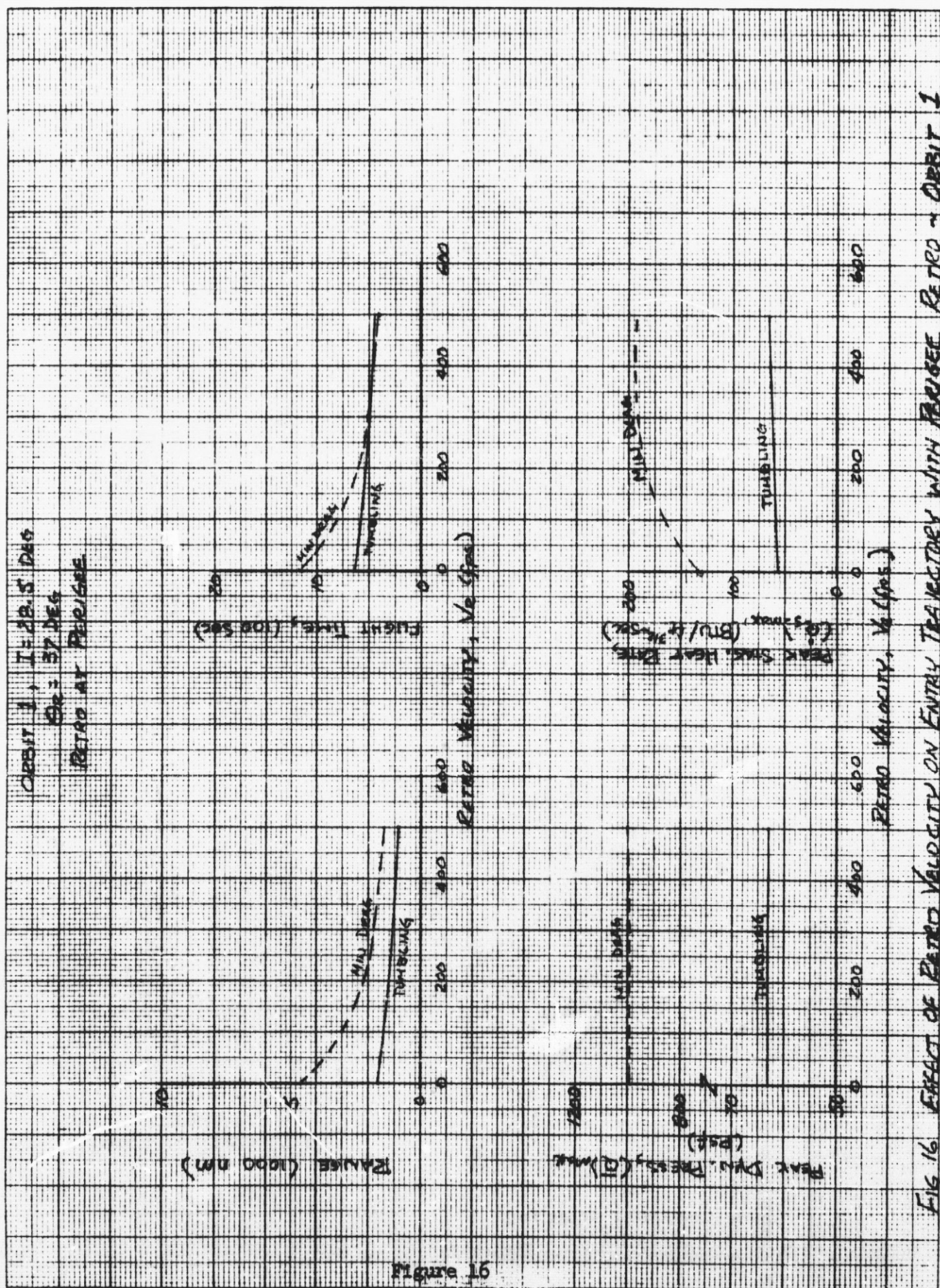


FIG 16 EFFECT OF RETRO VELOCITY ON ENTRY TRAJECTORY WITH REUSEE RETRO ~ ORBIT 1

EM NO: 12-12-05-M1-8

DATE: 18 June 1971

Figure 17 shows a summary of impact locations from data in Tables 6, 7 and 8. Matching these results to shipping density data in Figure 4 indicates minimum to low danger impacts in all cases shown.

Also important to impact location selection is the sensitivity of entry range to various trajectory parameter deviations. Figures 18 through 21 present such sensitivities for tumbling tank entry to an Indian Ocean impact. Parameter deviations include orbital elements retro characteristics, vehicle configuration and atmospheric effects.* Most critical to range sensitivity of the parameters shown are orbit conditions at retro and rocket impulse. Ballistic coefficient effects and initial azimuth (ΔAz) errors are the least contributors along with small changes in θ_R and retro yaw angle, ψ_R . Note, that range errors due to both θ_R and ψ_R are symmetric about the nominal value ($\Delta\theta_R = \Delta\psi_R = 0$) indicating retro at θ_R (and ψ_R) for minimum downrange.**

The data also show only small effects on range sensitivity of orbit inclination and differences in orbital retro conditions.

Sensitivities for minimum drag entry from orbits 1 through 4 to Indian Ocean impacts (Figs. 22 through 25) also show little change due to inclination and are of the same magnitudes as tumbling drag sensitivities. Only range variations due to $\Delta\theta_R$ show differences because of the non-optimum pitch angle condition.

Sensitivities for perigee-retro trajectories from orbits 1 and 4 are presented in Figs. 28 through 29. Though range deviation similarities again exist between minimum and tumbling drag data for both retro conditions, relative magnitudes are decreased considerably. The effect of orbital inertial flight path (γ_{I_0}) is decreased almost 50%, the effect of orbital velocity reduced to relatively negligible magnitudes, and the effect of retro total impulse lowered by about 75%. The effects of $\Delta\theta_R$ are somewhat more amplified because of the non-optimum condition.

Reducing V_R to zero at perigee eliminates the sensitivity similarities between tumbling and minimum drag cases but the effects of inclination angle and perigee location are still small (Figs. 30 through 33). Range sensitivities due to orbit conditions at retro are still prime factors, however.

Conversely, increasing V_R (to 300 fps or 500 fps) decreases range deviations due to all parameters except $\Delta\theta_R$ (Figs. 34 through 41).

Dispersion computations based on the foregoing sensitivities are discussed later in this report.

*Vehicle weight, drag and atmospheric density effects are included in range deviations due to variations in $W/C_D A$.

** $(\theta_R)_{opt}$ for tumbling entry was previously selected as a representative retro pitch angle for all entry trajectories.

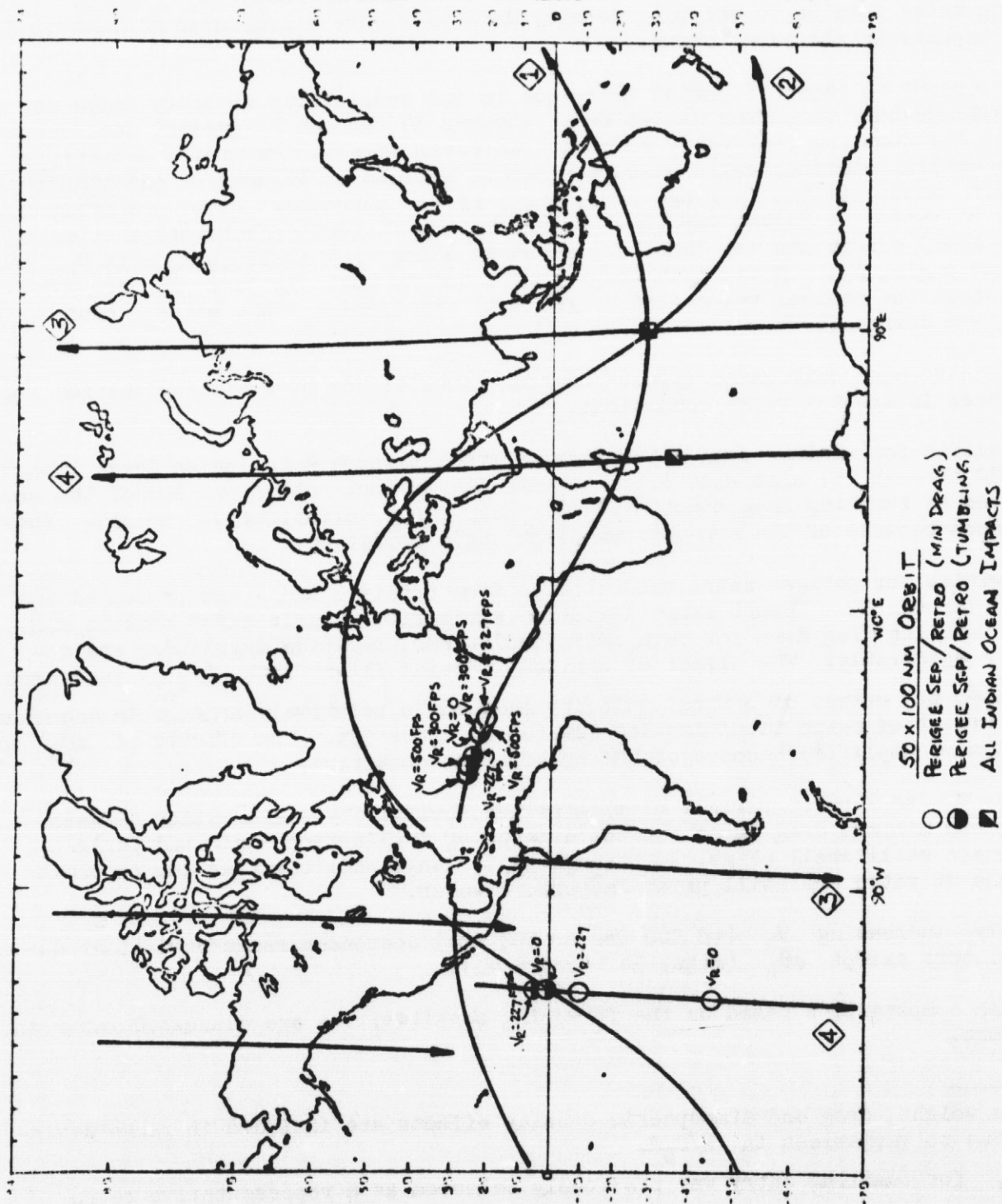


Figure 17 Impact Location Summary

Figure 17

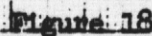
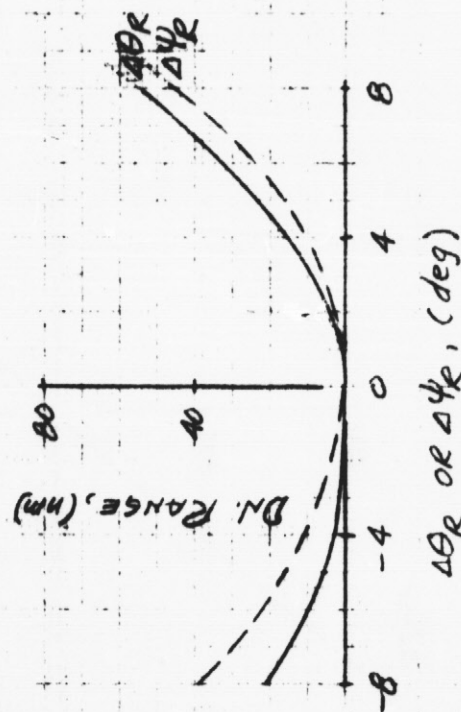
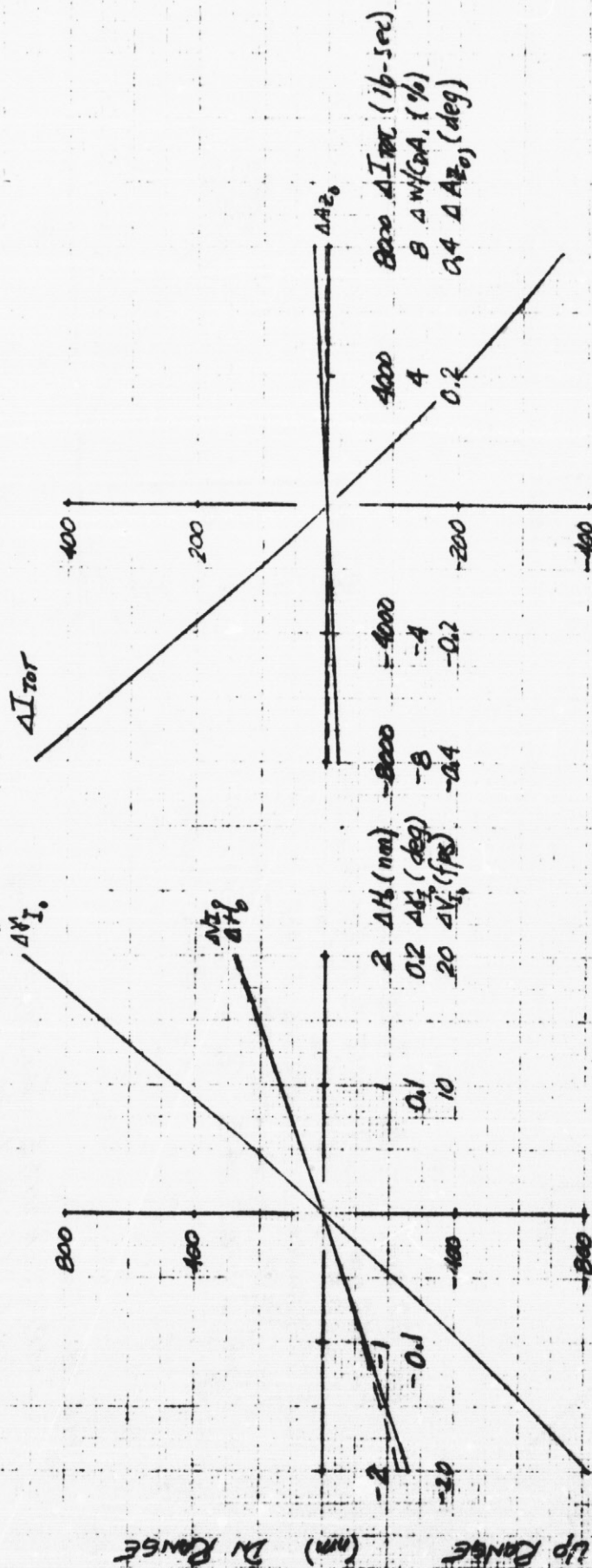


FIG 18
IMPACT RANGE SENSITIVITIES-
INDIAN OCEAN IMPACT- ORBIT 1
(TUMBLING)



FM NO: L2-12-05-M1-8
DATE: 18 June 1971



HP = 50 nm
HA = 100 nm
I = 55 deg
EPR LAUNCH
TANK RETRO - 22.1 MIN FROM INJECTION
NON IMPACT AT
BURN TIME = 5 sec
THRUST = 14,500 lb
OPT DR = 39.5 deg
TUMBLING DRAG
TANK RETRO - 22.1 MIN FROM INJECTION
NON IMPACT AT
T_E = 89.3° EAST
T_E = 29.5° SOUTH

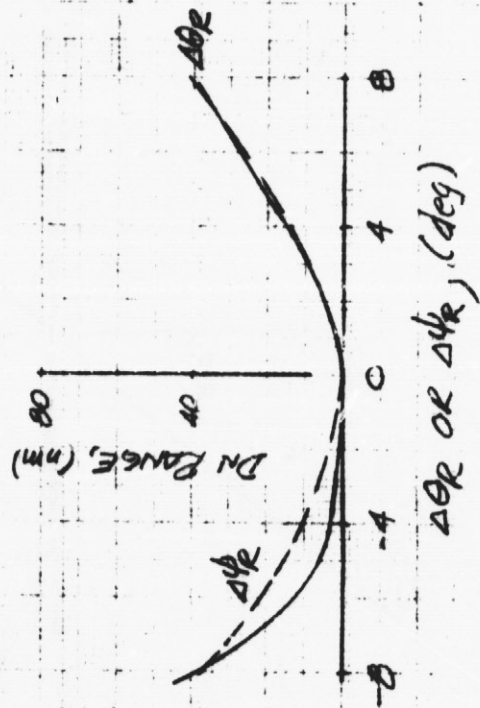
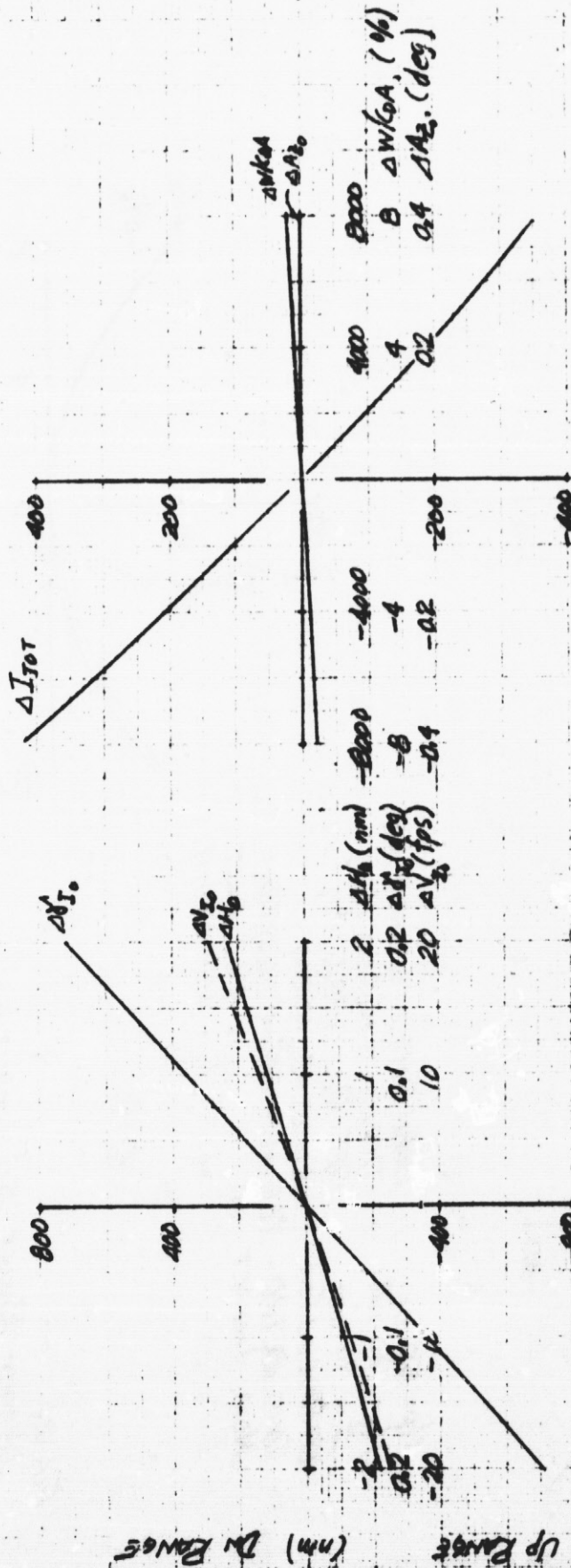


Fig. 19
IMPACT RANGE SENSITIVITIES
- INDIAN OCEAN IMPACT - ORBIT 2
(TUMBLING)

E.A.V

EM NO: I2-12-05-M1-8
DATE: 18 June 1971



HP = 50 mm
HA = 100 mm
I = 90 deg
RETRO LAUNCH
TANK RETRO - 14.6 MIN FROM INJECTION
NOM IMPACT AT:
BURN TIME = 5 sec
THRUST = 14,500 lb
OPT. OR = +32.4 deg
TUMBLING DRAG
2E = 88.6 EAST
A = 28.5 SOUTH

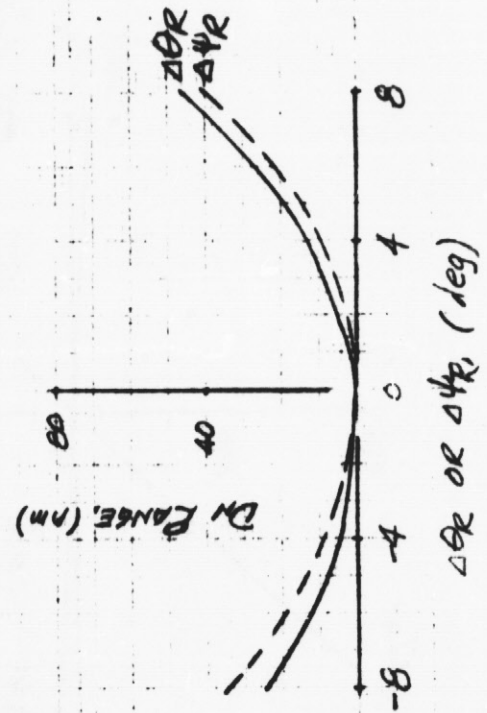


FIG 20
IMPACT RANGE SENSITIVITIES
- INDIAN OCEAN IMPACT - ORBIT 3
(TUMBLING)

EX-10

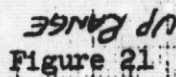
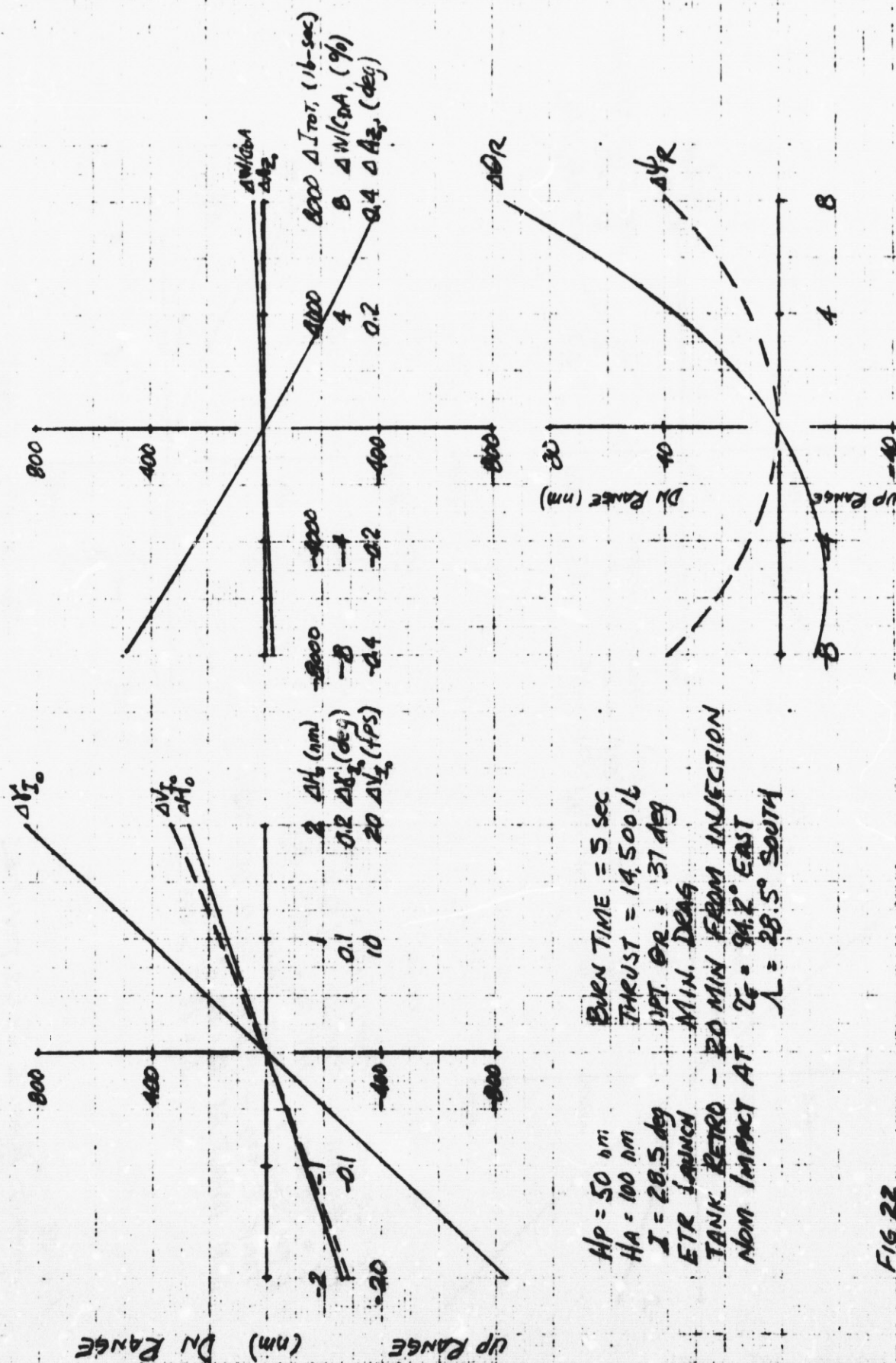


FIG 21
IMPACT RANGE SENSITIVITIES
(INDIAN OCEAN IMPACT - ORBIT 4
(TUMBLING))

DATE: 18 June 1971



HP = 50 nm
 HA = 100 nm
 I = 28.5 deg
 ETR LAUNCH
 TANK RETRO - 20 MIN FROM INJECTION
 NOM IMPACT AT 28.5° EAST
 $\lambda = 28.5^\circ$ SOUTH

BURN TIME = 5 sec
 THRUST = 14,500 lb
 OPT. OR = 37 deg
 MIN. DRAG

FIG 22
 IMPACT RANGE SENSITIVITIES -
 - INDIAN OCEAN IMPACT - DRIBIT 1
 (MINIMUM DRAG)

OR OR 44° , (deg)

5/12

EM NO: L2-12-05-M1-8

DATE: 18 June 1971

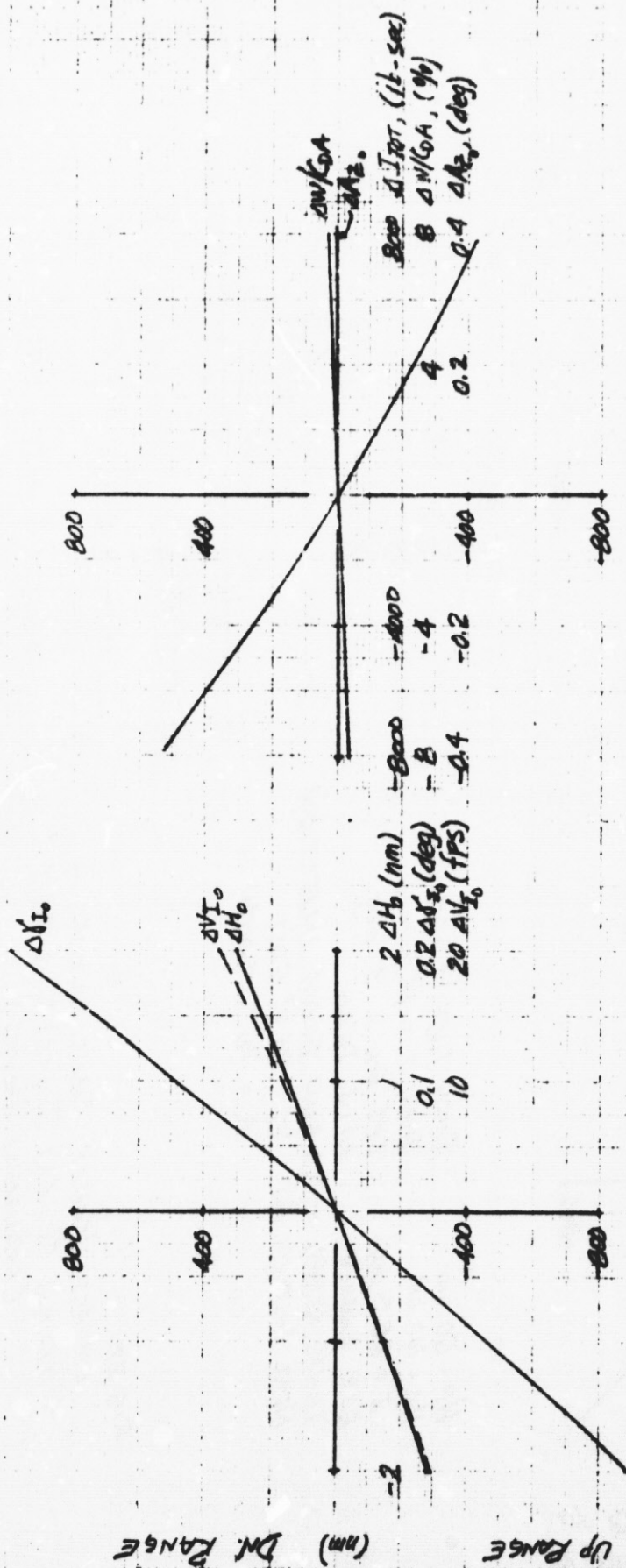


Figure 23

$H_p = 50$ nm Burn Time = 5 sec
 $H_a = 100$ nm Thrust = 14,500 lb
 $I = 55$ deg Opt. $\theta_r = 39.5$ deg
 ETR Launch Min. Drag
 Tank Retro - 19.8 min from Injection
 Nom. Impact at $\theta_r = 88.3^\circ$ East
 $\lambda = 28.5$ South

FIG 23.
 IMPACT RANGE SENSITIVITIES
 - INDIAN OCEAN IMPACT - ORBIT 2
 (MINIMUM DRAG)

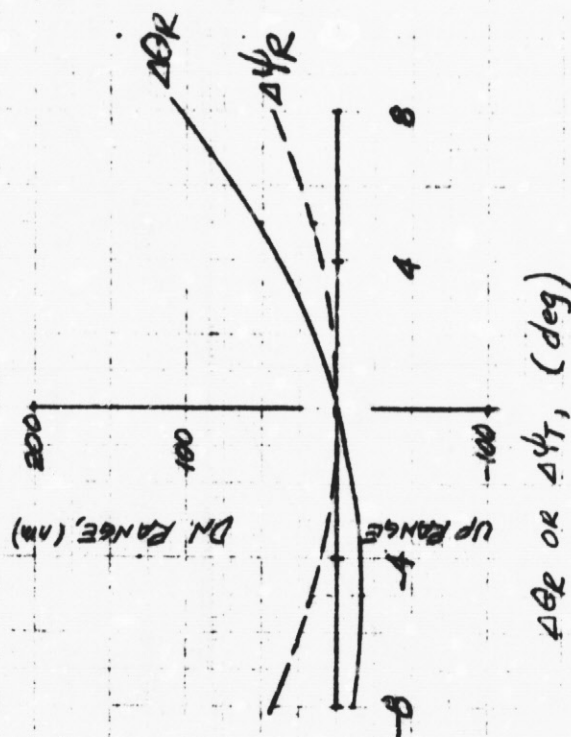


FIG 24.
 IMPACT RANGE SENSITIVITIES
 - INDIAN OCEAN IMPACT - ORBIT 2
 (MINIMUM DRAG)

EXC

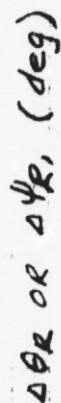


FIG. 28
- IMPACT RANGE SENSITIVITIES
- INDIAN OCEAN IMPACT - ORBIT 3
(MINIMUM DEAS)

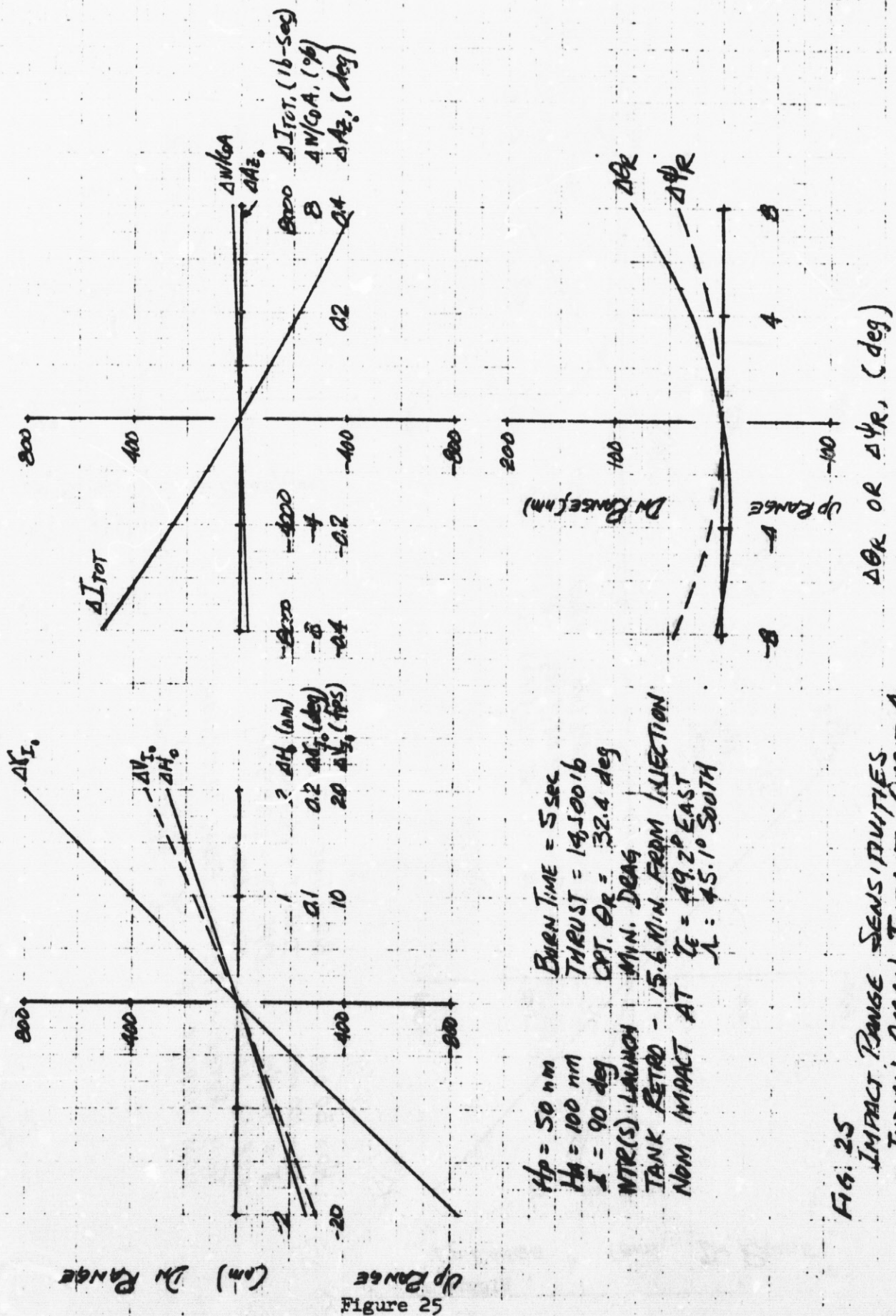
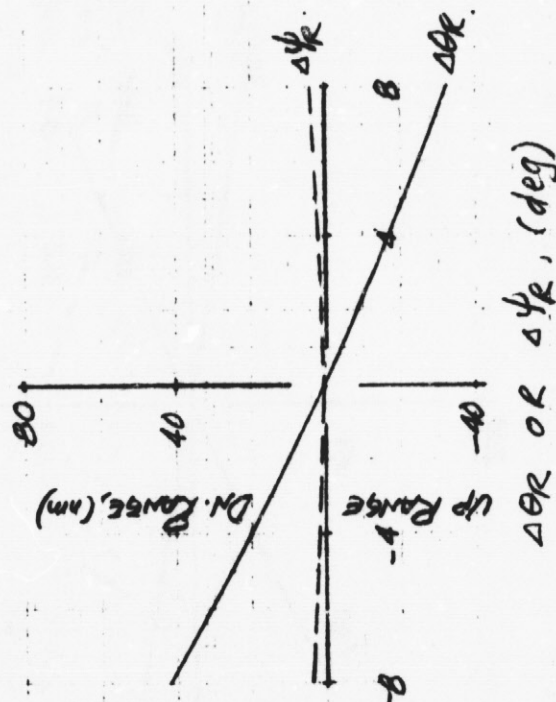


FIG. 25
IMPACT RANGE SENSITIVITIES
-- INDIAN OCEAN IMPACT - ORBIT 4
(MINIMUM DEATHS)

SKW


$$V_p = 227 \text{ FPS}$$

HP = 50 nm
HA = 100 nm
I = 28.5 deg
ETR LAUNCH
BURN TIME = 5 sec
THRUST = 14,500 lb
GR = +37 deg
TANK RETRO AT INJ

NbM. Impact:
 $\tau_E = 49^\circ W$, $\Delta = 24.2^\circ N$
 (ATLANTIC OCEAN)

FIG 26 IMPACT RANGE SENSITIVITIES - PERIGEE
-RETRO - ORBIT 1.

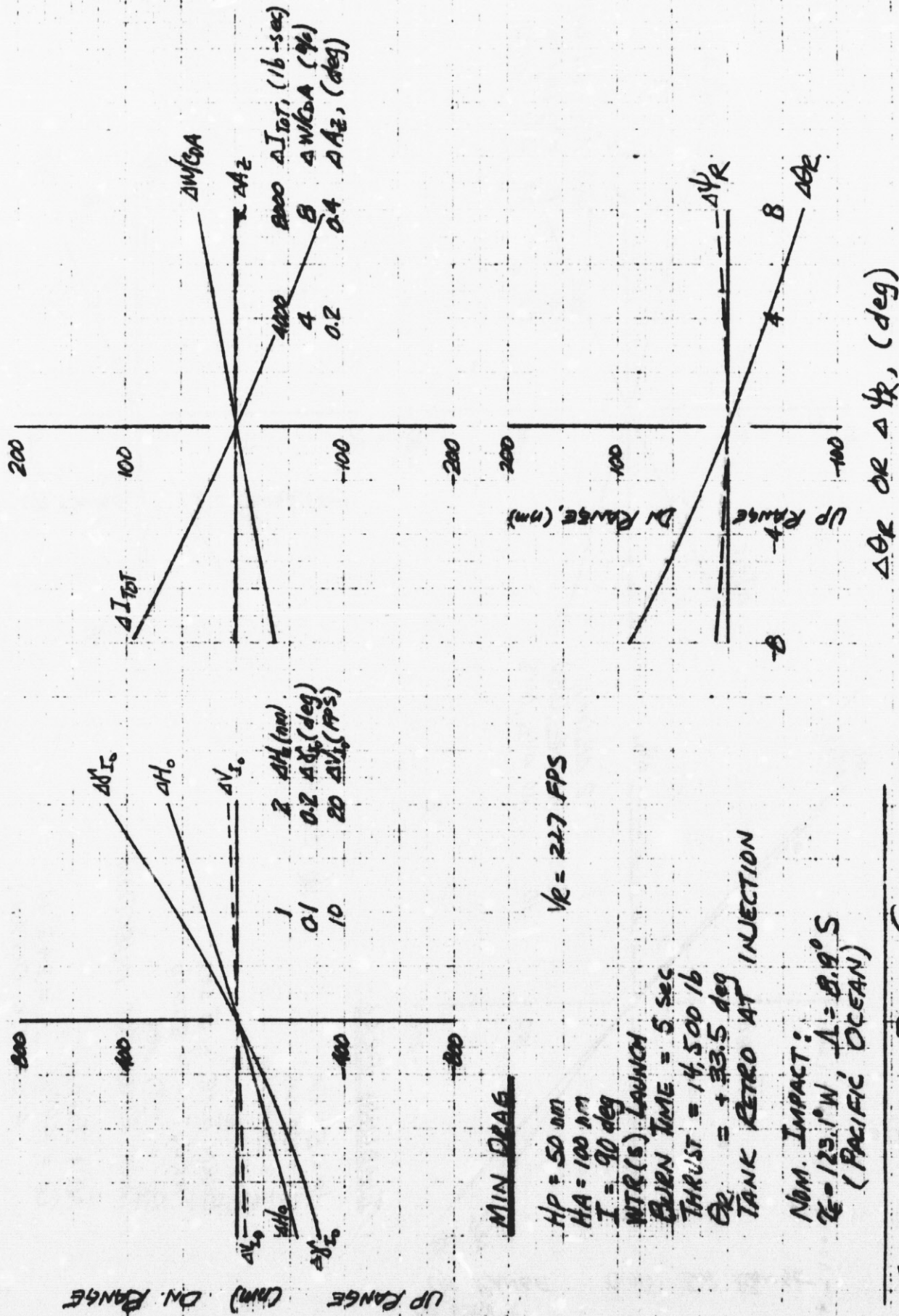


Figure 27

FIG 27 IMPACT RANGE SENSITIVITIES
- PERIGEE RETRO - ORBIT 1

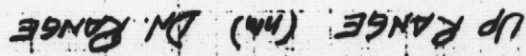
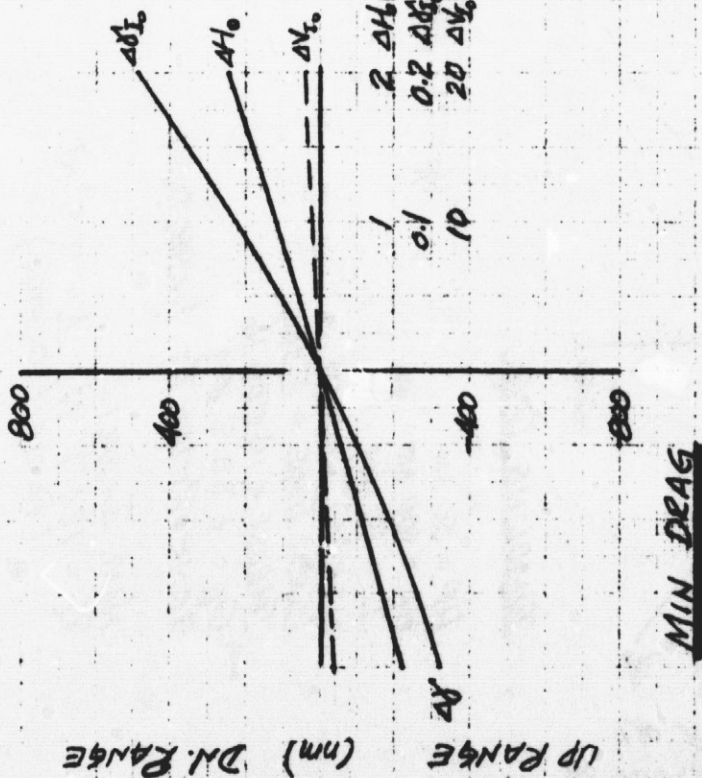
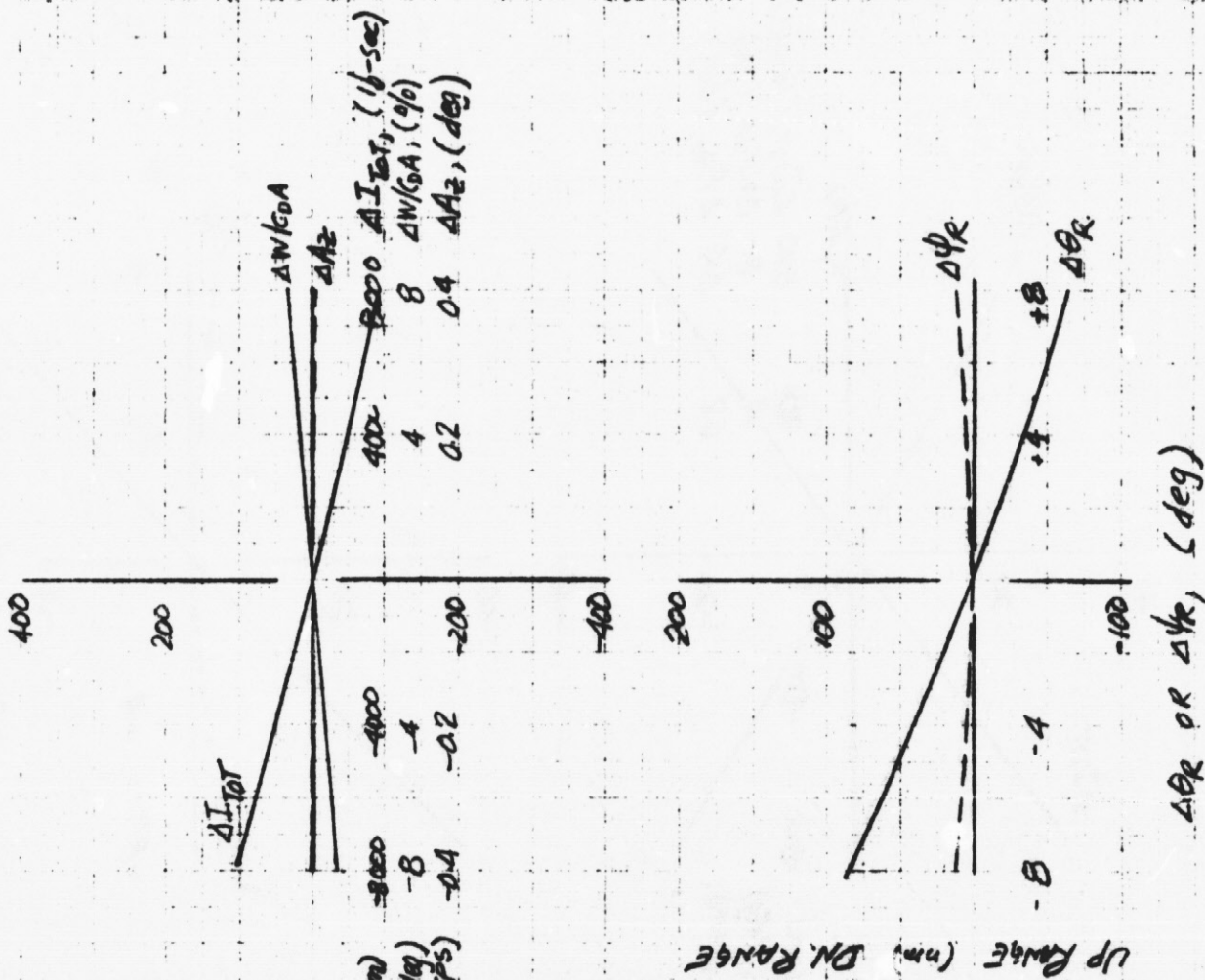


Figure 28

FIG 28 IMPACT RANGE SENSITIVITIES
- PERIGEE RETD - ORBIT 4


$$V_e = 227 \text{ FPS}$$

$H_p = 50 \text{ mm}$

 $H_A = 100 \text{ mm}$
$$I = 20.5 \text{ deg}$$

512-1-1010

Even Time = 5 col

Tracey - 14 Sep 16

14-27-60

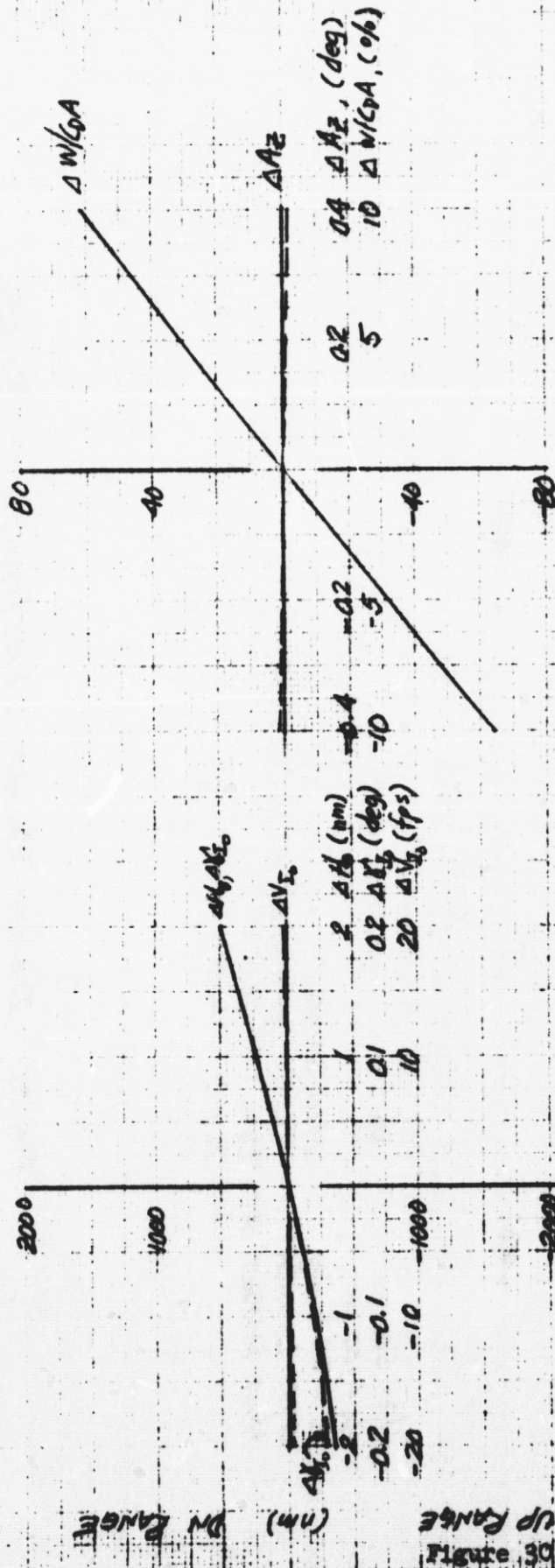
RE. - 12/14/49
TANK RETRO AT INJECTION

Now. Impact!

$$\lambda = 348^\circ \text{W} \quad \lambda = 195^\circ \text{W}$$

/ ATLANTIC OCEAN

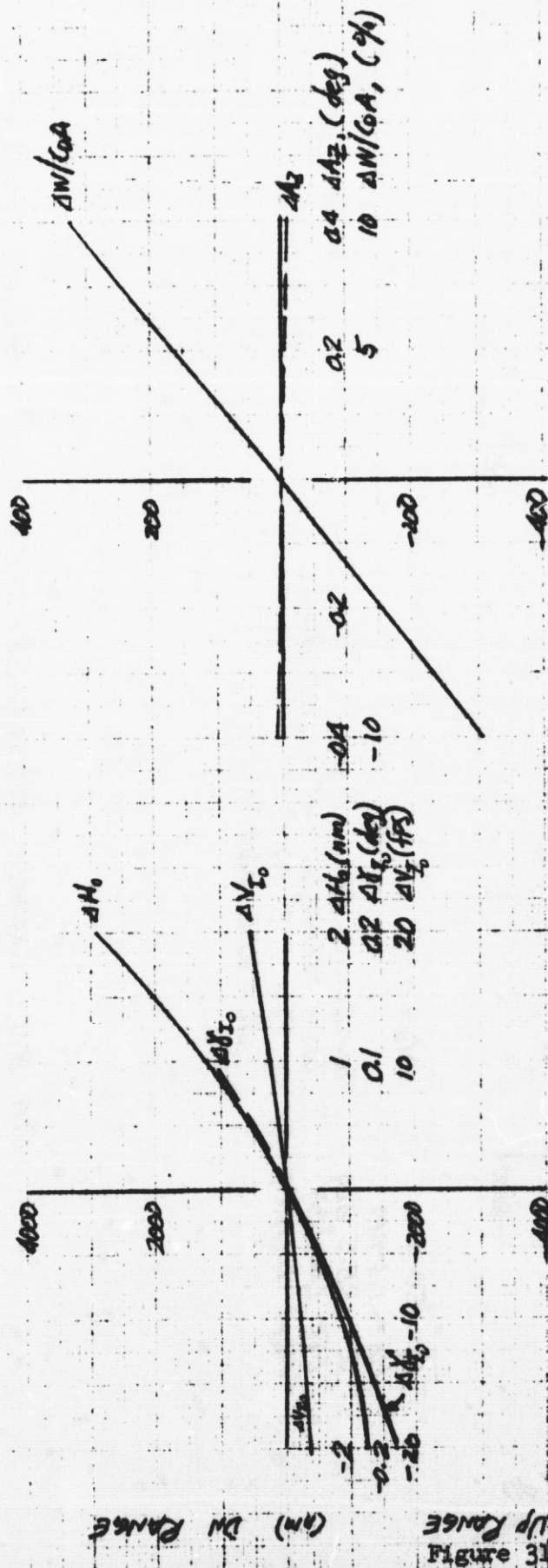
Fig 29 IMPACT RANGE SENSITIVITIES
- PER 155E RETRO - ORBIT 4



HP: 50 nm
HA: 180 nm
I: 28.5 deg
ETR CAUTION
NOM. IMPACT AT
TUMBLING DEAG
TANK SEPARATION AT INJECTION
TE: 41.3 WEST
A: 21.8 NORTH
V_E = 0

FIG. 30 IMPACT RANGE SENSITIVITIES - PERIGEE SEPARATION (ORBIT 1)

EXH

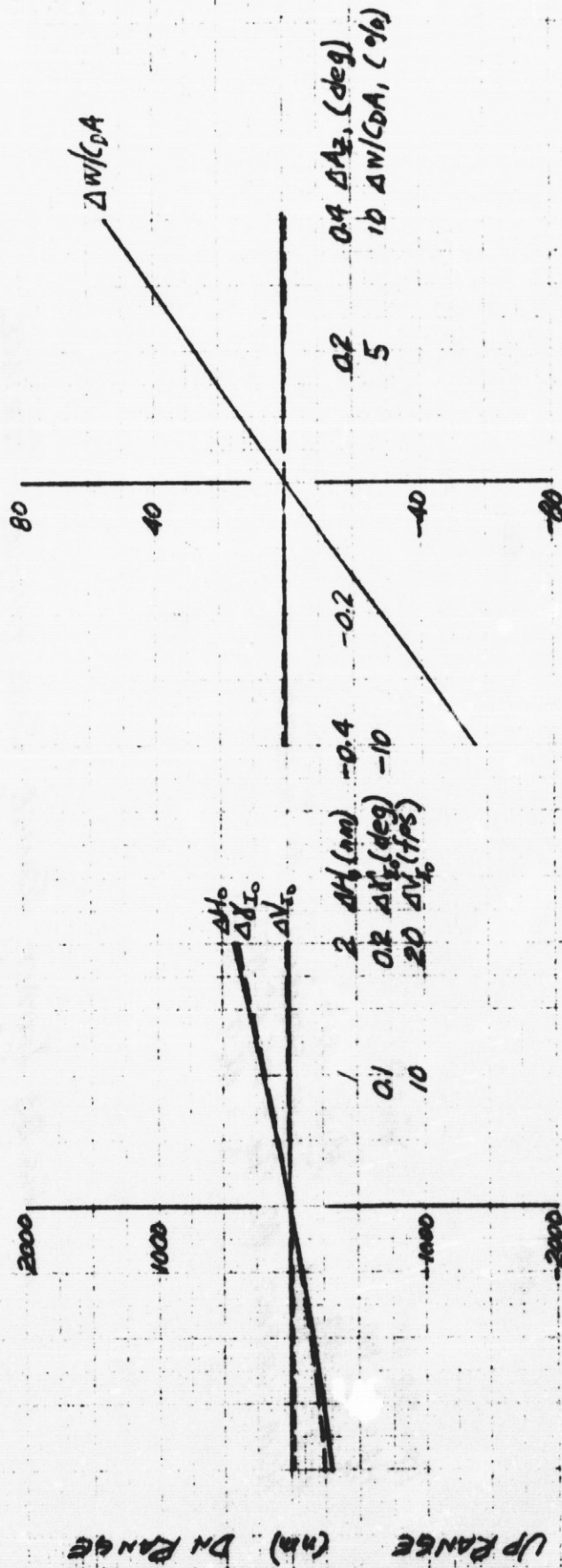


HP = 50 nm
HA = 100 nm
I = 28.5 deg
ETR LAUNCH
NON IMPACT AT
 $\lambda = 0.5^\circ$ NORTH

MIN DRAG
TANK SEPARATION AT INJECTION
 $\lambda = 1.9^\circ$ EAST
 $\lambda = 0.5^\circ$ NORTH

FIG 31 IMPACT RANGE SENSITIVITIES - PERIGEE SEPARATION - (ORBIT 1)

S. A. E. J.



HP = 50 nm
HA = 100 nm
I = 90 deg
WTR(S) LAUNCH
Nom. IMPACT AT 122.7° WEST
A = 0.7° SOUTH

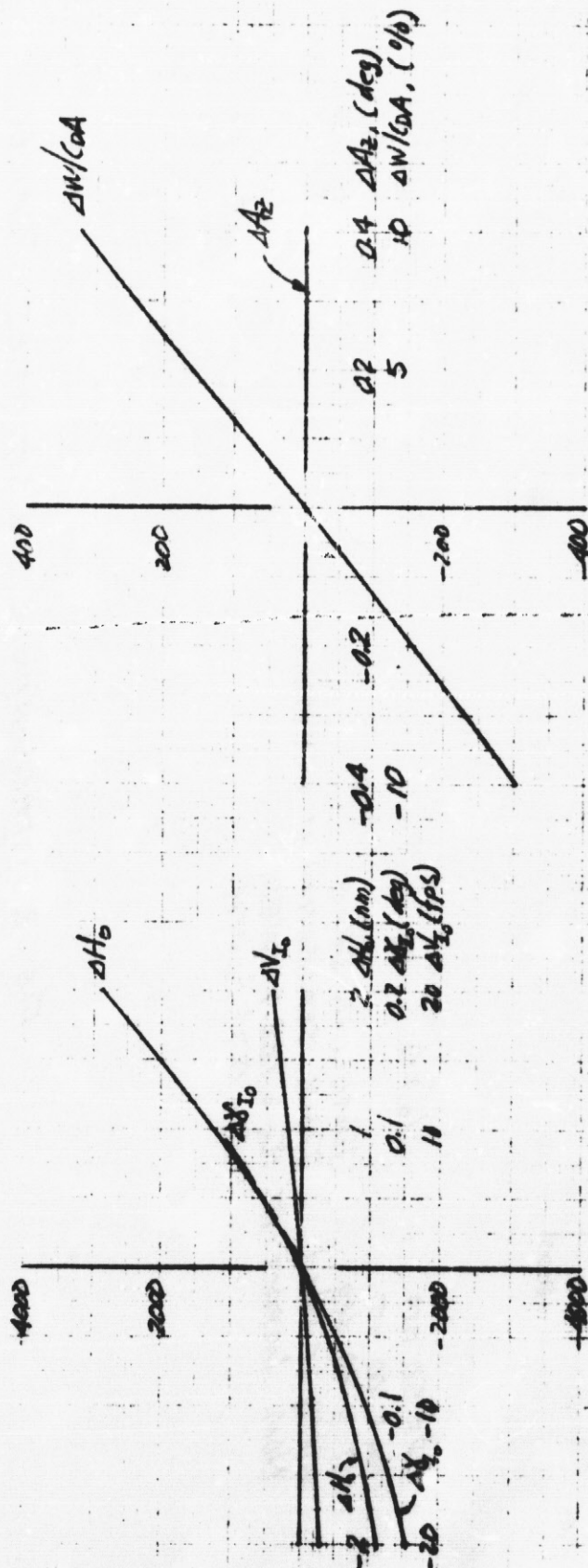
TUMBLING DRAG
TANK SEPARATION AT INJECTION

V₂ = 0

FIG 32 IMPACT RANGE SENSITIVITIES - PERIGEE SEPARATION - (ORBIT 4)

End

E. H. 0



HP = 50 nm
HA = 100 nm
I = 90 deg
WTR (s) LAUNCH
NDM. IMPACT AJ
VR = 0
MIN. URA 5
TANK SEPARATION AT INJECTION
Tg = 125.4° WEST
A = 46.9° SOUTH

FIG 33 IMPACT RANGE SENSITIVITIES - PERIGEE SEPARATION - (ORBIT 4)

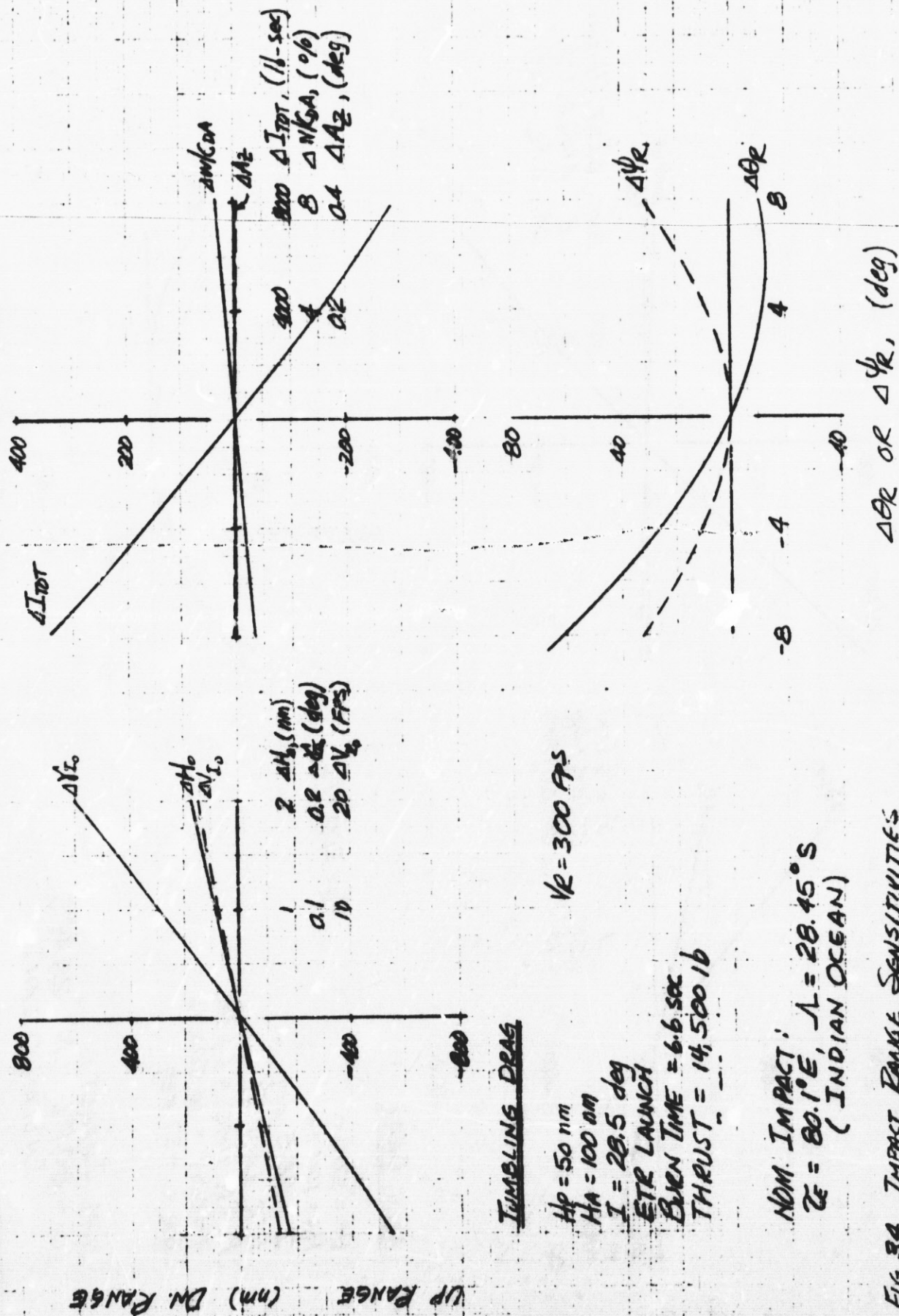


FIG 34 IMPACT RANGE SENSITIVITIES
-INDIAN OCEAN IMPACT - ORBIT 1

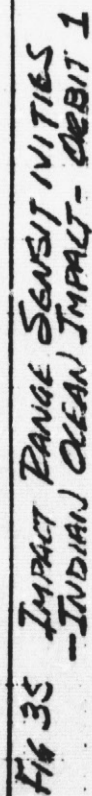


Figure 35

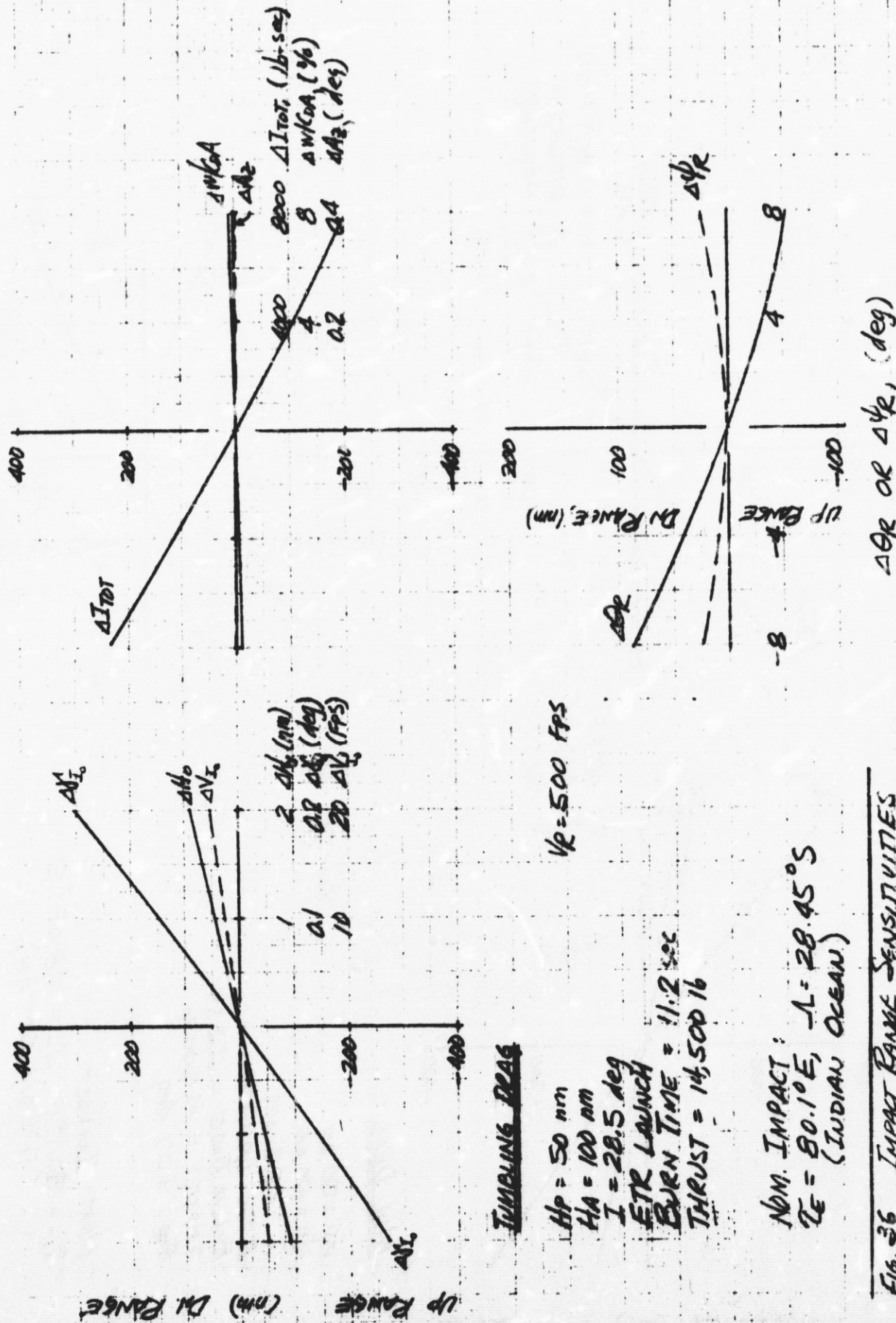


Figure 36

DATE: 18 June 1971

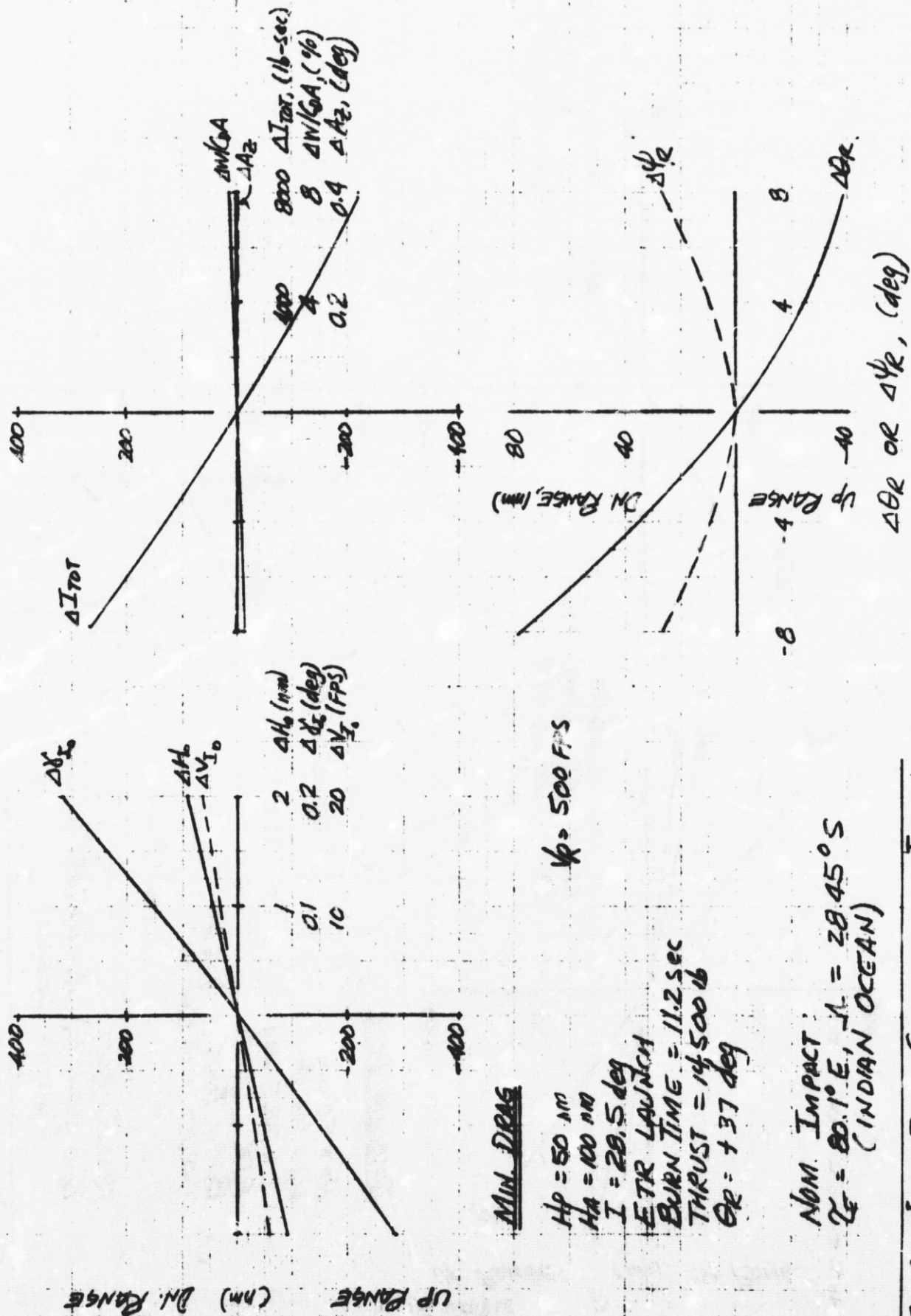


Figure 37

FIG 37 IMPACT RANGE SENSITIVITIES - INDIAN OCEAN IMPACT - ORBIT 1

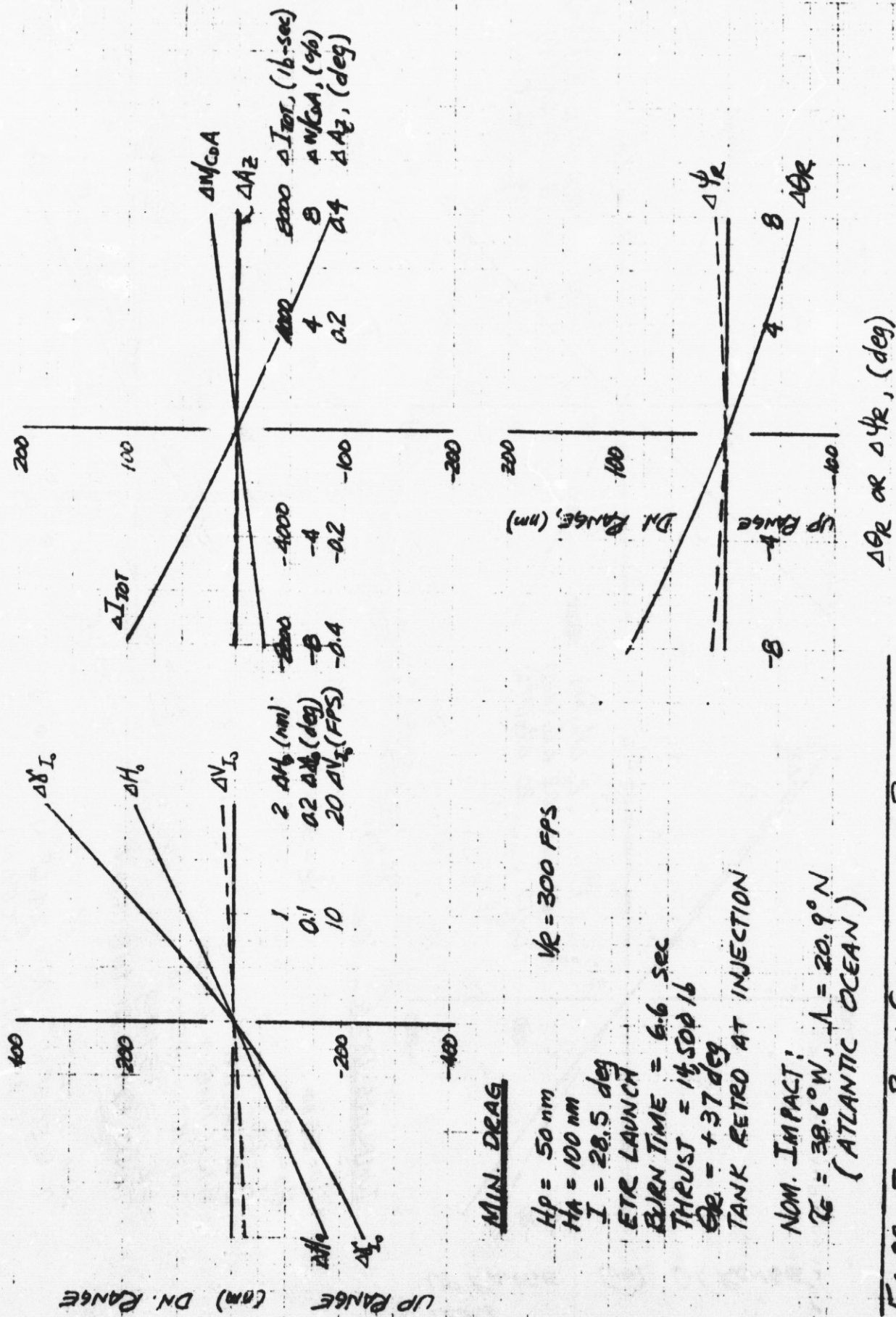


Figure 39

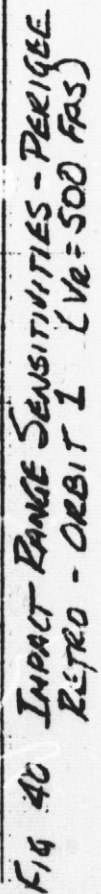
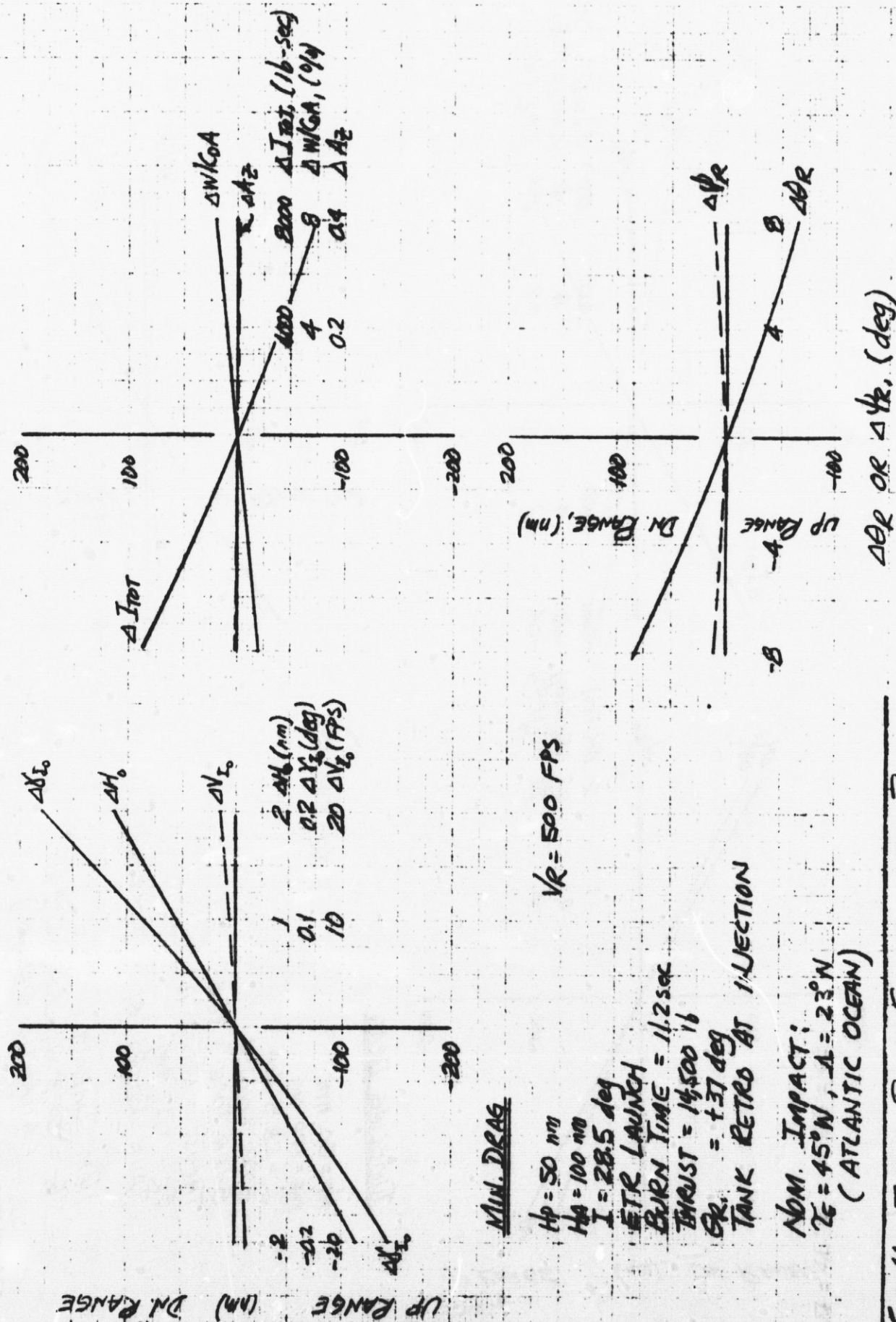


Figure 40



6D Separation and Entry Analysis

The likelihood of a droptank with center of gravity and configuration asymmetries trimming at a constant attitude from retro to impact (as assumed in the point mass simulations) is quite small. Under actual conditions, separation and/or retro induced angular rates, coupled with aerodynamic characteristics and mass property relationships, will most likely cause the tank to tumble or precess about the aerodynamic (relative) velocity vector, (\vec{V}_A) before assuming a final trim condition. Body motion histories, each peculiar to a given set of parametric conditions, may cause the tank to skip as it encounters the sensible atmosphere, or dive deeply into more dense regions. The corresponding aerodynamic and thermal environments will vary over a large range.

The LMSC Arbitrary Body 6D Program combines detailed aerodynamic, propulsion and mass property characteristics to define both translational and rotational body motion over an oblate rotating earth. In this study, the program was used to define both droptank separation histories and entry trajectory profiles.

A single retro condition is assumed for the 6D analysis, that of entry from orbit 1 to an Indian Ocean impact. Assumed time of retro is 21 minutes after perigee injection (see Table 1). Nominal retro rocket characteristics (Table 3) are used with the thrust vector aligned to the average center of gravity (c.g.) location during retro-burn, ($l_{cg_{ave}} = 38.3$ ft, $ycg = 0.9$ ft, $zcg = -0.37$ ft*). Pitch angle at separation is 37° (corresponding to θ_R in point mass simulations). Flight sequence is as described in previous discussion.

Separation Analysis. Analyses of droptank translational motion using a point mass comparison program and angular motion using the 6D program were performed to ascertain separation histories from the orbiter. Figure 42 shows nomenclature and conventions used in the study. Intrack, crosstrack and vertical distances - X_s , Y_s , Z_s , respectively - are all measured with respect to the orbit radius-velocity plane. Angular deviations in pitch ($\Delta\theta$) and yaw ($\Delta\psi$) are related to the initial droptank attitude. Geometry of separation velocity/orbital velocity relationships is in Fig. 43 where V_s is separation velocity and ϵ the separation angle from the tank vertical reference axis, Z_p . ($\epsilon = 29.5$ degrees for all cases.)

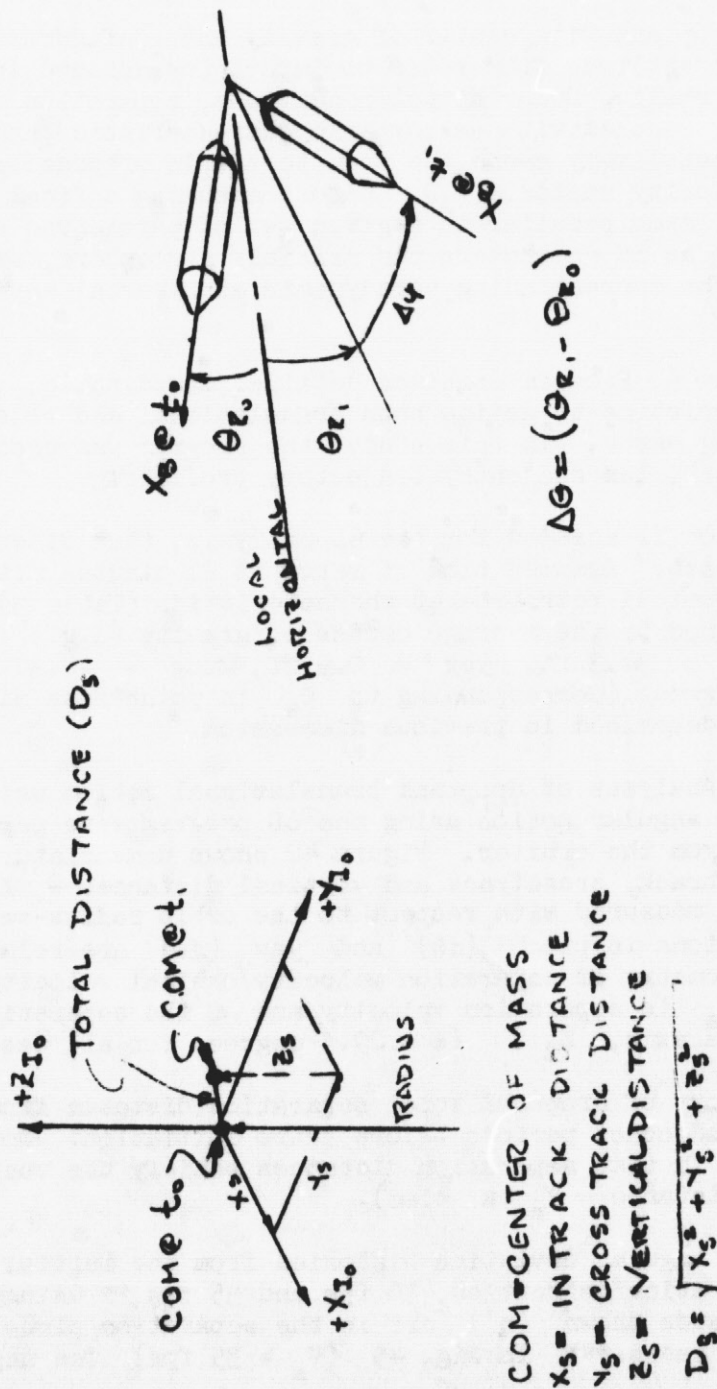
Figure 44 shows a history of droptank total separation distance from the orbiter. The data are for assumed coast periods before retro initiation. Note the insensitivity to drag effects in that separation distances satisfy the vacuum (ideal) distance equation, (distance = $V_s \times$ time).

Figures 45 and 46 show angular deviation histories from the initial droptank attitude generated for two separation velocities, 10 fps and 35 fps,** using the 6D arbitrary body program. Pitch rates shown (q') are in the separation plane. Roll rate (p) is assumed zero in all cases.*** In Fig. 45 ($V_s = 35$ fps) the angular $\Delta\psi/\Delta\theta$

*See Appendix A for definitions and sign conventions.

**Coast period before retro with $V_s = 10$ fps is 10 sec; with $V_s = 35$ fps there is a 2 sec coast.

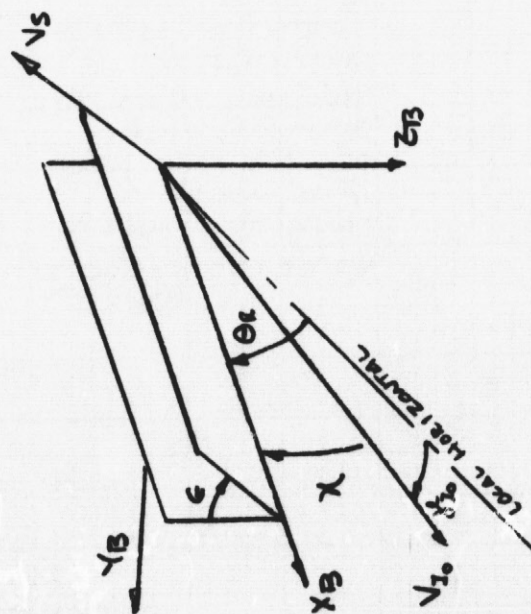
***Separation device angular misalignments will produce roll rates of about 0.05 deg/sec (Ref. 11).



NOMENCLATURE FOR SEPARATION ANALYSIS
FIG 42

Figure 42

$$\begin{aligned}
 V_Y &= -V_S \sin \epsilon \\
 V_Z &= V_S \cos \epsilon \\
 V_{I_0}^2 &= \left\{ (V_{I_0} \cos \chi)^2 + (V_{I_0} \sin \chi + V_Z)^2 \right\}^{1/2} \\
 V_{I_1} &= \left\{ V_{I_0}^2 + V_Y^2 \right\}^{1/2} \\
 \Delta \delta_{I_1}^2 &= \tan^{-1} \left\{ \frac{V_{I_0} \sin \chi + V_Z}{V_{I_0} \cos \chi} \right\} - \chi \\
 \Delta A_2 &= \tan^{-1} \left\{ \frac{V_Y}{V_{I_0}} \right\}
 \end{aligned}$$



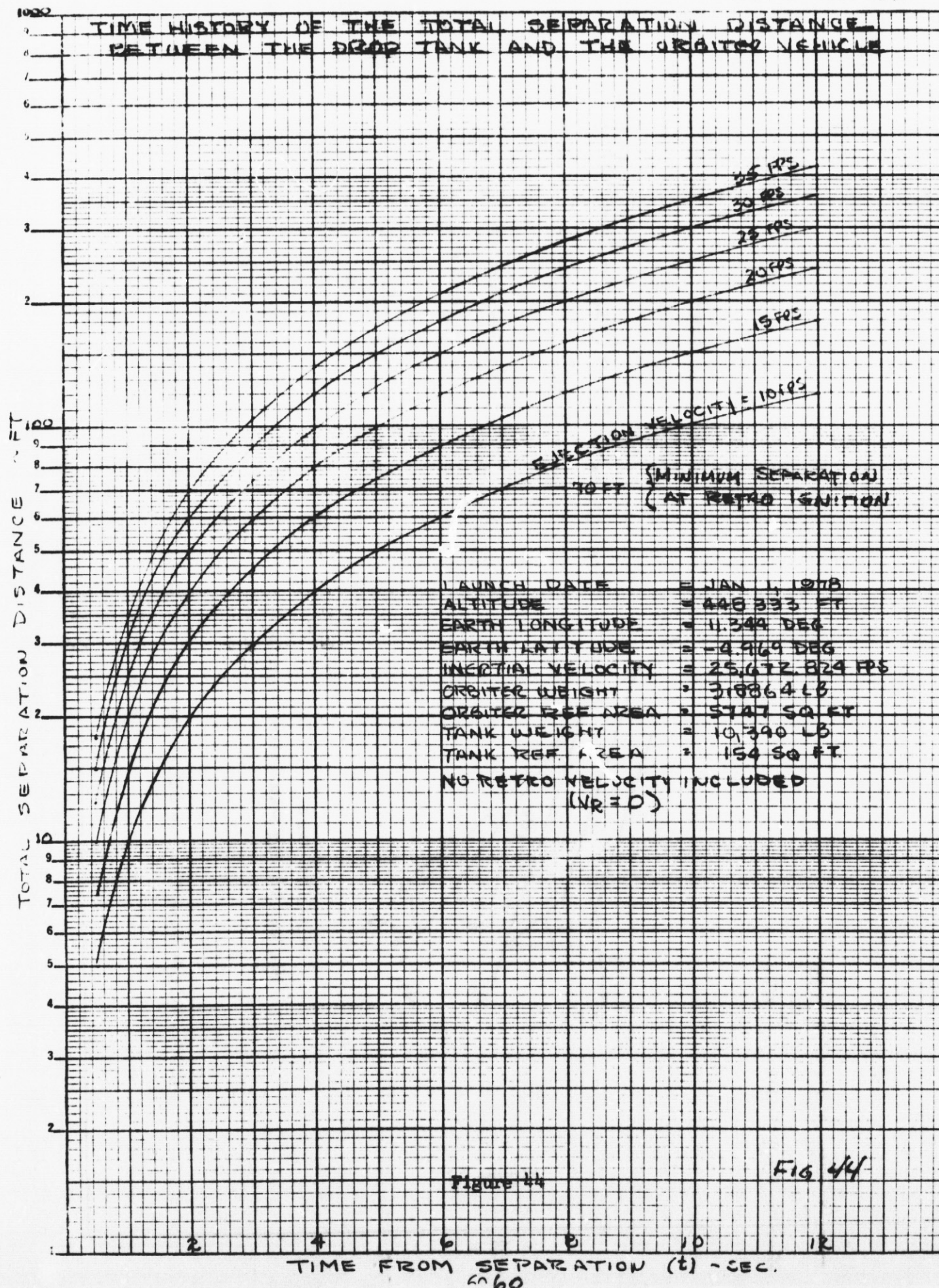
$\epsilon = 29.5 \text{ DEG}$
 χ IS SEPARATION PLANE

NOMENCLATURE FOR DETERMINING ORBIT VELOCITY FOR TANK

FIG. 43

Figure 43

DATE: 18 June 1971



PREPARED BY _____
DATE 18 June 1971
CHECKED BY _____

LOCKHEED MISSILES & SPACE COMPANY
A GROUP DIVISION OF LOCKHEED AIRCRAFT CORPORATION

PAGE _____
MODEL _____
REPORT NO. EM 12-12-05-
M1-8

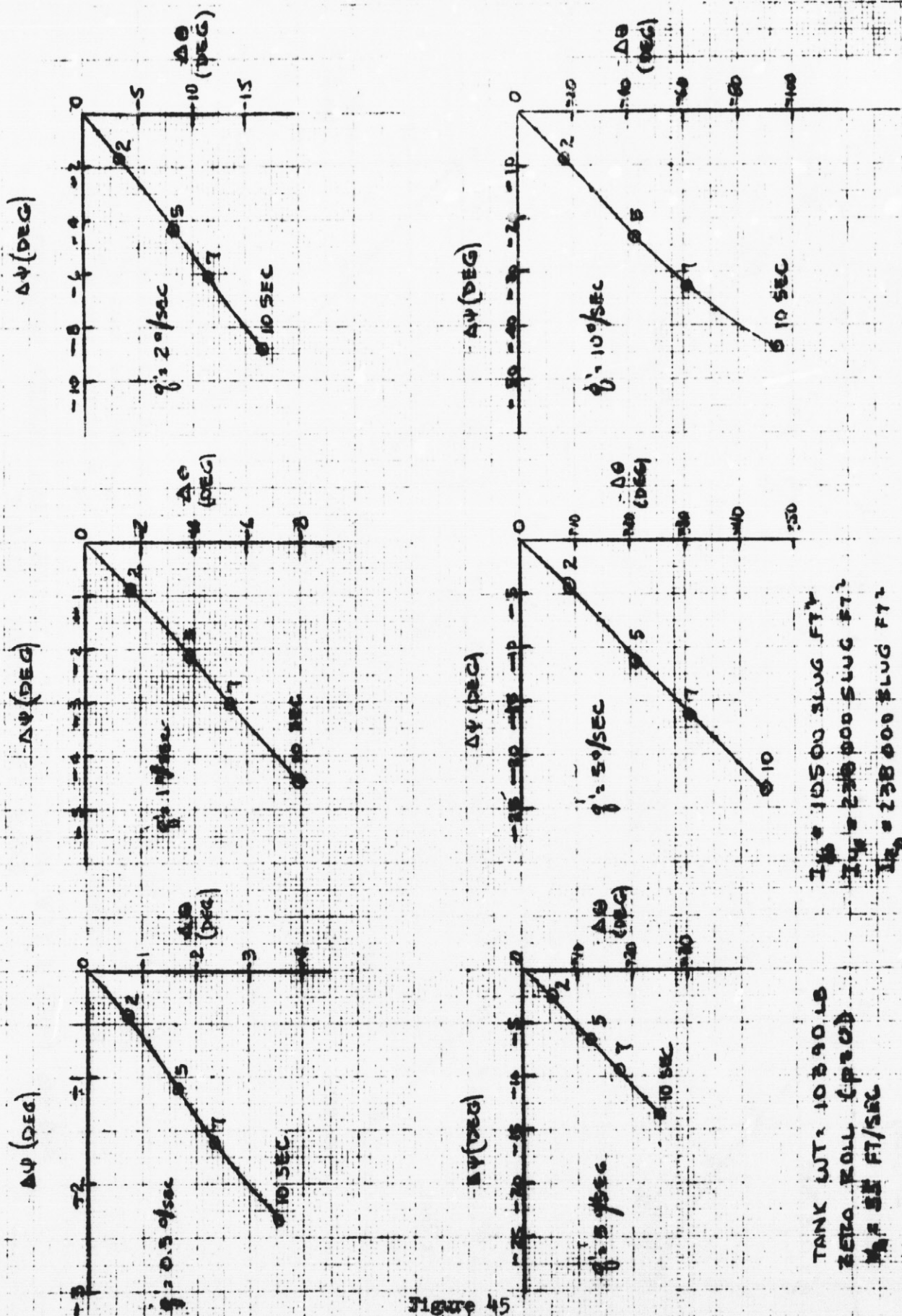
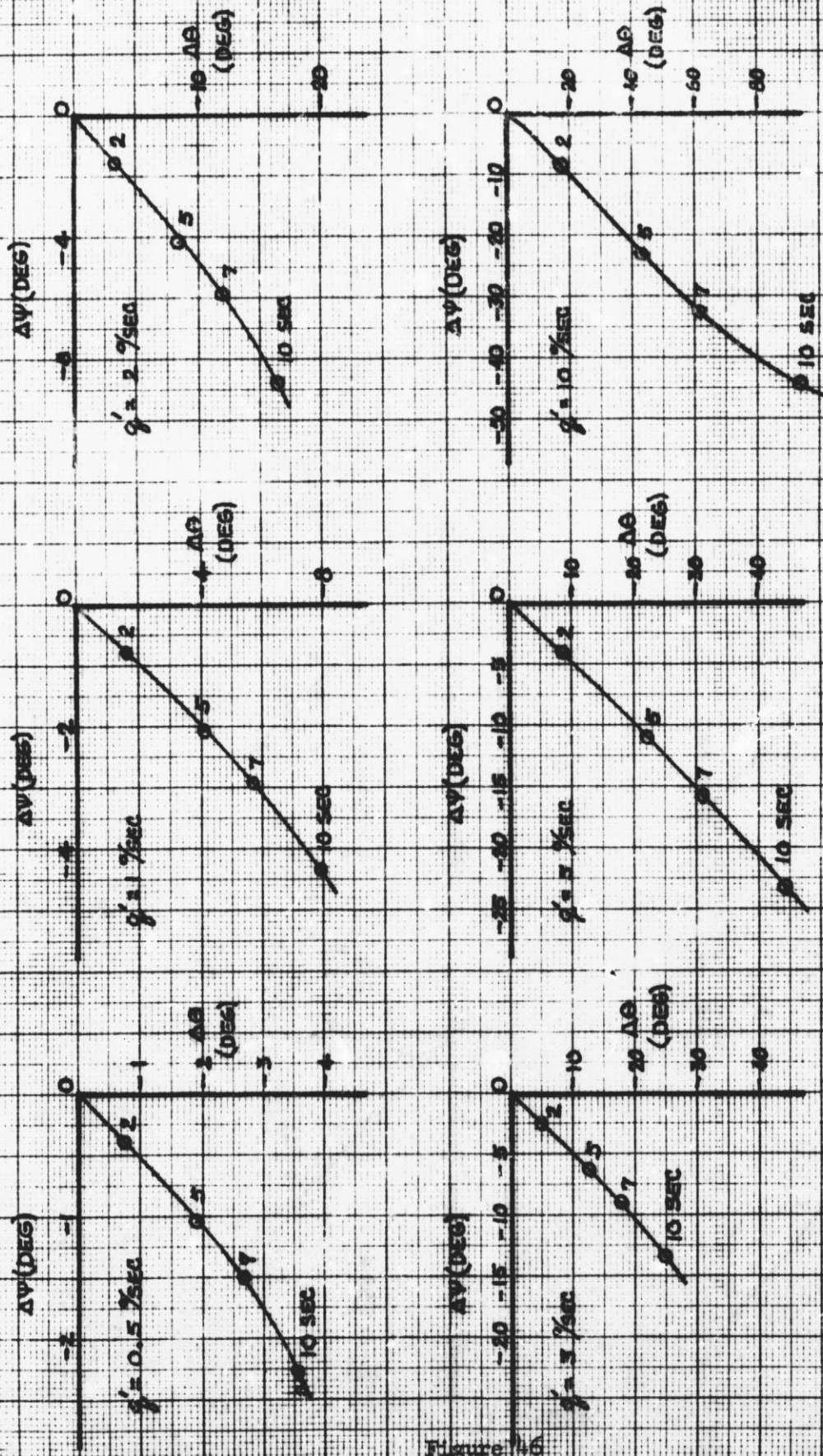


Figure 45

FIG. 45 PITCH & YAW ANGLE FOR THE ORBITER TANK DURING SEPARATION FROM ORBITER VEHICLE

6/17/71



TANK MT = 10,500 SLUG FT²
ZERO ROLL ($\dot{\phi}=0$)
 $V_z = 10$ FT/SEC

FIG 46 PITCH & YAW ANGLE FOR THE ORBITER TANK DURING SEPARATION FROM THE ORBITER VEHICLE

histories are essentially linear through coast (2 sec), retro fire, (2 sec to 7 sec), and post-retro coast for all cases. Only when $q' = 10$ deg/sec does the relationship $\Delta\psi/\Delta\theta$ become nonlinear. With $q' = 0.5$ deg/sec, the effects of varying thrust moments due to the longitudinal c.g. motion during retro are illustrated by the S-shaped curve. As pitch rate increases, the effects of c.g. travel are overshadowed by the effects of q' .

Lowering separation velocity to 10 fps has little effect on angular deviations for the assumed pitch rates (Fig. 46). These results again indicate insensitivity to drag as well as coupled angular rate/velocity effects.

Selection of a realistic pitch rate depends on the alignment and performance uncertainties of the separation devices. Reference 11 indicates that performance of a gas generator-piston separation device is subject to fairly large uncertainties from small deviations in propellant temperatures. A reasonable estimate of minimum uncertainties shows that pitch rates of 5 deg/sec to 10 deg/sec may be produced. Consequently, an optimistic assumption of nominal $q' = 5$ deg/sec is used in subsequent simulations.

A composite plot of intrack, crosstrack, radial and angular separation histories of the droptank relative to its initial position on the orbiter is shown in Fig. 47 for $V_s = 35$ fps, $q' = 5$ deg/sec. The left hand plot, is a view looking aft along the orbiter X_B axis showing the radial (vertical)/crosstrack separation distance relationship. The center plot is looking down (relative to local horizontal) to view both intrack/crosstrack relationships and $\Delta\psi$ history as indicated by the attitude of the tank X_B axis. At retro initiation, the tank is 70 feet from the orbiter and rotated by $\Delta\psi = -4$ degree. At retro termination, $\Delta\psi = -15$ degrees at distance of 245 feet $\left(\text{total distance} = \left[(R_s)^2 + (CT)^2 + (IT)^2 \right]^{1/2} \right)$.

The pitch attitude history is shown together with the vertical/intrack relationship (right hand plot). The tank begins deboost at $\Delta\theta = -9$ degrees rotating to $\Delta\theta = -31$ degrees at burnout. Average pitch deviation for the retro period is -20 or a $(\theta_R)_{ave} = (37-20) = 17$ degrees. Referring to curves of impact deviations due to $\Delta\theta_R$ (Fig. 18), the corresponding range error is about ± 160 nm.

The separation composite for $V_s = 10$ fps is shown in Fig. 48. Of particular interest is the pitch and yaw deviation with respect to retro initiation. Since coast time must be extended to 10 seconds to accommodate the minimum separation distance requirement (~ 70 feet), $\Delta\theta$ at retro initiation (10 sec) will be -44 degrees. The corresponding θ_R at ignition is $(37-44) = -7$ degrees. Assuming a similar $\Delta\theta$ growth rate (as in Fig. 47), $(\theta_R)_{ave} = -27$. At this attitude, the retro velocity vector is directed up and aft (relative to the local horizontal and orbital direction respectively, with the result of increased time and range to impact. (The effect is further amplified by the added deviation in yaw). Further analysis is required to define these effects in detail, but it suffices to say at this time, increased ranges decrease the accuracy of impact predictions and dispersions, and

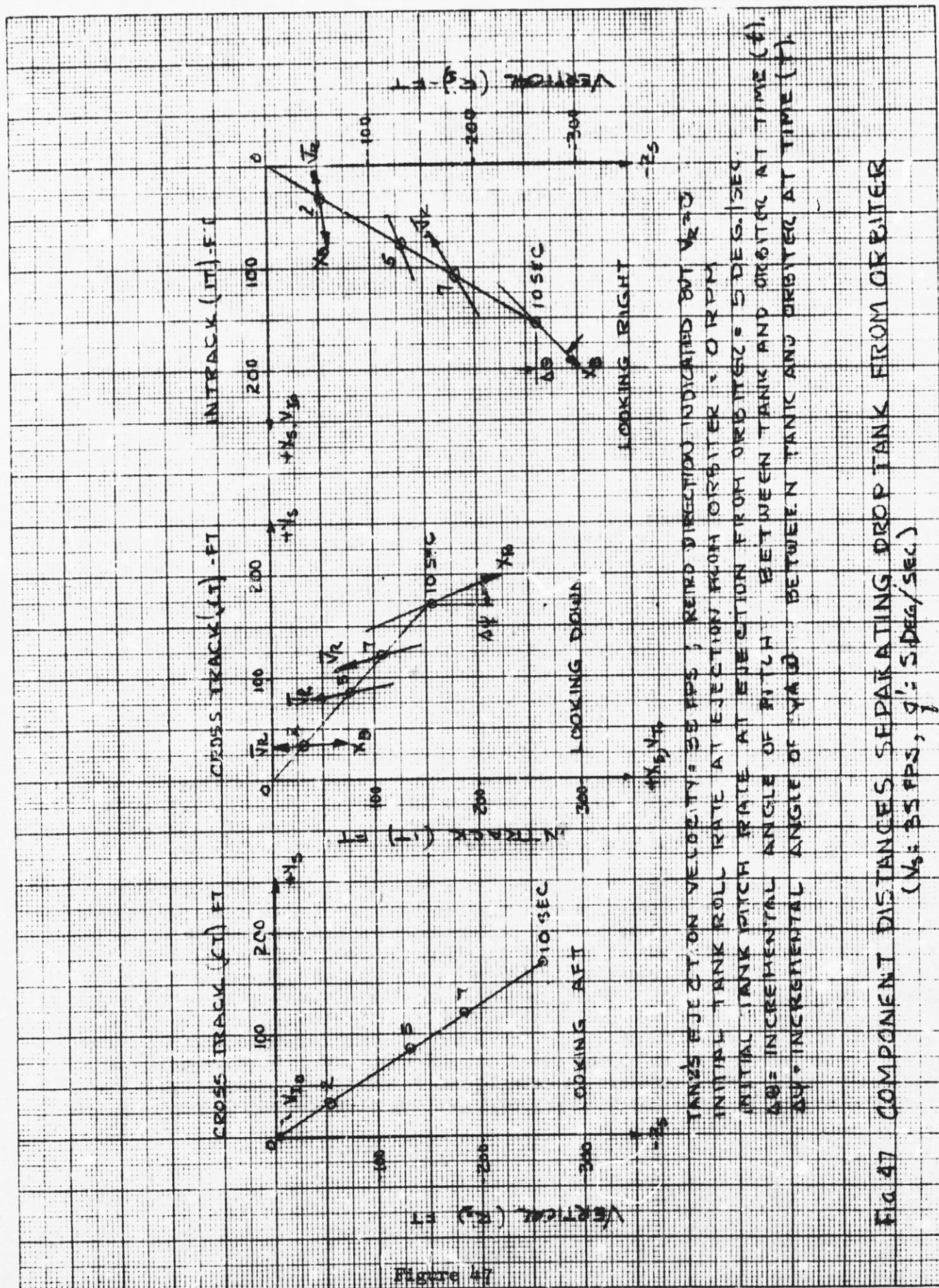




FIG 4B COMPONENT DISTANCES SEPARATING DROP TANK FROM ORBITER
($V_s = 10 \text{ FPS}$, $\theta' = 5 \text{ DEG/SEC}$)

are therefore undesirable. Consequently, it appears that higher separation velocities are required to offset large pitch rates. For the remainder of this study $V_s = 35$ fps shall be assumed.

6D Entry Simulations. The 6D portion of the separation analysis was extended to define the total droptank entry profile from separation to impact (at 50,000 ft). Body motion changes, center of gravity deviations, and thrust misalignments were investigated parametrically to determine their individual and generalized collective effect on entry characteristics. Nominal initial conditions are the same as those assumed or specified earlier in the report. They are repeated below for convenience.

- Orbit 1 $I = 28.5^\circ$ (ETR)
 - Indian Ocean Impact
 - Separation Time, 21.0 min
 - Separation Velocity, 35 fps
 - Separation Pitch Rate, 5 deg/sec
 - Retro velocity, 227 fps
 - Retro pitch angle, 37 deg
 - Separation/retro Sequence
- } See Table 5

Time = 0 to 2 sec, coast
 = 2 to 7 sec, retro-fire
 = 7 to 8 sec, coast
 = 8 sec, jettison retrorocket and hardware

Table 9 lists the various configurations evaluated in the analysis. Case 1 is the nominal trajectory using tank mass properties in Table 2, aerodynamic characteristics in Appendix B, and nominal conditions given above. Cases 2 and 3 assume tumble rates induced at 10 seconds with a thrust moment applied for 0.5 sec about the Y_B axis.* Center of gravity shifts (Cases 4 and 5) represent 3σ deviation in estimates of longitudinal c.g. location. Shifted locations are tabulated in Table 10.

Thrust misalignments are directional deviations in the applied retro velocity. Angular errors are $\Delta\theta_T = +0.12$ deg (in pitch plane) and $\Delta\psi_T = +0.12$ deg (in yaw plane). These are Cases 6 through 9.

Figure 49 presents trajectory parameter histories for the nominal case (1) entry. The droptank follows an essentially ballistic path to about 230000 ft ($t = 1050$ sec) where it executes a pullup as indicated by the reversal in flight path angle γ . Following a slight altitude skip, the tank dives more steeply into the atmosphere. Peak dynamic pressure ($(\bar{q})_{\max} = 750$ psf) occurs during the final dive at $t = 1170$ sec. Peak heating rate is about $78 \text{ BTU/ft}^{3/2}$ -seconds at 1150 sec.

* $M_{TYB} = 145,037 \text{ ft-lb}$ for 5 RPM tumble, $M_{TYB} = 290,074 \text{ ft-lb}$ for 10 RPM tumble.

Table 9

LIST OF INITIAL BODY CONDITION VARIATIONS FOR
PARAMETRIC SIX-DEGREE-OF-FREEDOM TRAJECTORIES

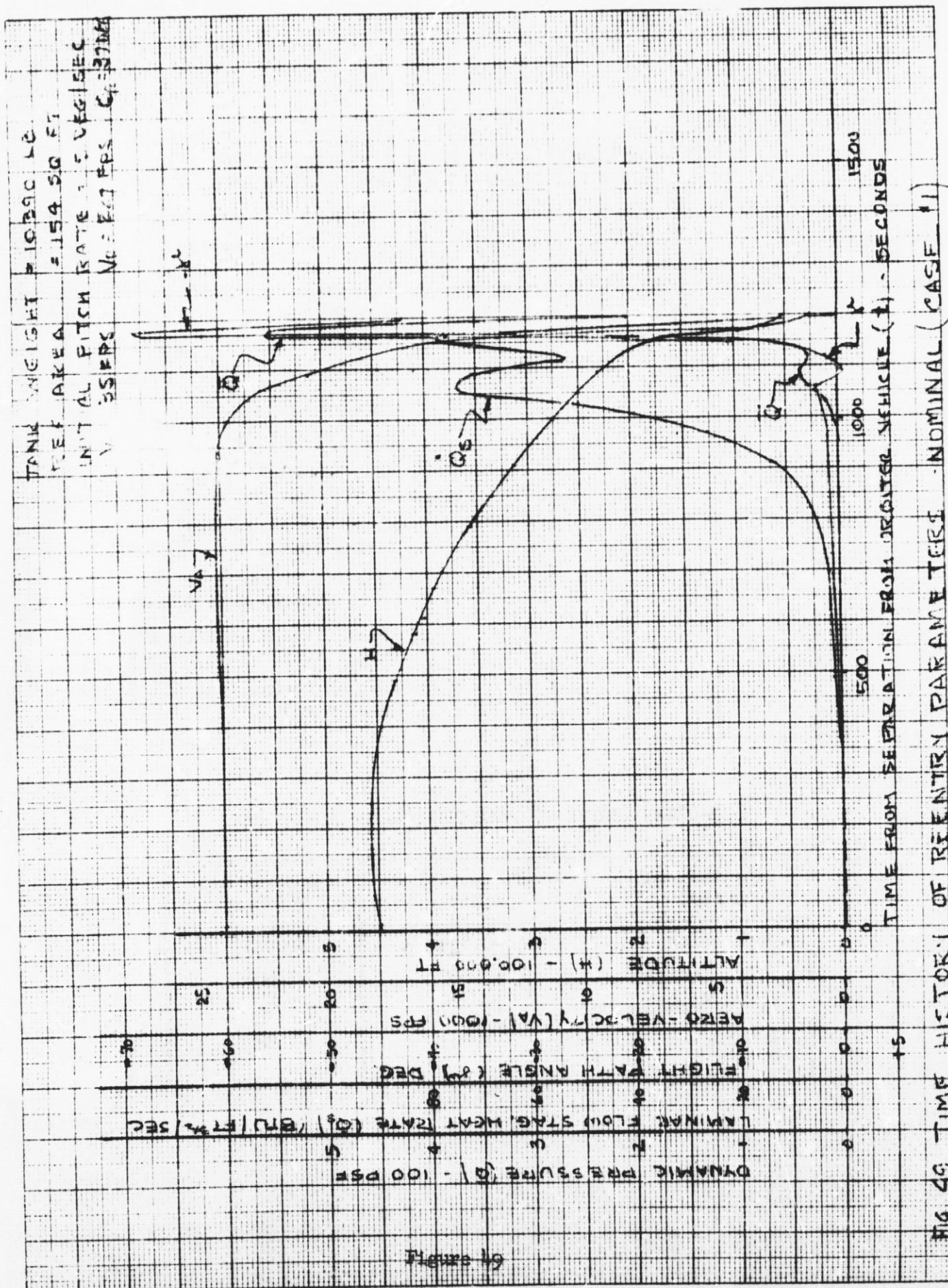
Case No.	θ_R (deg)	η_o (deg)	p_o	q' (deg/sec)	Remarks
1	37	36.7	0	5	Nominal case
2	"	"	"	"	Induced Tumble - 5 RPM @ 10 sec
3	"	"	"	"	Induced Tumble - 10 RPM @ 10 sec
4	"	"	"	"	Forward C.G. Shift
5	"	"	"	"	Aft C.G. Shift
6	"	"	"	"	Plus Yaw Misalignment of Thrust Vector (+0.12 deg)
7	"	"	"	"	Minus Yaw Misalignment of Thrust Vector (-0.12 deg)
8	"	"	"	"	Plus Pitch Misalignment of Thrust Vector (+0.12 deg)
9	"	"	"	"	Minus Pitch Misalignment of Thrust Vector (-0.12 deg)
10	"	"	"	0	Same as nominal but all angular rates zero.

Table 10

3-SIGMA CENTER OF GRAVITY LOCATION DEVIATIONS

Longitudinal (Δl_{cg})	Aft Deviation (ft)	Fwd Deviation (ft)
Separation	+0.833	-0.917
Retro Ignition	+1.667	-1.666
Retro Termination	+1.667	-1.666
Entry	-1.667	-1.583

DATE: 18 June 1971



Total angle of attack history for Case 1 is shown in Fig. 50, as a function of altitude together with V_A -H and \bar{Q} -H profiles. The η -band from 0 to 180 deg denotes the tank is tumbling. This is not surprising considering the initial separation pitch rate and the small atmospheric effects indicated in the previous section. As atmospheric density increases, the η -band begins converging, changing the tumbling motion to a wide pendulum-swing motion. Increasing atmospheric effects eventually cause convergence to an aerodynamic trim angle of about 40 degrees and then, as Mach number decreases to about $\eta = 0$.*

The altitude skip is obvious in V_A -H profile data of Fig. 50.

Figures 51 and 52 were prepared to better define motion of the droptank in the region of η -convergence. The figures show the trace of the X_B reference axis as it moves about the aerodynamic velocity vector and as viewed when looking into \bar{V}_A . Conventions for defining η and the displacement (bank) angle, X , are defined in Appendix A, Fig. A-2. Solid lines in Fig. 51 and 52 denote angular motion for $-90 \text{ deg} \leq \eta \leq +90 \text{ deg}$ (front spatial hemisphere) whereas dashed lines indicate $+90 \text{ deg} < \eta < 270 \text{ deg}$ (rear spatial hemisphere).

Figure 51 shows the η - X motion starting after atmospheric effects have begun forcing η -convergence ($t = 837 \text{ sec}$). The tank X_B axis swings through $\eta = 90 \text{ deg}$ during the first indicated oscillation to a maximum of 96 degrees. With each succeeding swing, η decreases and the tank enters a slow precessional motion about \bar{V}_A . As the body approaches the final time point on the plot, precession rate, \dot{X} , is slightly less than 3 deg/sec.

Figure 52 begins with the final time-point shown in Fig. 51. As the body motion continues, the tank converges more rapidly to a trim η of about 40 degrees. By $t = 1150 \text{ seconds}$, only small perturbations in η ($\pm 4 \text{ deg}$) are discernible. The tank, however, is trimmed in an attitude resulting in a downward net down force relative to the local horizontal. This trim attitude at first appears inconsistent with aerodynamic data which show trim at positive angles of attack (α) with positive net lift forces. The solution to the inconsistency lies in the relationship of \dot{X} and p . Precession rate between $t = 1124 \text{ seconds}$ and 1150 seconds is about 1 deg/sec. Roll rate is near zero** throughout the trajectory which means the droptank assumes the inverted position established for retro fire. Therefore, even though the body trims to a positive α , producing a positive lift force relative to the droptank, the net lift force is oriented downward for an effective negative lift-to-drag ratio, $(-L/D)$. In this time period (from 1100 seconds to 1150 seconds) the droptank is forced into a steep dive (by the $-L/D$) as indicated by the altitude history plot in Fig. 49 and the V_A -H plot in Fig. 50. The magnitude of lift-to-drag ratio produced by this trim condition (i.e. $\eta = 40 \text{ deg}$, $X = 180 \text{ deg}$) is $L/D = -0.9$.

Since total angles of attack only measure angular displacement of the body axis from the velocity vector, the trim attitude producing a net downforce does not show up in the η -H plot in Fig. 50.

*Note, tank trim angle characteristics are shown by the aero-moment data of Appendix B.

**Roll rate is available in 6D simulation computer output but is not plotted for presentation herein.

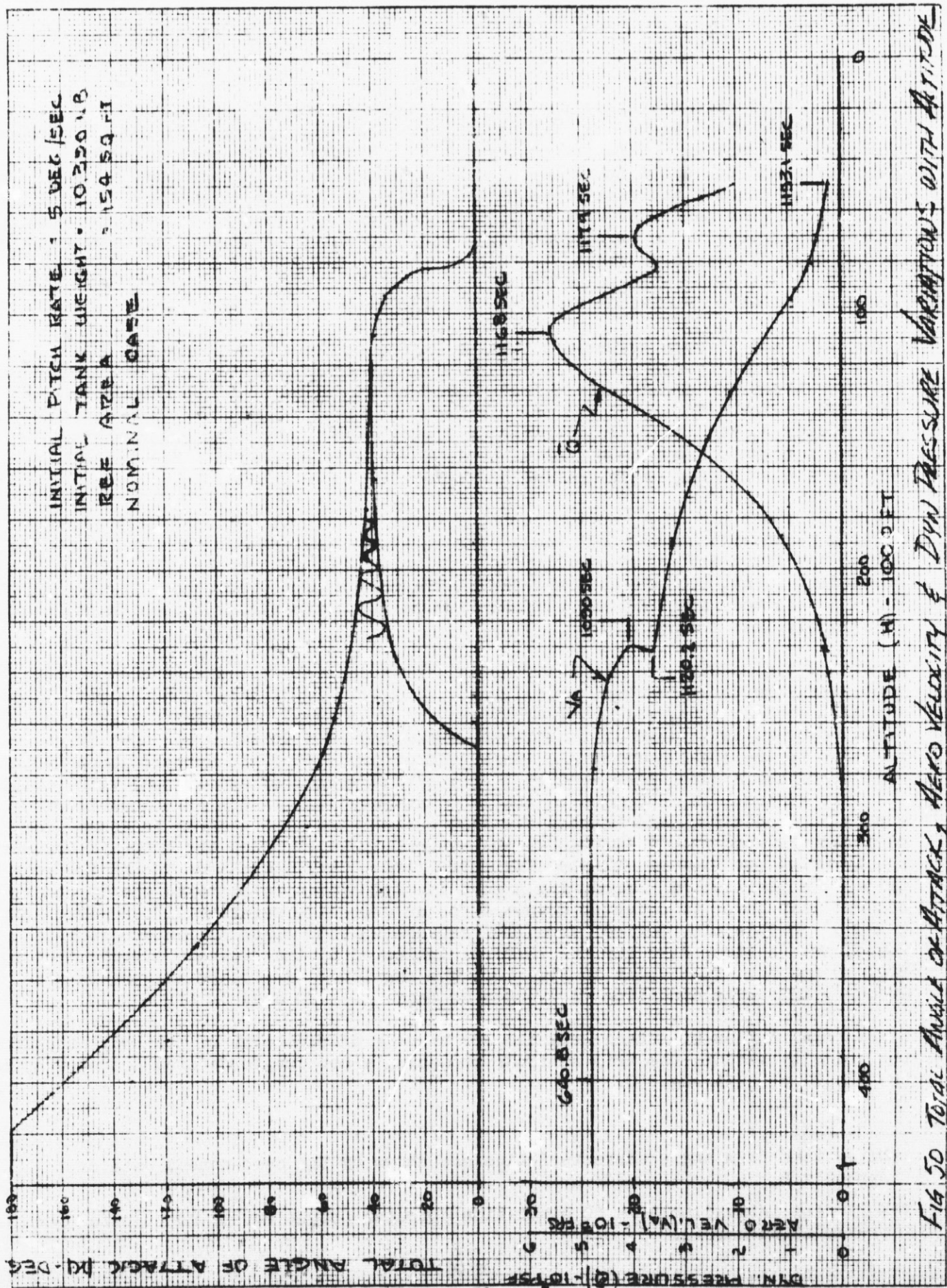
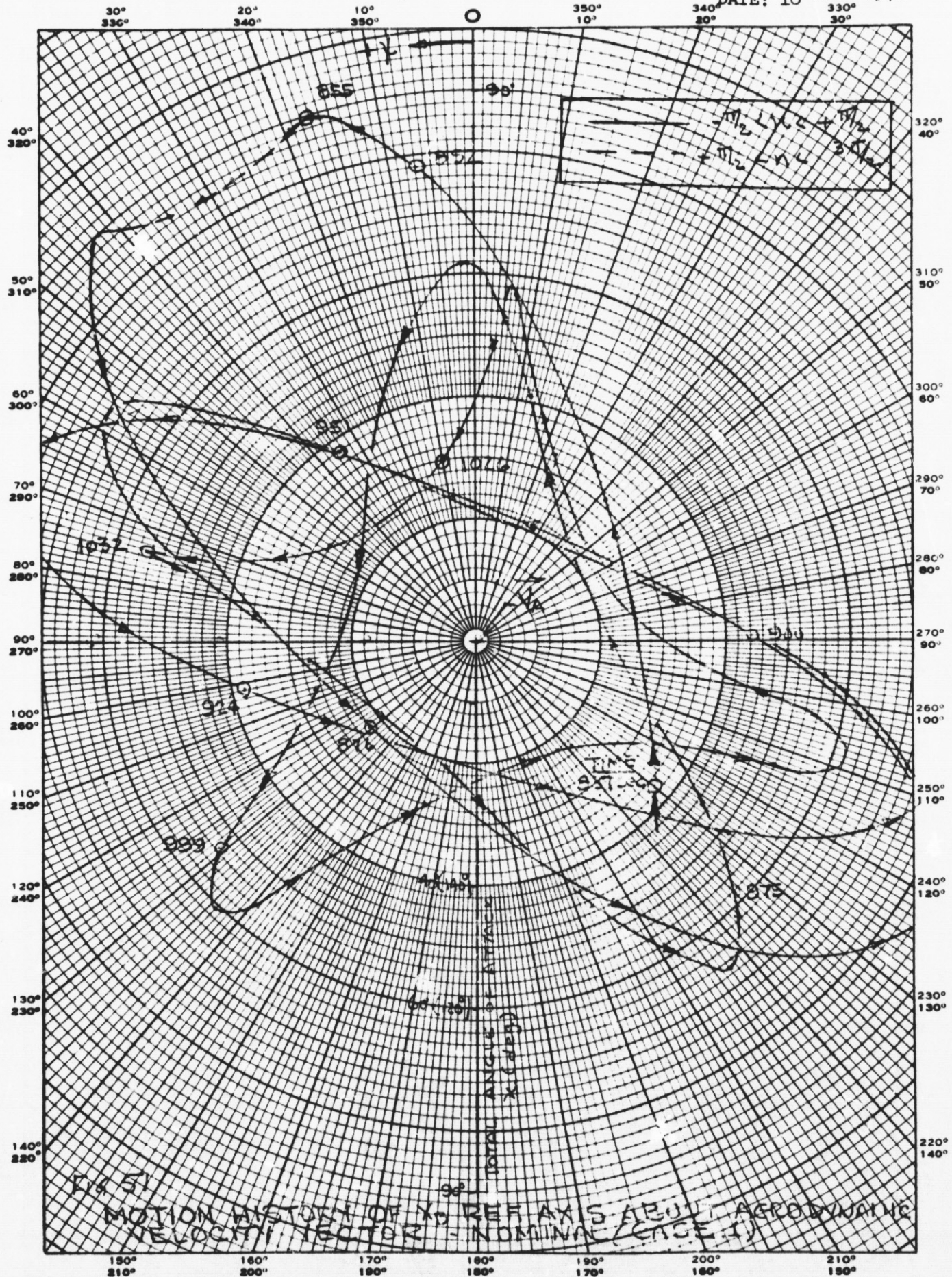


Figure 50
- 70 -

EM NO: L2-12-05-M1-8
DATE: 18 June 1971



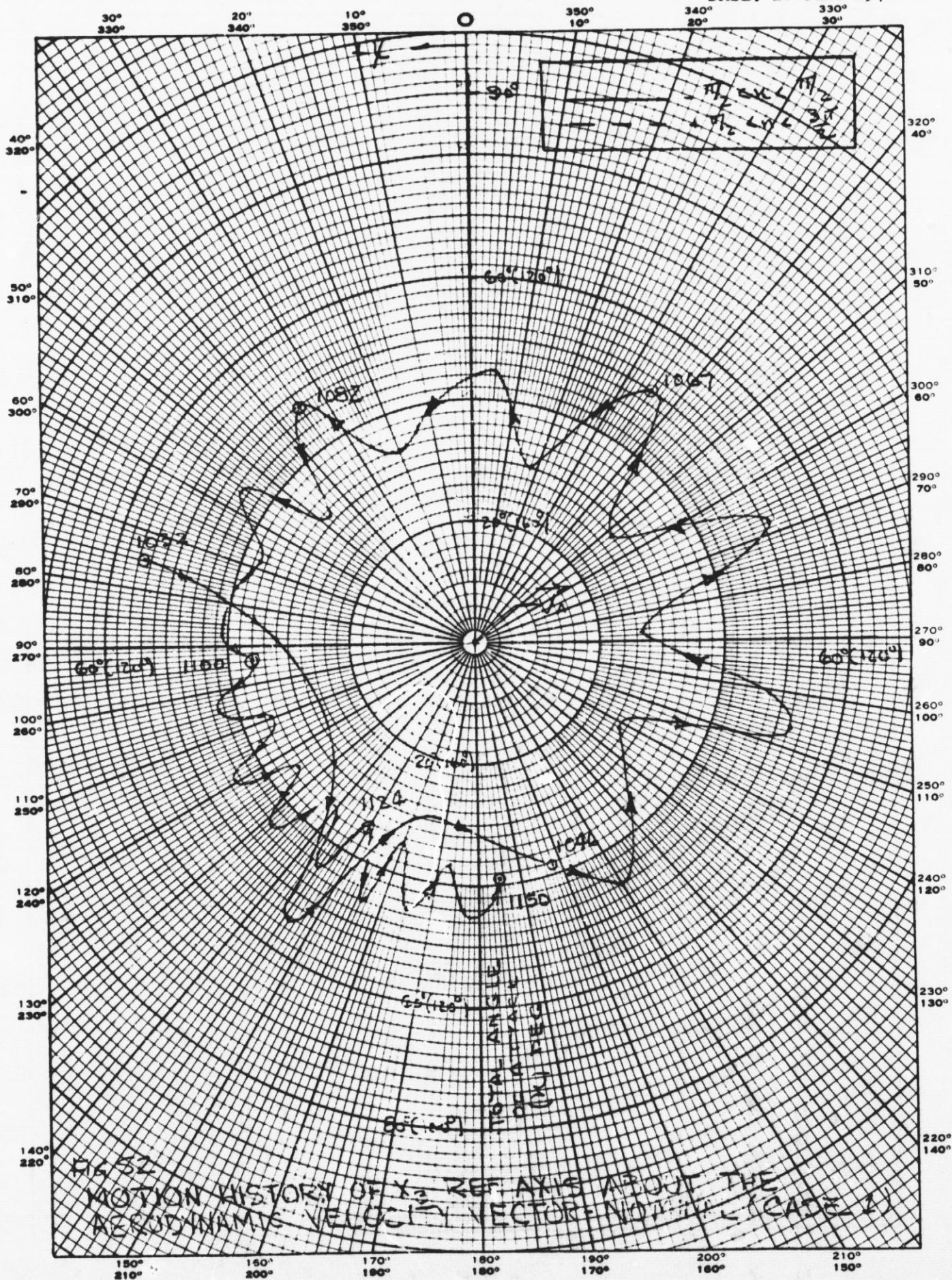
EUGENE DIETZEN CO.
MADE IN U. S. A.

NO. 340R-P DIETZEN GRAPH PAPER
POLAR CO-ORDINATE

EM NO: L2-12-05-M1-8
DATE: 18 June 1971

EUSENE DIETZEN CO.
MADE IN U. S. A.

NO. 3408-R DIETZEN GRAPH PAPER
POLAR CO-ORDINATE



From a dispersions point of view, entering the droptank at a trimmed angle of attack which results in an L/D greater than 1, is not desirable. Ideally, entry should occur either at maximum drag conditions, $\eta \sim 90$ deg, or tumbling. In an effort to accomplish the latter, a 5 RPM tumble rate was imposed on the droptank 10 seconds after separation by assuming a large pitching moment provided by a tumble-rocket. The resulting entry trajectory history is in Fig. 53. The tank again, enters ballistically, and apparently achieves its trim attitude at low enough velocity to prevent a significant pullup. The V_A -H plot in Fig. 54 verifies the elimination of a skip maneuver whereas the η -H history indicates convergence to a trim- η occurs at lower altitudes. Figure 53 also shows a dive after 1200 seconds, but when referring again to Fig. 54, the data show the tank has slowed to supersonic velocities by about $t = 1160$ seconds and vehicle trim η reduces to zero. Since $\eta = 0$ is a minimum drag condition, the droptank will dive.

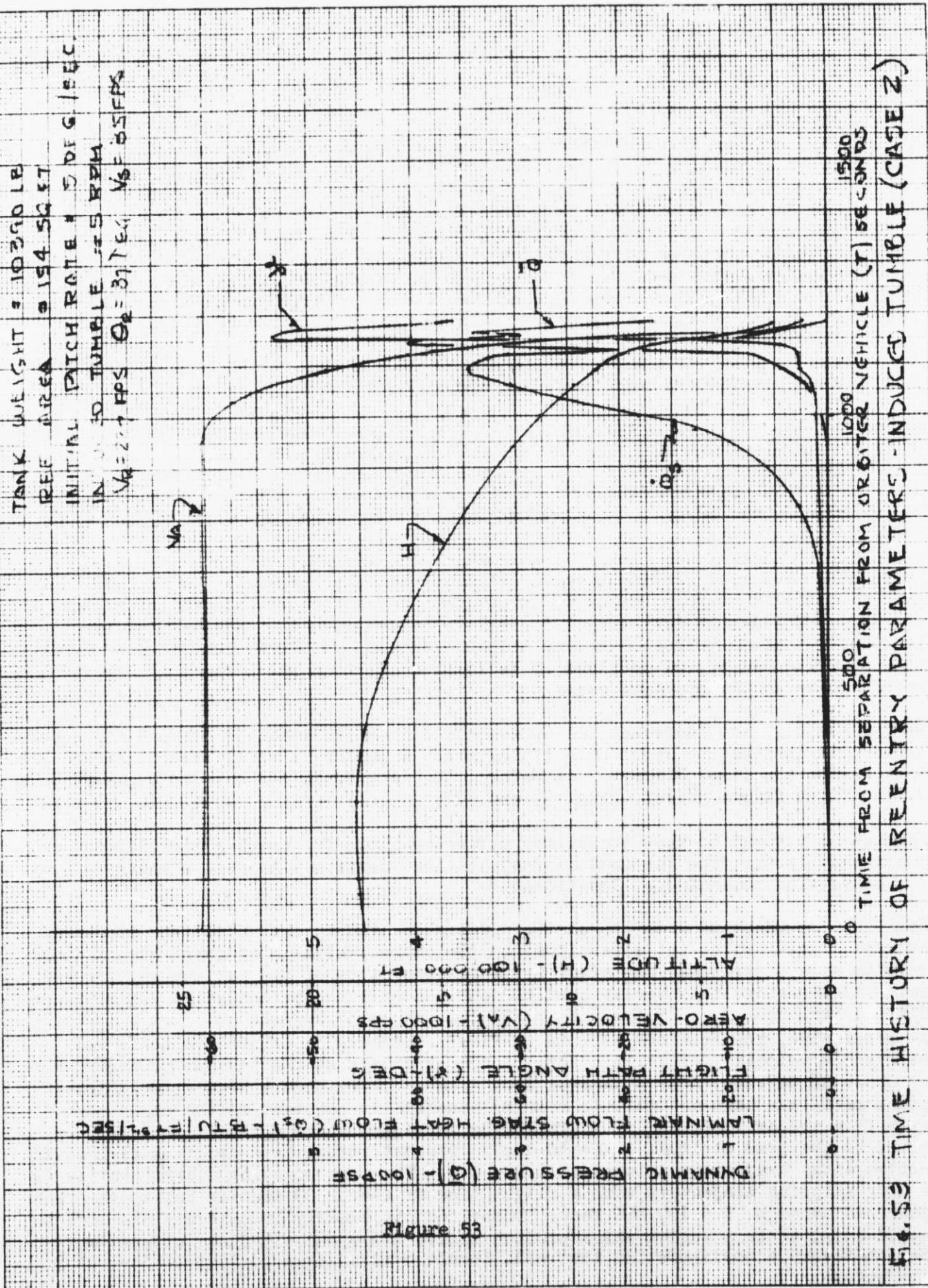
Increasing the induced tumble rate to 10 RPM produces an unexpected flight profile if one were to extrapolate from Cases 1 and 2 (Figs. 55 and 56). The tank continues tumble through an altitude of 280,000 feet (about 990 seconds) followed by a rapid trim to $\eta = 40$ degrees. The tank executes a skip at 193,000 feet before continuing its descent. Deceleration to supersonic conditions occurs by about 1300 seconds and trim $\eta \sim 0$.

Moving the center of gravity forward (Figs. 57 and 58) increases the droptank aerodynamic stability margin resulting in earlier convergence to trim η (at higher H and V_A). The result is a long skipping trajectory with the tank gaining about 160,000 feet after pullout. A long trimmed descent profile follows with an apparently $-L/D$ as evidenced by the continually increasing \bar{Q} history. Trim angle eventually goes zero as in the previous cases.

Moving the c.g. aft increases the hypersonic trim- η to about 52 degrees and supersonic trim attitude to about $\eta = 37$ degrees. A pullup is still evident before the tank begins its final descent. As before, the data again indicate an apparent $-L/D$ during final flight phases, (Fig. 59 and 60).

Figures 61 through 68 show trajectory parameter plots for angular misalignment of the thrust vector from the nominal installation position. All are similar to previous cases with nominal c.g. locations.

Case 10 (for which no data are plotted) was generated to determine the effects of initial angular rates (at separation) on the entry profile. At first glance, the results were surprising, but after brief consideration of the various angular and rate relationships they became credible and valuable to the analysis. Initial conditions included $V_g = 35$ fps, $V_R = 227$ fps, $\theta_R = 37$ degrees and $p = q = 0$. At separation, the combined effects of flight path angle, orbital velocity and separation velocity result in a total angle of attack at the instant of separation of about 36 degrees, only 4 degrees from trim- η . Without a separation induced pitch rate, the angular attitude remains essentially constant as the tanks move away from the orbiter, and then, following retro and as aero-forces build up, η moves to the trim attitude ($\eta = 40$ deg). The net result is a droptank flying its entire entry trajectory trimmed at $L/D = 0.9$. The corresponding flight profile is a long skipping trajectory with a flight time of over 2300 seconds before the tank descends through $H = 100,000$ feet. These results clearly demonstrate the need to avoid entry at trim angles which produce finite L/D 's and, in fact, direct tank design toward a configuration that will tumble over a large portion of its entry trajectory.



K&E 10 X 10 TO THE CENTIMETER 46 1513
KEUFFEL & ESSER CO

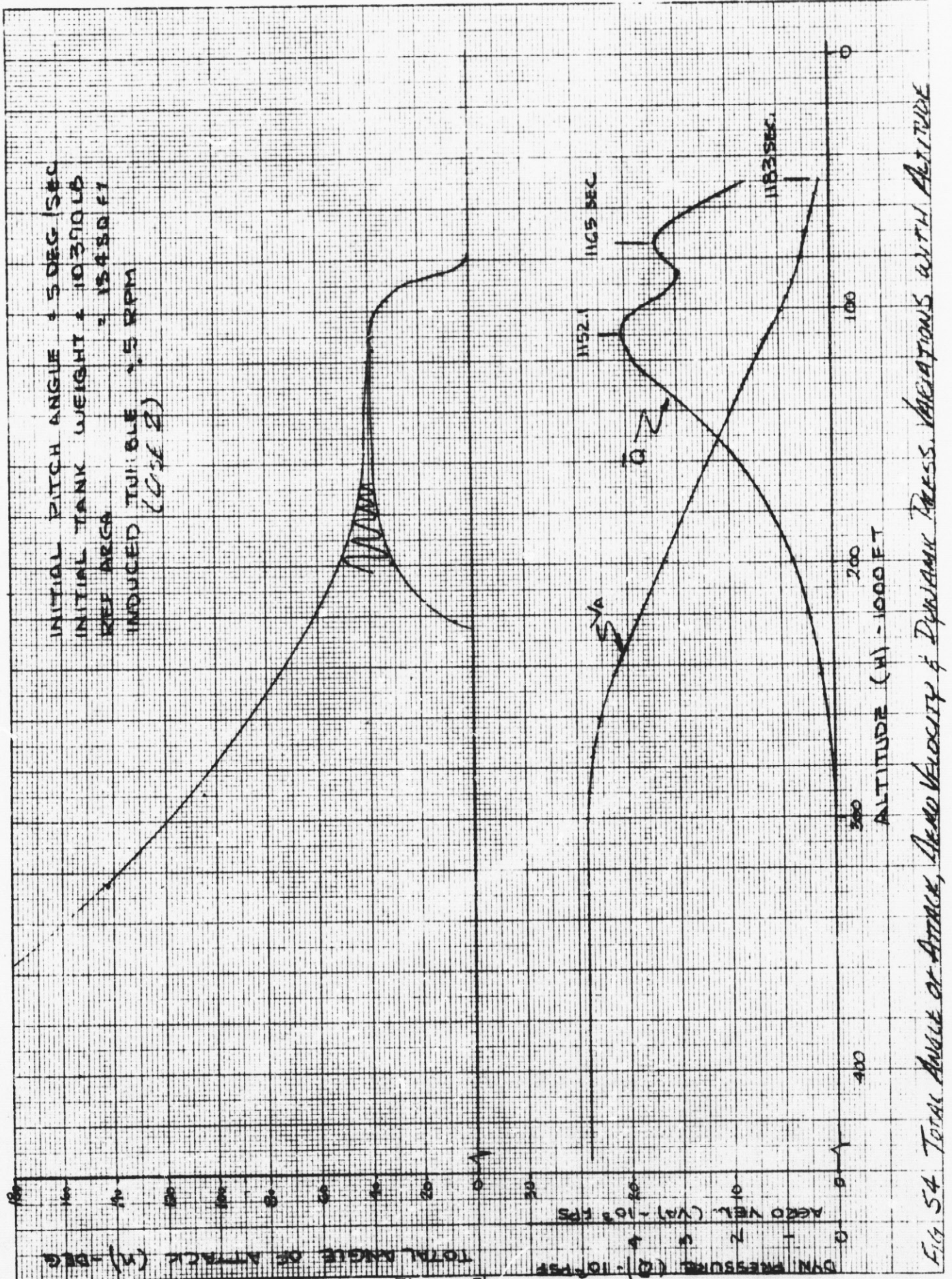


Figure 54
- 75 -

Fig. 54 Total Angle of Attack, Aero Velocity & Dynamic Pressure Variations with Altitude

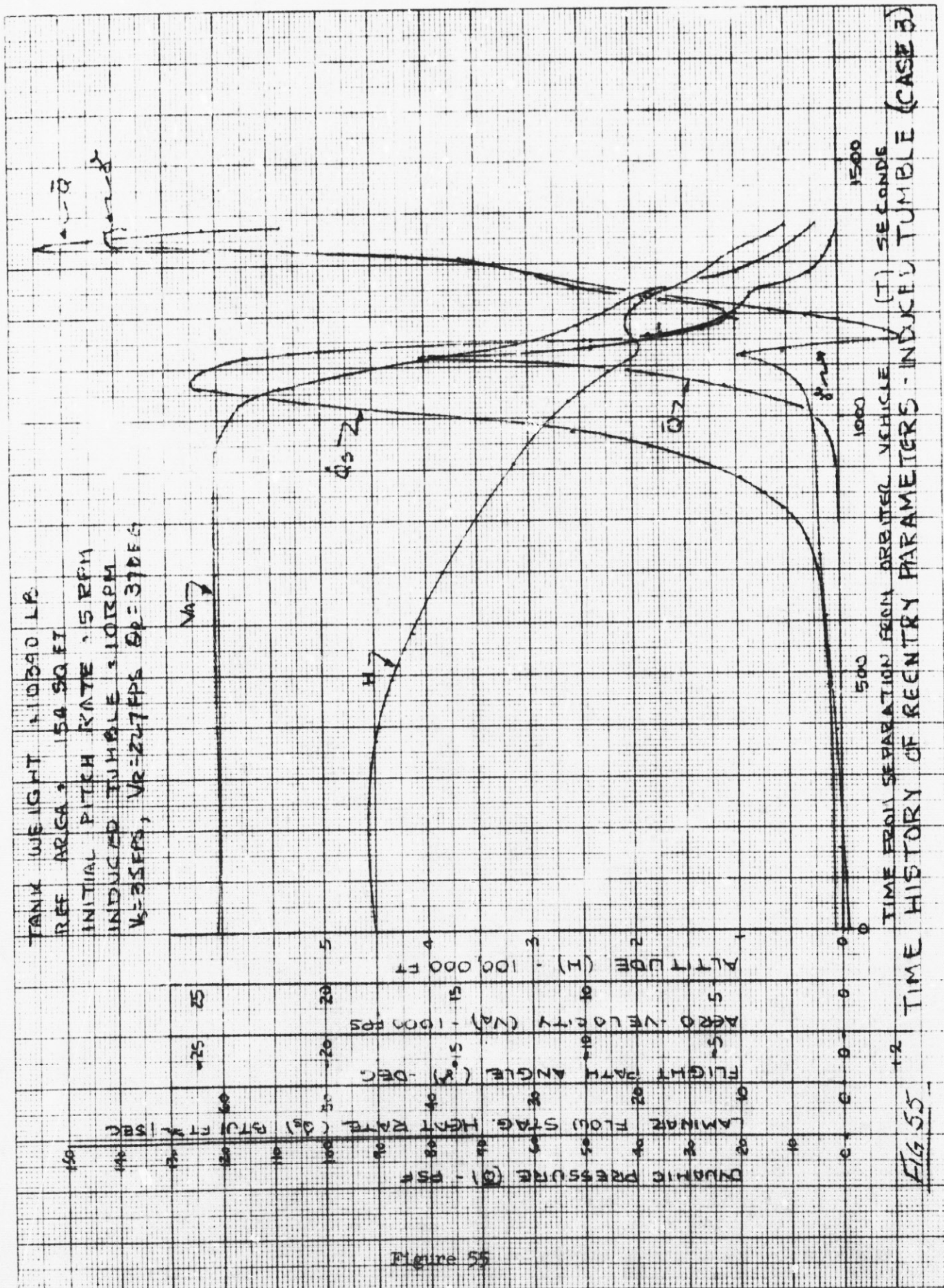


Figure 55

SQUARE 10 X 10 TO THE CENTER 15 1514

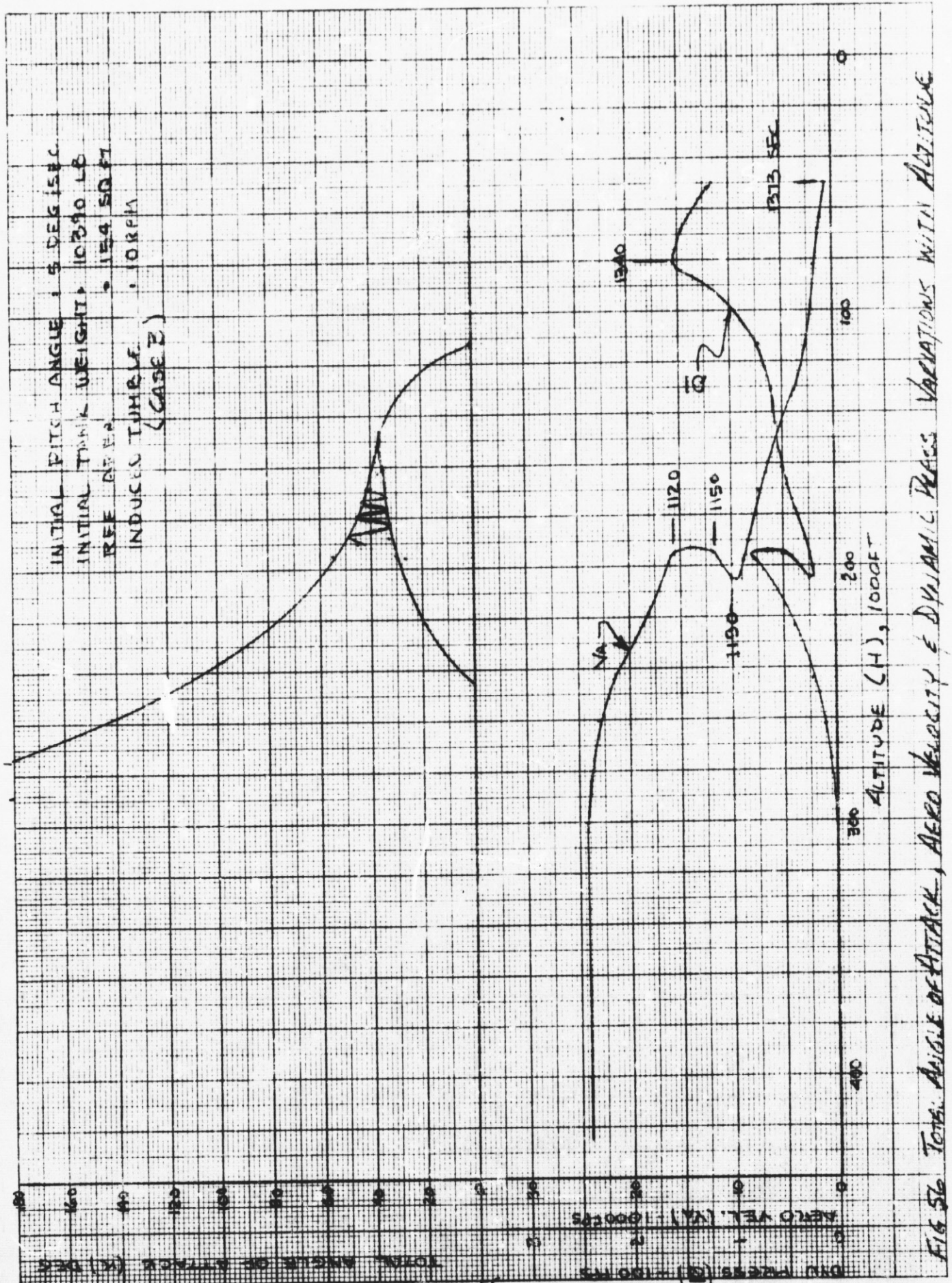


FIG 56 TOTAL ANGLE OF ATTACK, AERO VELOCITY & DYNAMIC PRESS VARIATIONS WITH ALTITUDE

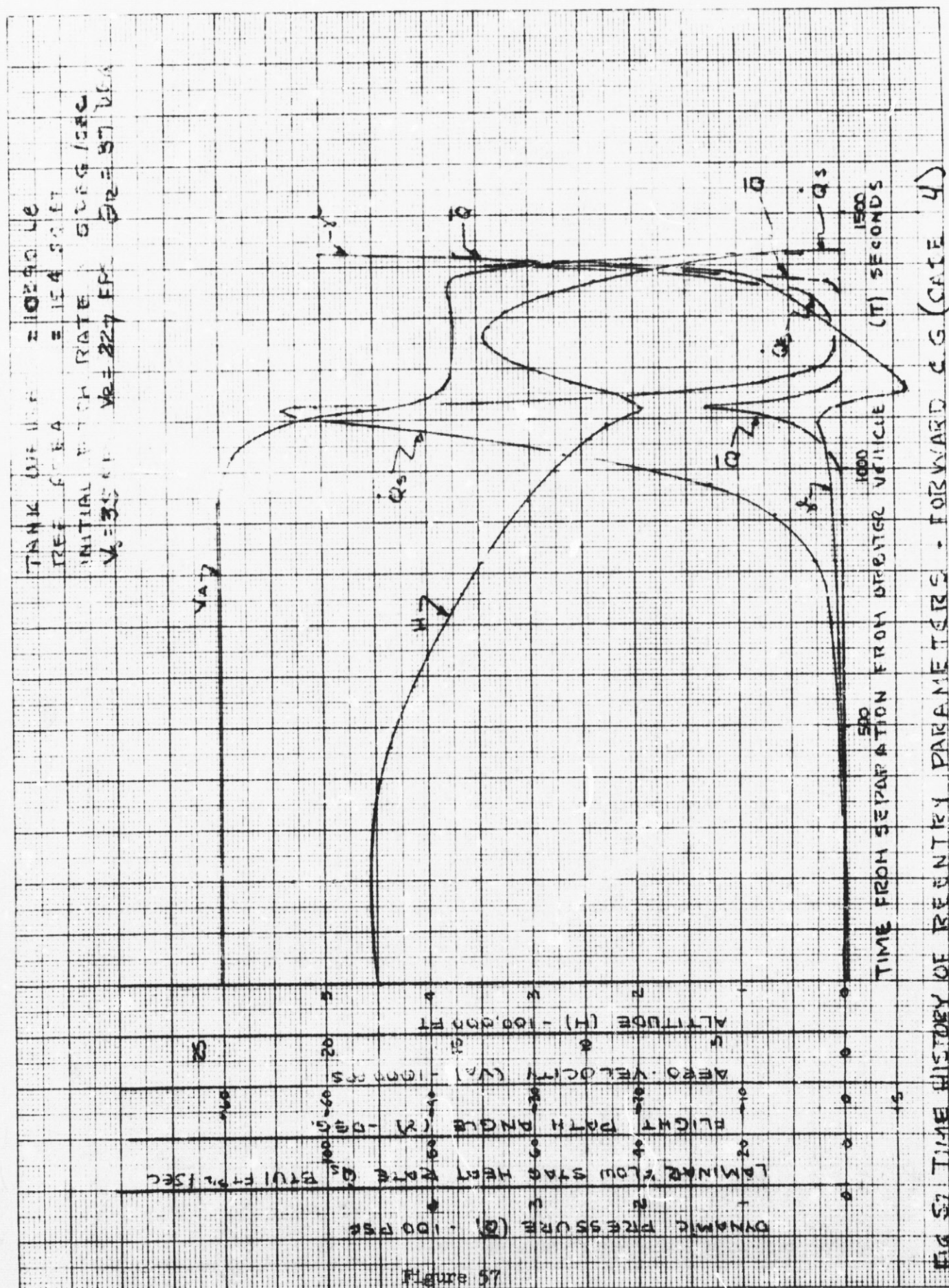


Figure 57

DATE: 18 June 1971

AS 2013 SV 2:13m.00:00.00 1000000

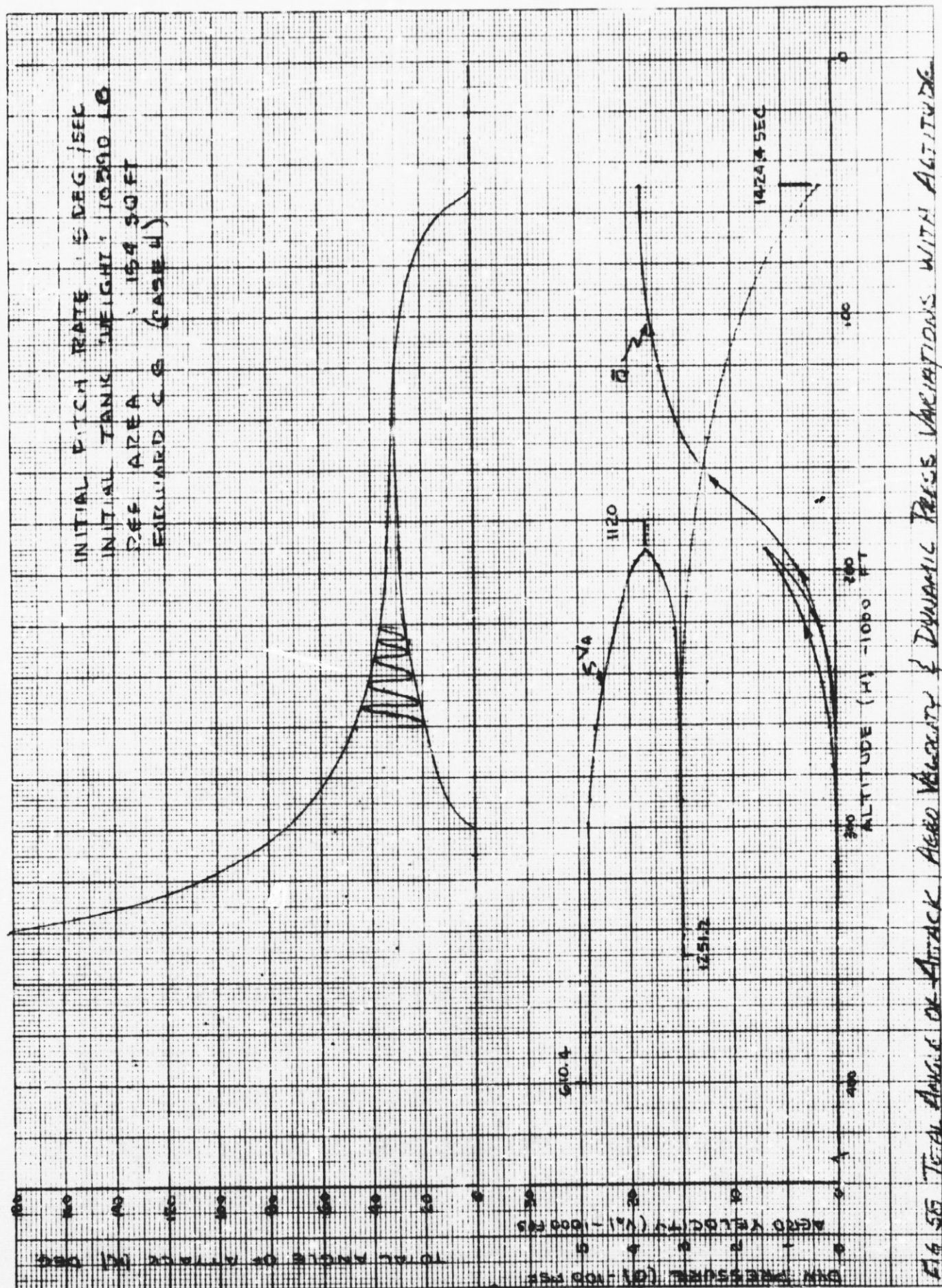


Figure 58

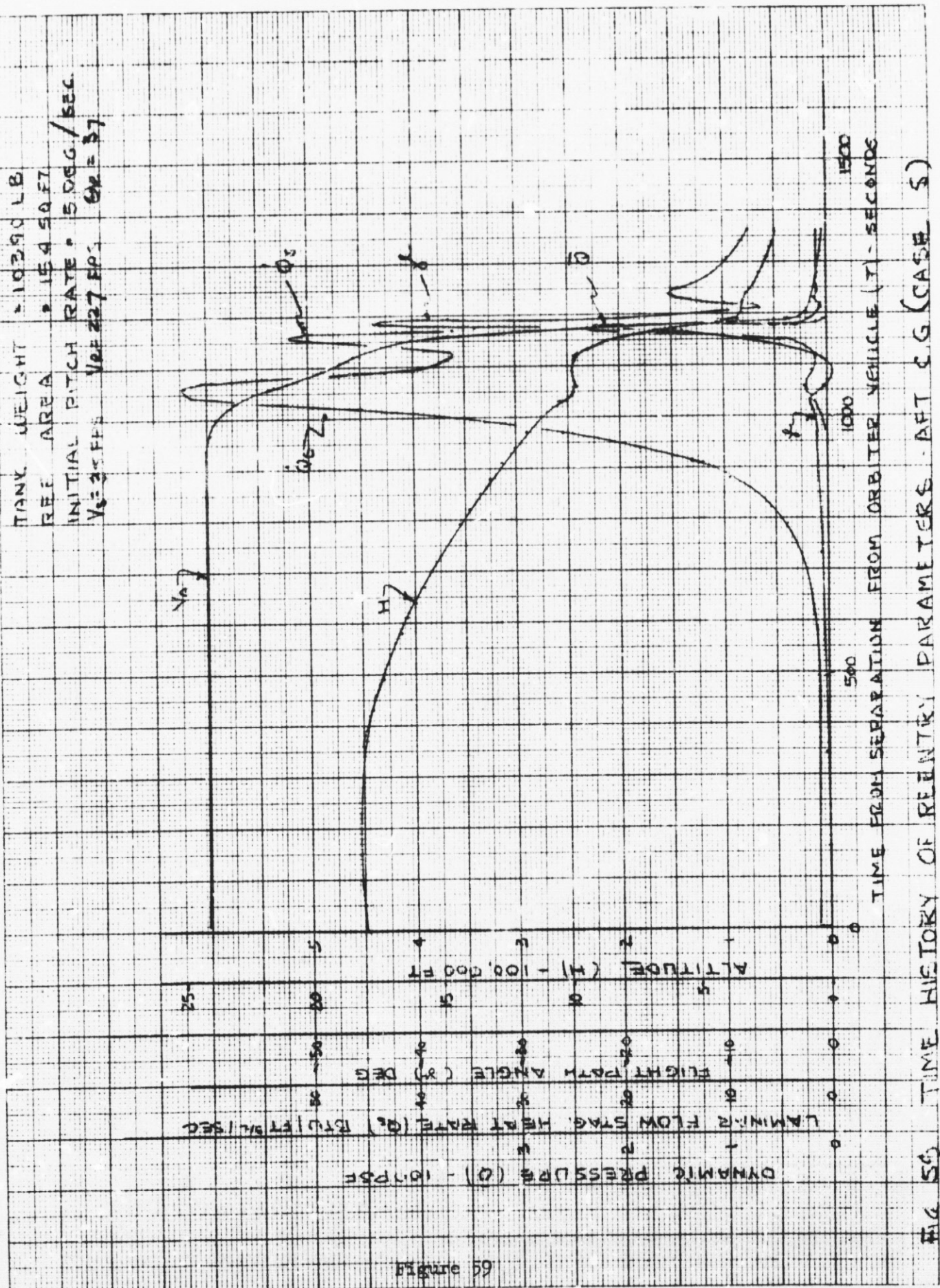


Figure 59

DATE: 18 June 1971

SQUARES TO X TO THE CENTIMETER AS ABOVE

INITIAL PITCH ANGLE = 5 DEG/SEC
INITIAL TANK WEIGHT = 10,390 LB
REF AREA = 154 SQ FT
AS - C.G. (CASE 5)

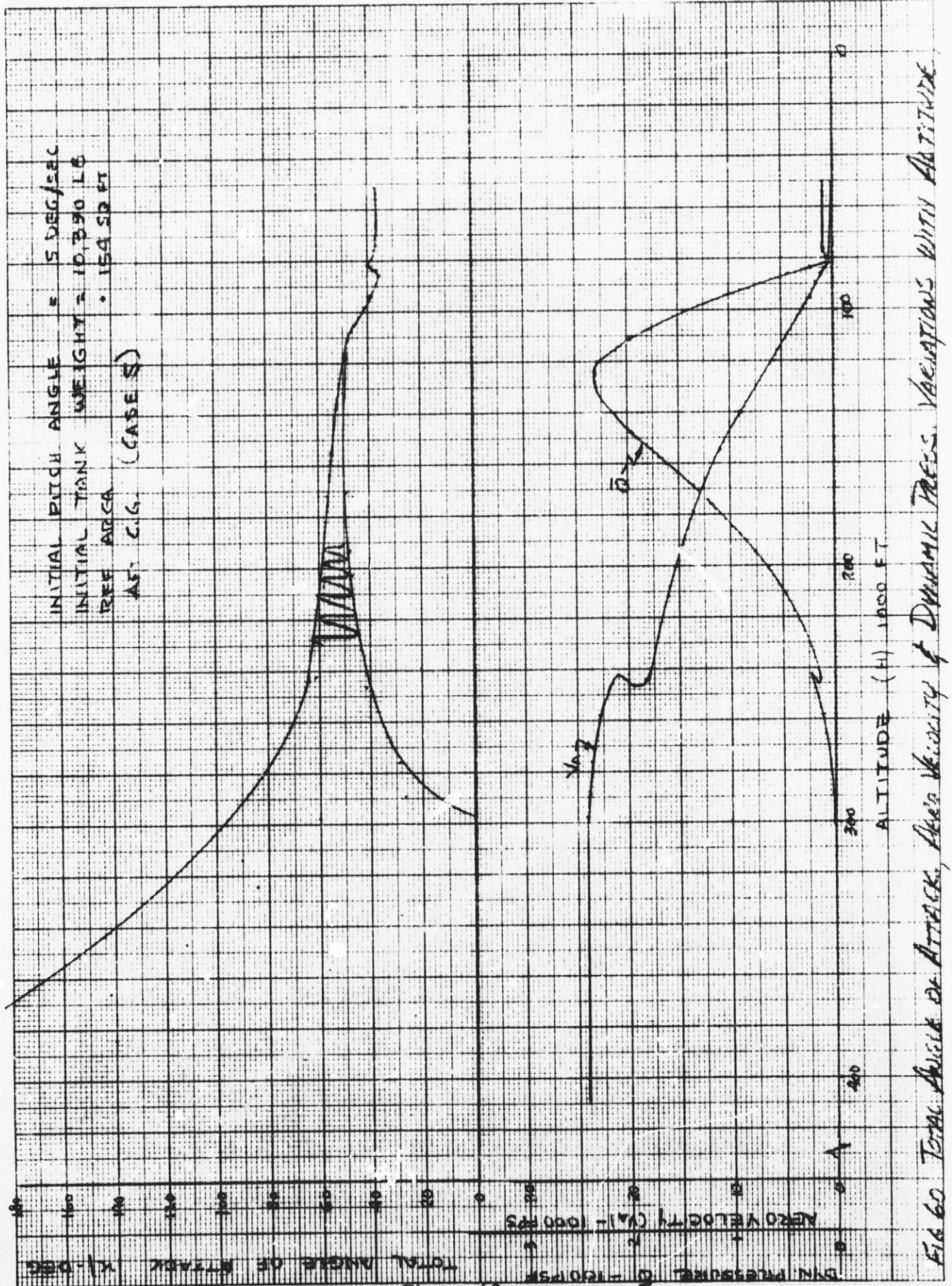
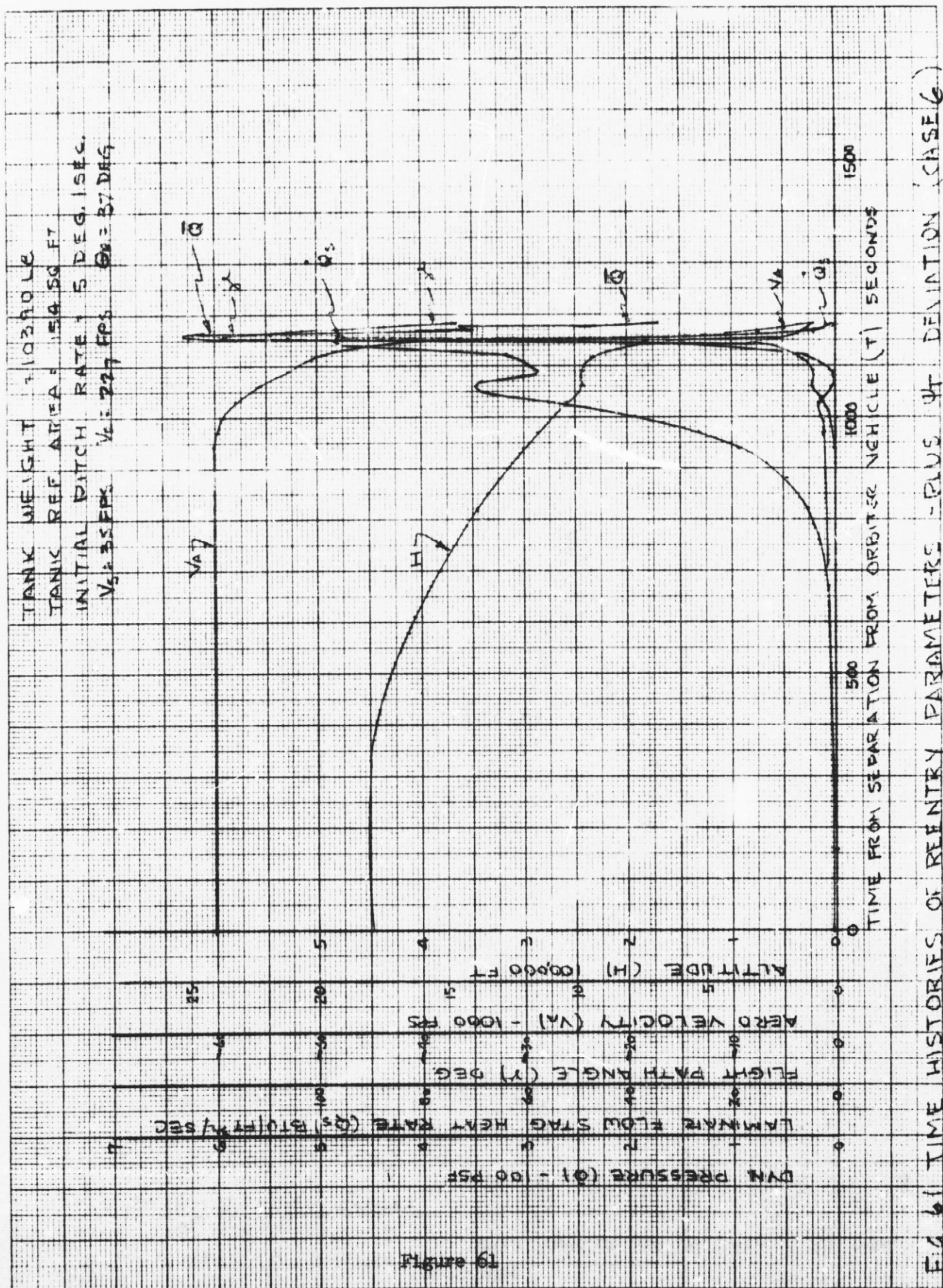


FIG 60 Total Shield or Attack, Area Velocity & Dynamic Press. Variations with Altitude.



SQUARE 1 X 10 TO THE CENTIMETER AS 6014 01

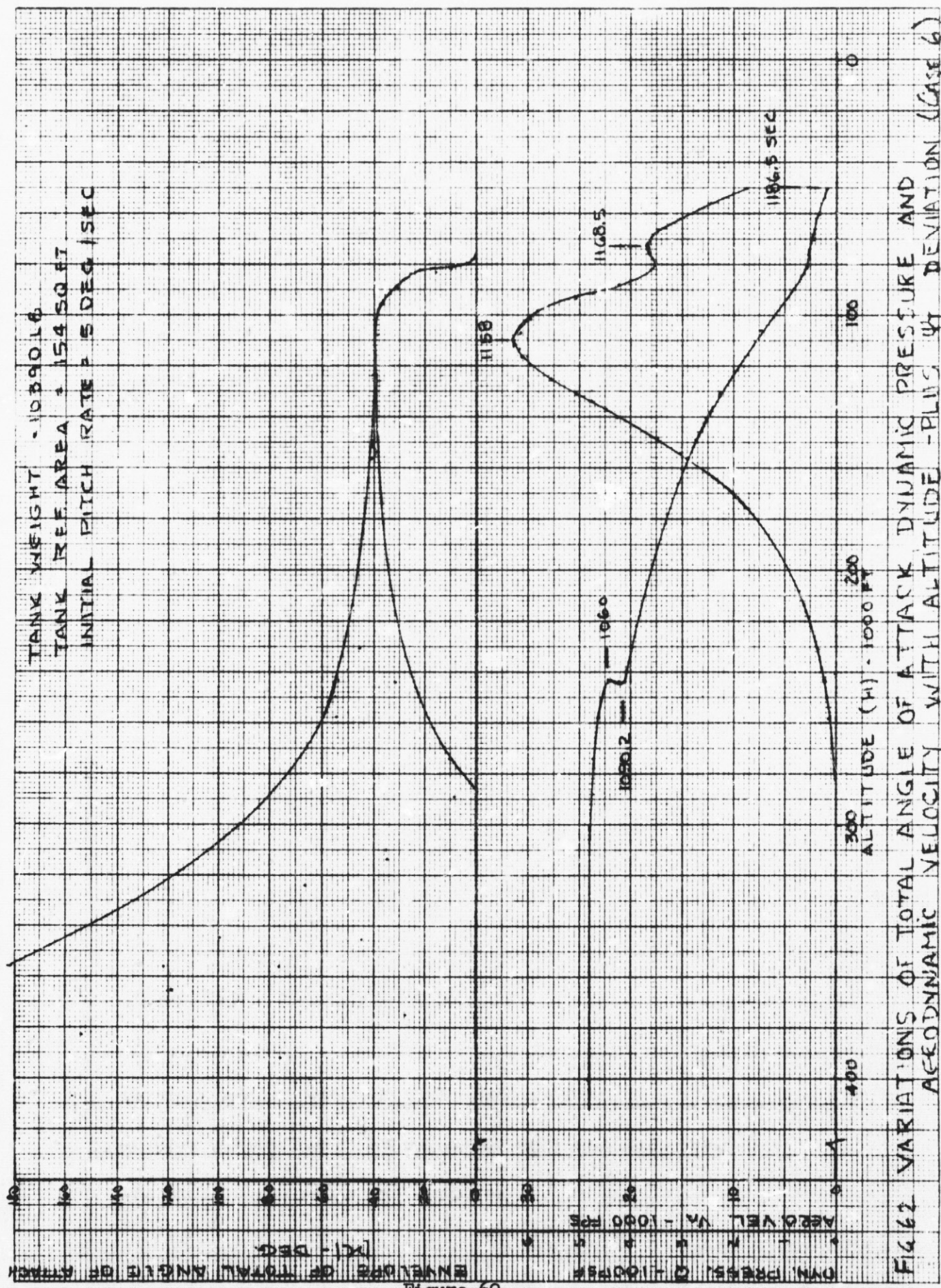
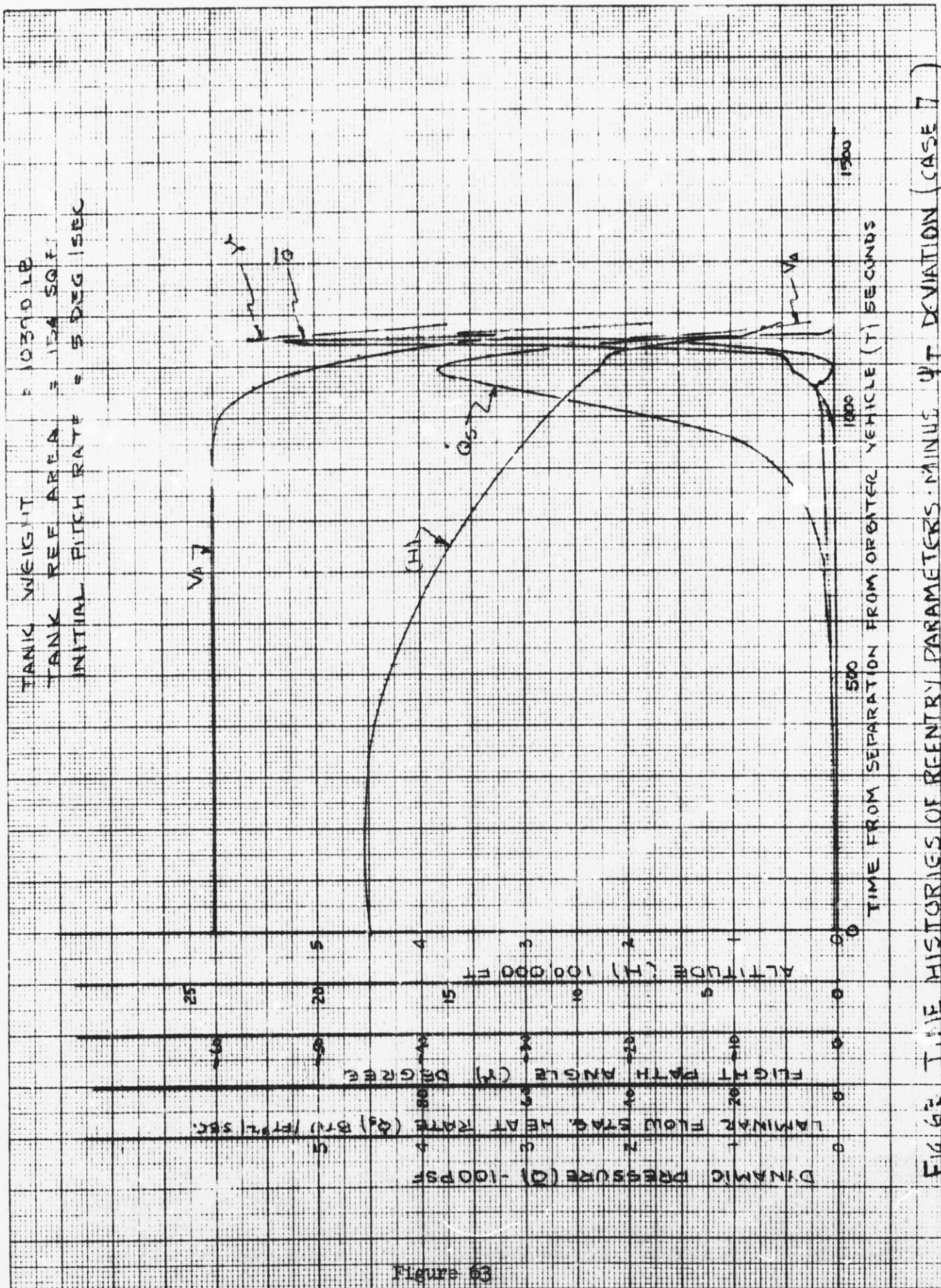


Figure 62
- 83 -

FIG 62 VARIATIONS OF TOTAL ANGLE OF ATTACK, DYNAMIC PRESSURE AND
AERO DYNAMIC VELOCITY WITH ALTITUDE - PLUS WT DEVIATION (CASE 6)



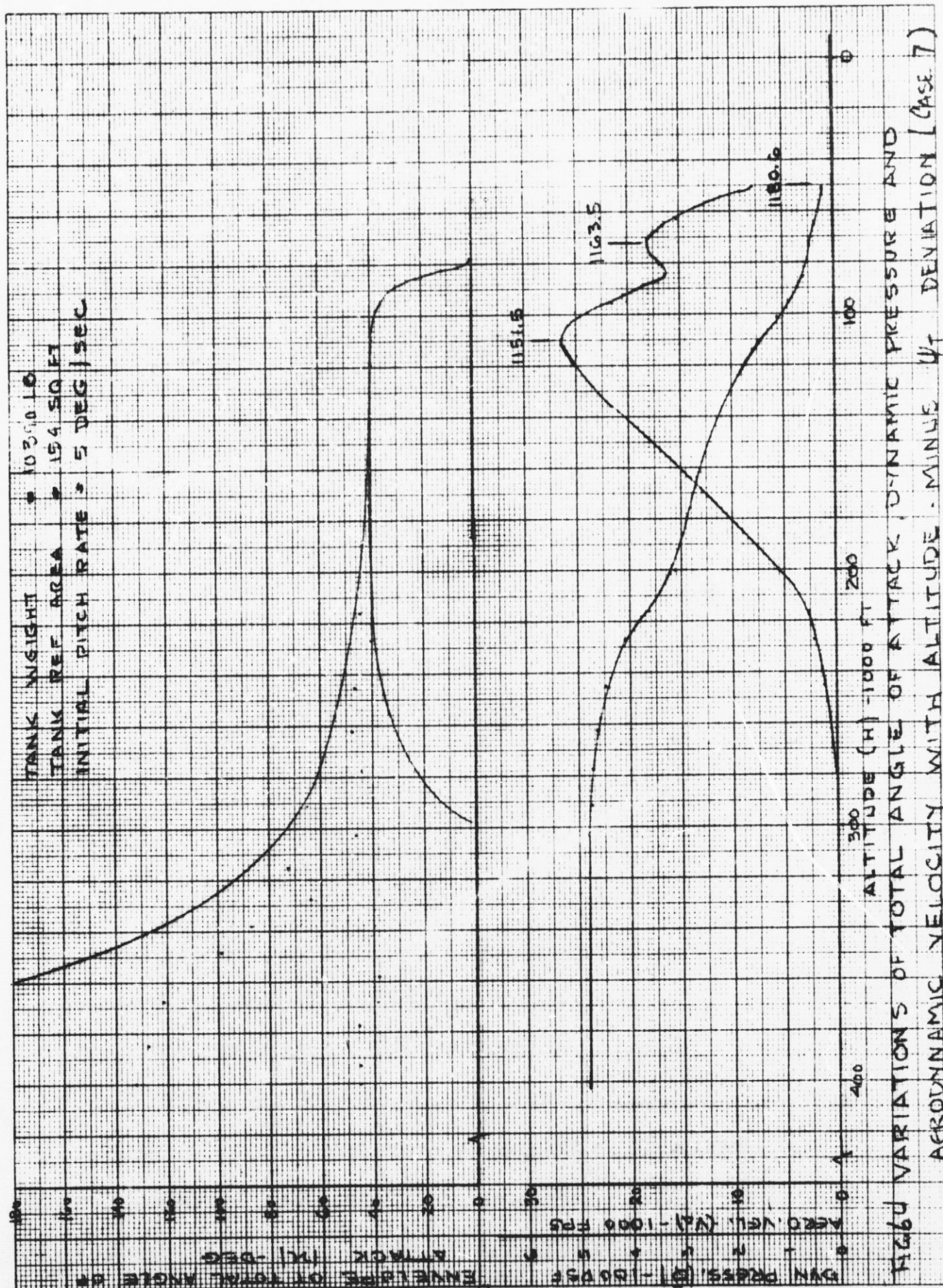
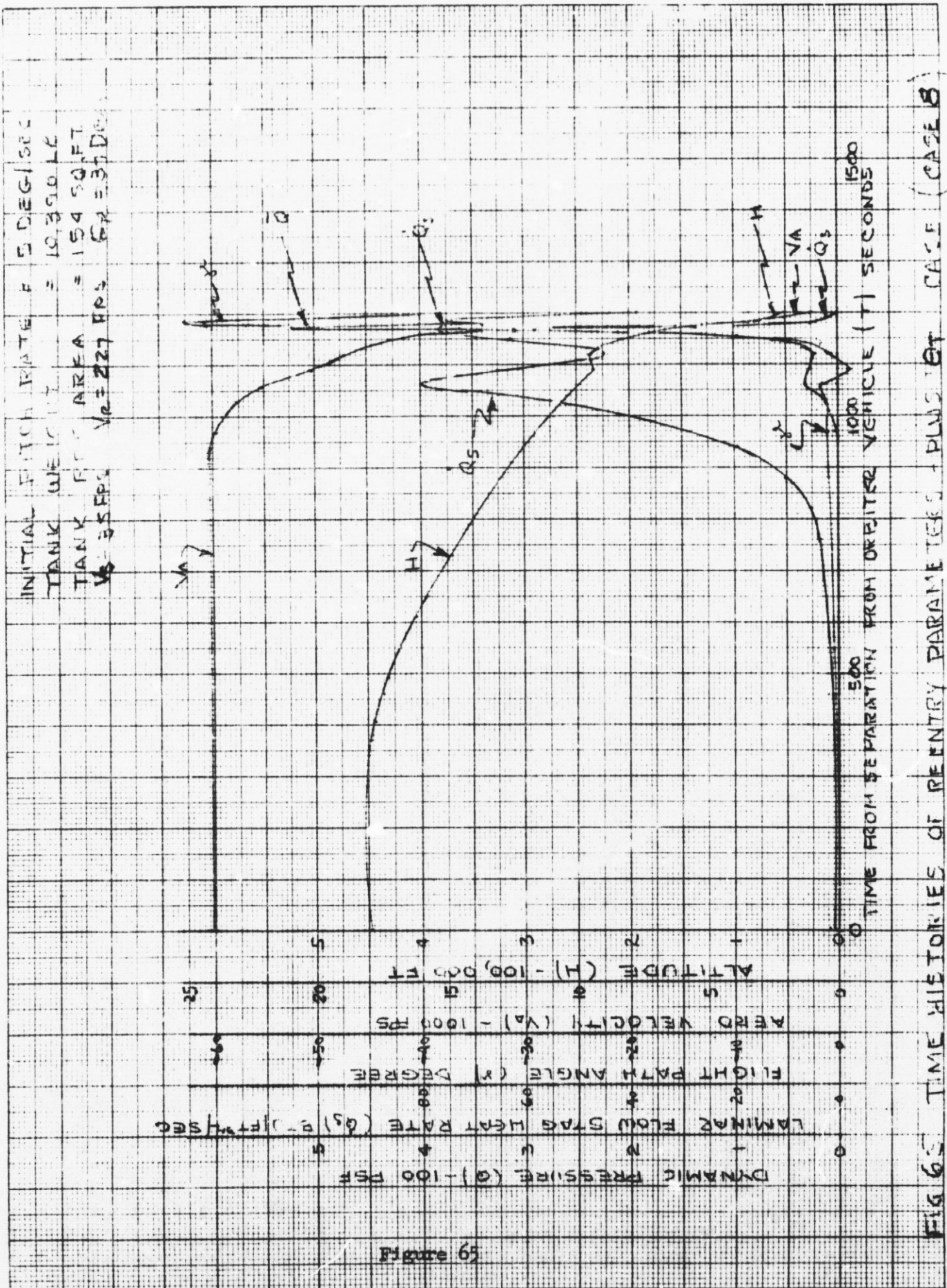


Figure 64
- 85 -

EM NO: L2-12-05-M1-8
DATE: 18 June 1971



DATE: 18 June 1971

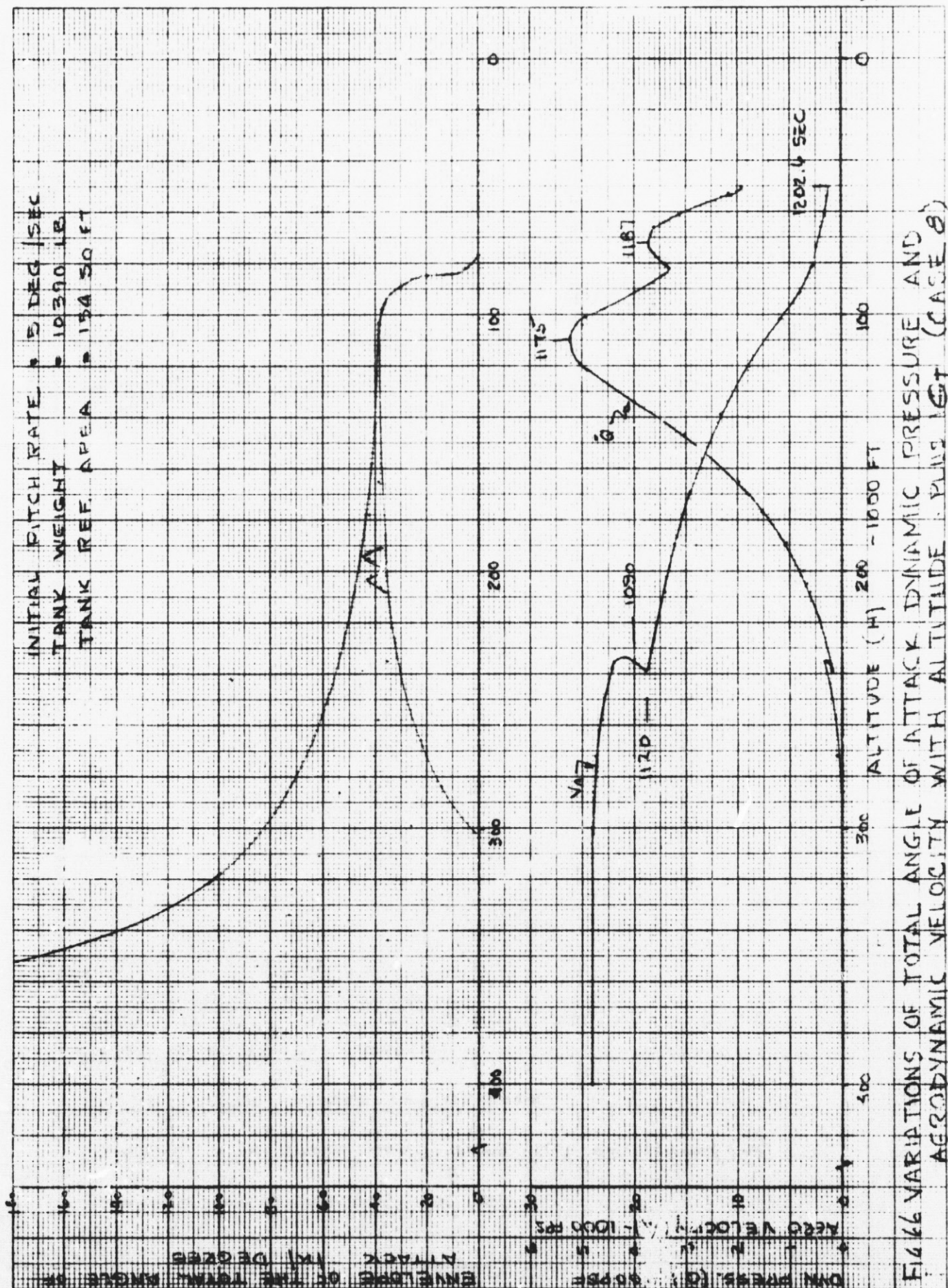


FIG. 66 VARIATIONS OF TOTAL ANGLE OF ATTACK, DYNAMIC PRESSURE AND AERODYNAMIC VELOCITY WITH ALTITUDE (CASE 8)



EM NO: 12-12-05-M1-8

DATE: 18 June 1971

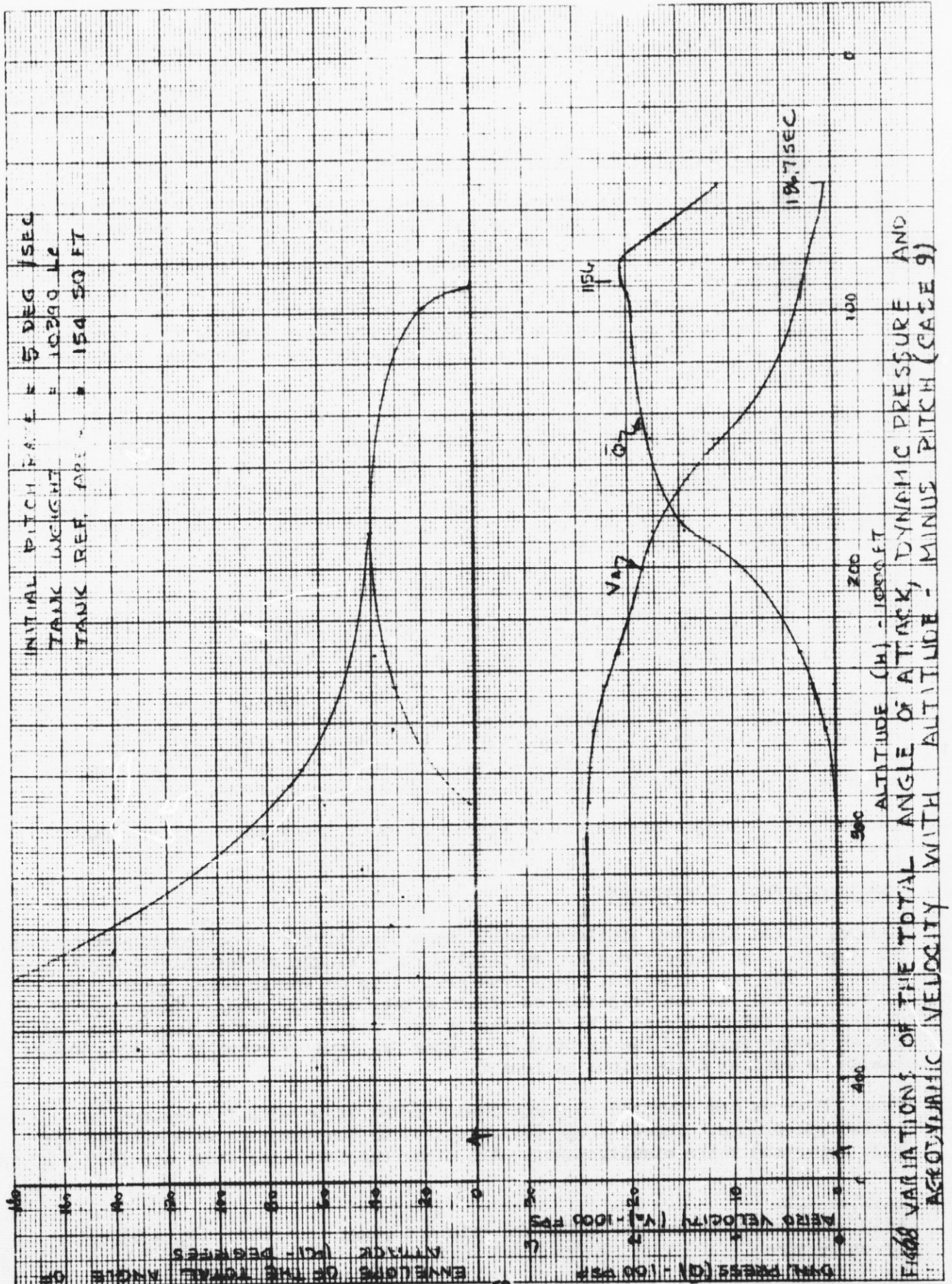


Figure 68

Comparison of Point Mass and 6D Analysis Results

Each of the 6D trajectories generated in the foregoing analysis is the singular product of a unique set of conditions and will, therefore, have a unique effect on droptank design, entry flight profiles and impact location predictions. The extent of these effects can be illustrated by comparing equivalent 3D point mass trajectories with the 6D results. Figure 69 shows such a comparison in the form of altitude-velocity profiles. In all cases, conditions for entry from orbit 1 to impact in the Indian Ocean were assumed. Separation/retro time is 20.3 minutes for the point mass, minimum drag case and 21 minutes for the point mass, tumbling and 6D nominal profiles.

As expected, the 6D profile exhibits the characteristics of a composite entry mode, i.e., combined tumbling and lifting. Initially the droptank is entering along a ballistic (tumbling) flight path but as η begins converging, the profile deviates from a tumbling entry profile. Following the pullout maneuver the tank dives (as earlier discussed) because of a net, downward lift force which simulates a decreased drag condition. Consequently the 6D profile approaches a minimum drag path, finally achieving it as the tank trim angle goes to zero at around Mach 2.

Table 11 lists flight time, $(\bar{Q})_{\max}$ and $(\dot{Q}_s)_{\max}$ for the 6D trajectory simulations (Cases 1 through 9). When comparing with corresponding 3D point mass data in Table 6, note that flight times are shorter and both $(\bar{Q})_{\max}$ and $(\dot{Q}_s)_{\max}$ are between corresponding values for tumbling and minimum drag entry.

Comparative impact locations are shown in Fig. 70 in relation to the point mass trajectory impact for a tumbling entry. All 6D cases fall within a 125 nm radius of the point mass condition except Case 4, entry with a forward c.g. location. Early convergence to trim η and the resulting high lift trajectory extends the relative range over 600 nm downrange with a crossrange of about 160 nm.

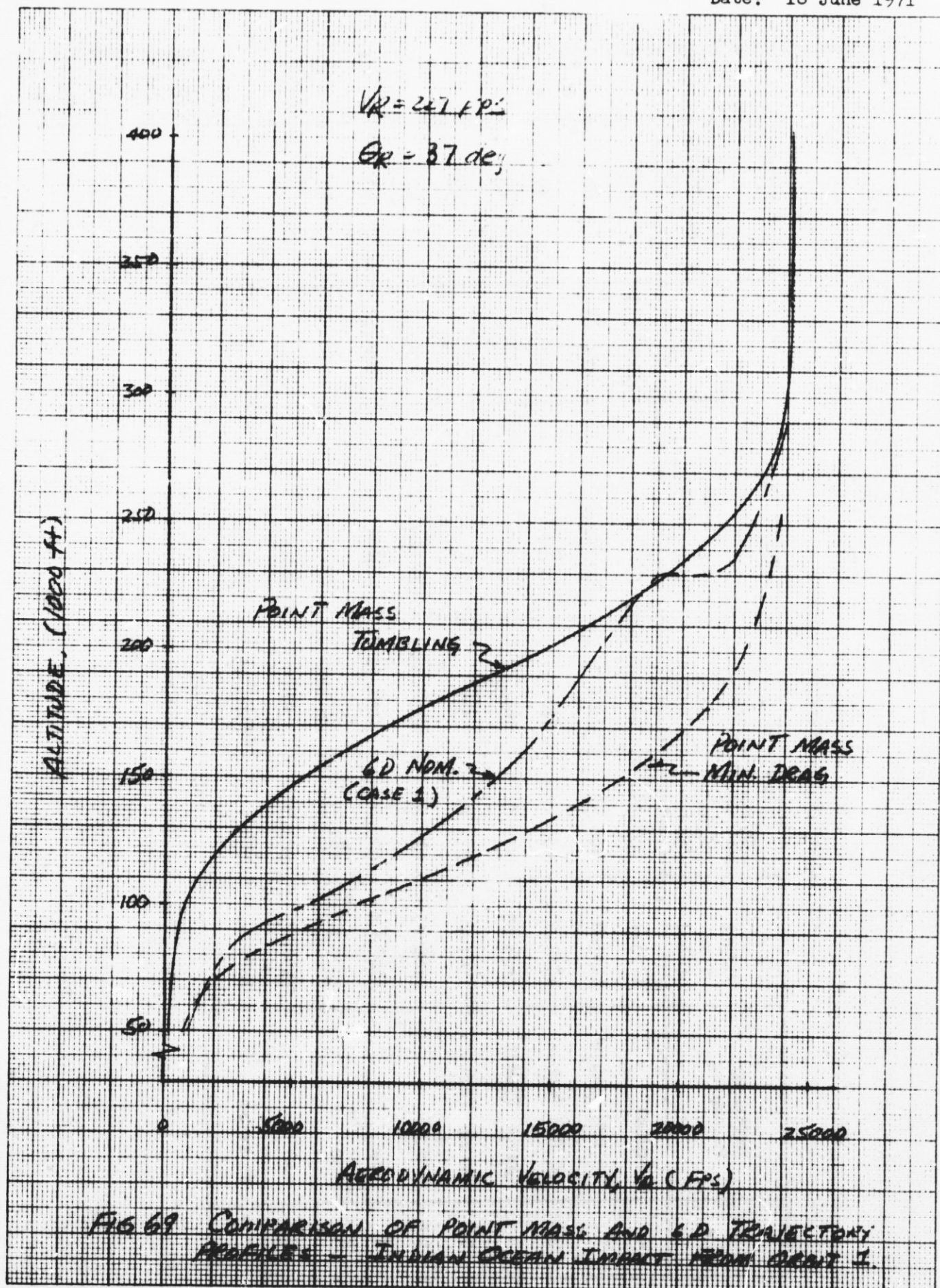
The nominal 6D trajectory impact is within 10 nm of the predicted point mass location.

RSS Impact Range Dispersion

Because of the apparent similarities of range sensitivity to parametric variations, 3σ impact range dispersions are calculated for a single representative entry trajectory. The case selected, entry from orbit 1 to an Indian Ocean impact, is typical of the various trajectories offering near maximum range. Consequently, dispersions for this case will represent a near maximum expected impact envelope for an intact entry of the droptank.* Higher V_R and/or retro at perigee should result in smaller dispersions at impact.

Table 12 shows the computed root-sum-square (RSS) dispersion for assumed 3σ parametric errors. Impact range deviations of 6D trajectories were assumed for c.g. error and retro misalignments. All other sensitivities shown are from Fig. 18,

*The correlation is not valid for the extended range non-retro ($V_R = 0$) entry from perigee.



EM NO: 12-12-05-M1-8
DATE: 18 June 1971

Table 11

6D TRAJECTORIES PARAMETER SUMMARY

Case No.	Defining Parameter	Flight Time (Sec)	Maximum Dynamic Pressure		Maximum Laminar Heat Rate		Trim Angle of Attack (Deg)
			Value (psf)	Time (Sec)	Value (BTU/ft ^{3/2} -Sec)	Time (Sec)	
1	Nominal	1193.1	554.16	1168	77.835	1156.535	40
2	5 RPM Tumble	1183.0	404.42	1152.1	68.82	1090.07	40
3	10 RPM Tumble	1372.93	155.0	1340	61.93	1060.0	40
4	Δl cg (fwd)	1424.40	377.8	1424	107.74	1120.0	30
5	Δl cg (aft)	1361.6	232.4	1175	62.2	1060	52
6	+ $\Delta\psi$	1186.45	629.04	1158.53	95.624	1150.53	40
7	- $\Delta\psi$	1180.63	529.534	1151.51	76.437	1090.1	40
8	+ $\Delta\theta$	1202.6.	523.79	1175.58	79.9	1060	40
9	- $\Delta\theta$	1196.67	205.89	1158.5	103.17	1120.0	40
10	No rates	2427.55	154.1	2427.55	32.857	1430.4	40

Table 11

DATE: 18 June 1971

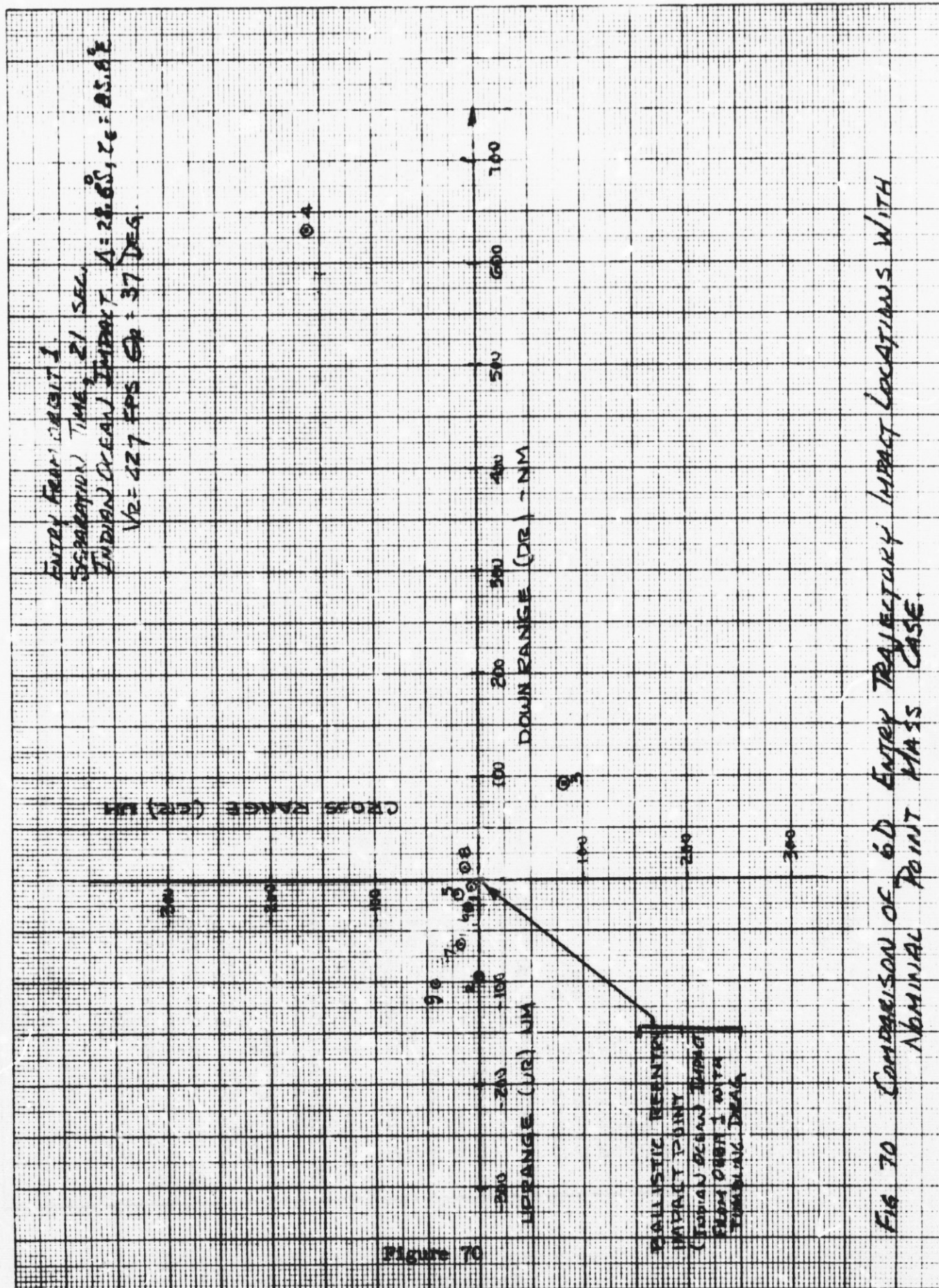


FIG 70 COMPARISON OF 6D ENTRY TRAJECTORY IMPACT LOCATIONS WITH NOMINAL POINT MASS CASE.

Table 12

IMPACT RANGE DISPERSIONS

- Entry from Orbit 1, Indian Ocean Impact
- Separation Time, 21 Min $V_R=227$ FPS, $\theta_R=37$ Deg

Error Source	Dn Range (nm)	Up Range (nm)	+X-Range (nm)	-X-Range (nm)
Orbit Elements				
Position	3	- 3	0.5	-0.5
Altitude (+2 nm)	280	-280	-	-
Velocity (+20 fps)	300	-260	-	-
Flt Path (+0.1 deg)	430	-430	-	-
Azimuth (+0.1 deg)	-	-	10	-10
RSS Dispersion Due to Orbit Elements	+594	-575	10.0	10.0
Retro Conditions				
Pitch Angle (+ 10 deg)	+ 85	- 40	-	-
Yaw Angle (+ 12 deg)	100	- 55	30	-30
Total Impulse (+ 11 pct)	500	480	-	-
Thrust Misalign, $\Delta\theta_T$ (+0.12 deg)	12	100	-	-40
$\Delta\psi_T$ (+0.12 deg)	-	-62	-	-18
Retro Initiation (+ 1.4 sec)	6	- 6	-	-
RSS Dispersion Due to Retro	517	-499	30	53
Mass Properties				
W/C.A (+ 10 pct)	30	- 30	-	-
Long. C.G. (+ 0.02 L_{REF})	+630	- 15	-	-165
RSS Dispersion Due to Mass Properties	631	- 34	-	-165
Atmosphere/Aerodynamics				
Density (+ 10%)	30	- 30	-	-
Drag (+ 10%)	30	- 30	-	-
RSS Dispersion Due to Atmosphere/Aero	42	- 42	0	0
TOTAL RSS DISPERSION	1010	-753	32	-174

Lockheed Missiles & Space Company

Space Shuttle Project

 EM NO: 12-12-05-M1-8
 DATE: 18 June 1971

Table 12

- 94 -

which is for a tumbling entry condition. The total dispersion is 1010 nm down-range, 763 nm uprange and +32 nm, -174 nm in crossrange. The effect of a forward c.g. shift is the prime contributor to the asymmetry in both intrack and crossrange about the nominal.

Errors shown for orbit elements reflect lack of tracking information on a vehicle which has just recently been injected into orbit. After one orbit pass, tracking data inputs can be used to reduce these contributions significantly.*

In the separation analysis, the average θ_R during retro was established at 17 degrees based on an initial $\theta_R = 37$ degrees. The 20 degrees difference was reduced to $\Delta\theta_R = \pm 10$ degrees assuming orbiter attitude is adjusted to somewhat compensate for expected retro pitch errors. This assumption is not valid for retro yaw angle errors.

The resulting dispersion envelope is illustrated in Fig. 71 for both LH₂ droptanks relative to an assumed impact location. The two points which fall just outside the boundary are the range errors for the forward c.g. configuration. Accurate weight and balance data before launch can be used to adjust nominal predictions to include these points.

Tank Breakup Considerations

All of the data presented so far, assume the LH₂ droptanks will enter structurally intact to impact. In actual operations, however, the tanks will probably fail structurally, either by design or by chance, scattering fragments as they descend. A brief analysis of fragment ranges was performed to aid in prediction of any extension of the dispersion envelope which may be necessary because of breakup.

Figures 72, 73 and 74 show range to impact, $(\dot{Q}_s)_{\max}$ and $(\bar{Q})_{\max}$ for an assumed breakup at retro. Ballistic coefficient is used as the parametric factor for defining fragment size. The data are for ballistic descent since likelihood of a totally trimmed fragment trajectory with finite L/D is only a small possibility. Initial trajectory conditions are shown in Table 13.

Fragment ranges vary from 4400 nm to 6650 nm for the $W/C_D A$ range considered. Assuming a particle spectrum of $5 \text{ psf} \leq (W/C_D A) \leq 500 \text{ psf}$, an impact range increase (over intact point mass tumbling entry) of about 1500 nm can be expected. Peak dynamic pressure will vary to about 4200 psf and $(\dot{Q}_s)_{\max}$ to approximately 500 BTU/ft^{3/2}-sec.

Figures 75 through 78 show fragment ranges for assumed tank breakup at the times of peak heating and peak dynamic pressure for entry from each of the four orbit conditions.** The effect of breakup along a tumbling vs. a minimum drag trajectory

*With updated tracking, 3 σ orbit element errors are reduced to $\Delta H = \pm 0.5$ nm, $\Delta V_{Io} = \pm 4.0$ fps, $\Delta \gamma_{Io} = 0.03$ degree.

**Trajectory conditions at $(\dot{Q}_s)_{\max}$ and $(\bar{Q})_{\max}$ are from nominal 3D point mass entry trajectories for Indian Ocean impact.

EM NO: L2-12-05-M1-8
 DATE: 18 June 1971

SCAPRE 10 x 10 INE C14 INETER 40 8014 11

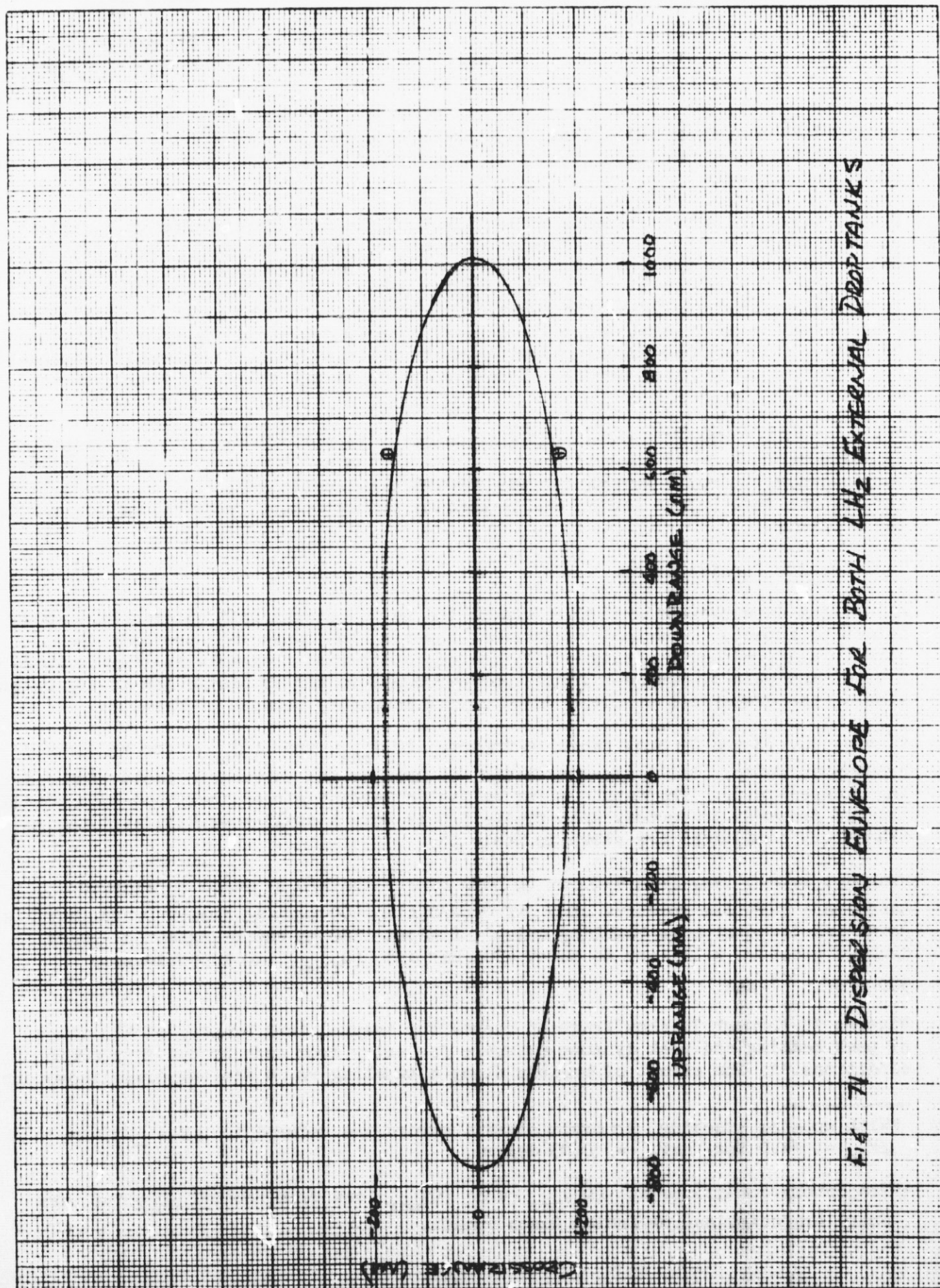


Figure 71

EM NO: L2-12-05-M1-8
DATE: 18 June 1971

10000

ENTRY FOR INDIAN OCEAN IMPACT

$V_R = 227 \text{ fps}$

1000

100

BALLISTIC COEFFICIENT, W/CDA (psf)

10

$I = 55^\circ$
 $I = 40.5^\circ$
 $I = 30^\circ (\text{MFR} - S)$
 $I = 20^\circ (\text{MFR} - S)$

FIG 72 FRAGMENT ENTRY RANGES FOR BREAKUP AT RETRO

RANGE (1000 nm)

12

3

4

5

6

7

8

9

- 97 -

EM NO: 12-12-05-M1-8

DATE: 18 June 1971

ENTRY FOR INDIAN OCEAN IMPACT

10000

1000

100

10

BALLISTIC COEFFICIENT, W/CDA, (psf)

$I = 28.5^\circ$ $I = 55^\circ$ $I = 90^\circ$ (END & WTR)

$V_R = 227$ fps

FIG. 7. PEAK LAMINAR STAGNATION POINT HEAT RATE FOR ENTRY AT INDIAN OCEAN

PEAK LAMINAR STAGNATION POINT HEAT RATE $(Q_s)_{max}$, (BTU/ft^{3/2}-sec)

0

500

1000

1500

2000

2500

EM NO: L2-12-05-M1-8
DATE: 18 June 1971

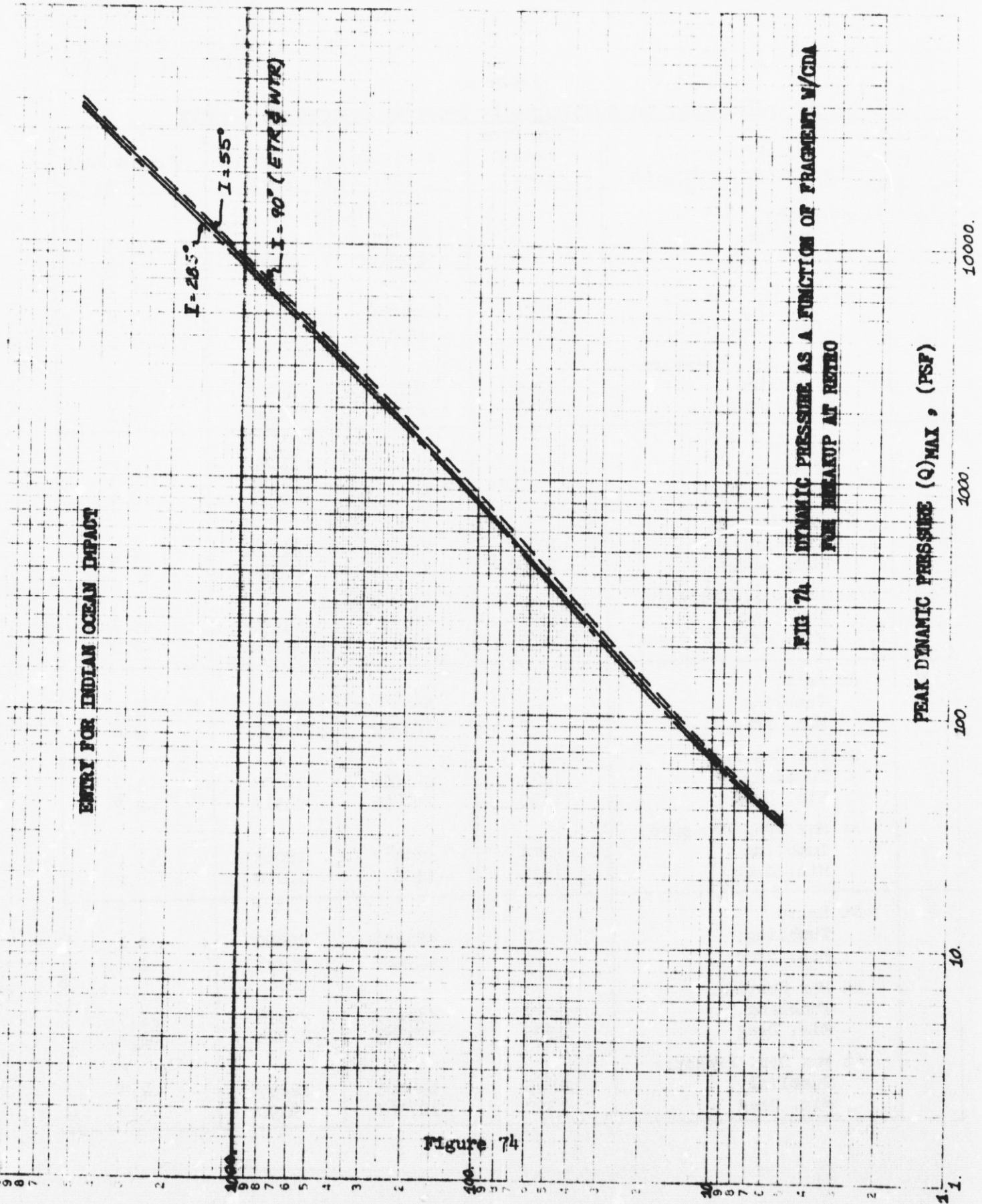


FIG 74. DYNAMIC PRESSURE AS A FUNCTION OF FRAGMENT W/CDA FOR BREAKUP AT RETRO

Figure 74

BALLISTIC COEFFICIENT, W/CDA, (PSF)

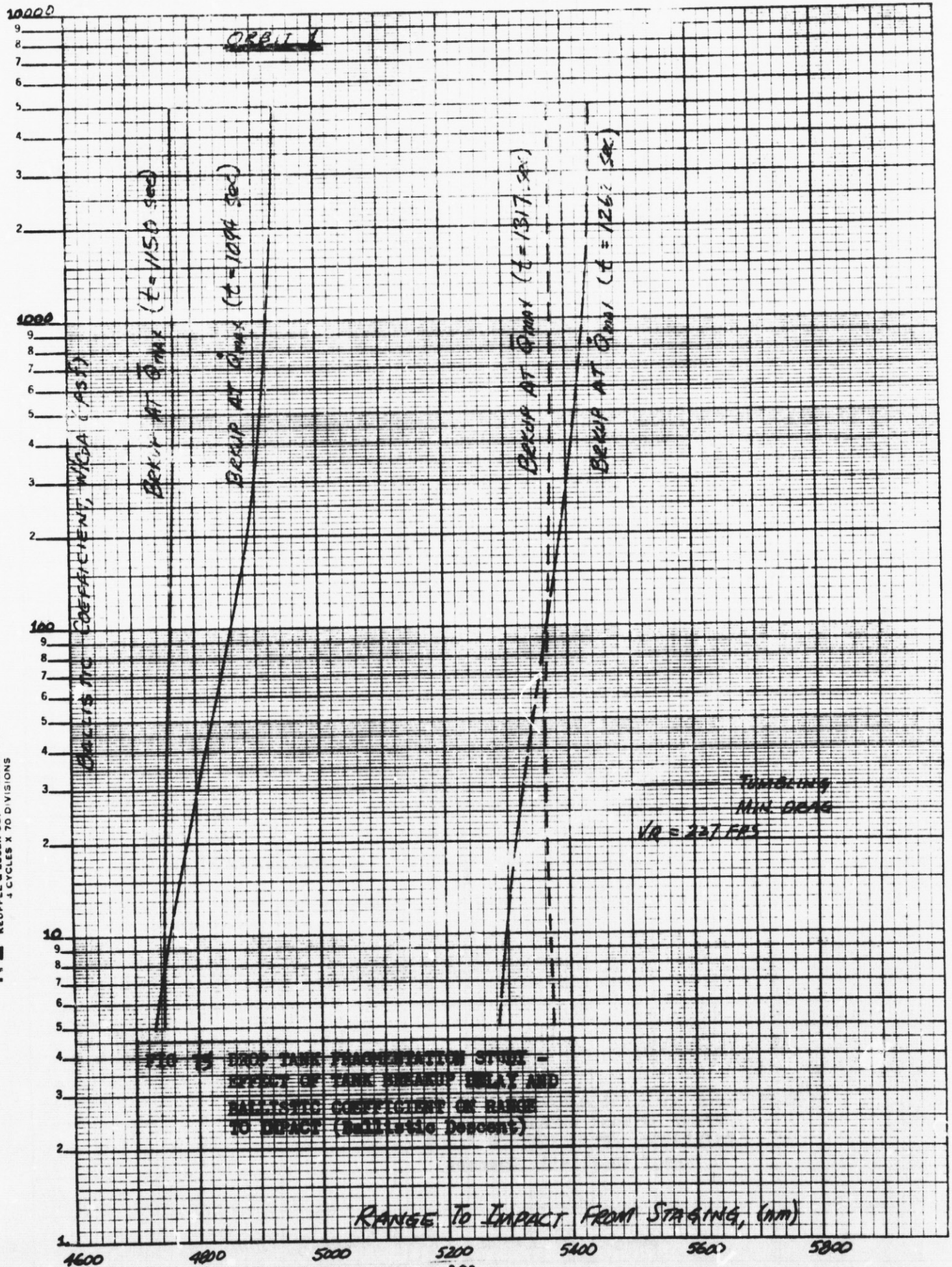
Table 13

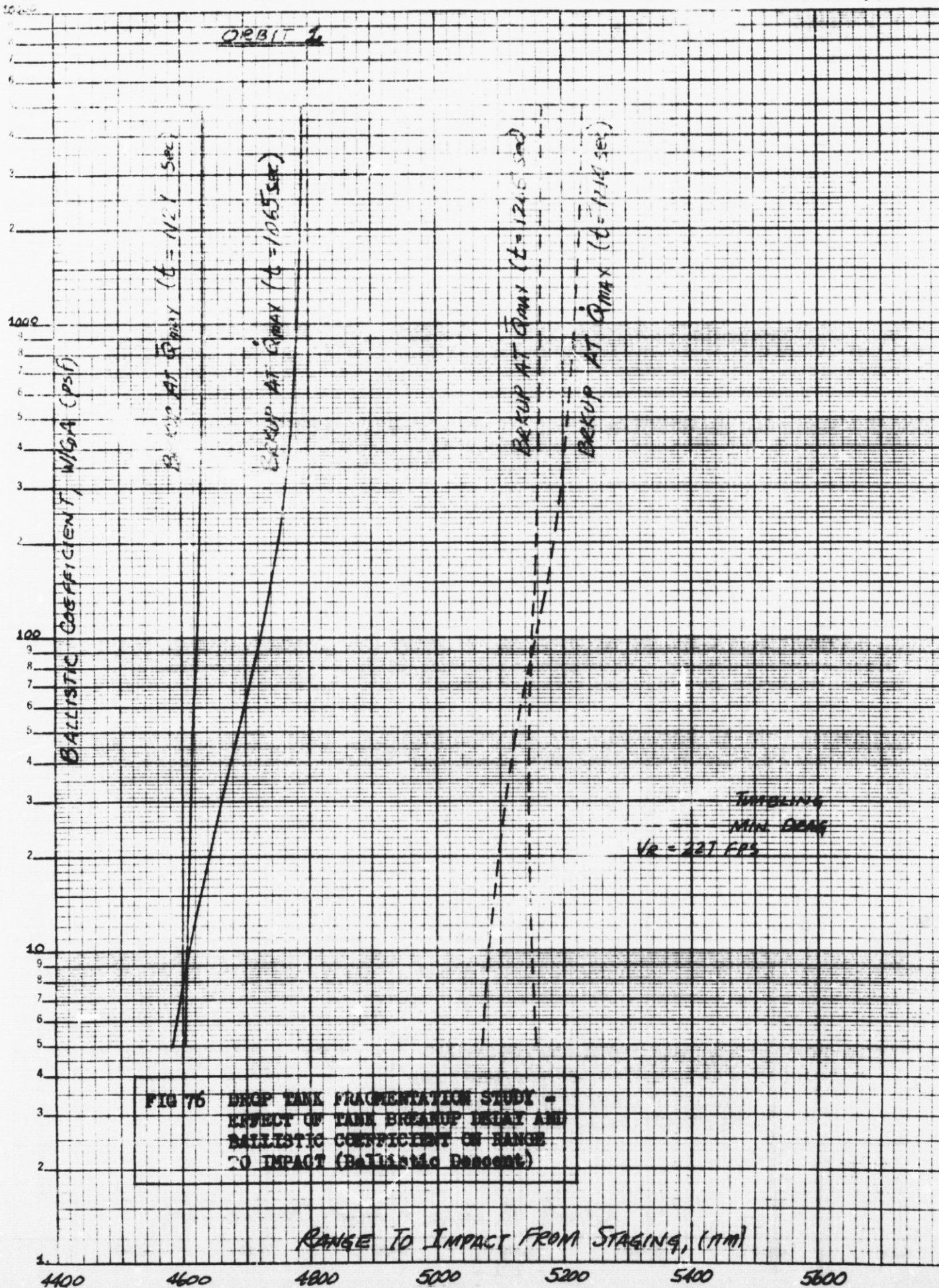
ASSUMED TRAJECTORY CONDITIONS AT DROPTANK STRUCTURAL FAILURE

Orbit	Tank Entry Trajectory Conditions	Time From Retro (sec)	Altitude (ft)	Velocity (fps)	Flight Path (deg)
1	At Retro				
	Tumbling	0	448333	25673	0.4
	Min. Drag	0	439697	25683	0.4
	At Max Heating				
	Tumbling	109 ¹ / ₄	234271	21337	-2.0
	Min. Drag	1262	164140	20551	-2.5
	At Max Dyn. Pressure				
	Tumbling	1150	182239	12143	-5.2
	Min. Drag	1317	106845	10336	-6.1
2	At Retro				
	Tumbling	0	468796	25650	0.4
	Min. Drag	0	450181	25677	0.4
	At Max Heating				
	Tumbling	1065	234101	21113	-2.1
	Min. Drag	1214	163809	20304	-2.7
	At Max Dyn. Pressure				
	Tumbling	1121	181496	11700	-5.5
	Min. Drag	1265	109165	10506	-6.2
3	At Retro				
	Tumbling	0	495725	25657	0.4
	Min. Drag	0	461222	25691	0.4
	At Max Heating				
	Tumbling	1221	235058	21193	-1.9
	Min. Drag	1359	167895	20517	-2.3
	At Max Dyn. Pressure				
	Tumbling	1273	186487	12063	-5.1
	Min. Drag	1431	110677	10210	-6.2
4	At Retro				
	Tumbling	0	453258	25690	0.4
	Min. Drag	0	419105	25723	0.4
	At Max Heating				
	Tumbling	1177	235179	20974	-1.9
	Min. Drag	1305	176383	21024	-2.1
	At Max Dyn. Pressure				
	Tumbling	1225	190805	12257	-4.8
	Min. Drag	1370	107367	9290	-6.9

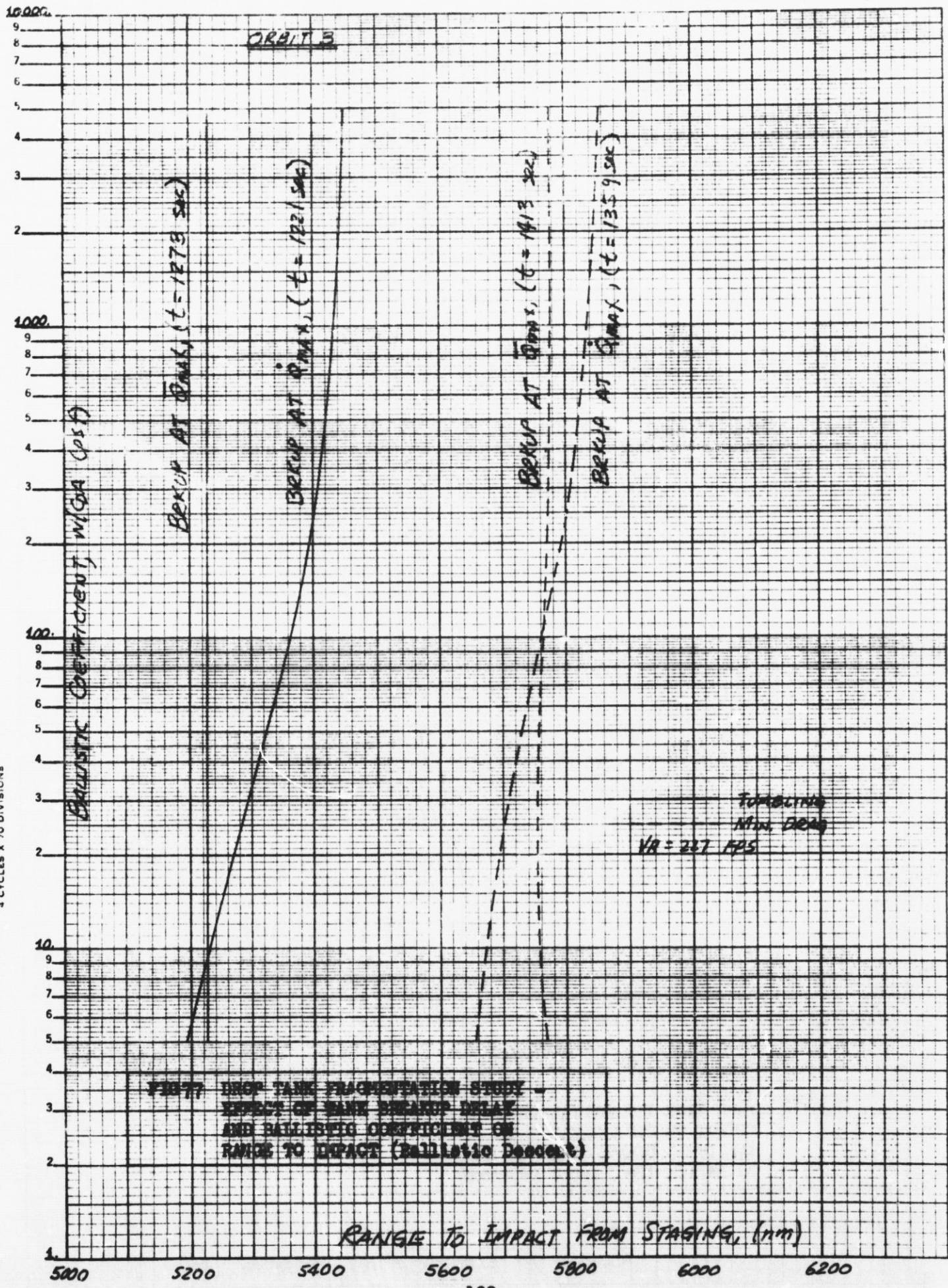
DATE: 18 June 1971

K-E SEMI-LOGARITHMIC 359-81
KEUFFEL & ESSER CO. MADE IN U.S.A.
4 CYCLES X 70 DIVISIONS

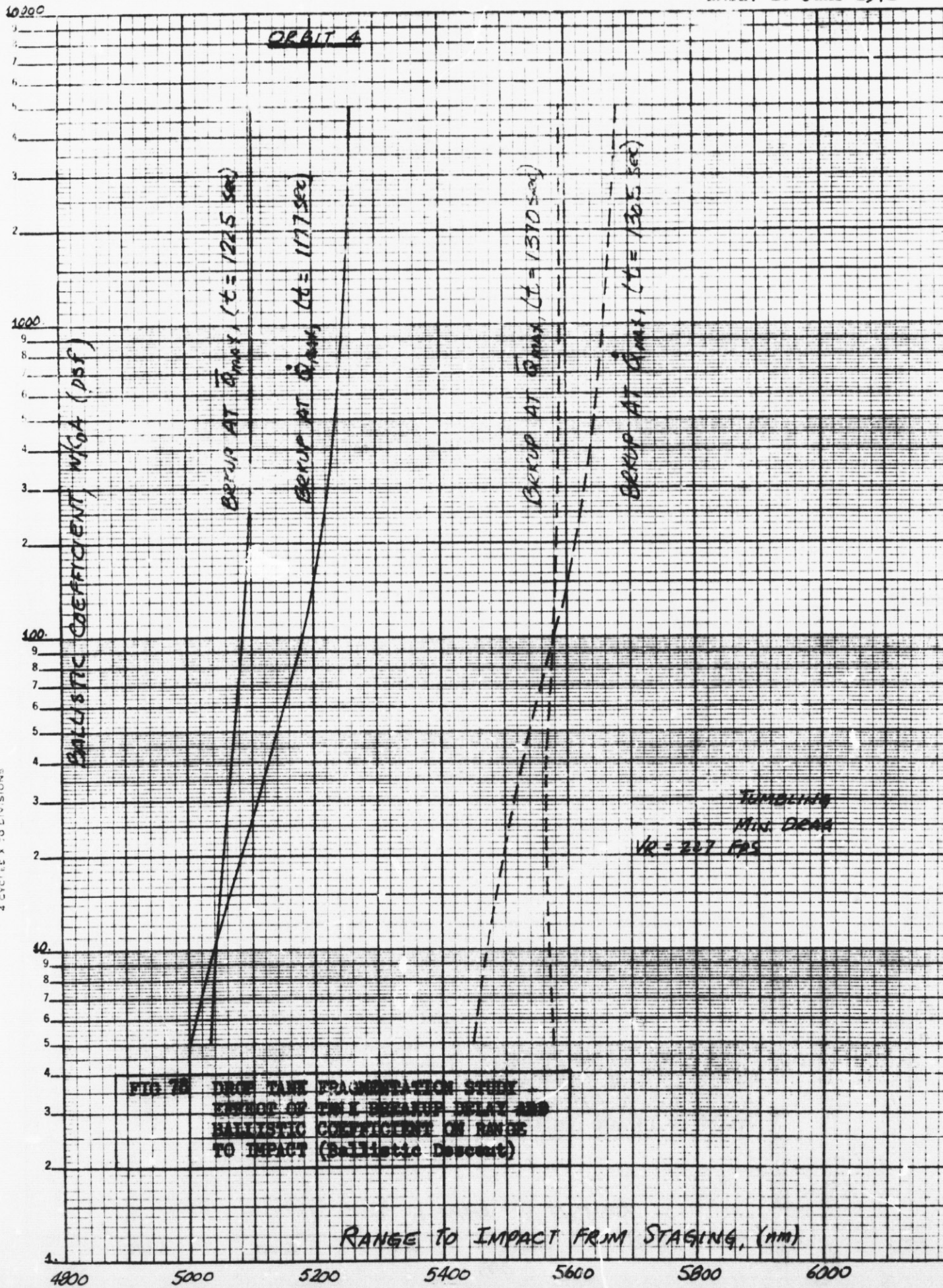




K&E SEMI-LOGARITHMIC 359-81
KEUFFEL & ESSER CO. MADE IN U.S.A.
4 CYCLES X 70 DIVISIONS



DATE: 18 June 1971



is also indicated. Fragment ranges are reduced considerably for corresponding magnitudes of $W/C_D A$ when compared with Fig. 72, indicating that it is desirable to delay breakup as long as possible to reduce resulting fragment impact range envelopes.

CONCLUSIONS

The foregoing separation and entry analysis was based on an assumed LH_2 droptank configuration with an aerodynamically symmetric cross-section and with slight center of gravity offsets. Given a set of orbit conditions, separation and retro velocities, and nominal angular rates, the tank tumbles until it encounters the sensible atmosphere at which time it begins total angle of attack convergence to a trim attitude of $\eta = 40$ degrees. The body experiences a slight precessing motion about the aerodynamic (relative) velocity vector which slows down as trim η is approached. Total range to impact is from 1900 nm to 6000 nm depending on assumed retro location.

Considering now, a non-aerodynamically symmetric body, the results represent optimistic entry characteristics since the symmetric aero-properties of the assumed droptank make performance predictions somewhat simpler. An asymmetric body would also trim to some angle of attack, but orientation of total force vector may be either in or out of the trajectory plane. Furthermore, body dynamic motion becomes increasingly complicated adding to the requirements for sound structural/thermal design.

Several conclusions to general tank design can be made based on results of this analysis. They are as follows:

- Tank design should provide minimum aerodynamic stability to delay η -convergence as long as possible. Related loads, range and dispersions will be minimized.
- Separation characteristics relating to coast before retro initiation require additional analysis to optimize tolerable angular rates with separation distance requirements and separation velocity.
- Extreme retro pitch attitudes affect orbiter performance, therefore, θ_R should be relatively low (below approximately 30 degrees).
- Higher retro velocities offer advantages of shorter range and reduced dispersions.
- Indian Ocean impact locations are practical for all the shuttle missions considered. Perigee-retro is only practical for WTR launched orbits or 28.5 deg inclined orbits launched from ETR.
- Non-retro entry is possible from perigee of orbits 1 and 4 but must be made with a tumbling body.
- Orbit elements, retro conditions and droptank c.g. characteristics are critical contributors to impact range dispersions.
- An elliptic dispersion envelope with axes of 2020 nm and 400 nm will contain all predicted range errors and most of the anticipated fragment impact locations.

REFERENCES

1. "Gravitational Constants Being Used by the Astrodynamics Department," R. J. Yoo, IDC 55-31-181, Lockheed Missiles and Space Co., Sunnyvale, Ca., 30 Sept 1965.
2. "Influence of Solar Activity on Atmospheric Density and Its Impact on Space Design," S. K. Lew, LMSC/D006304, (TM 62-12-002), Lockheed Missiles and Space Co., Sunnyvale, Ca., 9 January 1970.
3. "Prediction Curve For $\bar{F}_{10.7}$ For The Remainder of the Twentieth Sunspot Cycle (February 1970 Update)," S. K. Lew, IDC 62-12/155, Lockheed Missiles and Space Co., Sunnyvale, Ca., 2 February 1970.
4. "External Droptank Orbital System Ascent Trajectories For 50 X 100 NM Orbit Injection," E. T. Fitzgerald, EM L2-12-05-M1-6, Lockheed Missiles and Space Co., Sunnyvale, Ca., 7 June 1971.
5. "Effects of Earth Oblateness Atmospheric Drag on a Space Shuttle Vehicle in Low Perigee Orbits," L. A. Bleich, EM No. L2-12-05-M1-7, Lockheed Missiles and Space Co., Sunnyvale, Ca., 7 June 1971.
6. "Mass Property Estimates For Orbiter External LH_2 Tank," R. A. Byers, EM No. L2-12-M1-1, Lockheed Missiles and Space Co., Sunnyvale, Ca., 3 May 1971.
7. "Hypersonic Arbitrary Body Aerodynamic Computer Program (Mark III Version)," A. F. Gentry, DAC 61552, Douglas Aircraft Co., April 1968.
8. "Retro Rocket Parametrics For Orbiter External LH_2 Tank," R. A. Byers, EM No. L2-12-01-M1-1, Lockheed Missiles and Space Co., Sunnyvale, Ca., 18 May 1971.
9. "Determination of Droptank Impact Hazards," R. R. Roush, EM L2-05-M3-2, Lockheed Missiles and Space Co., Sunnyvale, Ca., 22 Mar 1971.
10. "A Study of Maritime Mobile Satellites - Volume I - Merchant Vessel Population/Distribution Present and Forecast," DOT-CG-00505A(1), Automated Marine International, Newport Beach, Ca., 1 Sept 1970.
11. "Gas Generator-Piston Separation Analysis for the Orbiter External LH_2 Tank," R. A. Byers, EM No. L2-12-02-M1-1, Lockheed Missiles and Space Co., Sunnyvale, Ca., 12 May 1971.

Appendix A

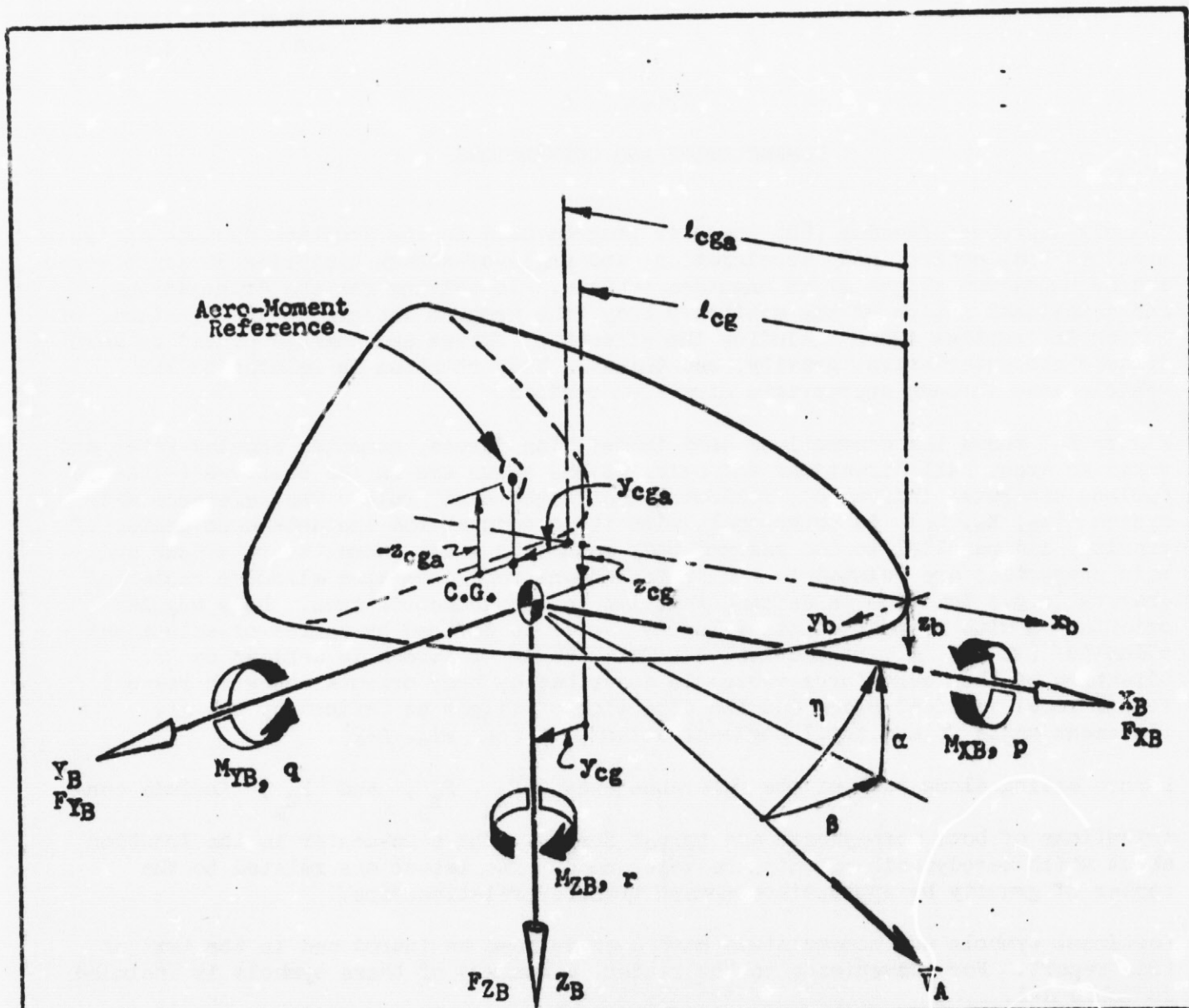
NOMENCLATURE AND CONVENTIONS

The six-degree-of-freedom (6D) computer program used in the droptank dynamic analysis predicts body motion, body acceleration, and angle-of-attack histories during powered and/or unpowered flight of an unguided vehicle. In solving for the translational and rotational motion of the arbitrary body, the program integrates the equations of motion in inertial space including the effects of forces and moments caused by aerodynamic characteristics, gravity, and thrust. Body rotation is related to the vehicle axes through appropriate direction cosines.

Figure A-1 shows the conventions used in defining forces, moments, angular rates and vehicles axes. All directions and orientations shown are in the positive (+) sense (unless otherwise indicated), following the "right-hand" rule. The reference axis system (X_B , Y_B , Z_B) is orthogonal, with its origin at the instantaneous center of gravity, and parallel to the assumed body geometric axes. Moments, rotations and mass properties are related to the instantaneous reference axes although center of gravity (c.g.) location is defined relative to the geometric axes. Body angular orientation with respect to the velocity vector is defined by angles-of-attack and sideslip (α and β , respectively). Total angle of attack is defined by η . Direction of the aero-force vector is described by body orientation with respect to the local vertical plane and the direction of flight as defined by the displacement angle X and total angle-of-attack, η (see Fig. A-2).

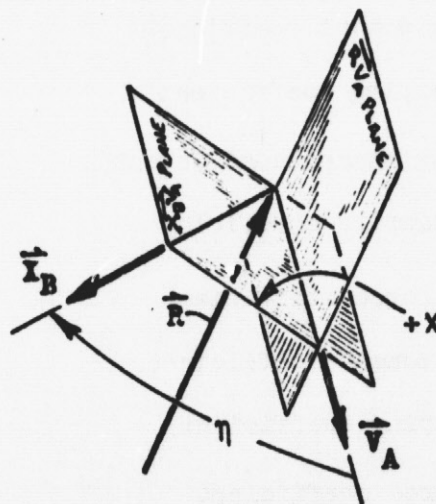
Forces acting along each of the reference axes (F_{X_B} , F_{Y_B} , and F_{Z_B}) include contributions of both aerodynamic and thrust forces. The aero-center is the location about which aerodynamic moments are referenced. The latter are related to the center of gravity by appropriate moment transfer relationships.

Pertinent symbols and nomenclature have been defined as introduced in the text of this report. For convenience to the reader, a summary of these symbols is included in Table A-1.



- | | |
|--------------------------------|---|
| X_B, Y_B, Z_B | Instantaneous Body Reference Axes (Origin at C.G.) |
| x_b, y_b, z_b | Body Geometric Axes (Parallel to Reference Axes) |
| F_{XB}, F_{YB}, F_{ZB} | Force Components Along (Parallel to) Body Reference Axes |
| M_{XB}, M_{YB}, M_{ZB} | Moment Components About Body Reference Axes |
| l_{cg}, y_{cg}, z_{cg} | Center of Gravity (C.G.) Location Relative To Geometric Axes |
| $l_{cg_a}, y_{cg_a}, z_{cg_a}$ | Aero-Moment Reference Location Relative To Geometric Axes |
| p, q, r | Angular Rates Along Reference Axes Relative To Inertial Reference |
| α, β, η | Angle of Attack, Angle of Sideslip, Total Angle of Attack |
| \vec{V}_A | Aerodynamic (Relative) Velocity Vector |

FIG. A-1 DEFINITION OF REFERENCE AXES, FORCES, MOMENTS, AND ROTATIONS
A-2



- \vec{R} Radius vector from Inertial Reference to body center of mass.
- \vec{V}_A Aerodynamic (relative) velocity vector
- \vec{X}_B Instantaneous body longitudinal reference axis
- η Total angle of attack
- x Angular displacement of $\vec{X}_B \vec{V}_A$ -plane from $\vec{R} \vec{V}_A$ -plane

FIG. A-2 DEFINITION OF BODY AXIS DISPLACEMENT ABOUT AERODYNAMIC (RELATIVE) VELOCITY VECTOR

NOMENCLATURE

<u>Symbol</u>	<u>Definition</u>	<u>Units</u>
A, A_{ref}	Reference area	ft^2
C_A	Axial force coefficient	-
C_D	Drag Coefficient	-
c.g.	Center of gravity	-
C_l	Rolling moment coefficient	-
C_{l_p}	Roll damping coefficient	-
C_m	Pitching moment coefficient	-
C_{m_q}	Pitch damping coefficient	-
C_N	Normal force coefficient	-
C_n	Yawing moment coefficient	-
C_{n_r}	Yaw damping coefficient	-
C_Y	Side force coefficient	-
DR	Downrange from staging point	nm
$F_{A_{X_B}}$	Aero-force along X_B -axis ($= -C_A \bar{Q} A_{ref}$)	lb
$F_{A_{Y_B}}$	Aero-force along Y_B -axis ($= C_Y \bar{Q} A_{ref}$)	lb
$F_{A_{Z_B}}$	Aero-force along Z_B -axis ($= -C_N \bar{Q} A_{ref}$)	lb
$F_{T_{X_B}}, F_{T_{Y_B}}, F_{T_{Z_B}}$	Thrust forces along body ref. axes	lb
F_{X_B}	Force along body X_B - axis $\left(= F_{A_{X_B}} + F_{T_{X_B}} \right)$	lb
F_{Y_B}	Force along body Y_B - axis $\left(= F_{A_{Y_B}} + F_{T_{Y_B}} \right)$	lb

NOMENCLATURE (Continued)

<u>Symbol</u>	<u>Definition</u>	<u>Units</u>
F_{Z_B}	Force along body Z_B - axis $\left(= F_{A_{Z_B}} + F_{T_{Z_B}} \right)$	lb
H	Altitude	ft
I	Orbit inclination angle	deg
I_{SP}	Specific impulse	sec
I_{tot}	Total impulse	lb-sec
I_x	Roll moment of inertia	slug-ft ²
I_y	Pitch moment of inertia	slug-ft ²
I_z	Yaw moment of inertia	slug-ft ²
I_{xy}, I_{xz}, I_{yz}	Products of inertia	slug-ft ²
L/D	Lift-to-drag ratio	-
L_{ref}	Reference length	ft
l_{cg}	Longitudinal c.g. location (aft of nose ref.)	ft
l_{cga}	Longitudinal location of aero-moment reference (aft of nose ref.)	ft
M_{X_B}	Moment about X_B -axis $\left(= M_{A_{Y_B}} + M_{T_{X_B}} \right)$	ft-lb
M_{Y_B}	Moment about Y_B -axis $\left(= M_{A_{Y_B}} + M_{T_{Y_B}} \right)$	ft-lb
M_{Z_B}	Moment about Z_B -axis $\left(= M_{A_{Z_B}} + M_{T_{Z_B}} \right)$	ft-lb
$M_{A_{X_B}}$	Aero-rolling moment	ft-lb
$M_{A_{Y_B}}$	Aero-pitching moment	ft-lb
$M_{A_{Z_B}}$	Aero-yawing moment	ft-lb

EM NO: L2-12-05-M1-8

DATE: 18 June 1971

NOMENCLATURE (Continued)

<u>Symbol</u>	<u>Definition</u>	<u>Units</u>
$M_{T_{X_B}}, M_{T_{Y_B}}, M_{T_{Z_B}}$	Thrust moments about body ref. axes	ft-lb
p	Roll rate about X_B -axis	deg/sec
\bar{Q}	Dynamic pressure	psf
\dot{Q}_s	Laminar stagnation point heat rate	Btu/ft ^{3/2} -sec
q	Pitch rate about Y_B -axis	deg/sec
\vec{R}	Radius vector from inertial reference to body center of mass	ft
r	Yaw rate about Z_B -axis	deg/sec
T_V	Vacuum thrust	lb
t	Time from separation	sec
V_A	Aerodynamic (relative) velocity	fps
V_I	Inertial (orbit) velocity	fps
V_R	Retro velocity	fps
V_S	Separation velocity	fps
W	Weight	lb
X_B, Y_B, Z_B	Body reference axes	-
x_b, y_b, z_b	Body geometric axes	-
y_{cg}	Lateral c.g. displacement from x_b -axis	ft
y_{cga}	Lateral displacement of aero-moment reference from x_b -axis	ft
z_{cg}	Vertical c.g. displacement from x_b -axis	ft
z_{cga}	Vertical displacement of aero-moment reference from x_b -axis	ft
α	Angle-of-attack	deg
β	Angle of sideslip	deg

NOMENCLATURE (Continued)

<u>Symbol</u>	<u>Definition</u>	<u>Units</u>
γ_I	Inertial flight path angle	deg
γ	Aerodynamic (relative) flight path angle	deg
θ_R	Retro pitch angle	deg
θ_T	Thrust pitch misalignment angle	deg
η	Total angle of attack	deg
Λ	Geodetic latitude	deg
λ	Geocentric latitude	deg
τ_E	Earth longitude	deg
χ	Displacement (bank) angle from \vec{V}_A R plane	deg
$\dot{\chi}$	Precession rate about \vec{V}_A	deg/sec
ψ_R	Retro yaw angle	deg
ψ_T	Thrust yaw misalignment angle	deg
$(\vec{})$	Vector	

Subscripts

ave	Average
max	maximum or peak magnitude
o	Initial condition
opt	Optimum

Appendix B

LH₂ DROPTANK AERODYNAMIC CHARACTERISTICS

Aerodynamic force, moment and damping coefficient data are shown in Figures B-1 through B-4. The data are presented as a function of total angle of attack* ($0 \leq |\eta| \leq 180$ deg) altitude, H, and Mach number for continuum flow regimes and as a function of η in free molecule flow. (The roll damping coefficient was assumed zero and therefore not included.) Reference parameters pertinent to the coefficients are as follows:

$$\text{Reference area, } A_{\text{ref}} = 154 \text{ ft}^2$$

$$\text{Reference length, } L_{\text{ref}} = 86.6 \text{ ft}$$

$$\text{Aero-moment center, } l_{cg_a} = 34.8 \text{ ft}$$

$$y_{cg_a} = 0.38 \text{ ft}$$

$$z_{cg_a} = 0.01 \text{ ft}$$

*See Appendix A, Fig. A-1 for the relationship of η to angles of attack and sideslip (α and β respectively) and the aerodynamic, or relative velocity vector, \vec{V}_A .

PREPARED BY
DATE June 1951
CHECKED BY

LOCKHEED MISSILES & SPACE COMPANY
A GROUP DIVISION OF LOCKHEED AIRCRAFT CORPORATION

PAGE
MODEL
REPORT NO. EM No. 1, -1,
05-M1-8

REF AREA = 15.4 FT²
REF LENGTH = 86.6 FT.
AERO-MOMENT CENTER, x_{cg} = 24.8 FT
 y_{cg} = 0.29 FT
 z_{cg} = 0.01 FT.

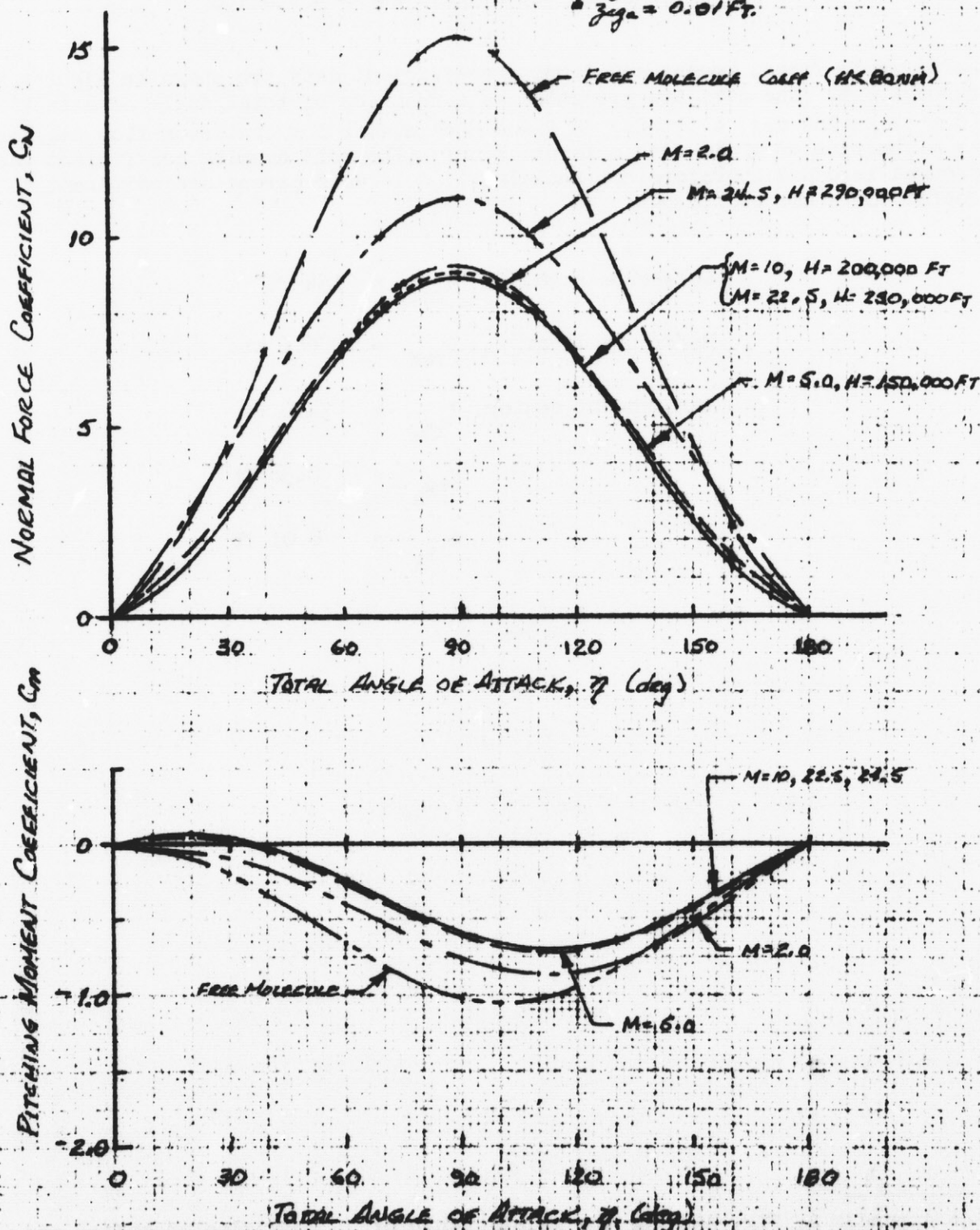


FIG. B1. DROP TANK NORMAL FORCE AND PITCHING MOMENT COEFFICIENTS VS. TOTAL ANGLE OF ATTACK.

PREPARED BY: June 1957
 DATE: June 1957
 CHECKED BY:

LOCKHEED MISSILES & SPACE COMPANY
 A GROUP DIVISION OF LOCKHEED AIRCRAFT CORPORATION

PAGE 1
 MODEL LM No: 1-1
 REPORT NO. 05-M1-8

REF AREA = 15.4 FT²
 REF LENGTH = 86.6 FT.
 AERO-MOMENT CENTER, x_{cg} = 34.8 FT
 y_{cg} = 0.28 FT
 z_{cg} = 0.01 FT

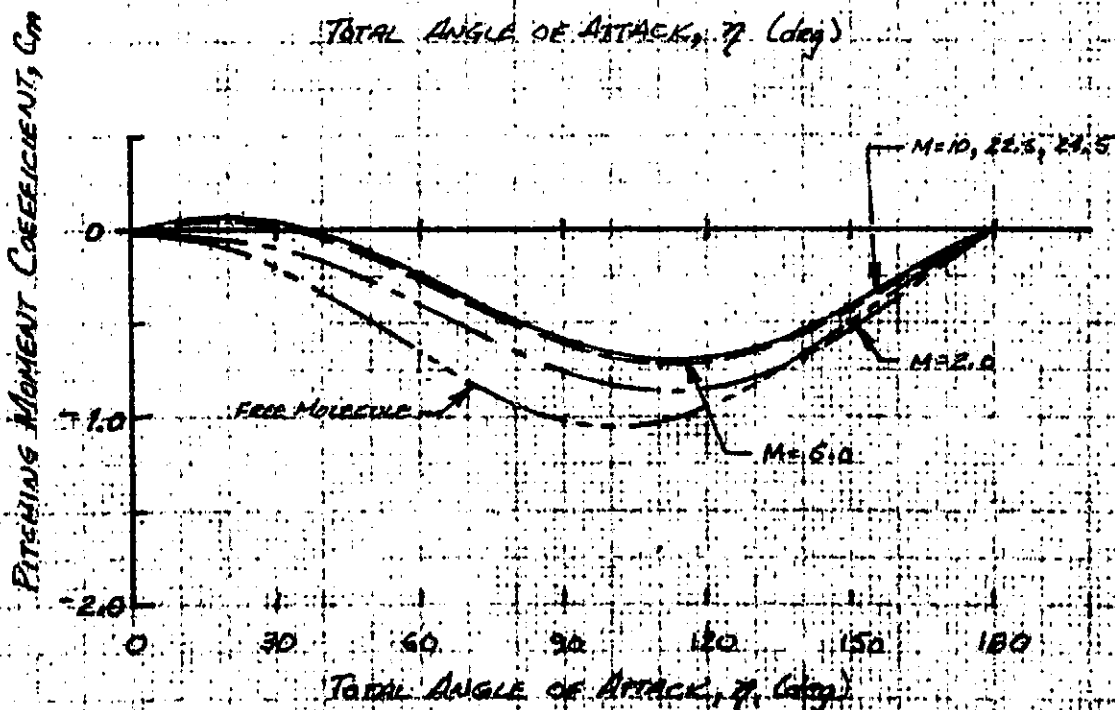
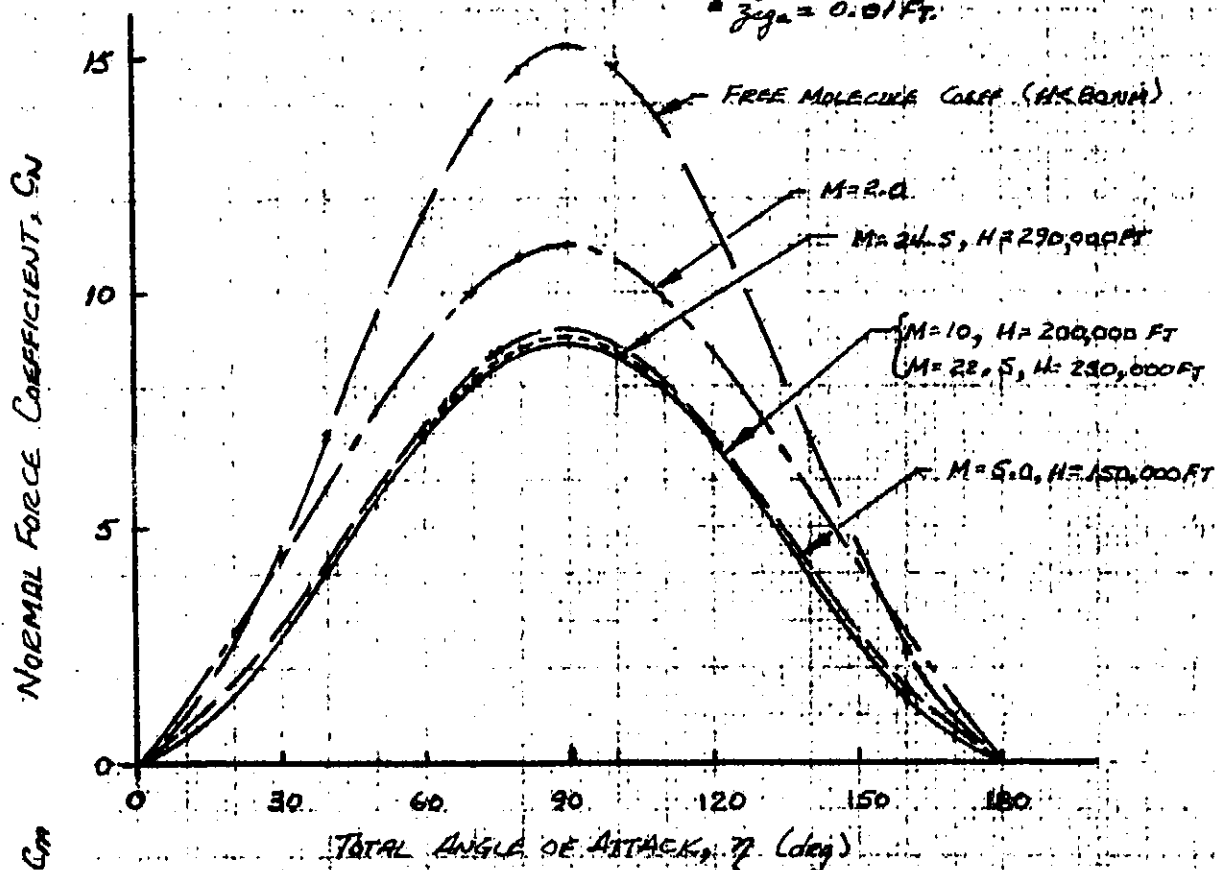


FIG. B1 DROP TANK NORMAL FORCE AND PITCHING MOMENT COEFFICIENTS VS TOTAL ANGLE OF ATTACK

DATE 10/10/54
CHECKED BY

LOCKHEED MISSILES & SPACE COMPANY
A GROUP DIVISION OF LOCKHEED AIRCRAFT CORPORATION

MODEL
REPORT NO.

Ref. Area: 154 FT²

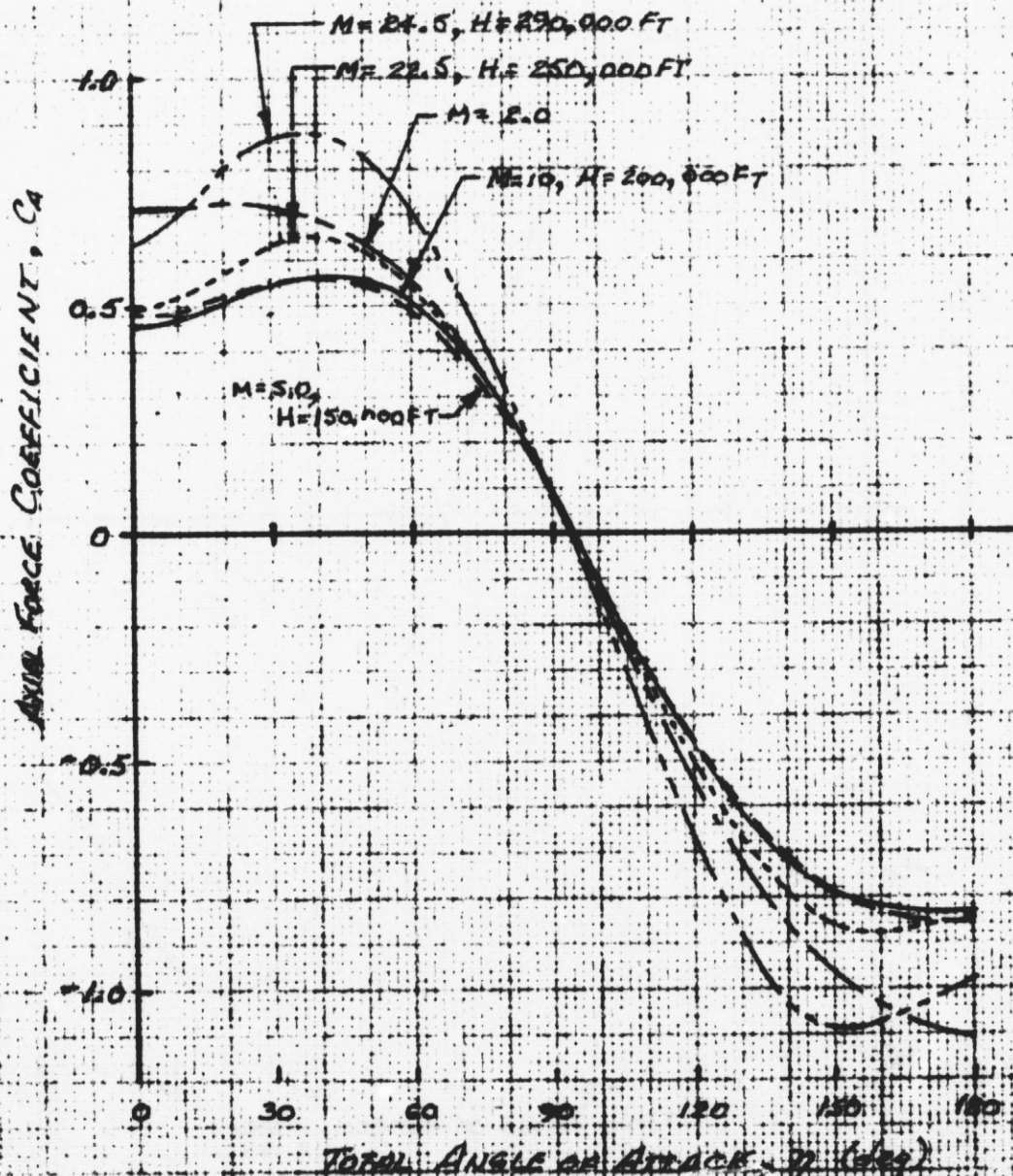


FIG B2 AXIAL FORCE COEFFICIENT VS. TOTAL ANGLE OF ATTACK - CONTINUUM FLOW

PREPARED BY _____
 DATE 13 June 57
 CHECKED BY _____

EM NO: 12-12-05-M2-8
LOCKHEED MISSILES & SPACE COMPANY
 A GROUP DIVISION OF LOCKHEED AIRCRAFT CORPORATION

PAGE _____
 MODEL _____
 REPORT NO _____

REF AREA: 154 FT²
 (H > 80 NM)

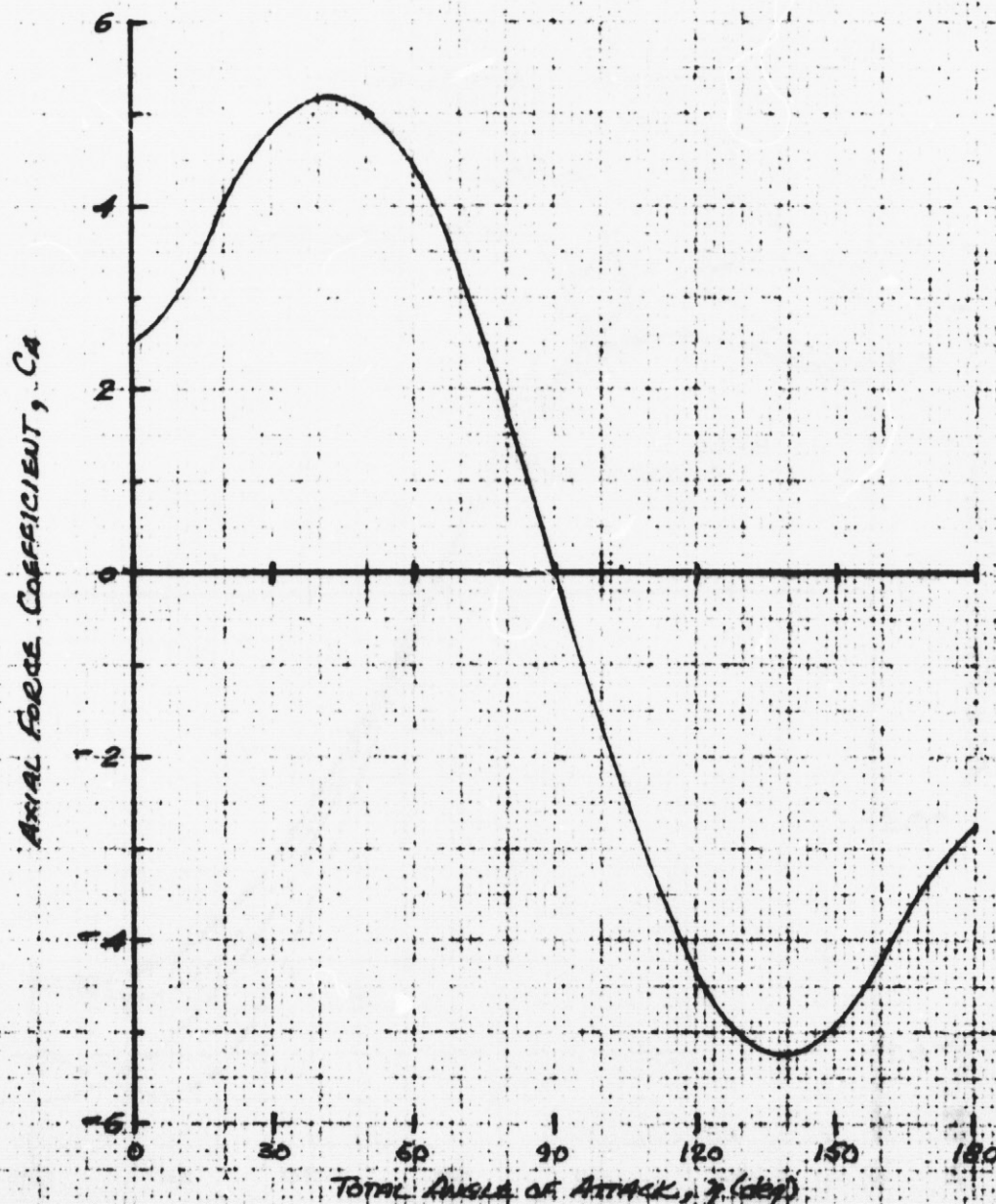


FIG 83 AXIAL FORCE COEFFICIENT VS TOTAL ANGLE OF ATTACK - FREE MOLECULE FLOW

PREPARED BY
DATE 18 June 1971
CHECKED BY

EM NO: 12-12-05-M1-8
LOCKHEED MISSILES & SPACE COMPANY
A GROUP DIVISION OF LOCKHEED AIRCRAFT CORPORATION

PAGE
MODEL
REPORT NO

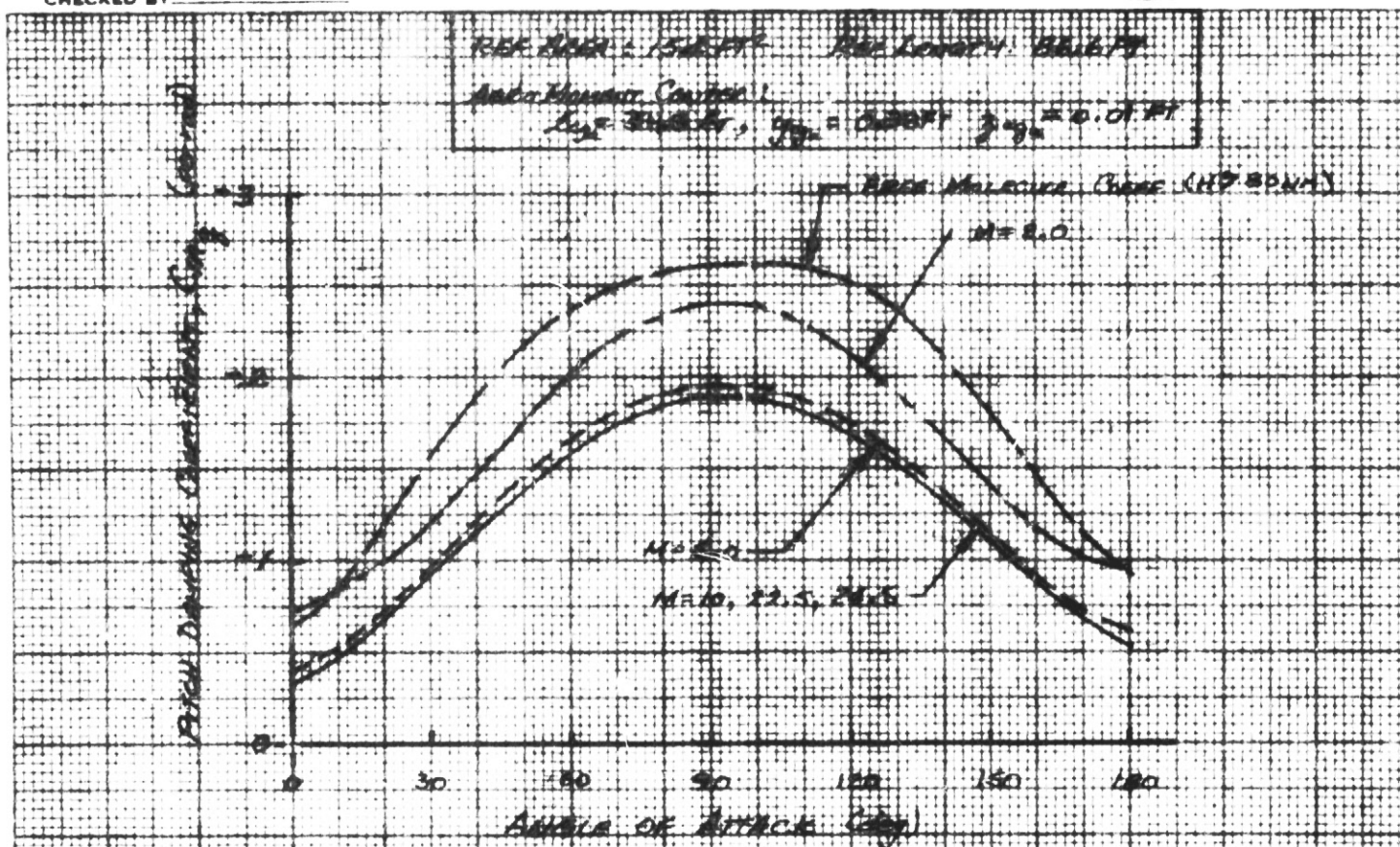


Fig. 34 Pitch Damping Coefficient vs. Angle of Attack

ENGINEERING MEMORANDUM

TITLE: PERFORMANCE AND DESIGN REQUIREMENTS FOR THE EXTERNAL LIQUID HYDROGEN DROPTANK	EM NO: 1.2-12-M1-3 REF: DATE: 20 June 1971
AUTHORS: L. Harris	APPROVAL: ENGINEERING SYSTEM ENGRS <i>C.A. Byers</i>

PROBLEM STATEMENT

Establish the requirements and basic restraints/constraints imposed on the design for External Liquid Hydrogen (LH₂) Droptank. The droptank is used to provide storage for the propellant (LH₂) used in the propulsion system of an orbiter.

RESULTS

The performance and design requirements are presented in a format similar to a CEI (Contract End Item) Specification.

AFFECTED WORK BREAKDOWN STRUCTURE ELEMENTS

- Performance Requirements
- Design Requirements
- Quality Assurance Provisions

ASSUMED CONDITIONS

The droptank requirements presented in this EM are based on a design generated by Lockheed Missiles & Space Co. (LMSC) for a droptank used in connection with the GAC orbiter documented in SKT 100723

DISCUSSION OF RESULTS1.0 SCOPE

1.1 General. This EM establishes the requirements and basic restraints/constraints imposed on the design for External Liquid Hydrogen (LH₂) Droptank, hereinafter referred to as the droptank.

1.2 Function. The droptank is used to provide storage for the propellant (LH₂) used in the propulsion system of an orbiter.

2.0 APPLICABLE DOCUMENTS. (To be determined)3.0 REQUIREMENTS3.1 Performance

3.1.1 Ascent. The droptank shall be capable of withstanding the ascent environments to reach a 50 x 100 nm orbit.

3.1.2 Tank Capacity. The LH₂ weight per droptank shall be 56,654 lb at 37 deg R at 4.274 lb per cu ft. plus a 3 percent ullage volume allowance.

3.1.3 Tank Attachment and Separation.

3.1.3.1 Detailed Interface.

3.1.3.1.1 Electrical. The electrical interface shall be as specified in EM No. L2-12-03-M1-1 and L2-12-03-M1-2.

3.1.3.1.2 Mechanical. The mechanical interface shall be as specified in Drawing No. SKG 100719.

3.1.3.2 Separation. The droptank shall be capable of separating from the orbiter during the 50 by 100 nm orbit coast in a nominal time of 0.2 sec, at a velocity of 35 fps, and an angular deviation of ± 1 deg maximum, ± 3 deg per sec maximum. Orbiter attitude shall be with nose rotated downward, in the plan of motion, to an angle of $127 \text{ deg} \pm 1 \text{ deg}$ with respect to the horizon.

3.1.4 Droptank Entry (at Retro-Rocket ignition). The rotation angle at retro-rocket ignition shall be limited to a maximum of 6 deg. An intact entry shall be required. The firing of the retro-rocket shall start as shown in Table I. The retro-rocket burn time shall be limited to a maximum of 5 sec and the thrust shall be commensurate with the tank weight and deorbit ΔV of 230 fps. The droptank should be configured to enter at a low trimmed angle of attack unless there is inherent neutral stability, in which case the droptank shall be configured as balanced as possible to encourage tumbling.

Table I

<u>Launch Site</u>	<u>Orbit Inclination (deg)</u>	<u>Time After Perigee Injection (Minutes)</u>
ETR	28.5	21.0
ETR	55.0	22.1
ETR	90.0	19.6
WTR	90.0	17.8

3.1.5 Thermal Protection System. The droptank shall have an insulation/ablator type thermal protection system. During ground hold, the thermal protection system shall be capable of keeping the outer surface of the insulation at a temperature sufficient to prevent excessive ice formation. During entry, the thermal protection system shall be sized to assure that the droptank remains intact.

3.1.6 Propulsion System

3.1.6.1 Pressurization and Venting. The propulsion system shall be capable of pressurizing and venting the droptank during prelaunch, ascent, and post separation and entry as follows:

3.1.6.1.1 Prelaunch. The droptank shall have the capability of a purge, chill, and fill operation through a ground coupling device. The droptank shall be capable of being purged through a pressurization and fill-coupling at a nominal pressure of 25 psia. After the droptank has been completely purged, it shall be capable of a chill and fill cycle, which shall consist of introducing LH_2 at a very slow rate at a nominal pressure of 25 psia. The droptank shall be capable of being vented during fill.

3.1.6.1.2 Ascent. The droptank valves shall be closed until an altitude of approximately 80,000 ft has been achieved, at which time the droptank shall have the capability of being vented to reduce vapor pressure of the upper layer of propellant. After separation from the booster, the droptank shall be capable of being pressurized with a gaseous hydrogen to a level which exceeds the rocket engine start NPSP (Net Positive Suction Pressure) requirement. The droptank shall be capable of maintaining adequate pressure to continuously satisfy engine NPSP requirement for steady state operation until shutdown (approximately 400 sec after liftoff).

3.1.6.1.3 Post Separation and Entry. Prior to droptank separation the venting pressurization, propellant feed and recirculation lines shall be isolated from the orbiter. After separation the droptank shall be capable of decreasing pressure to a level to assure an intact entry.

3.1.6.2 Propellant and Feed System.

3.1.6.2.1 Main Feed System. The main feed system shall be capable of filling the droptank on the ground and supplying the LH_2 to the orbiter during orbiter operation.

3.1.6.2.2 Recirculation System. The recirculation system shall be capable of maintaining the rocket engine pumps in a chilled condition on the ground and during booster operation until the orbiter is separated and the main rocket engines are started.

3.1.7 Electrical System

3.1.7.1 Input Power. The input power shall be furnished from batteries capable of furnishing a nominal 28 vdc at 110 amperes.

3.1.7.2 Instrumentation. The instrumentation shall be as specified in EM No. L2-12-03-M1-2.

3.1.7.3 Separation System. The electrical separation system shall be as specified in EM No. L2-12-03-M1-1.

3.2 Design and Construction. Design and construction of the droptank shall be in accordance with LMSC Drawing SKT 100723 and the following.

3.2.1 Design Load Criteria. The droptank shall be capable of withstanding the following loading environments:

- a. Maximum Bending Moment: 10^6 in. lb at 525 in. aft of the droptank nose
- b. Maximum Axial Acceleration: 3g

3.2.2 Weight. Weight of the droptank shall not exceed the following:

<u>Item</u>	<u>Weight (lb)</u>
Structure	3101
Insulation (Intact Entry)	3677
Separation System	85
Deorbit System	340
Propulsion System	694
Contingency	789
Total	<u>8686</u>

EM NO: L2-12-M1-3

DATE:

3.2.3 Dimensions. The dimensions of the droptank shall not exceed those specified on LMSC Drawing SKG 100719 and SKG 100721. The approximate length shall be 94.5 ft and a diameter of approximately 15 ft.

3.2.4 Nose Cone. The design of the nose cone shall be as shown on LMSC Drawing SKS 100718.

3.2.5 Separation System. The droptank shall be separated from the orbiter by two gas type generator devices located fore and aft in the attach struts. The dimensions shall not exceed 6 in. in diameter by 42 in. long. The nominal effective working pressure shall be 1000 psia. The gas generator grain temperature shall be limited to ± 20 deg each ± 3 percent on combustion pressure.

3.2.6 Storage. The droptank shall be designed to withstand storage for one year without degradation to the performance requirements specified herein.

3.3 Environmental. (To be determined)

4.0 QUALITY ASSURANCE PROVISIONS

4.1 Verification. Each requirement specified herein shall be verified by either inspection, analysis, demonstration, or test.

5.0 PREPARATION FOR DELIVERY. Not applicable.

ENGINEERING MEMORANDUM

TITLE: MATERIAL SELECTION FOR LIQUID HYDROGEN DROPTANK	PM NO: L2-12-01-M1-18 REF: DATE: 18 June 1971
AUTHORS: Elliott Willner	APPROVAL: ENGINEERING SYSTEM ENGINEER <i>R. A. Byers</i>

PROBLEM STATEMENT:

Select from candidate alloys materials for design and fabrication that would result in low cost, light weight, and high reliability liquid hydrogen drop tankage.

RESULTS

Two materials have been selected which meet the criteria for drop tankage: maximum reliability, minimum weight, and minimum cost. The two materials are aluminum alloy in the -T87 and -T81 temper, and the stainless steel alloy 301 in the extra full hard (XFH) temper.

DISCUSSION OF RESULTS

1.1 Material Considerations

Minimum cost, maximum reliability, and minimum weight are fundamental criteria for consideration in selection of a material from available candidates.

Basic Material Costs:

As a first approximation for the costing of materials the following tabulation indicates the relative range of cost for the as-received material prior to fabrication:

<u>Material</u>	<u>Cost Range (\$/lb)</u>
Aluminum Alloys	1-3
Austenitic Stainless Steel	
Magnesium Alloys	
Titanium Alloys	6-20
Glass Filament Winding	40-100
Carbon Composites	100-300
Boron Composites	
Wrought Beryllium	

Contributing Factors For Tank Reliability

Maximum reliability of a material for shuttle liquid hydrogen drop tankage must be predicated not only on experience but also on characterization and knowledge of the chemical and mechanical behavior of the processed product. Minimum cost to fabricate a product does not necessarily relate to the cost of the basic material because additional costs are required in the fabrication to assure maximum reliability as well as a minimum weight tank. To design a tank for minimum weight requires the application of a material and those processes which would provide for the maximum in reliability at minimum cost. For example, a material may demonstrate the highest strength to weight relationship for design of the lightest tank. However, this material may possess a low tolerance to imperfections. Consequently, the approach for manufacture would demand extremely sophisticated (costly) procedures to minimize flaws and of necessity the associated costs for non-destructive inspection would be high. Non-destructive inspection could never be absolute in assuring the tank would be free from deleterious flaws. Proof testing is the only positive

method to detect assuredly deleterious flaws. Nevertheless, on proof testing, the tank must not fail catastrophically if the candidate material does possess a flaw. Sole reliance on the proof test to screen fabricated high strength-to-weight tankage that has a low tolerance for flaws, when the probability of their presence is high, can be a very costly procedure.

Alternatives would include increasing the thickness of the high strength-to-weight material to effectively operate and be proof tested at lower stress levels in order to provide a tolerance level for imperfections, or implement tankage design with a candidate material that not necessarily compromises weight, but assures both maximum reliability with attendant tolerances to imperfections and minimum cost.

This philosophy is the basis from which the evaluation of candidate materials have been analyzed. Where discrete fracture toughness test data are not available as for the case of the Magnesium alloys, other comparable indicators are used, i.e., notched-to-unnotched tensile strengths.

On the basis of strength-to-weight ratios in conjunction with fracture toughness, three classifications of alloys offer the most promise for cryogenic tankage. They are (1) aluminum alloys that contain copper, (2) alpha phase titanium alloys, and (3) cold worked stable and meta stable stainless steels. These three alloy systems exhibit the highest strength-to-weight ratios. Recent experimental efforts have been devoted to determining the fracture toughness, threshold stress intensity factors and cyclic flaw growth behavior of the more promising alloys. These include aluminum alloys 2219, 2021, 2014, titanium alloy Ti-5Al-2.5Sn fracture toughness for the materials were evaluated at -423°F (Liquid Hydrogen), -320°F (Liquid Nitrogen), and ambient air in all of the referenced studies. Only crude estimates can be made in terms of plane strain threshold stress intensity for the fracture toughness behavior for the cold worked stainless alloy 301KFH. These estimates are based on plane stress fracture toughness and notched-to-unnotched tensile strength.

Date: 18 June 1971

Rationalization For Alloy Selection

Analysis of available information indicates that for material thicknesses required for drop tank usage, aluminum alloy 2219 in either the -T81 or -T87 tempers has a distinct advantage over the Ti-5Al-2.5 Sn, see Tables I, II, III, IV, and V, and Figures I and 2. The advantage is based largely on the disparity on the flaw growth behavior of the alloys.

Other alloy considerations will be discussed later. In addition to the obvious economic advantages of fabricating the drop tank from the aluminum alloy 2219, another prime consideration to substantiate this selection relates to a comparison of sizes for initial allowable imperfections. With all material design configurations assumed to be equivalent (which they are not because of mill suppliers limitations -- to be discussed in a later section), the lightest vessel that could be built would be made from the titanium alloy. However, the maximum allowable flaw size, i.e., the critical flaw size at the proof stress, will be smaller than a similar 2219-T87 structure and, more than likely, too small to detect by presently available non-destructive testing techniques. See Figure II. With undetected flaws in excess of the maximum allowable flaw size, a distinct possibility arises that some of the pressure vessels made of the titanium alloy can be expected to fail during proof test. The same arguments may be presented for application of cold worked stainless 301XFH. Although no discrete -423°F plane strain stress intensity information is available for 301XFH, plane stress data and notched-to-unnotched tensile strength indicates the capacity to withstand the influence and detection of small flaws at -423°F . See Figure II. Because of weight savings at low cost, 301XFH is considered as candidate. However, discrete testing should be performed to characterize actual flaw size allowables.

Titanium alloys might be considered where the lightest weight vessel would be absolutely mandatory. Not only is titanium more expensive to procure as a raw material, requirements for welding are extremely demanding. Welding large structures in an atmospheric environment creates the hazard of interstitial elements contaminating the weld regardless of any sophisticated inert atmosphere

shield that may be employed. Therefore, with the high probability that contamination will occur and also that macroscopic mechanical imperfections may be created beyond the capacity for detection by non-destructive techniques, give sufficient logic to discard titanium alloys as candidates for the liquid hydrogen drop tankage. Further, as noted, the costs for manufacturing would demand sophisticated procedures and these would be approximately five-fold those for the aluminum or stainless tankage.

Consequently, the alloy selection may be narrowed to the aluminum alloy 2219 in either the -T87 or -T81 temper or possibly the stainless alloy 301 in the extra-full-hard condition (60 percent cold work).

The 2219-T87 or -T81 may be used for the cylindrical section and the 2219-T81 or 2219-T87 for tank ends dependent on final design configuration and manufacturing processes used. Simplicity for processing cylinders will relate to welding cylinders from the as-received 2219-T8X stock. No heat treatment of cylinders would be required.

The end sections may require intermediate thermal treatments, and these heat treatments would obviously relate to processing the final configuration. The processes are well established and fully understood. However, manufacturing of complex configurations to the 2219-T87 condition will require special and possibly costly procedures. It is far more economically advantageous to fabricate to the final 2219-T81 condition for acceptable properties with equal reliability at low costs. The -T87 temper requires a minimum of 6 percent strain, whereas the -T81 requires only 1 percent of strain.

The 2219 alloy is readily weldable by both fusion and resistance welding methods. Reliability is further enhanced by the probable occurrence of fewer imperfections in conjunction to the "forgiveness" or tolerance of the material to imperfection (discussed previously).

The alloy readily lends itself to forming, or machining either by mechanical or chemical means,

Lockheed Missiles & Space Co. has developed a special starting temper for the aluminum alloy when complex forming processes are employed. This condition permits in-process thermal treatment for stress-relieving when subsequent operations are required. The significance of this starting temper, designated -H210, permits complex forming operations without suffering intermediate forming problems associated with grain coarsening or attendant degradation to ductility after final heat treatment prior to finishing to either the -T81 or -T87 tempers are required.

Utilization of 30LXFH would follow the same pattern outlined for the 2219 aluminum alloy. However, strengthening cannot be achieved by heat treatments. Nevertheless, in process thermal treatments may be necessary to enhance fabricability of end or complex sections. Further, limitations will be imposed upon complex tank-end configurations. The 30LXFH will lend itself readily to cylinder-type fabrication; compound or complex configurations may be formed to generous radii and then joined.

Fusion welding of 30LXFH causes creation of a heat affected zone and a lowering of mechanical properties and sensitization. Weldments will require roll planishing to overcome this degradation. Sensitization is a condition that may be conducive to intergranular corrosion if exposed to an aggressive marine atmosphere. Nevertheless, many years of space vehicle experience in such environments indicates the problem, if any, is minimal. The 30LXFH although it is basically an austenitic alloy does convert to some degree of martensite on cold working. This condition causes the material to become ferromagnetic. Final selection of a material for the shuttle system must recognize this phenomenon to avoid electromagnetic flight systems interference, if any.

Also, dependent on final design and process selection 30LXFH may also be readily resistance-welded.

Date: 18 June 1971

Selection of the aluminum alloy 2219 in the -T87 and -T81 tempers as well as the 301XFH relates to reliability, cost, and weight. Both these candidate materials have been used extensively in space vehicle cryogenic application. Final design must of necessity have limitations established for acceptable imperfections. In the case of 2219 much effort has been performed and reported. Similarly much effort has been expended on characterizing the 301XFH. However, a limited effort should be undertaken to establish threshold stress intensity limitations for the 301 XFH.

Other Alloys Considered

A new alloy of the aluminum-copper family, designated 2021, shows even greater promise than 2219 as a cryogenic tankage material. The alloy possesses a strength-to-weight ratio that is greater than 2219. Information on the fabrication characteristics as well as fracture toughness data indicate the alloy is comparable to 2219 in every category. The advantage of the 2021 over 2219 is that the new alloy does not require for its strength a predetermined degree of cold work or strain. An area that requires further exploration is a definitive analysis of the need to post-weld age. Initial development revealed freedom from stress corrosion cracking after postweld aging; however, later work revealed that processing parameters for the weldment may be the cause of such tendencies without the benefit of postweld aging. More recent work has presented the argument that excessive heat on welding the aluminum copper systems, whether it is 2219 or 2021, would reduce its capacity to withstand stress corrosion cracking regardless of postweld aging. Nevertheless, lacking a comprehensive program or real experience for comparative analysis, the need for postweld aging negates any strength advantages of the 2021 because of the increased processing costs.

Aluminum alloy 2021 might be a candidate except for the added cost required for postweld aging processes or the additional characterization required to eliminate this as a requirement. Advantages might be gained to use 2021 for

tank ends if no postweld aging were required. Maximum strengths could then be achieved at minimal manufacturing costs. For these reasons the material has been considered as a candidate for the study, but of necessity is deleted from further evaluation.

Another aluminum-copper alloy that has found application as a cryogenic tank-age material is 2014. However, some difficulty is encountered in joining the alloy by means of fusion welding and is therefore given no further consideration.

Although much is known about the 5XXX magnesium aluminum series of alloys, the poor tensile yield strength-to-weight ratios at cryogenic temperature give cause to eliminate the 5456-H321 as candidate. The alloy also requires a predetermined percentage of cold work for its basic strength, and this requirement too makes the material unattractive particularly by restricting the design and subsequent fabrication of the tank ends resulting in weight penalties.

The magnesium alloys which are also tabulated Table I and graphically illustrated in Figure I reveal strength to weight advantage based on ultimate strength. However, two other factors give cause for discrimination. Tensile yield strength-to-weight ratios are low, and above all, its fracture toughness based on notched-to-unnotched tensile strength is extremely low at cryogenic temperatures. Thus, the loss for cryogenic reliabilities negates its potential, unless a specific effort is undertaken to characterize the stress intensity fracture toughness for the ZEL0A-H24, and this may only further prove the alloy to be a poor candidate for cryogenic usage.

Conclusion

Two candidate materials have been selected which meet the criteria for drop tankage: Maximum reliability, minimum weight, and minimum cost. The two materials are aluminum alloy 2219 in the -T87 and -T81 temper, and the 301XFH.

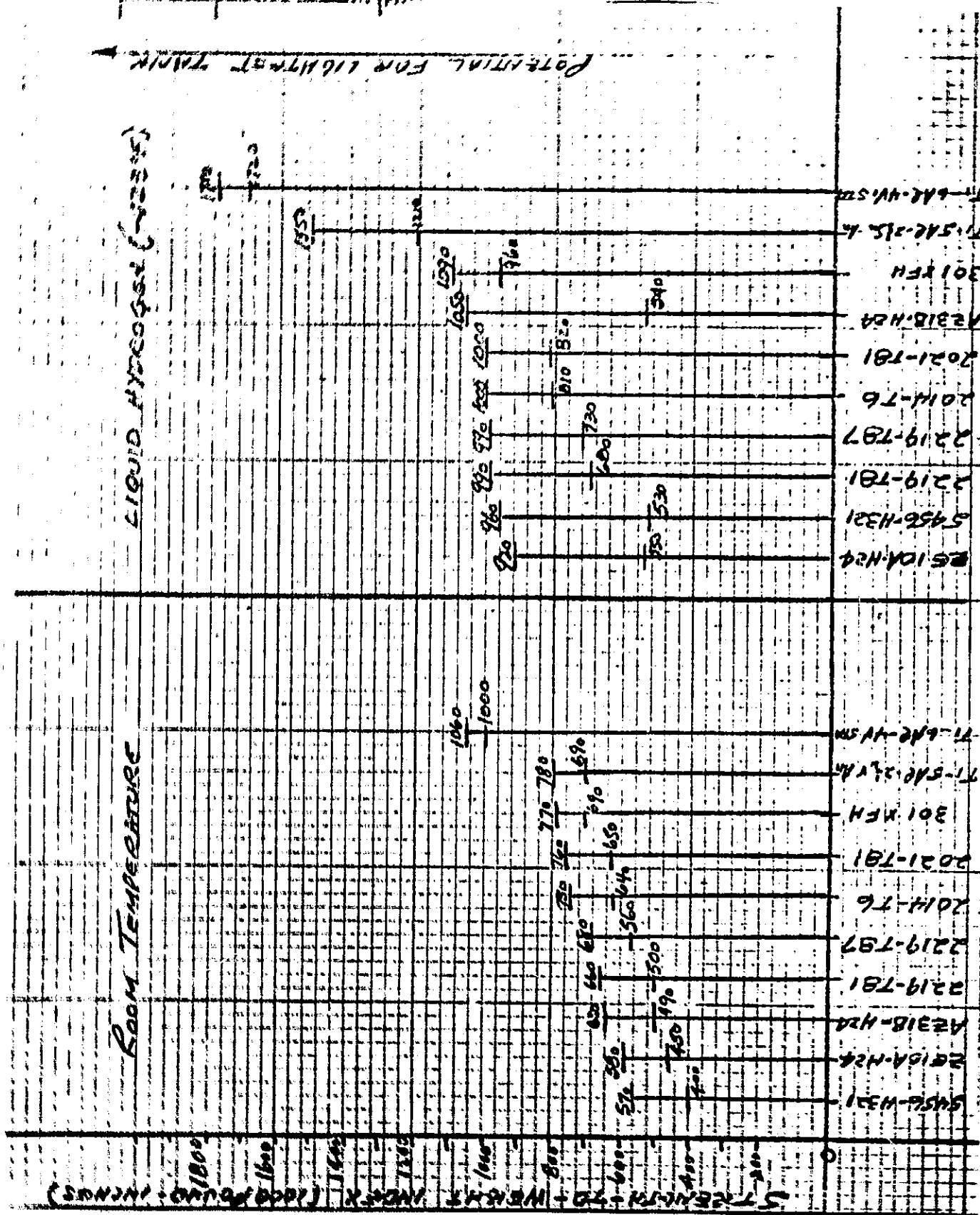
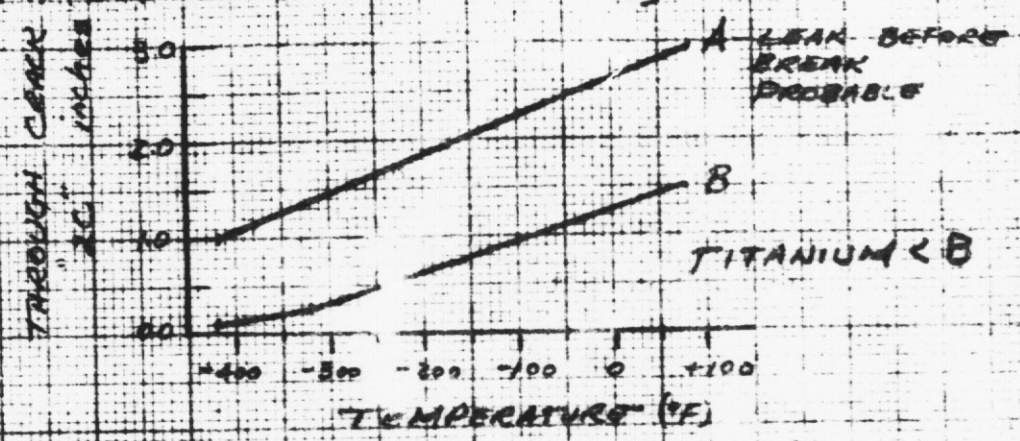
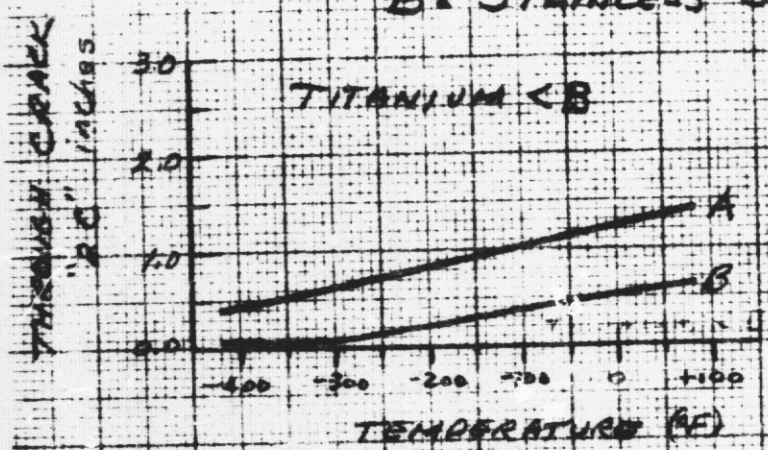
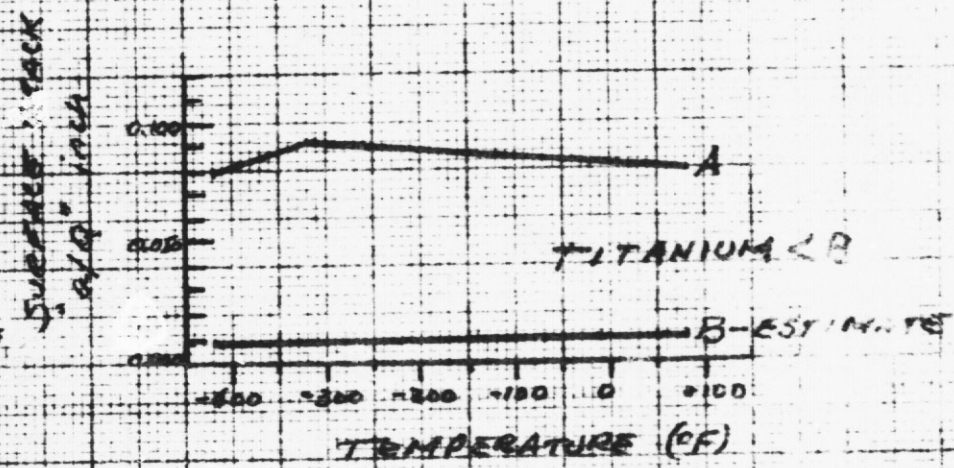
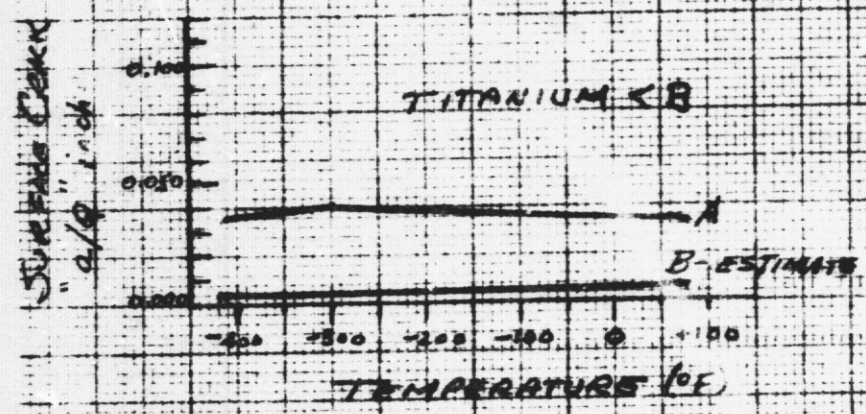


Fig. 1 Strength to Weight Comparison for Candidate Alloys for LH₂ Droptank

A = ALUMINUM ALLOYS 2219-T81, 2219-T87, AND 2021-T81 (0.003 inch)
 B = STAINLESS 301 XEH (60% COLD WORK) - 0.025 inch



($a_c = \frac{1}{2}$ LENGTH OF FLAW)



PROOF TEST
 CRITICAL CRACK SIZE

PROOF STRESS = YIELD STRENGTH

OPERATING APPLICATION
 CRITICAL CRACK SIZE

STRESS = $\frac{2}{3}$ YIELD STRENGTH

a = DEPTH OF FLAW; Q = SHAPE FACTOR

Fig. 2 Approximate Allowable Flaw Sizes for Thin Wall Droptank

EM NO. 12-12-01-M-18
 Date: 18 June 1971

EM NO: 12-12-01-M1-18
DATE: 18 June 1971

Table I
Comparison of Candidate Alloys -- Typical Properties

Alloy	Room Temperature					Liquid Hydrogen Temperature (-423°F)				
	UTS	UTS DENSITY	TYS	TYS DENSITY	NTS UTS	UTS	UTS DENSITY	TYS	TYS DENSITY	NTS UTS
Base Metal	KSI		KSI			KSI		KSI		
Aluminum										
2219-T81	66	660	50	500	.84	99	990	68	680	.71
2219-T87	68	680	56	560	.80	99	990	73	730	.72
2014-T6	73	730	64	640	.91	100	1000	81	810	.66
2021-T81	76	760	65	650	.84	100	1000	82	820	.90
5456-H321	57	570	40	400	.83	96	960	53	530	.59
Magnesium										
AZ31B-H24	42	650	32	490	0.90	68	1050	35	540	.28
ZE10A-H24	38	580	29	450	1.05	60	920	36	550	.30
Titanium-E21										
6Al-4Sn STA	170	1060	160	1000	.71	285	1780	275	1720	.38
5Al-2½ Sn Ann	125	780	110	690	1.20	250	1550	195	1210	.63
Stainless										
301 XPH	223	770	200	690	.70	315	1090	280	960	.41

Table III

Recommended Design Mechanical Properties of Some Copper-Aluminum Alloys and 301 XFH Stainless at Various Temperatures

FORM	7719 Sheet & Plate						2219	2024	2012 Sheet & Plate ***						301	304
CONDITION	-162	-78	-185	-185	-185	-185	MBD	-78	-78	-78	-78	-78	-78	-78	301	304
WORKING	2.000	0.070	0.250	1.000	1.000	0.039	0.039	0.039	0.039	0.039	0.039	0.039	0.039	0.039	0.039	0.039
Temp.	(-162°F)															
F _{UT} , ksi	85	94	94	94	95	95	95	95	96	92	96	96	92	96	96	275
F _{TY} , ksi	49	61	61	61	68	69	68	79	75	78	78	75	75	78	75	260
- percent	9	9	11	10	8	9	10	-	-	-	-	-	-	-	-	1
Temp.	(-120°F)															
F _{UT} , ksi	67	77	77	77	78	78	78	87	77	80	80	77	80	80	80	290
F _{TY} , ksi	43	55	55	55	61	62	61	73	68	70	70	68	70	68	68	200
- percent	8	7	10	9	6	7	8	-	-	-	-	-	-	-	-	2
Temp.	(-112°F)															
F _{UT} , ksi	57	66	66	66	67	67	67	76	67	70	70	67	70	70	70	200
F _{TY} , ksi	38	49	49	49	54	55	54	65	61	64	64	61	64	61	61	160
- percent	6	6	9	8	5	6	7	-	-	-	-	-	-	-	-	2
Temp.	(-100°F)															
F _{UT} , ksi	51	64	64	64	66	66	66	75	65	68	68	65	68	68	68	200
F _{TY} , ksi	37	47	47	47	53	54	53	61	59	61	61	59	61	59	59	160
- percent	6	6	8	7	5	6	7	-	-	-	-	-	-	-	-	2
Temp.	(75°F)															
F _{UT} , ksi	56	62	62	62	63	63	63	75	64	64	67	67	64	67	67	200
F _{TY} , ksi	36	46	46	46	51	52	51	64	59	57	59	59	57	59	57	160
- percent	6	6	8	7	5	6	7	(a)	6	8	6	6	6	8	6	8
Temp.	(212°F)															
F _{UT} , ksi	49	56	56	56	56	56	56	59	59	61	61	59	61	61	61	
F _{TY} , ksi	33	41	41	41	46	46	46	58	52	54	54	52	54	54	52	
- percent	7	8	10	9	7	8	9	-	6	8	6	6	6	8	6	

(a) The elongation values are 6, 5 and 3 for 0.030-0.249, 0.250-0.499 and 0.500-1.000 inches at 75°F

* Values based on proposed revision to MIL-REK-5

on Values given are tentative expected - minimum design properties

see Values based on MIL-REK-5

*** May be modified on development of actual weld schedules including repair - ***** Values are roll planned

Table IV

TYPICAL MECHANICAL PROPERTIES
OF Ti-5Al-2.5Sn

CONDITION	ELI Base Metal						Weldments		
THICKNESS	0.200		0.25		1.000		1.000	0.500	0.200
DIRECTION	L	T	L	T	L	T			
Temperature (-423°F)									
F _{TU} ksi	208	206	223	192	240	250	258	216	205
F _{TY} ksi	206	202	196	180	-	-	245	185	-
-percent	-		13	30	8	4			-
Temperature (-320°F)									
F _{TU}	188	186	180	183	210	222	242		185
F _{TY}	178	178	170	175	202	210	220		176
-percent	17	15	24	23	11	8			11
Temperature (-110°F)									
F _{TU}			132	132					
F _{TY}			126	128					
-percent			24	22					
Temperature (75°F)									
F _{TU}	117	116	115	115				110	117
F _{TY}	111	113	101	103				93	111
-percent	17	17	24	24				-	11
Temperature (212°F)									
F _{TU}	103	103	101	101					
F _{TY}	101	101	98	99					
-percent	-	-	-	-					

Table V

Typical Static Fracture Toughness and Threshold
Stress Intensity Values

2219 Aluminum										2021 Aluminum				Ti-5Su-2½Su		301 XFH	
Condition	Base Metal					Weldments					Base Metal Weldments			Base Metal	Weld	Base Metal	Weld
	-T87		-T81		-T87	-T81		-T81 Repair		-T81		AGED	As Weld	Eli		60°/cm	
Thickness	0.25 0.625	1.000 1.25	0.063 0.25	0.700 1.00	0.25 1.00	.063	1.00	0.063	1.00	.063 0.500	1.00	.063 0.50	1.00	0.20	0.20	0.25	
K _{IC} Temp. Rt (°F)	36	33	41	49	28	36	25	32	15	20	28	13	28	72	68	KC 150	NO DATA AVAILABLE
-110	-	34	-	-	-	-	-	-	-	22	-	-	-	-	-	-	
-320	41	37	43	56	30	19	27	48	18	30	37	-	35	66	63	90	
-423	44	37	74	47	18	33	22	47	15	36	40	-	28	52	47	83	
K _{TH} /K _{IC} Temp. Rt (°F)	.75				.82						.77	.73	.58	-			
-320°	.8				.8						.82		.62	.8			
-423	.85										.76		.69	.9			

EM No. 12-12-01-MI-18
Date: 18 June 1971

ENGINEERING MEMORANDUM

TITLE: BASELINE DROPTANK LOADS	EM NO L2-12-01-MI-12 REF: DATE: 21 June 1971
AUTHORS: D. A. Rumbaugh/H. Sims <i>D.A. Rumbaugh</i>	APPROVAL: ENGINEERING <i>[Signature]</i> SYSTEM ENGRG <i>R. A. Byers</i>

PROBLEM STATEMENT

Establish preliminary design loads on the droptanks of the two-and-one-half-stage orbiter.

RESULTS

Two ascent loading conditions were considered. The first condition is the maximum aerodynamic loading condition, maximum α , β q. The second condition occurs when the launch vehicle reaches maximum longitudinal acceleration. The droptank reactions, acting on the tanks, are shown in Table 1 for the baseline tank configuration and in Table 2 for the G.A.C. configuration. An estimate of tank bending moment for the baseline tank, at the maximum α q condition is shown in Figure 1. Axial load distributions for the ascent load conditions are included in Figure 2. Tank reentry loads are shown on Figures 6, 7 and 8.

Criteria and Assumptions

The criteria used in generating loads on the two-and-one-half-stage droptanks has been compiled from previous space shuttle vehicle analysis and from newly generated data where new data is available. The criteria used in loads analysis is as follows:

- Dynamic pressure at maximum α , β q = 500 psf
- α and β = ± 4 deg
- Normal and lateral load factor at maximum α , β q = ± 0.4 g
- Maximum axial load factor = 3g

General

The determination of preliminary design loads for the droptank structure has been based on the evaluation of three loading events, these being considered the most severe for design of the major structural elements of the droptanks. The three events are maximum α , β q, maximum axial acceleration, and reentry.

ASCENT LOADS

Preliminary estimates of aerodynamic loading at maximum α , β , q have been found to be nonconservative based on wind tunnel data for the two-and-one-half-stage vehicle. The revised aerodynamic loading distribution, based on wind tunnel data is shown on Figure 5. The airload distribution has been unitized to $C_N = 1$ and is considered to apply in both the pitch and yaw planes. The wind tunnel data reflects larger interference effects than were anticipated in the preliminary estimates.

The revised droptank reactions and bending moments, shown in Table 1 and Figure 1 respectively, reflect the effects of the increased loading. The preliminary estimates of tank bending moments and reactions are shown in Table 3 and Figure 6. Axial loads for the maximum α , β , q condition and the maximum axial acceleration conditions are shown in Figure 2. The inertia distribution used in calculation of the loads at maximum α , β , q is shown in Figure 7.

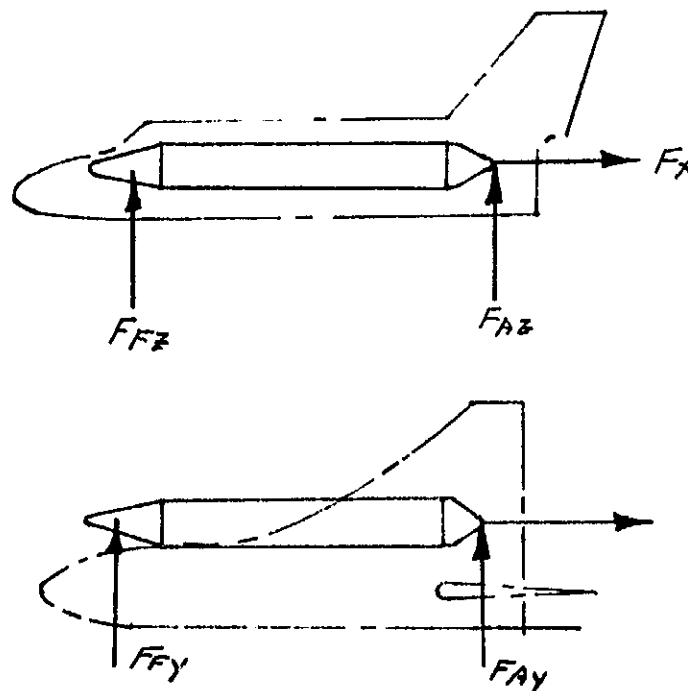
REENTRY LOADS

Tank reentry loads were calculated for two conditions. Before detailed six degrees-of-freedom reentry studies were completed, the tank was assumed to be tumbling so that $\alpha = 90^\circ$ could occur at any point on the trajectory. These moments and tension loads, in unit form, are shown in Figures 6 and 7. An estimated dynamic pressure (\bar{q}) of 100 psf and rotational velocity (ω) of 0.6 rad/sec were used in the load calculation.

The six degrees-of-freedom studies show the tank to be stable, and reentering nose first, for all conditions investigated. Rotational velocities of approximately 0.1 rad/sec were obtained so that the tension caused is negligible. Total angles-of-attack of the order of 40° resulted. Unit moment and axial load for these conditions are shown in Figure 8. A dynamic pressure of 630 psf results for the most severe condition.

Newtonian concepts were used to calculate the unit normal airload distributions shown in Figure 9. Inertia distributions were obtained by multiplying the weight distribution shown in Figure 9 by a unit load factor ($\eta_{N/\bar{q}} = F_N/\bar{q} W$). It can be seen from the load factor equation that the total unit loads and moments are independent of tank weight and vary only with the distribution of weight and angle-of-attack. The unit rotational inertia distributions were determined from the weight distribution and are included in the total load curves.

TABLE 1

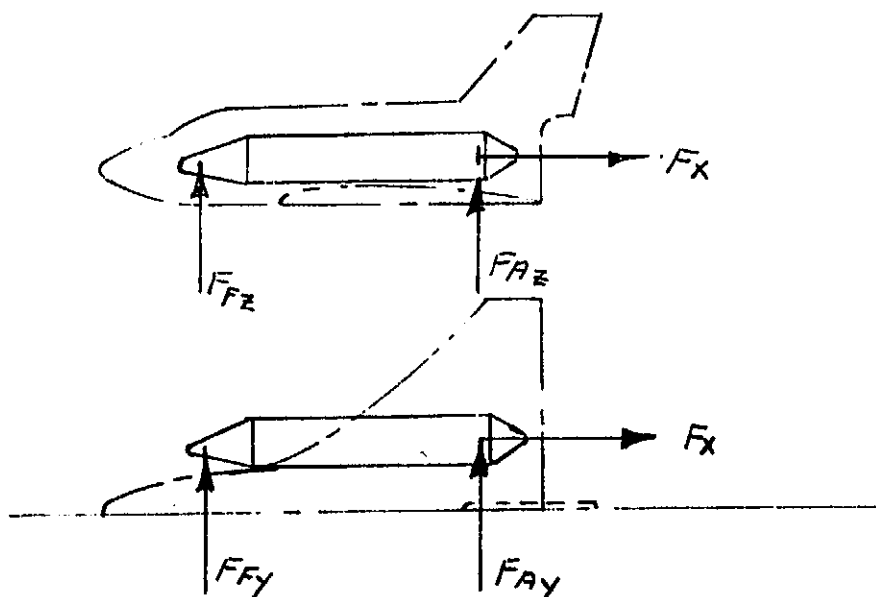
BASE LINE DROP TANK REACTIONS

REACTIONS ON THE DROP TANKS

CONDITION	F_x	FF_z	FF_y	FA_z	F_{AY}
MAX AXIAL g's	-145,500				
MAX + α g	-140,000	+23,350	+31,000	+18,150	+17,500
MAX - α g	-140,000	+15,350	+4,910	+6,050	+2,790
MAX + β g	-140,000	+21,700	+21,400	+12,300	+28,000
MAX - β g	-140,000	+19,200	+20,200	+10,800	+21,500
MAX $\pm \beta$ g INERTIA ONLY		$\pm 10,000$	$\pm 10,000$	$\pm 10,750$	$\pm 10,750$

TABLE 2

G A C DROP TANK REACTIONS



REACTIONS ON THE DROP TANKS

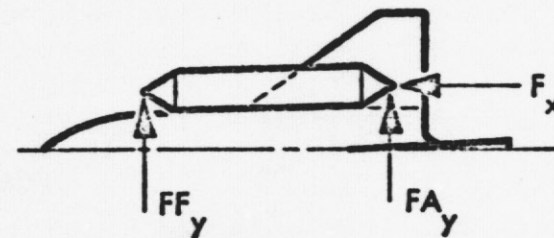
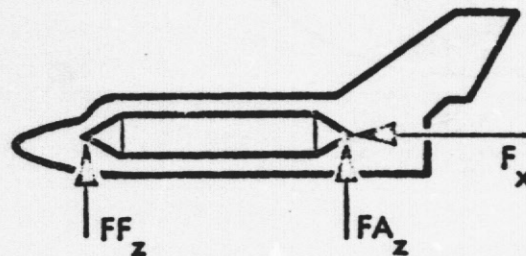
CONDITION	F_x	FF_z	FF_y	FA_z	FA_y
MAX AXIAL g's	-216 000				
MAX + α g	-167 400	+20,000	+24,200	+32,600	+31,200
MAX - α g	-167 400	+13,520	+10,950	+10,780	+6,750
MAX + β g	-167 400	+17,100	+21,500	+22,100	+34,500
MAX - β g	-167 400	+15,050	+21,200	+19,500	+21,700

Table 3

DROPTANK DESIGN LOAD CRITERIA

● LIFTOFF	NONCRITICAL
● MAXIMUM DYNAMIC PRESSURE	
MAXIMUM αq , DEG-PSF	2000
LONGITUDINAL LOAD FACTOR, q	1.4
NORMAL LOAD FACTOR, q	0.4
DYNAMIC AXIAL LOAD FACTOR, q	0.3
● MAXIMUM AXIAL LOAD FACTOR, q	3.0

TANK ATTACH REACTION CRITERIA



CONDITION	F_x (LB)	FA_z (LB)	FA_y (LB)	FF_z (LB)	FF_y (LB)
MAX AXIAL g	145,000	0	3,200	0	2970
MAX q	140,000	+16,000 - 9,960	+9,960 -	+9,440 -9,890	+ 9,440 -34,000

EM NO. L2-12-01-M-12
Date: 21 June 1971

FIG. 4

BASE LINE DROP TANK
ESTIMATED BENDING MOMENT
MAX @ 2 CONDITION

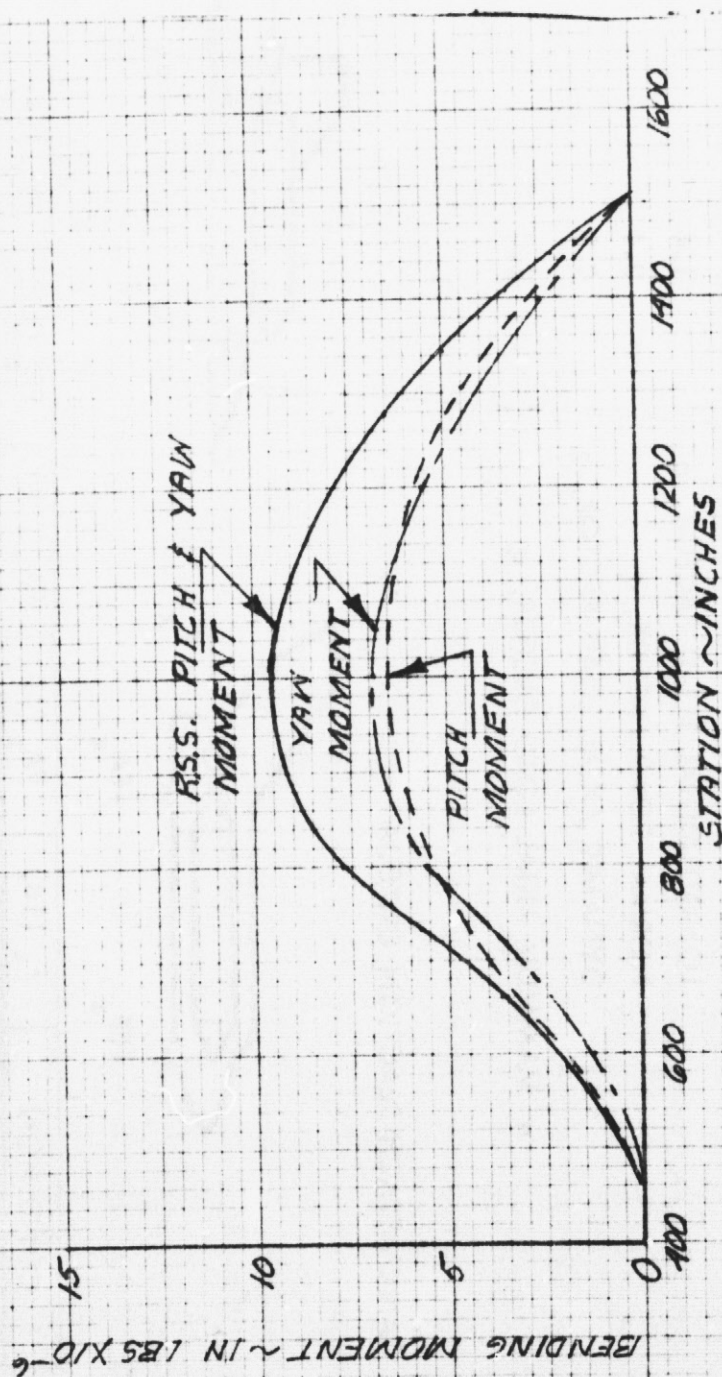


FIG. 1

EM NO. L2-12-01-M1-12

DATE 21 June 1971

PREPARED BY DAR 11 MAY

PAGE OF

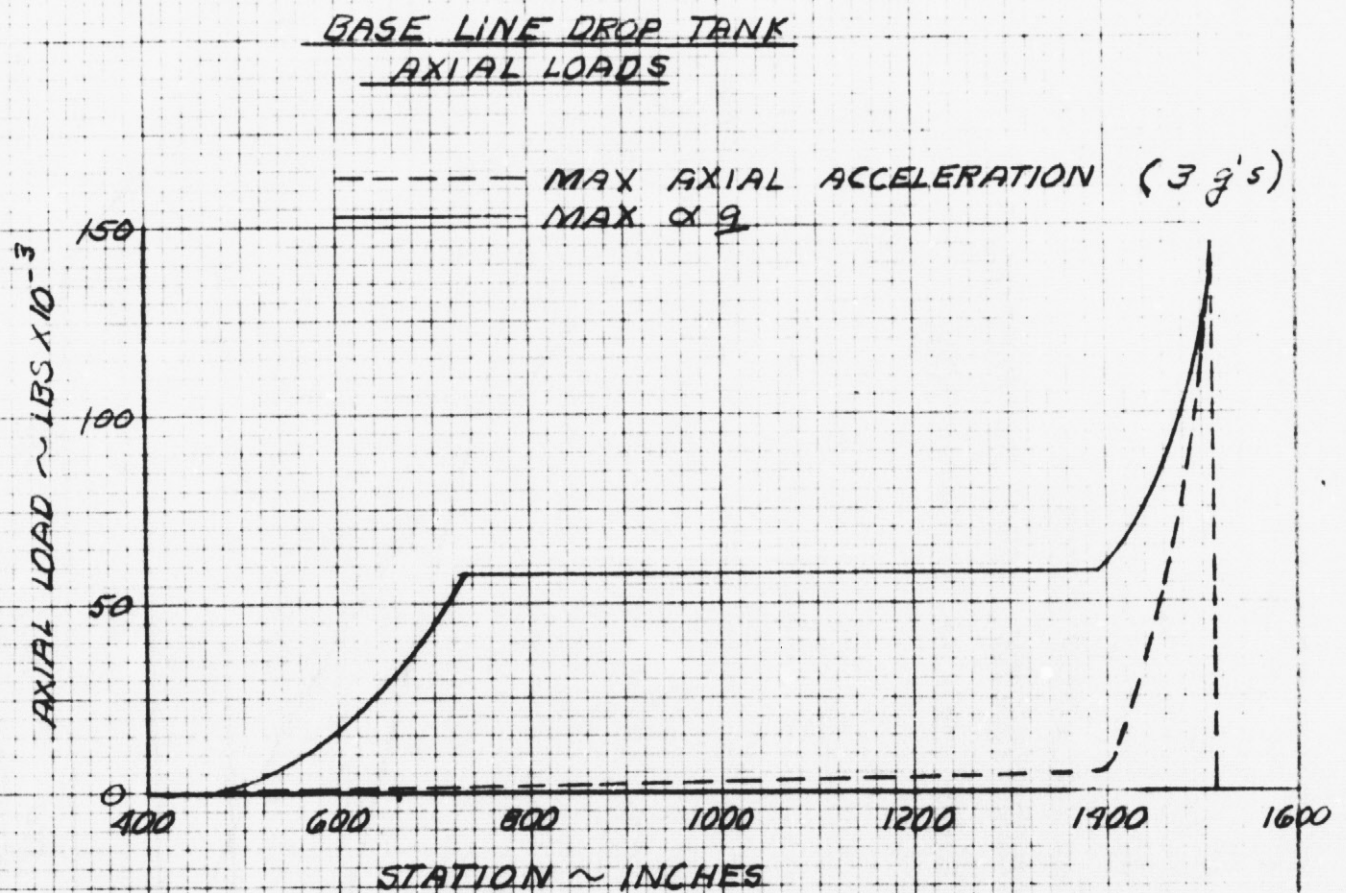


Figure 2

EM NO. L2-12-01-M1-12

DATE 21 June 1971

PAGE OF

PREPARED BY

BASE LINE DROP TANK
UNIT AERODYNAMIC LOAD DISTRIBUTION
MAXIMUM α , β & γ CONDITION

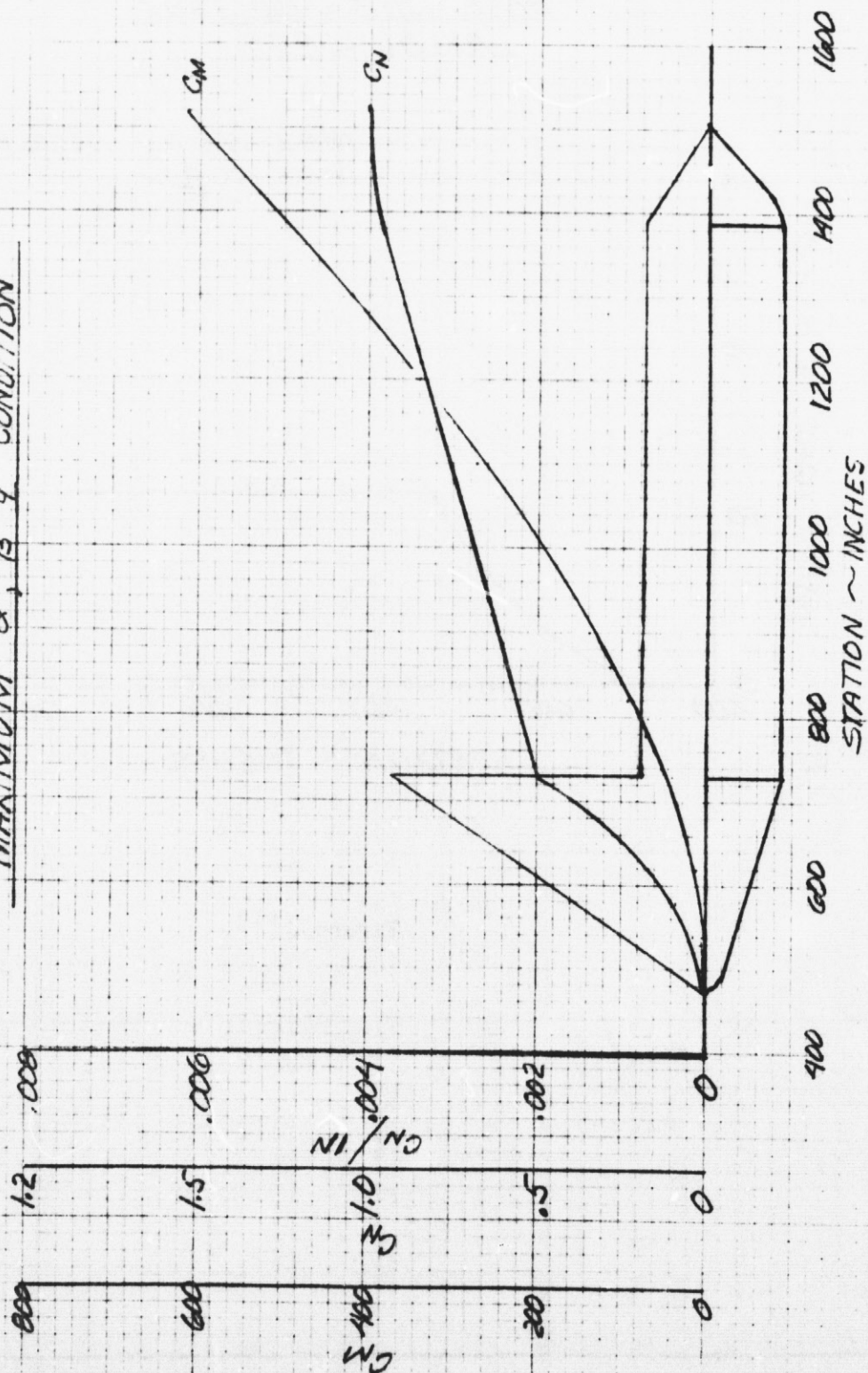


Figure 3

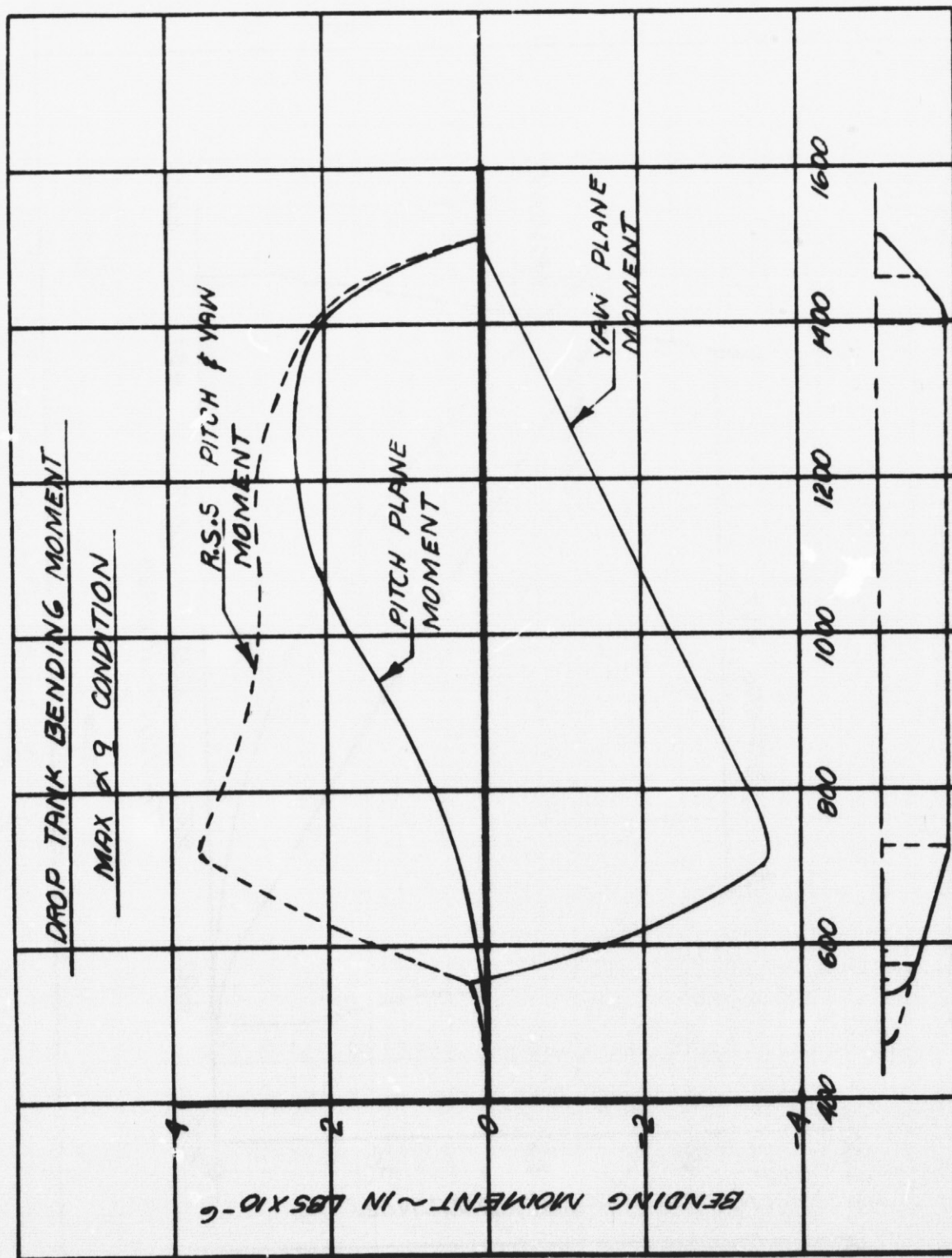


Figure 4

EM NO. L2-12-01-M1-12

DATE 21 June 1971

PREPARED BY

PAGE OF

BASELINE DROP TANK

UNIT INERTIA DISTRIBUTION

TANK FULL CONDITION

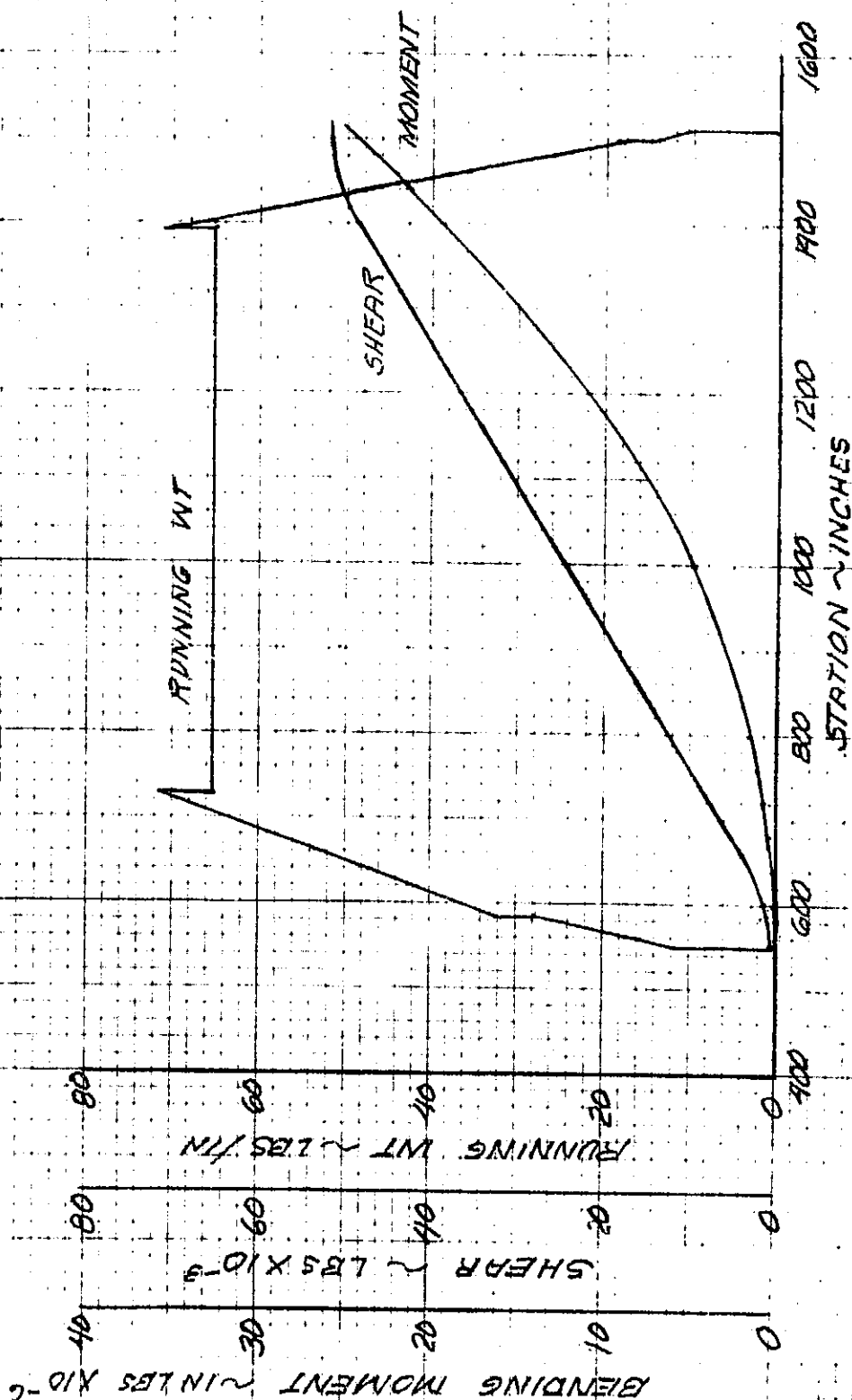


Figure 5

BASE LINE DROP TANK RE-ENTRY
MOMENT / q , $\alpha = 90^\circ$

EM NO. L2-12-01-M1-12

DATE 21 June 1971

PREPARED BY HJS

PAGE OF

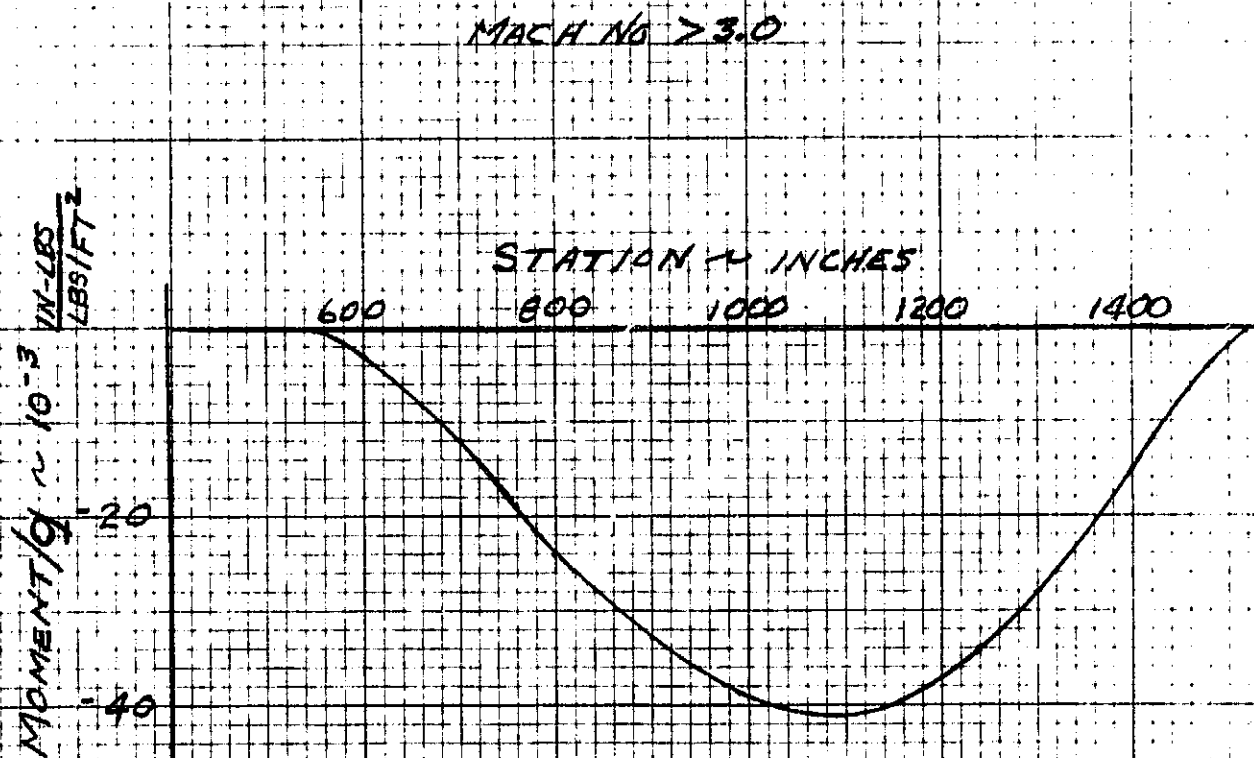


Figure 6

BASE LINE LOCKHEED MISSILES & SPACE COMPANY
DROP TANK TENSION DURING RE-ENTRY
DUE TO PITCH/YAW RATE PER RADIAN
PER SECOND

SPACE SHUTTLE PROJECT

EM NO. L2-12-01-M1-12

DATE 21 June 1971

PREPARED BY HJS

PAGE OF

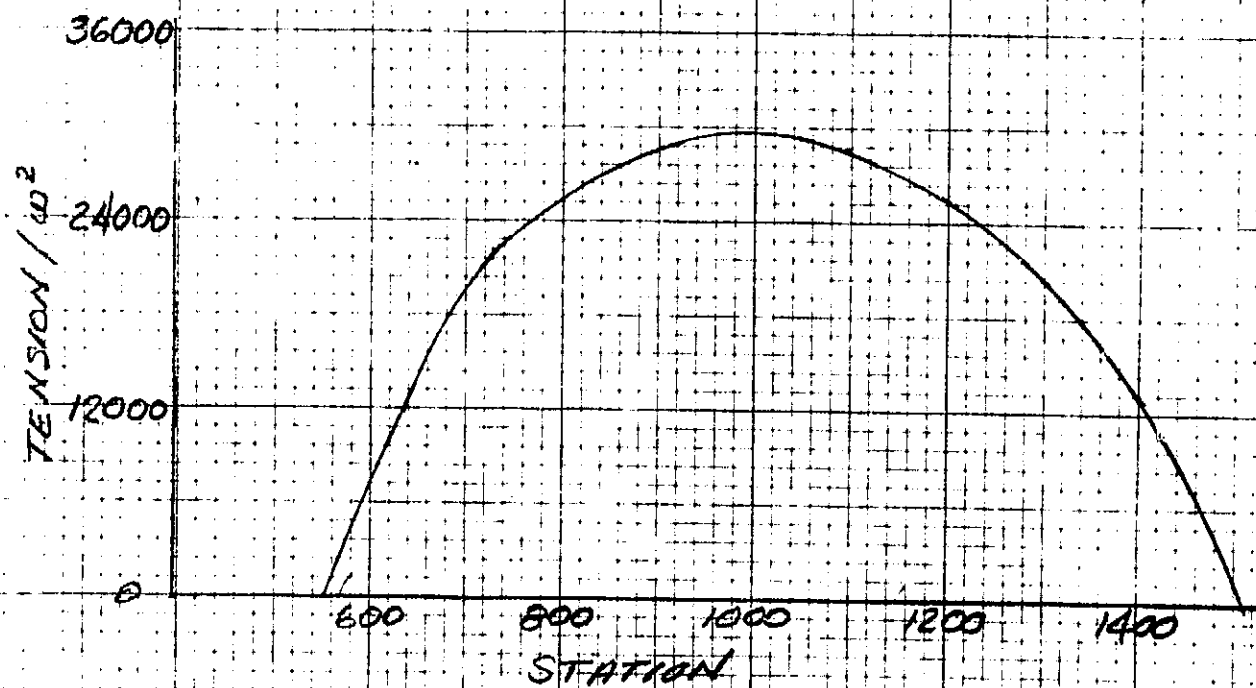


Figure 7

EM NO. L2-12-01-M1-12

DATE 21 June 1971

PAGE OF

PREPARED BY HJS

BASE LINE
UNIT BENDING MOMENT
AND AXIAL LOAD
 $(\alpha = 40^\circ)$

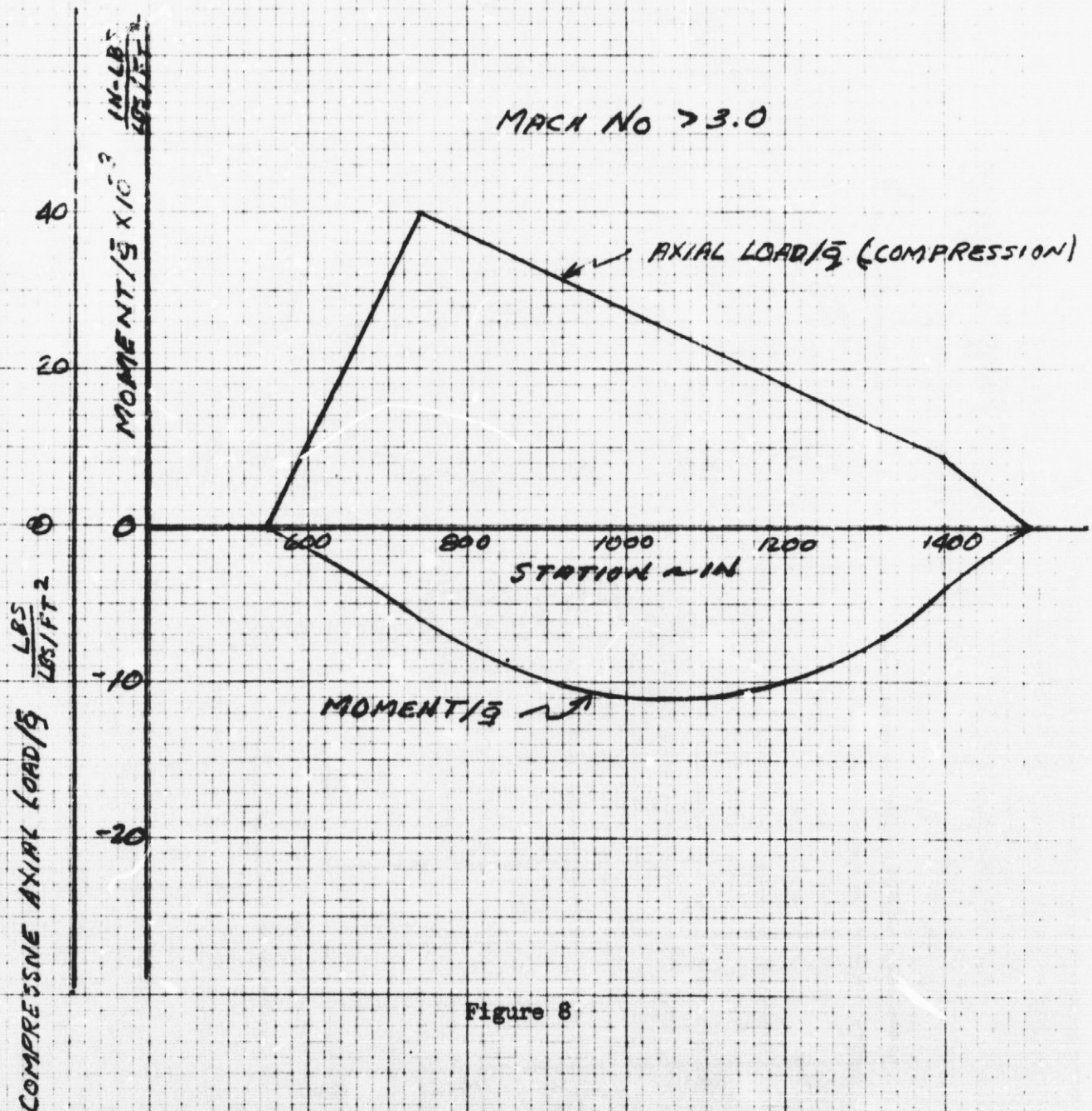


Figure 8

EM NO. L2-12-01-M1-12

DATE 21 June 1971

PAGE OF

PREPARED BY H.J. SIMS

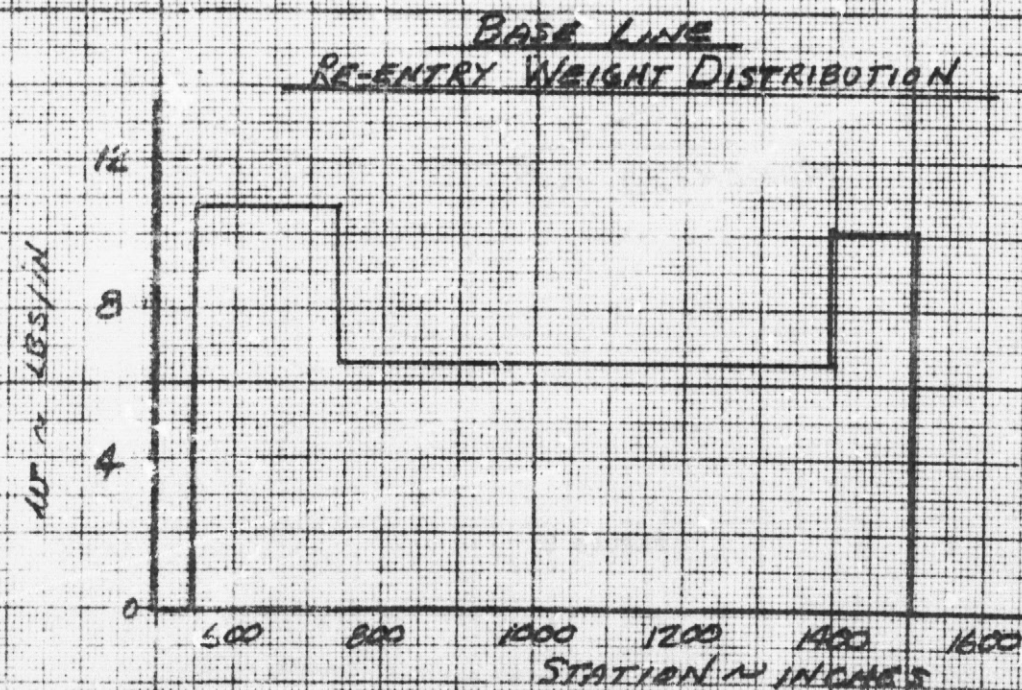
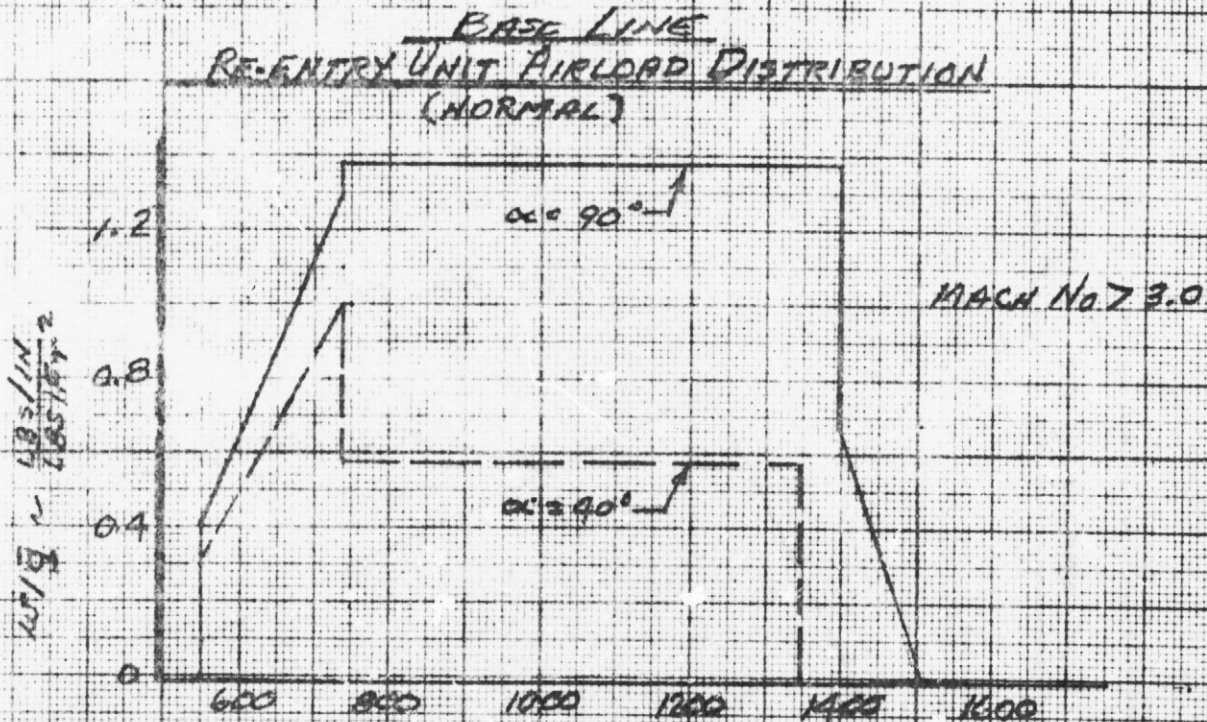


Figure 9

ENGINEERING MEMORANDUM

TITLE: BASELINE DROPTANK STRUCTURAL ANALYSIS	EM NO: 12-12-01-M1-13 REF: 12-12-01-P1 DATE: 21 June 1971
AUTHORS: S. A. Carter/H. Baserga	APPROVAL: ENGINEERING <i>[Signature]</i> SYSTEM ENGRG <i>[Signature]</i>

PROBLEM STATEMENT

Perform preliminary structural analyses on the Baseline Droptank configuration proposed for use on the Two-and-One-Half Stage Space Shuttle Orbiter, for the purpose of determining realistic meaningful weights and fabrication requirements in order to project total program cost. Consideration will be given to intact entry, ground handling, and ullage pressure variations.

RESULTS

The analyses contained herein show that externally supported LH₂ nonreusable droptanks are sized on the basis of internal pressure while subjected to the ascent environment. The tank membrane, sized for pressure, is capable of sustaining all ascent load conditions without the requirement of additional stiffening. The results also show that intact entry can be achieved if the tanks are insulated with cork which limits the tank bondline temperature to 500°F. Limiting the tank wall temperature to 500°F requires the internal tank pressure to 12 psia ⁺⁰. This requirement permits the tank to enter the atmosphere and collapse at a low ⁻³ altitude (5000 ft < h < 15,000 ft). The study further shows that the droptank can be subjected to handling from its extremities without damage through all stages of assembly if the tank is internally pressurized to 2 psig. A significant weight penalty results, however, if the tank is required to be handled unpressurized. Since this study was predicated on a very preliminary tank ullage pressure requirements curve, an analysis was performed to assess the weight penalty associated with increased ullage pressures.

ANALYSIS

1.0 INTRODUCTION

In support of the Task 4 study requirements of the ACS Study (NAS 8-26362) to evaluate the weight and program costs for an LH₂ droptank configuration developed for the Two-and-One-Half Stage Space Shuttle System, preliminary structural analyses of the GAC configuration were performed. This system employs a delta-wing orbiter in combination with two nonrecoverable LH₂ propellant tanks, externally simply-supported along the side of the fuselage. Each droptank assembly is attached to the orbiter at two locations: one forward in the nose section, reacting only transverse loads, and one aft at the orbiter aft payload compartment bulkhead, reacting omnidirectional loads.

After careful screening of candidate materials, two were selected; 2219 aluminum and 301 CRES steel (extra-hard temper). Two tempers in the aluminum were investigated: the -81 temper and -87 temper, the reason being that while -T87 is slightly stronger, the -T81 is available in wider sheet widths. This characteristic was only advantageous in the fusion welded (Configuration A) design. When the weldbonded design is considered, both tempers are available, and therefore, the -87 temper was selected.

2.0 DESIGN CRITERIA

Two design load environments were evaluated; ascent loading (Booster and Orbiter ascent conditions) and intact entry. The design loads criteria from which design loads are obtained are presented in EM 12-12-01-M1-12. In addition to the external loads environment, tank design criteria was required. For this preliminary study, the tank ullage pressure history curve provided by GAC was used. The ultimate factor of safety is 1.40.

3.0 BASELINE DROPTANK SIZING

3.1 LOAD CONDITIONS

Preliminary tank membrane sizing is based on internal pressure requirements from launch release through orbiter separation. The following load conditions are considered:

A. Tank Full:

Ullage gas temperature = 360°R , Wetted wall temperature = 40°R

Condition 1: Maximum Booster Acceleration

$$n_x = 3.0g @ t = 154 \text{ sec}, p_{ull} = 24.5 \text{ psia}$$

Condition 2: Orbiter Ignition

$$n_x = 1.4g @ t = 186 \text{ sec}, p_{ull} = 29.0 \text{ psia}$$

B. Tank Empty:

Tank Wall Temperature Varies Linearly:

$$\begin{aligned} \text{Tank Top Temperature} &= 360^{\circ}\text{R} \\ \text{Tank Bottom Temperature} &= 40^{\circ}\text{R} \end{aligned}$$

Condition 3: Orbiter Ascent Burnout

$$n_x \approx 0, p_{ull} = 25 \text{ psia}$$

A verification of the assumption that the tank wall temperature varies linearly when it is empty was made by a one dimensional thermodynamic analysis. A comparison of these results with the assumed values is shown in Fig. 1.

3.2 BASELINE DROPTANK MEMBRANE SIZING ANALYSIS

The LH_2 tank geometry is taken from Engineering Drawing SKT 100703. The pertinent details used for this analysis are shown in Fig. 2.

Of the three design conditions, maximum acceleration proved not to be critical because of the higher ullage pressure occurring at orbiter ignition. A combination of the latter two conditions (orbiter ignition and orbiter burnout) establishes the membrane requirements. This is shown in the subsequent analysis in Table 1.

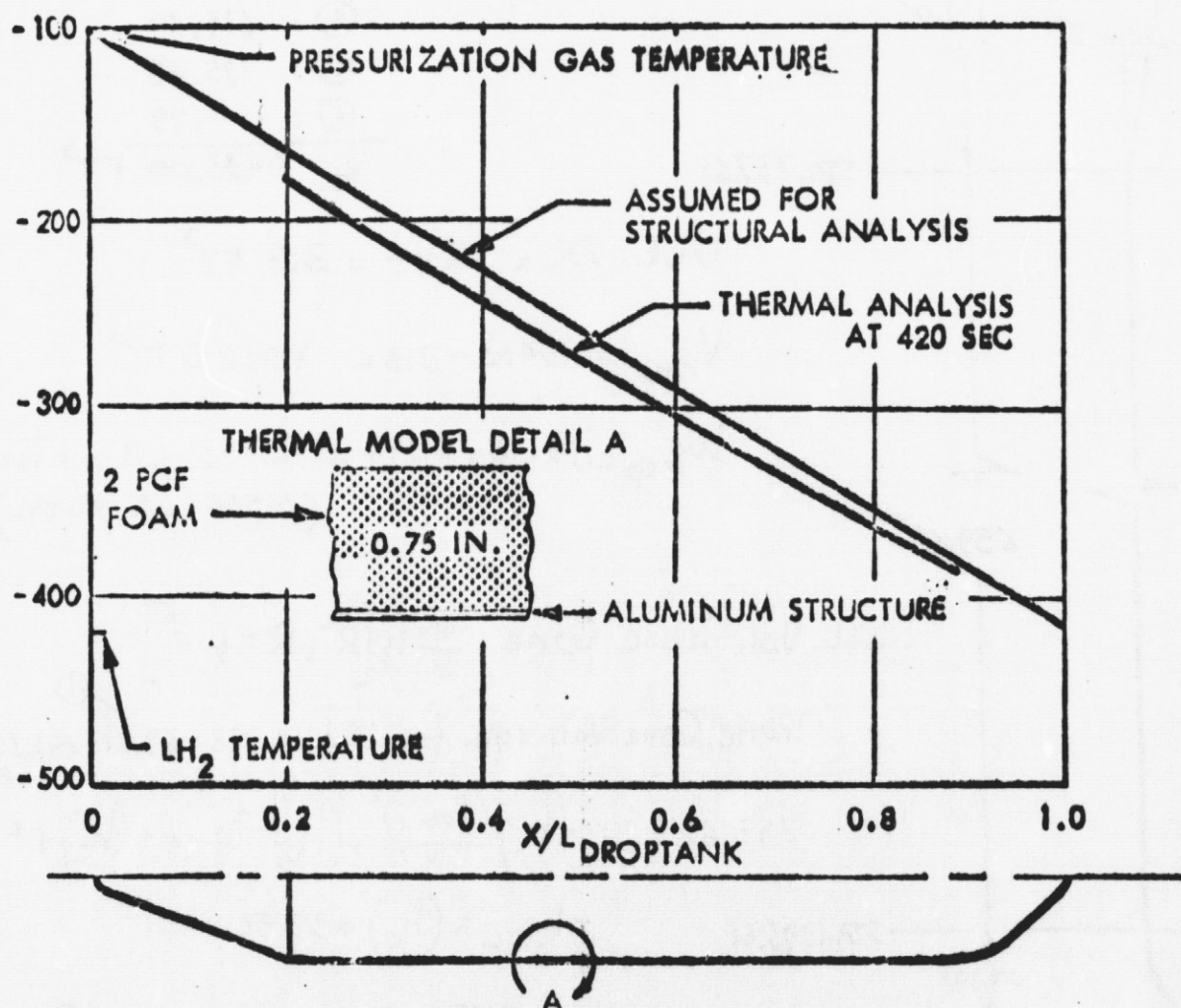
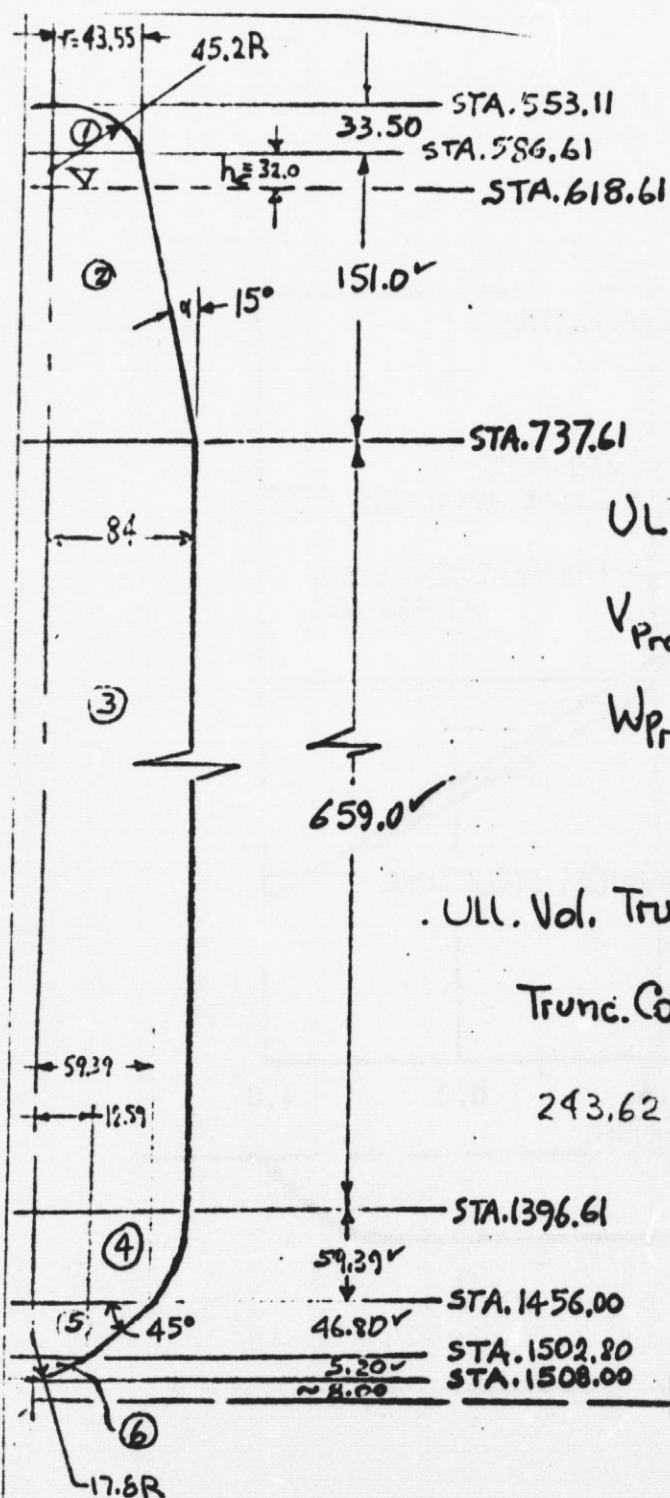


Fig. 1 Droptank Critical Structure Temperature



VOLUMES

① : 69.38

② : 1153.00

③ : 8919.69

④ : 634.49

⑤ : 125.65

⑥ : .79

$$V_T = 10433.00 \text{ FT}^3$$

$$ULL \text{ VOL.} = 3\% V_T = 313 \text{ FT}^3$$

$$V_{Prop} = 10433 - 313 = 10120 \text{ FT}^3$$

$$W_{Prop} = 10120 \times 4.274 = 43253 \text{ LB per tank}$$

(86506 LB TOTAL)

$$ULL \text{ Vol. Trunc. Cone} : \frac{\pi}{3} h_c [R^2 + Rr + r^2]$$

$$\text{Trunc. Cone Vol. req'd. for ULL} : 313 - 69.38 = 243.62 \text{ FT}^3$$

$$243.62 = \pi \left[(h_c) \frac{(\tan \alpha)^2}{3} + (h_c) r \tan \alpha + (h_c) r^2 \right]$$

$$H_{ULL} = (h_c) + 33.50$$

$$ULL \text{ HEIGHT} = 32.0 + 33.5 = 65.5''$$

PROPELLANT (LH₂) : Temp = -420°F (40°R), $\delta = 4.274 \text{ LB/FT}^3$

ULL HE TEMP. = -100°F (360°R) (°R = °F + 460)

Fig. 2 LH₂ Droptank Geometry (SKT 100703)

Table 1
DESIGN LOADS (LIMIT)

LOADING CONDITIONS

A. TANK FULL OF PROPELLANT (LH₂) @ -420°F

COND. ① : Max. Booster Accel., $n=3.0g/s$. @ 154 sec $p_{ULL}=24.5$ PSIA

COND. ② : 2nd. Stage Ignition, Accel. $n=1.4g/s$. @ 186 sec $p_{ULL}=29.0$ PSIA

B. TANK EMPTY, ULLAGE TEMP. = -100°F

COND. ③ : 2nd. Stage Drop Tank Staging, $p_{ULL}=25.0$ PSIA

JUNCTURE SHELL/SHELL	STA.	LH ₂ Height (IN)	P _{HYD} (PSI)	COND. ①			COND. ②			COND. ③	
				(β)(P _{HYD})	P _{ULL}	P _{T①}	(1.4)(P _{HYD})	P _{ULL}	P _{T②}	-T(°F)	p _③
①, Top	553.11	—	—	—	—	24.50	—	—	29.0	100.0	—
①/②	586.61	—	—	—	—	24.50	—	—	29.0	111.2	—
②/③	737.61	119.0	.2943	.8828	24.5 PSIA	25.383	.412	29.0 PSIA	29.412	161.8	25.0 PSIA
	940.0	321.39	.795	2.385		26.885	1.113		30.113	230.0	
	1150.0	531.39	1.314	3.942		28.442	1.840		30.840	300.0	
③/④	1396.61	778.0	1.924	5.772		30.272	2.694		31.694	382.7	
	1456.0	837.39	2.071	6.213		30.713	2.8994		31.90	402.6	
④/⑤	1502.8	884.2	2.187	6.560		31.060	3.0612		32.061	418.2	
	1508.0	889.39	2.1995	6.598		31.098	3.079		32.079	420.0	

NOTE: $P_{T①L} < P_{T②i}$ & $T_{①i} = T_{②i}$. Hence COND. ① IS NOT CRITICAL.

$$P_{HYD} = \left(\frac{4.274 \text{ LB/FT}^3}{1728 \text{ IN}^3/\text{FT}^3} \right) (\text{LH}_2 \text{ Height, IN}) = (.002473) (\text{LH}_2 \text{ Ht})$$

$$\text{Temp. @ STA}_i : -T_i = 100^\circ + \left(\frac{420^\circ - 100^\circ}{1508 - 553.11} \right) (\text{STA}_i - 553.11) = 100^\circ + (.3351) (\text{STA}_i - 553.11)$$

The analytical procedure used for tank membrane sizing is shown in Table 2. The material ultimate strength versus temperature is taken from Mil Handbook 5A. Minimum gage requirements were established at .025 and .010 for the aluminum and steel tank configurations, respectively. The resulting tank gages are summarized for all three material selections in Table 3, followed by the detailed calculations which lead to this summary.

3.3 TANK ANALYSIS FOR EXTERNAL ASCENT LOADS

Having established gage requirements for internal pressure, a check on ascent load capability was performed to determine whether that consideration is critical to design. The ascent axial load and bending moment occurring at maximum αq (Ref. EM L2-12-01-M1-12), results in the most severe ascent load condition. Preliminary loads were developed without the aid of wind tunnel data. When wind tunnel data became available (late in the study), the loads had to be revised because of the significant differences between the assumed aerodynamic load distribution and the test results. Both these are converted to maximum compression stress resultants (line loads) and compared to the structural capability of the membrane while at maximum αq (ambient pressure 1.5.3 psi). For this condition, the tank internal pressure is assumed to be 3 psia lower for the compression side to account for valve tolerance. This comparison is shown in Fig. 3, followed by the detailed calculations which lead to the plot of this figure, in Tables 4A, 4B and 5. It is noted from Fig. 3, that ascent loads are not critical, and no additional stiffening is required.

3.4 TANK ANALYSIS FOR ENTRY LOADS

Using the membrane wall thicknesses established for ascent internal pressure (for the 2219-T87 aluminum configuration) as shown in Table 3, an analysis was performed to determine the droptank structural capability during intact entry as a function of tank wall temperature and internal pressure. The purpose for this analysis is to determine the cork insulation requirements for intact entry. This thermal analysis is presented in EM L2-12-01-M1-10. Figure 4 presents the burst strength capability for discrete locations along the tank as a function of tank wall temperature. The calculations which lead to the construction of this figure are shown in Table 6. It can be seen from Fig. 4, that if the droptank is vented to a low internal pressure, the allowable wall temperature can be permitted to reach a high value; e.g., venting the tank to 8 psia permits the tank wall temperature to reach 620°F before failure. No factor of safety is associated with these values, but these values are slightly conservative in the cylinder membrane area where inherent biaxial strength provides a fifteen percent margin.

Calculations for allowable compression and tension stress resultants (line loads) were performed for several values of tank internal pressure. A valve pressure tolerance of 3 psia was included for compression loads to account for reduced load relief. The resulting allowables for the tank are shown in Figs. 5 and 6 for compression and tension, respectively. The tension side establishes the limiting wall temperature of vented pressure. The calculations which lead to the construction of these figures are presented in Tables 7 through 12.

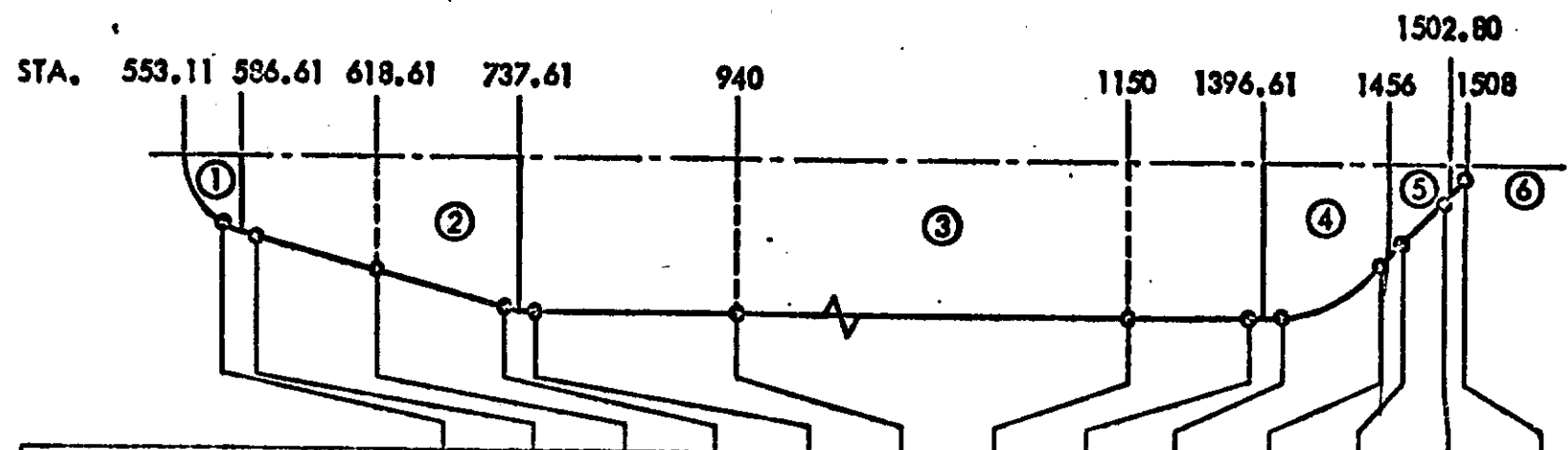
The load environment to which the tank is subjected during entry is directly a function of what kind of trajectory the tank assumes during entry. Point-mass trajectories were initially run, and from these, it was assumed that the tank never trimmed, but tumbled to impact at 0.6 radians per second. These trajectory analyses

TABLE 2: 2219-T87AL ALLY. WALL THICKNESS SIZING

COND. ②	T, °F	G _T , ksi	COND. ③: p=25.0 PSI	ROUND-OFF THICK.
$t_1 = \frac{(P_{1-2})(R_0)}{2 \sigma_{ULL}} (1.4) = \frac{29.0 \times 45.2}{2 \times 66.5} (1.4) = .0138"$	-100	66.5	NON CRITICAL	.014
$t_2 = \frac{(P_{1-2})(r_1)}{\sigma_{ULL} \cos \alpha} (1.4) = \frac{29.0 \times 43.55}{66.5 \times .9659} (1.4) = .0275"$	-111.2	67.0	N.C. .024	.028
$t_3 = \frac{(P_{1-2})(r_2)}{\sigma_{ULL} \cos \alpha} (1.4) = \frac{29.0 \times 52.1}{66.5 \times .9659} (1.4) = .0329"$	-122	67.5	N.C. .028	.033
$t_4 = \frac{(P_{2-3})(r_3)}{\sigma \cos \alpha} (1.4) = \frac{29.412 \times 84}{94.5 \times .9659} (1.4) = .0379"$	-162	68.0	$\frac{25 \times 84}{68 \times .9659} (1.4) = .0448$.045
$t_5 = \frac{(P_{2-3})(R_3)}{\sigma} (1.4) = \frac{29.412 \times 84}{94.5} (1.4) = .0365"$	-162	68.0	$\frac{25 \times 84}{68} (1.4) = .0433$.044
$t_6 = \frac{(P_1)(R_0)}{\sigma} (1.4) = \frac{30.113 \times 84}{94.5} (1.4) = .0375"$	-230	70.0	$\frac{25 \times 84}{70} (1.4) = .0420$.042
$t_7 = \frac{(P_j)(R_0)}{\sigma} (1.4) = \frac{30.840 \times 84}{94.5} (1.4) = .0384"$	-300	75.5	$\frac{25 \times 84}{75.5} (1.4) = .0390$.039
$t_8 = \frac{(P_{3-4})(R_0)}{\sigma} (1.4) = \frac{31.694 \times 84}{94.5} (1.4) = .0395"$	-383	87.5	$\frac{25 \times 84}{87.5} (1.4) = .0336$.040
$t_9 = \frac{(P_{3-4})(R_0)}{2 \sigma} (1.4) = \frac{31.694 \times 84}{2 \times 94.5} (1.4) = .0197"$	-383	87.5	$\frac{25 \times 84}{2 \times 87.5} (1.4) = .0168$.020
$t_{10} = \frac{(P_{4-5})(R_0)}{2 \sigma} (1.4) = \frac{31.90 \times 84}{2 \times 94.5} (1.4) = .0199"$	-402.6	91.5	$\frac{25 \times 84}{2 \times 91.5} (1.4) = .0161$.020
$t_{11} = \frac{(P_{4-5})(r_4)}{\sigma \cos \beta} (1.4) = \frac{31.90 \times 59.39}{94.5 \times .7071} (1.4) = .0397"$	-402.6	91.5	$\frac{25 \times 59.39}{91.5 \times .7071} (1.4) = .0321$.040
$t_{12} = \frac{(P_{5-6})(r_5)}{\sigma \cos \beta} (1.4) = \frac{32.061 \times 12.59}{94.5 \times .7071} (1.4) = .0085"$	-418.2	94.5	N.C.	.010
$t_{13} = \frac{(P_{5-6})(R_0)}{2 \sigma} (1.4) = \frac{32.061 \times 17.8}{2 \times 94.5} (1.4) = .0043"$	-418.2	94.5	N.C.	.006
$t_{14} = \frac{(P_6)(R_0)}{2 \sigma} (1.4) = \frac{32.079 \times 17.8}{2 \times 94.5} (1.4) = .0043"$	-420	94.5	N.C.	.006

NOTE: BLUE FIGURES ARE FOR $t_{min} = .010"$

Table 3

14-FOOT DIA LH₂ DROPTANK


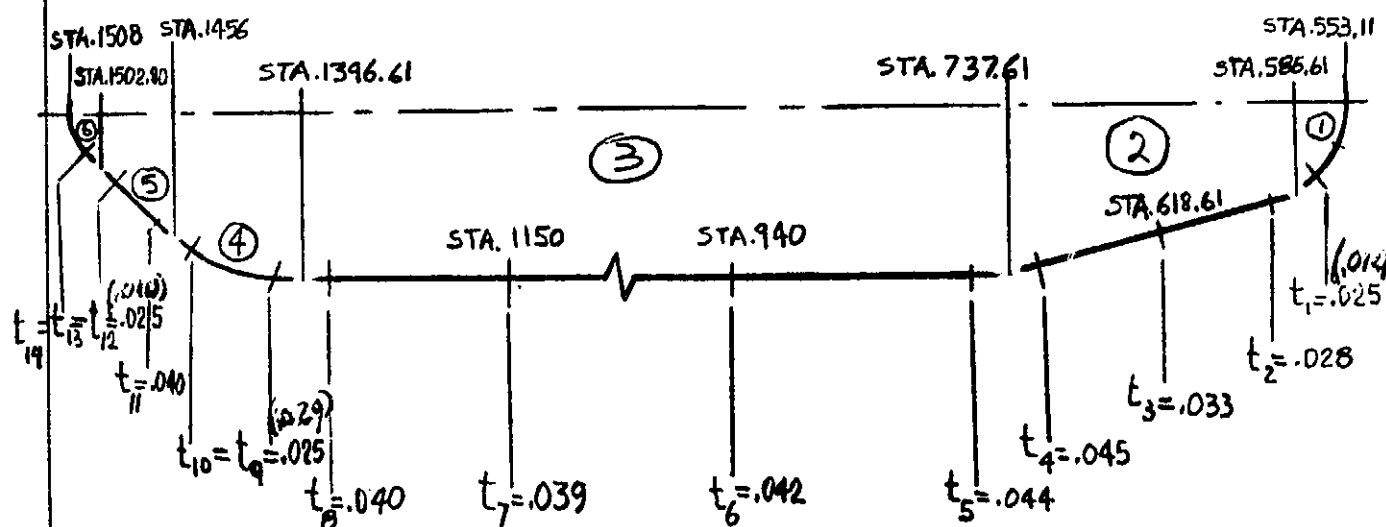
THICKNESS (IN.)	t ₁	t ₂	t ₃	t ₄	t ₅	t ₆	t ₇	t ₈	t ₉	t ₁₀	t ₁₁	t ₁₂	t ₁₃
2219-T-87 FLT COND (INT PRESS.) WT = 1352 LB	.025	.023	.033	.045	.044	.042	.039	.040	.025	.025	.040	.025	.025
2219-T-31 FLT COND (INT PRESS.) WT = 1670 LB	.025	.023	.034	.046	.044	.043	.040	.040	.025	.025	.040	.025	.025
301 CRES EXTRA HARD FLT COND (INT PRESS.) WT = 1555 LB	.010	.010	.010	.012	.012	.012	.012	.012	.010	.010	.012	.010	.010

EM NO: 12-12-01-M-13
DATE: 21 June 1971

Space Shuttle Project

THICKNESS DISTRIBUTION (2219-T87 AL-ALLY)

Using $t_{min} = .025"$ and round-off values from Page 3 the LH_2 tank wall thicknesses are as sketched below

2219-T87 AL-ALLY TANK WEIGHT

a) Constant thickness shells

$$\text{Spherical Cap, Shell ①: } W_1 = 2\pi \times 42.5 \times 33.5 \times .025 \times .102 = 22.8 \sim 23.^\#$$

$$\text{Spherical Segment, Shell ④: } W_4 = 2\pi \times 84.0 \times 59.39 \times .025 \times .102 = 79.9 \sim 80.^\#$$

$$\text{Spherical Cap, Shell ⑥: } W_6 = 2\pi \times 17.8 \times 5.20 \times .025 \times .102 = 1.48 \sim 2.^\#$$

b) Varying thickness shells

$$\text{Fwd. Cone, Shell ②: } t_{Av} = \frac{1}{2}(.028 + .045) = .0365"$$

$$W_2 = \pi(84 + 43.55) \left((151)^2 + (84 - 43.55)^2 \right)^{1/2} (.0365)(.102) = 239.6 \sim 240.^\#$$

Cylinder, Shell ③.

$$\text{STA. 1396.61 to STA. 1150 : } W = 2\pi(84)(246.61)(.0395)(.102) = 524.41 \#$$

$$\text{STA. 1150 to STA. 737.61 : } t_{Av} = \frac{1}{3}(.039 + .042 + .044) = .0416 \sim .042''$$

$$W = 2\pi(84)(412.39)(.042)(.102) = 932.43 \#$$

$$W_{\textcircled{3}} = 524.41 + 932.43 = 1456.83 \sim 1457 \#$$

$$\text{Aft Cone, Shell ⑤ : } t_{Av} = \frac{1}{2}(.025 + .040) = .0325''$$

$$W_{\textcircled{5}} = \pi(59.39 + 12.59)\left((46.80)^2 + (59.39 - 12.59)^2\right)^{1/2}(.0325)(.102) = 49.6 \sim 50 \#$$

$$\text{TOTAL WEIGHT: } W = \sum_{\textcircled{1}}^{\textcircled{6}} W_{\textcircled{i}} = 1852 \text{ LB (shells only).}$$

Assuming 35% weight increase due to transition sections, flanges etc. the total preliminary weight estimate is:

$$\underline{\underline{W_T = 1.35 W \sim 2500 \text{ LB}}}$$

NOTE: Thicknesses at the Aft portion of tank near the Aft Support attachment points (say, t_{10} , t_{11} & t_{12}) may be increased after a buckling analysis for non-symmetrical loads is performed.

WALL THICKNESSES USING 2219-T81 AL ALLY

From MIL-HDBK 5A, Fig. 3.2.25.4.1 (a) the tensile allow. are:

T, °F	-100	-111.2	-122	-162	-230	-300	-383	-402.6	-418.2	-420
(%)	106	106.3	107	108.2	112	120	140	146	152	152
(%)(62)	65.7	66.0	66.3	67.1	69.4	74.4	86.8	90.5	94.2	94.2

Ratioing values shown in Pg. 3 & using above allowables the new thicknesses are:

$$t_1 = (.0138) \left(\frac{66.5}{65.7} \right) = .0139 \sim .014" (.025" \text{ min. thick})$$

$$t_2 = (.0275) \left(\frac{66.5}{65.7} \right) = .02783 \sim .028"$$

$$t_3 = (.0329) \left(\frac{66.5}{65.7} \right) = .03333 \sim .034"$$

$$t_4 = (.0448) \left(\frac{68.0}{67.1} \right) = .0454 \sim .046"$$

$$t_5 = (.0433) \left(\frac{68.0}{67.1} \right) = .04388 \sim .044"$$

$$t_6 = (.0420) \left(\frac{70}{69.4} \right) = .04236 \sim .043"$$

$$t_7 = (.0390) \left(\frac{75.5}{74.4} \right) = .03957 \sim .040"$$

$$t_8 = (.0395) \left(\frac{94.5}{94.2} \right) = .03962 \sim .040"$$

$$t_9 = (.0197) \left(\frac{94.5}{94.2} \right) = .01976 \sim .020" (.025")$$

$$t_{10} = (.0199) \left(\frac{94.5}{94.2} \right) = .01996 \sim .020" (.025")$$

$$t_{11} = (.0397) \left(\frac{94.5}{94.2} \right) = .03982 \sim .040"$$

$$t_{12} = (.0085) \left(\frac{94.5}{94.2} \right) = .00852 \sim .010" (.025")$$

$$t_{13} = t_{14} = (.0043) \left(\frac{94.5}{94.2} \right) = .00431 \sim .010" (.025")$$

REMARK: See NOTE in page 5.

2219-T 81 AL ALY TANK WEIGHT

Using data from page 4 in conjunction with new thicknesses (where applicable) one has:

$$\text{Shell } \textcircled{1}, W_{\textcircled{1}} = 23. \#$$

$$\text{Shell } \textcircled{4}, W_{\textcircled{4}} = 80. \#$$

$$\text{Shell } \textcircled{6}, W_{\textcircled{6}} = 2. \#$$

$$\text{Shell } \textcircled{2}, t_{Av} = \frac{1}{2}(.028 + .046) = .0370", V_{\textcircled{2}} = (240) \left(\frac{.0370}{.0365} \right) = 243.3 \#$$

Shell $\textcircled{3}$,

$$\text{STA. 1396.61 to STA 1150: } W = (524.41) \left(\frac{.0400}{.0395} \right) = 531.04 \#$$

$$\text{STA 1150 to STA 737.61: } t_{Av} = \frac{1}{3}(.040 + .043 + .044) = .0423"$$

$$W = (932.43) \left(\frac{.0423}{.0420} \right) = 939.09 \#$$

$$W_{\textcircled{3}} = 531.04 + 939.09 = 1470.13 \#$$

$$\text{shell } \textcircled{5}, W_{\textcircled{5}} = 50. \#$$

$$\sum_{\textcircled{1}}^{\textcircled{6}} W_{\textcircled{i}} = 1868.43 \sim 1870 \text{ LB (shell only)}$$

$$\underline{\text{TOTAL WT: } 1.35(\sum W_i) = 2524.5 \text{ LB}}$$

FeA

FERROUS ALLOYS

AEROSPACE STRUCTURAL METALS HDBK, 1967

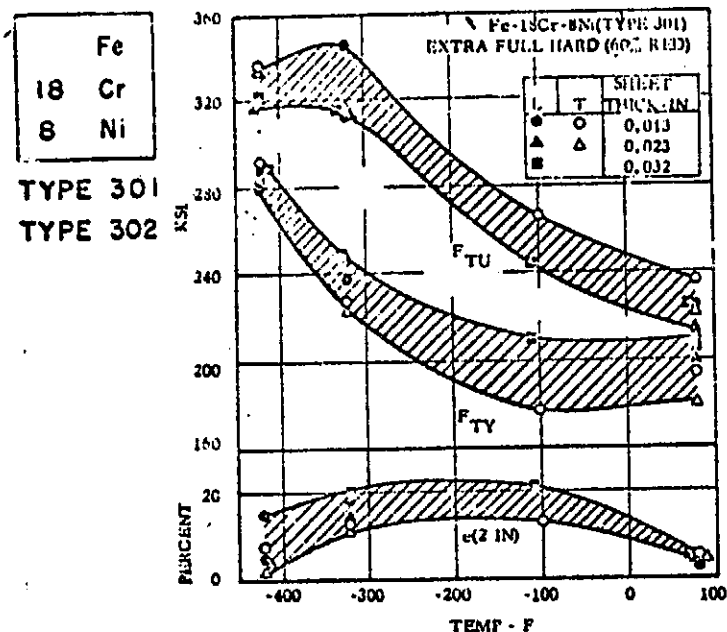


FIG. 3.03166 EFFECT OF LOW TEST TEMPERATURE AND THICKNESS ON TENSILE PROPERTIES OF 60 PERCENT REDUCED SHEET (31, p. 21, 22, 23)

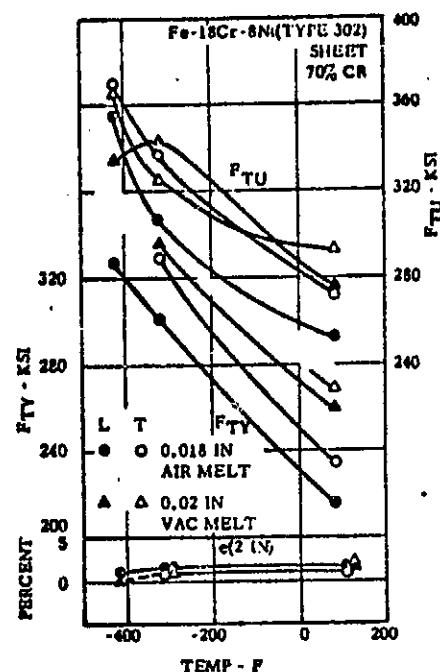


FIG. 3.03168 EFFECT OF LOW TEST TEMPERATURE AND MELT METHOD ON TENSILE PROPERTIES OF 70 PERCENT REDUCED SHEET (23)

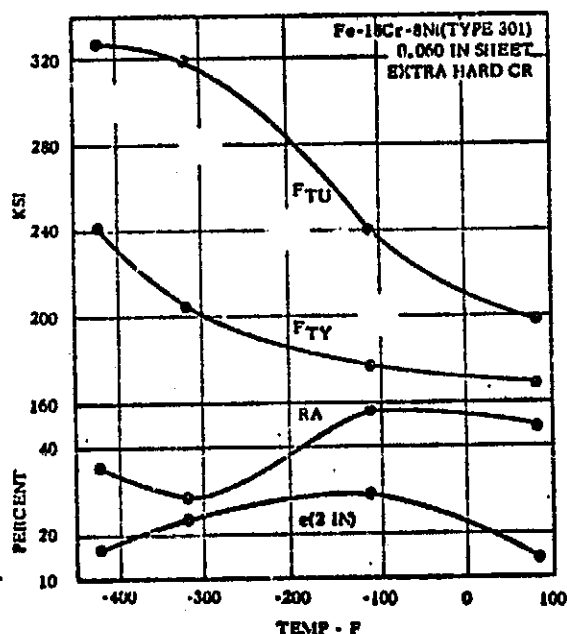


FIG. 3.03167 EFFECT OF LOW TEMPERATURE ON TENSILE PROPERTIES OF EXTRA HARD COLD ROLLED SHEET (32, p. 26)

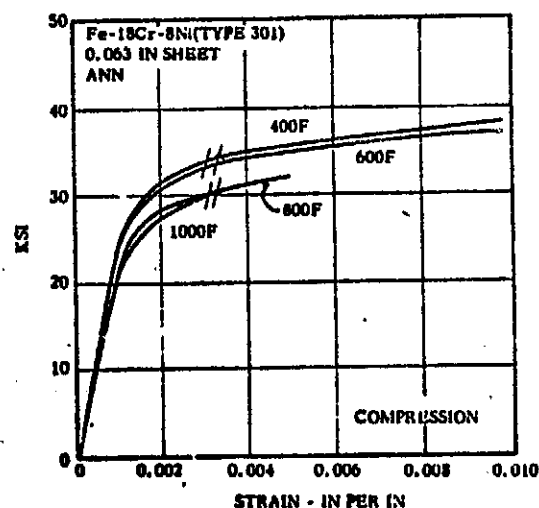
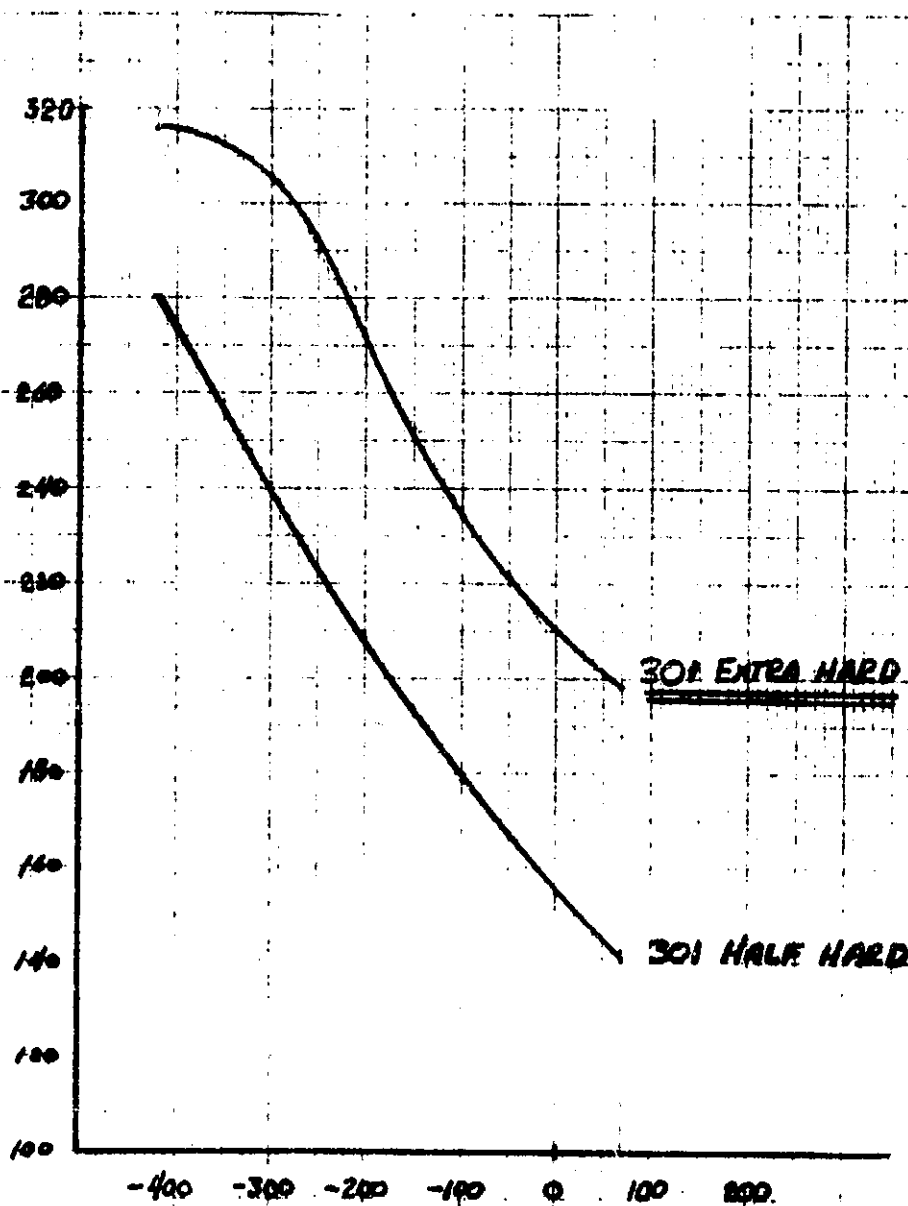


FIG. 3.03211 STRESS-STRAIN CURVES IN COMPRESSION FOR TYPE 301 ANNEALED SHEET AT ELEVATED TEMPERATURES (19, p. 57)

Prepared by: <i>H. BASERGA</i>	Date <i>5-21-71</i>	LOCKHEED MISSILES & SPACE COMPANY A GROUP DIVISION OF LOCKHEED AIRCRAFT CORPORATION	Page <i>13</i>	Temp.	Form.
Checked by:	Date	Title	EM No. <i>L2-12-01-M1-13</i>		
Approved by:	Date		Date: <i>21 June 1971</i>		

301 CRES ST'L. TENSILE PROPERTIES

For purposes of a preliminary tank wall thickness sizing tensile properties as shown below are used.



Prepared by: <i>H. EASERGA</i>	Date <i>5-21-71</i>	LOCKHEED MISSILES & SPACE COMPANY A GROUP DIVISION OF LOCKHEED AIRCRAFT CORP.	Page 1	Temp. 1	Form. 1
Checked by:	Date	Title	EM No. L2-12-01-M1-13	Date: 21 June 1971	
Approved by:	Date		Report No.		

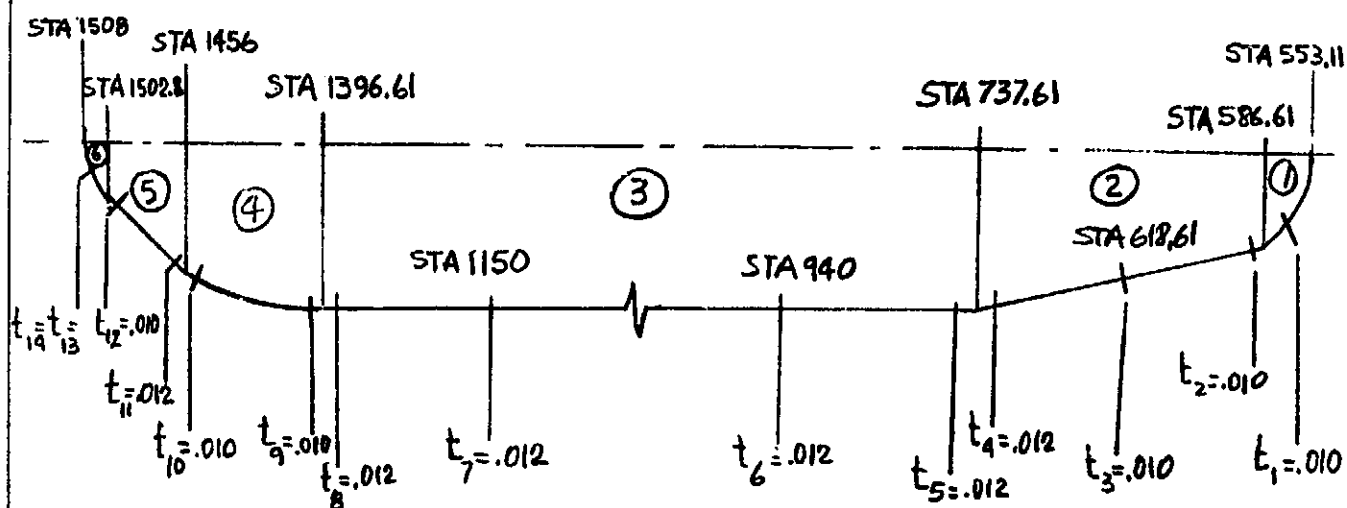
301 EXTRA HARD ST'L. WALL THICKNESS SIZING

		COND. (2)	T, °F	$\bar{\sigma}_T$, KSI	COND. (3): $p=25$ PSI	ROUND OFF THICK.
①	$t_1 = \frac{(P_{1-2})(R_0)}{2 \bar{\sigma}_{ULL}} (1.4)$	$\frac{29.0 \times 45.2}{2 \times 234} (1.4) = .0039$	-100	234	NON CRITICAL	.010
②	$t_2 = \frac{(P_{1-2})(r_1)}{\bar{\sigma}_{ULL} \cos \alpha} (1.4)$	$\frac{29.0 \times 43.55}{234 \times .9659} (1.4) = .0078$	-111.2	238	N.C.	.010
	$t_3 = \frac{(P_{1-2})(r_2)}{\bar{\sigma}_{ULL} \cos \alpha} (1.4)$	$\frac{29 \times 52.10}{234 \times .9659} (1.4) = .0098$	-122	240	N.C.	.010
	$t_4 = \frac{(P_{2-3})(r_3)}{\bar{\sigma} \cos \alpha} (1.4)$	$\frac{29.412 \times 84}{316 \times .9659} (1.4) = .0113$	-162	256	$\frac{25 \times 84}{256 \times .9659} (1.4) = .0119$.012
	$t_5 = \frac{(P_{2-3})(R_3)}{\bar{\sigma}} (1.4)$	$\frac{29.412 \times 84}{316} (1.4) = .0109$	-162	256	$\frac{25 \times 84}{256} (1.4) = .0115$.012
STA. 940	$t_6 = \frac{(P_1)(R_3)}{\bar{\sigma}} (1.4)$	$\frac{30.113 \times 84}{316} (1.4) = .0112$	-230	284	$\frac{25 \times 84}{284} (1.4) = .0104$.012
③	$t_7 = \frac{(P_j)(R_3)}{\bar{\sigma}} (1.4)$	$\frac{30.840 \times 84}{316} (1.4) = .0115$	-300	305	$\frac{25 \times 84}{305} (1.4) = .0097$.012
STA. 1150	$t_8 = \frac{(P_{3-4})(R_3)}{\bar{\sigma}} (1.4)$	$\frac{31.694 \times 84}{316} (1.4) = .0118$	-383	315	$\frac{25 \times 84}{315} (1.4) = .0093$.012
	$t_9 = \frac{(P_{3-4})(R_3)}{2 \bar{\sigma}} (1.4)$	$\frac{31.694 \times 84}{2 \times 316} (1.4) = .0059$	-383	315	$\frac{25 \times 84}{2 \times 315} (1.4) = .0047$.010
	$t_{10} = \frac{(P_{4-5})(R_4)}{2 \bar{\sigma}} (1.4)$	$\frac{31.90 \times 84}{2 \times 316} (1.4) = .0059$	-402.6	316	N.C.	.010
	$t_{11} = \frac{(P_{4-5})(r_4)}{\bar{\sigma} \cos \beta} (1.4)$	$\frac{31.90 \times 59.39}{316 \times .7071} (1.4) = .0119$	-402.6	316	N.C.	.012
	$t_{12} = \frac{(P_{5-6})(r_5)}{\bar{\sigma} \cos \beta} (1.4)$	$\frac{32.061 \times 12.59}{316 \times .7071} (1.4) = .0025$	-418.2	316	N.C.	.010
	$t_{13} = \frac{(P_{5-6})(R_6)}{2 \bar{\sigma}} (1.4)$	$\frac{32.061 \times 17.8}{2 \times 316} (1.4) = .0012$	-418.2	316	N.C.	.010
	$t_{14} = \frac{(P_6)(R_6)}{2 \bar{\sigma}} (1.4)$	$\frac{32.079 \times 17.8}{2 \times 316} (1.4) = .0012$	-420	316	N.C.	.010

Prepared by: H. BASERGA	Date 5-21-71	LOCKHEED MISSILES & SPACE CO A GROUP DIVISION OF LOCKHEED AIRCRAFT CO. EM No. L2-12-01-M1-13 Date: 21 June 1971
Checked by:	Date	
Approved by:	Date	
		Report No.

THICKNESS DISTRIBUTION (301 CRES EXTRA HARD)

Using $t_{min} = .010$ " and rounding off values from Table the LH₂ tank wall thicknesses are as sketched below.



ST'L. TANK WEIGHT

Spherical Cap, Shell ① : $W_① = (23) \frac{.010 \times .286}{.025 \times .102} = 25.8$

Fwd. Cone, Shell ② : $W_② = (240) \frac{.0106 \times .286}{.0365 \times .102} = 195.4$

Cylinder, Shell ③ : $W_③ = 2\pi \times 84 \times 659 \times .012 \times .286 = 1,193.7$

Spherical Segm., Shell ④ : $W_④ = (80) \frac{.010 \times .286}{.025 \times .102} = 89.7$

Aft Cone, Shell ⑤ : $W_⑤ = (50) \frac{.011 \times .286}{.0325 \times .102} = 47.5$

Aft Sph. Cap, Shell ⑥ : $W_⑥ = (2) \frac{.010 \times .286}{.025 \times .102} = 2.3$

$\Sigma W_① = 1554.4 \text{ LB}$

TOTAL WEIGHT: $W_T = (1.35)(1554.4) = 2098.44 \sim 2100 \text{ LB}$

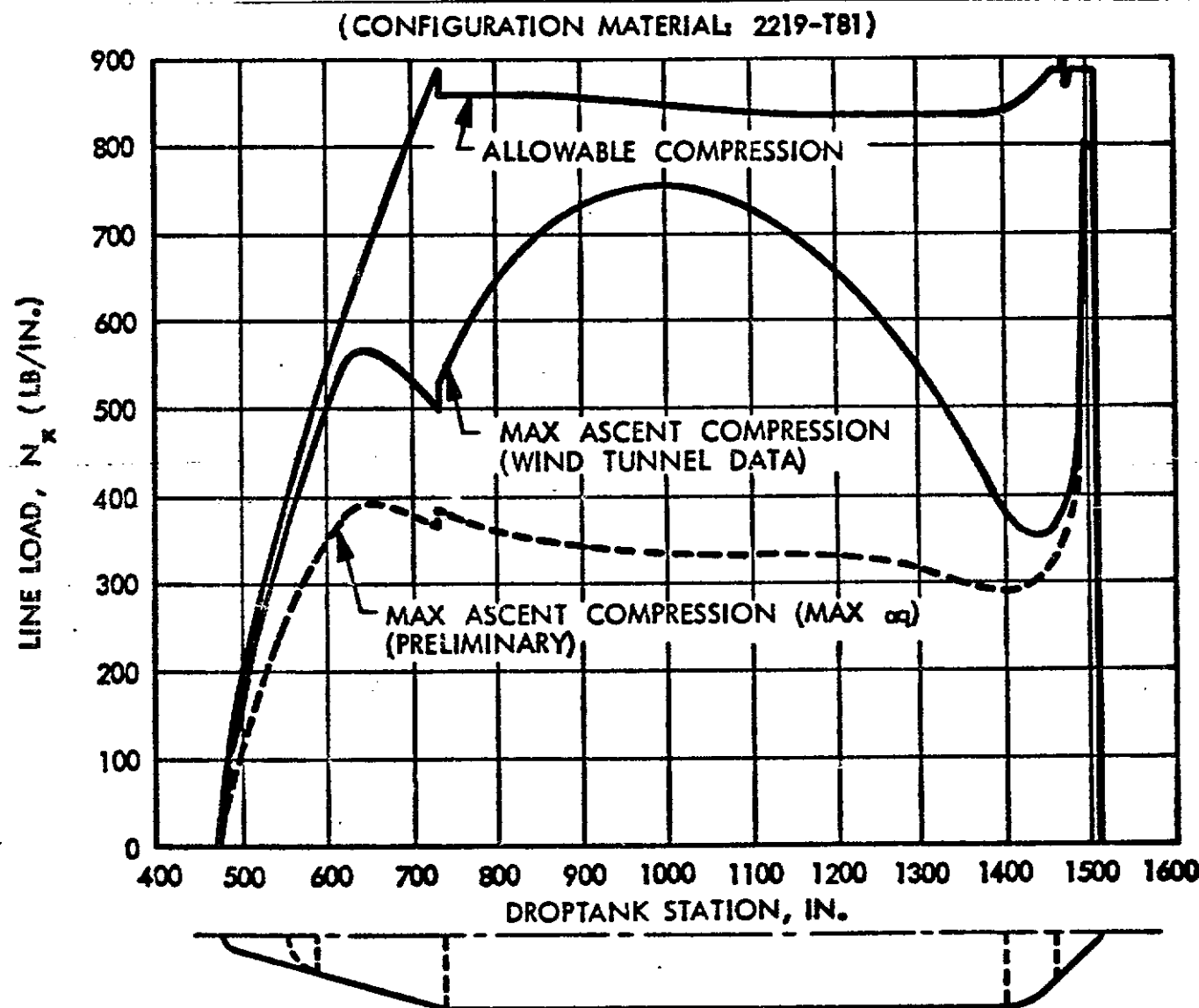


Fig. 3 Droptank Ascent Compression Line Load

DC3568(1)

Prepared by: S. A. CARTER	Date: MAY 26 1971	LOCKHEED MISSILES & SPACE COM A GROUP DIVISION OF LOCKHEED AIRCRAFT CORP	EX NO. L2-12-01-M1-13
Checked by:	Date:	Title:	Date: 21 June 1971
Approved by:	Date:		Report No.

TABLE 4A
PRELIMINARY DROPTANK ASCENT LINE LOADS
(MAX $g \ll$ CONDITION)

STATION (IN)	RADIUS (IN)	MOMENT (LB-IN/10 ⁶)	AXIAL LOAD (LB x 10 ³)	$\pm N_{XB}$ ⁽¹⁾ (LB/IN)	N_{XA} ⁽²⁾ (LB/IN)	N_{VCOMP} (LB/IN)	N_{XTEN} (LB/IN)
587	45.2	1.2	13	262	64	326	198
617	53.9	1.85	25	284	103	387	181
737	87	3.70	57.5	217	147	364	70
738	84	3.70	57.5	234	153	387	81
800	84	3.40	57.5	215	153	368	62
900	84	3.07	57.5	194	153	347	41
1000	84	2.90	57.5	183	153	336	30
1100	84	2.90	57.5	183	153	336	30
1200	84	2.90	57.5	183	153	336	30
1300	84	2.65	57.5	167	153	320	14
1397	84	2.20	57.5	139	153	292	-14 (comp)
1456	84	1.50	87.0	95	231	326	-136 (comp)

(1) $N_{XB} = \frac{1.4M}{\pi R^2}$

(2) $N_{XA} = \frac{1.4A}{2\pi R}$

Prepared by: S. A CARTER	Date	LOCKHEED MISSILES & SPACE COM A GROUP DIVISION OF LOCKHEED AIRCRAFT CORP	FM NO. 12-12-01-M1-13
Checked by:	Date	Title	Date: 21 June 1971
Approved by:	Date		Report No.

TABLE 4B
DROPTANK ASCENT LINE LOADS : MAX α g CONDITION
BASED ON WIND TUNNEL AIR LOAD PREDICTIONS

STATION (IN)	RADIUS (IN)	MOMENT (LB-IN x 10 ⁻⁶)	AXIAL LOAD (LB x 10 ⁻³)	$\pm N_{XB}^{(1)}$ (LB/IN)	$- N_{XB}^{(2)}$ (LB/IN)	N_{XCOMP} (LB/IN)	N_{XTENS} (LB/IN)
567	45.2	1.89	13	412	64	476	348
619	53.9	3.0	25	460	103	563	357
738(-)	87	6.0	57.5	353	147	500	206
738(+)	84	6.0	57.5	379	153	532	226
800	84	7.7	57.5	486	153	639	333
900	84	9.2	57.5	581	153	734	428
1000	84	9.5	57.5	600	153	753	447
1100	84	9.1	57.5	575	153	728	422
1200	84	8.0	57.5	505	153	658	352
1300	84	6.2	57.5	392	153	545	239
1397	84	3.7	57.5	234	153	387	81
1456	84	2.0	87.0	126	231	357	-105 (comp)

(1) $N_{XB} = \frac{1.4M}{\pi R^2}$

(2) $N_{XB} = \frac{1.4A}{2\pi R}$

Prepared by: S. A. CARTER	Date MAY 26 1971	LOCKHEED MISSILES & SPACE COMF A GROUP DIVISION OF LOCKHEED AIRCRAFT CORP	EM No. L2-12-01-M1-13 Date: 21 June 1971
Checked by:	Date	Title	
Approved by:	Date		Report No.

TABLE 5 **DROP TANK ALLOWABLE LINE LOADS**

ASCENT αg CONDITION

ASSUME INTERNAL PRESSURE = 25 psia $\begin{cases} +0 \\ -3 \text{ psia} \end{cases}$ for valve Tol.

TANK TEMP = -420°F , $E_c = 12.5 \times 10^6 \text{ psi}$, $F_{tu} = 94,000 \text{ psi}$

STA (IN)	r IN	t (IN)	R/t	K	P ⁽¹⁾ psig	P ⁽²⁾	λ	N _{cr} ⁽³⁾	N _{comp} ⁽⁴⁾	N _{cr} ⁽⁵⁾	N _{TEM}	M _{ALL} $\times 10^{-6} \text{ in-lb}$
587	45.2	.028	1615	.63	16.7	5.76	.865	114	491	2632	2186	3.151
619	53.9	.034	1585	.635	16.7	5.55	.861	140	590	3196	2665	5.385
737	87	.046	1892	.62	17.2	8.14	.901	166	892	4324	3467	21.211
738	84	.044	1909	.62	17.2	8.28	.903	157	858	4136	3309	19.019
910	84	.043	1955	.62	18.0	9.09	.911	152	853	4042	3215	18.909
1150	84	.040	2100	.61	18.9	11.02	.925	133	834	3760	2933	18.487
1397	84	.040	2100	.61	20.0	11.66	.929	134	835	3760	2933	18.510
1456	84	.040	2100	.61	20.2	11.78	.930	134	835	3760	2933	18.510

(1) $P_{amb} = 5.3 \text{ psi @ } \alpha g \therefore P_g = 25 - 3 - 5.3 = 16.7 \text{ psig}$, $P_{gh} = \gamma h + P_g$

(2) $\bar{P} = \left(\frac{P}{E_c}\right) \left(\frac{R}{t}\right)^2 \sqrt{3(1-\mu^2)}$

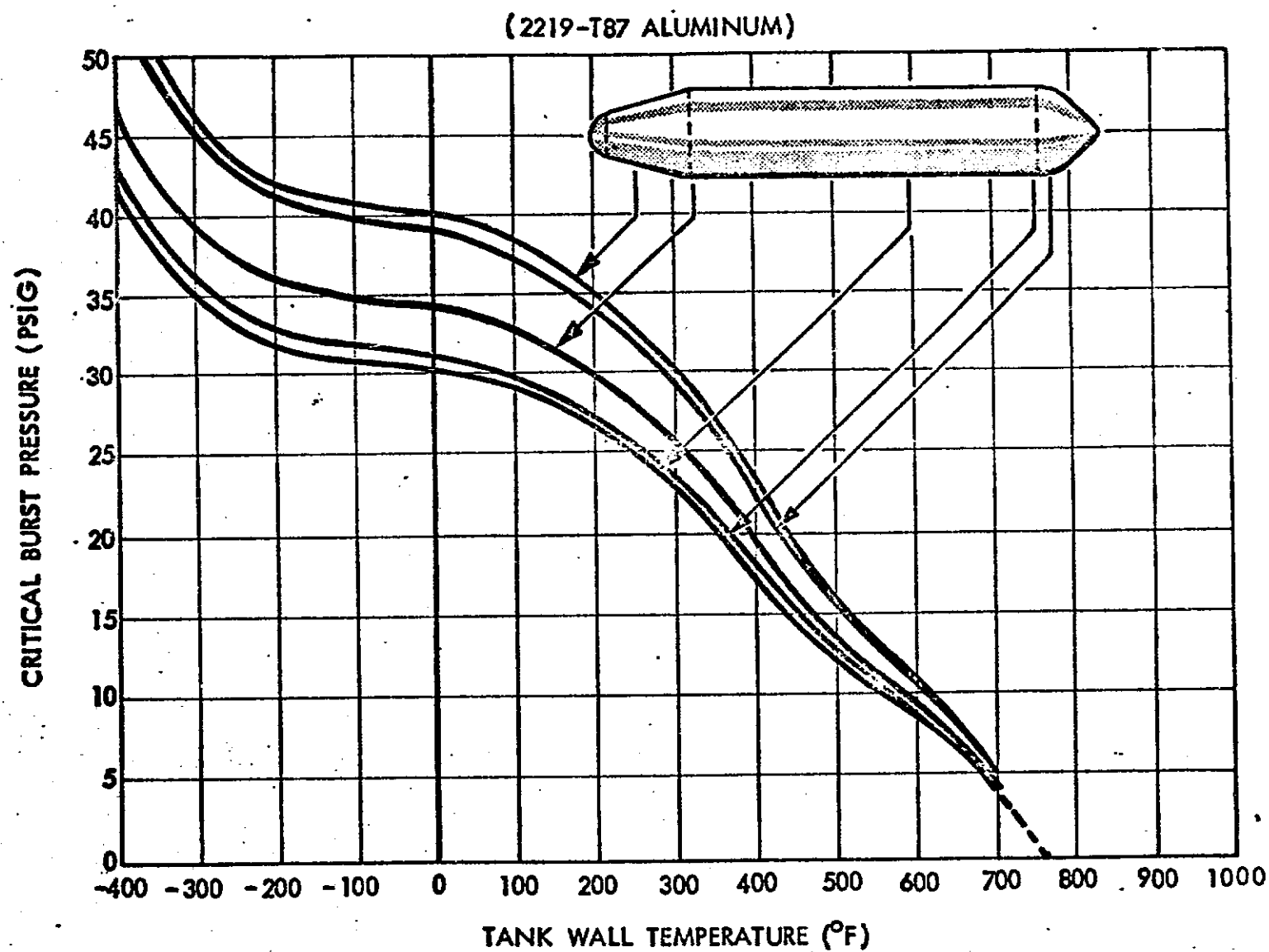
(3) $N_{cr} = \lambda \left[E / \sqrt{3(1-\mu^2)} \left(\frac{t}{R}\right)^2 \right]$; See Fifth Letter Rept, EM L2-01-02-M5-2

(4) $N_{comp} = N_{cr} + \frac{PR}{2}$

(5) $N_{XT} = F_{tu}(t)$; $N_{XP} = \frac{19.7R}{2} \therefore N_{XTEN} = N_{XT} - N_{XP}$



FIGURE 4
DROPTANK CRITICAL BURST PRESSURE



D03594

EM No. 12-12-01-M-1
Date: 21 June 1971

Prepared by: S. A. CARTER	Date: MAY 14 1971	LOCKHEED MISSILES & SPACE COMPANY A GROUP DIVISION OF LOCKHEED AIRCRAFT CORP.	EM No. L2-12-01-M1-13 Date: 21 June 1971
Checked by:	Date:	Title:	
Approved by:	Date:		Report No.

TABLE 6
CRITICAL TANK BURST PRESSURE ANALYSIS

TEMP., °F	F _{t0} (psi)	FWD DOME t: .025 R: 45.2	CONE t: .033 R: 53.94	FWD CYL t: .044 R: 84	FWD/MID CYL t: .042 R: 84	AFT/MID CYL t: .039 R: 84	AFT CYL t: .040 R: 84	AFT SPH t: .015 R: 84	AFT CONE t: .033 R: 50.90	AFT DOME t: .025 R: 17.8
-420	94,500	104.5	57.8	49.5	47.25	43.9	45.0	56.2	61.3	265.4
-350	82,000	90.7	50.2	42.95	41.0	38.1	39.0	48.8	53.2	230.3
-300	75,500	83.5	46.2			35.1				
-250	71,000	78.5	43.4	37.2	35.5	33.0	33.8	42.3	46.0	199.4
-200	69,000	76.3	42.2			32.0				
-150	68,000	75.2	41.6	35.6	34.0	31.6	32.4	40.5	44.1	191.0
-100	66,500	73.6	40.7			30.9				
-50	66,000	73.0	40.4	34.6	33.0	30.6	31.4	39.3	42.8	185.4
0	65,500	72.5	40.1			30.4				
+50	64,500	71.3	39.5	33.8	32.3	29.9	30.7	38.4	41.8	181.2
+100	62,000	68.6	37.9			28.8				
+150	60,000	66.4	36.7	31.4	30.0	27.9	28.6	35.7	38.9	168.5
+200	56,500	62.5	34.6			26.2				
+250	54,000	59.7	33.0	28.3	27.0	25.1	25.7	32.1	35.0	151.7
+300	50,000	55.3	30.6			23.2				
+350	44,000	48.7	26.9	23.0	22.0	20.4	21.0	26.2	28.5	123.6
+400	38,000	42.0	23.2			17.6				
+450	31,500	34.8	19.3	16.5	15.8	14.6	15.0	18.7	20.5	88.5
+500	26,000	28.8	15.9			12.1				
+550	22,000	24.3	13.5	11.5	11.0	10.2	10.5	13.1	14.3	61.8
+600	19,000	21.0	11.6			8.8				
+650	14,000	15.5	8.6	7.3	7.0	6.5	6.7	8.3	9.1	39.3
+700	8,200	9.1	5.0	4.3	4.1	3.8	3.9	4.9	5.3	23.0

$$P_{cr} = \frac{KF_{t0} \cdot t}{R}, \quad K_{sph} = 2.0, \quad K_{cyl} = K_{cone} = 1.0$$

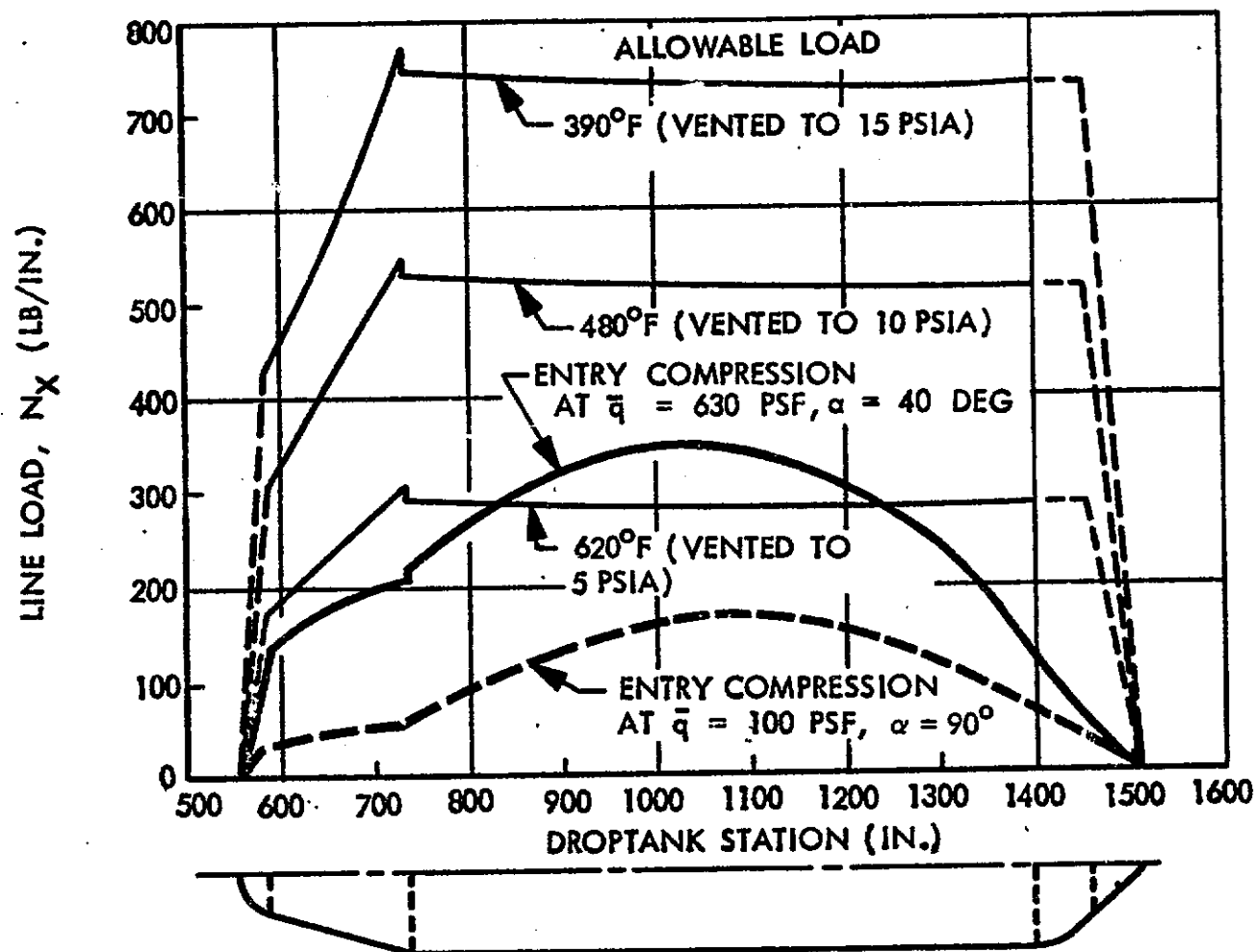


Fig. 5 Droptank Compression Line Load

D03590(1)

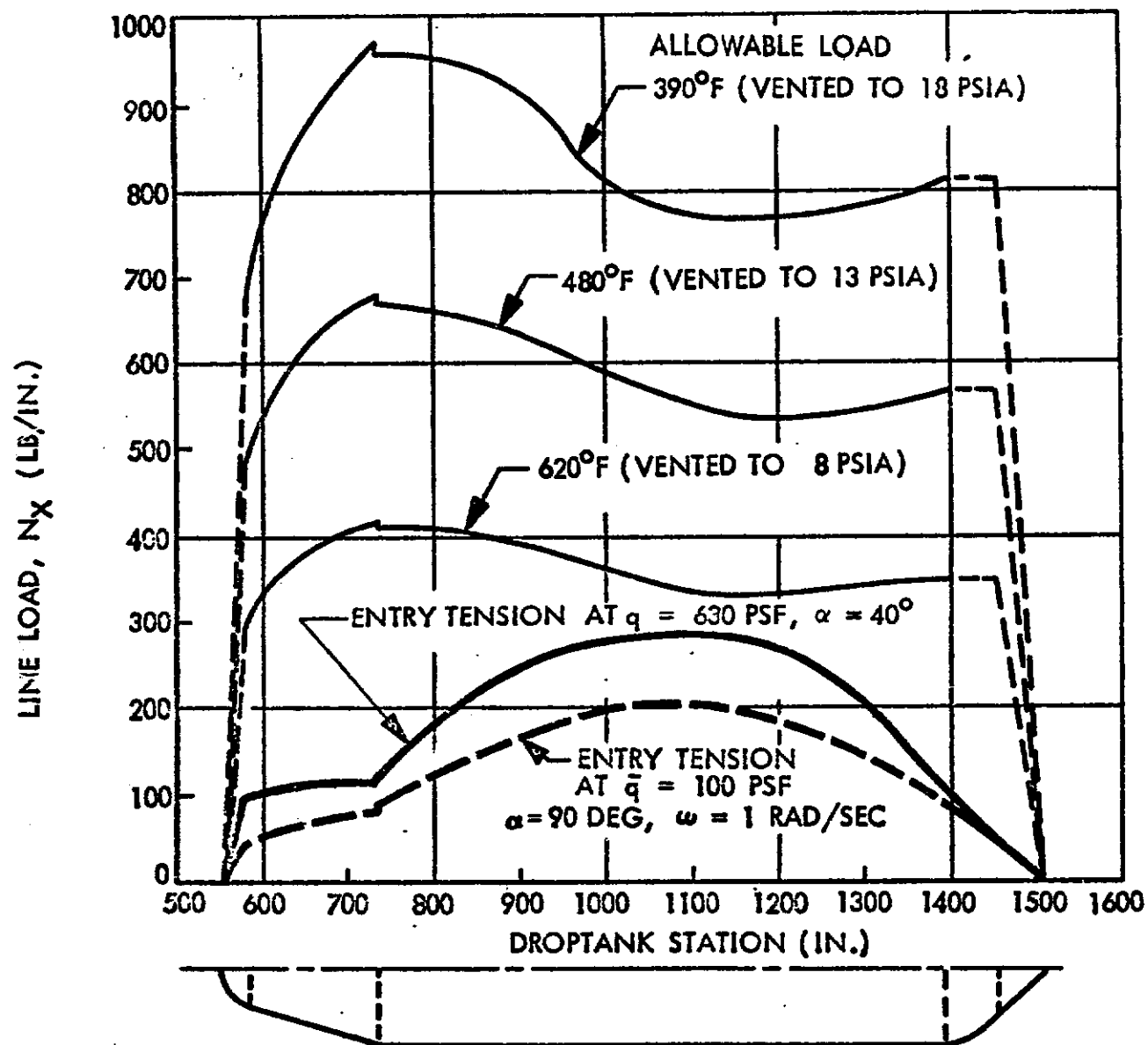


Fig. 6 Droptank Tension Line Load

D03591(1)

Prepared by: S. A. CARTER	Date: MAY 27 1971	LOCKHEED MISSILES & SPACE COM A GROUP DIVISION OF LOCKHEED AIRCRAFT CORP	EM No. L2-12-01-M-13
Checked by:	Date:		Title
Approved by:	Date:		Report No.

Table 7
DROP TANK ALLOWABLE COMPRESSION LINE LOAD
 • DURING ENTRY: VENTED PRESSURE = 18-3 = 15 psia

GEOMETRY	STA (IN)	R (IN)	t (IN)	R/t	L/R	K	P ⁽¹⁾ (PSIA)	P ⁽¹⁾	λ ⁽²⁾	N _{ter} ⁽³⁾ (LB/IN)	N _{yp} (LB/IN)	N _{ALL COMP} ⁽⁴⁾ (LB/IN)
	587	45.2	.028	1614	> 2	.63	15	6.80	.88	87	339	426
	619	53.9	.033	1634	> 2	.63		6.97	.89	103	404	507
	737	87	.045	1932	> 2	.62		9.74	.92	123	650	773
	738	84	.044	1909	> 2	.62		9.51	.91	121	630	750
	940	84	.042	2000	> 2	.61		10.44	.92	111	630	741
	1150	84	.039	2154	> 2	.61		12.10	.93	97	630	729
	1397	84	.040	2100	> 2	.61		11.50	.93	102	630	732
	1456	84	.040	2100	> 2	.61	15	11.50	.93	102	630	732

TANK WALL TEMPERATURE = 390°F, E_c = 9.5 x 10⁶ psi

(1) $\bar{P} = \left(\frac{P}{E_c} \right) \left(\frac{R}{t} \right)^2 \sqrt{3(1-\mu^2)}$

(2)

(3) $N_{ter} = \lambda \left[\frac{K \cdot F}{E / \sqrt{3(1-\mu^2)}} \right] \left(\frac{t^2}{R} \right)$

(4) $N_{ALL} = N_{ter} + N_{yp} = N_{ter} + \frac{PR}{2}$

(5) Max Tank wall pressure is based on the critical vented pressure during re-entry. Using P_{cr} = 18 psia (@ 390°F) ± 3 (For Valve Tolerance)

Prepared by: S. A. CARTER	Date: MAY 17 1971	LOCKHEED MISSILES & SPACE COMPANY <small>A GROUP DIVISION OF LOCKHEED AIRCRAFT CORP.</small>	Page Temp. Form.
Checked by:	Date	Title	EM No. 12-12-01-M1-13 Date: 21 June 1971
Approved by:	Date		Report No.

Table 8

DROP TANK ALLOWABLE TENSION LINE LOAD

DURING ENTRY: VENTED PRESSURE = (18-0) = 18 psia

GEOMETRY	STA (IN)	R (IN)	t (IN)	P ⁽¹⁾ (PSIA)	TEMP. ⁽²⁾ °F	F _{tu} (PSI)	N _{xt} ⁽³⁾ (LB/IN)	N _{xp} ⁽⁴⁾ (LB/IN)	N _{YALL TENS.} ⁽⁵⁾ (LB/IN)
	587	45.2	.028	18	390	39000	1092	407	685
	619	53.9	.033	↑	↑	↑	1287	485	802
	737	87	.045	↑	↑	↑	1755	783	972
	738	84	.044	↑	↑	↑	1716	756	960
	940	84	.042	↑	↑	↑	1638	756	882
	1150	84	.039	↑	↑	↑	1521	756	765
	1397	84	.040	↓	↓	↓	1560	756	804
	1456	84	.040	18	390	39000	1560	756	804

(1) MAX. INTERNAL PRESSURE = 15 psi + VALVE TOLERANCE = 18 psi

(2) FROM CRITICAL BURST PRESSURE CHART, ALLOWABLE TEMP = 390 °F

(3) $N_{xt} = F_{tu}(t)$

(4) $N_{xp} = PR/2$

(5) $N_{YALL TENS} = N_{xt} - N_{xp}$

Prepared by: S. A. CARTER	Date MAY 26 1971	LOCKHEED MISSILES & SPACE COM A GROUP DIVISION OF LOCKHEED AIRCRAFT CORP.	EM No. L2-12-01-M1-13	
Checked by:	Date		Title	Date: 21 June 1971
Approved by:	Date		Report No.	

Table 9
DROP TANK ALLOWABLE COMPRESSION LINE LOAD
(DURING RE-ENTRY)

ASSUME TANK INTERNAL PRESSURE = $13 - 3 = 10$ psia
ASSUME TANK WALL TEMPERATURE = 480°F , $E_c = 8.8 \times 10^6$ psi

STA (IN)	R (IN)	t (IN)	K	P (psia)	\bar{P}	λ	N_{xcr} (LB/IN)	N_{xsp} (LB/IN)	N_{xallow} (LB/IN)
587	45.2	.028	.63	10	4.89	.84	77	226	303
619	53.9	.033	.63	↑ ↓	5.01	.85	91	270	361
737	87	.045	.62		7.02	.89	110	435	545
738	84	.044	.62		6.84	.88	108	420	528
940	84	.042	.61		7.51	.89	100	420	520
1150	84	.039	.61		9.17	.91	88	420	508
1397	84	.040	.61		8.28	.90	91	420	511
1456	84	.040	.61	10	8.28	.90	91	420	511

Prepared by: S. A. CARTER	Date MAY 26 1971	LOCKHEED MISSILES & SPACE COM A GROUP DIVISION OF LOCKHEED AIRCRAFT CORP.	PM No. 12-12-01-M1-13
Checked by:	Date	Title	Date: 21 June 1971
Approved by:	Date		Report No.

Table 10
DROP TANK ALLOWABLE COMPRESSION & TENSION LINE LOAD

ASSUME TANK INTERNAL PRESSURE = 8 psia \pm 3 psia
 ASSUME TANK WALL TEMPERATURE = 620°F
 $E_c = 7.2 \times 10^6$ psi, $F_{t0} = 17,000$ psi

STA (IN)	R (IN)	t (IN)	P _{TEN} (PSIA)	F _{t0} KSI	N _{xTEN} ⁽¹⁾	K	P _{com} (PSIA)	\bar{P} ⁽²⁾	λ	N _{xcr} ⁽³⁾	N _{xp} ⁽⁴⁾	N _{xcom} ⁽⁵⁾
587	45.2	.028	8	17	295	.63	5	2.99	.762	58	113	171
619	53.9	.033	↑	↑	354	.63	↑	3.06	.761	67	135	202
737	87	.045			417	.62		4.29	.823	83	218	301
738	84	.044			412	.62		4.18	.819	82	210	292
940	84	.042			378	.61		4.59	.831	76	210	286
1150	84	.039			327	.61		5.32	.852	67	210	277
1397	84	.040			344	.61		5.06	.845	70	210	280
1456	84	.040	↓	↓	344	.61	5	5.06	.845	70	210	280

(1) $N_{xTEN} = F_{t0}(t) - \frac{PR}{2}$

(2) $\bar{P} = \left(\frac{P}{E}\right)\left(\frac{R}{t}\right)^2 \sqrt{3(1-\mu^2)}$

(3) $N_{xcr} = \lambda \left[E / \sqrt{3(1-\mu^2)} \left(\frac{t}{R} \right) \right]$

(4) $N_{xp} = \frac{PR}{2}$

(5) $N_{xcom} = N_{xcr} + \frac{PR}{2}$

Prepared by: S. A. CARTER	Date MAY 28 1971	LOCKHEED MISSILES & SPACE COM A GROUP DIVISION OF LOCKHEED AIRCRAFT CORP		EM No. L2-12-01-MI-13
Checked by:	Date	Title		Date: 21 June 1971
Approved by:	Date			Report No.

Table 11.1

DROP TANK ALLOWABLE TENSION LINE LOAD (DURING RE-ENTRY)

ASSUME TANK INTERNAL PRESSURE = 13 psia

ASSUME TANK WALL TEMPERATURE = 480°F, $F_{t0} = 27,700$

STA (IN)	R (IN)	t (IN)	P (psig)	TEMP. °F	F_{t0} (psi)	N_{xt} (LB/IN)	N_{xp} (LB/IN)	$N_{xall TEN}$ (LB/IN)
587	45.2	.028	13	480	27,700	776	294	482
619	53.9	.033	↑	↑	↑	914	350	564
737	87	.045	↑	↑	↑	1247	566	681
738	84	.044	↑	↑	↑	1219	546	673
940	84	.042	↑	↑	↑	1163	546	617
1150	84	.039	↑	↑	↑	1080	546	534
1397	84	.040	↓	↓	↓	1108	546	562
1456	84	.040	13	480	27,700	1108	546	562

Prepared by: S. A. CARTER	Date MAY 27 1971	LOCKHEED MISSILES & SPACE COMP A GROUP DIVISION OF LOCKHEED AIRCRAFT CORP.	EM No. L2-12-01-11-13	
Checked by:	Date		Title	Date: 21 June
Approved by:	Date		Report No.	

Table 12
DROP TANK ALLOWABLE COMPRESSION & TENSION LINE LOAD

ASSUME TANK INTERNAL PRESSURE = 6 psia ± 3

ASSUME TANK WALL TEMPERATURE = 665 °F

$E_c = 6.6 \times 10^6 \text{ psi}$, $F_{tu} = 12000 \text{ psi}$

STA (IN)	R (IN)	t (IN)	P _{TEN} (psig)	F _{tu} (psi)	N _{TEN} ⁽¹⁾ (LB/IN)	K	P _{COMP} (psig)	\bar{P} ⁽²⁾	λ	N _{YCR} ⁽³⁾	N _{YP}	N _{YCOMP}
587	4.2	.028	6	12000	200	.63	3	1.957	.675	47	68	115
619	53.7	.033	↑	↑	234	.63	↑	2.004	.680	55	81	136
737	87	.045	↑	↑	279	.62	↑	2.807	.748	70	131	201
738	84	.044	↑	↑	276	.62	↑	2.737	.743	68	126	194
940	84	.042	↑	↑	252	.61	↑	3.004	.758	64	126	190
1150	84	.039	↑	↑	216	.61	↑	3.464	.786	57	126	183
1397	84	.040	↓	↓	228	.61	↓	3.312	.777	59	126	185
1456	84	.040	6	12000	228	.61	3	3.312	.777	59	126	185

$$(1) N_{TEN} = F_{tu}(t) - \frac{PR}{2}$$

$$(2) \bar{P} = \left(\frac{P}{E}\right) \left(\frac{R}{t}\right)^2 \sqrt{3(1-\mu^2)}$$

$$(3) N_{YCR} = \lambda \left[E / \sqrt{3(1-\mu^2)} \left(\frac{t}{R}\right)^2 \right]$$

EM NO: L2-12-01-M1-13

DATE: 21 June 1971

indicated that the maximum dynamic pressure never exceeded 70 psf for this condition. Since these analyses were incomplete at the time the structures analysis was pursued, a \bar{q} of 100 psf was selected for initial investigation. The results from 6-D trajectories showed that the droptank stabilizes, nose first, to an angle-of-attack, α , of 40 deg., and the maximum dynamic pressure reaches 630 psf. The line loads from both these conditions (shown in EM L2-12-01-M1-12) were converted to maximum line loads in compression and tension, shown in Tables 13 and 14, and superimposed on Figures 5 and 6 for comparison with the allowable tank line loads. It is readily seen that the maximum entry loads are not critical if the tank wall temperature is limited to 500°F by cork insulation. The temperature 500°F is the limiting value for the bond line of the cork. Thus, intact entry can be achieved with cork insulation to an attitude range of 5000 to 15,000 ft, before collapse occurs when the ambient pressure becomes greater than the vented tank pressure which is set at 12 psia ± 3 . The reader is referred to EM L2-12-01-M1-10 for the thermal analyses associated with this study.

3.5 TANK ANALYSIS FOR HANDLING CONSIDERATIONS

Generally, aerospace philosophy assumes that ground handling load environments will not dictate flight hardware strength and stiffness requirements. Preliminary investigations were made for handling the baseline tank configuration in the horizontal and vertical positions to assess its strength capabilities and determine what is required for normal handling environments through the various stages of final assembly. The results of this investigation show that the empty tank, supported at its extremities, either in the horizontal or vertical position (except in tension) will require various amounts of internal pressure to prevent the tank from collapsing under its own weight. The pressurization requirements are a function of the tank weight, and are summarized at the conclusion of the following calculations in Table 15. For this analysis, an assumed handling load factor of 2 gs was used. If these values of internal pressure are maintained, handling can be achieved without compromising flight weight. In order to be able to handle the droptank without internal pressure, the tank wall must be thickened beyond that which is required for flight requirements. The following calculations show the thickness required for each condition and the resulting weight penalties are summarized in Table 15.

It should be pointed out that internal pressurization has other advantages and safeguards. Once the tank is cleaned and prepared for flight use, internal pressure will guarantee total cleanliness required for flight operation, and secondly, an unpressurized tank could inadvertently collapse during a sudden change in temperature. Final judgements regarding the handling considerations must be postponed until a more detailed evaluation of total program requirements are more defined.

Prepared by: S. A. CARTER	Date MAY 27 1971	LOCKHEED MISSILES & SPACE CO. A GROUP DIVISION OF LOCKHEED AIRCRAFT CORP.	EM No. 12-12-01-M1-13
Checked by:	Date		Date: 21 June 1971
Approved by:	Date	Title	Report No.

Table 13

DROP TANK ENTRY LINE LOADS

 $\text{MAX } \bar{q} = 100 \text{ PSF}, \alpha = 90^\circ, \omega = 0.6 \text{ RAD/SEC}$

STATION (IN)	RADIUS (IN)	MOMENT (LB-IN $\times 10^6$)	AXIAL LOAD (LB $\times 10^3$)	$\pm N_{XB}^{(1)}$ (LB/IN)	$+ N_{XA}^{(2)}$ (LB/IN)	N_{XCOMP} (LB/IN)	N_{XTENS} (LB/IN)
587	45.2	.25	1.8	39	6	33	45
619	53.9	.45	2.4	49	7	42	56
737	87	1.60	7.4	67 72	13 14	54 5	80 86
738							
800	84	2.40	8.4	108	16	92	124
900	84	3.27	9.5	148	18	130	166
1000	84	3.90	9.9	176	19	157	195
1100	84	4.10	9.5	185	18	167	203
1200	84	3.70	8.4	167	16	151	183
1300	84	2.80	6.8	126	13	113	139
1397	84	1.60	4.4	72	8	64	80
1456	84	0.70	2.4	32	5	27	37

$$(1) N_{XB} = \frac{M}{\pi R^2}$$

$$(2) N_{XA} = \frac{A}{2\pi R}$$

Prepared by: S. A. CARTER	Date: JUN 17 1971	LOCKHEED MISSILES & SPACE COM A GROUP DIVISION OF LOCKHEED AIRCRAFT CORP.		IN No. 12-12-01-M-13
Checked by:	Date:	Title:		Date: 21 June 1971
Approved by:	Date:			Report No.

Table 14
DROP TANK ENTRY LINE LOADS
 MAX \bar{q} = 630 psf, α = 40°

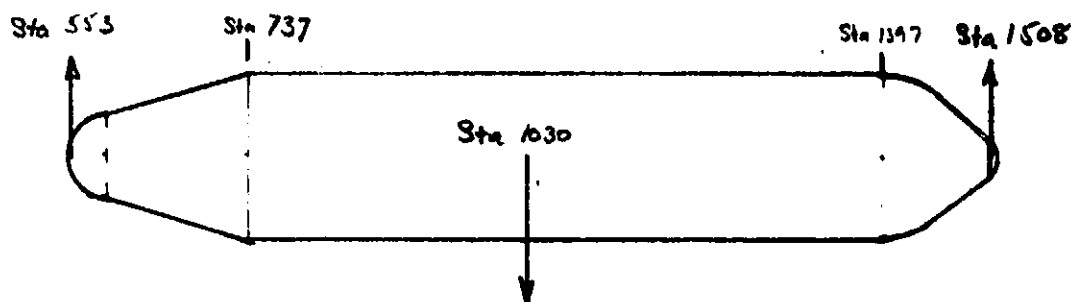
STATION (IN)	RADIUS (IN)	MOMENT (LB-IN $\times 10^3$)	AXIAL LOAD (LB $\times 10^3$)	$\pm N_{PB}$ ⁽¹⁾ (LB/IN)	$-N_{SA}$ ⁽²⁾ (LB/IN)	N_{COMP} (LB/IN)	N_{TEN} (LB/IN)
587	45.2	.765	5.04	119	18	137	101
619	53.9	1.26	7.875	138	23	161	115
738(-)	87	3.78	25.20	159	46	205	113
738(+)	84	3.78	25.20	171	48	219	123
800	84	4.851	23.310	219	44	263	175
900	84	6.30	20.475	284	39	323	245
1000	84	6.93	17.64	313	33	346	280
1100	84	6.867	14.49	310	28	338	282
1200	84	6.3	11.34	284	22	306	262
1300	84	5.04	8.505	227	16	243	211
1397	84	2.583	5.67	117	11	128	106
1456	84	1.197	2.52	54	5	59	49

(1) $N_{PB} = \frac{M}{R/L}$

(2) $N_{SA} = \frac{A}{L/R}$

Prepared by: S. A. CARTER	Date JUN 9 1971	LOCKHEED MISSILES & SPACE CO. A GROUP DIVISION OF LOCKHEED AIRCRAFT CORP.		EM No. 12-12-01-M1-13
Checked by:	Date	Title		Date: 21 June 1971
Approved by:	Date			Report No.

DROP TANK SELF-SUPPORT



- Cond (1) WEIGHT (STORED) = 6900 lbs ; Assume 2g
 Cond (2) WEIGHT (Launch Ready) = 9050

$$M_1 \text{ [Max. Moment. (center)]} = \frac{WL}{8} = \frac{(2)(6900)(955)}{8} = 1,647,400 \text{ in-lb}$$

$$M_2 = 2,160,700 \text{ in-lb}$$

$$N_{x1} = \frac{M}{\pi R^2} = 74.3 \text{ ppi} \quad , \quad N_{x1}(\text{ULT}) = 104 \text{ ppi}$$

$$N_{x2} = 97.5 \text{ ppi} \quad , \quad N_{x2}(\text{ULT}) = 137 \text{ ppi}$$

$$\text{Shell thickness, } t = .040, \quad R/t = \frac{84}{.040} = 2100, \quad K_b = .61 (1.3) = .79$$

$$\therefore N_{xcrb} = \frac{K}{2\pi} E_c t^2 / R = \frac{.79}{2\pi} (10.8 \times 10^6) (.040)^2 / 84 = 26 \text{ ppi}$$

$$\text{Pressurized with 2 psig, } \frac{PR}{2} = \frac{2 \times 84}{2} = 84 \text{ psi}$$

$$\bar{P} = \frac{P}{E_c} \left(\frac{R}{t} \right)^2 \sqrt{1 - \mu^2} = 1.35, \quad \lambda = .59, \quad N_{xcr} = .59 \left[E_c / \sqrt{1 - \mu^2} \right] t^2 / R = 73 \text{ ppi}$$

$$N_{xALL} = 73 + 84 = 157 \text{ ppi} > N_{x2}$$

$$\text{Axial Load Req'd to Release Bending Load} = (137 - 26) [2\pi R] = 58,000 \text{ lbs}$$

Prepared by: S. A. CARTER	Date JUN 9 1971	LOCKHEED MISSILES & SPACE CO. A GROUP DIVISION OF LOCKHEED AIRCRAFT CORP.	EM No. L2-12-01-11-13 Date: 21 June 1971
Checked by:	Date	Title	Report No.
Approved by:	Date		

SHELL THICKNESS REQ'D FOR SELF-SUPPORT

STORED CONDITION

$$\text{Axial } N_{x_t} = \frac{104}{1.30} = 80 \text{ ppi}, \quad \frac{N_x}{RE} = \frac{80}{84 \times 1.08 \times 10^7} = 8.6 \times 10^{-8}$$

$$t \approx 84 (.0009) \approx .076$$

$$\text{try } t = .076, \quad R/t = 1100, \quad 1/R \approx 2, \quad K = .695, \quad K_b = 1.3(.695) = .90$$

$$N_{x_b} = \frac{.90}{2\pi} (10.8 \times 10^6) (.076)^2 / 84 = 106 \text{ ppi} \sim N_{x_{all}} \therefore \text{OK}$$

$$\text{Mom. @ Fwd Cyl Station} = \frac{6900(184)}{2} - \frac{6900(184)^2}{955 \cdot 2} = 512,500 \text{ in-lb.}$$

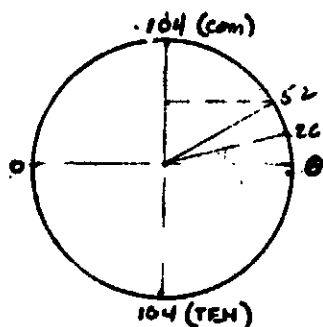
$$N_{x_{STA 737}} = \frac{512500 \times 1.4}{\pi(84)^2} = 32 \text{ ppi}$$

$$t_c = .044, \quad R/t = 1909, \quad K_b = .62(1.3) = .805$$

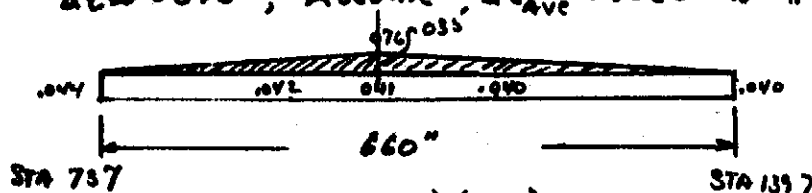
$$N_{x_{cr}} = \frac{.805}{2\pi} (10.8 \times 10^6) (.044)^2 / 84 = 32 \text{ ppi} \sim N_{x_{all}} \therefore \text{OK}$$

$$\text{Mom. @ Aft Cyl Station} = \frac{6900(111)}{2} - \frac{6900(111)^2}{955 \cdot 2} = 338,440 \text{ in-lb}$$

$$N_{x_{STA 1397}} = \frac{338,440 \times 1.4}{\pi(84)^2} = 22 \text{ ppi}, \quad \text{for } t = .040, < N_{x_{cr}} \therefore \text{OK}$$



By thickening only one-half of the shell cylinder at station 1030 from .040 to .076 and tapering that thickness from both ends; $\Delta t_{cr} = .018$, Assume $\Delta t_{ave} = .020$ for π Radians



$$\therefore \Delta W = .020(660)(\pi)(84)(.102) = 355 \text{ lbs/Tank}$$

Prepared by: S. A. CARTER	Date JUN 9 1971	LOCKHEED MISSILES & SPACE COMB No. L2-12-01-M1-13 A GROUP DIVISION OF LOCKHEED AIRCRAFT CORP.	
Checked by:	Date	Title	Date: 21 June 1971
Approved by:	Date	Report No.	

LAUNCH READY CONDITION

$$\text{try } t = .084, R/t = 1000, L/R = 2, K = .72, K_b = 1.3(.72) = .936$$

$$N_{xb} = \frac{.936}{2\pi} (10.8 \times 10^6) (.084)^2 / 84 = 135 \text{ ppi} \approx N_{xall}$$

$$\therefore \Delta t \approx .018 + .008 \approx .026 \quad \therefore \text{Assume } \Delta t_{ave} \approx .030$$

$$\Delta W = 355 \left(\frac{.030}{.020} \right) = 533 \text{ lbs / Tank}$$

STORED CONDITION - SUPPORTED VERTICALLY

$$\text{Axial Load at aft end} \approx 6900 \text{ lbs} \times 2g$$

$$N_{xa} = \frac{6900 \times 2 \times 1.4}{2\pi(84)} = 37 \text{ ppi}$$

$$\text{Shell } t = .040, N_{xcra} = \frac{.61}{2\pi} (10.8 \times 10^6) (.040)^2 / 84 = 20 \text{ ppi}$$

$$\text{Pressurized with } \frac{1}{4} \text{ psig, } \frac{PR}{2} = \frac{(.25)(84)}{2} = 10.5 \text{ ppi}$$

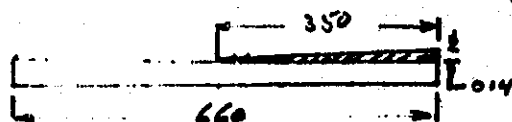
$$\bar{P} = \frac{P}{E} \left(\frac{R}{t} \right)^2 \sqrt{3(1-\mu^2)} = .169, \lambda = .228, N_{xcra} = .228 \left[\frac{E_c}{13(1-\mu^2)} \right] \frac{t^2}{R} = 28 \text{ ppi}$$

$$\therefore N_{xall} = 28 + 10.5 = 38.5 \text{ ppi} > N_{xa} \quad \therefore \text{ok}$$

Thickness req'd for no pressurization:

$$\text{Shell } t = .054, \frac{R}{t} = 1560 \rightarrow K = .635, N_{xcra} = \frac{.635}{2\pi} (10.8 \times 10^6) \left(\frac{.054}{84} \right)^2 = 38 \text{ ppi}$$

$$\text{Axial Load @ STA 1000} = 37 \left(\frac{1}{2} \right) = 18 \text{ ppi} \\ \text{@ STA 1250} = 37 \left(\frac{3}{4} \right) = 28 \text{ ppi} > \therefore \text{TAPER Shell From STA 1050}$$



$$\therefore \Delta t_{ave} = .007, \text{ for } 350 \text{ cyl length}$$

$$\Delta W = .007(350)(2\pi)(84)(.102) = 132 \text{ lbs}$$

Prepared by: E. A. CARTER	Date JUN 11 1971	LOCKHEED MISSILES & SPACE CO. A GROUP DIVISION OF LOCKHEED AIRCRAFT CO.	EM No. L2-12-01-M1-13 Date: 21 June 1971
Checked by:	Date	Title	Report No.
Approved by:	Date		

STORED CONDITION -

Add rings to stiffen shell in lieu of added thickness:

Using $L/R = 0.1$ or Rings @ 8.4 inches, $R/t = 2100$

$$\therefore K_b \approx 1.18 (1.3) = 1.535, N_{yb} = \frac{1.535}{2\pi} (10.8 \times 10^6) \left(\frac{0.040}{8.4} \right) = 50 \text{ psi}$$

It is concluded from the above, that simply adding rings to the membrane design will not adequately cover the load capability deficiency in the unpressurized state.

The following table summarizes all of the results:

Table 15

HANDLING CONDITION (2g DYNAMIC AMPLIFICATION)	PRESSURE REQUIRED (PSIG)	MEMBRANE WEIGHT PENALTY (LBS)	SYSTEM WT. PENALTY (LBS)
HORIZONTALLY STORED	1.50	0	0
	0	355	890
HORIZONTALLY TRANSPORTED TO PAD ON ORBITER	2.0	0	0
	0	533	1330
VERTICALLY STORED	0.25	0	0
	0	132	330

* TWO TANKS, ASSUMING 1.25 NOF

3.6 TANK ANALYSIS FOR PROOF PRESSURE CONSIDERATIONS

Proof testing a pressure vessel designed for a variety of design environments becomes a difficult problem. The baseline droptank critical design environment is a complex one because the critical condition is a combination of two ascent conditions: orbiter ignition and orbiter burnout. This is based on the GAC pressurization requirements. Later analysis by IMSC (Ref: Report, Section 12.1) shows the orbiter ignition ullage pressure can be reduced to 25 psia. If this is true, that condition goes away, and the critical condition becomes the empty burnout condition throughout the tank. Simulating this condition in the laboratory, however is no small problem, since the tank wall temperature varies (linearly) from 360°R (pressurization gas temperature) to 40°R (LH₂ temperature). At this condition, the tank pressure is constant: in this case, 25 psia. Compromising any part of this environment will detract from the validity of the proof test and may cause a weight penalty.

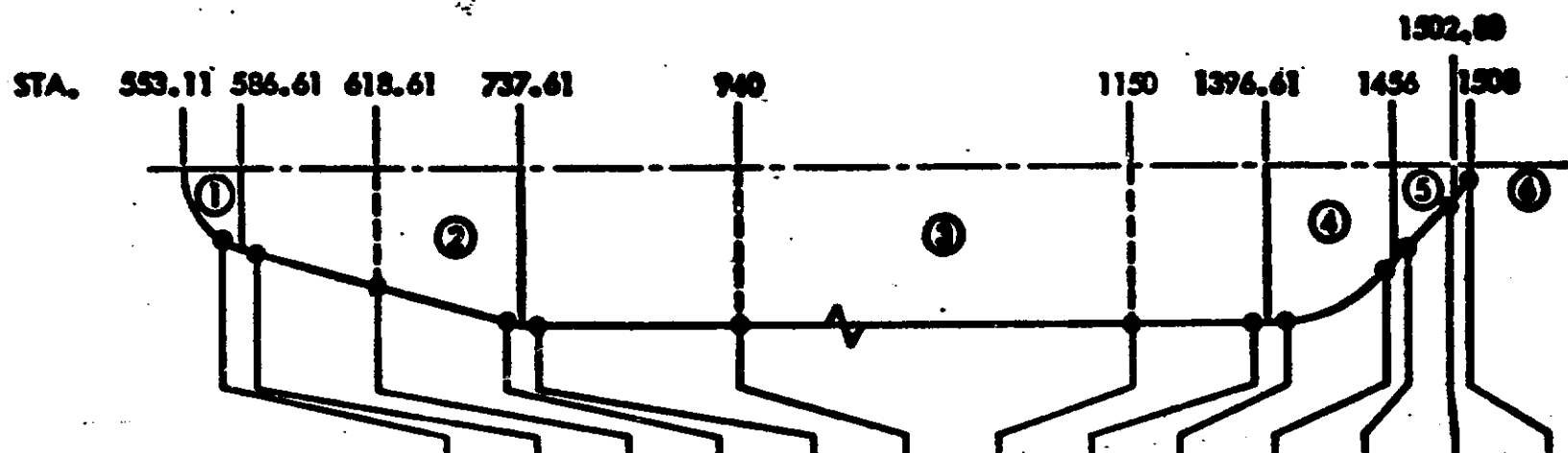
The simplest approach to proof testing pressure vessels is a pneumatic pressure test. Table 16 shows the tank gage increases that are necessary if an equivalent proof pressure is established for one critical tank location. In this case, the critical location selected is Station 680. Comparing these gage values to those established for the true environment (See Table 3), it is noted that a severe weight penalty results for both candidate materials. These weight penalties are based only on theoretical dimensions, and thus increase another 35 percent over that shown.

An alternative to the simple pneumatic test is shown in Fig. 7. Deviation from cryogenic temperature still results, however, but by turning the tank upside down and filling it with a fluid to the level shown that provides the fluid density as shown, will result in a total proof test of the tank without compromising the tank membrane thickness required for the true environment.

The detailed calculations which lead to the results shown in Table 16 and to the construction of Figure 7 are presented in the following pages.

Table 16

14-Foot DIA LH₂ Droptank Thickness Requirements
for Room Temperature Proof Test



THICKNESS (IN.)	' ₁	' ₂	' ₃	' ₄	' ₅	' ₆	' ₇	' ₈	' ₉	' ₁₀	' ₁₁	' ₁₂	' ₁₃
2219-T-87 PROOF PRESS. @ RT WT = 2282 *	.025	.030	.033	.054	.052	.052	.052	.052	.026	.026	.052	.025	.025
301 CRES EXTRA HARD PROOF PRESS. @ RT WT = 1874 LB *	.010	.010	.010	.015	.015	.015	.015	.015	.010	.010	.015	.010	.010

*PNEUMATIC TEST

Space Shuttle Project

EM NO: 12-12-01-MI-13
DATE: 21 June 1971

14-FOOT DIAMETER TANK (BASELINE)

HYDRO-PNEUMATIC PROOF TEST

MATERIAL: 2219-T81 ALUMINUM ALLOY

$$F_{t_u} = 62 \text{ KSI, MAX. } \sigma_{\text{PROOF}} = (62) \left(\frac{1.05}{1.40} \right) = 46.5 \text{ KSI}$$

EQUIVALENT $\Delta P_{\text{REQUIRED}} = 2.2 \text{ PSIG (CYLINDER SECTION)}$

REQUIRED FLUID DENSITY $= 71.7 \text{ LB/FT}^3$

ADVANTAGES

- TEST MAY BE CONDUCTED AT ROOM TEMPERATURE
- CRITICAL SECTIONS ARE PROOF-TESTED TO ALMOST MAX. σ_{PROOF}
- NO SIGNIFICANT WEIGHT INCREASE WHEN COMPARED WITH TANK DESIGNED FOR FLIGHT CONDITIONS
- REQUIRES SIMPLE TEST STAND (TANK MAY BE SUSPENDED FROM HARD POINT AT STA 1508)

DISADVANTAGES

- DIFFICULTY OF FORMULATING FLUID DENSITY
- TANK NEEDS EXTENSIVE REMOVAL OF FLUID TRACES AFTER PROOF TEST
- TANK NOT PROOFED AT CRYOGENIC TEMPERATURES

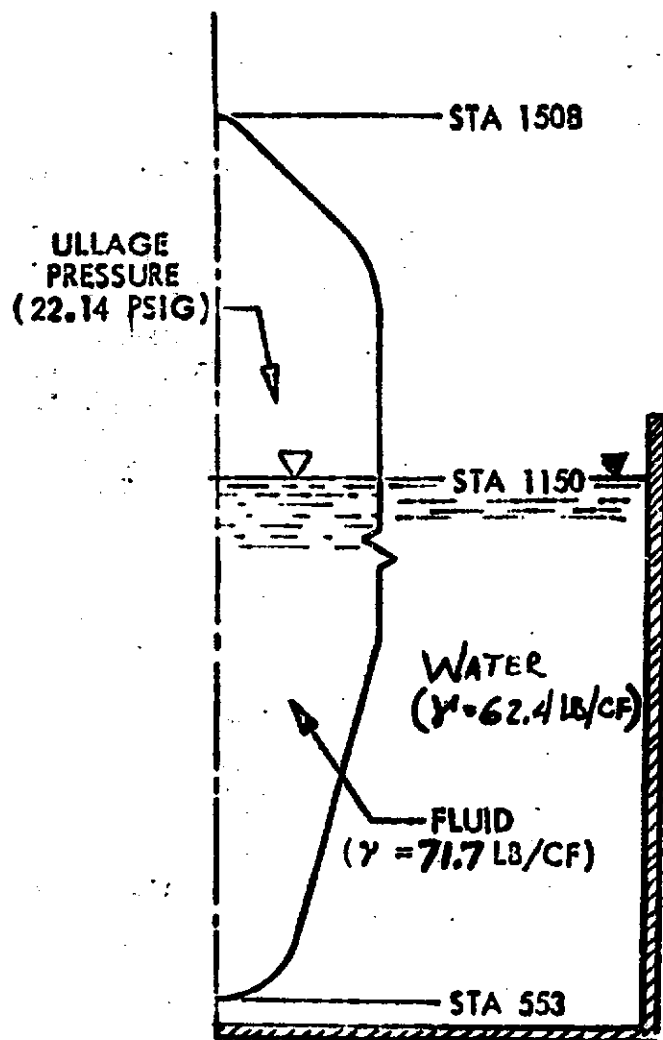


Figure 7

Space Shuttle Project

EM NO: 12-12-01-M-13
DATE: 21 June 1971

Prepared by: H. BAKER	Date 5-3-71	LOCKHEED MISSILES & SPACE COM. No. 12-12-01-M1-13 A GROUP DIVISION OF LOCKHEED AIRCRAFT CORP.	
Checked by:	Date	Title	Date 21 June 1971
Approved by:	Date		Report No.

2219-T87 TANK DESIGN FOR PROOF PRESSURE AT ROOM TEMP.

From ps. 3: $\frac{29.0 \text{ PSI}}{66.5 \text{ KSI}} = \frac{P_{R.T.}}{63 \text{ KSI}} \therefore P_{R.T.} = 27.5 \text{ PSI}$

Using $t_3 = .033"$, $\sigma = \frac{27.5 \times 52.1}{.033 \times .9659} (1.4) = 62930 \text{ PSI} < \sigma_{ALL} = 63 \text{ KSI}$

CHECKING THICKNESSES FOR $p = 27.5 \text{ PSI} \neq \sigma_T = 63 \text{ KSI} (@ R.T.)$

$t'_1 = \frac{27.5 \times 45.2}{2 \times 63000} \times 1.4 = .0135 < (t_1 = .025")$ NO THICK. INCR. Use $t'_1 = .025"$
(.014") (0.04")

$t'_2 = \frac{27.5 \times 43.55}{63 \times .9659} \times 1.4 = .027 < (t_2 = .030")$ NO THICK. INCR. Use $t'_2 = .030"$

$t'_3 = \frac{27.5 \times 52.1}{63 \times .9659} \times 1.4 = .0326 < (t_3 = .033")$ NO THICK. INCR. Use $t'_3 = .033"$

$t'_4 = \frac{27.5 \times 84}{63 \times .9659} \times 1.4 = .0531 > (t_4 = .045")$ CH'G. THICK. Use $t'_4 = .054"$

$t'_5 = \frac{27.5 \times 84}{63} \times 1.4 = .0513 > (t_5 = .044")$ CH'G. THICK. Use $t'_5 = .052"$

$t'_6 = t'_5 = .0513 > (t_6 = .042")$ CH'G. THICK. Use $t'_6 = .052"$

$t'_7 = t'_5 = .0513 > (t_7 = .039")$ CH'G. THICK. Use $t'_7 = .052"$

$t'_8 = t'_5 = .0513 > (t_8 = .040")$ CH'G. THICK. Use $t'_8 = .052"$

$t'_9 = t'_{10} = \frac{27.5 \times 84}{2 \times 63} \times 1.4 = .0256 > (t_9 = t_{10} = .025")$ CH'G. THICK. Use $t'_9 = .026"$

Prepared by: <u>H. BASERGA</u>	Date: <u>5-3-71</u>	LOCKHEED MISSILES & SPACE COM. A GROUP DIVISION OF LOCKHEED AIRCRAFT CORP.	
Checked by:	Date:	Title:	Report No. <u>L2-12-01-M1-13</u> Date: <u>21 June 1971</u>
Approved by:	Date:	Report No.	

$$t'_{11} = \frac{27.5 \times 59.39}{63 \times 1.7071} \times 1.4 = .0513 > (t_{11} = .040") \text{ CH'G. THICK. Use } t'_{11} = .052"$$

$$t'_{12} = \frac{27.5 \times 12.59}{63 \times 1.7071} \times 1.4 = .0109 < (t_{12} = .025") \text{ NO THICK. INCR. Use } t'_{12} = .025"$$

$$t'_{13} = t'_{14} = \frac{27.5 \times 17.8}{2 \times 63} \times 1.4 = .0054 < (t_{13} = t_{14} = .025") \text{ NO THICK. INCR. Use } t'_{13} = t'_{14} = .025" \text{ (.010")}$$

PROOF PRESSURE @ ROOM TEMP.

Using 5% above operating pressure one has

$$p_{\text{PROOF}} = (27.5) \left(\frac{1.05}{1.40} \right) = 20.625 \sim 20.6 \text{ PSI}$$

WEIGHT INCREASE

Weight increase at the different portions is obtained by simple ratioing of thicknesses, where applicable

$$\text{Shell ① : } W'_{\text{①}} = W_{\text{①}} = 23. \#$$

$$\text{Shell ② : } t'_{Av} = \frac{1}{2} (.030 + .054) = .042", W'_{\text{②}} = 240 \left(\frac{.042}{.0375} \right) = 269 \#$$

$$\text{Shell ③ : } W'_{\text{③}} = 517.77 \left(\frac{.052}{.039} \right) + 932.43 \left(\frac{.052}{.042} \right) = 1845 \#$$

$$\text{Shell ④ : } W'_{\text{④}} = 80 \left(\frac{.026}{.025} \right) = 83.2 \#$$

$$\text{Shell ⑤ : } t'_{Av} = \frac{1}{2} (.052 + .025) = .0385, W'_{\text{⑤}} = 50 \left(\frac{.0385}{.0325} \right) = 59.3 \#$$

$$\text{Shell ⑥ : } W'_{\text{⑥}} = W_{\text{⑥}} = 2 \#$$

$$\text{TOTAL WT.} = \sum_{\text{①}}^{\text{⑥}} W'_{\text{①}} = 2281.5 \sim 2282 \#$$

Prepared by: H. BASERGA	Date: 5-4-71	LOCKHEED MISSILES & SPACE COM A ROCKET DIVISION OF LOCKHEED AIRCRAFT CORP.		No. 12-12-01-11-13
Checked by:	Date:	Title:		Date: 21 June 1971
Approved by:	Date:			Report No.

2219-T87 AL-ALCY TANK, CONT'D.)

$$\text{TOTAL WEIGHT: } \sum_{\text{O}}^{\text{O}} W_{\text{L}}^{\text{I}} = 2281.5 \approx 2282 \#$$

$$\text{Using 35\% as before, } W_T = 1.35 \times 2282 = 3080.7 \approx 3081 \#$$

$$\text{WEIGHT INCR.} = 3081 - 2500 = 581 \#, \text{ say, } 600 \#$$

Prepared by: H. BASERGA	Date 5-25-71	LOCKHEED MISSILES & SPACE COMPANY No. L2-12-01-11-13 A GROUP DIVISION OF LOCKHEED AIRCRAFT CORP.	Date: 21 June 1971
Checked by:	Date	Title	Report No.
Approved by:	Date		

301 ST'L. TANK DESIGN FOR PROOF PRESSURE @ ROOM TEMP.

8 From pg. 14 : $\frac{29}{234} = \frac{P_{R.T.}}{198} \therefore P_{R.T.} = 24.54 \text{ PSI}$

CHECKING THICKNESSES FOR $p = 24.54 \text{ PSI}$ & $\sigma_T = 198 \text{ KSI}$ (@ R.T.)

$$t'_1 = (1.4) \left(\frac{24.54}{198} \right) \left(\frac{45.2}{2} \right) = .0039" < (t_1 = .010") \text{ NO THICK INCR. , use } t'_1 = .010"$$

$$t'_2 = (1.4) \left(\frac{24.54}{198} \right) \left(\frac{43.55}{.9659} \right) = .0078" < (t_2 = .010") \text{ NO THICK INCR. , use } t'_2 = .010"$$

$$t'_3 = (1.4) \left(\frac{24.54}{198} \right) \left(\frac{52.10}{.9659} \right) = .0093" < (t_3 = .010") \text{ NO THICK INCR. , use } t'_3 = .010"$$

$$t'_4 = (1.4) \left(\frac{24.54}{198} \right) \left(\frac{84}{.9659} \right) = .0150" > (t_4 = .012") \text{ CH'G. THICK. , use } t'_4 = .015"$$

$$t'_5 = (1.4) \left(\frac{24.54}{198} \right) (84) = .0145" > (t_5 = .012") \text{ CH'G. THICK. , use } t'_5 = .015"$$

$$t'_6 = t'_5 = .0145" > (t_6 = .012") \text{ CH'G. THICK. , use } t'_6 = .015"$$

$$t'_7 = t'_5 = .0145" > (t_7 = .012") \text{ CH'G. THICK. , use } t'_7 = .015"$$

$$t'_8 = t'_5 = .0145" > (t_8 = .012") \text{ CH'G. THICK. , use } t'_8 = .015"$$

$$t'_9 = t'_{10} = (1.4) \left(\frac{24.54}{198} \right) \left(\frac{84}{2} \right) = .0073" < (t_9 = .010) \text{ NO THICK. INCR. , use } t'_9 = t'_{10} = .010"$$

Prepared by: H. BASERGA	Date: 5-25-71	LOCKHEED MISSILES & SPACE CO. A GROUP DIVISION OF LOCKHEED AIRCRAFT CORP. No. 12-12-01-11-13 Date: 21 June 1971
Checked by:	Date:	
Approved by:	Date:	Report No.

$$t'_{11} = (1.4) \left(\frac{24.54}{198} \right) \left(\frac{59.39}{.7071} \right) = .0145" > (t_{11} = .012") \text{ CH'G. THICK. , use } t'_{11} = .015"$$

$$t'_{12} = (1.4) \left(\frac{24.54}{198} \right) \left(\frac{12.59}{.7071} \right) = .0031" < (t_{12} = .010") \text{ NO THICK INCR, use } t'_{12} = .010"$$

$$t'_{13} = t'_{14} = (1.4) \left(\frac{24.54}{198} \right) \left(\frac{17.8}{2} \right) = .0015" < (t_{13} = .010") \text{ NO THICK INCR, use } t'_{13} = .010"$$

PROOF PRESSURE @ ROOM TEMP: $p_{\text{PROOF}} = (24.54) \left(\frac{1.05}{1.40} \right) = 18.4 \text{ PSI}$

WEIGHT INCREASE

Shell ①: $W'_1 = W_1 = 25.8$

Shell ②: $W'_2 = (195.4) \left(\frac{.0116}{.0106} \right) = 213.8$

Shell ③: $W'_3 = (1,193.7) \left(\frac{.015}{.012} \right) = 1492.2$

Shell ④: $W'_4 = W_4 = 89.7$

Shell ⑤: $W'_5 = (47.9) \left(\frac{.0116}{.0110} \right) = 50.1$

Shell ⑥: $W'_6 = W_6 = 2.3$

$$\Sigma W'_i = 1873.9$$

TOTAL WT. = $(1.35)(1873.9) = 2529.76 \sim 2530 \text{ LB}$

WT increase : $2530 - 2100 = 430 \text{ LB}$

Prepared by: H. BASEPRA	Date 5-26-71	LOCKHEED MISSILES & SPACE CO. A GROUP DIVISION OF LOCKHEED AIRCRAFT CO.		Item No. 12-12-01-M1-13
Checked by.	Date	Title		Date: 21 June 1971
Approved by:	Date			Report No.

HYDRO-PNEUMATIC PROOF TEST

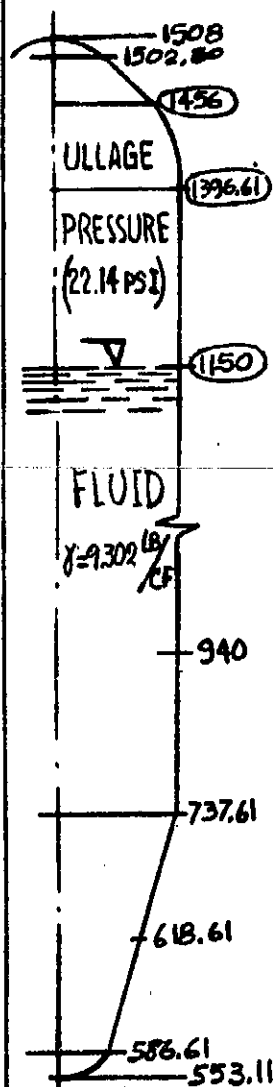
To reduce the weight penalty introduced in the tank design when a fully pneumatic test at room temp. is considered, a design where the pressure is provided by both fluid height and ullage is presented here. Only one mat'l. is studied.

From MIL-HDBK 5, Table 3.2.25.0 (b), for 2219-TB1 AL ALLY at Room Temp., $F_{tu} = 62 \text{ KSI}$. Then, the allowable stress at Proof Pressure is: $\sigma_{\text{Proof}} = (62) \left(\frac{1.05}{1.40} \right) = 46.5 \text{ KSI}$. (On basis "A" tension yield allowables are: $F_{ty} = 47 \text{ KSI (L)}$ & $F_{ty} = 46 \text{ KSI (LT)}$).

Using thicknesses shown in page 6 the pressures req'd. to produce $\sigma_{\text{Proof}} = 46.5 \text{ KSI}$ at each location are

STA.	THICKN.	$P_{\text{CRIT.}}, \text{PSI}$	
553.11	$t_1 = \begin{smallmatrix} (.014) \\ .025 \end{smallmatrix}$	$(46.5)^K \left(\frac{2 \times .025}{45.2} \right) = 51.43$	$(51.43) \left(\frac{.014}{.025} \right) = 28.6$
583.61	$t_2 = .028$	$(46.5)^K \left(\frac{.9659 \times .028}{43.55} \right) = 28.88$	
618.61	$t_3 = .034$	$(46.5)^K \left(\frac{.9659 \times .034}{52.1} \right) = 29.31$	
737.61	$t_4 = .046$	$(46.5)^K \left(\frac{.9659 \times .046}{84} \right) = 24.60$	

Prepared by: H. BASERGA	Date 5-26-71	LOCKHEED MISSILES & SPACE CO. No. 12-12001-M1-13 A GROUP DIVISION OF LOCKHEED AIRCRAFT CORP.	Date: 21 June 1971
Checked by:	Date	Title	Report No.
Approved by:	Date		



STA	THICKN.	P _{CRIT.} , PSI
737.61	$t_5 = .044$	$(46.5)^K \left(\frac{.044}{84} \right) = 24.36$
940.0	$t_6 = .043$	$(46.5)^K \left(\frac{.043}{84} \right) = 23.80$
1150.0	$t_7 = .040$	$(46.5)^K \left(\frac{.040}{84} \right) = (22.14)$
1396.61	$t_8 = .040$	$= (22.14)$
1396.61	$t_9 = .025$	$(46.5)^K \left(\frac{2 \times .025}{84} \right) = 27.68$
1456.0	$t_{10} = .025$	" " = 27.68
1456.0	$t_{11} = .040$	$(46.5)^K \left(\frac{.7071 \times .040}{59.39} \right) = (22.14)$
1502.80	$t_{12} = .025$	$(46.5)^K \left(\frac{.7071 \times .025}{12.69} \right) = 65.29$
1508.0	$t_{13} = .025$	$(46.5)^K \left(\frac{2 \times .025}{17.8} \right) = 130.62$

$$(27.68) \left(\frac{.020}{.025} \right) = (22.14)$$

$$(") (") = (22.14)$$

$$(130.62) \left(\frac{.010}{.025} \right) = 52.25$$

By inspection of critical pressures the portion of tank between STA 1150 \pm STA 1508 may be proof tested at $p_{ull} = 22.14 \text{ PSI}$ without any redesign of wall thicknesses, i.e., no weight penalty is involved. From STA 1150 to STA 553 (Fwd. end of tank) a hydrostatic pressure (fluid column) may be superimposed to the ullage pressure to generate larger pressures so that more sections

Prepared by: H. BASEKGA	Date 5-26-71	LOCKHEED MISSILES & SPACE CO. EM No. 12-12-01-M1-13 A GROUP DIVISION OF LOCKHEED AIRCRAFT CO. Date: 21 June 1971	
Checked by:	Date	Title	muon
Approved by:	Date		Report No.

of the tank can be proof tested. The density of the fluid is established as follows.

$$\Delta p = (p_{STA 737.61}) - (p_{STA 1150}) = 24.36 - 22.14 = 2.22 \text{ PSI}$$

Equating $\Delta p = p_{HYD} = \gamma h$, where $h = 1150 - 737.61 = 412.39"$,

the reqd. density is $\gamma = \frac{2.22}{412.39} = .00538 \text{ LB/IN}^3 (= 9.302 \text{ LB/FT}^3)$

Stresses resulting from the combined pressure ($p_{HYD} + p_{PULL}$) from STA 1150 to STA 553 (wet shell) are:

STA	h	p_{HYD}	p_{PULL}	$p_{HYD} + p_{PULL}$	$(\sigma_m)_{PROOF}$, PSI
1150	0	0		22.14	$\frac{22.14 \times 84}{.040} = 46494$
940	210	1.13		23.27	$\frac{23.27 \times 84}{.043} = 45458$
737.61	412.39	2.22		24.36	$\frac{24.36 \times 84}{.045 \times .9659} = 47077 > 46.5 (*)$
618.61	531.39	2.86		25.00	$\frac{25.0 \times 52.10}{.034 \times .9659} = 39661$
586.61	563.39	3.03		25.17	$\frac{25.17 \times 43.55}{.028 \times .9659} = 40530$
553.11	596.89	3.21		25.35	$\frac{25.35 \times 45.20}{2 \times .025} = 22916$

(*) Using $t = .046"$, $\sigma_m = (47077) \left(\frac{.045}{.046} \right) = 46054 < 46.5 \text{ KSI}$

Prepared by: H. BASERGA	Date 5-26-71	LOCKHEED MISSILES & SPACE CO A GROUP DIVISION OF LOCKHEED AIRCRAFT CO	EN No. 12-12-01-M1-13 Date: 21 June 1971
Checked by:	Date	Title	
Approved by:	Date	Report No.	

From STA 1150 to STA 1508 (dry shell) the membrane stresses under the constant internal pressure $p_{\text{ULL}} = 22.14 \text{ PSI}$ are as follows

STA	(\bar{U}_m) _{PROOF} , PSI
1396.11	$\frac{22.14 \times 84}{.040} = 46494$
1456.	$\frac{22.14 \times 59.39}{.040 \times .7071} = 46488$
1502.80	$\frac{22.14 \times 12.59}{.023 \times .7071} = 15768$
1508	$\frac{22.14 \times 17.80}{2 \times .025} = 7882$

CONCLUSION

As shown by the membrane stress levels resulting from the combined hydro-pneumatic test only a minor wall thickness increase is req'd. (from .045" to .046") to proof-test all the critical areas at near the max. allowable stress of the material. Hence no significant weight penalty is involved with respect to the tank when designed for flight conditions.

EM NO: 12-12-01-M1-13

DATE: 21 June 1971

3.7 TANK ANALYSIS FOR ULLAGE PRESSURE CONSIDERATIONS

All of the analyses contained in this Engineering Memo have thus far been based on the preliminary GAC ullage pressure sequence. Establishing a design ullage pressure profile is beyond the scope of this study, but a knowledge of the impact of ullage pressure on tank weight would aid in establishing the optimum pressure profile.

An analysis was performed for a range of ullage pressures from 25 psia to 33 psia using the 2219-T81 Aluminum baseline tank configuration. Two considerations were made: first, to vary the ullage pressure while the tank is full, venting down to 25 psia at burnout, and second, to hold the ullage pressure constant. Using 25 psia as the baseline value, Figure 8 shows the weight penalty associated with both considerations. The calculations which lead to the construction of Figure 8 are presented in Tables 17 through 19. These weight values are for one tank, and represent theoretical changes. True weight penalties are approximately 25 to 35 percent higher.

3.8 DROPTANK SHROUD ANALYSIS

The droptank shroud design is a function of the design requirements. Initially, its purpose was to support a small rocket, used for entry. Later design alternates show the rocket motor supported from the aft cone of the droptank. Initially, the cone analysis was based on the criteria and geometry shown in Fig. 9. The purpose of this trade study was to establish weights for two candidate materials and two structural concepts. The weight results shown in Fig. 9 indicate that significant weight savings are achieved using magnesium HM21A-T8. It was therefore concluded to use HM21A-T8 as the baseline material for the nose shroud. The calculations shown on the following pages lead to the final baseline design, presented in Eng. Drawing SKM 100717. The analysis included here shows a magnesium nose cap. Last minute changes to the design incorporated a Sitka-Spruce formed plywood nose cap. Both weight and cost are reduced using the wood nose cap. The nose cap is mechanically fastened to a chem-milled ring-stiffened cone, which in turn is mechanically fastened to the forward (aluminum) stub skirt of the droptank. Variations of this design were incorporated into the NAR and GAC tank designs.

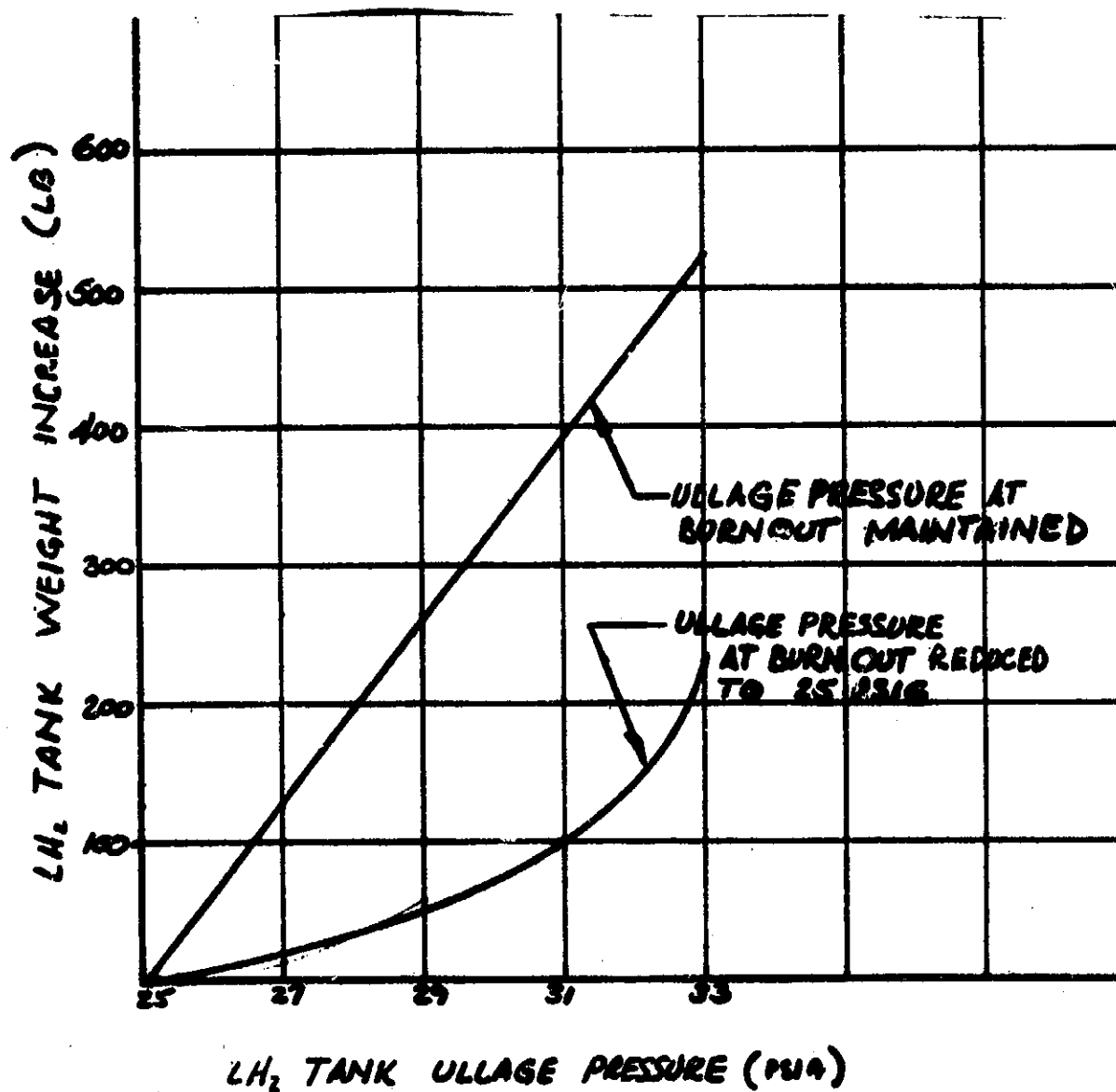


Figure 8 Ullage Pressure Weight Penalty

Prepared by: S. A. CARTER	Date JUN 11 1971	LOCKHEED MISSILES & SPACE COMPANY A GROUP DIVISION OF LOCKHEED AIRCRAFT CORP.	EM No. L2-12-01-M-13
Checked by:	Date		Date: 21 June 1971
Approved by:	Date		Report No.

TANK PRESSURIZATION STUDY

Table 17 Ullage Pressure At Burnout = 25 psig

GEOMETRY	STA	HEAD HEIGHT	PHD @ 3g	Wall Temp °F	P _T @ Pull = Following (psig)					F _{to} (K ₃₀)	Membrane t @ Pull = (in)				
					25	27	29	31	33		25	27	29	31	33
	553			-100	25	27	29	31	33	65.7	.012	.013	.014	.015	.016
	587				↓	↓	↓	↓	↓		.024	.026	.028	.030	.032
	618	0	0	-420	25	27	29	31	33	94.2	.020	.022	.024	.025	.027
	120	.89			25.9	27.9	29.9	31.9	33.9		.034	.036	.039	.042	.044
											.033	.035	.038	.040	.043
	940	322	2.39		27.4	29.4	31.4	33.4	35.4		.035	.037	.040	.042	.045
	1150	532	3.95		29.0	31.0	33.0	35.0	37.0		.037	.039	.042	.044	.047
	1397	779	5.78		30.8	32.8	34.8	36.8	38.8		.039	.041	.044	.046	.049
	1456	838	6.22		31.2	33.2	35.2	37.2	39.2		.020	.021	.022	.023	.025
	1503	885	6.57		31.6	33.6	35.6	37.6	39.6		.020	.021	.022	.023	.025
	1508	890	6.60	-420	31.6	33.6	35.6	37.6	39.6	94.2	.040	.042	.044	.047	.049
											.008	.009	.010	.011	
											.004	.005	.005	.005	.006
											.004	.005	.005	.005	.006

Prepared by: S. A. CARTER	Date JUN 11 1971	LOCKHEED MISSILES & SPACE COM. A GROUP DIVISION OF LOCKHEED AIRCRAFT CORP.	EM No. L2-12-01-M1-13
Checked by:	Date	Title	Date: 21 June 1971
Approved by:	Date		Report No.

Table 17 (Cont'd)

TANK PRESSURIZATION STUDY (Cont'd)

STA	t_m Empty Cond	Δt_m - 3g COND. @ $P_{ULL} = (in)$					Δt_m $t_{m,0.020}$	Δt_m $t_{m,0.025}$	P_{ULL} CRITICALITY
		25	27	29	31	33			
553	.012	0	+0.001	+0.002	+0.003	+0.004	+0.008	+0.013	N/C
587	.024	0	+0.002	+0.004	+0.006	+0.008	0	+0.001	25'
618	.029	-0.009	-0.007	-0.005	-0.004	-0.002	0	0	N/C
738(-)	.046	-0.012	-0.010	-0.007	-0.004	-0.002	0	0	N/C
738(+)	.044	-0.011	-0.009	-0.006	-0.004	+0.001	0	0	33
940	.043	-0.008	-0.006	-0.003	-0.001	+0.004	0	0	33
1150	.040	-0.003	-0.001	+0.002	+0.004	+0.009	0	0	28
1392	.034	+0.005	+0.007	+0.010	+0.012	+0.015	0	0	25'
1397(+)	.017	+0.003	+0.004	+0.005	+0.006	+0.008	+0.003	+0.008	N/C
1456(-)	.017	+0.003	+0.004	+0.005	+0.006	+0.008	+0.003	+0.008	N/C
1456(+)	.033	+0.007	+0.009	+0.011	+0.014	+0.016	0	0	25'
1503	.007	+0.001	+0.002	+0.003	+0.003	+0.004	+0.013	+0.018	N/C
1508	.004	0	+0.001	+0.001	+0.001	+0.002	+0.016	+0.021	N/C

Prepared by: S: A CARTER	Date	LOCKHEED MISSILES & SPACE CO. A GROUP DIVISION OF LOCKHEED AIRCRAFT CO. EM No. L2-12-01-M1-13 Date: 21 June 1971
Checked by:	Date	
Approved by:	Date	
		Report No.

TANK PRESSURIZATION STUDY (CONT'D)

Table 18 Ullage Pressure At Burnout = Pull

STN	WALL TEMP °F	F ₆₀ (ksi)	R (in)	Membrane t @ Pull =					ΔDesign t @ Pull =				
				25	27	29	31	33	25	27	29	31	33
553	-100	65.7	45.2	.012	.013	.014	.015	.016	0	0	0	0	0
587	-111	66.0	45.2	.024	.026	.028	.030	.032	0	+0.002	+0.004	+0.006	+0.008
618	-122	66.3	53.9	.029	.031	.033	.036	.038	0	+0.002	+0.004	+0.007	+0.009
738(-)	-162	67.1	87	.046	.049	.053	.057	.060	0	+0.003	+0.007	+0.011	+0.014
738(+)	-162	67.1	84	.044	.048	.051	.055	.058	0	+0.004	+0.007	+0.011	+0.014
940	-230	69.4	84	.043	.046	.050	.053	.056	0	+0.002	+0.007	+0.010	+0.013
1150	-300	74.4	84	.040	.043	.046	.049	.053	0	+0.003	+0.006	+0.009	+0.013
1377(-)	-383	86.8	84	.034	.037	.040	.042	.045	0	+0.003	+0.006	+0.008	+0.011
1377(+)	-383	86.8	84	.017	.019	.020	.021	.023	0	+0.002	+0.003	+0.004	+0.006
1456(-)	-403	90.5	84	.017	.018	.019	.020	.022	0	+0.001	+0.002	+0.003	+0.005
1456(+)	-403	90.5	84	.033	.035	.038	.041	.043	0	+0.002	+0.005	+0.008	+0.010
1503	-418	94.1	17.8	.007	.008	.008	.009	.009	0	+0.001	+0.001	+0.002	+0.002
1508	-420	94.2	17.8	.004	.004	.004	.005	.005	0	0	0	+0.001	+0.001

Prepared by: SI A CARTER	Date JUN 11 1971	LOCKHEED MISSILES & SPACE COM A GROUP DIVISION OF LOCKHEED AIRCRAFT CORP	EM No. L2-12-01-M1-13 Date: 21 June 1971
Checked by:	Date	Title	Report No.
Approved by:	Date		

TABLE 19: ULLAGE PRESSURE WEIGHT PENALTY

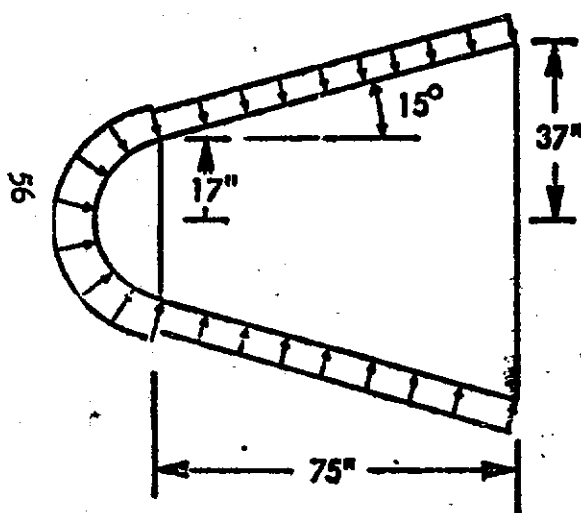
ELEMENT WEIGHT FORMULA	Δ WEIGHTS @ Pull =				
	25	27	29	31	33
FWD CONE WEIGHT = $\pi \left(\frac{32.0}{.9659} \right) [52.1 + 43.55] (.102) \Delta t_{AVE}$	0	1	2	3	4
CYLINDER WEIGHT = $2\pi (84) (940 - 738) (.102) \Delta t_{AVE}$	0	0	0	0	27
CYLINDER WEIGHT = $2\pi (84) (1150 - 940) (.102) \Delta t_{AVE}$	0	0	11	23	74
CYLINDER WEIGHT = $2\pi (84) (1397 - 1150) (.102) \Delta t_{AVE}$	0	13	46	73	126
TOTAL DELTA MEMBRANE WEIGHT (IF ULLAGE PRESSURE REDUCED TO 25 PSI @ B.O.)	0	14	59	99	231

ELEMENT WEIGHT FORMULA	Δ WEIGHTS @ Pull =				
	25	27	29	31	33
FWD CONE WEIGHT = $\pi \left(\frac{151}{.9659} \right) [84 + 43.55] (.102) \Delta t_{AVE}$	0	.0025 16	.0055 35	.0085 54	.0110 70
CYLINDER WEIGHT = $2\pi (84) (940 - 738) (.102) \Delta t_{AVE}$	0	.0035 38	.007 76	.0105 114	.0135 147
CYLINDER WEIGHT = $2\pi (84) (1150 - 940) (.102) \Delta t_{AVE}$	0	.003 34	.0065 73	.0095 107	.013 147
CYLINDER WEIGHT = $2\pi (84) (1397 - 1150) (.102) \Delta t_{AVE}$	0	.003 40	.006 80	.0085 113	.012 160
TOTAL DELTA MEMBRANE WEIGHT (IF ULLAGE PRESSURE HELD THRU B.O.)	0	128	264	388	524

FORM LMSC 302 B-2

DROPTANK FORWARD SHROUD

- FACTOR OF SAFETY - 1.4
- DESIGN TEMPERATURE - 300°F
- DESIGN LIMIT PRESSURE (MAX αq):
 NOSE CAP - 3.5 PSIG (STAGNATION)
 CONE - 2.6 PSIG
- CAP DESIGN (MONOCOQUE SHELL):
 ALUMINUM 2219-T87, THICKNESS = 0.030 IN.
 MAGNESIUM HM21A-T8, THICKNESS = 0.039 IN.
- CONE DESIGN:



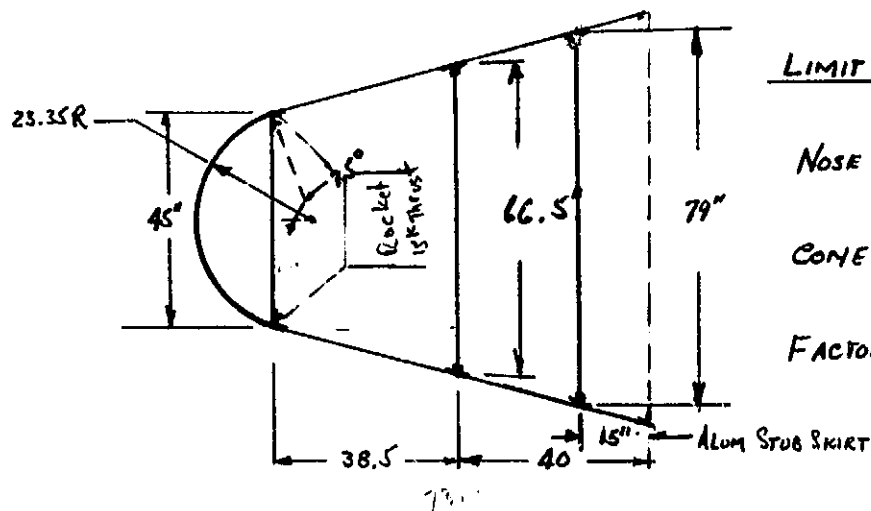
MATERIAL	CONCEPT	\bar{r} (IN.)	WEIGHT (LB)
2219-T87 AL	MONOCOQUE	0.130	175
2219-T87 AL	RING-STIFFENED	0.051	68
HM21A-T8	MONOCOQUE	0.159	134
HM21A-T8	RING-STIFFENED	0.060	51

Figure 9

Space Shuttle Project
 EM NO: L2-12-01-M-13
 DATE: 21 June 1971

Prepared by: S. A. CARTER	Date JUN 8 1971	LOCKHEED MISSILES & SPACE CO. A GROUP DIVISION OF LOCKHEED AIRCRAFT CORP.	EM No. L2-12-01-M1-13
Checked by:	Date:	Title	Date: 21 June 1971
Approved by:	Date:		Report No.

DROP TANK FORWARD SHROUD



LIMIT PRESSURE :

NOSE CAP = 3.5 psig

CONE = 2.6 psig

FACTOR OF SAFETY = 1.4

SPHERICAL CAP ANALYSIS (METHOD - REF NASA SP8032)

Assume Temp = 300°F

MATERIAL = HM 21A - T8 MAGNESIUM

$$F_{cy} = 13,200 \text{ psi} \quad , \quad E_c = 6 \times 10^6 \text{ psi}$$

$$F_{tu} = 19,200 \text{ psi}$$

$$P_{cl} = 1.21 E_c \left(\frac{t}{R} \right)^2 \quad , \quad P_{cr} \approx 0.14 P_{cl}$$

$$t_{req} \approx \left(\frac{P_{cr}}{.17 E_c} \right)^{1/2} R = \left(\frac{3.5 \times 1.4}{.17 \times 6 \times 10^6} \right)^{1/2} (23.35) = .052 \text{ "}$$

$$\lambda = 2 \left[12(1-\mu^2) \right]^{1/4} \left(\frac{R}{t} \right)^{1/2} \sin \sigma \approx 2 \left[12(.91) \right]^{1/4} \left(\frac{23.35}{.051} \right)^{1/2} (.607) = 47.30$$

$$P_{cr} = \left(.14 + \frac{3.2}{\lambda^2} \right) P_{cl} = .141$$

$$P_{cr} = .1718 E_c \left(\frac{t}{R} \right)^2 = .1718 (6 \times 10^6) \left(\frac{.051}{23.35} \right)^2 = 4.90 \text{ psi} \quad , \quad MS = 0$$

$$\text{Use Shell } t = .051 \quad ; \quad \text{Weight} = 2\pi (23.35) (17.3) (.051) (.064) = 8.3 \text{ lbs}$$

Prepared by: S. A. CARTER	Date JUN 8 1971	LOCKHEED MISSILES & SPACE CO. EM No. L2-12-01-M1-13 A GROUP DIVISION OF LOCKHEED AIRCRAFT CORP.	Date: 21 June 1971
Checked by:	Date	Title	
Approved by:	Date		Report No.

CONE ANALYSIS

Using monocoque analysis (Ref NASA SP 8019)

$$R_{eff} = \frac{R_1 + R_2}{2 \cos \alpha} = \frac{22.5 + 33.25}{2 \cos 15^\circ} = 28.9", \quad L_{eff} = \frac{38.5}{\cos 15^\circ} = 40"$$

$$\gamma = 0.75$$

$$P_{cr} \frac{0.92 \gamma E}{\left(\frac{L}{R}\right) \left(\frac{R}{t}\right)^{5/2}} = \frac{(0.92)(.75)(6 \times 10^6)}{\left(\frac{40}{28.9}\right) \left(\frac{R}{t}\right)^{5/2}} = 2.6 \times 1.4$$

$$\left(\frac{R}{t}\right)_{req} = \left[\frac{(0.92)(.75)(6 \times 10^6)}{\left(\frac{40}{28.9}\right) (2.6 \times 1.4)} \right]^{0.4} = (8.217 \times 10^3)^{0.4} = 232.5$$

$$t_{req} = \frac{R}{232.5} = \frac{28.9}{232.5} = .125"$$

Using Ring Stiffened analysis

$$\left(\frac{R}{t}\right)_{req} = \left(\frac{11.374 \times 10^5}{L/R} \right)^{0.4} = \frac{264.5}{(L/R)^{0.4}}$$

$$\text{Using } t = .030, \quad L = \frac{11.374 \times 10^5}{R^{1.5}} (t)^{2.5} = \frac{177.3}{R^{1/2}}$$

$$\left. \begin{array}{l} \text{at } R = 23.3, \quad L = 1.58" \\ \text{at } R = 34.4, \quad L = 0.88" \end{array} \right\} \text{spacing too small}$$

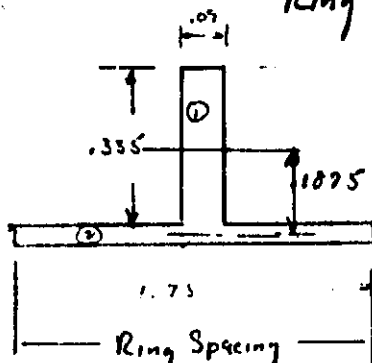
$$\text{Using } t = .040, \quad L = \frac{364}{R^{1/2}} \quad \left\{ \begin{array}{l} R_c = 23.3, \quad L = 3.24" \\ R_c = 34.4, \quad L = 1.80" \\ R_c = 40.9, \quad L = 1.39" \end{array} \right\} \text{Use } t_s = .040$$

Ring Schedule : 1 @ 3 $\frac{1}{4}$ ", 2 @ 3", 2 @ 2 $\frac{3}{4}$ ", 2 @ 2 $\frac{1}{2}$ ", 4 @ 2 $\frac{1}{4}$ ", 4 @ 2", 4 @ 1 $\frac{3}{4}$ "
12 @ 1 $\frac{1}{2}$ "

Prepared by: SA CARTER	Date JUN 9 1971	LOCKHEED MISSILES & SPACE CO A GROUP DIVISION OF LOCKHEED AIRCRAFT CO		EM No. L2-12-01-M1-13
Checked by:	Date	Title		Date: 21 June 1971
Approved by:	Date			Report No.

Ring Area requirements:

Assume Ring height = 0.375
Ring thickness = 0.090



EI	A	Y	A _Y	A _Y ²	I _b
①	.03015	.1875	.00565	.00106	.000282
②	.07000	0	0	0	.0000093
Σ	.1000	.0565	.00565	.00106	.0002913

$$I_R = .001361 - (.0565)(.00565) = .001032 \text{ in}^4$$

$$I_R' = \frac{.001032}{1.75} = .000590 \text{ in}^3$$

$$I_S' = \frac{(.04)^3}{12(1-.42)} = .00000586 \text{ in}^3$$

$$I_R'/I_S' = 100.64, (I_R'/I_S')^{3/4} = 31.8$$

$$P_{CRG} = \frac{(1.04)\pi^2 E \left(\frac{t_3}{R}\right)^{5/2}}{12(1-.42)^{3/4} \lambda/R} \left(\frac{I_R'}{I_S'}\right)^{3/4} = \frac{.92 E \left(\frac{t_3}{R}\right)^{5/2}}{(\lambda/R)} \left(\frac{I_R'}{I_S'}\right)^{3/4}$$

$$P_{CRG} = \frac{(.92)(6 \times 10^6) \left(\frac{.04}{32.1}\right)^{5/2}}{\left(\frac{85.73}{32.1}\right)} (31.8) = 4.70 > P_{ULF} = 3.64 \therefore \text{OK}$$

$$\Sigma \text{ Ring Length} \approx 6032", \Sigma V_R = 181.86 \text{ ei}, W_R \approx 12 \text{ lbs}$$

$$\text{Weight of shell} = \pi \left(\frac{63.5}{.966}\right) [22.5 + 39.5] (.04) (1.064) = 33 \text{ lbs}, W_{TOTAL} = 45 \text{ lbs}$$

ALUMINUM STUB SKIRT:

$$\text{Assume } t = .045, R/t = \frac{39.5}{.966(.045)} = 910, Y_R = .38, k = 1.05$$

$$\therefore P_{CR} = K E_c t^2 = 1.05 (10 \times 10^6) (.045)^2 = 21,250 \text{ lbs} > 15000 \times 1.4$$

$$\frac{R}{t} = \left[\frac{.92 (.75) (10 \times 10^6)}{(.38) (2.6 \times 1.4)} \right]^{.40} = (49.884 \times 10^5)^{.40} = 477; t_{req} = \frac{43}{477} = .090$$

$$R_{eq} = \frac{43.55 + 39.5}{2 (.966)} = 43 \text{ or use } t = .090, Wt = \pi \left(\frac{15}{.966}\right) [39.5 + 43.55] (.09) (1.02) = 37 \text{ lbs}$$

Prepared by: S. A. CARTER	Date JUN 9 1971	LOCKHEED MISSILES & SPACE CO. EM No. L2-12-01-M1-13 A GROUP DIVISION OF LOCKHEED AIRCRAFT CORP. Date: 21 June 1971
Checked by:	Date	Title
Approved by:	Date	Report No.

Should Capability to resist Axial Load (Rocket Thrust)

$$\text{Forward End} \sim R/t = \frac{22.5}{.966(.04)} = 583, \quad Y/R = 0.145, \quad K \approx 2.1$$

$$P_{cr} = K E_c t^2 = 2.1 (6.0 \times 10^6) (.040)^2 = 20,000 \text{ lbs}$$

$$\text{Aft End} \approx R/t = \frac{39.5}{.966(.04)} = 1020, \quad Y/R < .1, \quad K > 1.87$$

$$P_{cr} = 1.87 (6.0 \times 10^6) (.040)^2 > 18,000 \text{ lbs}$$

Support Cone For Rocket

$$\text{Using Mag. HM 21A-T8 @ } 200^\circ \text{F}, \quad F_{tu} = 24,400 \text{ psi}$$

$$\text{Load on Cone} = \frac{15000 \times 1.4}{\pi (20) 0.707} = 475 \text{ ppi}$$

$$t_{req} = \frac{475}{24,400} = .020$$

Mounting Ring for Rocket

$$\text{Using Mag HM 21A-T8 @ } 300^\circ \text{F}, \quad E_c = 6 \times 10^6$$

$$I_{req} = \frac{P R^3}{3 E} \quad ; \quad P = \frac{15000 \times 1.4}{\pi (45)} = 149 \text{ ppi}$$

$$I_{req} = \frac{149 (22.5)^3}{6 \times 10^6} = 0.283 \text{ in}^4, \quad \text{use } 2 \times 1\frac{1}{4} \times \frac{1}{8} \text{ [} A = .53 \text{ in}^2 \text{]}$$

$$\text{Rocket Support Struct Weight} = \pi \left(\frac{10}{.707} \right) [22.5 + 10] (.020)(.064) + \pi (45)(.53)(.064) = 7 \text{ lbs}$$

3.9 DROPTANK ORBITER SUPPORT STRUCTURE ANALYSIS

An analysis of five different configurations is presented here to establish preliminary sizes and weights for the droptank supporting structure. A schematic of configurations is shown in Fig. 10. It should be noted that Configuration 1 was analyzed for three sizes of the baseline tank (12, 14 and 18 ft diameters) whereas Configurations 2 and 3 were analyzed only for the 14 ft DIA baseline tank and Configurations 4 and 5 were considered only for the GAC tank. The calculated weight of all configurations does not include end fittings (no NOF factor) and is plotted in terms of tank DIA in Fig. 11. For all cases Ti-6AL-4V material is assumed.

The analysis of the supporting structure assumes that tension members (here noted by "rods") do not have compression capabilities thus simplifying statically indeterminate cases. This assumption is supported by the rods' large L/ρ ratio. It is also assumed the structure is supported at frictionless rigid joints. The results of the detail analysis presented here are summarized in Fig. 2. It should be noted, however, that the analysis performed for Configurations 1, 2 and 3 (baseline) is based on preliminary loads which were superseded by loads reflecting wind tunnel data. Time did not permit these loads to be incorporated in the baseline configurations but an estimate on weight impact shows an increase in the order of 10% for the Aft Support and 30% for the Fwd. Support.

Loads used in the analysis of Configurations 4 and 5 (GAC tank) include wind tunnel data.

3.10 GAC/NAR DROPTANK MEMBRANE SIZING ANALYSIS

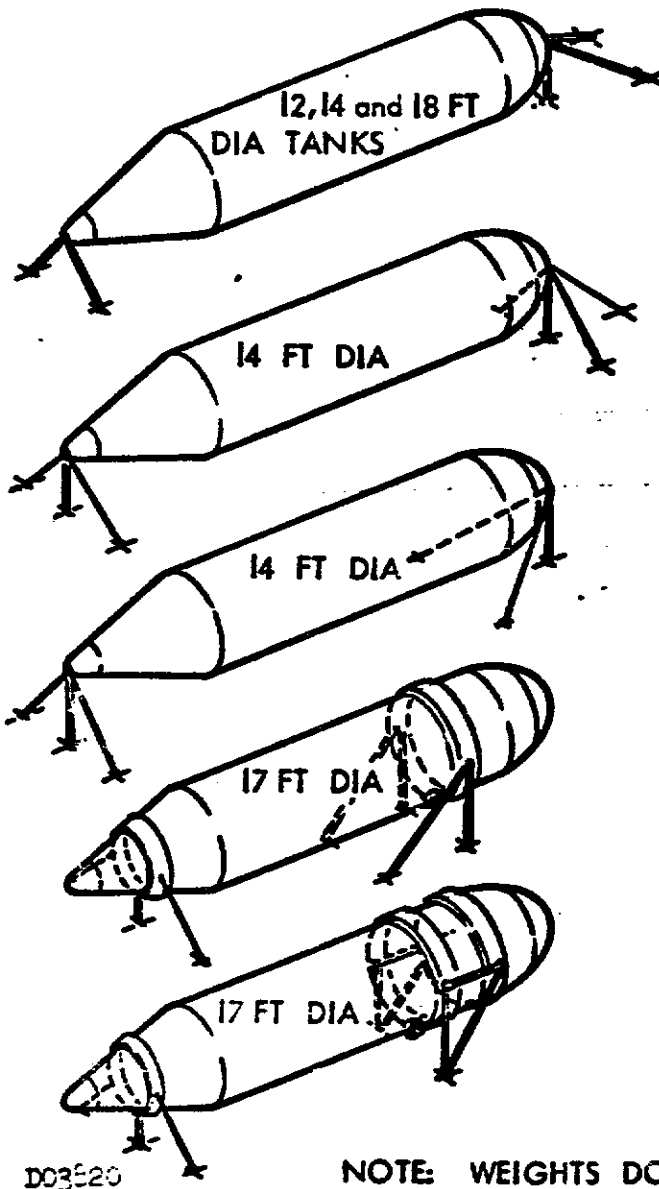
Time did not permit detail analyses of the GAC configuration (Eng. Dwg. SKG 100719) or the NAR configuration (Eng. Dwg. SKG 100718), but tank membrane sizing was performed and included here on the following pages. An evaluation of the support structure for the GAC tank was also made (see Section 3.9).

Based on the analyses performed on the baseline configurations, good weight estimates (and costs) can be made using weight scaling laws. This procedure was followed to establish the final weights for both configurations (see Sections 16 and 17, in Part 3, ACS Final Report, Task IV).



Fig. 10

DROPTANK SUPPORT CONFIGURATIONS



CONFIG. 1 BASELINE DROPTANK
(ALL TUBULAR MEMBERS)
WEIGHT FOR 14 FT DIA = 259 LB.

CONFIG. 2 BASELINE DROPTANK
(TWO TUBES AND FIVE RODS) WEIGHT = 118 LB

CONFIG. 3 BASELINE DROPTANK
(TWO TUBES AND FOUR RODS) WEIGHT = 93 LB

CONFIG. 4 GAC DROPTANK
(THREE TUBES AND FOUR RODS,
ONE RING AT TANK) WEIGHT = 136 LB

CONFIG. 5 GAC DROPTANK
(FRONT SUPPORT SAME AS CONFIG.
4, AFT SUPP. REQUIRES TWO RINGS AND
INTERCOSTAL AT TANK). WEIGHT = 148 LB

D03520

NOTE: WEIGHTS DO NOT INCLUDE FITTINGS, RINGS, AND NOF

EM No. 12-12-01-21-13
Date: 21 June 1971



LH₂ TANK STRUT WEIGHT

MATERIAL: Ti-6AL-4V (NOF NOT INCLUDED)

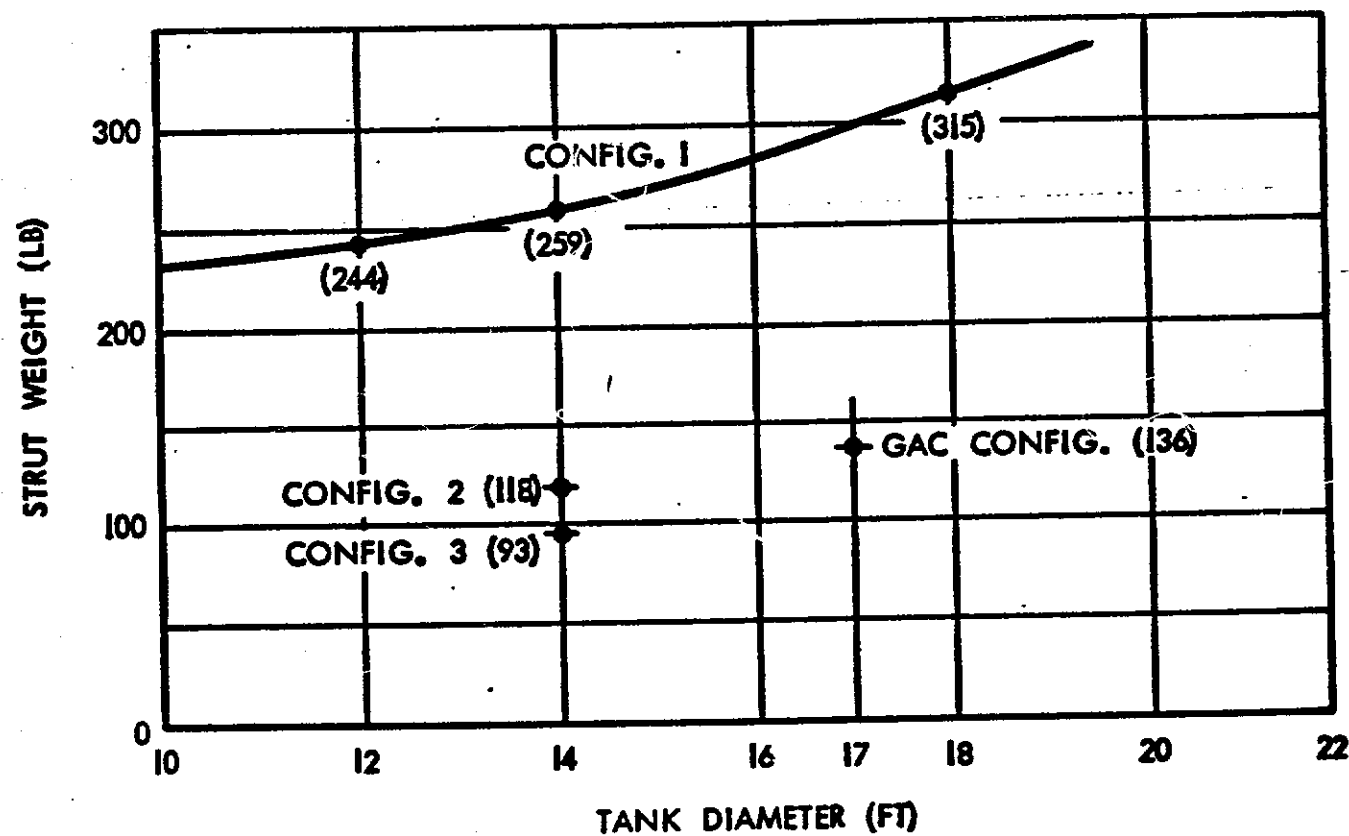


Fig. 11

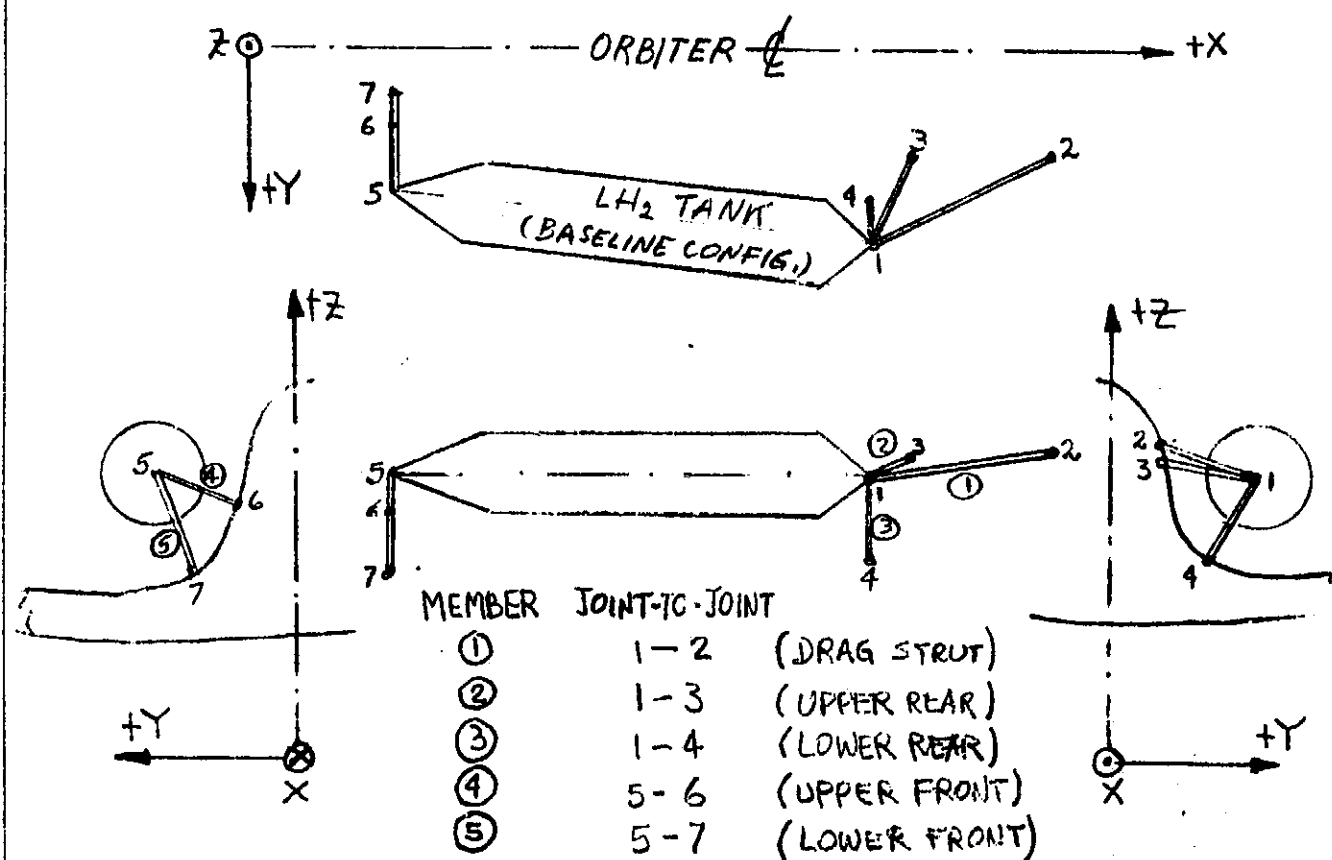
D03819

EM No. 12-12-01-M1-13
Date: 21 June 1971

Prepared by: H. BASERGA	Date 5-4-71	LOCKHEED MISSILES & SPACE CO A GROUP DIVISION OF LOCKHEED AIRCRAFT CO	EM No. L2-12-01-M1-13
Checked by:	Date		Date: 21 June 1971
Approved by:	Date		Report No.

CONFIGURATION 1

The supporting structure for three different baseline tanks (12 FT, 14 FT & 18 FT in diameter) is analyzed using a space truss program ("STAF," Stiffness Techniques to Analyze Frames, LMSC No. A847688, by R. Kidder). Unit loads of 100^{lb} at the loader joints are applied in pertinent directions so that actual forces at members can be obtained by simple ratioing of the actual applied loads. In all cases sign convention and notation as sketched below is kept constant.



Prepared by: H. BASERGA	Date 5-6-71	LOCKHEED MISSILES & SPACE CO A GROUP DIVISION OF LOCKHEED AIRCRAFT CO.		EM No. L2-12-01-M1-13
Checked by:	Date	Title		Date: 21 June 1971
Approved by:	Date			Report No.

SPACE TRUSS ANALYSIS DATE 06 MAY 71

LH2 TANK SUPPORTING STRUCTURE, 12FT DIA TANK CONFIG.

COORDINATES OF JOINTS

JOINT	X	Y	Z
1	1522.000	243.000	438.000
2	1712.000	120.000	488.000
3	1572.000	120.000	475.000
4	1522.000	185.000	336.000
5	548.000	201.000	438.000
6	548.000	105.000	442.000
7	548.000	144.000	340.000

MEMBER DESIGNATIONS AND PROPERTIES

MEMBER	JJ END	JK END	L	CX	CY	CZ
1	1	2	231.795	.819689	-.530641	.215708
2	1	3	137.833	.362757	-.892383	.268440
3	1	4	117.337	.000000	-.494302	-.869290
4	5	6	96.083	.000000	-.999133	.041631
5	5	7	113.371	.000000	-.502774	-.864418
6	1	5	974.905	-.999072	-.043081	.000000

NOTE: For ALL Configurations (12FT, 14FT & 18FT DIA TANKS)
the joint coordinates are referred to the orbiter
global system of coordinates.

Prepared by: H. BASERGA	Date 5-8-71	LOCKHEED MISSILES & SPACE CO. <small>A GROUP DIVISION OF LOCKHEED AIRCRAFT CORP.</small>		EM No. 12-12-01-13
Checked by:	Date	Title		Date: 21 June 1971
Approved by:	Date	Report No.		

12 FT. DIA. TANK, CONT'D.

LOADING CASES, FORCES AND REACTIONS

LOADING, JOINT 1: $PX = +100K$					
JOINT	REACTIONS			MEMBER	AXIAL FORCE
	RX	RY	RZ		
2	-138.248	89.447	-36.381	1	-168.659
3	38.248	-90.090	28.304	2	105.437
4	0.0	4.593	8.077	3	-9.292

LOADING, JOINT 1: $PY = -100K$					
JOINT	REACTIONS			MEMBER	AXIAL FORCE
	RX	RY	RZ		
2	47.990	-31.067	12.629	1	58.546
3	-47.990	118.055	-35.512	2	-132.292
4	0.0	13.012	22.883	3	-26.324

LOADING, JOINT 1: $PZ = -100K$					
JOINT	REACTIONS			MEMBER	AXIAL FORCE
	RX	RY	RZ		
2	-27.288	17.666	-7.181	1	-33.291
3	27.288	-67.129	20.193	2	75.225
4	0.0	49.464	86.988	3	-100.068

LOADING, JOINT 5: $PY = -100K$					
JOINT	REACTIONS			MEMBER	AXIAL FORCE
	RX	RY	RZ		
6	0.0	97.634	-4.068	4	-97.718
7	0.0	2.366	4.068	5	-4.706

LOADING, JOINT 5: $PZ = -100K$					
JOINT	REACTIONS			MEMBER	AXIAL FORCE
	RX	RY	RZ		
6	0.0	-56.787	2.366	4	56.836
7	0.0	56.787	97.634	5	-112.948

Prepared by: H. BASERGA	Date: 5-6-71	LOCKHEED MISSILES & SPACE CO A GROUP DIVISION OF LOCKHEED AIRCRAFT CO		EM No. L2-12-01-M1-13
Checked by:	Date:	Title:		Date: 21 June 1971
Approved by:	Date:			Report No.

SPACE TRUSS ANALYSIS DATE 06 MAY 71

LH2 DRUP TANK SUPPORTING STRUCTURE, 14FT DIA TANK (BASELINE)

COORDINATES OF JOINTS

JOINT	X	Y	Z
1	1522.000	250.000	450.000
2	1712.000	120.000	488.000
3	1572.000	120.000	475.000
4	1522.000	185.000	336.000
5	548.000	208.000	450.000
6	548.000	105.000	442.000
7	548.000	144.000	340.000

MEMBER DESIGNATIONS AND PROPERTIES

MEMBER	JJ END	JK END	L	CX	CY	CZ
1	1	2	233.932	.814289	-.557145	.162858
2	1	3	141.510	.353333	-.918665	.176666
3	1	4	131.229	.000000	-.495318	-.868712
4	5	6	103.310	.000000	-.996997	-.077437
5	5	7	127.264	.000000	-.502894	-.864348
6	1	5	974.905	-.999072	-.043081	.000000

Prepared by: <i>W. B. K. A. A.</i>	Date: <i>5-8-71</i>	LOCKHEED MISSILES & SPACE COMPANY A GROUP DIVISION OF LOCKHEED AIRCRAFT CORP.	Page: <i>Temp.</i> Part: <i>1</i>
Checked by:	Date:	Title:	EM No. <i>L2-12-01-M1-13</i> Date: <i>21 June 1971</i>
Approved by:	Date:		Report No.

14 FT. DIA. TANK, CONT'D.

LOADING CASES, FORCES AND REACTIONS

LOADING, JOINT 1: $PX = +100K$					
JOINT	REACTIONS			MEMBER	AXIAL FORCE
	RX	RY	RZ		
2	-138.251	94.593	-27.650	1	-169.782
3	38.251	-99.453	14.125	2	108.259
4	0.0	4.860	8.524	3	-9.813

LOADING, JOINT 1: $PY = -100K$					
JOINT	REACTIONS			MEMBER	AXIAL FORCE
	RX	RY	RZ		
2	47.919	-32.787	9.583	1	58.846
3	-47.919	124.590	-23.959	2	-135.621
4	0.0	8.197	14.376	3	-16.546

LOADING, JOINT 1: $PZ = -100K$					
JOINT	REACTIONS			MEMBER	AXIAL FORCE
	RX	RY	RZ		
2	-27.322	18.694	-5.464	1	-35.554
3	27.322	-71.038	13.661	2	77.328
4	0.0	52.344	41.803	3	-105.677

LOADING, JOINT 5: $PY = -100K$					
JOINT	REACTIONS			MEMBER	AXIAL FORCE
	RX	RY	RZ		
6	0.0	104.733	8.134	4	-105.048
7	0.0	-4.733	-8.134	5	9.411

LOADING, JOINT 5: $PZ = -100K$					
JOINT	REACTIONS			MEMBER	AXIAL FORCE
	RX	RY	RZ		
6	0.0	-60.935	-4.733	4	61.119
7	0.0	60.935	104.733	5	-121.170

Prepared by: H. BASERGA	Date 5-6-71	LOCKHEED MISSILES & SPACE CO A GROUP DIVISION OF LOCKHEED AIRCRAFT CO	EM No. L2-12-01-M1-13
Checked by:	Date	Title	Date: 21 June 1971
Approved by:	Date		Report No.

SPACE TRUSS ANALYSIS DATE 05 MAY 71

LH2 TANK SUPPORTING STRUCTURE. 18FT DIA TANK CONFIG.

COORDINATES OF JOINTS

JOINT	X	Y	Z
1	1522.000	264.000	474.000
2	1712.000	120.000	488.000
3	1572.000	120.000	475.000
4	1522.000	185.000	336.000
5	548.000	222.000	474.000
6	548.000	105.000	442.000
7	548.000	144.000	340.000

MEMBER DESIGNATIONS AND PROPERTIES

MEMBER	JJ END	JK END	L	CX	CY	CZ
1	1	2	238.814	.795599	-.602980	.058623
2	1	3	152.437	.328005	-.944653	.006560
3	1	4	159.013	.000000	-.496816	-.867856
4	5	6	121.297	.000000	-.964573	-.263815
5	5	7	155.048	.000000	-.503069	-.864246
6	1	5	974.905	-.999072	-.043081	.000000

Prepared by: H. BAKER	Date: 5-8-71	LOCKHEED MISSILES & SPACE CO. A GROUP DIVISION OF LOCKHEED AIRCRAFT CORP.	EM No. L2-12-01-M1-13
Checked by:	Date:		Date: 21 June 1971
Approved by:	Date:	Title	Report No.

18 FT. DIA. TANK, CONT'D.

LOADING CASES, FORCES AND REACTIONS

LOADING, JOINT 1: $PX = +100K$					
JOINT	REACTIONS			MEMBER	AXIAL FORCE
	RX	RY	RZ		
2	-138.256	104.783	-10.187	1	-173.776
3	38.256	-110.177	.765	2	116.633
4	0.0	5.394	9.422	3	-10.857

LOADING, JOINT 1: $PY = -100K$					
JOINT	REACTIONS			MEMBER	AXIAL FORCE
	RX	RY	RZ		
2	47.815	-56.239	3.523	1	60.100
3	-47.815	137.708	-.956	2	-145.777
4	0.0	-1.469	-2.567	3	2.958

LOADING, JOINT 1: $PZ = -100K$					
JOINT	REACTIONS			MEMBER	AXIAL FORCE
	RX	RY	RZ		
2	-27.372	20.745	-2.016	1	-34.405
3	27.372	-78.833	.547	2	83.452
4	0.0		101.469	3	-116.920

LOADING, JOINT 5: $PY = -100K$					
JOINT	REACTIONS			MEMBER	AXIAL FORCE
	RX	RY	RZ		
6	0.0	118.935	32.529	4	-123.303
7	0.0	-18.935	-32.529	5	37.639

LOADING, JOINT 5: $PZ = -100K$					
JOINT	REACTIONS			MEMBER	AXIAL FORCE
	RX	RY	RZ		
6	0.0	-69.230	-18.935	4	71.773
7	0.0	69.230	118.935	5	-137.617

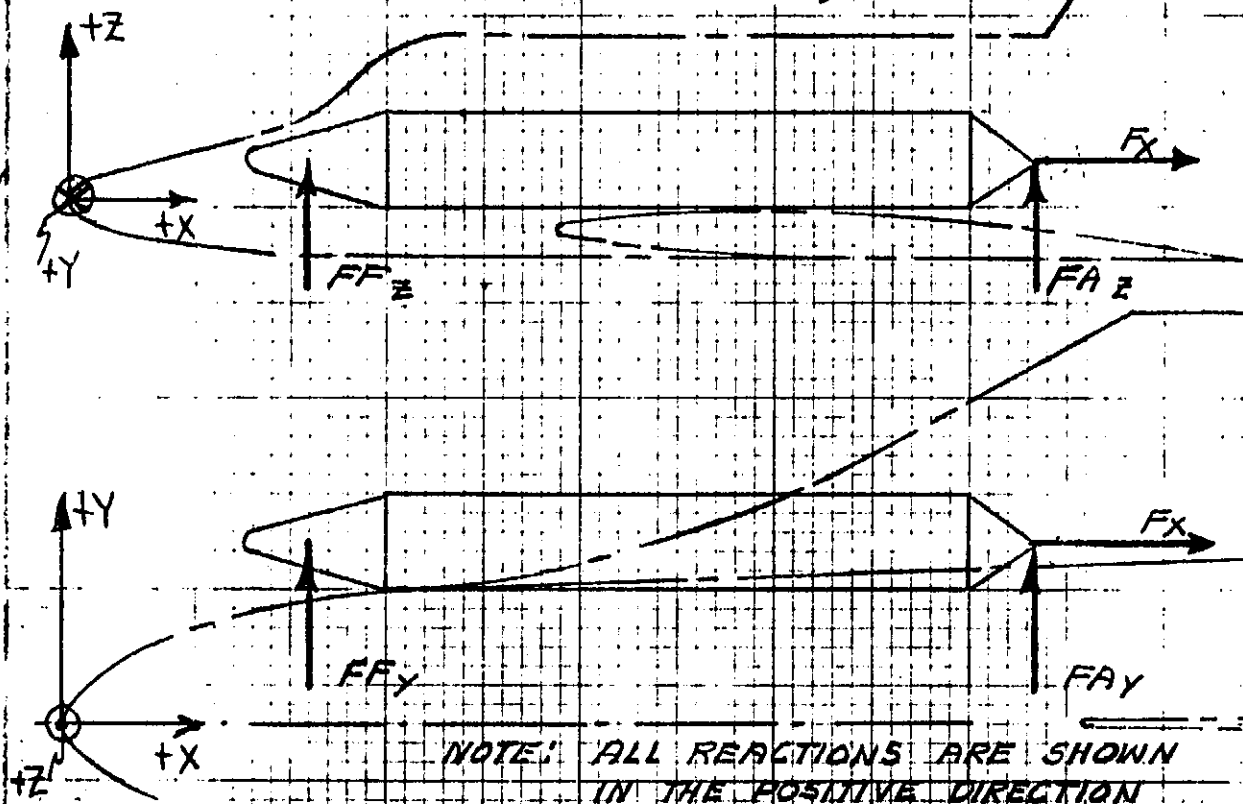
EM No. 12-12-01-M-13

Date: 21 June 1971

PREPARED BY

PAGE OF

BASELINE DROP TANK / ORBITER INTERFACE REACTIONS (PRELIMINARY)



REACTIONS ~ LBS

CONDITION	F_x	FF_z	FA_z	FF_y	FA_y
COND. ① MAX AXIAL g's	-145,500	0	0	0	0
COND. ② MAX α_z	-140,000	-450	+16,000	-34,000	+3,950
COND. ③ MAX α_z INERTIA LOAD ONLY ($\pm 1.7g$)	N.A.	$\pm 9,440$	$\pm 9,960$	$\pm 9,440$	$\pm 9,960$
COND. ④ MAX α_z AIR LOAD ONLY	N.A.	-9,890	+6,040	-34,000	+3,950

Prepared by: H. BASERGA	Date 5-12-71	LOCKHEED MISSILES & SPACE COM A GROUP DIVISION OF LOCKHEED AIRCRAFT CORP.		EM No. L2-12-01-M1-13
Checked by:	Date	Title		Date: 21 June 1971
Approved by:	Date			Report No.

SUPPORTING STRUCTURE LOADING ANALYSIS

Notation & sign convention is same as for the preceeding unit-load analysis. Basic loads listed below are from preceeding preliminary loads.

LOADING CONDITION	AFT, JOINT No. 1			FWD., JOINT No. 5	
	FA _X	FA _Y	FA _Z	FF _Y	FF _Z
① MAX. Axial (3 G's)	+145,500	0	0	0	0
② MAX. αq	+140,000	-3950	-16,000	+34,000	+450
Max αq Inertia					
③ load only ($\pm 4G$'s)	Not App.	$\pm 9,960$	$\pm 9,960$	$\pm 9,440$	$\pm 9,440$
Max. αq Air					
④ load only	Not App.	-3950	-6,040	+34,000	+1,890

Influence coefficients for each member are found by rationing above listed values into the unit load of 100^k used in the Space Truss Analysis. Final load on each member is found by superposition of partial values. Loading analysis is carried out separately for 12 FT DIA, 14 FT DIA & 16 FT DIA configurations.

NOTE: AFT supporting strut is not critical for COND. ③ & ④.

Prepared by: H. BASERGA	Date 5-12-71	LOCKHEED MISSILES & SPACE CO. A GROUP DIVISION OF LOCKHEED AIRCRAFT CORP.	Form No. L2-12-01-M1-13
Checked by:	Date	Title	Date: 21 June 1971
Approved by:	Date		Report No.

LOADING COND. ①

Loaded structure is the Aft Support with no significant loads being reacted at the Fwd. Support. The influence coeff. for loads in the "X" direction is: $K_x = \frac{+145.5}{+100} = 1.455$

Member No.	12 FT DIA TANK		14 FT DIA TANK		18 FT DIA TANK	
	Axial Unit Force	$K_x(A.U.F.)$	Axial Unit Force	$K_x(A.U.F.)$	Axial Unit Force	$K_x(A.U.F.)$
1	-168,659	-245,399	-169,782	-247,033	-173,776	-252,844
2	+105,437	+153,411	+108,259	+157,517	+116,633	+169,701
3	-9,292	-13,520	-9,813	-14,278	-10,857	-15,797

LOADING COND. ②: Loads are simultaneously applied along the three axis.

MEMBER No. 1 (DRAG STRUT).

Influence Coefficient	12 FT DIA TANK		14 FT DIA TANK		18 FT DIA TANK	
	Axial Unit Force	$K_L(A.U.F.)$	Axial Unit Force	$K_L(A.U.F.)$	Axial Unit Force	$K_L(A.U.F.)$
$K_x = \frac{140}{100} = 1.400$	-168,659	-236,123	-169,782	-237,695	-173,776	-243,287
$K_y = \frac{-3.95}{-100} = .0395$	+58,546	+2313	58,848	+2,325	+60,100	+2374
$K_z = \frac{-16.00}{-100} = .160$	-33,291	-5327	-33,554	-5,367	-34,405	-5505
Actual Force		-239,137		-240,737		-246,418

Prepared by: H. BASERGA	Date 5-12-71	LOCKHEED MISSILES & SPACE CO. A GROUP DIVISION OF LOCKHEED AIRCRAFT CORP.		EM No. L2-12-01-M1-13
Checked by:	Date	Title		Date: 21 June 1971
Approved by:	Date			Report No.

LOADING COND. (3), CONT'D.)

MEMBER No. 2 (UPPER REAR STRUT)

Influence Coefficient	12 FT DIA TANK		14 FT DIA TANK		18 FT DIA TANK	
	Axial Unit Force	K _i (A.U.F.)	Axial Unit Force	K _i (A.U.F.)	Axial Unit Force	K _i (A.U.F.)
$K_X = \frac{140.0}{100.} = 1.400$	+105,437	+147,612	+108,259	+151,563	+116,633	+163,286
$K_Y = \frac{-3.95}{-100.} = .0395$	-132,292	- 5225	-135,621	- 5,357	-145,777	- 5758
$K_Z = \frac{-16.00}{-100.} = .160$	+75,225	+12036	+77,328	+12,373	+83,452	+13352
Actual Force		+154,423		+158,579		+170,880

MEMBER No. 3 (LOWER REAR STRUT)

Influence Coefficient	12 FT DIA TANK		14 FT DIA TANK		18 FT DIA TANK	
	Axial Unit Force	K _i (A.U.F.)	Axial Unit Force	K _i (A.U.F.)	Axial Unit Force	K _i (A.U.F.)
$K_X = \frac{140.0}{100.} = 1.400$	-9,292	-13009	-9,813	-13,738	-10,857	-15200
$K_Y = \frac{-3.95}{-100.} = .0395$	-26,324	- 1040	-16,548	- 654	+2,958	+117
$K_Z = \frac{-16.00}{-100.} = .160$	-100,068	-16011	-105,677	-16,908	-116,920	-18707
Actual Force		-30060		-31,300		-33790

Prepared by: H. BASERGA	Date 5-13-71	LOCKHEED MISSILES & SPACE COMP A GROUP DIVISION OF LOCKHEED AIRCRAFT CORP.		EM No. 12-12-01-M-13 Date: 21 June 1971
Checked by:	Date	Title		
Approved by:	Date	Report No.		

LOADING COND. ②, CONT'D.)

MEMBER No 4 (UPPER FRONT STRUT), COND. ②

Influence Coefficient	12 FT DIA TANK		14 FT DIA TANK		18 FT DIA TANK	
	Axial Unit Force	K _i (A.U.F.)	Axial Unit Force	K _i (A.U.F.)	Axial Unit Force	K _i (A.U.F.)
K _x = 0.0	0.0	0.0	0.0	0.0	0.0	0.0
K _y = $\frac{+34.0}{-100.} = -.340$	-97,718	+ 33224	-105,048	+ 35,716	-123,303	+41923
K _z = $\frac{+.450}{-100.} = -.0045$	56,836	- 255	61,119	- 275	71,773	- 323
Actual Force		+ 32969		+35441		+41600

MEMBER No. 5 (LOWER FRONT STRUT), COND. ②

Influence Coefficient	12 FT DIA TANK		14 FT DIA TANK		18 FT DIA TANK	
	Axial Unit Force	K _i (A.U.F.)	Axial Unit Force	K _i (A.U.F.)	Axial Unit Force	K _i (A.U.F.)
K _x = 0.0	0.0	0.0	0.0	0.0	0.0	0.0
K _y = $\frac{+34.0}{-100.} = -.340$	-4,706	+1600	9,411	-3200	37,639	-12797
K _z = $\frac{+.450}{-100} = -.0045$	-112,948	+ 508	-121,170	+ 545	-137,617	+ 619
Actual Force		+ 2108		-2655		-12178

Prepared by: <u>H. BASTENIA</u>	Date <u>5-13-71</u>	LOCKHEED MISSILES & SPACE COMF A GROUP DIVISION OF LOCKHEED AIRCRAFT CORP.		Date <u>21 June 1971</u>	Temp. <u>12</u>	Perm. <u>12</u>
Checked by:	Date	Title		EM No. <u>L2-12-01-M1-13</u>		
Approved by:	Date			Date: <u>21 June 1971</u>		
				Report No.		

LOADING COND. ③ , Max. Inertia load only.

MLMBER No 4 (UPPER FRONT STRUT), COND. ③_a: +F_y, +F_z

Influence Coefficient	12 FT DIA TANK		14 FT DIA TANK		18 FT DIA TANK	
	Axial Unit Force	K _i (A.U.F.)	Axial Unit Force	K _i (A.U.F.)	Axial Unit Force	K _i (A.U.F.)
K _x = 0.0	0.0	0.0	0.0	0.0	0.0	0.0
K _y = $\frac{+9.44}{-100} = -.0944$	-97,718	+9225	-105,048	+9917	-123,303	+11640
K _z = $\frac{+9.44}{-100} = -.0944$	+56,836	-5365	+61,119	-5770	+71,773	-6775
Actual Force		+3860		+4147		+4865

MEMBER No 5 (LOWER FRONT STRUT), COND. ③_a: +F_y, +F_z

Influence Coefficient	12 FT DIA TANK		14 FT DIA TANK		18 FT DIA TANK	
	Axial Unit Force	K _i (A.U.F.)	Axial Unit Force	K _i (A.U.F.)	Axial Unit Force	K _i (A.U.F.)
K _x = 0.0	0.0	0.0	0.0	0.0	0.0	0.0
K _y = $\frac{+9.44}{-100} = -.0944$	-4,706	+444	+9,411	-888	+37,639	-3553
K _z = $\frac{+9.44}{-100} = -.0944$	-112,948	+10662	-121,170	+11438	-137,617	+12991
Actual Force		+11106		+10550		+9438

Prepared by: <i>[Signature]</i>	Date: <i>5-13-71</i>	LOCKHEED MISSILES & SPACE CO. A GROUP DIVISION OF LOCKHEED AIRCRAFT CORP.	EM No. <i>L2-12-01-M1-13</i>
Checked by:	Date:	Title:	Date: <i>21 June 1971</i>
Approved by:	Date:		Report No.

LOADING COND. (3), CONT'D.)

MEMBER NO 4 (UPPER FRONT STRUT), COND. (3)_b: -F_y, -F_z

Influence Coefficient	12 FT DIA. TANK		14 FT DIA TANK		18 FT DIA TANK	
	Axial Unit Force	K _i (A.U.F.)	Axial Unit Force	K _i (A.U.F.)	Axial Unit Force	K _i (A.U.F.)
<i>0.0</i>	<i>0.0</i>	<i>0.0</i>	<i>0.0</i>	<i>0.0</i>	<i>0.0</i>	<i>0.0</i>
<i>$-\frac{9.44}{-100} = +.0944$</i>	<i>-97,718</i>	<i>-9225</i>	<i>-105,048</i>	<i>-9917</i>	<i>-123,303</i>	<i>-11640</i>
<i>$-\frac{9.44}{-100} = +.0944$</i>	<i>+56,836</i>	<i>+5365</i>	<i>+61,119</i>	<i>+5770</i>	<i>+71,773</i>	<i>+6775</i>
<i>Actual Force</i>		<i>-3860</i>		<i>-4147</i>		<i>-4865</i>

MEMBER NO 5 (LOWER FRONT STRUT), COND. (3)_b: -F_y, -F_z

Influence Coefficient	12 FT DIA TANK		14 FT DIA TANK		18 FT DIA TANK	
	Axial Unit Force	K _i (A.U.F.)	Axial Unit Force	K _i (A.U.F.)	Axial Unit Force	K _i (A.U.F.)
<i>K_x = 0.0</i>	<i>0.0</i>	<i>0.0</i>	<i>0.0</i>	<i>0.0</i>	<i>0.0</i>	<i>0.0</i>
<i>$K_y = \frac{-9.44}{-100} = +.0944$</i>	<i>-4,706</i>	<i>-444</i>	<i>+9,411</i>	<i>+888</i>	<i>+37,639</i>	<i>+3553</i>
<i>$K_z = \frac{-9.44}{-100} = +.0944$</i>	<i>-112,948</i>	<i>-10662</i>	<i>-121,170</i>	<i>-11438</i>	<i>-137,617</i>	<i>-12991</i>
<i>Actual Force</i>		<i>-11106</i>		<i>-10550</i>		<i>-9438</i>

Prepared by: <u>W. J. S. 5A</u>	Date: <u>5-14-71</u>	LOCKHEED MISSILES & SPACE CO A GROUP DIVISION OF LOCKHEED AIRCRAFT CO.	EM No. <u>L2-12-01-M1-13</u>
Checked by:	Date:	Title:	Date: <u>21 June 1971</u>
Approved by:	Date:	Report No.	

LOADING COND. ③, CONT'D.)

MEMBER No 4 (UPPER FRONT STRUT), COND. ③: $+F_y, -F_z$

Influence Coefficient	12 FT DIA TANK		14 FT DIA TANK		18 FT DIA TANK	
	Axial Unit Force	$K_i(A.U.F.)$	Axial Unit Force	$K_i(A.U.F.)$	Axial Unit Force	$K_i(A.U.F.)$
$K_x = 0.0$	0.0	0.0	0.0	0.0	0.0	0.0
$K_y = \frac{+9.44}{-100} = -.0944$	-97,718	+ 4225	-105,048	+ 9917	-123,303	+ 11640
$K_z = \frac{-9.44}{-100} = +.0944$	+56,836	+ 5365	+61,119	+ 5770	+71,773	+ 6775
Actual Force		+14590		+15687		+18415

MEMBER No 5 (LOWER FRONT STRUT), COND. ③: $+F_y, -F_z$

Influence Coefficient	12 FT DIA TANK		14 FT DIA TANK		18 FT DIA TANK	
	Axial Unit Force	$K_i(A.U.F.)$	Axial Unit Force	$K_i(A.U.F.)$	Axial Unit Force	$K_i(A.U.F.)$
$K_x = 0.0$	0.0	0.0	0.0	0.0	0.0	0.0
$K_y = \frac{+9.44}{-100} = -.0944$	-4,706	+ 444	+ 9,411	- 888	+37,639	- 3553
$K_z = \frac{-9.44}{-100} = +.0944$	-112,948	- 10662	-121,170	-11438	-137,617	-12991
Actual Force		-10218		-12326		-16544

Prepared by: <u>H. BASEMAN</u>	Date <u>5-14-71</u>	LOCKHEED MISSILES & SPACE CO. A SUBDIVISION OF LOCKHEED AIRCRAFT CO.	EM No. <u>12-12-01-10-13</u>
Checked by:	Date	Title	Date: <u>21 June 1971</u>
Approved by:	Date		Report No.

LOADING COND. ③, CONT'D.)

MEMBER No 4 (UPPER FRONT STRUT), COND. ③ $-F_y, +F_z$

Influence Coefficient	12 FT DIA TANK		14 FT DIA TANK		18 FT DIA TANK	
	Axial Unit Force	$K_i(A.U.F.)$	Axial Unit Force	$K_i(A.U.F.)$	Axial Unit Force	$K_i(A.U.F.)$
$K_x = 0.0$	0.0	0.0	0.0	0.0	0.0	0.0
$K_y = \frac{-9.44}{-100} = +0.0944$	-97,718	-9225	-105,048	-9917	-123,308	-11640
$K_z = \frac{+9.44}{-100} = -0.0944$	+56,836	-5365	+61,119	-5770	+71,773	-6775
Actual Force		-14590		-15687		-18415

MEMBER No 5 (LOWER FRONT STRUT), COND. ③ $-F_y, +F_z$

Influence Coefficient	12 FT DIA TANK		14 FT DIA TANK		18 FT DIA TANK	
	Axial Unit Force	$K_i(A.U.F.)$	Axial Unit Force	$K_i(A.U.F.)$	Axial Unit Force	$K_i(A.U.F.)$
$K_x = 0.0$	0.0	0.0	0.0	0.0	0.0	0.0
$K_y = \frac{-9.44}{-100} = +0.0944$	-4,706	-444	+9,411	+888	+37,639	+3553
$K_z = \frac{+9.44}{-100} = -0.0944$	-112,948	+10662	-121,170	+11438	-137,617	+12991
Actual Force		+10218		+12326		+16544

Prepared by: H. B. S. S. A.	Date 5-17-71	LOCKHEED MISSILES & SPACE CO. A GROUP DIVISION OF LOCKHEED AIRCRAFT CORP.	EM No. L2-12-01-M1-13
Checked by:	Date	Title	Date: 21 June 1971
Approved by:	Date		Report No.

LOADING COND. ④: Max. kg Air Load Only.

MEMBER No 4 (UPPER FRONT STRUT), COND. ④

Influence Coefficient	12 FT DIA TANK		14 FT DIA TANK		18 FT DIA TANK	
	Axial Unit Force	$K_i(A.U.F.)$	Axial Unit Force	$K_i(A.U.F.)$	Axial Unit Force	$K_i(A.U.F.)$
$K_x = 0.0$	0.0	0.0	0.0	0.0	0.0	0.0
$K_y = \frac{+34.0}{-100} = -.34$	-97,718	+ 33224	-105,048	+ 35716	-123,303	+ 41923
$K_z = \frac{+9.89}{-100} = -.0989$	+56,836	- 5621	+61,119	- 6045	+71,773	- 7098
Actual Force		+27603		+29671		+34825

MEMBER No 5 (LOWER FRONT STRUT), COND. ④

Influence Coefficient	12 FT DIA TANK		14 FT DIA TANK		18 FT DIA TANK	
	Axial Unit Force	$K_i(A.U.F.)$	Axial Unit Force	$K_i(A.U.F.)$	Axial Unit Force	$K_i(A.U.F.)$
$K_x = 0.0$	0.0	0.0	0.0	0.0	0.0	0.0
$K_y = \frac{+34.0}{-100} = -.34$	-4,706	+1600	+9,411	-3200	+37,639	-12797
$K_z = \frac{+9.89}{-100} = -.0989$	-112,948	+11171	-121,170	+11984	-137,617	+13610
Actual Force		+12771		+8784		+813

Prepared by: H. BASERGA	Date 5-19-71	LOCKHEED MISSILES & SPACE COMPANY A GROUP DIVISION OF LOCKHEED AIRCRAFT CO	Page 15	Temp.	Form.
Checked by:	Date	Title	EM No. 12-12-01-M1-13 Date: 21 June 1971		
Approved by:	Date		Report No.		

SUMMARY OF STRUT AXIAL LOADS (LIMIT)

LOADING CONDITION	MEMBER No. 1: DRAG STRUT		
	12 FT DIA	14 FT DIA	18 FT DIA
① MAX AXIAL (3G's)	-245,399	-247,033	-252,844
② MAX αq	-239,137	-240,737	-246,418

MEMBER No. 2: UPPER REAR STRUT			
① MAX AXIAL (3G's)	+153,411	+157,517	+169,701
② MAX αq	+154,423	+158,579	+170,820

MEMBER No. 3: LOWER REAR STRUT			
① MAX AXIAL (3G's)	-13,520	-14,278	-15,797
② MAX αq	-30,060	-31,300	-33,790

MEMBER No. 4: UPPER FRONT STRUT			
② MAX αq	+32,969	+35,441	+41,600
③a	+3,860	+4,147	+4,865
③b	-3,860	-4,147	-4,865
③c	+14,590	+15,687	+18,415
③d	-14,590	-15,687	-18,415
④ MAX αq (AIR LOAD ONLY)	+27,603	+29,671	+34,825

Prepared by: H. BASERGA	Date 5-19-71	LOCKHEED MISSILES & SPACE C A GROUP DIVISION OF LOCKHEED AIRCRAFT C		EM No. L2-12-01-M1-13
Checked by:	Date	Title		Date: 21 June 1971
Approved by:	Date			Report No.

SUMMARY OF STRUT AXIAL LOADS, CONT'D.

LOADING CONDITION	MEMBER No. 5 : LOWER FRONT STRUT		
	12 FT DIA	14 FT DIA	18 FT DIA
② MAX αq	+2,108	-2,655	-12,178
③a	+11,106	+10,550	+9,438
③b	-11,106	-10,550	-9,438
③c	-10,218	-12,326	-16,544
③d	+10,218	+12,326	+16,544
④ MAX αq (AIR LOAD ONLY)	+12,771	+8,784	+813

NOTE : Pending an investigation on loads including wind tunnel data the aft support structure (members 1, 2 & 3) is sized on the basis of Conditions ① & ②.

Prepared by: H. BASERGA	Date 5-19-71	LOCKHEED MISSILES & SPACE CO A GROUP DIVISION OF LOCKHEED AIRCRAFT CO	Form No. L2-12-Q1-M1-13 Date: 21 June 1971
Checked by:	Date	Title	Report No.
Approved by:	Date		

STRUT CRITICAL LOADS

By inspection of "SUMMARY OF STRUT AXIAL LOADS" the critical loads are:

MEMBER	AXIAL LOADS (LIMIT)			CRITICAL CASE
	12 FT DIA	14 FT DIA	18 FT DIA	
1, DRAG STRUT	-245,399	-247,033	-252,844	COND. ①
2, UPPER REAR	+154,423	+158,579	+170,880	COND. ②
3, LOWER REAR	-30,060	-31,300	-33,790	COND. ②
4, UPPER FRONT	-14,590	-15,687	-18,415	COND. ③ d
5, LOWER FRONT	-11,106	-12,326	-16,544	COND. ③ b & c

STRESS ANALYSIS

ALL CONFIG. : $P_{ult.} = (1.4) P_{lim.}$

MAT'L. : Ti-6Al-4V, solution treated & aged sheet, $t < .187"$

12 FT DIA TANK

P/t	STRUT	SIZE	A	P	L	L/p	F_c	$P_{col.}$	$P_{ult.}$	M.S.	WT.
63.5	1	14.0 x .110	4.800	4.910	231.80	47.21	72500	-348,000	-343,559	.012	179.0
23	2	4.5 x .098	1.355	—	137.84	—	—	(+216,300)	(+216,93)	.002	30.0
37	3	6.0 x .045	.841	2.106	117.34	55.71	52000	-43732	-42,084	.039	16.0
56.5	4	4.5 x .035	.490	1.580	96.09	60.8	44000	-21560	-20,426	.055	8.0
56.5	5	4.5 x .040	.560	1.577	113.38	71.89	31000	-17360	-15,544	.116	11.0
											244.0

Prepared by: H. BASLERGA	Date 5-20-71	LOCKHEED MISSILES & SPACE CO <small>A GROUP DIVISION OF LOCKHEED AIRCRAFT CO.</small>		PM No. L2-12-01-M1-13
Checked by:	Date	Title		Date: 21 June 1971
Approved by:	Date			Report No.

14 FT DIA TANK

STRUT	SIZE	A	P	L	L/p	F _c	P _{col.}	P _{ult.}	M.S.	WT.
1	14.0x.110	4.800	4.910	233.34	47.52	72200	-346560	-345,846	.002	180.0
2	4.75x.095	1.389	—	141.51	—	—	(+222,240)	(+220,011)	.010	32.0
3	6.0x.063	1.175	2.095	131.23	63.0	40500	-47587	-43820	.046	25.0
4	5.0x.035	.545	1.756	103.31	59.0	46000	-25070	-21962	.140	9.0
5	5.0x.040	.623	1.754	127.27	73.0	30500	-19000	-17257	.101	13.0
										259.0

18 FT DIA TANK

STRUT	SIZE	A	P	L	L/p	F _c	P _{col.}	P _{ult.}	M.S.	WT.
1	14.0x.125	5.448	4.906	238.82	48.67	70000	-381,360	-353,982	.077	209.0
2	4.75x.103	1.503	—	152.44	—	—	(+240,480)	(+239,232)	.005	37.0
3	7.0 x .060	1.308	2.453	159.02	64.8	39000	-51012	-47306	.078	34.0
4	5.5x.040	.686	1.930	121.30	62.8	41500	-28469	-25781	.104	14.0
5	6.0x.045	.841	2.106	155.05	73.6	29000	-24389	-23162	.052	21.0
										315.0

Prepared by: H. BASERGA	Date 5-20-71	LOCKHEED MISSILES & SPACE A GROUP DIVISION OF LOCKHEED AIRCRAFT	EM No. L2-12-01-M1-13
Checked by:	Date	Title	Date: 21 June 1971
Approved by:	Date		Report No.

References for the STRESS ANALYSIS

Column Stress Allow. (F_c) values are taken from Stress Memo No. 83b, Fig. 30 (Ti-6Al-4V, $t \leq .187"$, curve 1, Room Temp.)

Crippling Strength. Refer to Stress Memo No. 126.

Extending curve of Fig. 11 given for Curved Element- No Edge Free to values $R/t > 36$ the basic Crippling Stress asymptotically tends to 30 KSI.

From Table I, pg. 16, the Mat'l. Correction Factor for Ti-6Al-4V, solution treated & aged sheet is 2.477.

Hence the Allow. Crippling Strength is

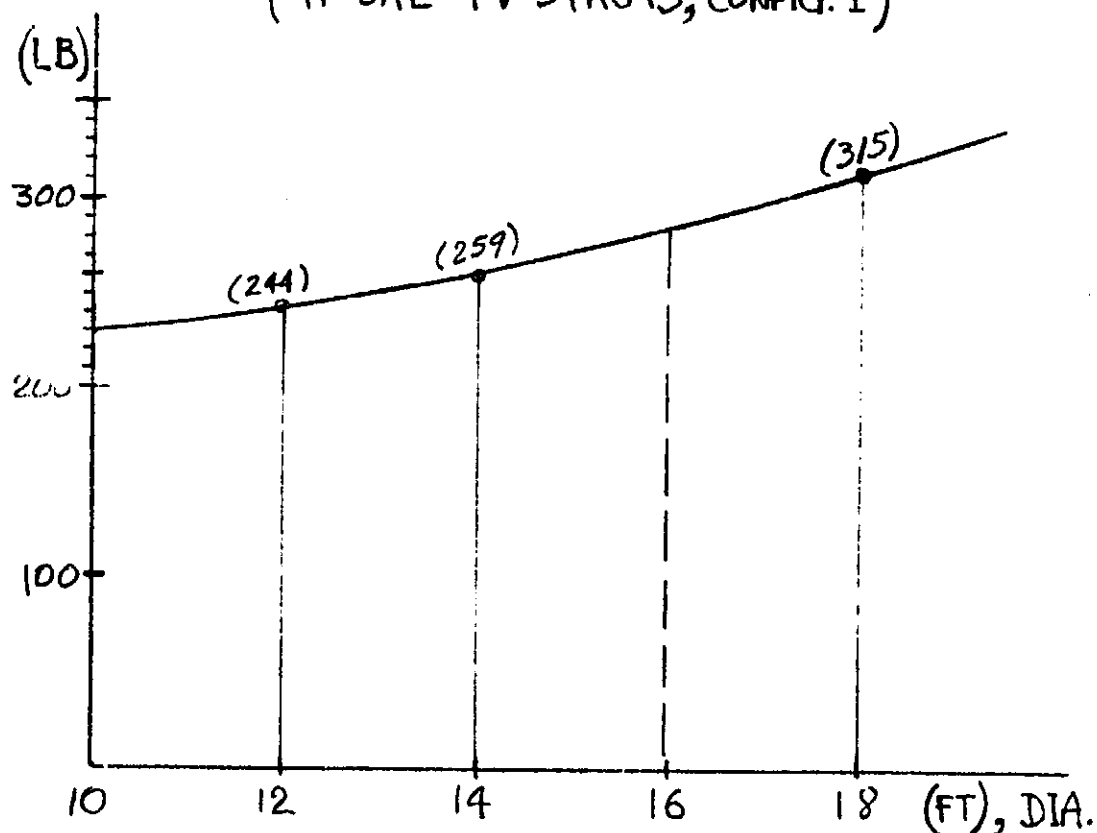
$$F_{cc} = (2.477)(30000) = 74310 \text{ PSI}$$

For all analyzed configurations the Column Stress F_c is less than F_{cc} . Therefore, for weight comparison purposes, it is assumed that crippling mode of failure is precluded.

Prepared by: H. BASEGA	Date 5-20-71	LOCKHEED MISSILES & SPACE COMPANY A GROUP DIVISION OF LOCKHEED AIRCRAFT CO	Page 1	Temp. 1	Perm. 1
Checked by:	Date	Title	EM No. L2-12-01-M1-13 Date: 21 June 1971		
Approved by:	Date		Report No.		

TANK ATTACHMENT TO ORBITER

(Ti-6AL-4V STRUTS, CONFIG. 1)



From above curve the estimated weights for 10 FT DIA & 18 FT DIA tanks supporting structure are 230 LB and 285 LB respectively. Strut ends weight is not included.

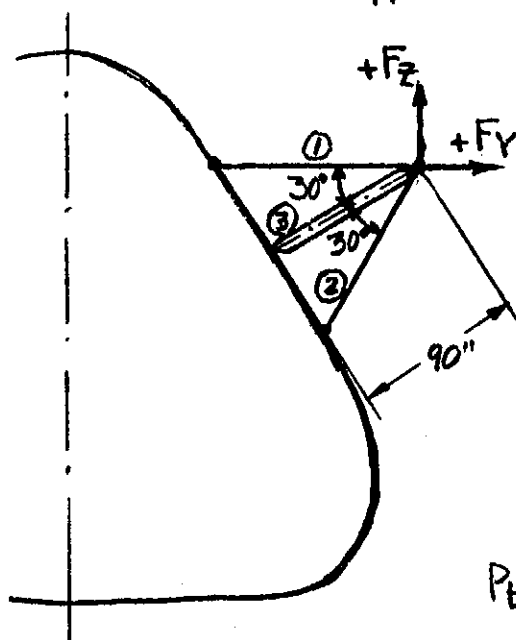
Prepared by: H. BASERGA	Date 6-2-71	LOCKHEED MISSILES & SPACE CO A GROUP DIVISION OF LOCKHEED AIRCRAFT CO	EM No. L2-12-01-M1-13
Checked by:	Date	Title	Date: 21 June 1971
Approved by:	Date		Report No.

CONFIG. 2

A supporting structure where tension rods are used is considered. For purposes of a weight evaluation and preliminary member sizing a simplified analysis is presented here.

FRONT SUPPORT: Two tension rods and one compression strut, all in one plane normal to orbiter.

CRITICAL LOADING: COND. ④, Max. αq , Air Load Only, where forces applied to support are as shown below.



TENSION RODS

$$P_{t①} = \frac{(-)F_z}{\tan 30^\circ} + (+)F_y = \frac{9440}{.5774} + 9440 = 25789 \text{ LB}$$

$$(P_{t①})_{\text{Max}} = F_y = 34000 \text{ LB LIM}$$

$$A_{①} = \frac{34000}{160000} (1.4) = .298 \text{ IN}^2$$

$$\text{ROD ①, DIA} = \sqrt{\frac{4 \times .298}{\pi}} = .620 \text{ IN}$$

$$P_{t②} = (+)F_z \left(\frac{\sin 120^\circ}{\sin 30^\circ} \right) = 9890 \left(\frac{.866}{.5} \right) = 17130 \text{ LB LIM.}$$

$$A_{②} = \frac{17130}{160000} (1.4) = .150 \text{ IN}^2$$

$$\text{ROD ②, DIA} = \sqrt{\frac{4 \times .150}{\pi}} = .437 \text{ IN}$$

$$\text{WEIGHT OF RODS: } (.150 + .298) \left(\frac{90}{\cos 30^\circ} \right) (.16) = 7.5 \text{ LB}$$

Prepared by: H. BASERGA	Date: 6-2-71	LOCKHEED MISSILES & SPACE CO A GROUP DIVISION OF LOCKHEED AIRCRAFT CO.	EM No. L2-12-01-M1-13
Checked by:	Date:	Title:	Date: 21 June 1971
Approved by:	Date:		Report No.

FRONT SUPPORT, CONT'D

COMPRESSION STRUT, LOAD: $P_C \textcircled{3} = F_z = 9890 \text{ LB LIM.}$

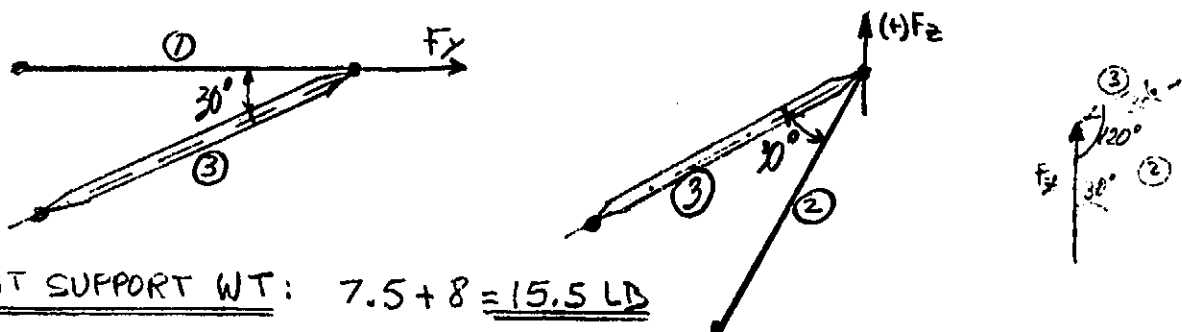
SIZING STRUT ③:

3.5 DIA x .049 WALL, $A = .531 \text{ in}^2$, $p = 1.22$, $L/p = 74$

From S.M. 836, Fig. 30 (Ti-6AL-4V): $F_c = 29500 \text{ PSI}$

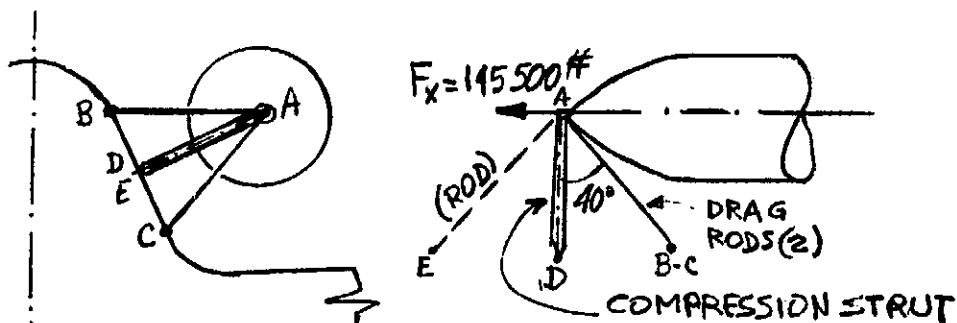
$$P_{\text{tot}} = .531 \times 29500 = 15664 \text{ LB ULT.}, \text{ M.S.} = \frac{15664}{(1.4)(9890)} - 1 = \underline{.131}$$

WEIGHT $\sim 90 \times .531 \times .16 = 8 \text{ LB}$



FRONT SUPPORT WT: $7.5 + 8 = \underline{15.5 \text{ LB}}$

AFT SUPPORT: LOADING COND. ① (MAX. AXIAL G'S).



$$P_c = \frac{F_x}{\tan 40^\circ} = \frac{145500}{.8391} = 173400 \text{ LB LIM}$$

$$P_{\text{TOTAL}} = \frac{F_x}{\sin 40^\circ} = \frac{145.5}{.6428} = 226,350 \text{ LB}; \text{ TENSION PER ROD: } P_t = \left(\frac{1}{2}\right) \frac{226350}{\cos 30^\circ} = 130690 \text{ LB LIM.}$$

NOTE: COND. ① IS LESS CRITICAL THAN FOLLOWING COND. ②.

Prepared by:
H. BASEGADate
6-2-71LOCKHEED MISSILES & SPACE CO. EM No. L2-12-01-M1-13
A GROUP DIVISION OF LOCKHEED AIRCRAFT CO.

Date: 21 June 1971

Checked by:

Date

Title

Approved by:

Date

Report No.

LOADING COND. ② (Max. $\times 9$)

NOTE: Loads marked (*) are preliminary findings from Loads Report.

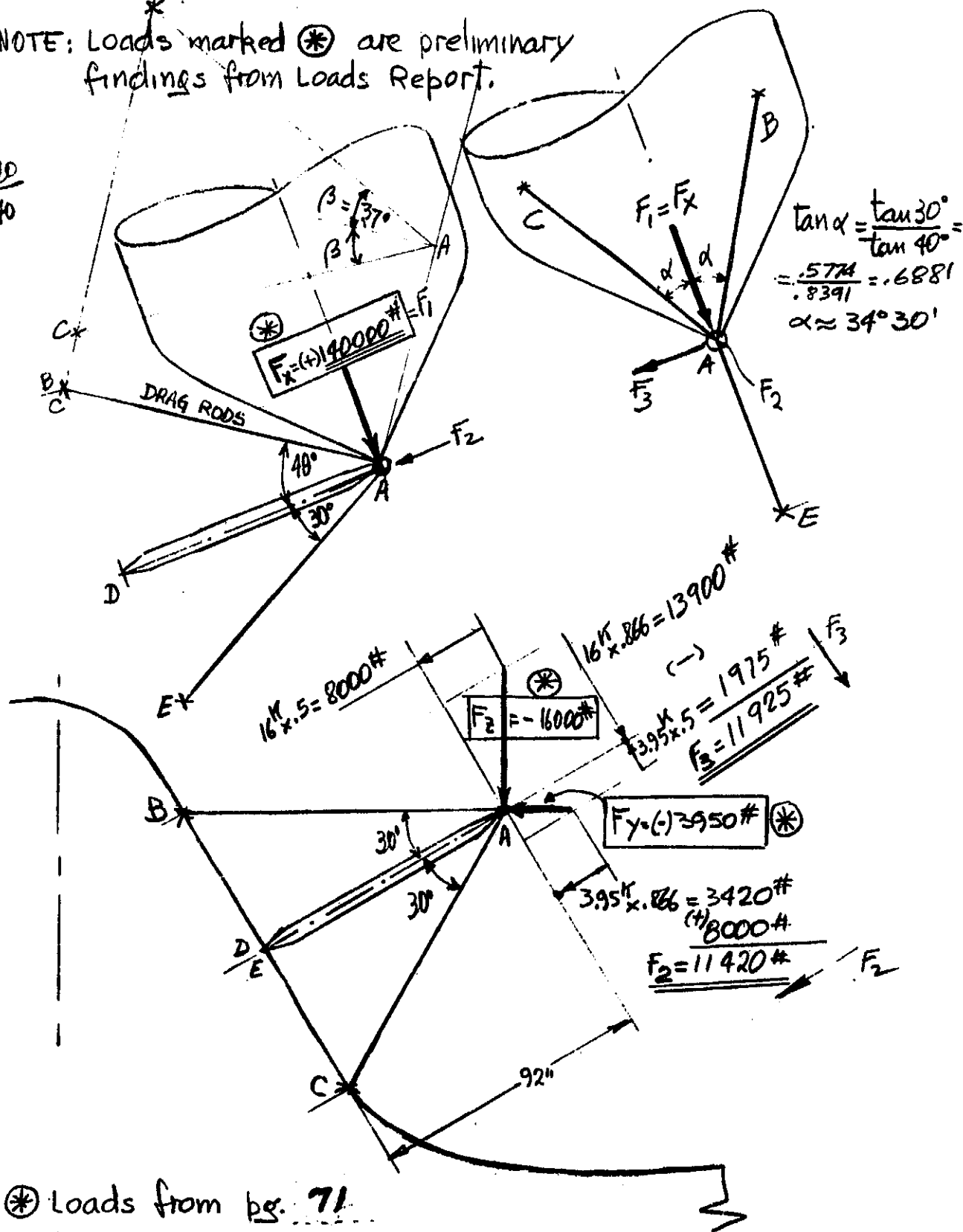
$$\tan \beta = \frac{\tan 30}{\tan 40}$$

$$\beta = 37^\circ$$

$$\tan 40 = .8391$$

$$\sin \beta = .7986$$

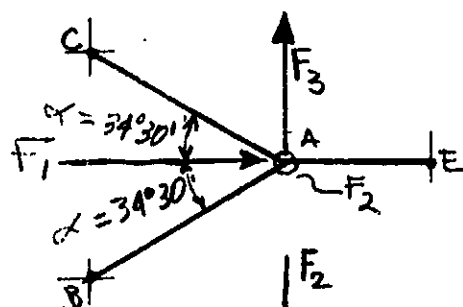
$$\tan 30 = .5774$$



Prepared by: H. BASERGA	Date 6-2-71	LOCKHEED MISSILES & SPACE CO. A GROUP DIVISION OF LOCKHEED AIRCRAFT CO.	Form No. L2-12-01-M1-13
Checked by:	Date	Title	Date: 21 June 1971
Approved by:	Date		Report No.

COND (2), CONT'D.)

Using limit loads as shown below the supporting structure is analyzed assuming that tension members (rods) do not take any compressive load.

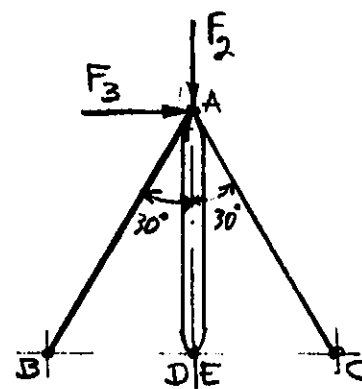
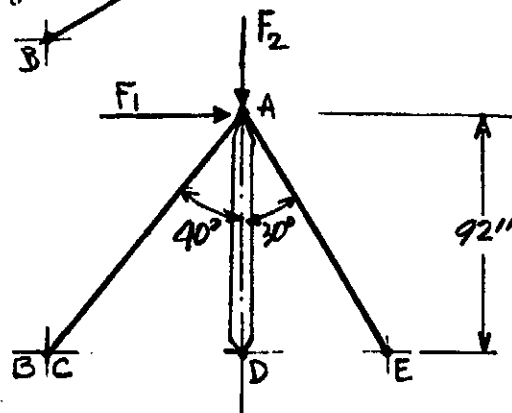


SIMULTANEOUS LOADING

$$F_1 = 140000 \text{ LB}$$

$$F_2 = 11420 \text{ LB}$$

$$F_3 = 11925 \text{ LB}$$



F1 LOAD

$$P_{AB} = P_{AC} = \left(\frac{1}{2}\right) \frac{F_1}{\sin 40^\circ \cos \beta} = \left(\frac{1}{2}\right) \frac{140000}{.6428 \times .7986} = 136362 \text{ LB}$$

$$P_{AD} = \frac{F_1}{\tan 40^\circ} = \frac{140000}{.8391} = -166846 \text{ LB}$$

F2 LOAD

Since F_2 is in the direction of STRUT \overline{AD} ,

$$P_{AD} = F_2 = -11420 \text{ LB}$$

Prepared by: H. BASERGA	Date 6-3-71	LOCKHEED MISSILES & SPACE CON A GROUP DIVISION OF LOCKHEED AIRCRAFT CORP.	EM No. 12-12-01-M1-13
Checked by:	Date	Title	Date: 21 June 1971
Approved by:	Date		Report No.

COND. (2), CONT'D.)

$$\alpha = 21^\circ 30' \quad \begin{cases} \sin \alpha = .5664 \\ \tan \alpha = .6873 \end{cases}$$

F₃ LOAD

$$P_{tAB} = \frac{F_3}{\sin \alpha \sin 40^\circ} = \frac{11925}{(.5664)(.6428)} = 32754 \text{ LB}$$

$$P_{tAE} = \frac{F_3}{\sin \alpha \tan 30^\circ} = \frac{11925}{(.5664)(.5774)} = 36463 \text{ LB}$$

$$P_{AD} = \left(\frac{F_3}{3} \right) \left(\frac{1}{(\sin \alpha \tan 40^\circ)} + \frac{1}{(\tan \alpha \tan 30^\circ)} \right) =$$

$$= (11925) \left(\frac{1}{(.5664 \times .8391)} + \frac{1}{(.6873 \times .5774)} \right) = 55140 \text{ LB}$$

SUMMARY OF MEMBER LOADING (LIM.)

MEMBER LOAD	AB	AC	AE	AD
F ₁	136362	136362	0	-166846
F ₂	0	0	0	-11420
F ₃	32754	0	36463	-55140
TOTAL	169116	136362	36463	-233406

SIZING TENSION MEMBERS: $A_{reqd} = \frac{P_t}{\sigma_t} \text{ (F.S.)}$; $DIA = \sqrt{\frac{4A}{\pi}}$

$$\overline{AB}, A = \frac{169116}{160000} (1.4) = 1.480 \text{ in}^2, D = 1.373", L = 131.327", WT = 32 \text{ LB}$$

$$\overline{AC}, A = \frac{136362}{160000} (1.4) = 1.194 \text{ in}^2, D = 1.233", L = 131.327", WT = 26 \text{ LB}$$

$$\overline{AE}, A = \frac{36463}{160000} (1.4) = .320 \text{ in}^2, D = .639", L = 100.25", WT = 6 \text{ LB}$$

TENSION RODS WEIGHT: 64 LB

Prepared by: H. BASERGA	Date: 6-3-71	LOCKHEED MISSILES & SPACE COMPANY A GROUP DIVISION OF LOCKHEED AIRCRAFT CORP.	Page 12-12-01-M1-13
Checked by:	Date:	Title	Date: 21 June 1971
Approved by:	Date:		Report No.

COND. ②, CONT'D.)

SIZING COMPRESSION STRUT ($P_c = -233,406$ LB, LIM.)

$$8.00 \text{ DIA} \times .105 \text{ WALL}, A = 2.604 \text{ IN}^2, p = 2.792, \frac{L}{p} = \frac{92}{2.792} = 33$$

From S.M. 83b, Fig. 30, $F_c = 131,000$ PSI (Ti-6AL-4V)

$$P_{col} = 131,000 \times 2.604 = 341,124 \text{ LB ULT}$$

$$M.S. = \frac{341,124}{(1.4)(233,406)} - 1 = \underline{.043}$$

$$\text{COMP. STRUT WEIGHT} \sim 2.604 \times 92 \times .16 = 38.5 \text{ LB}$$

$$\text{AFT SUPPORT WT. : Rods (64 LB) + Strut (38.5 LB) = 102.5 LB}$$

PRELIMINARY WT. ESTIMATE (CONFIG. II)

Not including rod & strut end fittings but assuming rods & struts extending from end to end the weight of CONFIG II is :

$$\text{FRONT SUPPORT : } 15.5 \text{ LB}$$

$$\text{AFT SUPPORT : } \underline{102.5 \text{ LB}}$$

$$\text{TOTAL (NET) WT. } 118.0 \text{ LB}$$

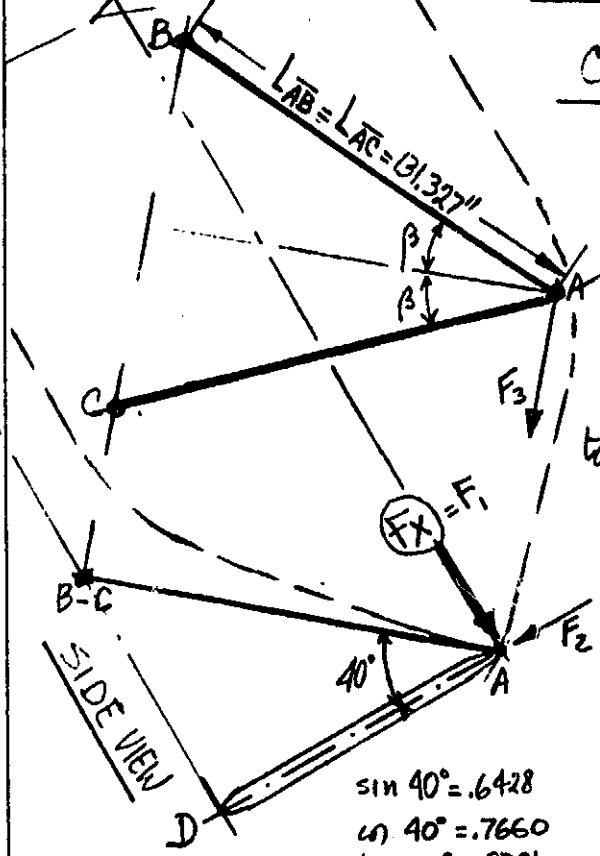
NOTE : Above weight estimate is for the 14FT DIA tank (baseline dsg'n.). Small weight variation may be anticipated for 12FT & 18FT DIA tanks.

Prepared by: H. BASERGA	Date 6-10-71	LOCKHEED MISSILES & SPACE COMPANY A GROUP DIVISION OF LOCKHEED AIRCRAFT CORP.	Page Temp. Perm.
Checked by:	Date	Title	EM No. L2-12-01-M1-13 Date: 21 June 1971
Approved by:	Date		Report No.

GEOMETRY & LOADING

CONFIG. 3

PLAN VIEW



$\tan \alpha = \tan 30^\circ / \tan 40^\circ$
 $= .6881$
 $\alpha = 34^\circ 30'$
 $\sin \alpha = .5664$
 $\cos \alpha = .8241$

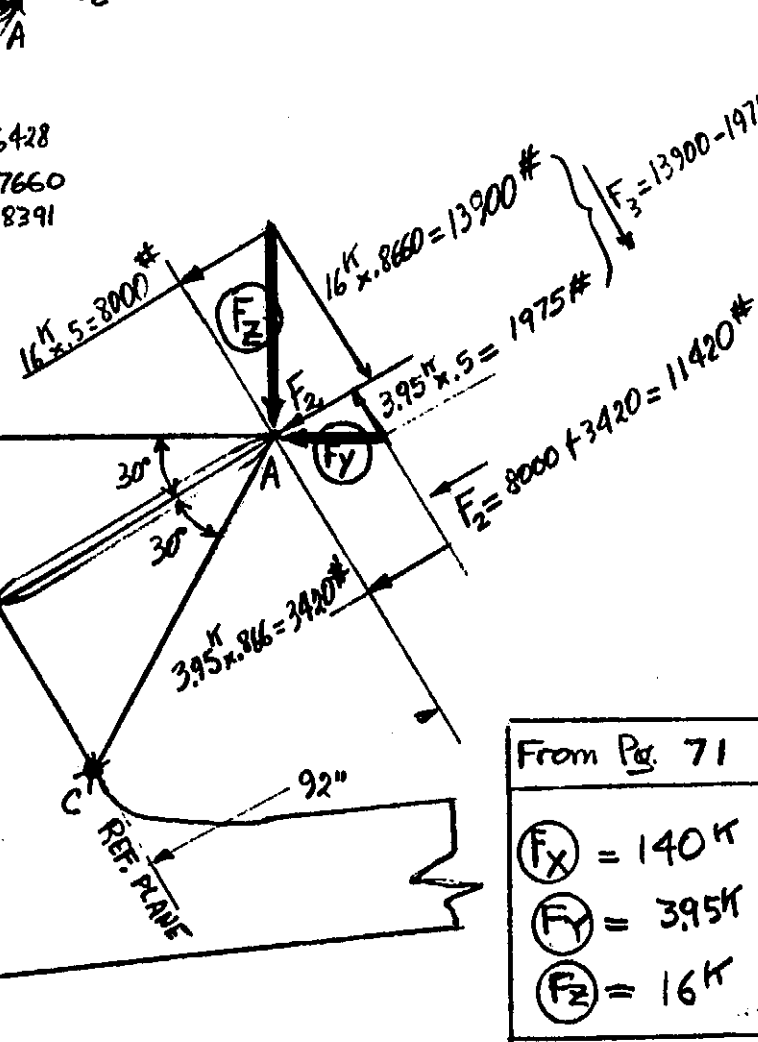
$\tan \beta = \tan 30^\circ \cos 40^\circ$
 $= .44223, \beta = 23^\circ 50'$
 $\sin \beta = .4041, \cos \beta = .9147$

SIDE VIEW

$\sin 40^\circ = .6428$
 $\cos 40^\circ = .7660$
 $\tan 40^\circ = .8391$

AFT VIEW

$\sin 30^\circ = .5$
 $\cos 30^\circ = .8660$
 $\tan 30^\circ = .5774$

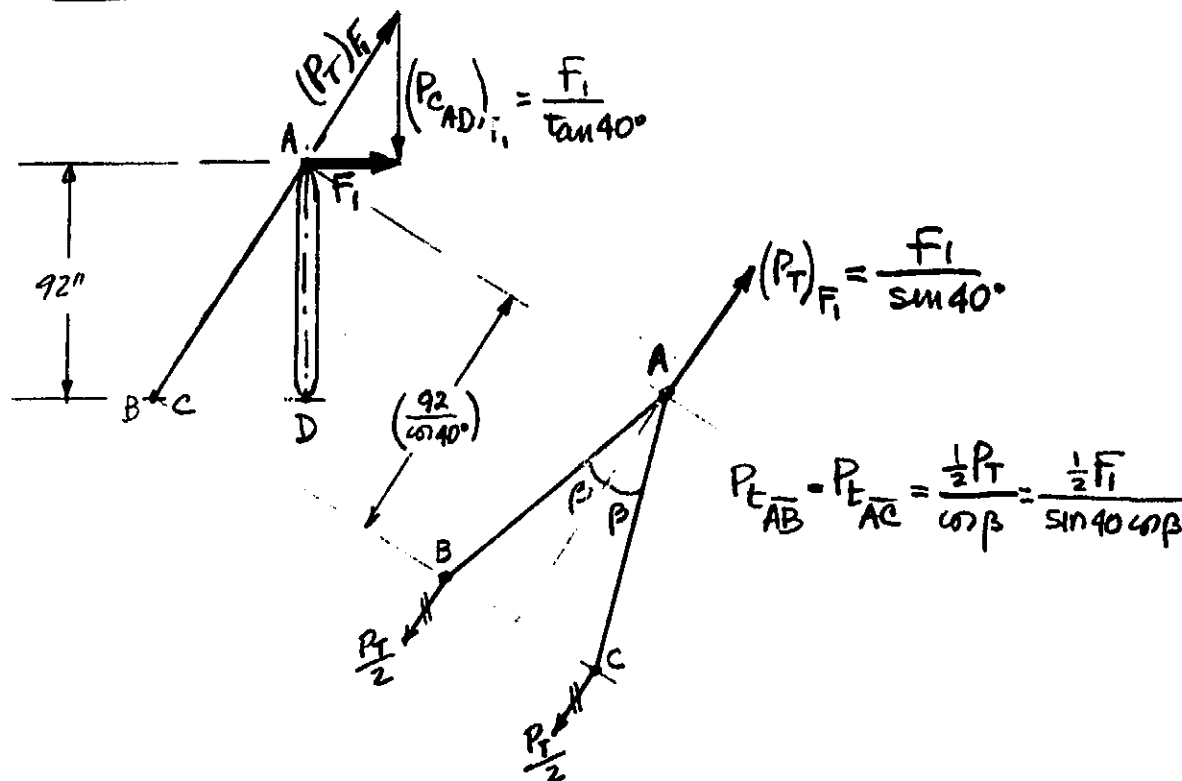


From Pg. 71

$F_x = 140K$
$F_y = 3.95K$
$F_z = 16K$

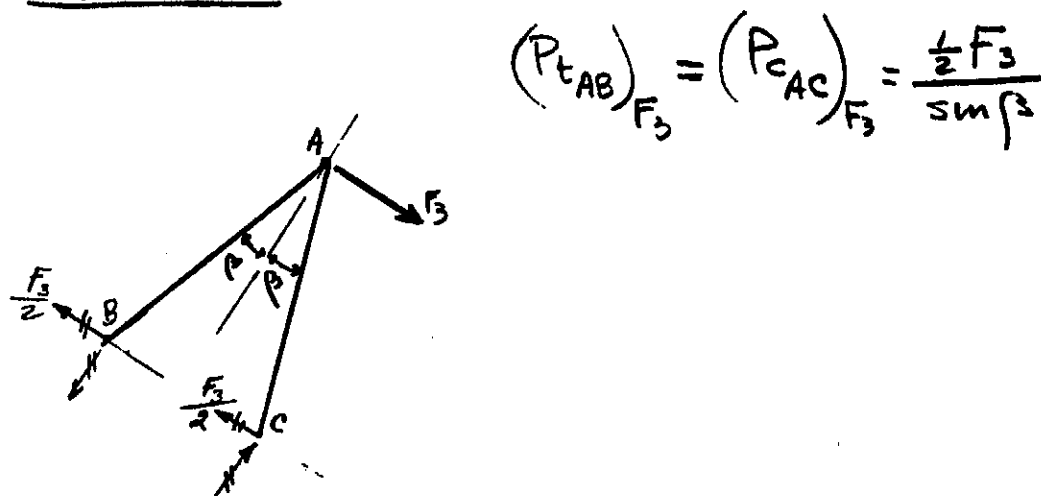
Prepared by: H. BASERGA	Date 6-10-71	LOCKHEED MISSILES & SPACE COMPANY A GROUP DIVISION OF LOCKHEED AIRCRAFT CO.	Report No.
Checked by:	Date	Title	SM No. 12-12-01-11-13 Date: 21 June 1971
Approved by:	Date		Report No.

F₁ LOAD



F₂ LOAD : $(P_{cAD})_{F_2} = F_2$, $(P_{AB})_{F_2} = (P_{AC})_{F_2} = 0$

F₃ LOAD



Prepared by: H. BASERGA	Date 6-10-71	LOCKHEED MISSILES & SPACE COM A GROUP DIVISION OF LOCKHEED AIRCRAFT CORP.	Report No. L2-12-01-M1-13
Checked by:	Date	Title	Date: 21 June 1971
Approved by:	Date		Report No.

CONFIG. 3

FRONT SUPPORT : Same as for CONFIG. II

WT = 15.5 LB

AFT SUPPORT : Rod $\overline{A-E}$ is removed.

LOADING COND. ① (MAX. AXIAL G's) is not critical.

LOADING COND. ②. Using notation and sign convention as per CONF. II the resulting loads normal & parallel to the reference plane are :

$$F_1 = 140000 \text{ LB}$$

$$F_2 = 11420 \text{ LB}$$

$$F_3 = 11925 \text{ LB}$$

F_1 LOAD.

$$(P_{\overline{AD}})_{F_1} = \frac{F_1}{\tan 40^\circ} = \frac{140^k}{.8391} = 166845 \text{ LB (comp.)}$$

$$(P_T)_{F_1} = \frac{F_1}{\sin 40^\circ} = \frac{140^k}{.6428} = 217797 \text{ LB}$$

$$P_{\overline{AB}} = P_{\overline{AC}} = \left(\frac{1}{2}\right) \frac{(P_T)_{F_1}}{\cos \beta} = \left(\frac{1}{2}\right) \frac{(217797)}{.9147} = 119054 \text{ LB}$$

F_2 LOAD.

$$P_{\overline{AB}} = P_{\overline{AC}} = 0, \quad P_{\overline{AD}} = F_2 = 11420 \text{ LB (comp.)}$$

Prepared by: <u>H. BASERGA</u>	Date <u>6-10-71</u>	LOCKHEED MISSILES & SPACE COMPANY A GROUP DIVISION OF LOCKHEED AIRCRAFT CORPORATION	Page <u>9</u>	Temp.	Perm.
Checked by:	Date	Title	EM No. L2-12-01-M1-13 Date: 21 June 1971		
Approved by:	Date		Report No.		

CONF. 3, (CONT'D.)

F_3 LOAD

$$P_{AD}=0, \quad P_{t_{AB}} = P_{c_{AC}} = \frac{\frac{1}{2} F_3}{\sin \beta} = \frac{\frac{1}{2} (11925)}{.4041} = 14755 \text{ LB}$$

SUMMARY OF MEMBER LOADS

$$\overline{AB}: 119054 + 14755 = +133809 \text{ LB LIM. (tension)}$$

$$\overline{AC}: 119054 - 14755 = +104299 \text{ LB LIM. (tension)}$$

$$\overline{AD}: -(166845 + 11420) = -178265 \text{ LB LIM. (comp.)}$$

SIZING TENSION RODS.

$$\overline{AB}: A = \frac{133809}{160000} (1.4) = 1.171 \text{ IN}^2 \quad \text{DIA} = 1.222 \text{ IN}$$

$$\overline{AC}: A = \frac{104299}{160000} (1.4) = .913 \text{ IN}^2 \quad \text{DIA} = 1.079 \text{ IN}$$

$$L_{\overline{AB}} = L_{\overline{AC}} = \left((92.00)^2 \left((\tan 30^\circ)^2 + \left(\frac{1}{\cos 40^\circ} \right)^2 \right) \right)^{1/2} = 131.327 \text{ IN}$$

$$\text{Weight of Rods} : (1.171 + .913)(131.327)(.16) = 43.78 \sim 44 \text{ LB}$$

$$\text{SIZING COMP. STRUT, } W_T = (2.236)(92.0)(.16) = 32.9 \sim 33 \text{ LB}$$

$$8.00 \text{ DIA} \times .090 \text{ WALL, } A = 2.236 \text{ IN}^2, \rho = 2.797, L/\rho = 32.89 \sim 33$$

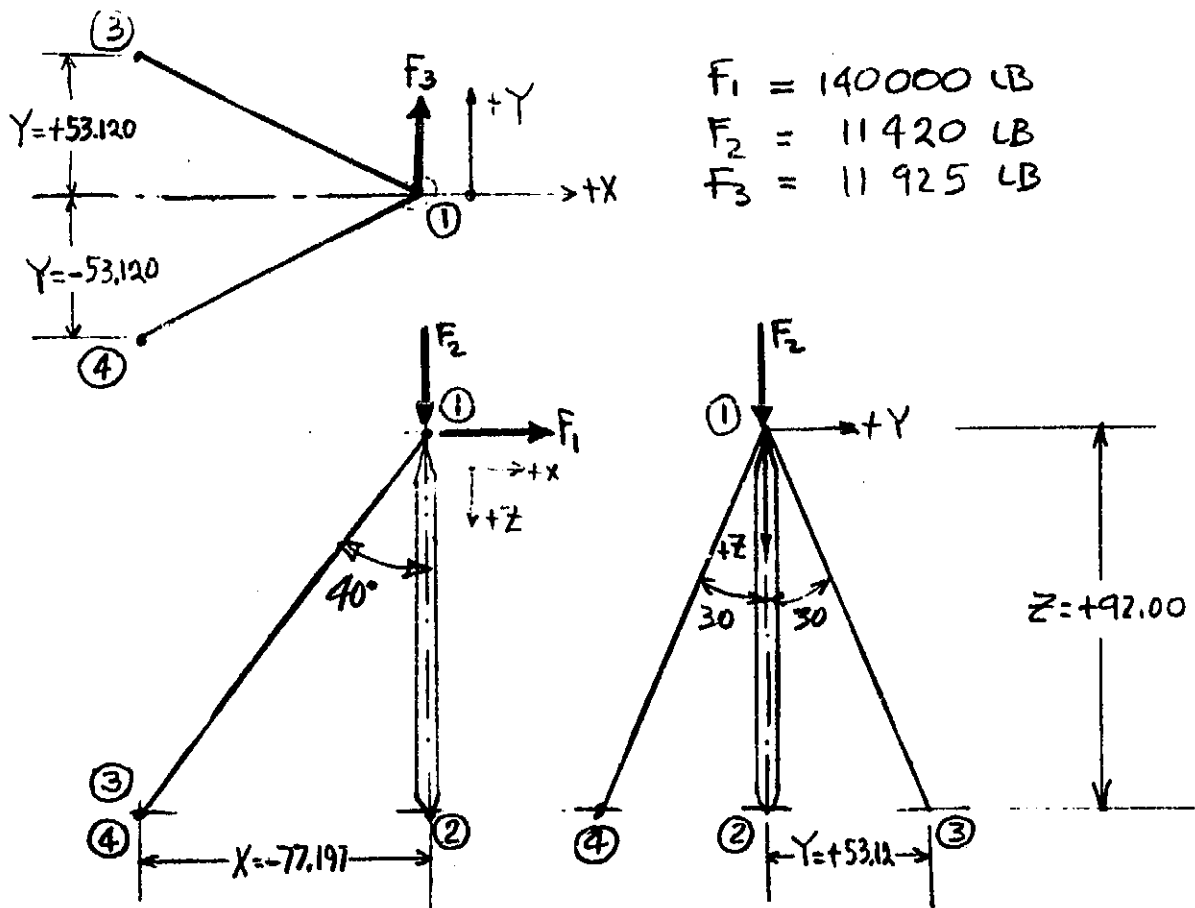
$$F_c = 130000 \text{ PSI} \quad \text{M.S.} = \frac{130000 \times 2.236}{(1.4)(178265)} - 1 = \underline{.16}$$

$$\text{TOTAL WT. (1st. ESTIMATE)} : 44 + 33 = 77 \text{ LB (Aft Supp.)}$$

$$\text{TOTAL WT. CONF. III (")} : 77 + 15.5 (\text{Front Supp.}) = \underline{\underline{\sim 93 \text{ LB}}}$$

Prepared by: H. BASERSA	Date 6-11-71	LOCKHEED MISSILES & SPACE COMPANY A GROUP DIVISION OF LOCKHEED AIRCRAFT CORPORATION	Page 2	Temp.	Perm.
Checked by:	Date		EM No. L2-12-01-M1-13 Date: 21 June 1971		
Approved by:	Date				

CHECKING EQUILIBRIUM



Member	X	Y	Z	L	$\cos \alpha$	$\cos \beta$	$\cos \gamma$
②	0	0	92.00	92.00	0	0	1.0
③	-77.197	53.120	92.00	131.327	-.5878	.4045	.7005
④	-77.197	-53.120	92.00	131.327	-.5878	-.4045	.7005

Direction Cos: $\cos \alpha = \frac{X}{L}$, $\cos \beta = \frac{Y}{L}$, $\cos \gamma = \frac{Z}{L}$

Prepared by: H. BASERSA	Date 6-11-71	LOCKHEED MISSILES & SPACE COMPANY A GROUP DIVISION OF LOCKHEED AIRCRAFT CORPORATION	Page 6	Temp.	Perm.
Checked by:	Date		EM No. L2-12-01-M-13 Date: 21 June 1971		
Approved by:	Date				

EQUILIBRIUM EQUATIONS

$$\Sigma P_x = ② \cos \alpha + ③ \cos \alpha + ④ \cos \alpha + F_x = 0$$

$$\Sigma P_y = ② \cos \beta + ③ \cos \beta + ④ \cos \beta + F_y = 0$$

$$\Sigma P_z = ② \cos \gamma + ③ \cos \gamma + ④ \cos \gamma + F_z = 0$$

Substituting direction cosines,

$$\Sigma P_x = ②(0) + ③(-.5878) + ④(-.5878) + F_x = 0$$

$$\Sigma P_y = ②(0) + ③(.4045) + ④(-.4045) + F_y = 0$$

$$\Sigma P_z = ②(1.0) + ③(.7005) + ④(.7005) + F_z = 0$$

Solving for the main determinant

$$D = \begin{vmatrix} 0 & -.5878 & -.5878 \\ 0 & .4045 & -.4045 \\ 1.0 & .7005 & .7005 \end{vmatrix} = \begin{vmatrix} 0 & -.5878 & -.5878 \\ 0 & .4045 & -.4045 \\ 1.0 & .7005 & .7005 \end{vmatrix} = (-)(1.0)(.4045)(-.5878) + (-)(.5878)(-.4045)(1.0) =$$

$$= -(-.23776) + (.23776) = .47552$$

AFT LOAD, $F_1 = -140,000$ LB : $\Sigma F_x = F_1$, $\Sigma F_y = 0$, $\Sigma F_z = 0$

$$② = \frac{\begin{vmatrix} F_1 & -.5878 & -.5878 \\ 0 & .4045 & -.4045 \\ 0 & .7005 & .7005 \end{vmatrix}}{.47552} = \frac{(-)(.7005)(-.4045)(F_1) + (F_1)(.4045)(.7005)}{.47552} =$$

$$= \frac{2F_1(.4045 \times .7005)}{.47552}$$

$$② = \frac{2(-140,000)(.4045 \times .7005)}{.47552} = -166,845 \text{ LB}$$

Prepared by: H. BASERGA	Date 6-11-71	LOCKHEED MISSILES & SPACE COMPANY A GROUP DIVISION OF LOCKHEED AIRCRAFT CO	Page 1	Temp. 	Perm.
Checked by:	Date	Title	EM No. L2-12-01-M1-13 Date: 21 June 1971		
Approved by:	Date		Report No.		

$$③ = \frac{\begin{vmatrix} 0 & F_1 & -.5878 \\ 0 & 0 & -.4045 \\ 1.0 & 0 & .7005 \end{vmatrix}}{.47552} = \frac{(+)(F_1)(-.4045)(1.0)}{.47552} = F_1(-.85064) = +119090 \text{ LB}$$

$$④ = \frac{\begin{vmatrix} 0 & -.5878 & F_1 \\ 0 & .4045 & 0 \\ 1.0 & .7005 & 0 \end{vmatrix}}{.47552} = \frac{(-)(1.0)(.4045)(F_1)}{.47552} = +119090 \text{ LB}$$

VERTICAL LOAD, $F_2 = 11420 \text{ LB}$; $\Sigma F_x = 0$, $F_y = 0$, $\Sigma F_z = F_2$

Load on members ③ & ④ is zero.

Checking member ②:

$$② = \frac{\begin{vmatrix} 0 & -.5878 & -.5878 \\ 0 & .4045 & -.4045 \\ F_2 & .7005 & .7005 \end{vmatrix}}{.47552} = \frac{(-)(F_2)(.4045)(-.5878) + (-.5878)(-.4045)(F_2)}{.47552}$$

$$= \frac{F_2(2 \times .4045 \times .5878)}{.47552} = F_2 \left(\frac{.47552}{.47552} \right) = F_2 = 11420 \text{ LB (comp.)}$$

SIDE LOAD, $F_3 = 11925 \text{ LB}$; $\Sigma F_x = 0$, $\Sigma F_y = F_3$, $\Sigma F_z = 0$

$$② = \frac{\begin{vmatrix} 0 & -.5878 & -.5878 \\ F_3 & .4045 & -.4045 \\ 0 & .7005 & .7005 \end{vmatrix}}{.47552} = \frac{(-)(.7005)(F_3)(-.5878) + (-.5878)(F_3)(.7005)}{.47552} = 0$$

Prepared by: H. BASERGA	Date 6-11-71	LOCKHEED MISSILES & SPACE COMPANY A GROUP DIVISION OF LOCKHEED AIRCRAFT CORPORATION	Page 5	Temp.	Form.
Checked by:	Date	Title	EM No. L2-12-01-M-13 Date: 21 June 1971		
Approved by:	Date				

$$③ = \frac{\begin{vmatrix} 0 & 0 & -5878 & 0 & 0 \\ 0 & F_3 & -4045 & 0 & F_3 \\ 1.0 & 0 & .7005 & 1.0 & 0 \end{vmatrix}}{.47552} = \frac{(-)(1.0)(F_3)(-5878)}{.47552} = F_3 \left(\frac{.5878}{.47552} \right) = +14741 \text{ LB}$$

$$④ = \frac{\begin{vmatrix} 0 & -5878 & 0 & 0 & -5878 \\ 0 & 4045 & F_3 & 0 & 4045 \\ 1.0 & .7005 & 0 & 1.0 & .7005 \end{vmatrix}}{.47552} = \frac{(+)(-5878)(F_3)(1.0)}{.47552} = F_3 \left(\frac{-5878}{.47552} \right) = -14741 \text{ LB}$$

CHECK FOR EQUILIBRIUM

$$\Sigma P_x = (0)(\cos \alpha) + (14741)(-5878) + (-14741)(-5878) + 0 = 0 \quad \text{OK}$$

$$\Sigma P_y = (0)(\cos \beta) + (14741)(4045) + (-14741)(-4045) - 11925 = .469 \approx 0 \quad \text{OK}$$

$$\Sigma P_z = (0)(\cos \gamma) + (14741)(.7005) + (-14741)(.7005) + 0 = 0 \quad \text{OK}$$

SUMMARY OF MEMBER LOADS

LOAD \ MEMBER	② = \overline{AD}	③ = \overline{AB}	④ = \overline{AC}
$F_1 = 140000 \text{ LB}$	-166845	+119090	+119090
$F_2 = 11420 \text{ LB}$	-11420	0	0
$F_3 = 11925 \text{ LB}$	0	+14741	-14741
LOAD ON MEMBER	-178265	+133831	+104349

CHECK OK

Prepared by: H. BASERGA	Date 6-11-71	LOCKHEED MISSILES & SPACE COMPANY <small>A GROUP DIVISION OF LOCKHEED AIRCRAFT CORPORATION</small>	Page 5	Temp.	Form.
Checked by:	Date	Title	EM No. L2-12-01-M1-13		
Approved by:	Date		Date: 21 June 1971		

CHECKING EQUILIBRIUM FOR F_1 LOAD (Ref pgs. b & c)

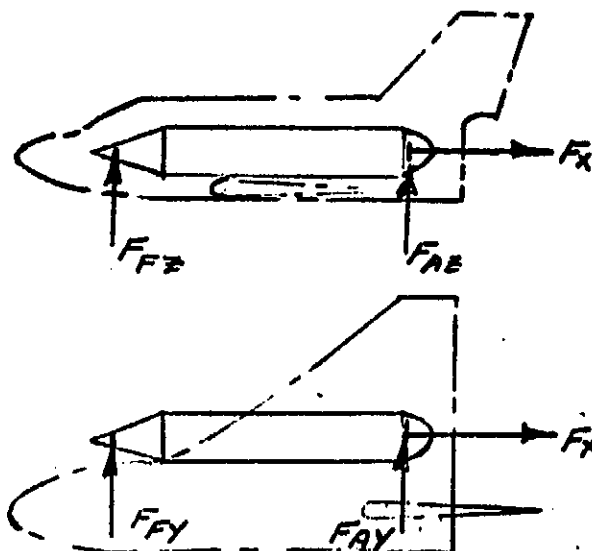
$$\Sigma P_x = (-166841)(0) + (+119090)(-.5878) + (+119090)(-.5878) + 140000 = -2.204 \approx 0$$

$$\Sigma P_y = (-166841)(0) + (+119090)(.4045) + (+119090)(-.4045) + 0 = 0$$

$$\Sigma P_z = (-166841)(1.0) + (+119090)(.7005) + (+119090)(.7005) + 0 = 4.09 \approx 0$$

Prepared by: DAR	Date: 15 JUNE	LOCKHEED MISSILES & SPACE COMPANY A GROUP DIVISION OF LOCKHEED AIRCRAFT CORPORATION	Page: 1/1	Temp:	Form:
Checked by:	Date:		EM No. L2-12-01-M1-13 Date: 21 JUNE 1971		
Approved by:	Date:				

G.A.C. DROP TANK REACTIONS



REACTIONS ON DROP TANKS

CONDITION	F_x	F_{Fz}	F_{Fy}	F_{Az}	F_{Ay}
MAX AXIAL g's	-216,000				
MAX + α g	-167,400	+20,000	-24,200	+32,600	-31,200
MAX - α g	-167,400	+13,520	-3,850	+10,780	-5,000
MAX + β g	-167,400	+17,100	-21,500	+22,100	-34,500
MAX - β g	-167,400	+15,050	-21,200	+19,500	-21,700

MAX $\pm \alpha, \beta$ g
INERTIA LOAD ONLY

$\pm 9,650$

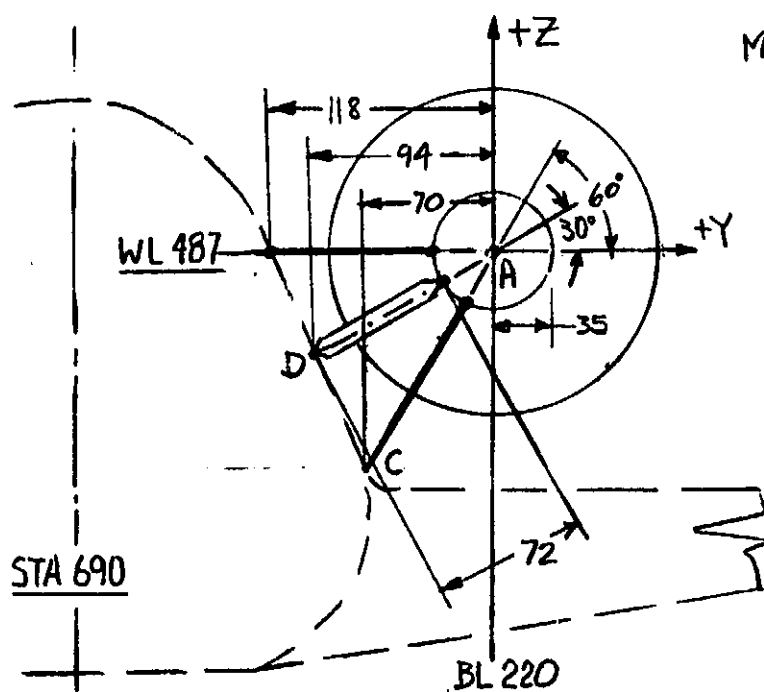
$\pm 19,150$

Prepared by: H. BASERGA	Date 6-15-71	LOCKHEED MISSILES & SPACE COMPANY A GROUP DIVISION OF LOCKHEED AIRCRAFT CORPORATION	Page	Temp.	Perm.
Checked by:	Date		EM No. L2-12-01-M1-13		
Approved by:	Date		Date: 21 June 1971		

CONFIGURATIONS 4 & E

FRONT SUPPORT (GAC TANK) GEOMETRY & LOADING

MAT'L. : Ti-6AL-4V



CONDITION	F _Z	F _Y
MAX AXIAL G's	0	0
MAX +αg	-20000	+24200
MAX -αg	-13520	+3850
MAX +βg	-17100	+21500
MAX -βg	-15050	+21200
MAX ±α/βg (INERTIA LOAD ONLY)	±9650	

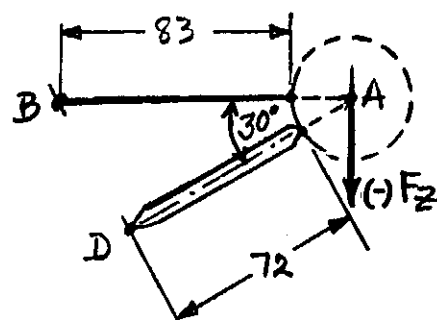
$$\overline{AB} = 118.00 \text{ IN}$$

$$\overline{AC} = 70 / \cos 60^\circ = 140 \text{ IN}$$

$$\overline{AD} = 94 / \cos 30^\circ = 108.545 \text{ IN}$$

$$\text{Column Length, } L = 72 \text{ IN}$$

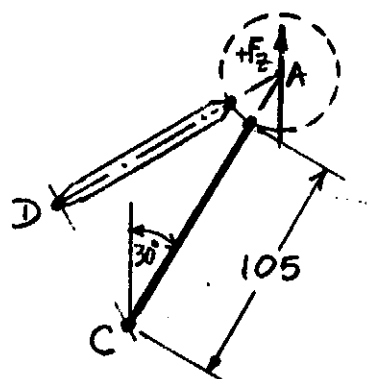
(-) F_Z LOAD : Only Rod \overline{AB} & Column \overline{AD} are considered.



$$P_{t\overline{AB}} = \frac{F_z}{\tan 30^\circ}$$

$$P_{c\overline{AD}} = \frac{F_z}{\sin 30^\circ}$$

(+) F_Z LOAD : Only Rod \overline{AC} & Column \overline{AD} are considered



$$P_{t\overline{AC}} = (+)F_z \frac{\cos 30^\circ}{\sin 30^\circ}$$

$$P_{c\overline{AD}} = (+)F_z \frac{\sin 30^\circ}{\sin 30^\circ} \text{ (NON CRITICAL)}$$

NA

Prepared by: H. BASERGA	Date	LOCKHEED MISSILES & SPACE COMPANY A GROUP DIVISION OF LOCKHEED AIRCRAFT CORPORATION	Page	Temp.	Perm.
Checked by:	Date		ITEM No. L2-12-01-M-13		
Approved by:	Date		Date: 21 June 1971		

GAC TR., FRONT SUPP., CONT'D.)

Rod AB, loading: $P_t = \frac{F_z}{\tan 30} + F_y$

CONDITION	$\frac{F_z}{.5774}$	F_y	P_t
MAX. (+) αq	34638	24200	58838
MAX. (-) αq	23415	3850	27265
MAX. (+) βq	29616	21500	51116
MAX. (-) βq	26065	21200	47265

CRITICAL COND.

$A_{req'd} = \frac{58838}{160000}(1.4) = .515 \text{ in}^2$, DIA = .810 IN, WT. = $83 \times .515 \times .16 = 7 \text{ LB}$

Member AD, loading: $P_{tAD} = \frac{F_z}{\sin 30^\circ}$, column length $L = 72 \text{ in}$

critical condition: MAX. (+) αq , $P_c = \frac{20000}{.5} = 40000 \text{ LB LIM.}$

6.00 DIA \times .040 WALL, $A = .755 \text{ in}^2$, $P = 2.120 \text{ in.}$, $L/p = 34$

From S.M. 83b. $F_c = 128000 \text{ PSI}$, $P_{col} = (.755)(128000) = 96640 \text{ LB ULT.}$

WT. $\sim 9 \text{ LB}$ M.S. = $\frac{96640}{(1.4)(40000)} - 1 = .725$

NOTE: A smaller tube could be used. Actuator dimensions, however, require a 6.00" DIA tube.

Rod AC: $P_{tAC} = (9650) \left(\frac{.866}{.5} \right) = 16714 \text{ LB LIM}$

$A_{req'd} = \frac{16714}{160000}(1.4) = .147 \text{ in}^2$, DIA = .433 IN

WT. = $72 \times .147 \times .16 = 1.69 \sim .2 \text{ LB}$

FRONT SUPPORT
TOTAL WT. = 18 LB

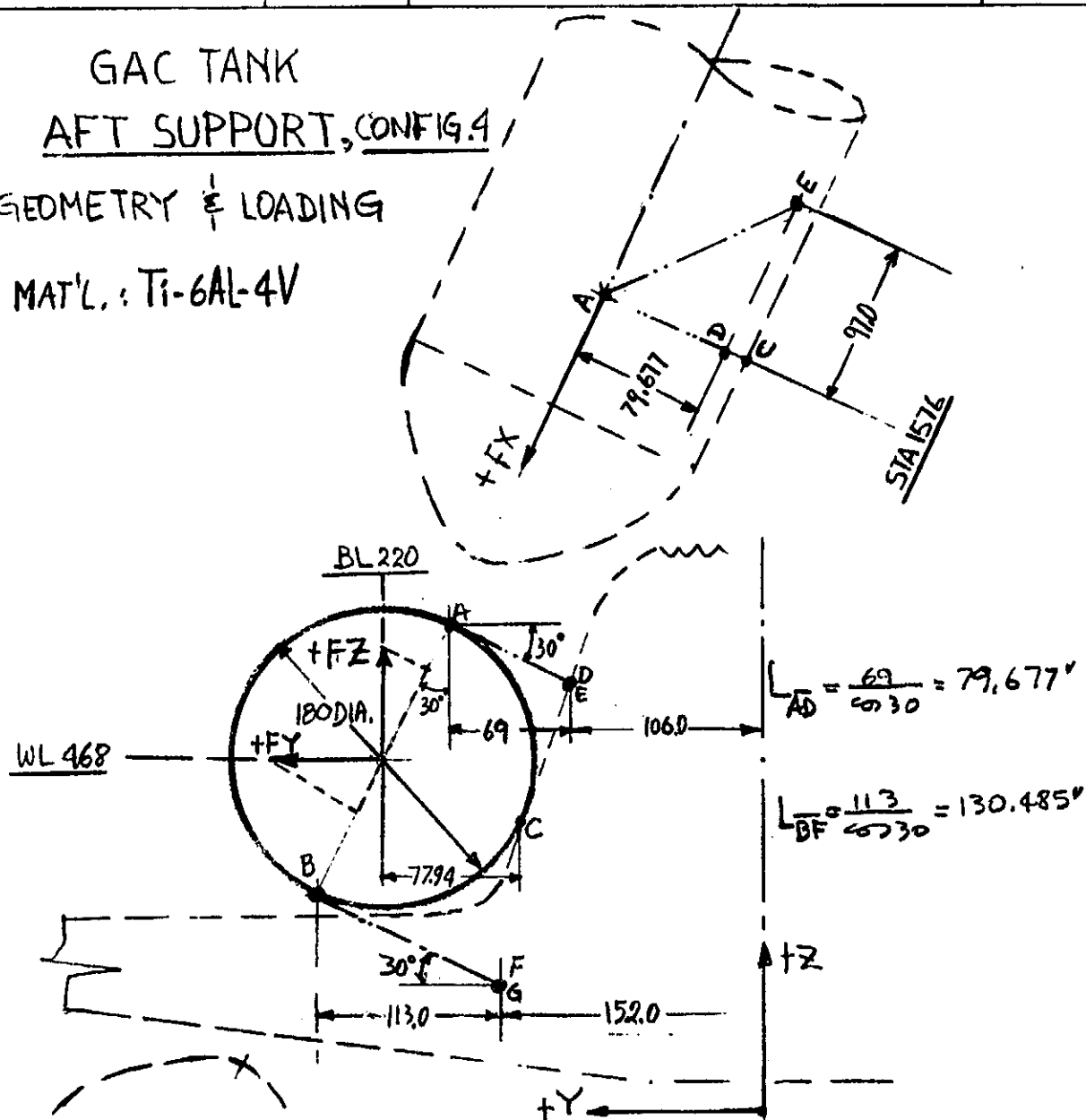
6AC 12111

Prepared by: H. BASERGA	Date 6-14-71	LOCKHEED MISSILES & SPACE CO A GROUP DIVISION OF LOCKHEED AIRCRAFT CO	EM No. L2-12-01-M1-13
Checked by:	Date	Title	Date: 21 June 1971
Approved by:	Date		Report No.

GAC TANK AFT SUPPORT, CONFIG. 4

GEOMETRY & LOADING

MAT'L: Ti-6AL-4V



FORCES AT SUPPORT STRUCT.

CONDITION	FX	FZ	FY
MAX. AXIAL G's	+216000	0	0
MAX. (+)αq	+167400	-32600	+31200
MAX. (-)αq	+167400	-10780	+5000
MAX. (+)βq	+167400	-22100	+34500
MAX. (-)βq	+167400	-19500	+21700

Prepared by: H. BASERGA	Date 6-16-71	LOCKHEED MISSILES & SPACE C A GROUP DIVISION OF LOCKHEED AIRCRAFT CO	EM No. 12-12-01-M1-13
Checked by:	Date	Title	Date: 21 June 1971
Approved by:	Date		Report No.

GAC TK. AFT SUPP. CONT'D.)

Solving $F_Y \neq F_Z$ into "P" directions (normal & parallel to reference line \overline{AB}) the center loading components at the aft support are: $P_X = F_X$,

$$P_Z = F_Z \sin 30^\circ + F_Y \cos 30^\circ, \quad P_Y = F_Z \cos 30^\circ - F_Y \sin 30^\circ$$

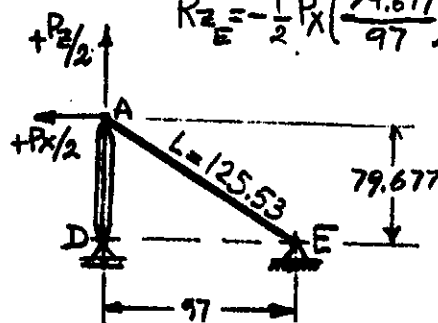
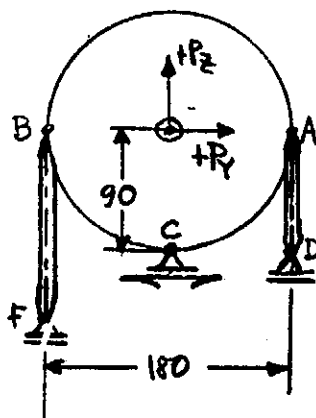
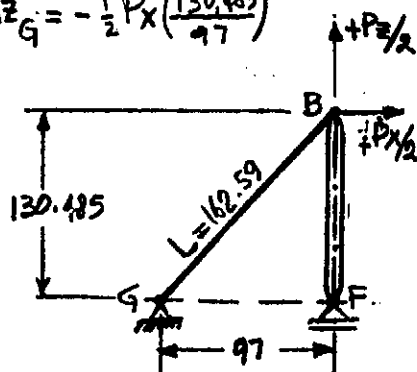
CONDITION	$F_Z \sin 30^\circ$	$F_Y \cos 30^\circ$	P_Z	$F_Z \cos 30^\circ$	$F_Y \sin 30^\circ$	P_Y
MAX (+) αq	-16300	27019.	10719	-28232	15600	-43832
MAX. (-) αq	-5390	4330	-1060	-933.6	2500	-11836
MAX. (+) βq	-11050	29877	18827	-19139	17250	-36389
MAX. (-) βq	-9750	18792	9042	-16887	10850	-37737

REACTIONS

$$R_{Z_D} = P_Y \left(\frac{90}{180} \right) - \frac{1}{2} P_Z + \frac{1}{2} P_X \left(\frac{79.677}{97} \right) \quad ; \quad R_{Z_F} = -P_Y \left(\frac{90}{180} \right) - \frac{1}{2} P_Z + \frac{1}{2} P_X \left(\frac{130.485}{97} \right)$$

$$R_{Z_G} = -\frac{1}{2} P_X \left(\frac{130.485}{97} \right)$$

$$R_{Z_E} = -\frac{1}{2} P_X \left(\frac{79.677}{97} \right)$$



6X TALK
⑤

Prepared by: H. BASERGA	Date: 6-16-71	LOCKHEED MISSILES & SPACE CO. A GROUP DIVISION OF LOCKHEED AIRCRAFT CO.	EM No. L2-12-01-M1-13
Checked by:	Date:	Title:	Date: 21 June 1971
Approved by:	Date:		Report No.

GAC TR. AFT SUPP. (CONT'D.)

1) REACTIONS @ C : Only Transverse reactions (parallel to P_y) are allowed

$$R_{x_c} = 0, \quad R_{z_c} = 0, \quad (R_{y_c})_{\text{Max}} = -(P_y)_{\text{Max}} = +43832 \text{ LB}$$

2) REACTIONS @ D : $R_{x_D} = 0, \quad R_{y_D} = 0$

CONDITION	$P_y(\frac{90}{180})$	$-(\frac{1}{2})P_z$	$(\frac{1}{2})P_x(\frac{79.677}{97})$	R_{z_D}
MAX. AXIAL G's	0	0	88712	<u>88712</u>
MAX. (+) αq	-21916	-5359.5	68752	41476.5
MAX. (-) αq	-5918	+530	68752	63364
MAX. (+) βq	-18194.5	-9413.5	68752	41144
MAX. (-) βq	-18868.5	-4521	68752	45362.5

($P_x = 216000$)
($P_x = 167400$)

3) REACTIONS @ E : $R_{y_E} = 0$

CONDITION	$R_{x_E} = -\frac{P_x}{2}$	$R_{z_E} = -\frac{P_x(79.677)}{2(97)}$
MAX. AXIAL G's	<u>-108000</u>	<u>-88712</u>
MAX. (+) αq	-83700	-68752
MAX. (+) βq	-83700	-68752

($P_x = 216000$)
($P_x = 167400$)

4) REACTIONS @ F : $R_{x_F} = 0, \quad R_{y_F} = 0$

CONDITION	$-P_y(\frac{90}{180})$	$-(\frac{1}{2})P_z$	$\frac{P_x(130.485)}{2(97)}$	R_{z_F}
MAX. AXIAL G's	0	0	145282	<u>145282</u>
MAX. (+) αq	21916	-5359.5	112593	129149.5
MAX. (-) αq	5918	+530	112593	119041
MAX. (+) βq	18194.5	-9413.5	112593	121374
MAX. (-) βq	18868.5	-4521	112593	126940.5

($P_x = 216000$)
($P_x = 167400$)

Prepared by: H. BASERGA	Date 6-16-71	LOCKHEED MISSILES & SPACE CO. A GROUP DIVISION OF LOCKHEED AIRCRAFT CORP.	Form EM No. L2-12-01-M1-13 Date: 21 June 1971
Checked by:	Date	Title	Report No.
Approved by:	Date		

SAC TR., AFT SUPP., CONT'D.)

REACTIONS @ G : $R_{Y_G} = 0$

CONDITION	$R_{X_G} = -\frac{P_X}{2}$	$R_{Z_G} = -\frac{P_X(130.485)}{2(97)}$
MAX. AXIAL G's	<u>-108000</u>	<u>-145282</u>
MAX. (\pm) αq	-83700	-112593
MAX. (\pm) βq	-83700	-112593

SUPPORT STRUCTURE STRESS ANALYSIS

COLUMN AD : Critical condition is MAX. AXIAL G's where

$$-P_c = (R_{Z_D})_{\text{Max.}} = 88712 \text{ LB LIM.}, L_{AD} = 79.677" (*)$$

6.5 DIA x .050 WALL, $A = 1.013 \text{ in}^2$, $p = 2.28 \text{ in}$, $L/p = 35$

From SM B3b, Fig. 30, $F_c = 125000 \text{ PSI}$, $P_{col} = 126625 \text{ LB ULT.}$

$$\text{M.S.} = \frac{126625}{(1.4)(88712)} - 1 = \underline{.019}$$

$$\text{WT.} = (1.013)(79.677)(.16) = 13 \text{ LB}$$

COLUMN BF : Critical condition is MAX. AXIAL G's where

$$-P_c = (R_{Z_F})_{\text{Max.}} = 145282 \text{ LB LIM.}, L_{BF} = 130.485" (*)$$

9.5 DIA x .070 WALL, $A = 2.073 \text{ in}^2$, $p = 3.33 \text{ in}$, $L/p = 39.2$

$$F_c = 104000 \text{ PSI}, \text{ M.S.} = \frac{(104000)(2.073)}{(1.4)(145282)} - 1 = \underline{.059}$$

$$\text{WT} = (2.073)(130.485)(.16) = 43.5 \text{ LB}$$

(*) Because of tank & orbiter connecting fittings actual column length is smaller. Hence above M.S. are conservative.

GAC TH. (7)

Prepared by: <u>H. BASERGA</u>	Date: <u>6-17-71</u>	LOCKHEED MISSILES & SPACE CO. A GROUP DIVISION OF LOCKHEED AIRCRAFT CO.	EM No. <u>L2-12-01-M1-13</u>
Checked by:	Date:	Title:	Date: <u>21 June 1971</u>
Approved by:	Date:		Report No.:

GAC TH., AFT SUPP., CONT'D.)

Rod AE: Critical Cond. is MAX. AXIAL G's where

$$R_{X_E} = -108000 \text{ LB}$$

$$R_{Z_E} = -88712 \text{ LB}$$

$$P_{t_{AE}} = ((108000)^2 + (88712)^2)^{1/2} = 139764 \text{ LB LIM}$$

$$A_{req'd} = \frac{139764}{160000} (1.4) = 1.223 \text{ IN}^2, \text{ DIA} = 1.25 \text{ IN}, \text{ WT} = 25 \text{ LB}$$

Rod BG: Critical Cond. is MAX. AXIAL G's where

$$R_{X_G} = -108000 \text{ LB}$$

$$R_{Z_G} = -145282 \text{ LB}$$

$$P_{t_{BG}} = ((108000)^2 + (145282)^2)^{1/2} = 181027 \text{ LB LIM}$$

$$A_{req'd} = \frac{181027}{160000} (1.4) = 1.584 \text{ IN}^2, \text{ DIA} = 1.42 \text{ IN}, \text{ WT} = 41.5$$

AFT SUPPORT TOTAL WT.: 118 LB

CONFIG. 4, FRONT & AFT SUPPORTS WT.: 18 + 118 = 136 LB

NOTE: Transverse support at "C" and member end fittings are not included in above WT.

Prepared by: <u>J. E. E. R. S. F.</u>	Date: <u>21 JUN 71</u>	LOCKHEED MISSILES & SPACE COMPANY A GROUP DIVISION OF LOCKHEED AIRCRAFT CORPORATION	Model
Checked by:	Date	Title	Report No. <u>EM</u> <u>L2-12-01-M1-B</u>
Approved by:	Date		

LOADING. Using MAX. AXIAL G's as critical condition the total load to be reacted at the Aft Support is $F_X = 216^K$. Without solving the redundant system, for preliminary member sizing and weight estimate purposes $F_X/2$ at each side is assumed.

$$P_{C_{\overline{AD}}} = (F_X/2) \tan \alpha = (108^K)(.8847) = 95,548 \text{ LB LIM } (L_{\overline{AD}} = 79.844")$$

$$P_{C_{\overline{BF}}} = (F_X/2) \tan \beta = (108^K)(1.4550) = 157,140 \text{ LB LIM } (L_{\overline{BF}} = 131.314")$$

$$P_{t_{\overline{AE}}} = \frac{(F_X/2)}{\cos \alpha} = \frac{(108^K)}{.7490} = 144,193 \text{ LB LIM } (L_{\overline{AE}} = 120.50")$$

$$P_{t_{\overline{BG}}} = \frac{(F_X/2)}{\cos \beta} = \frac{(108^K)}{.5664} = 190,678 \text{ LB LIM } (L_{\overline{BG}} = 159.34")$$

STRESS ANALYSIS

COLUMN \overline{AD} : $6.5 \times .060$ WALL, $A = 1.213 \text{ IN}^2$, $p = 2.277$, $WT = 15.5 \text{ LB}$

$$L/p = 35, \quad F_c = 125,000 \text{ PSI}, \quad P_{cd} = 151,625 \text{ LB ULT.}$$

$$M.S. = \frac{151,625}{(1.4)(95,548)} - 1 = \underline{.13}$$

COLUMN \overline{BF} : $9.5 \times .075$ WALL, $A = 2.220 \text{ IN}^2$, $p = 3.33$, $WT = 46.7 \text{ LB}$

$$L/p = 39.5, \quad F_c = 103,500 \text{ PSI}, \quad P_{cd} = 229,840 \text{ LB ULT.}$$

$$M.S. = \frac{229,840}{(1.4)(157,140)} - 1 = \underline{.044}$$

11. ZINSEKGA		21 JUN 71	ROCKET MISSILES & SPACE COMPANY A GROUP DIVISION OF LOCKHEED AIRCRAFT CORPORATION		1000
Checked by:	Date	Title	Model		
Approved by:	Date				Report No. EM L2-12-01-M-13

ROD AE : $A_{rod} = \frac{144193}{160000} (1.1) = 1.262 \text{ IN}^2$, DIA = 1.28", WT = 29.5 LB

ROD EG : $A_{rod} = \frac{190678}{160000} (1.1) = 1.670 \text{ IN}^2$, DIA = 1.458", WT = 42.6 LB

AFT SUPPORT TOTAL WT. = 129.3 ~ 130 LB

CONFIG. 5 STRUTS WT. = 18 + 130 = 148 LB

Total WT. above does not include rings at tank required to distribute the loading at attaching points.

Prepared by: S. A. CARTER	Date JUN 12 1971	LOCKHEED MISSILES & SPACE COM. A GROUP DIVISION OF LOCKHEED AIRCRAFT CORP.	RM No. L2-12-01-M1-13 Date: 21 June 1971
Checked by:	Date	Title	
Approved by:	Date		Report No.

GRUMMAN TANK - MEMBRANE SIZING

GEOMETRY	SA (in)	LOAD H. (in)	P _{H0} @ 3g	Wall Temp °F	F _w KSI	t _m (in)	Pull Empty	Wall Temp °F	F _w KSI	t _m (empty) (in)	Design t _m (in)
	719		25	+40°	64.0	.013	25	+40°	64.0	.013	.020
	753					.025		+26°	64.5	.025	.025
		0	25	-420°	94.5						
	92	92	25.7			.036		-48	66.2	.050	.050
						.035				.048	.048
	1176	342	27.5			.037		-153	68.0	.047	.047
	1436	602	29.5			.040		-263	72.0	.044	.044
	1686	852	31.3			.042		-369	85.6	.037	.042
						.021				.019	.025
	1750	916	31.8			.041		-396	90.0	.018	.025
						.043				.035	.035
	1801	967	32.2			.010		-418°	94.4	.010	.020
	1806	972	32.2	-420	94.5	.005	25	-420°	94.5	.005	.020

$$\text{TANK SURFACE AREA} = \frac{\pi}{4} \left[2(45.2)(33.5) + \left(\frac{173.4}{.966} \right) (43.55 + 90) + 2(760.5)(90) + 2(63.64)(90) \right. \\ \left. + \left(\frac{51.05}{.707} \right) (63.64 + 12.59) + 2(17.8)(5.2) \right]$$

$$= 3950 \text{ sq. ft.}$$

Prepared by: S. A. CARTER	Date JUN 12 1971	LOCKHEED MISSILES & SPACE CO A GROUP DIVISION OF LOCKHEED AIRCRAFT CORP	EM No. L2-12-01-M1-13
Checked by:	Date	Title	Date: 21 June 1971
Approved by:	Date		Report No.

GRUMMAN TANK (Cont'd)

TANK VOLUME

$$\text{FWD SPH CAP} = \frac{\pi}{3} \frac{(33.5)^2}{1728} [3(45.2) - 33.5] = 69.4 \text{ cf}$$

$$\text{CONE SEGMENT} = \frac{\pi}{3} \left(\frac{173.3}{1728} \right) [(43.55)^2 + (90)^2 + (43.55)(90)] = 1461.5 \text{ cf}$$

$$\text{CYLINDER SEGMENT} = \pi \left(\frac{760.5}{1728} \right) (90)^2 = 1199.3 \text{ cf}$$

$$\text{AFT SPH SEG} = \frac{1}{1728} \left[\frac{2\pi}{3} (90)^3 - \frac{\pi}{3} (26.4)^2 [3(90) - 26.4] \right] = 780.7 \text{ cf}$$

$$\text{AFT CONE SEG} = \frac{\pi}{3} \left(\frac{51}{1728} \right) [(63.6)^2 + (12.6)^2 + (63.6)(12.6)] = 154.7 \text{ cf}$$

$$\text{AFT SPH CAP} = \frac{\pi}{3} \frac{(5.2)^2}{1728} [3(17.8) - 5.2] = 0.8 \text{ cf}$$

$$\text{TOTAL VOLUME} = 13665.6 \text{ cf}$$

Using 3% ullage, = 510 cf, \therefore Propellant Volume = 13,255.6 cf

Cone ullage vol = 440.6 cf, \therefore Cone ullage height \approx 81"

TANK WEIGHTS

FORWARD CONE RICK RING

$$= 100$$

$$\text{FWD SPH CAP} = 2\pi (45.2)(33.5)(.020)(.102) = 19.4$$

$$\text{FWD CONE SEG} = \pi \left[\frac{173.4}{.962} \right] (43.55 + 90) \left[\frac{.030 + .025}{2} \right] (.102) = 288.1$$

$$\text{CYLINDER SEG} = 2\pi (760.5)(90) \left[\frac{.045 + .047 + .044 + .042}{4} \right] (.102) = 1984.9$$

$$\text{AFT SPH SEG} = 2\pi (63.64)(90)(.025)(.102) = 91.8$$

$$\text{AFT CONE SEG} = \pi \left[\frac{51.05}{.709} \right] (63.64 + 12.59) \left[\frac{.035 + .020}{2} \right] (.102) = 48.5$$

$$\text{AFT SPH CAP} = 2\pi (17.8)(5.2)(.020)(.102) = 1.2$$

$$\text{TOTAL TANK MEMBRANE WEIGHT} = 2534 \text{ lbs}$$

Prepared by: S. A. CARTER	Date JUN 12 1971	LOCKHEED MISSILES & SPACE CO. A GROUP DIVISION OF LOCKHEED AIRCRAFT CORP.	EM No. L2-12-01-M1-13 Date: 21 June 1971	
Checked by:	Date			Title
Approved by:	Date			

NAR TANK - MEMBRANE SIZING

GEOMETRY	STN	HEAD	P _{HD} @ 33 (PSIG)	Wall TEMP (°F)	F _{tu} (KSI)	t _m (in)	Pull Empty (PSIG)	Wall TEMP (°F)	F _{tu} (KSI)	t _m	Design t _m (in)
	0		25	+40	64.0	.013	25	+40	64.0	.013	.020
	84		25	+40	64.5	.025		+26	64.5	.025	.025
		0	25	-420	94.5						
	185	88	25.7			.034		-35	65.8	.047	.047
						.032				.045	.045
	396	299	27.2			.034		-120	67.4	.044	.044
	607	510	28.8			.036		-205	69.0	.043	.043
	818	721	30.4			.038		-290	74.4	.040	.040
	1028	931	31.9			.040		-375	86.3	.034	.040
						.020				.017	.025
	1088	991	32.4			.020		-399	90.7	.017	.025
						.040				.033	.040
	1135	1038	32.7			.010		-418	94.4	.008	.020
						.005				.004	.020
	1140	1043	32.7	-420	94.5	.005	25	-420	94.5	.004	.020

TANK SURFACE AREA = $\frac{\pi}{144} \left[2(45.2)(33.5) + \left(\frac{151}{.766} \right) [43.55 + 84] + 2(843.4)(84) + 2(59.39)(84) + \left(\frac{46.8}{.707} \right) (59.39 + 12.59) + 2(12.8)(5.2) \right]$

= 3918 sf.

Prepared by: S. A. CARTER	Date JUN 12 1971	LOCKHEED MISSILES & SPACE COM A GROUP DIVISION OF LOCKHEED AIRCRAFT CORP	EM No. L2-12-01-M1-13
Checked by:	Date		Date: 21 June 1971
Approved by:	Date		Report No.

NAR TANK (Cont'd)

TANK VOLUME

$$\text{FWD SPH CAP} = \frac{\pi}{3} \left(\frac{33.5}{1728} \right)^2 [3(45.2) - 33.5] = 69.4 \text{ cf}$$

$$\text{CONE SEGMENT} = \frac{\pi}{3} \left(\frac{151}{1728} \right) [(43.55)^2 + (84)^2 + (84)(43.55)] = 1,154.0 \text{ cf}$$

$$\text{CYLINDER SEGMENT} = \pi \left(\frac{843.4}{1728} \right) (84)^2 = 10,819.3 \text{ cf}$$

$$\text{AFT SPH SEGMENT} = \frac{1}{1728} \left[\frac{2\pi(84)^3}{3} - \frac{\pi}{3} (24.61)^2 [3(84) - 24.61] \right] = 634.9 \text{ cf}$$

$$\text{AFT CONE SEGMENT} = \frac{\pi}{3} \left(\frac{46.8}{1728} \right) [(59.39)^2 + (12.59)^2 + (59.39)(12.59)] = 125.7 \text{ cf}$$

$$\text{AFT SPH CAP} = \frac{\pi}{3} \left(\frac{5.2}{1728} \right)^2 [3(17.8) - 5.2] = 0.8 \text{ cf}$$

$$\text{TOTAL TANK VOLUME} = 12,804. \text{ cf}$$

Using 3% ULL = 384 cf, \therefore PROPELLANT VOL = 12,420 cf (53,083 lbs)

Cone ullage Vol = 314.6 cf \therefore Cone ullage height = 63.5"

TANK WEIGHT

$$\text{FWD CONE KICK RING} = 100$$

$$\text{FWD SPH CAP} = 2\pi(45.2)(33.5)(.020)(.102) = 19.4$$

$$\text{FWD CONE SEG} = \pi \left[\frac{151}{1728} \right] (43.55 + 84) \left[\frac{.047 + .025}{2} \right] (.102) = 230.0$$

$$\text{CYLINDER SEG} = 2\pi(843.4)(84) \left[\frac{.0451 + .044 + .043 + .040}{5} \right] (.102) = 1925.1$$

$$\text{AFT SPH SEG} = 2\pi(59.39)(84)(.025)(.102) = 79.9$$

$$\text{AFT CONE SEG} = \pi \left[\frac{46.8}{1728} \right] (59.39 + 12.59) \left[\frac{.040 + .020}{2} \right] (.102) = 45.8$$

$$\text{AFT SPH CAP} = 2\pi(17.8)(5.2)(.020)(.102) = 1.2$$

$$\text{TOTAL TANK MEMBRANE WEIGHT} = 2401 \text{ lbs}$$

ENGINEERING MEMORANDUM

TITLE: STRENGTH AND STABILITY ANALYSIS OF THE BASELINE DROPTANK THRUST CONE (ENG DWG SKT 100704)	EM NO: I2-12-01-M1-14 REF: I2-12-01-P1 DATE: 17 June 1971
AUTHORS: J. Skogh	APPROVAL: ENGINEERING <i>[Signature]</i> SYSTEM ENGRG <i>[Signature]</i>

PROBLEM

The Baseline Droptank is supported on a bolted flange at its aft end, as shown in Fig. 1. The concentrated support loads, although to some degree alleviated by the internal pressure, create relatively high compressive stresses which may cause the shell to buckle or collapse elastically before the ultimate strength of the material is reached. The geometry and loadings are complex, requiring a relatively sophisticated analysis.

RESULTS

Three different analyses were performed, using the computer code BOSOR (Ref. 1):

1. Linear, nonsymmetric stress analysis
2. Linear buckling analysis for nonsymmetric loading
3. Nonlinear, axisymmetric collapse analysis

It was found that the shell will buckle elastically at 1.33 times the ultimate load according to the classical buckling theory. Accounting for a conservative practical "knock-down" factor, this figure is reduced to about 0.83; therefore, it seems prudent to increase the shell thickness some 10 percent, which would increase the buckling load to 1.00+ times the ultimate load.

ANALYSIS

The analyses described here were all performed on the configuration shown in Fig. 1, with the conical part tapering from 0.150 inch at the meridional Station S = 15.38 to 0.050 inch at Station S = 80.8. Further details of the configuration may be gained from Drawing SKT 100704. The loading consists of an internal pressure, and axial and lateral concentrated loads introduced via a stiff bracket into the aft flange, as indicated in Fig. 1.

1. Linear, Nonsymmetric Stress Analysis. Stresses resulting from the loads shown in Fig. 1 were calculated. Figure 2 shows the meridional stresses for the "worst" circumferential station (i.e., in the plane of F_L). Note the rather small stresses, compared to the material ultimate strength, which is 94,500 psi. The strength-critical point occurs at the end of the transition region, at Station 15.38. At this point the meridional stress is 43,750 psi compression on the inside surface. Adding the hoop component, the effective stress

$$\sigma = \sqrt{\sigma_1^2 + \sigma_2^2 - \sigma_1 \sigma_2} \quad (1)$$

becomes

$$\sigma = 43,280 \text{ psi}$$

which results in a margin of safety of 1.18.

All other points in the shell have considerably lower stress.

2. Linear Buckling Analysis for Nonsymmetric Loading. The buckling analysis was made with the prebuckled state obtained from the linear analysis. Figure 3 shows a plot of the minimum eigenvalues obtained from the BOSOR analysis for various values of the number of circumferential waves. The critical load condition is obtained by multiplying the eigenvalue λ by the nominal load condition given in Fig. 1

$$\begin{bmatrix} P \\ F_X \\ F_L \end{bmatrix}_{\text{crit}} = \lambda \begin{bmatrix} p^* \\ F_X^* \\ F_L^* \end{bmatrix} \quad (2)$$

where the * denotes the nominal (in this case ultimate) load.

Thus the relative sizes of the loads are retained throughout the analysis. Particularly, the internal pressure has the value λp^* in the analysis. It is, however, desired to obtain a solution for a constant internal pressure of 28 psi. To do this, three different values of p^* were used, as shown in Fig. 3. The eigenvalues are relatively unaffected by the wave number. Figure 4 was prepared to facilitate interpolation. Note that there is a linear relationship, in the analysed region, between the $1/\lambda$ and $1/\lambda p^*$. This relationship may be expressed as

$$\lambda = \frac{2.75}{1 + \frac{30}{\lambda p^*}} \quad (3)$$

The quantity S_p in Fig. 4 is the meridional location of the maximum amplitude modal deformation, as indicated in Fig. 5. Note that, as the pressure is increased, the location of the buckles (critical region) moves toward the narrow end of the cone. The mode shapes and forces for one of the investigated configurations are shown in Figs. 5 through 7.

Equation (3) was used to construct the design graph in Fig. 8. The BOSOR analysis gives for $p = 28$ psi an eigenvalue of $\lambda = 1.33$. However, as is well known, the theory of buckling often predicts failure at higher loads than those encountered in practice, and so-called knock-down factors are employed to correct this discrepancy. In this case, the information contained in Ref. 2 (the pertinent part of which is shown in Fig. 9 here) was used to determine the knock-down factor shown in Fig. 8. With this factor the eigenvalue for $p = 28$ psi is reduced to 0.83 at the 99 percent probability level, giving the following values for the estimated buckling load:

$$\text{Buckle Load} \quad \left\{ \begin{array}{l} p = 28 \text{ psi} \\ F_X = 0.83 \times 196,000 = 163,000 \text{ lb} \\ F_L = 0.83 \times 23,000 = 19,000 \text{ lb} \end{array} \right.$$

The (classical) buckling load is proportional to $(t/R)^2$. Therefore, by increasing the thickness by a factor $\sqrt{1/0.85} = 1.09$ the buckling load will be brought up to the required level. This increase in thickness need only be made in the upper half ($S = 40$ to 80) of the cone.

3. Nonlinear Axisymmetric Collapse Analysis. In order to check for the possibility of large deformation collapse (as a Belleville washer) the tank was analyzed for nonlinear response. This type of analysis can only be made for axisymmetric loads, so the lateral component F_L was translated into an equivalent axial load.* The results of this analysis are shown in Fig. 10. It is found that the nonlinear deformations are only slightly larger than the linear deformations, and thus the possibility of axisymmetric collapse is remote.

REFERENCES

1. David Bushnell: "Stress, Stability and Vibration of Complex Shells of Revolution: Analysis and User's Manual for BOSOR3," SAMSO TR-69-375, 6 Sep 1969.
2. B. O. Almroth, A. B. Burns, E. V. Pittner: "Design Criteria for Axially Loaded Cylindrical Shells," J. Spacecraft, Vol. 7, No. 6, June 1970, pp. 714-720.

*This amounts to a 20 percent increase of the axial load.

Space Shuttle Project

ULT LOADS :

$$F_x^{\pi} = 196,000 \text{ LB}$$
$$F_L^* = 23,000 \text{ LB}$$

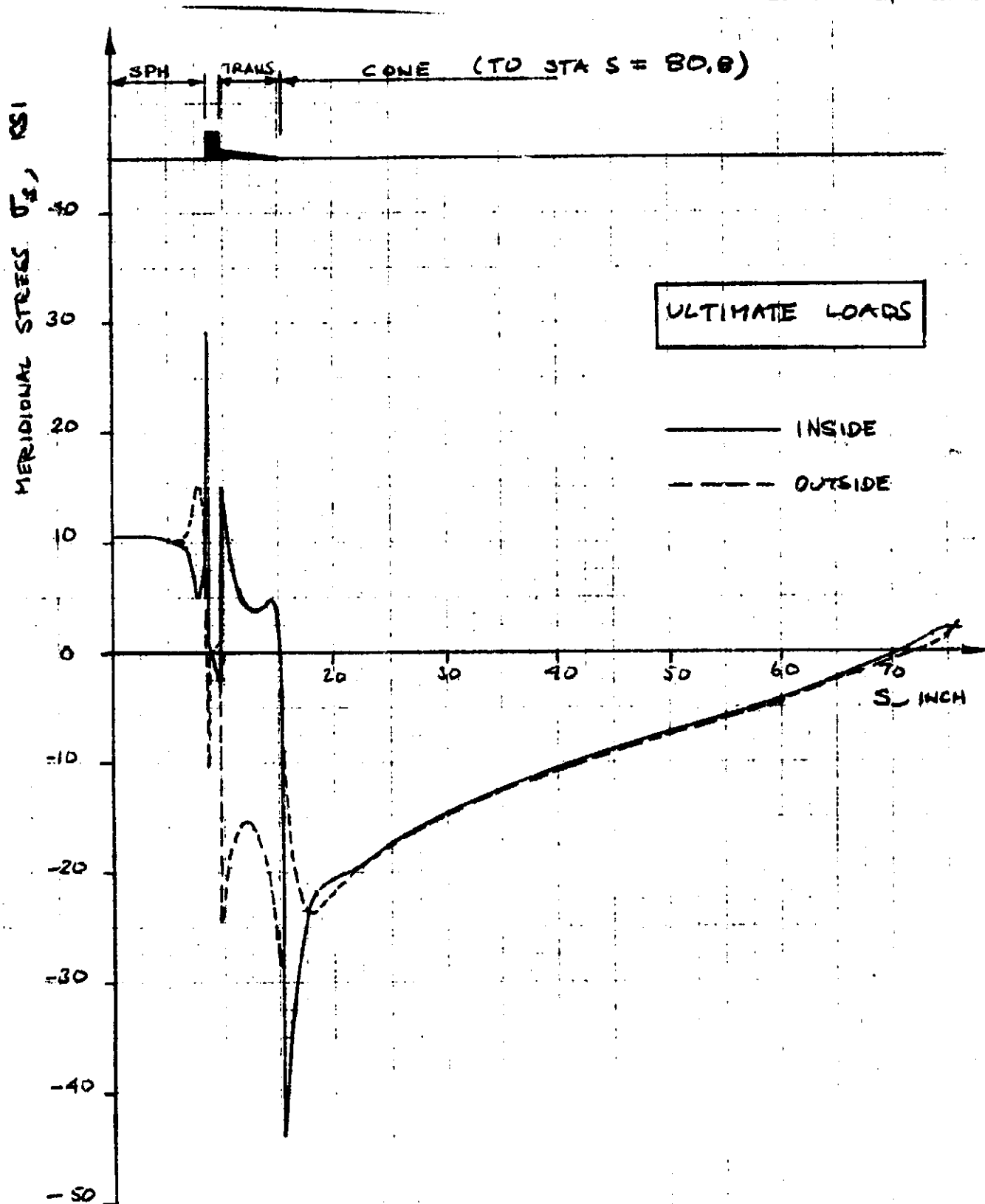



Fig. 2 Meridional Stress, Baseline Droptank

EM NO: 12-12-01-M1-14
DATE: 17 June 1971

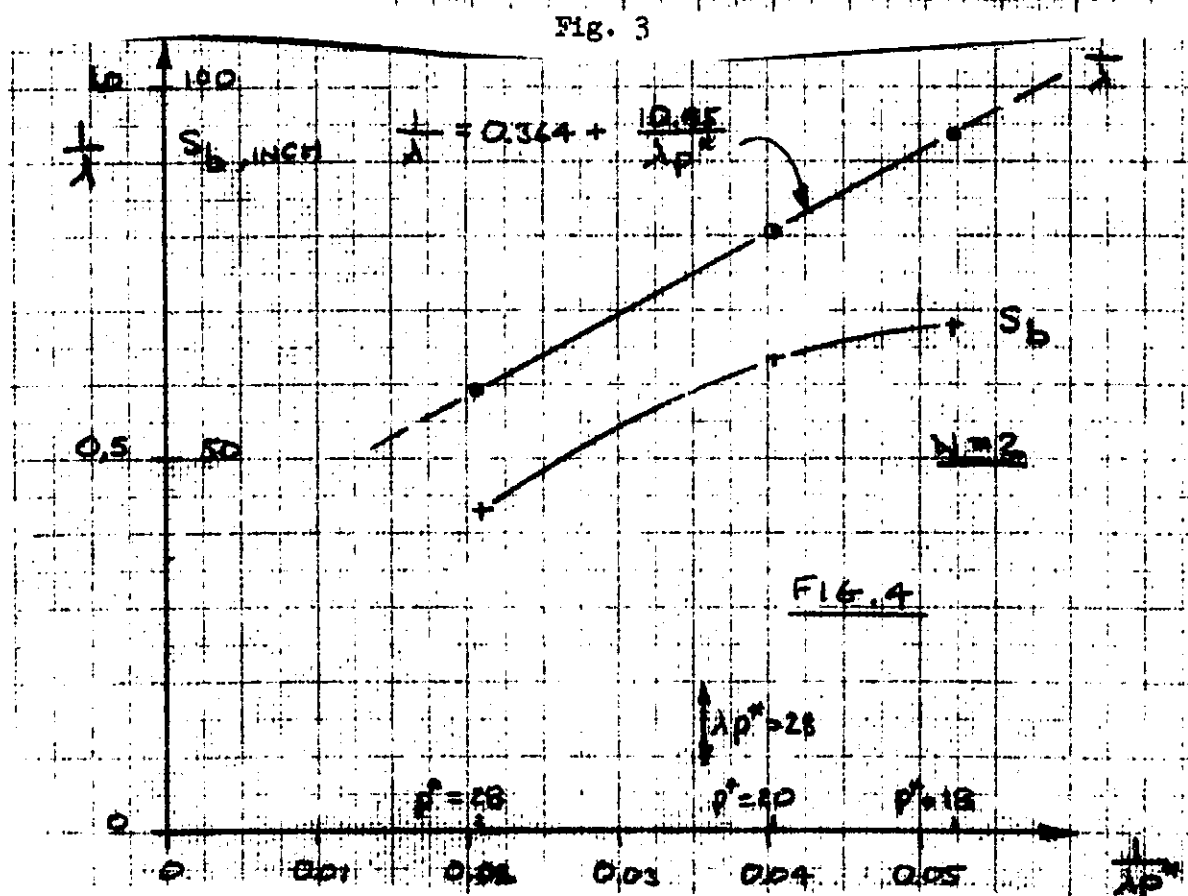
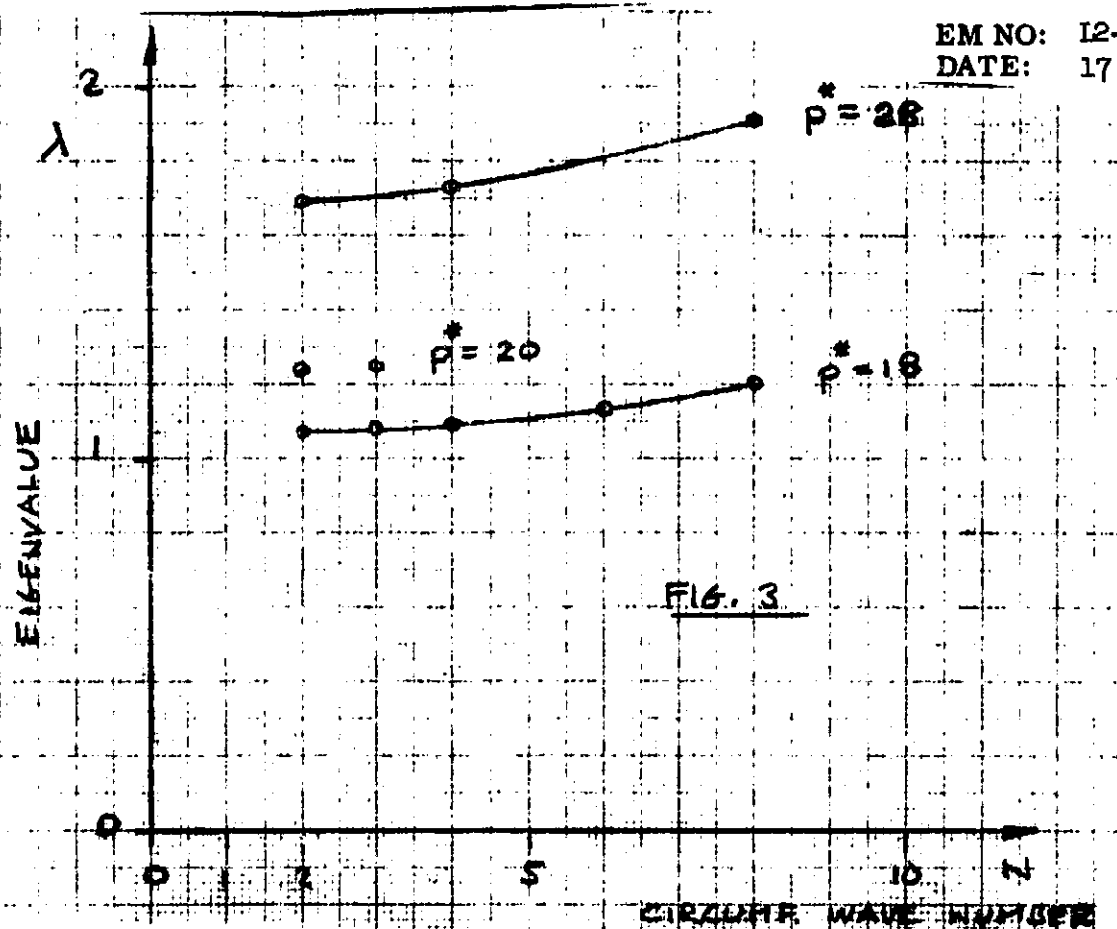


Fig. 4

BUCKLING OF LH2 TANK. $P_{INT} = 20 * EIGENVALUE$.

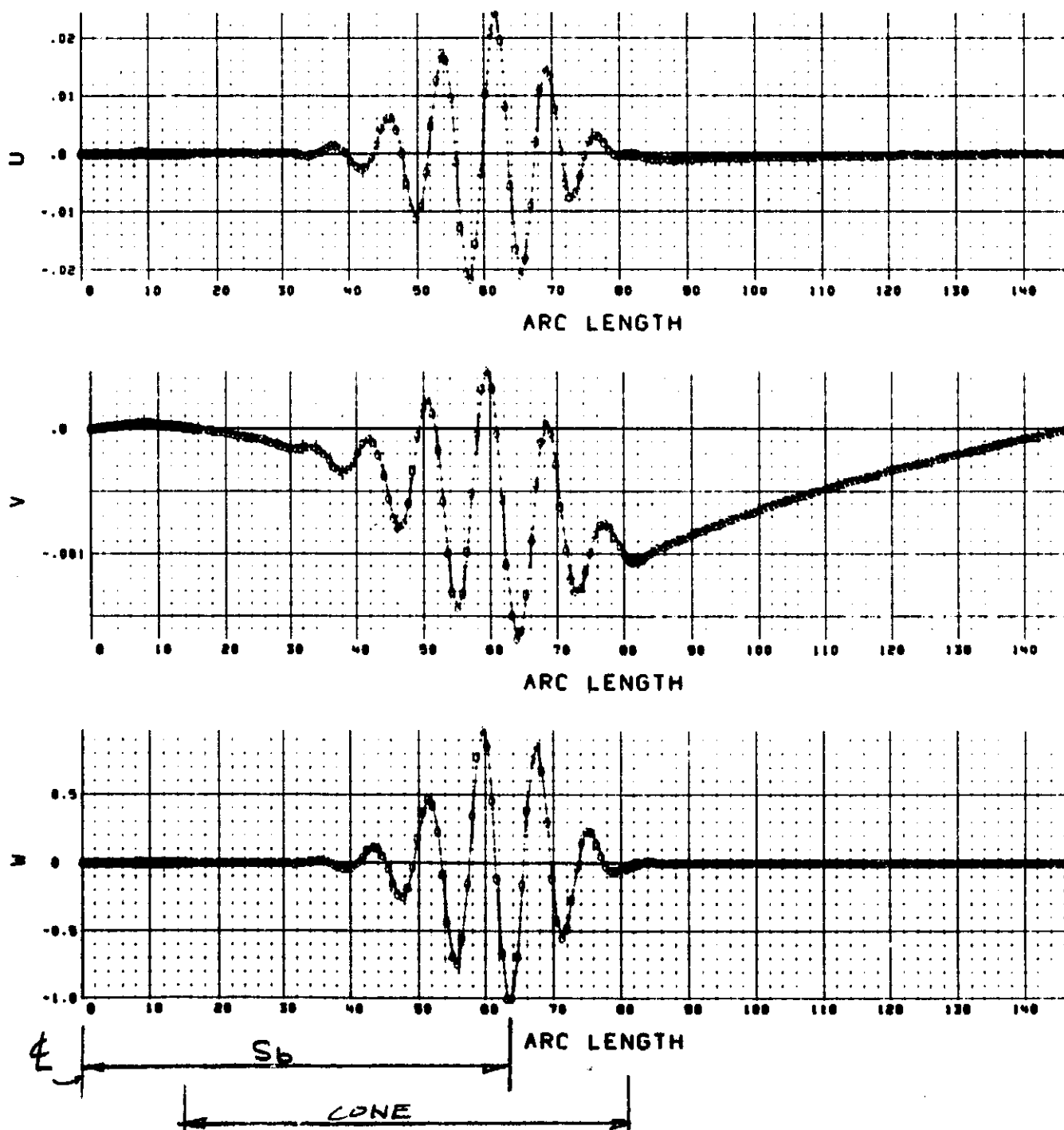


Fig. 5 Mode Shape for $N = 2$ Circumferential Waves, $p^* = 20$ psi

BUCKLING OF LH2 TANK. PINT=20*EIGENVALUE.

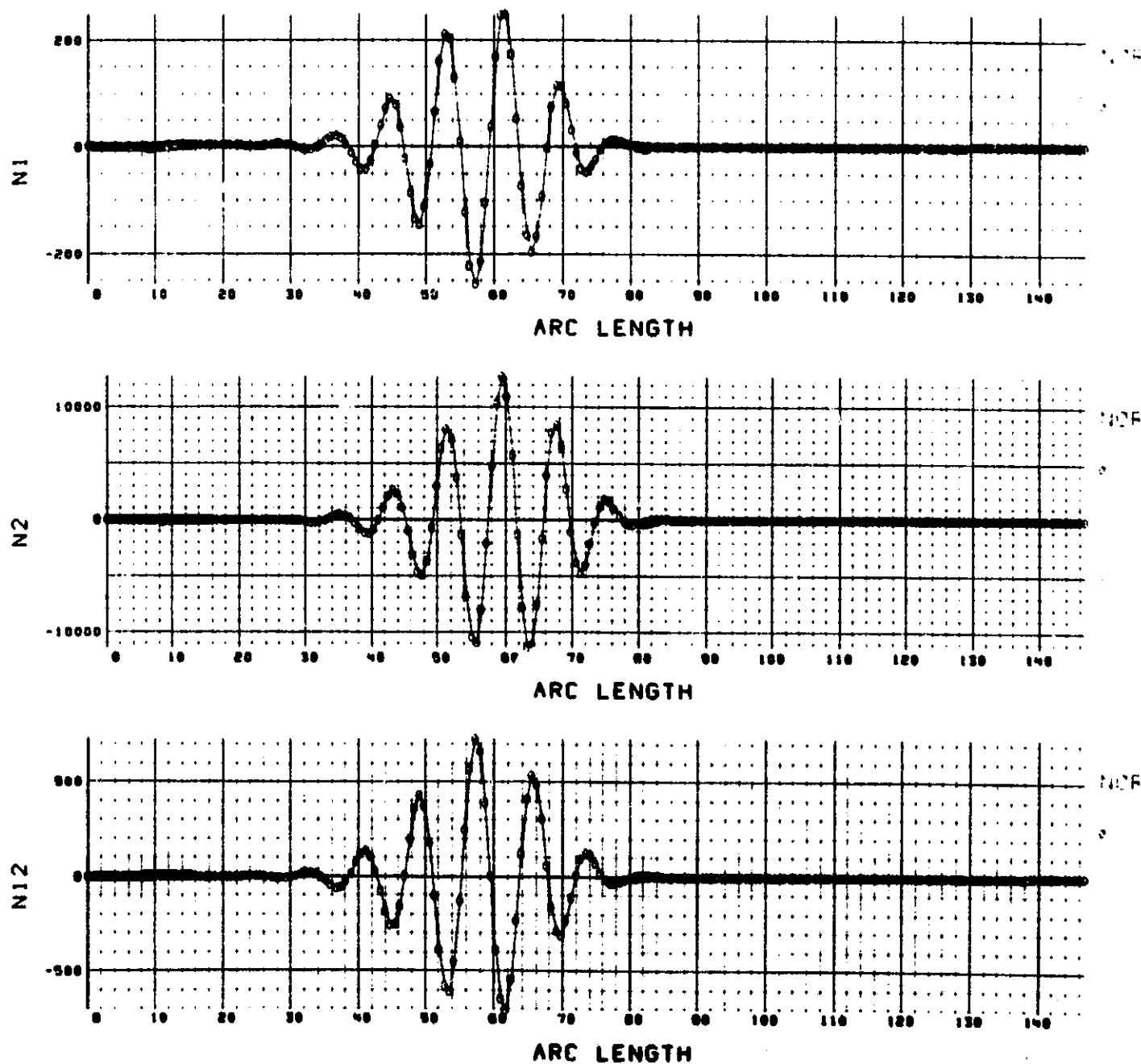


Fig. 6 Modal Forces, $N = 2$, $p^* = 20$

BUCKLING OF LH2 TANK. PINT=20*EIGENVALUE.

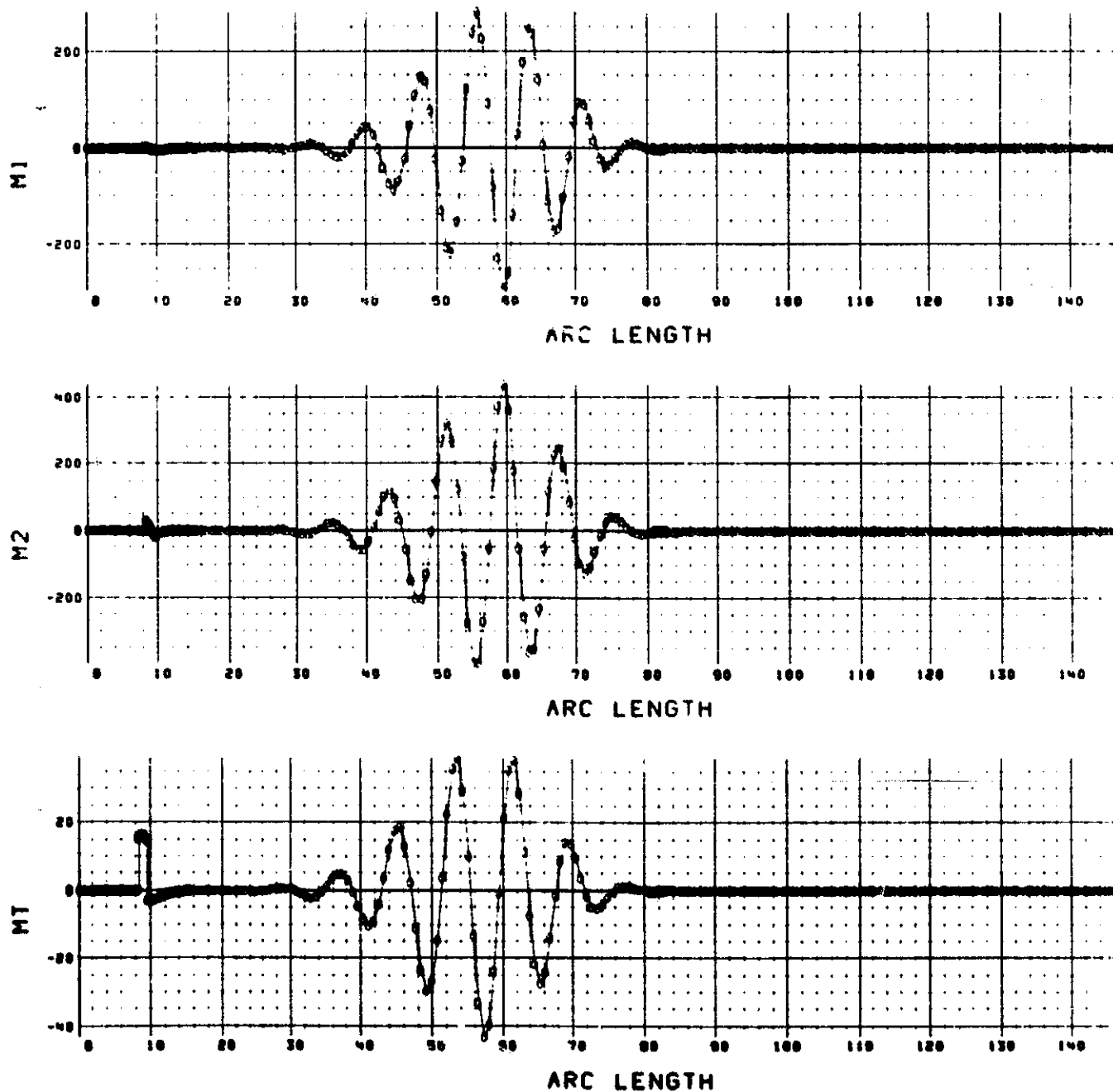


Fig. 7 Modal Forces, $N = 2$, $p^* = 20$

EM NO: 12-12-01-M1-14
DATE: 17 June 1971

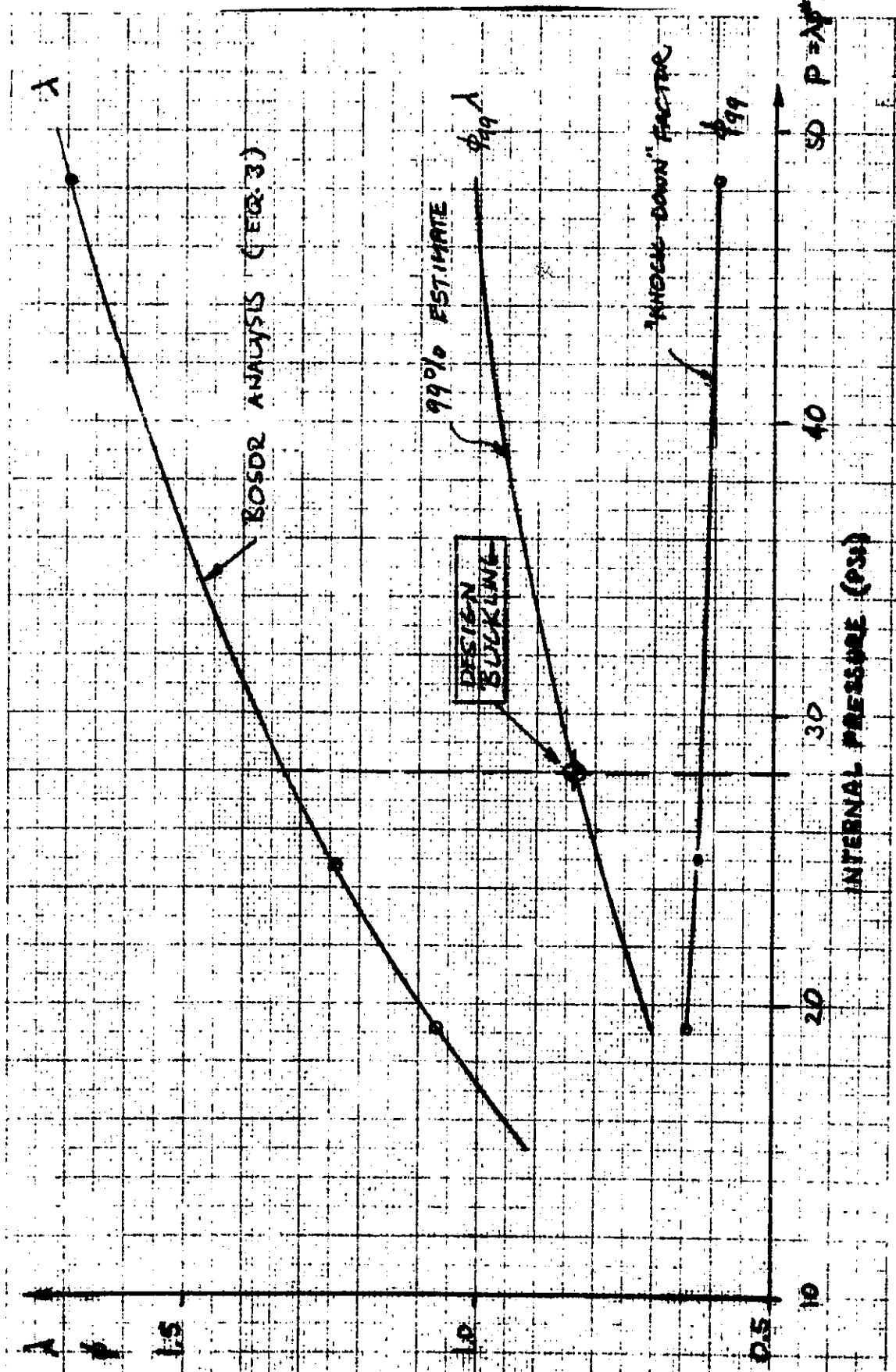
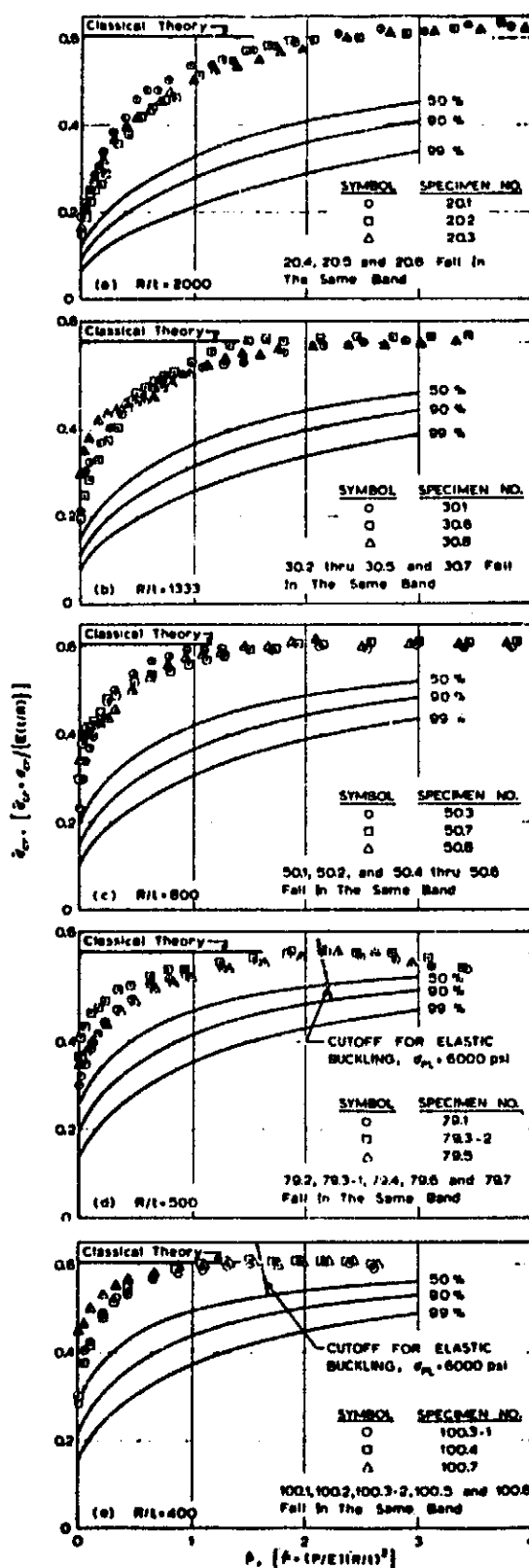


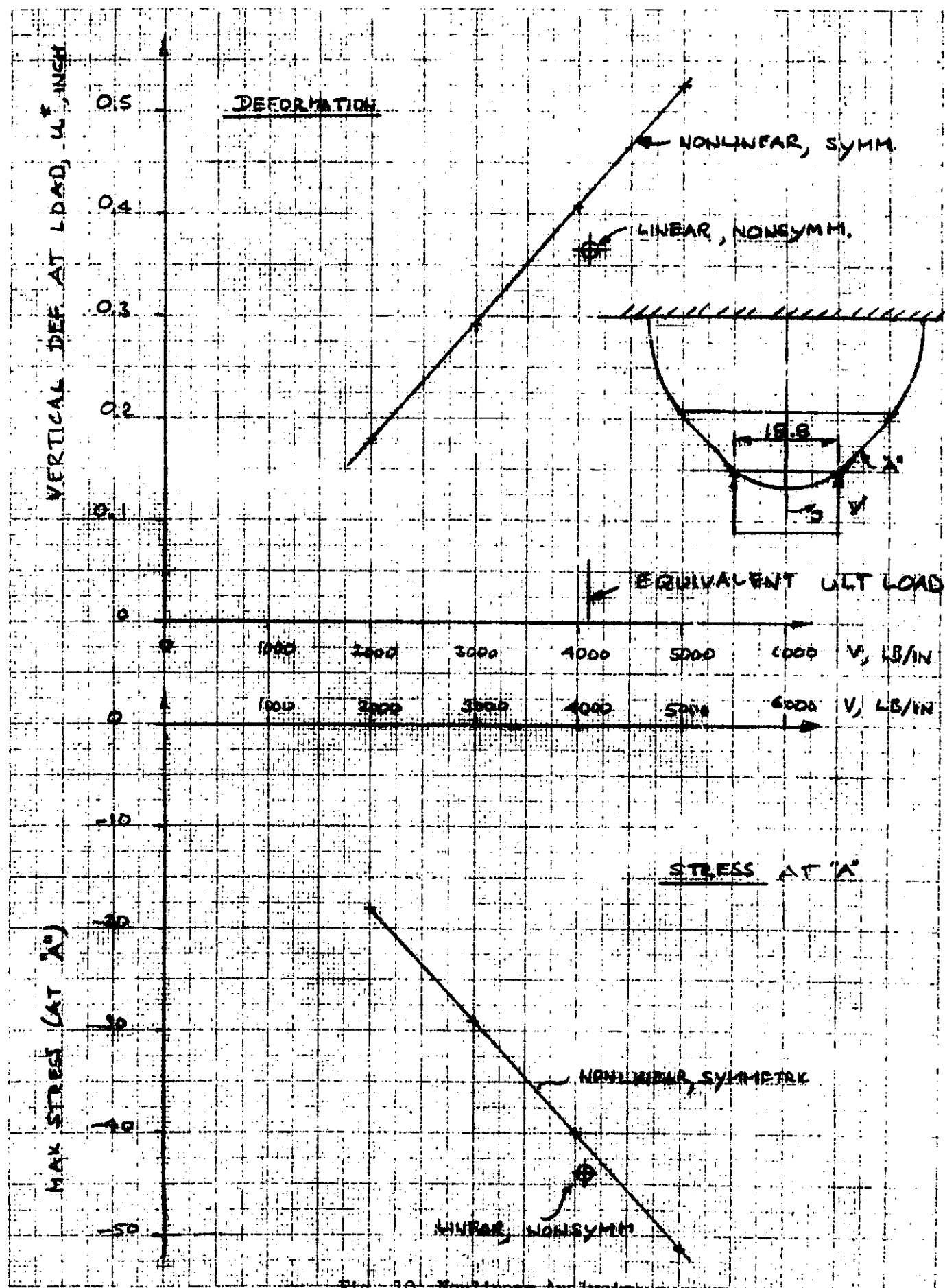
Fig. 8 LH₂ Tank Buckling Design Plot

EM NO: 12-12-01-M1-14
DATE: 17 June 1971



RANGE FOR LH₂ TANK

Fig. 9 Design Recommendations for Cylinders With Internal Pressure and Axial Compressive Loads (Ref. 2)



ENGINEERING MEMORANDUM

TITLE: NONLINEAR STRESS ANALYSIS OF LONGITUDINAL STRAP JOINTS IN WELDBOND LH ₂ DROPTANK	EM NO: I2-12-01-M1-15 REF: I2-12-01-P1 DATE: 17 June 1971
AUTHORS: J. Skogh	APPROVAL: ENGINEERING <i>[Signature]</i> SYSTEM ENGRG <i>[Signature]</i>

PROBLEM

The longitudinal joints in the spotbonded version of the baseline LH₂ droptank (Conf. B) (Fig. 1) are the critical feature of this design concept.² A realistic stress analysis, including the (as shown) very significant nonlinear effects in the joints is required. A complication is the fact that the problem is two-dimensional: the tank cross-section is not rotationally symmetric.

RESULTS

Nonlinear stress analysis results for three different configurations (variations in D and t, Fig. 1) have been obtained. It was found that the nonlinear effect is very large: a linear analysis would have underestimated the ultimate pressure capability of the LH₂ tank by more than 300 percent.

ANALYSIS

1. Elementary Analysis - An elementary linear uniaxial analysis gives the following maximum stresses for a joint where the gap $D \rightarrow 0$ (see Fig. 1):

$$\text{In shell:} \quad \sigma_{sh} = 4 \frac{N}{t_1} \quad (1)$$

$$\text{In strap:} \quad \sigma_{st} = 7 \frac{N}{t_2} \quad (2)$$

where

N = applied load, lb/in.

t₁ = shell thickness

t₂ = strap thickness

The membrane stress in the shell is

$$\sigma_o = \frac{N}{t_1} \quad (3)$$

Thus, the stress concentration in the strap is

$$K = 7 \frac{t_1}{t_2} \quad (4)$$

EM NO: 12-12-01-M1-15

DATE: 17 June 1971

The condition for equal maximum stress in the shell and strap is obtained by equating Eq. (1) to Eq. (2):

$$t_2 = 1.75 t_1 (\sigma_{sh} = \sigma_{st}) \quad (5)$$

2. Nonlinear Analysis - As the internal pressure is increased nonlinear elastic effects takes place: the structure strives to minimize the discontinuity by taking on a more advantageous shape. Since in the longitudinal strap joint deformations can take place inextensionally one would expect that the nonlinear effects are important. This expectation is fully borne out by the analysis results shown in Fig. 2 for a 0.05-inch thick strap. The lowest pressure used in the analysis was 0.01 psi, a pressure which may be considered too low to cause any nonlinear effects. For this pressure a stress concentration factor of 4.99 was realized. (This compares rather well with the factor 5.46 given by Eq. (4); the difference may be attributed to the finite gap D used in Fig. 2.) However, as the pressure is increased the stress concentration falls off rapidly, becoming 2.00 at about 10 psi pressure, and 1.65 at about 30 psi pressure.

The analysis on which Fig. 2 is based was done with the aid of the finite-difference computer program BOSOR (Ref. 1). While strictly speaking this program is applicable only to shells of revolution, an analytical "trick" makes it possible to apply it to noncircular cylinders. This is done by treating the cylinder as a toroidal shell with a huge radius - a shell that resembles a bicycle tire. The length of the cylinder is fixed by the wave number chosen for harmonic variation of stresses and displacements around the large circumference of the torus.* The analysis can therefore only be made for simply supported cylinders with arbitrary cross section shape and thickness distribution. The "axis" of the cylinder analyzed in this manner corresponds to the axis of centers of meridional curvature of the torus, and the circumference of the cylinder corresponds to the meridional direction of the torus. Thus, the analysis "trick" amounts to a reversal of the independent variables s and θ . Figure 3 shows the principle of the modeling, and Fig. 4 shows the actual dimensions used in the analysis. That this model is a good representation of the straight cylinder is shown by the fact that the maximum stresses at the inside joint (A in Fig. 4) agree to three figures with those at the outside joint (B). Better agreement could be had by increasing the radius R to, say, 10^5 inch, but the increased accuracy would not justify the increased run time.

A complete set of plotted output data is contained in Fig. 5. The terms "hoop" and "axial" refer to directions in the cylinder. By "equivalent stress" is meant the von Mises stress:

$$\sigma = \sqrt{\sigma_1^2 + \sigma_2^2 - \sigma_1 \sigma_2} \quad (6)$$

*In the cases described here the wave number was zero, making the cylinder length infinite. A finite length cylinder must be treated as a linear problem with this "trick." One does not get something for nothing.

EM NO: 12-12-01-M1-15

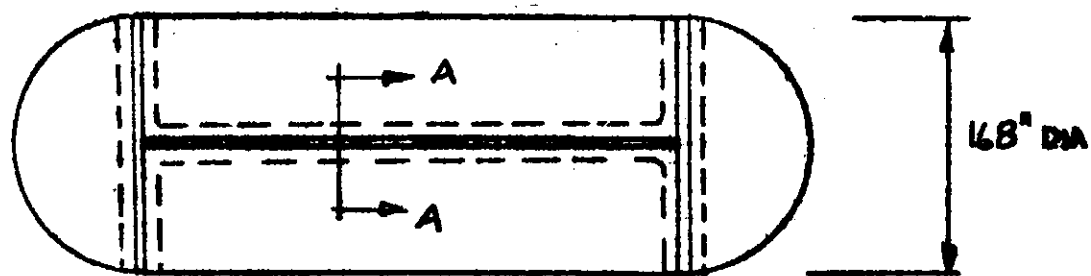
DATE: 17 June 1971

From a study of the results of the first configuration it was decided to continue the exploration of the strap joint by increasing the strap thickness to 0.067 inch, and to increase the gap D (Fig. 1) to 0.5 inch. The results of the analysis are shown in Fig. 6 (for $D = 0.25$ inch) and in Fig. 7 (for $D = 0.50$ inch). The maximum stress in the shell is practically unaffected by these changes, but the strap stress is considerably decreased. Note that the strap thickness to shell thickness ratio is $0.067/0.039 = 1.72$, which is close to the figure given by Eq. (5) as the condition for equal stress in strap and shell. Figures 6 and 7 show that for low pressures (i.e., linear response), the stress is indeed the same in the strap and in the shell, but as the pressure is increased the shell now becomes critical. This is, of course, due to the large step at "B" (see Figs. 6 and 7). By tapering the strap the shell should become less critical. Figure 8 shows that this is indeed the case, but that the tapering has a detrimental effect on the stress in the strap. From these analyses it appears that the ideal strap design would appear very much as in Fig. 9. Due to time limitations this configuration has not yet been analyzed.

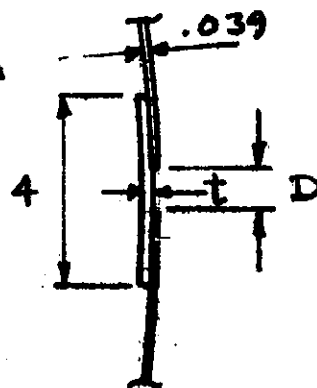
An interesting aspect of the strap design is the increase in the axial force in the strap itself, as shown in Fig. 5 (e). This increase is of the order of 50 percent, and implies that ends of the cylinder and therefore also the closures, will be subjected to a nonuniform circumferential load distribution, as shown in Fig. 10. The computer code BOSOR (Ref. 1) is capable of handling this problem, but only for the linear case. However, if a nonlinear analysis is required, the computer code STAGS (Ref. 2) is available.

REFERENCES

1. David Bushnell, "Stress, Stability and Vibration of Complex Shells of Revolution: Analysis and User's Manual for BOSOR3," SAMSO TR-69-375, 6 Sep 1969.
2. B. O. Almroth, et al., "User's Manual for the STAGS Computer Code, Buckling Analysis of General Shells," Vol. II of "Nosetip Design Analysis and Test (NDAT) Program," Lockheed Missiles & Space Company, Report LMSC-DO32008, December 1970.



SECT A-A



VARIABLES IN ANALYSIS:

D, t

MATERIAL: 2219-T87

Fig. 1 Strap Joint in LH₂ Tank

EM NO: L2-12-01-M1-15

DATE: 17 June 1971

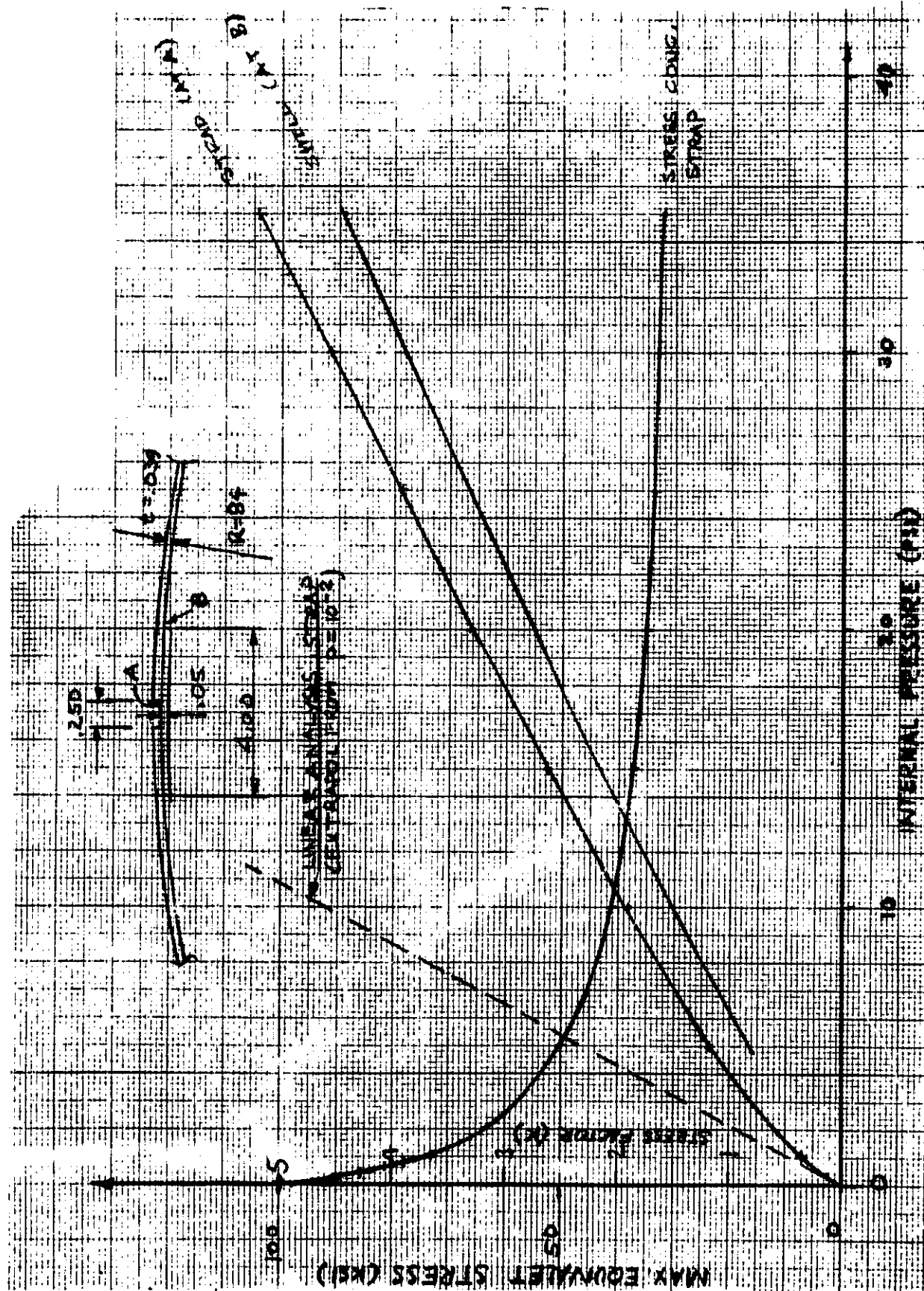


Fig. 2 Longitudinal Strap Joint Nonlinear Analysis

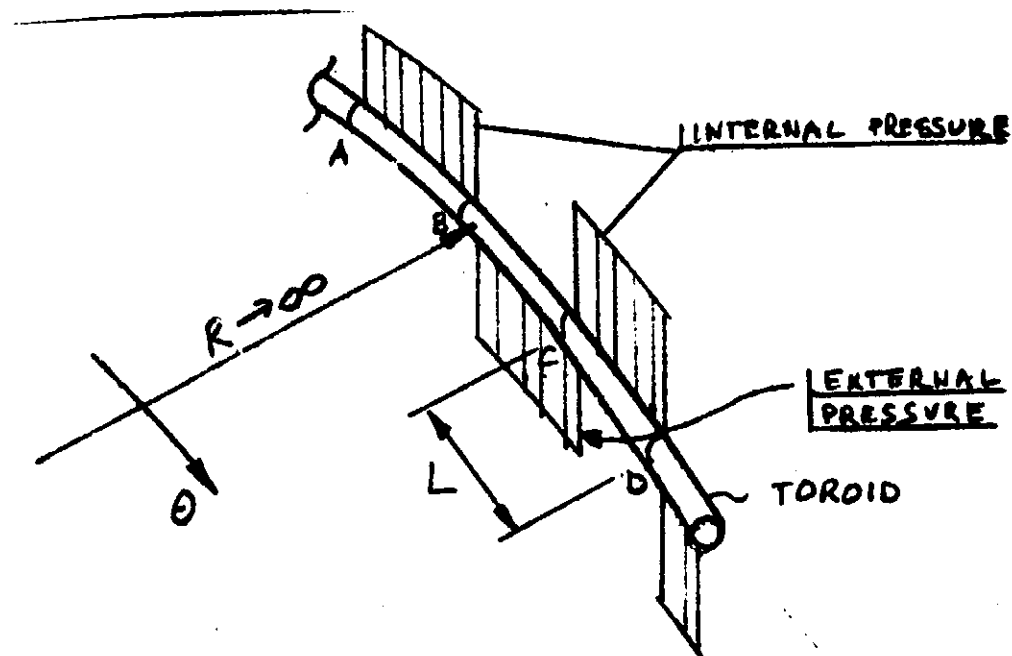


Fig. 3 Finite Length Cylinder Represented As Toroid

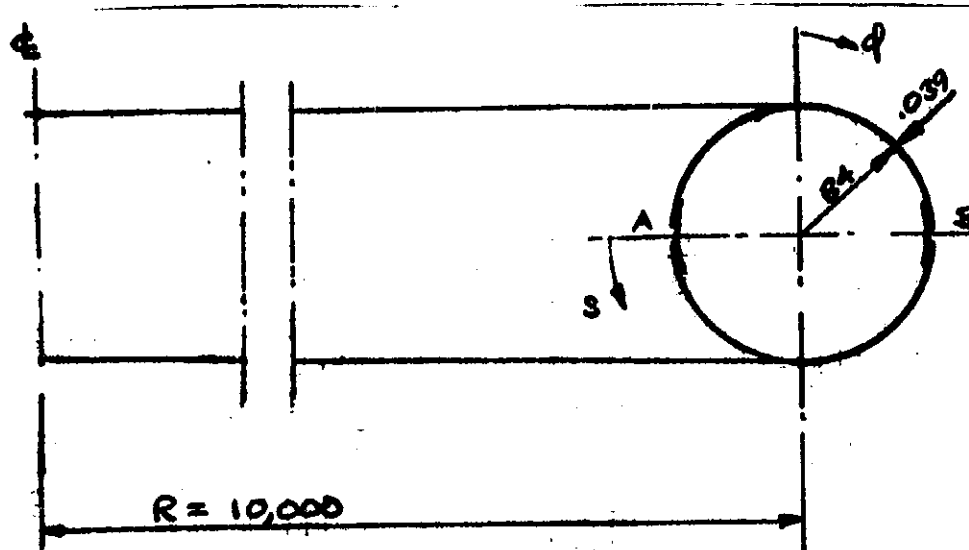


Fig. 4 Model Used in the Analysis

$P = 35 \text{ psi}$

AXIAL WELD BOND. $t_{\text{SKIN}} = 0.039$. $t_{\text{LAP}} = 0.050$

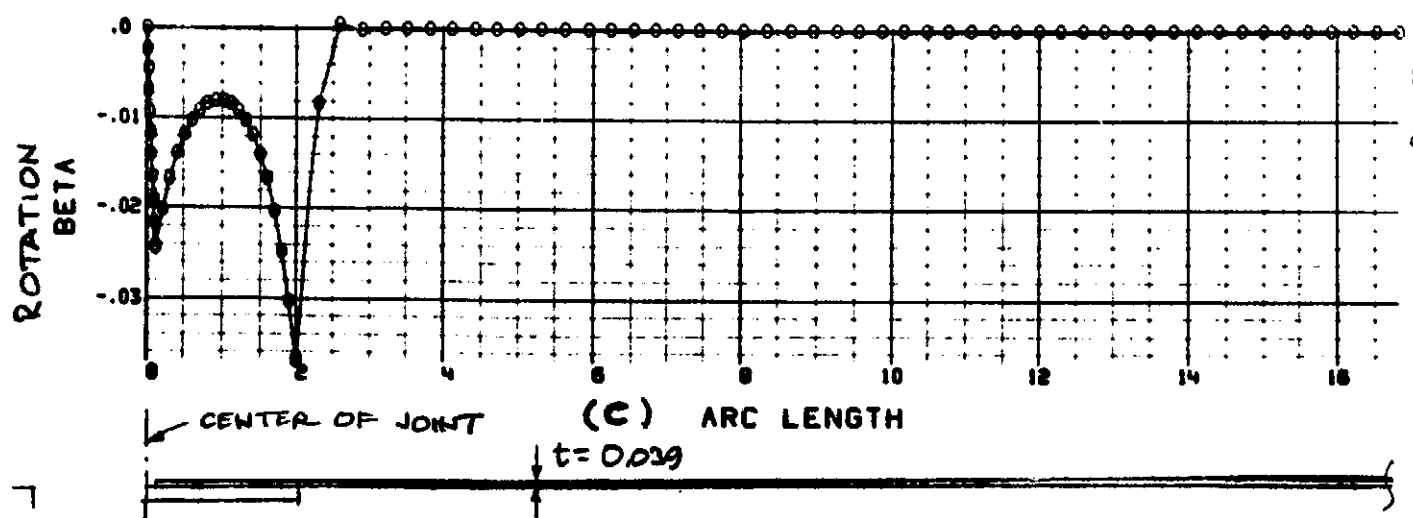
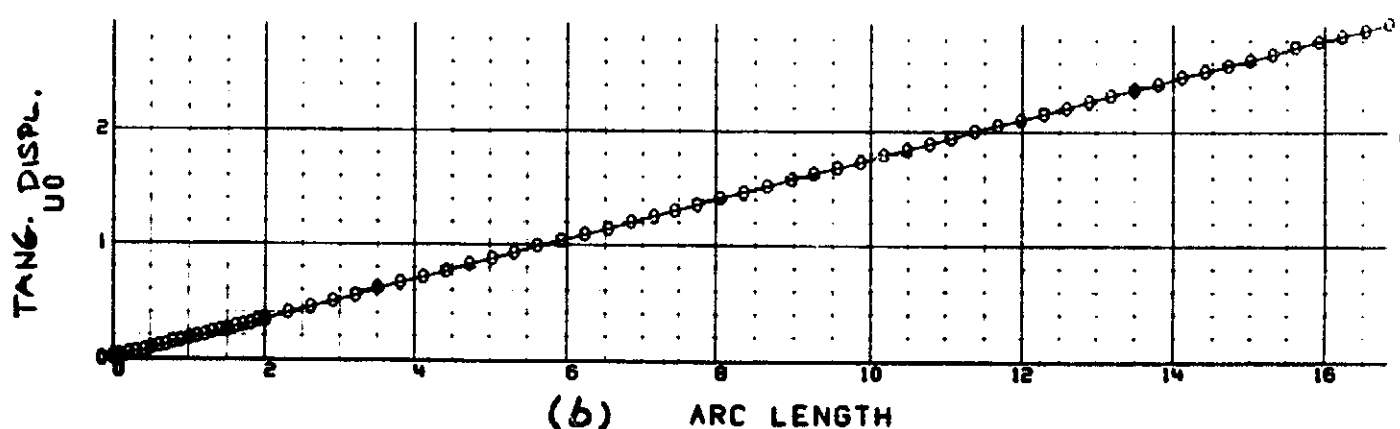
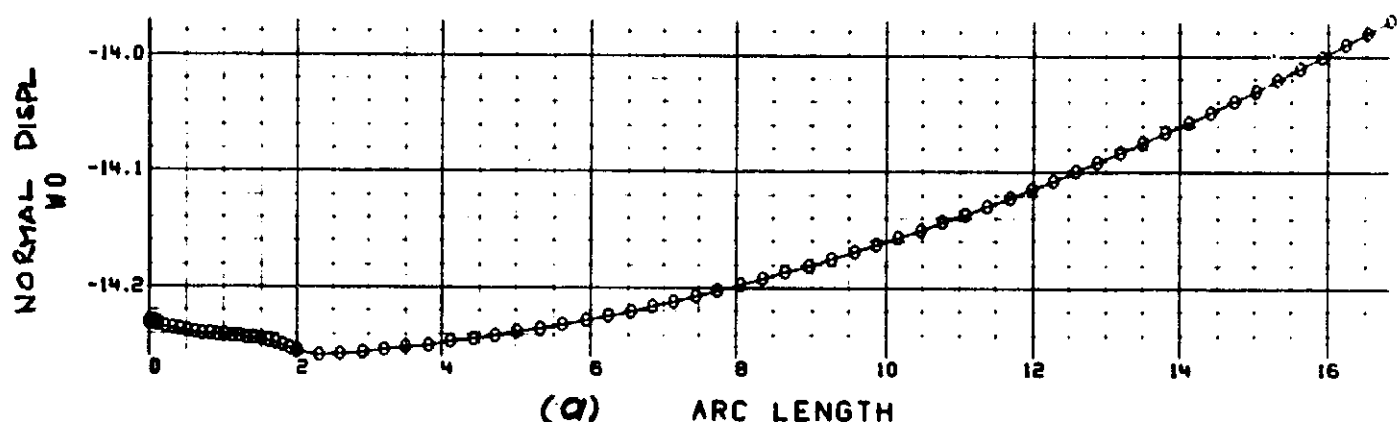


Fig. 5 Complete Analysis of Configuration According to Fig. 1, 35 psi Internal Pressure

AXIAL WELD BOND. TSKIN=0.039. TLAP=0.050

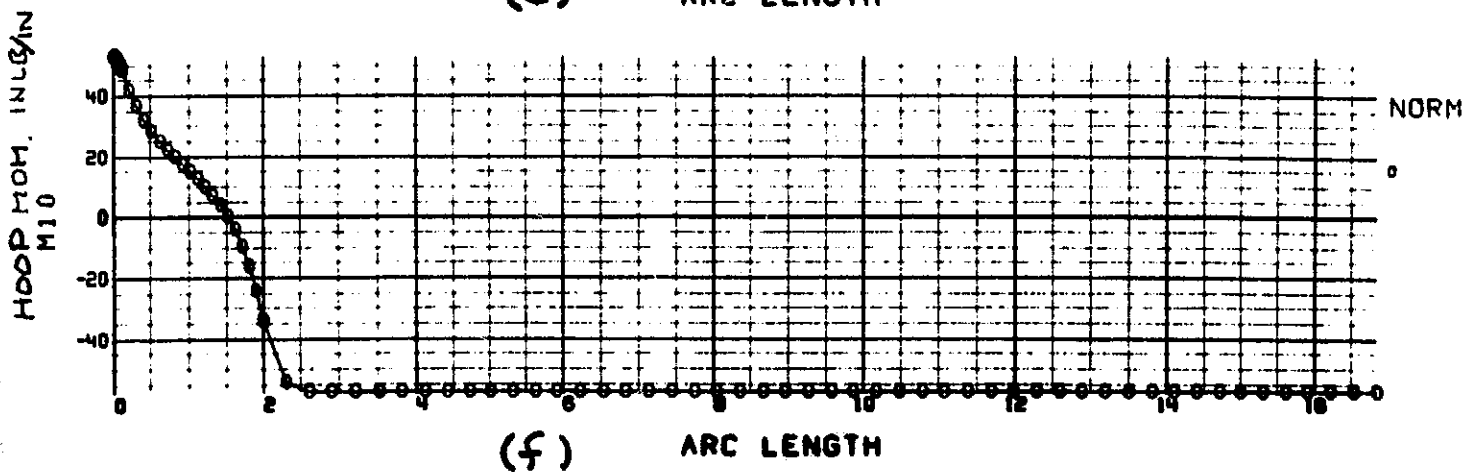
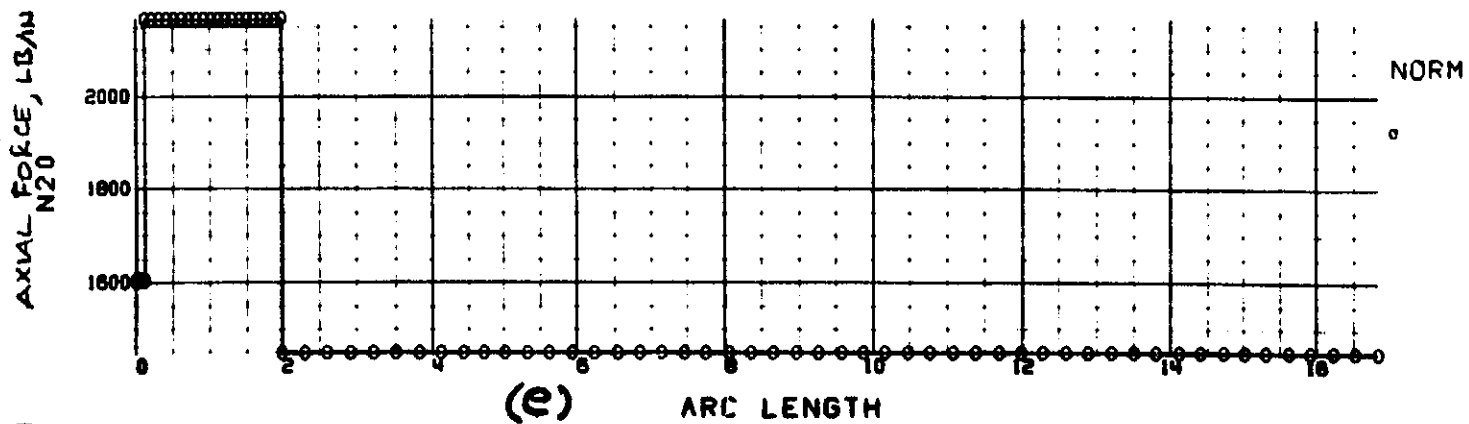
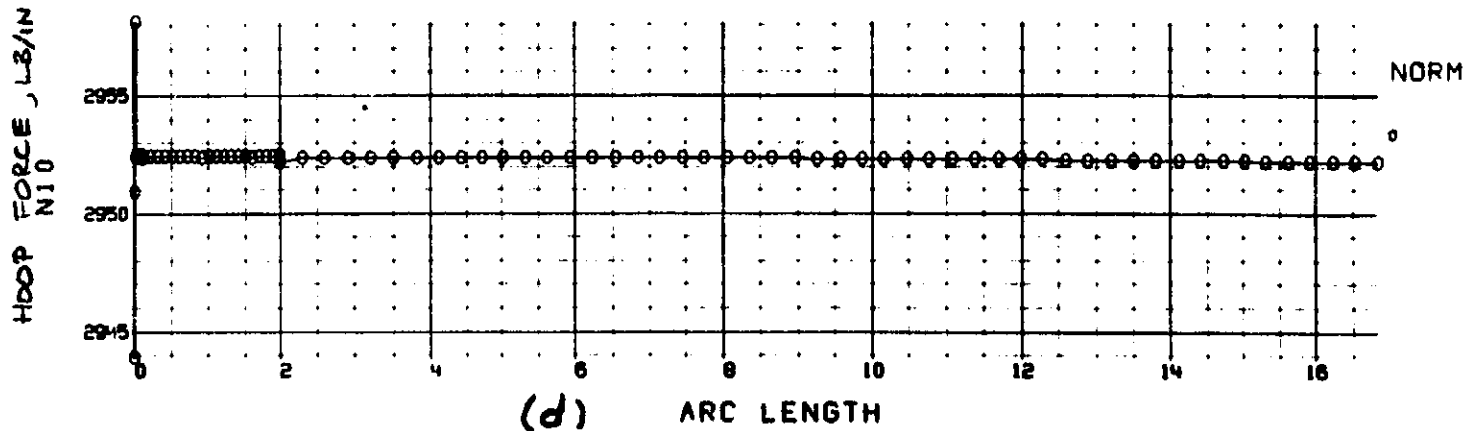


Fig. 5 (Cont'd)

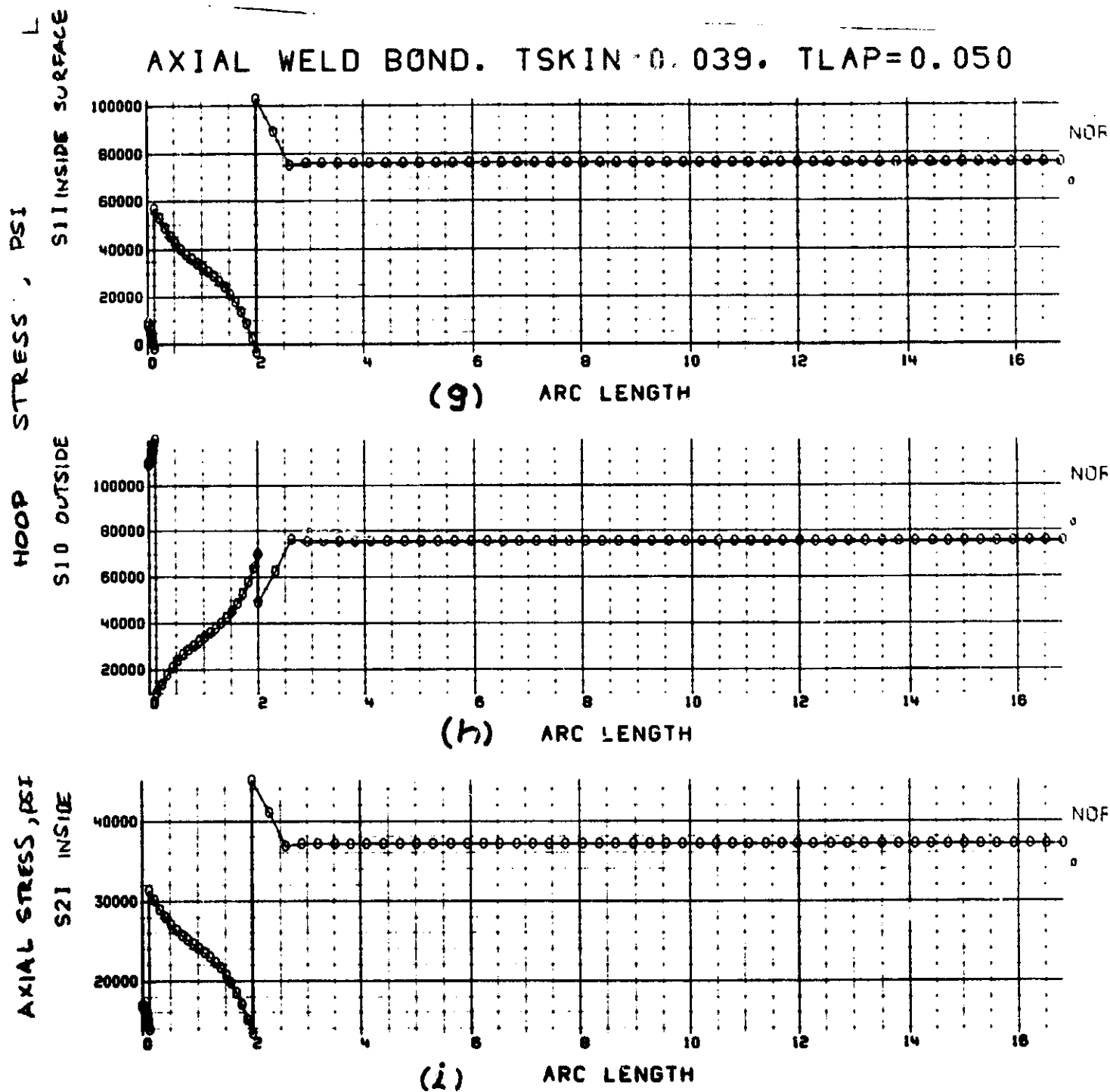
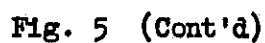
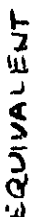


Fig. 5 (Cont'd)

Space Shuttle Project

DATE: 17 June 1971

AXIAL STRESS, PSI



EM NO: 12-12-01-M1-15
DATE: 17 June 1971

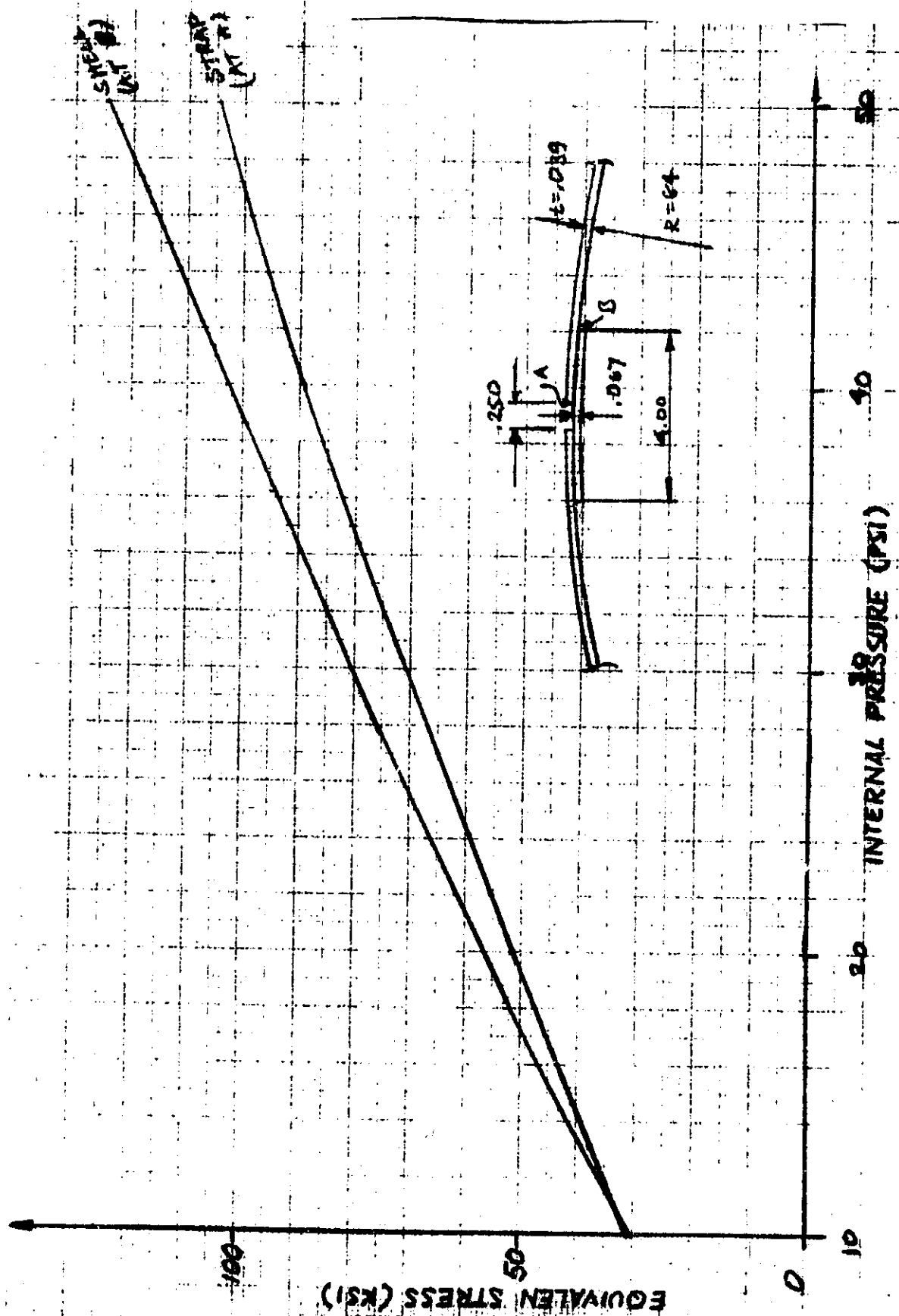


Fig. 6 Longitudinal Strap Joint Nonlinear Analysis

EM NO: 12-12-01-M1-15
DATE: 17 June 1971

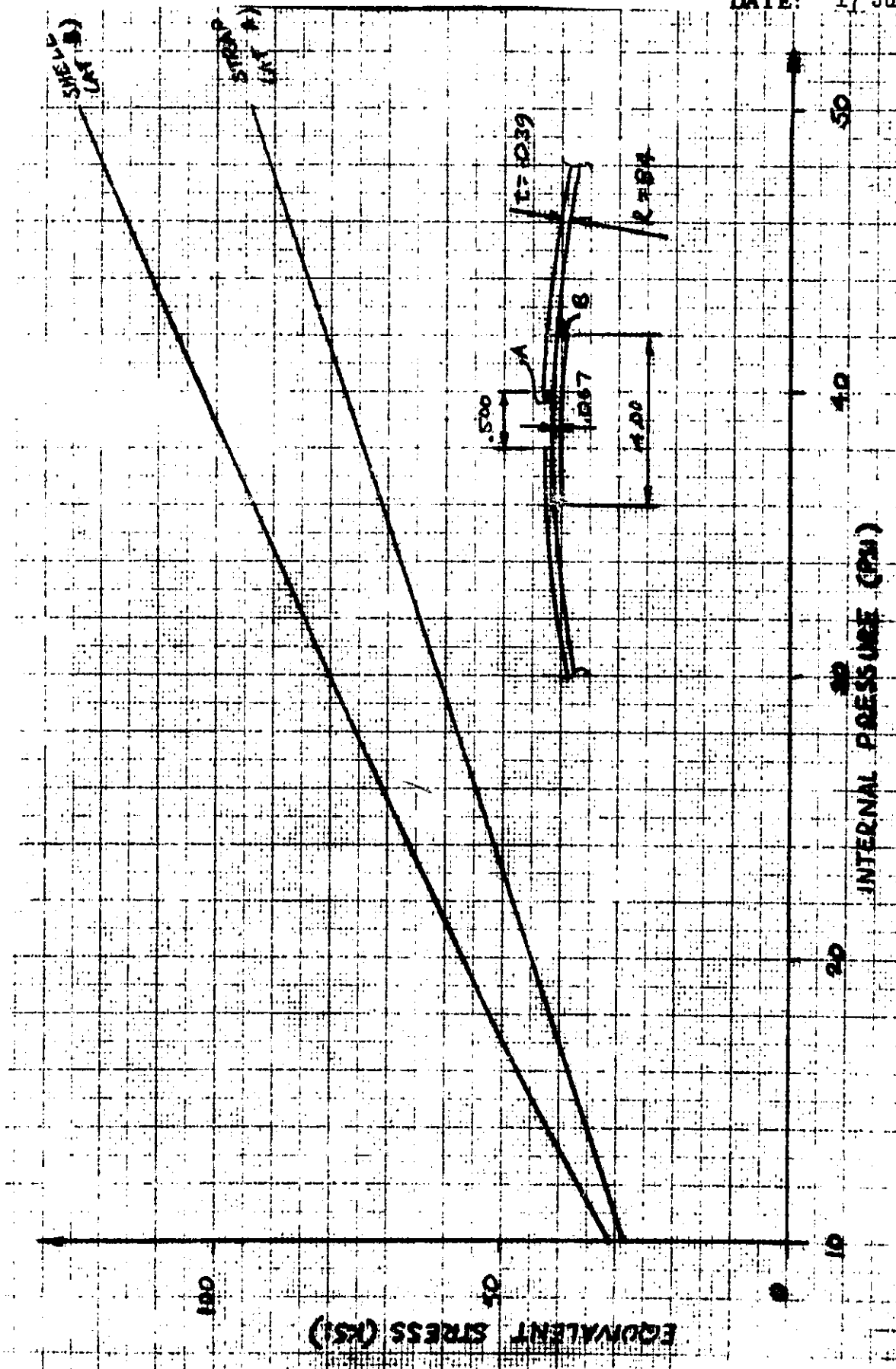


Fig. 7 Longitudinal Strap Joint Nonlinear Analysis

EM NO: 12-12-01-M1-15
DATE: 17 June 1971

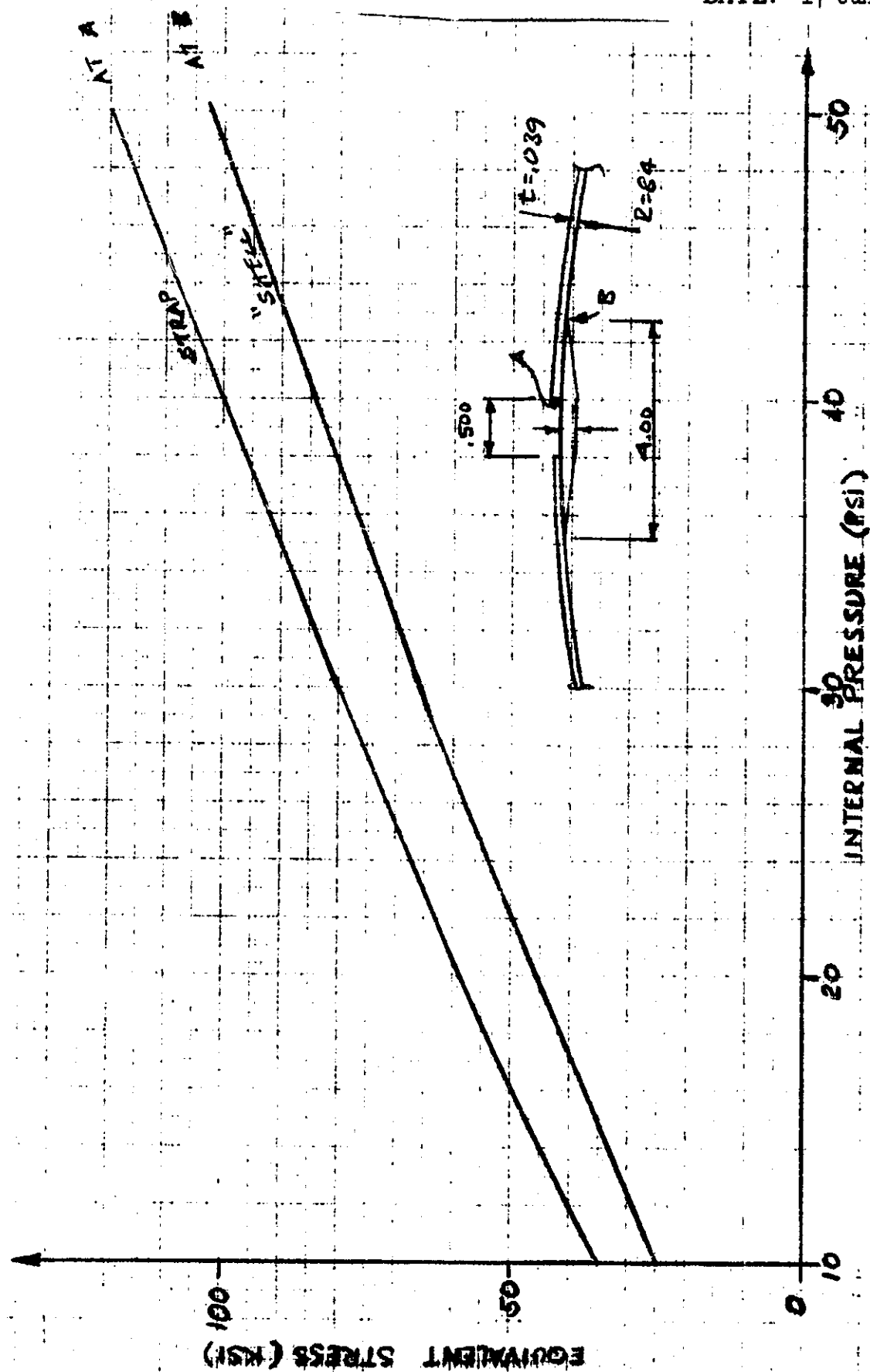


Fig. 8 Longitudinal Strap Joint Nonlinear Analysis Tapered Strap

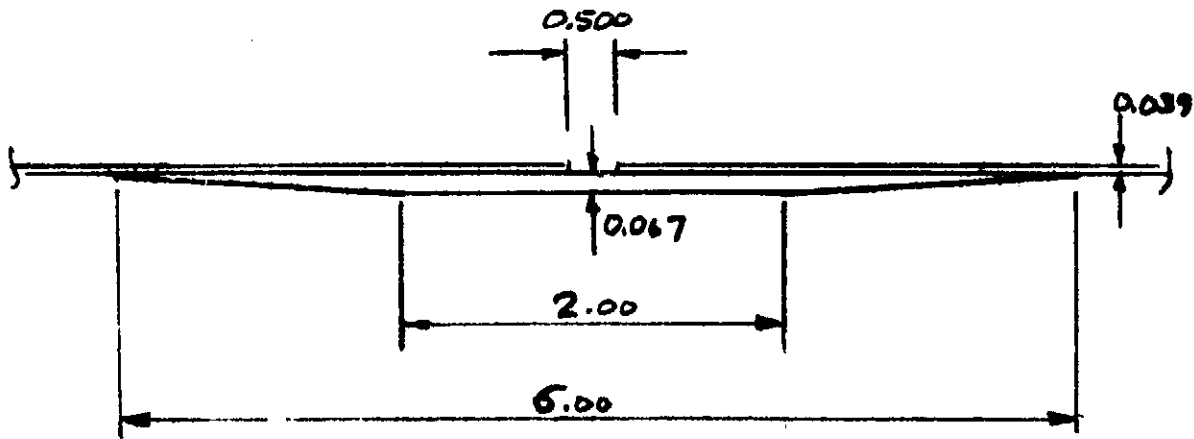


Fig. 9 "Ideal" Strap Design

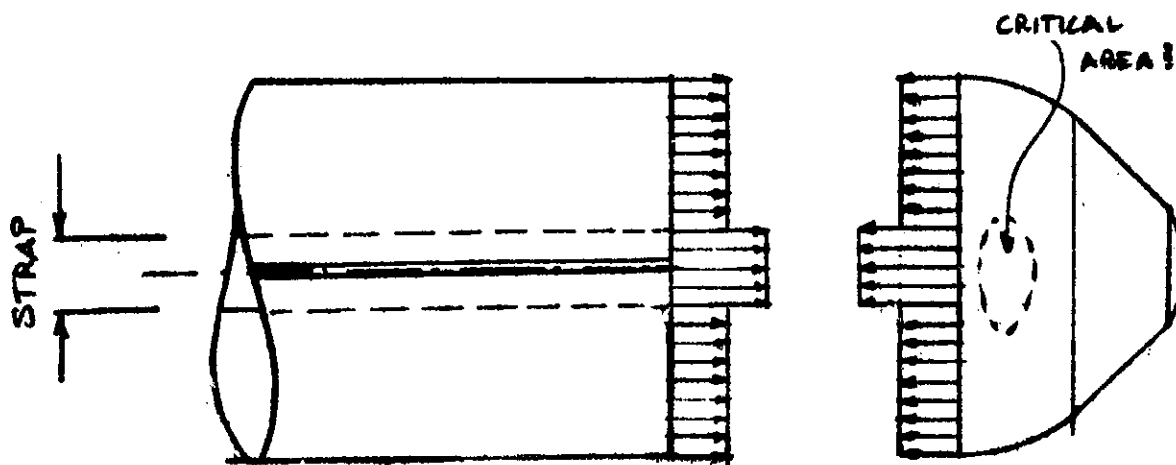


Fig. 10 Nonuniform Loading On Cylinder and Closure

ENGINEERING MEMORANDUM

TITLE: G.A.C. EXTERNAL DROPTANK ORBITER THERMAL EVALUATION	EM NO: L2-12-01-M1-7 REF: DATE: 11 May 1971
AUTHORS: K. W. McGee <i>K.W. McGee</i>	APPROVAL: ENGINEERING SYSTEM ENGRG <i>R. A. Byers</i>

PROBLEM STATEMENT

Evaluation of the Grumman (GAC) external LH₂ Droptank Orbiter concept (Ref 1) requires knowledge of the thermal environment and thermal protection system (TPS) requirements of the orbiter and droptanks. These data can then be used to determine validity of GAC data and to formulate LMSC predictions of the thermal characteristics of the system.

RESULTS

GAC thermal environment and TPS data were found to be generally comparable to LMSC calculations. Total droptank TPS weight was calculated at 4340 pounds, with an additional 960 pounds of TPS material required on the orbiter due to interference heating from the droptanks. Several different ablators were examined, with 30 pcf cork panels proving to be the most effective.

ANALYSIS

The GAC external droptank orbiter is shown in Figure 1 (Ref 2). All required ascent LH₂ is carried in the external droptanks, which are jettisoned in orbit. The orbiter overall length is 157 ft with a 106 ft wingspan and 55° leading edge sweep. The baseline droptanks are 14 ft in diameter and 85 ft long with an LH₂ capacity of 10,433 cubic feet per tank. As part of the present study, droptank length as a function of diameter was computed for a constant tank volume. Results are shown in Figure 2 for tank diameters from 10 to 20 ft. For a droptank diameter of 10.4 ft, the length is equal to the orbiter body length, 132 ft.

Thermal Environment

The GAC design ascent trajectory for the external droptank orbiter is shown in Figure 3 (Ref 3). Booster burn-out is 185 seconds after liftoff. Angle-of-attack was assumed to be zero for the entire ascent. Orbiter injection is into a 28.5° inclination orbit at 50 nm altitude. The droptanks are jettisoned in orbit where retro-rockets on the droptanks are fired to de-orbit the tanks. For the present study, no droptank reentry information was available, therefore the following analyses are for the ascent thermal environment only.

Data from a series of GAC tests were obtained from Langley Research Center and are presently being evaluated. The tests were run at LaRC in the Continuous Flow Hypersonic Tunnel at a nominal Mach number of 10. The test consisted of a thin-skin model with 44 thermocouples mounted on the orbiter side in the interference heating regions and 50 thermocouples on the droptank in the interference regions. The locations of the thermocouples along with the ratio of the local heat transfer coefficient (h_{LOCAL}) to the heat transfer coefficient on a 1 ft radius spherical stagnation point ($h_{1 FT SPHERE}$) are shown in Figure 4. These ratios ($h_{LOCAL}/h_{1 FT SPHERE}$) are plotted in Figure 5a for the orbiter body side as a function of distance along

the body. The peak at $X/L = 0.38$ is caused by the impingement of the droptank bow shockwave on the orbiter side. The peak for W.L. 412 corresponds to an interference heating factor of about 50. This is a localized effect though, and the interference factor for most of the body side is 8 or less near the droptank. Figure 5b plots h_{LOCAL}/h_1 FT SPHERE for the droptank side as a function of distance along the tank.

The various peaks correspond to impingement of orbiter shocks and shock reflection off the orbiter onto the droptanks. Interference factors from 20 to 40 are indicated on the conical section of the tank, while for the cylindrical section, the factors are generally less than 6.

Ascent heating predictions were based on Spalding-Chi heating theory with a transition Reynold's number of 100,000, based on boundary layer length. This relatively low transition Reynold's number was assumed to account for the flow disturbing effects of the orbiter shock system. Ascent heating histories for three locations on the droptank are shown in Figures 6a, b, and c. These heating rates are based on radiation equilibrium wall temperatures. The lower solid line in each figure represents the computed local undisturbed heat transfer rate, i.e., the local heat transfer rate for the droptank without the effect of interference between the orbiter and droptanks. Heating rate histories are shown for different multiples of the undisturbed heat transfer rate along with the GAC heating rate histories (Ref 3). The GAC curves reflect interference heating factors from 4 to 10 and more, depending upon location and boundary layer flow state (laminar or turbulent). The reason for the difference in time of peak heating between IMSC and GAC heating curves shown in Figure 6a is unknown but is probably due to the use of different transition criteria or boundary layer lengths in the calculations. Heating peaks at other locations occur at nearly identical times.

Comparison of GAC predicted tank heating rates (Fig. 6) with the test data of Figure 5b indicate reasonable agreement between this assumed and measured interference factors. Factors above 10 are indicated on the conical section in Figure 6a, which are confirmed by Figure 5b. On the cylindrical section, factors close to 6 for the forward part and near 3 for the aft portion are shown in Figures 6b and c. These factors also show reasonable agreement with the test data. The local undisturbed heat transfer coefficient ratio shown in Figure 5b is what would be appropriate for areas on the droptank where there is no interference heating. The value at which the ablator analysis was performed is shown in Figure 5b as the ablator evaluation interference factor at h_{LOCAL}/h_1 FT SPHERE = 0.19.

Figure 7 is a schematic of the droptank TPS proposed by GAC (Ref. 4). Their summary TPS weight statement is also shown. A constant thickness of 0.75 in. of 2 pcf polyurethane foam is used to cover the entire tank. As shown, GAC assumes 1000 ft² of ablative TPS is required to protect the tank in highly heated flow interference areas. No data are provided on the ablator type, thickness, or density. Figure 8 shows the orbiter surface areas assumed by GAC to require additional TPS due to interference heating. The total weight penalty is estimated at 924 lbs for the baseline droptank.

During the present study, TPS weights were computed as a function of tank diameter using the GAC data discussed above. The weight of the polyurethane foam was estimated assuming a thickness of 0.75 in. at 2 pcf plus an additional 0.125 in. to account for uncertainties in the spray application. An allowance of 0.104 pcf was also included to account for a waterproof and flame retardant surface coating (Ref. 5).

A 30 pcf ablator with an average thickness of 0.25 was assumed as representative for the 1000 ft² of tank area requiring ablative TPS (Fig. 7). Data of Figure 8 were modified to account for changes in tank geometry.

Figure 9 summarizes the results of this analysis and plots, for a fixed droptank volume (variable length and diameter), the weights of the various components of the TPS. Curves 2 and 3 of Figure 9 plot the computed weights of the ablator and foam, respectively, with Curve 4 being the total of Curves 2 and 3. A minimum droptank TPS weight (2 tanks) of 4340 pounds occurs at a tank diameter of about 14 ft, the GAC baseline design. TPS weight penalty on the orbiter wings and body due to the presence of the droptanks is plotted in Curve 1 of Figure 9. If this weight is added to the foam and ablator weights (Curve 4), the total TPS weight penalty due to the droptanks (Curve 5) is constant for diameters less than 14 ft at a value of 5300 pounds. The GAC droptank TPS weight shown in Figure 7 is 4750 pounds. This weight contains insulation items not included in the present analysis such as cryogenic insulation on the forward dome inside the conical nose cap. If these items are excluded, the GAC droptank TPS weight is about 4100 pounds, which is close to present prediction of 4340.

An analysis was performed to evaluate the thermal performance of five ablators on the cylindrical portion of the droptanks affected by interference heating. The local heating rate at the location examined ($X = 20$ ft) was assumed to be 0.19 and 0.30 times the stagnation point value for laminar and turbulent flow, respectively (see Fig. 5b). Table 1 lists the five materials that were examined and their densities. Ablator thicknesses were selected such that a constant unit weight of 0.625 pcf resulted. This is the unit weight that was assumed in the previous calculations.

The amount of ablative weight lost during ascent is shown in Table 1 for the five materials. Weight loss for all materials was one percent or less. Thermal protection was judged adequate if the ablator succeeded in maintaining the foam/ablator interface below 500°F (the assumed foam decomposition temperature) and the droptank structure below -200°F (the pressurization gas temperature) until time of separation. Only DC-325 did not meet these requirements, although two of the silicon elastomers allowed the foam/ablator interface to come within 30°F of the critical temperature, and therefore were judged to provide only marginal thermal protection. Ablator surface and foam/ablator interface temperatures are shown in Figure 10 for the five ablators studied. The difference in surface temperatures is due to the varying properties of the different ablators, such as specific heat, conductivity, and ablative characteristics. The only available GAC data on their ablator performance (Ref 2, page 3-61) is also shown in Figure 8. Their foam/ablator interface temperature history indicates that either an excessive thickness of ablator was assumed or that incorrect material properties were used for the ablator.

CONCLUSIONS

- 1) Preliminary analysis of wind tunnel heating data obtained by GAC shows average interference heating factors on the external tanks and orbiter side between 4 and 8, decreasing toward the aft end of the orbiter. Localized peak interference heating factors of 40 to 50 are indicated on both the orbiter and droptanks.
- 2) Comparison of GAC predicted heating rates at various droptank locations show reasonable agreement with wind tunnel test data.

- 3) Thermal analysis of the droptank TPS selected by GAC shows this concept to be adequate. A thickness of 0.75 in. of foam in the non-interference regions of the tank with interference regions of the tank having a coating of ablative material would be sufficient.
- 4) Comparison of GAC-computed TPS weights with IMSC weights, show fair agreement. The figures are within 300 pounds, depending upon how GAC data is interpreted.
- 5) An evaluation of five ablators showed that 0.25 in. of 30 pcf cork applied outside the foam, provides the best thermal protection for unit weight analyzed.

REFERENCES

1. Study Plan for Study of External LH₂ Droptank System Design, 30 March 1971, ACS-119
2. Grumman Aircraft Company Brochure MSC-03804, SS-884
3. GAC Data Package, 19 April 1971, SS-900
4. Alternate Space Shuttle Contract Study External Hydrogen Tank Orbiter/Heat Sink Booster, 25 March 1971, SS-832
5. Heathman, J. H. et al, "Analytical Investigation of a Low Cost Expendable Tankage System for an Advanced Staging Vehicle Concept," AFFDL-TR-70-42, June 1970

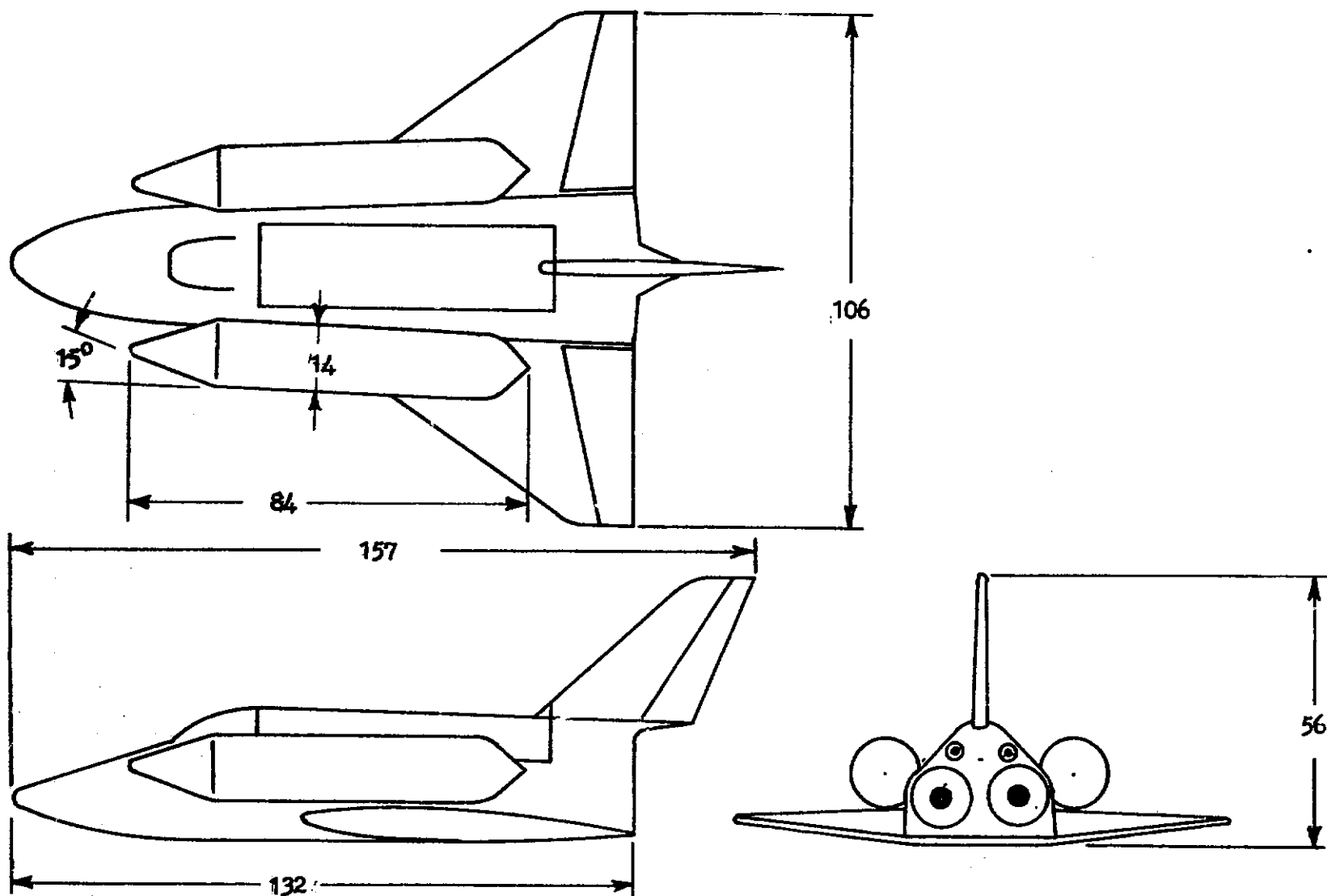


Figure 1 GAC External Tank Orbiter

DROPTANK LENGTH/DIAMETER VARIATIONS

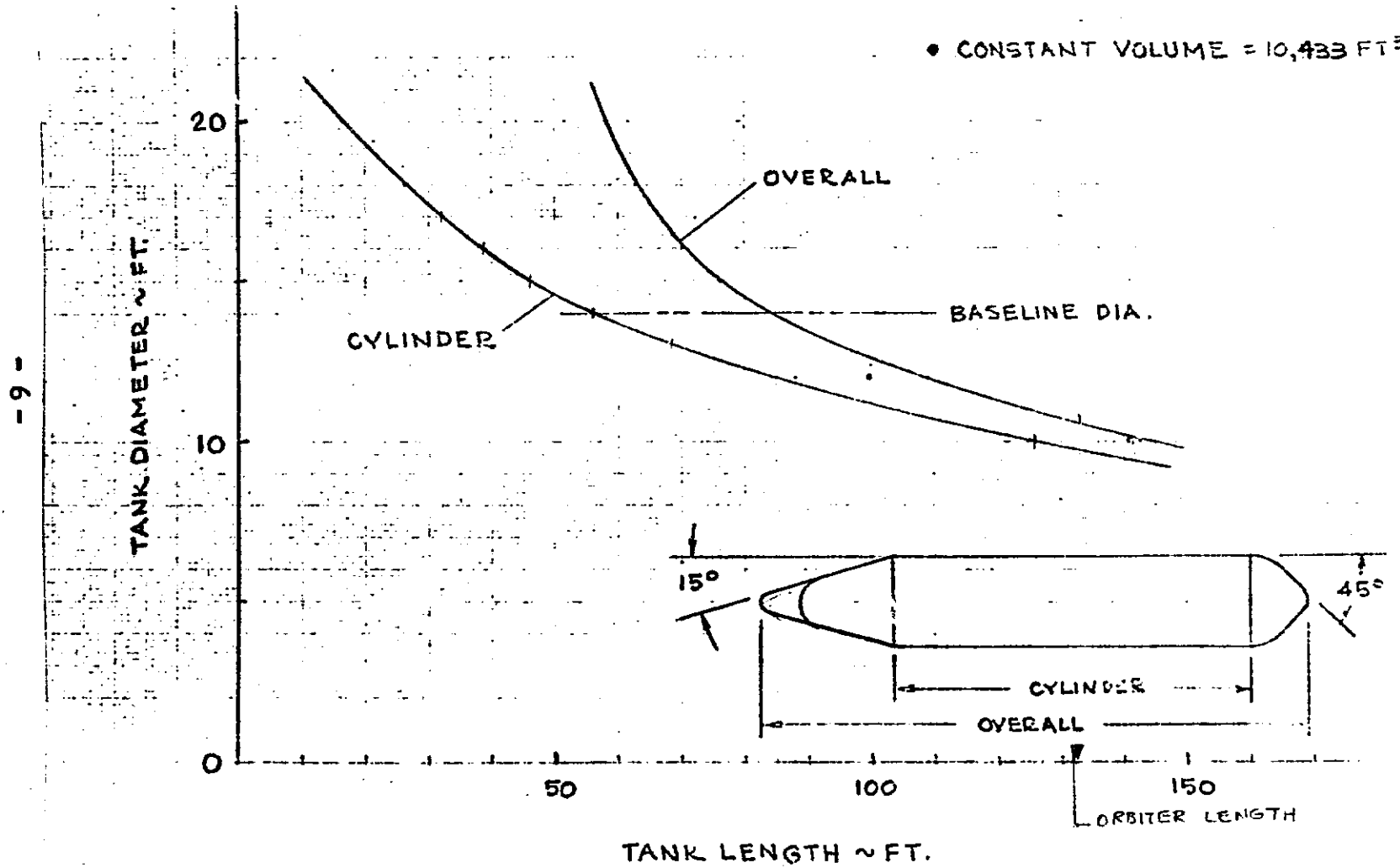


Figure 2 Droptank Length Vs. Diameter

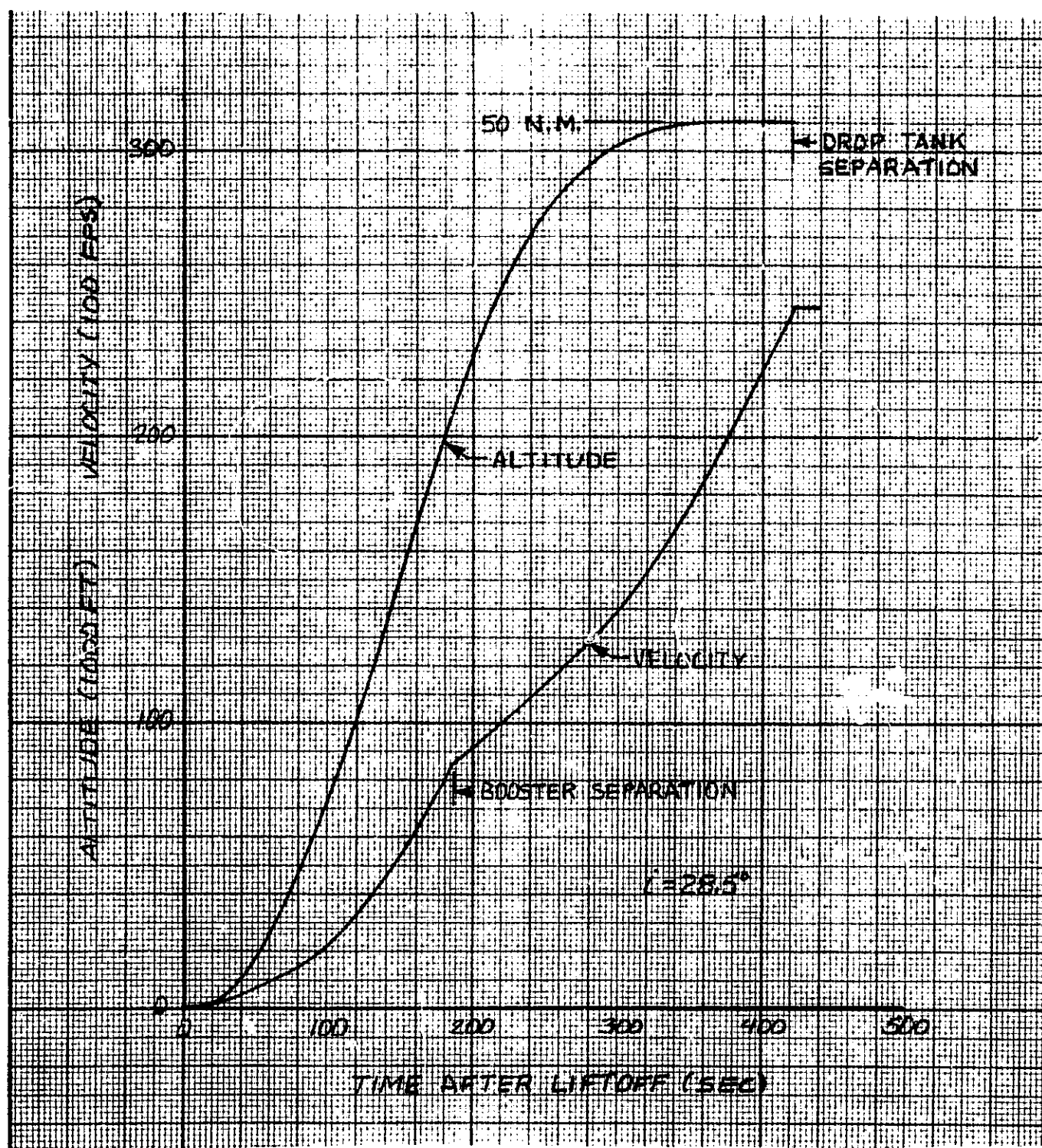
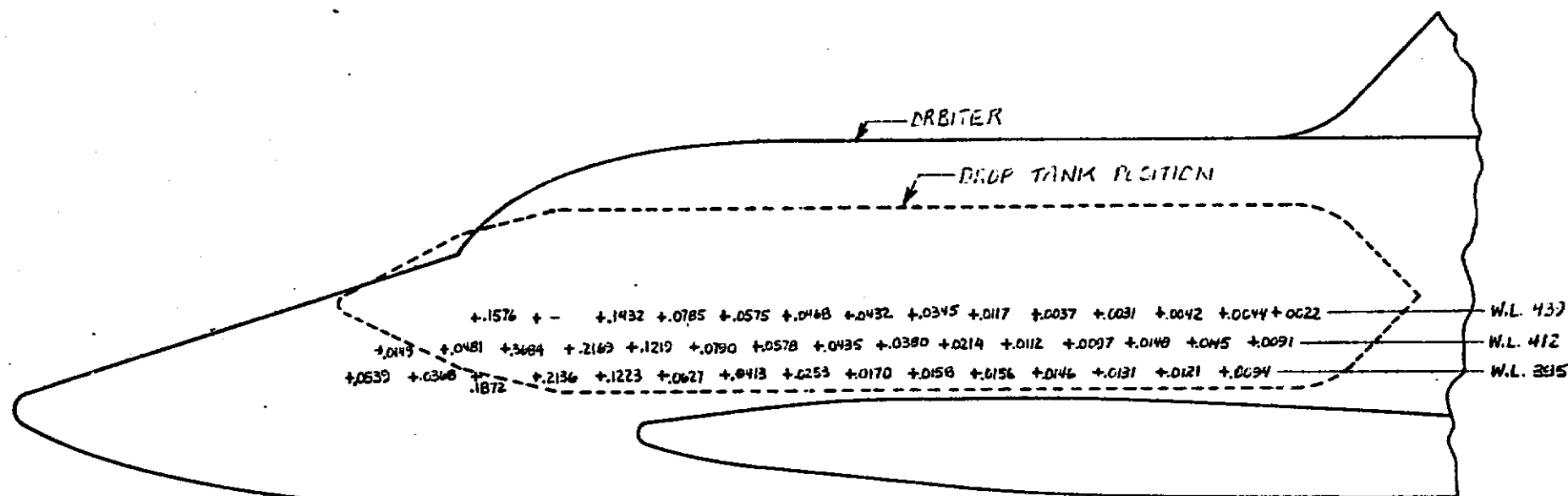


Figure 3 GAC 2-1/2 Stage Ascent Trajectory



ORBITER TEST RESULTS

GAC THERMOCOUPLE TEST RESULTS

 h_{LOCAL}/h_1 FT STAGNATION POINT

 $LY = 10.35$ LAMINAR FLOW

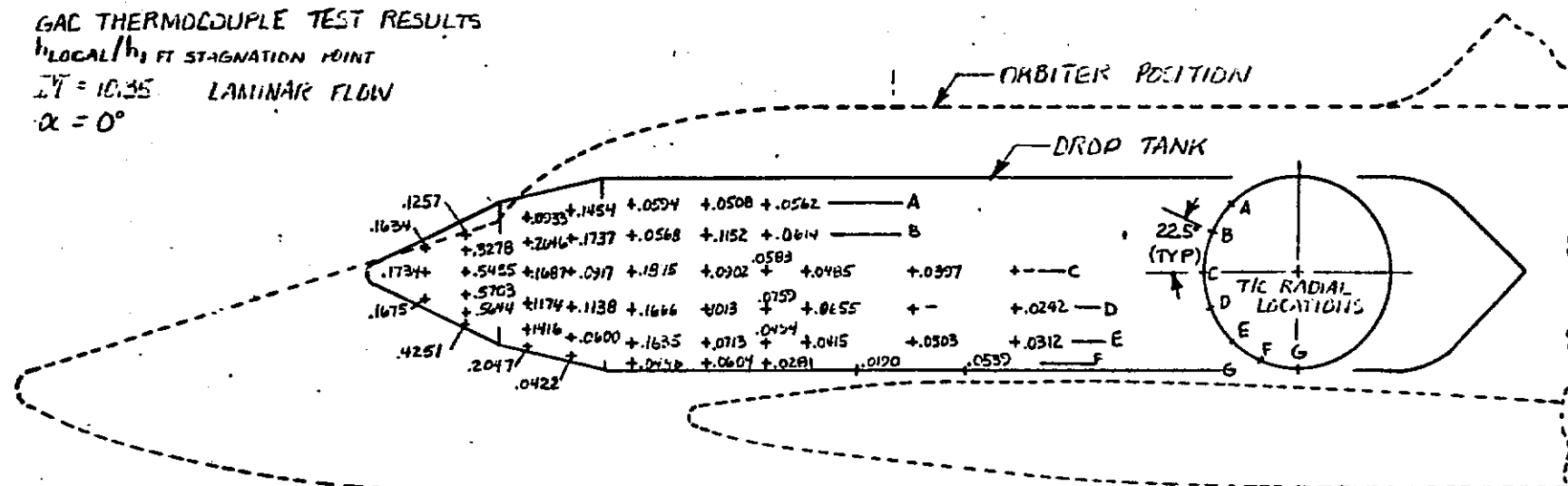
 $\alpha = 0^\circ$


FIG 4-1. TEST RESULTS

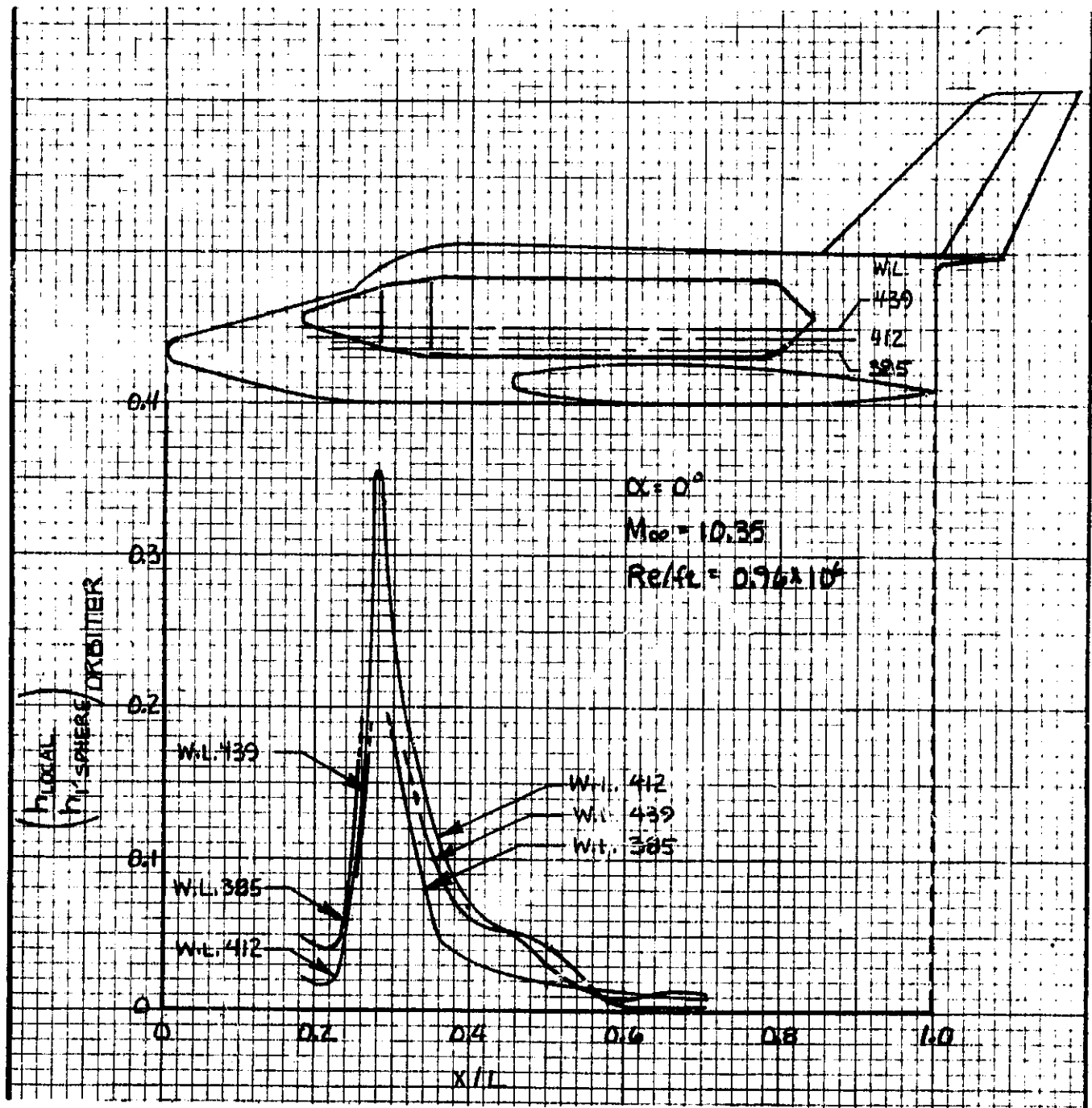


Figure 5a Orbiter Side Heating Rates

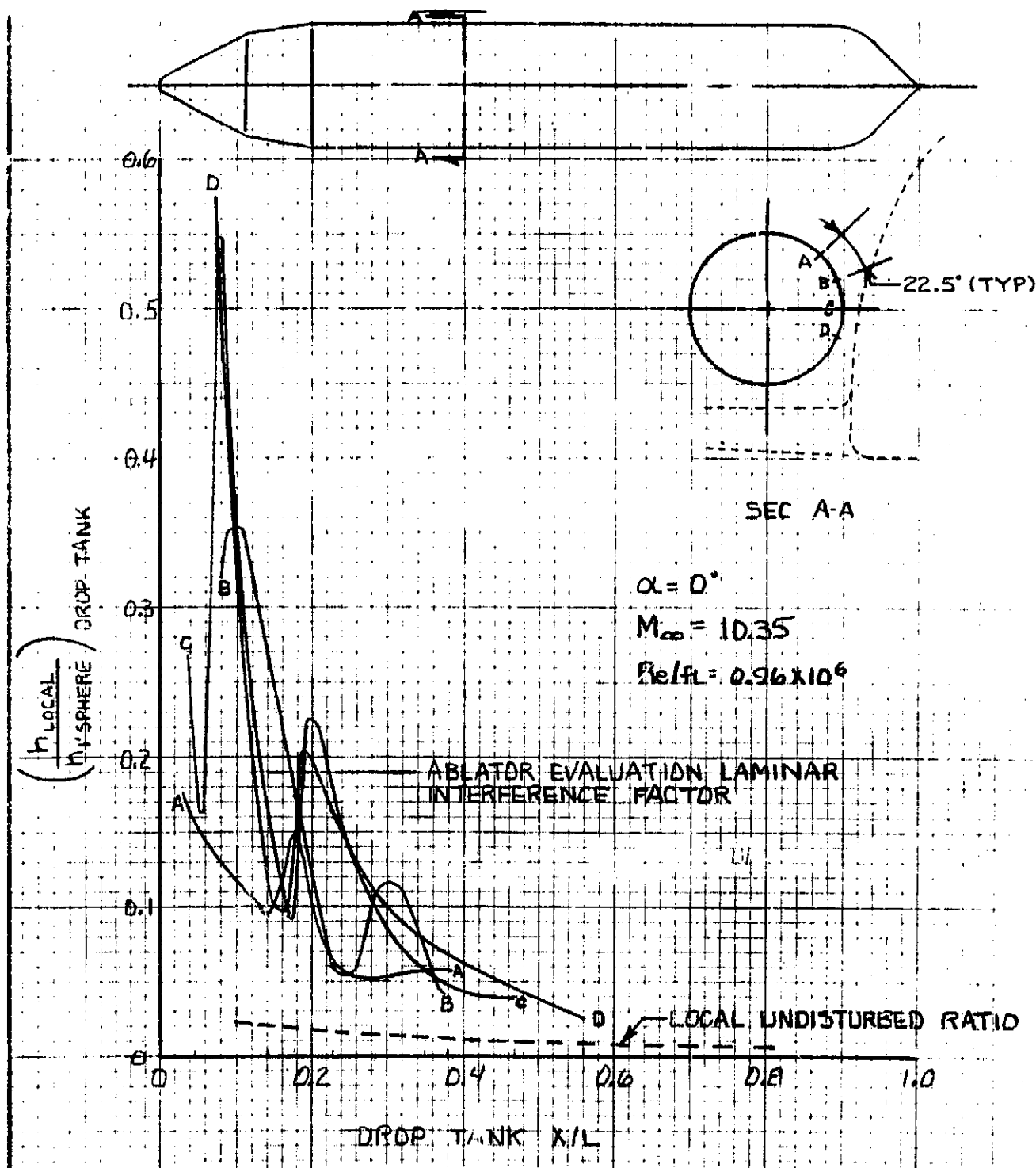


Figure 5b Droptank Side Heating Rates

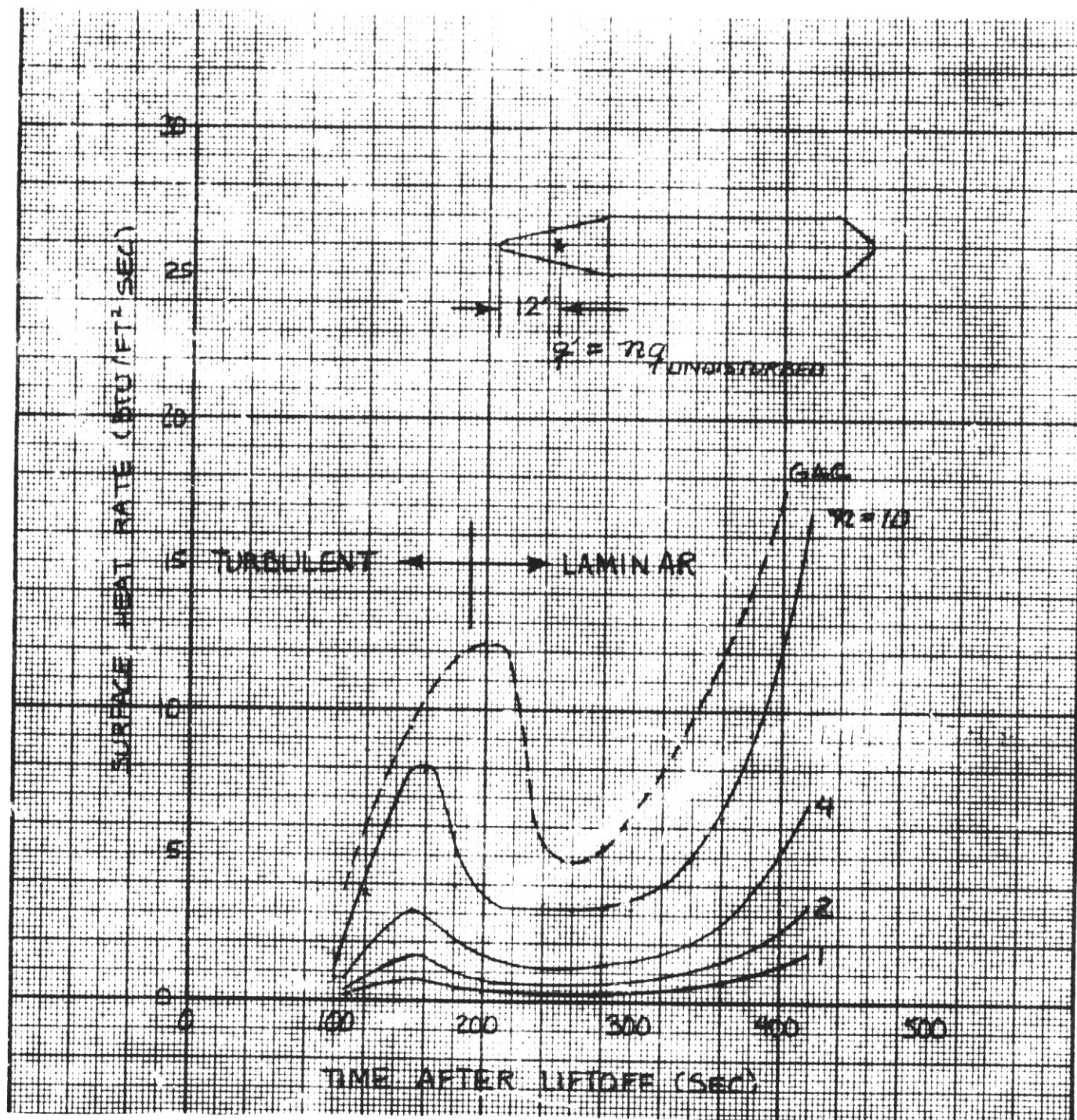


Figure 6a Droptank Ascent Heating Rates

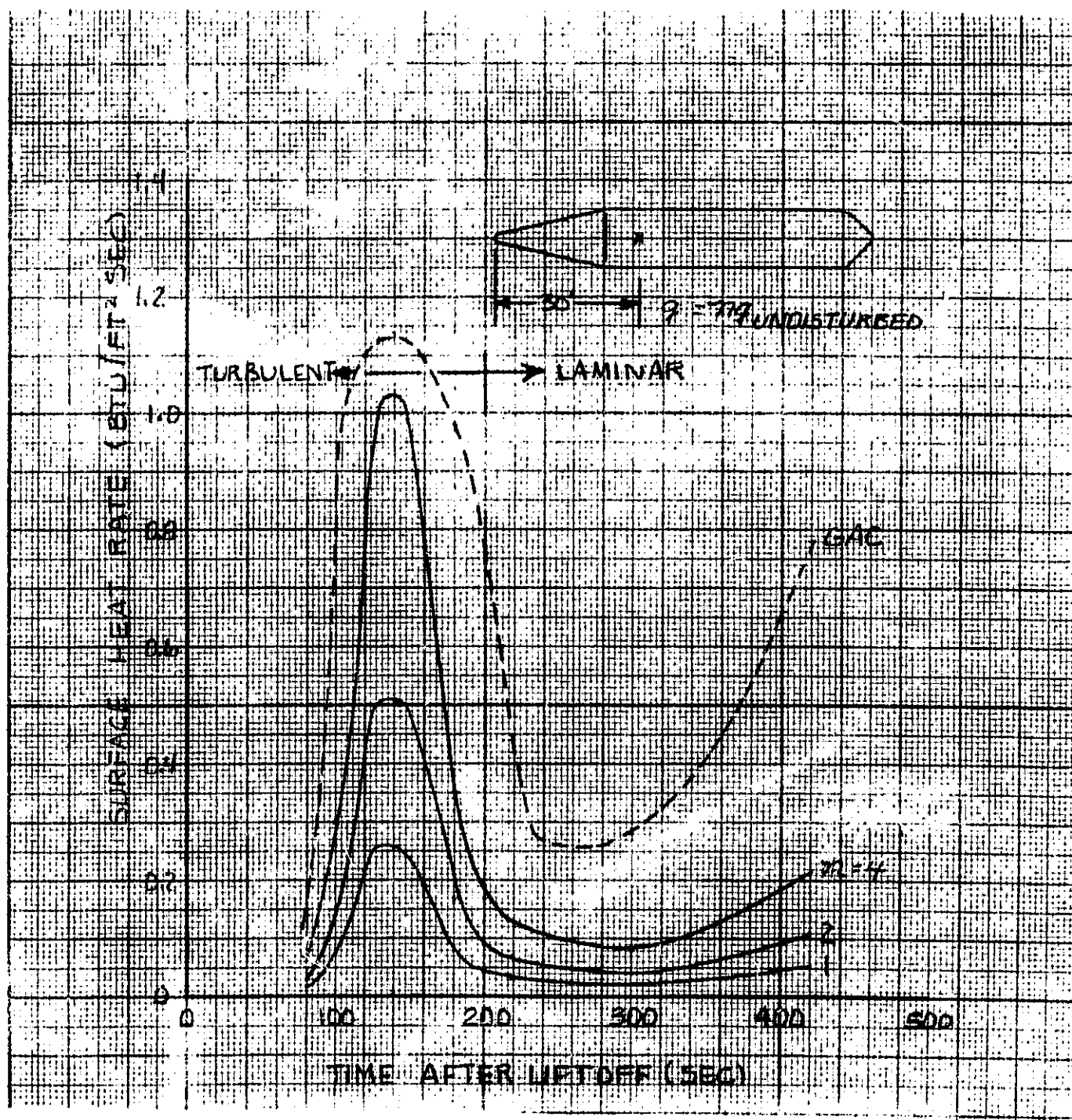


Figure 6b Droptank Ascent Heating Rates

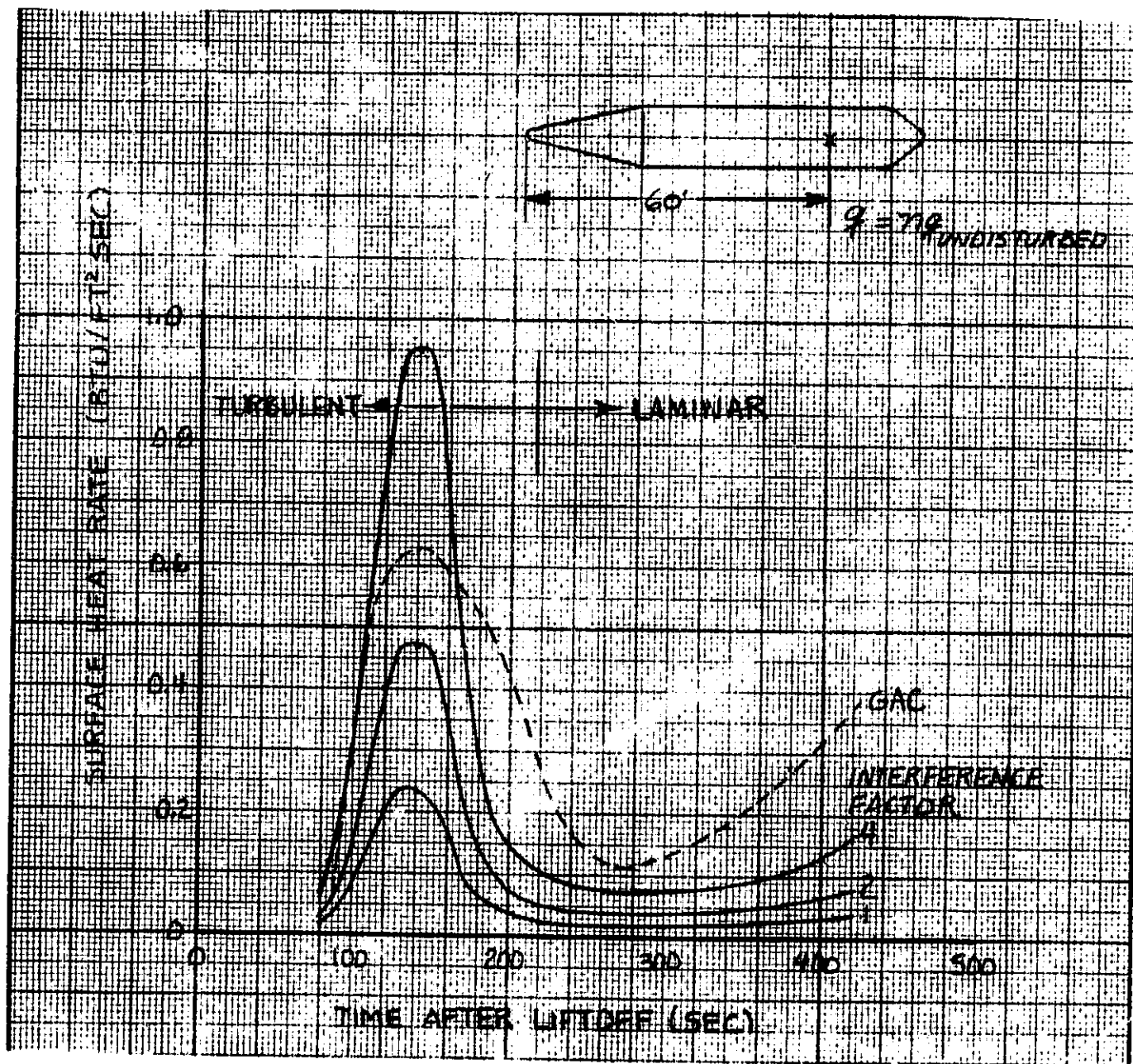
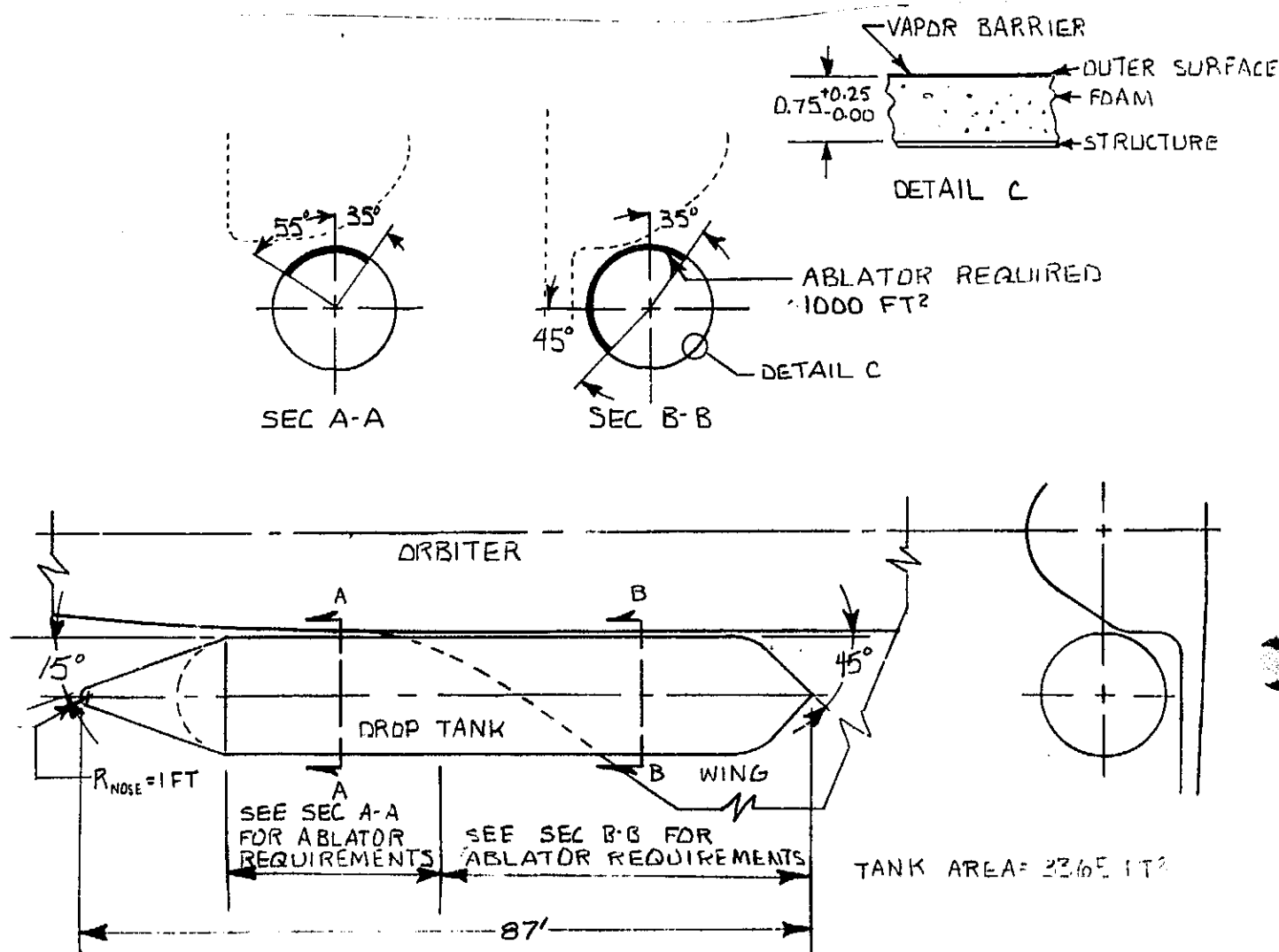


Figure 6c Droptank Ascent Heating Rates



A. TPS Schematic

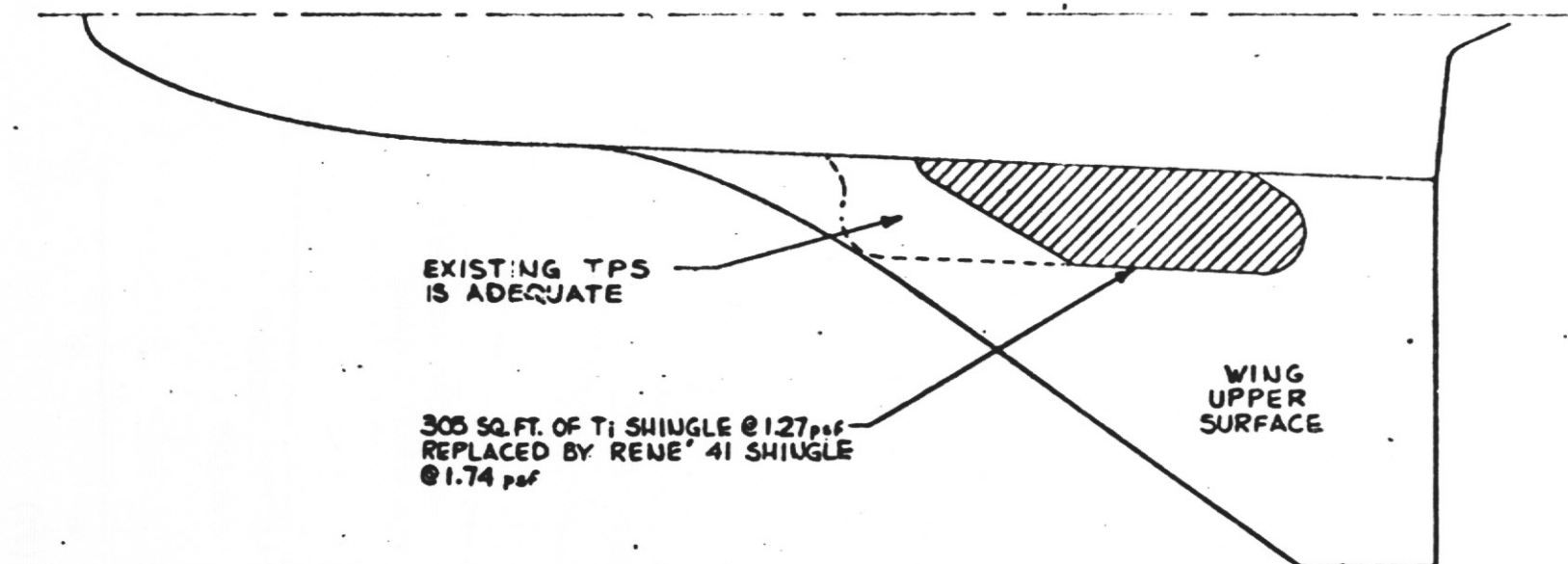
GAC DROPTANK TPS REQUIREMENTS

NOSE CONE	2104 LB
FORWARD DOME	184
AFT DOME	124
CRYOGENIC	912
SUPPORTS	374
INTERFERENCE HEATING	1052
INSULATION AND TPS	4750 LB

B. Summary Weight Statement (2 Tanks)

Figure 7 GAC Droptank TPS Concept (Ref 4)

EXTERNAL TANK ORBITER PENALTY DUE TO INTERFERENCE HEATING



TOTAL WEIGHT PENALTY
= 924 LBS/ORBITER

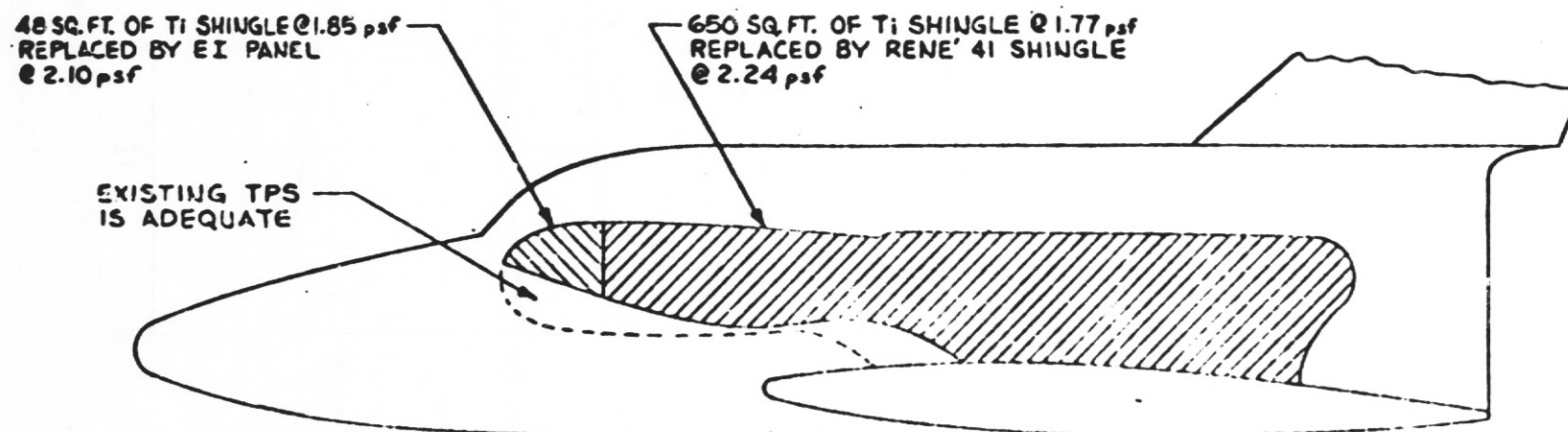


Figure 8 Orbiter Interference Heating Areas

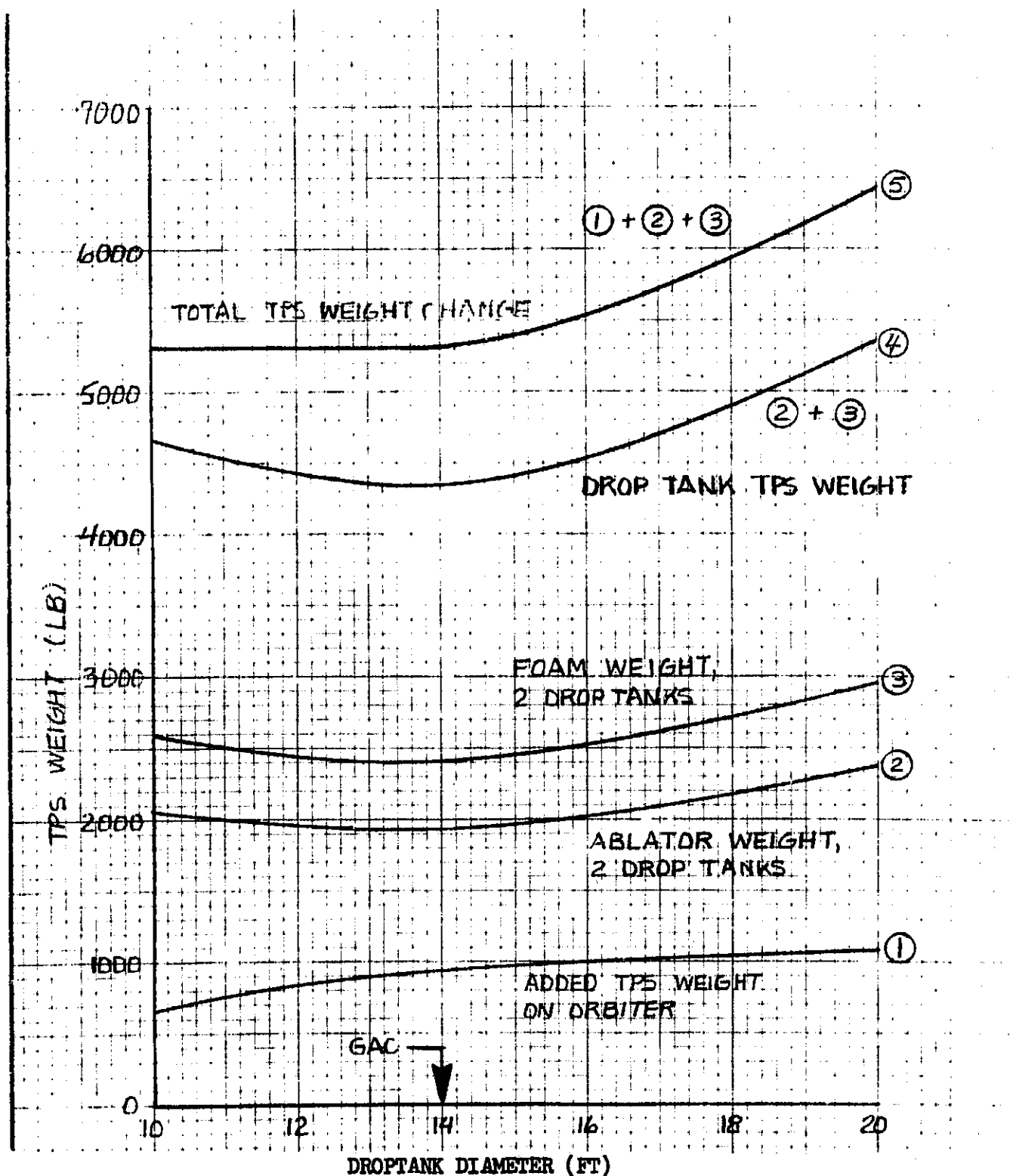
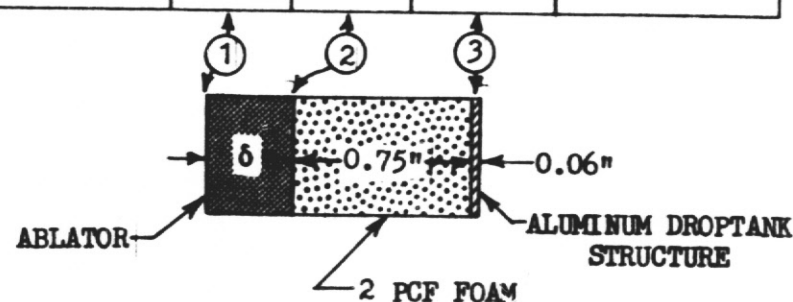


Figure 9 Droptank TPS Weights (Two Tanks)

Table 1

ABLATOR ANALYSIS RESULTS

Ablator Description	Density (pcf)	δ Thickness (inches)	% Weight Loss During Ascent	Max Temperature ($^{\circ}$ F)			Adequate Thermal Protection
				①	②	③	
Cork (Armstrong 2755)	30	0.25	~ 1	635	250	-300	Yes
TBS-757A; Silicon Ablator LMSC's Modification of RTV-757	32	0.25	< 1	685	470	-253	Marginal
Phenolic Nylon; filled with Phenolic Micro-Balloons	34.5	0.25	$\ll 1$	615	330	-281	Yes
Purple Blend; NASA/Langley Silicon Ablator	41	0.18	$\ll 1$	652	491	-242	Marginal
DC-325; Silicon Elastomer, High Temperature Capability	54	0.14	< 1	760	665	-194	No



EM NO: L2-12-01-M1-7
DATE: 11 May 1971

Space Shuttle Project

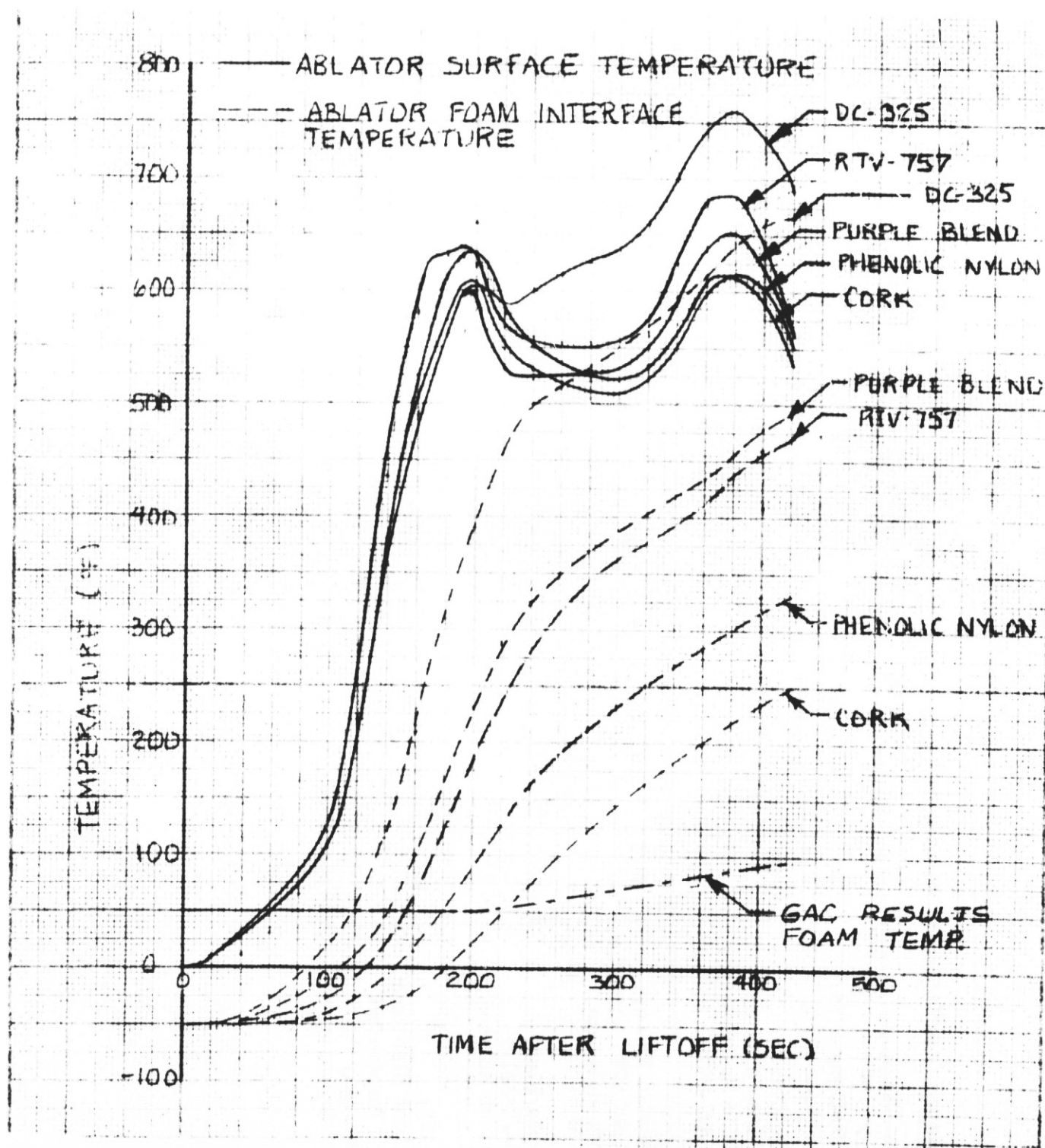


Figure 10 Droptank Ablator Temperatures

ENGINEERING MEMORANDUM

TITLE: GAC DROPTANK STABLE REENTRY ABLATOR REQUIREMENTS	EM NO: 12-12-01-M1-10 REF: 12-12-01-P1 DATE: 18 June 1971
AUTHORS: K. W. McGee <i>K.W. McGee</i>	APPROVAL: ENGINEERING SYSTEM ENGRG <i>R. A. Byers</i>

PROBLEM STATEMENT

Evaluation of various Grumman (GAC) droptank reentry modes has shown that the tank tends to stabilize at total angles of attack (η) greater than 0 deg instead of tumbling throughout reentry as previously assumed. In order to fully analyze the stable reentry modes, ablator thicknesses required to protect the tank for intact entry must be known.

RESULTS

For reentry with the droptank stabilized at $\eta = 5$ deg, cone first, 0.42 in. of cork is required on the conical section and 0.23 in. on the cylindrical section to protect the tank for intact impact. For reentry with the droptank stabilized at $\eta > 20$ deg, 0.42 in. of cork is required over the entire tank. Total thermal protection system weight (foam insulation and cork) is 7545 lb for $\eta = 5$ deg reentry and 10,783 lb for $\eta > 20$ deg reentry.

ANALYSIS

The GAC external droptank orbiter is shown in Fig. 1 (Ref. 1). All required ascent LH_2 is carried in the external droptanks, which are jettisoned in orbit. The orbiter overall length is 157 ft with a 106 ft wingspan and 55 deg leading edge sweep. The baseline droptanks are 15 ft in diameter and 94 ft long with an LH_2 capacity of 13,900 cubic ft per tank. The droptank forward cone semi-apex angle is 15 deg. The altitude and velocity histories of the droptank for a stable, trimmed reentry trajectory are shown in Fig. 2. Retro rocket firing is at 0 sec with droptank impact at about 1500 sec. Retro rocket firing is at the apogee of the droptank orbit, 1638 sec after liftoff and 1218 sec after orbit insertion. Also shown in Fig. 2 is the assumed maximum total angle of attack (η , the angle between velocity vector and droptank centerline). Angle of attack values are not shown prior to 900 sec because the droptank has not yet stabilized after the de-orbit maneuvers. The droptank stabilizes at $\eta \leq 40$ deg at altitudes less than 200,000 ft. Radiation equilibrium temperature histories for the droptank conical and cylindrical sections for $0 \leq \eta \leq 20$ deg are shown in Fig. 3. These temperature histories were computed assuming constant η throughout reentry. Constant η reentry is not consistent with the droptank trajectories, but was done to simplify the calculations required. Maximum surface temperatures on the cylindrical section are 1200°F for $\eta = 0$ deg reentry and 2920°F for $\eta = 20$ deg reentry. Maximum surface temperature on the conical section is 2640 deg. The conical section temperature history was assumed invariant for all reentry angles.

Figure 4 shows cork ablator requirements to protect the tank for intact impact for the conical and cylindrical sections of the droptank. The thermal environment used to determine the ablator thickness was based on the average circumferential droptank heating to account for tank spinning. For reentry at $\eta = 5$ deg and

EM NO: 12-12-01-M1-10

DATE: 18 June 1971

assuming a 500°F bondline temperature limit at impact, 0.42 in. of cork is required on the conical section and 0.23 in. is required on the cylindrical section. Total TPS weight, including spray on foam insulation, bonding agent, and surface coating is 7545 lb for 2 tanks. For reentry at $\eta \geq 20$ deg, 0.42 in. of cork is required over the entire droptank. TPS weight is 10,783 lb for two droptanks.

Assuming stabilized reentry, intact entry for the GAC droptank is feasible. The lower TPS weight requirements at the smaller trim angles indicates the advantage of tank stabilization.

REFERENCE

1. Grumman Aircraft Company Brochure MSC-03804, SS-884.

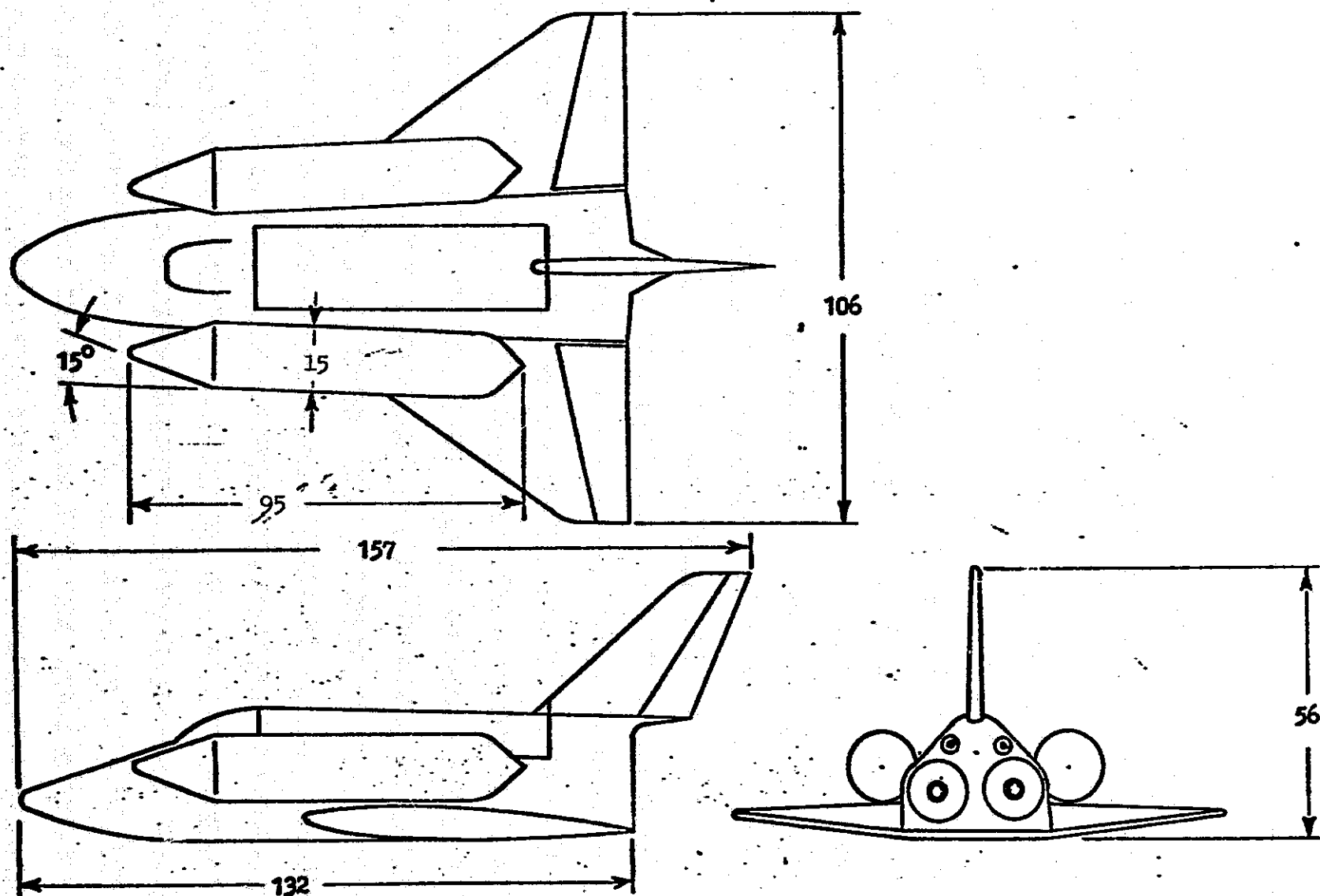


Figure 1 GAC External Tank Orbiter

EM NO. 12-12-01-M1-10

DATE 18 June 1971

PAGE OF

PREPARED BY

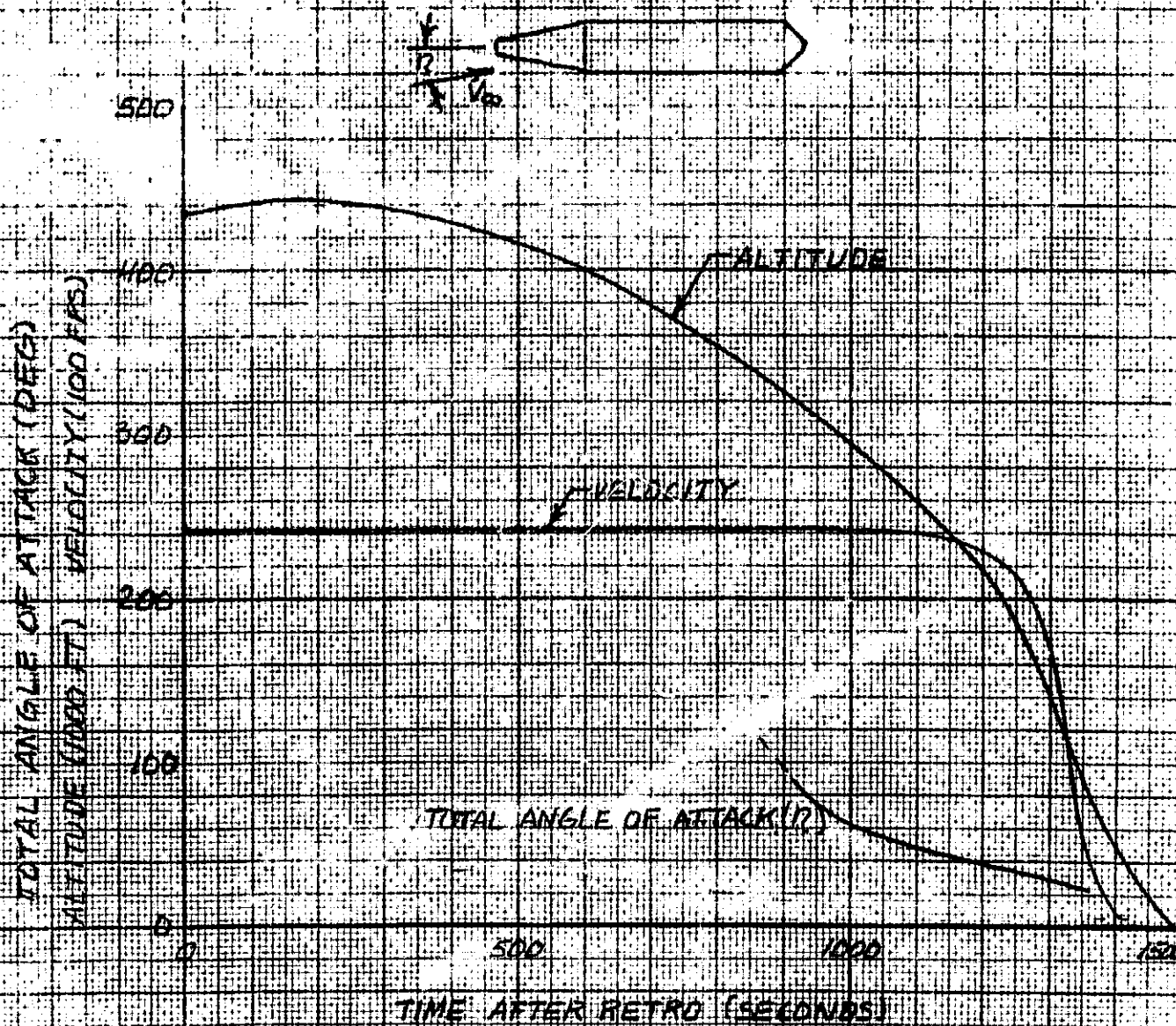


FIGURE 2 - DROP TANK STABLE REENTRY TRAJECTORY

EM NO. 12-12-01-M1-10

DATE 18 June 1971

PAGE OF

PREPARED BY

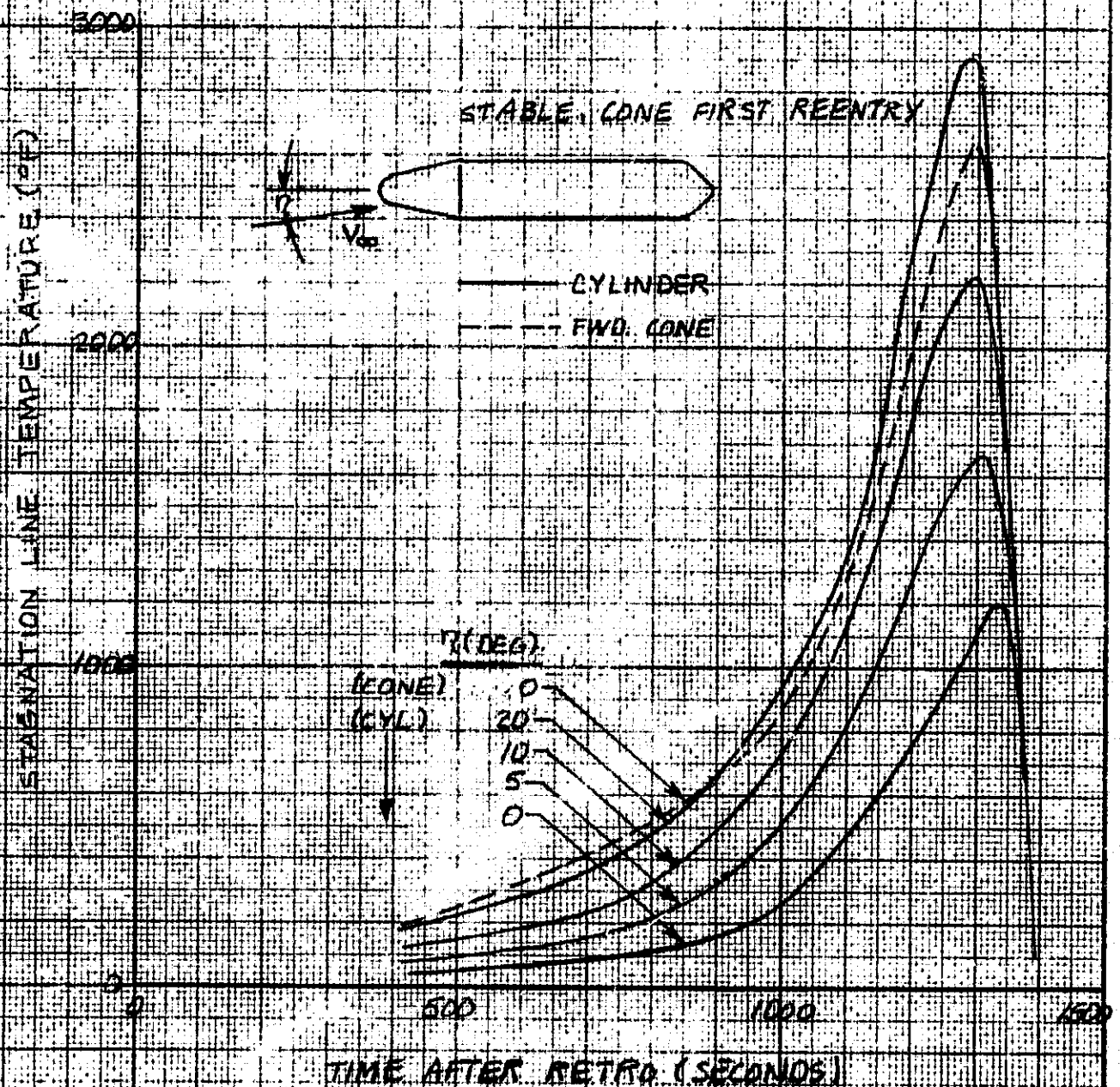


FIGURE 3- DROPTANK SURFACE TEMPERATURE HISTORIES

EM NO. 12-12-01-M1-10

DATE 18 June 1971

PAGE OF

PREPARED BY

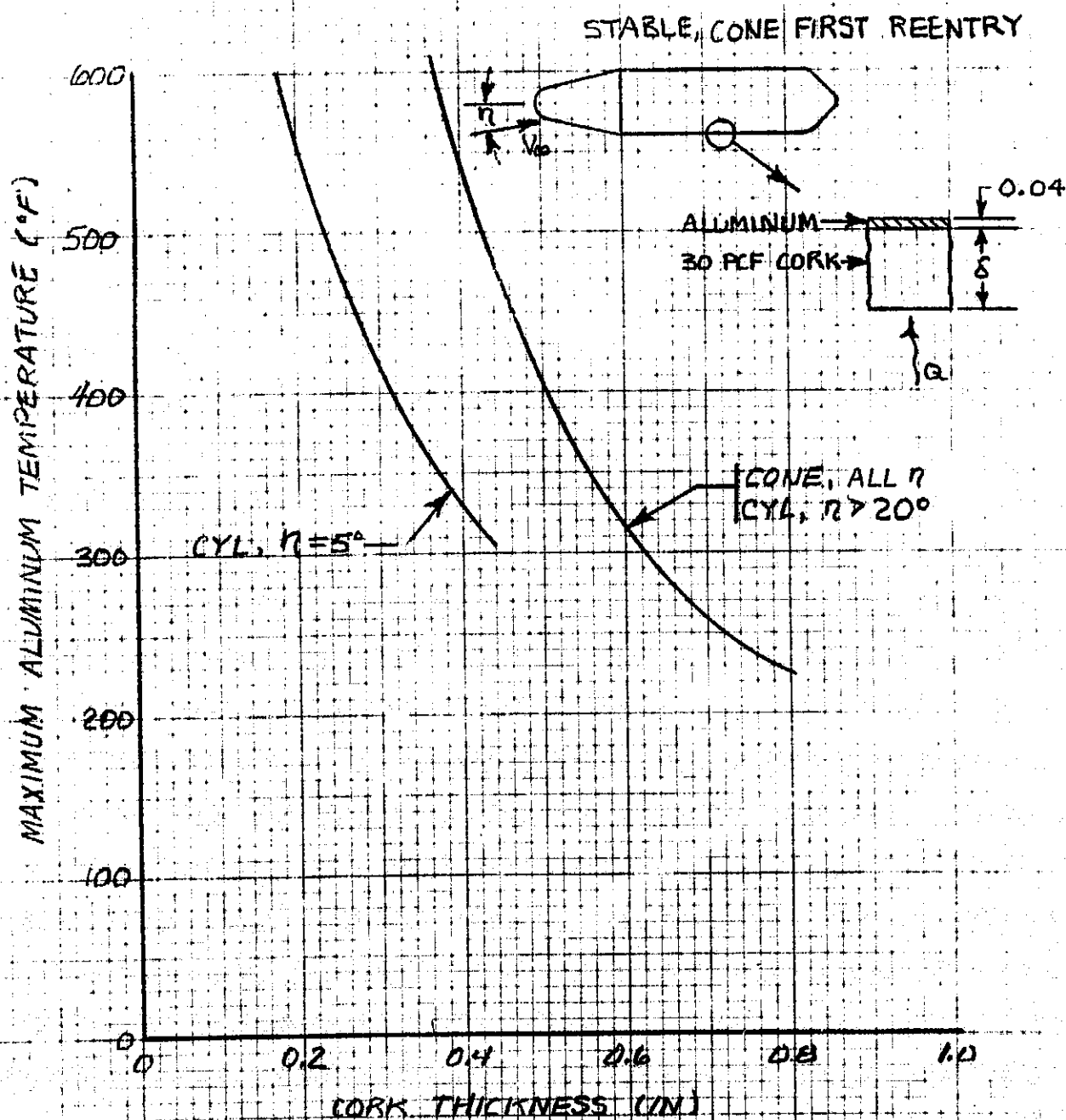


FIGURE 4 - STABLE REENTRY ABLATOR REQUIREMENTS

ENGINEERING MEMORANDUM

TITLE: DROPTANK PRESSURIZATION STUDY WITH ASCENT TPS	EM NO: L2-12-02-M1-2 REF: DATE: 18 June 1971
AUTHORS: R. M. Vernon/J. J. Gries <i>JJG</i>	APPROVAL: ENGINEERING SYSTEM ENGRG <i>R. A. Byers</i>

PROBLEM STATEMENT

To determine the effect of pressurization system design on the propellant tank and residual weights for tanks with thermal protection for ascent only.

RESULTS

Analyses indicate that the proposed pressurization/vent system provides a minimum of 4 psi NPSP throughout the propellant drain period without exceeding 26 psia ullage pressure at any time.

AFFECTED WORK BREAKDOWN STRUCTURE

Propellant Tank

Orbiter Pressurization System

Assumptions

The droptank configuration used in this analysis is shown in Fig. 1. A tank wall with a thickness of 0.057 in. was used and was assumed to be 2219 aluminum for thermal purposes. The insulation was 3/4 in. polyurethane foam with a thermal conductivity ranging from 0.0026 Btu/hr ft °R at 37°R to 0.022 Btu/hr ft °R at 600 °R.

DiscussionPressurizations Computations

The Asymmetric Propellant Heating Computer Program (1) was used to perform propellant heating, stratification and pressurization computations. The computer model treats a draining axisymmetric vessel with variable acceleration and allows for asymmetric heating effects. The liquid is treated in a stepwise-in-time manner and is stratified in horizontal layers due to assumed quasi-steady boundary layer flow along the heated vessel walls. The boundary layer flow is considered to be turbulent and includes wall heating as well as source (nuclear) heating. The asymmetric heating is treated by considering the vessel as a number of wedges about the vessel center-line. The pressurization is treated in a continuous manner and couples the ullage with the liquid and the wall through mass and/or energy transfer, and includes continuous or intermittent pressurizing or venting. The ullage region is considered to be a lumped system of mean properties as is the wall.

EM NO: L2-12-02-M1-2

DATE: 18 June 1971

For each specified time step, the program prints out a considerable amount of data including boundary layer characteristics, ullage conditions, pressurant and vented masses and properties of each liquid layer. During expulsion periods the properties of the drained propellant are also printed.

In the droptank study, the heat flux shown in Fig. 2 was applied to the tank wall. Input data for ascent acceleration and propellant flowrate are shown in Figs. 3 and 4 respectively. Table 1 presents the fixed input data and initial conditions. An engine bleed pressurization system to provide a constant flowrate of 0.5 lbm/sec of hydrogen at 500°R was assumed.

Analysis

Ullage pressure has a direct effect on tank weight and Fig. 5 shows ullage pressures for the droptank with 3/4 in. foam insulation. After venting the tank to 16 psia on the ground, the vent was closed at 50 seconds before lift-off. For safety reasons, the vent had to remain closed until 100 seconds after lift-off and there was a rise in ullage pressure as expected. However, venting was not required because the desired operating pressure level of 26 psia would not be reached until the engine starts operating and supplies pressurant gas. Very little gas was vented at this time since the expanding ullage during expulsion causes the ullage pressure to decrease. At 375 seconds after liftoff the ullage pressure was at a minimum as was the engine inlet pressure. The rise in pressure at the end of the burn was due to high wall heat fluxes resulting from the foam eroding away.

The pressures at the tank outlet and engine inlet show the effect of varying acceleration levels on the hydrostatic head developed in the liquid. During engine operation the lower engine inlet pressure reflects the pressure losses in the feed system. During the last 45 seconds of the burn, the propellant flowrate continuously decreased to maintain a constant acceleration of 3g. The resulting decrease in feedline pressure drop allowed the engine inlet pressure to surpass that of the tank outlet. The liquid temperature profiles (Fig. 6) show very little temperature rise of the bulk liquid during the first 180 seconds. The wall heat flux was small at this time but the boundary layer flow had already caused a substantial layer of warmed liquid on top. About half-way through the burn, the liquid delivered to the engine started to increase in temperature. However, all propellant entering the feedline remained below 39°R as shown by the temperature profile of the residual remaining at 422 seconds from liftoff. The minimum NPSP occurred just before engine shutdown when the propellant temperature was rising quite rapidly while the pressure at the engine inlet was increasing slowly. At shutdown the liquid at 38.9°R had a vapor pressure of 21.0 psia resulting in an NPSP of 4.6 psi based on an engine inlet pressure of 25.6 psia.

Lockheed Missiles & Space Company

Space Shuttle Project

EM NO: L2-12-02-M1-2

DATE: 18 June 1971

The residual vapor mass was about 220 lb. Earlier analyses with insulation thicknesses from $3/8$ to $1\ 1/8$ in. resulted in a variation of residual vapor with wall heating of less than 5%. However, the operating pressure in these cases was 23 psia which resulted in an NPSP too low for a suitable design.

References

1. Modular Nuclear Vehicle Study, Volume IV, Asymmetric Propellant Heating Computer Program, IMSC-A794909-A, 15 September 1968, Contract NAS8-20007

Table 1

Fixed Input Data For Pressurization Analyses

Propellant Loading, lbm	48,055 ⁽¹⁾
Total Tank Volume, ft ³	11,238 ⁽¹⁾
Initial Ullage Volume, ft ³	371 ⁽¹⁾⁽²⁾
Total Surface Area, ft ²	3,425 ⁽¹⁾
Initial Propellant Saturation Pressure (3), psia	17.0
Operating Pressure, psia	26.0
Ground Hold Duration, sec	100

Notes:

- (1) Values are per tank
- (2) Initial ullage includes vapor trapped during loading operation.
- (3) Saturation condition is at start of ground hold period.

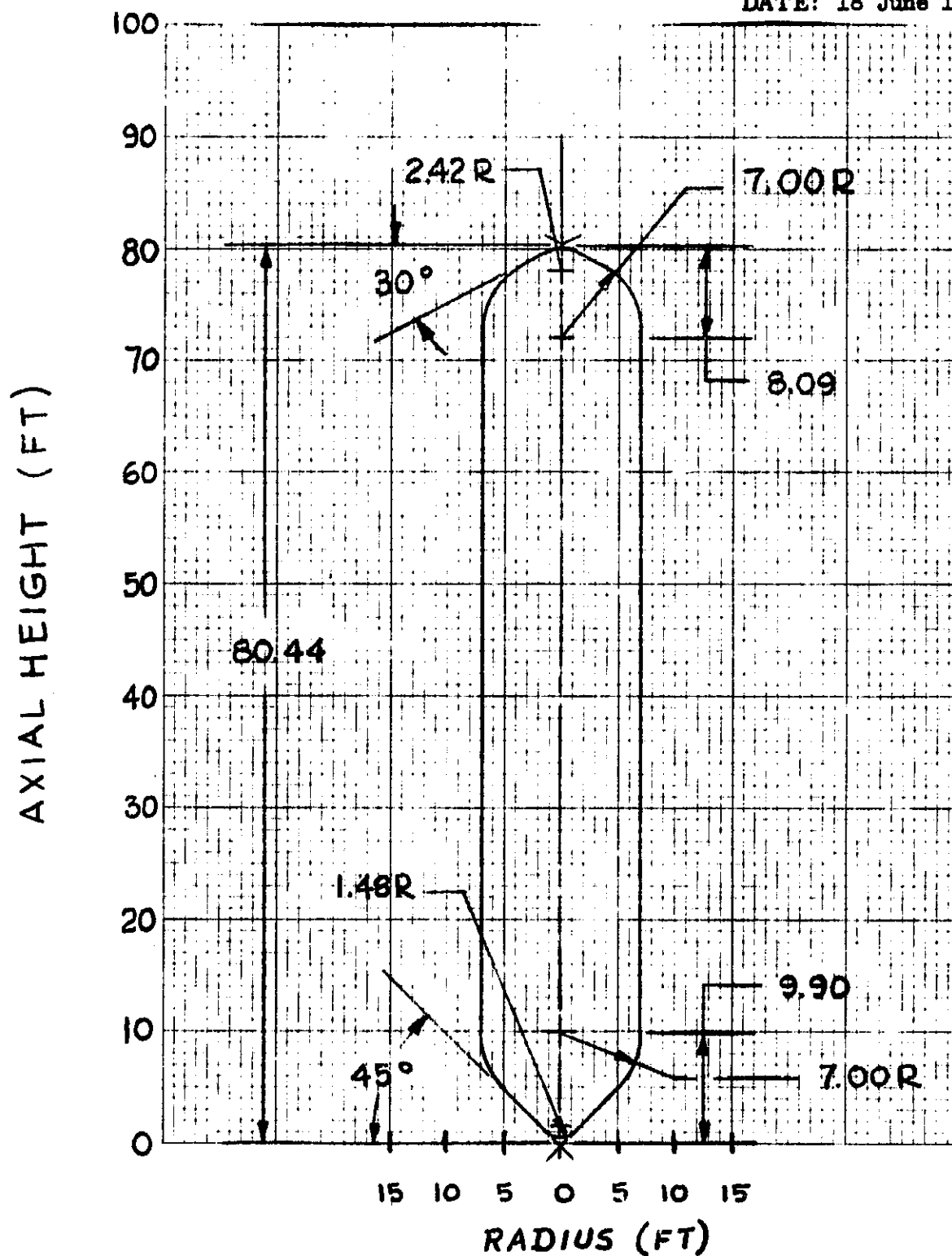
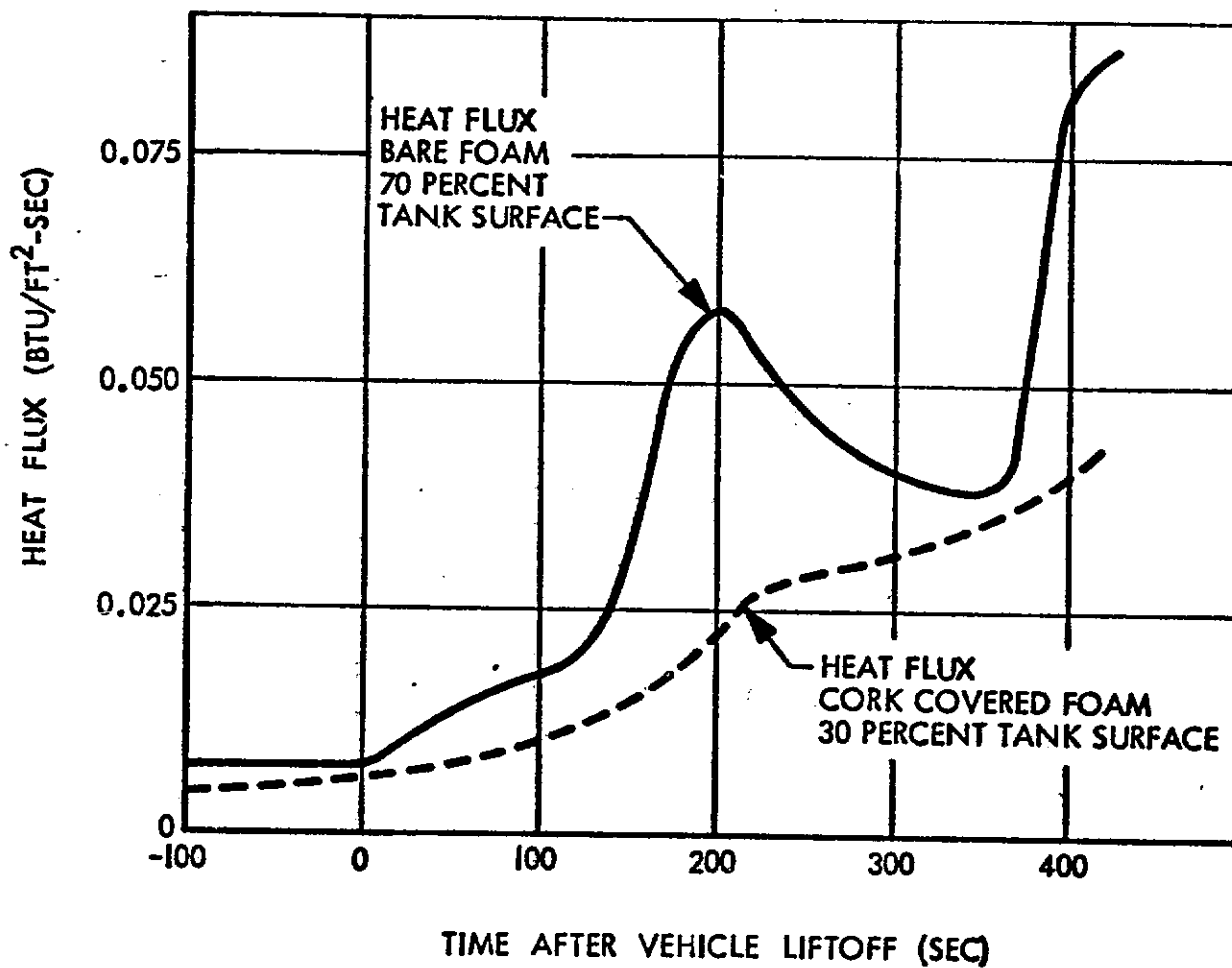


Fig. 1 External LH₂ Droptank Configuration

Fig. 2



LIQUID HYDROGEN DROPTANK WALL HEAT FLUX - 3/4 IN. EXTERNAL FOAM INSULATION



EM No. L2-12-02-M1-2
Date: 18 June 1971

DO3225

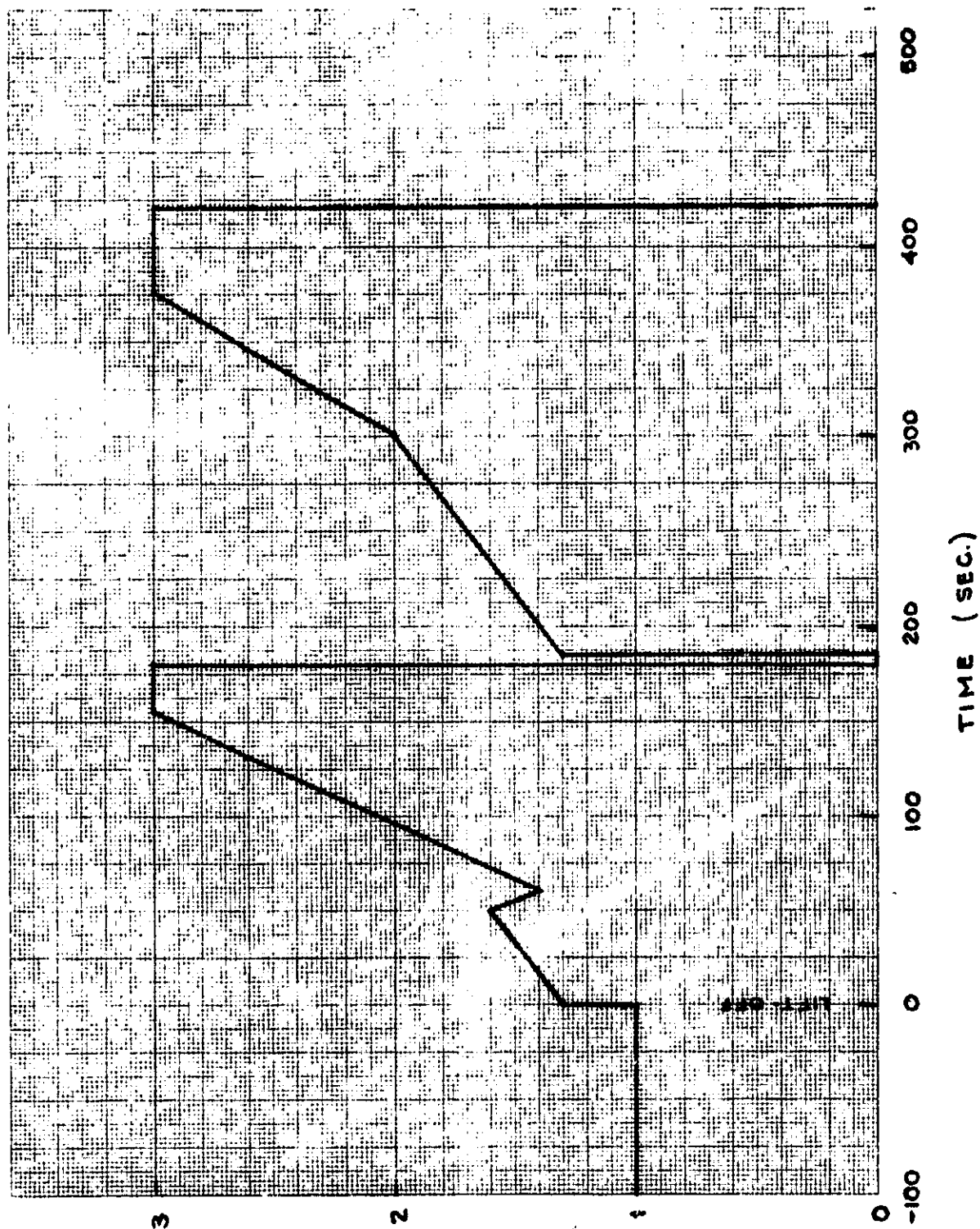


Fig. 3 Vehicle Acceleration History

ACCELERATION LOAD FACTOR (g)

Fig. 3

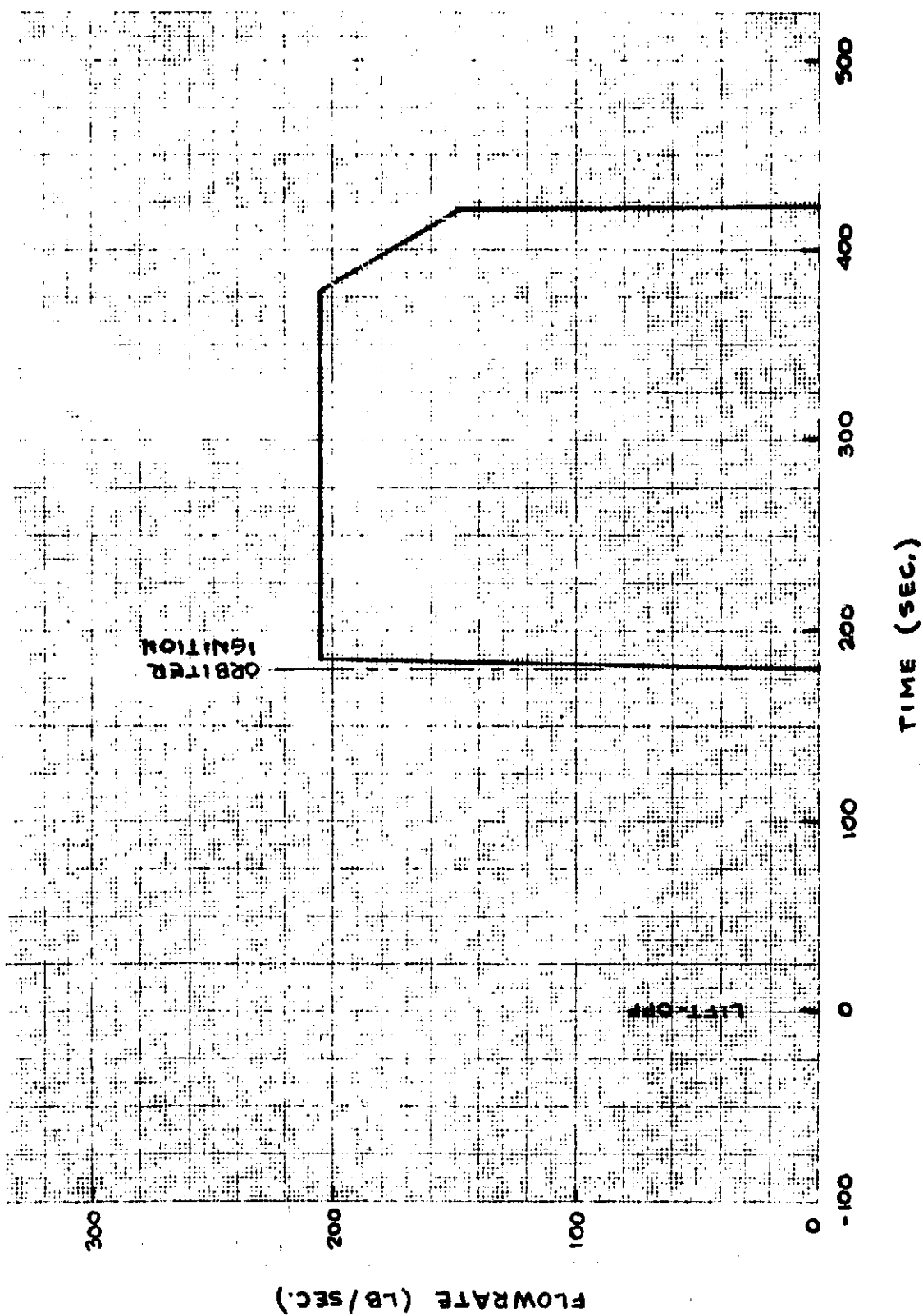


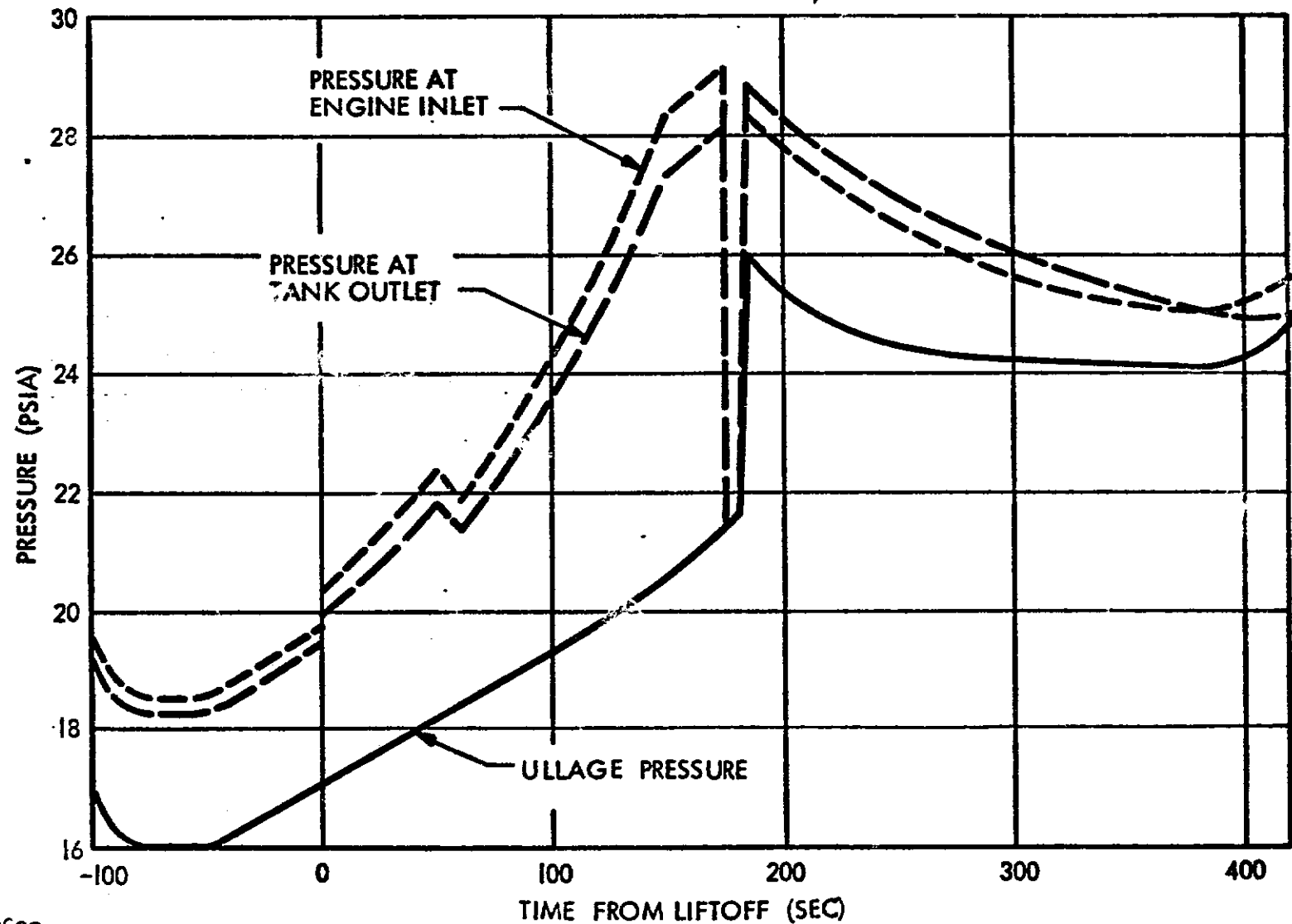
Fig. 4 Liquid Hydrogen Flowrate



Fig. 5

DROPTANK PRESSURE - TIME HISTORY

INSULATION THICKNESS - 3/4 IN.



EM No. 12-12-02-M1-2
Date: 18 June 1971

D03523



Fig. 6
LIQUID TEMPERATURE PROFILES
INSULATION THICKNESS - 3/4 IN.

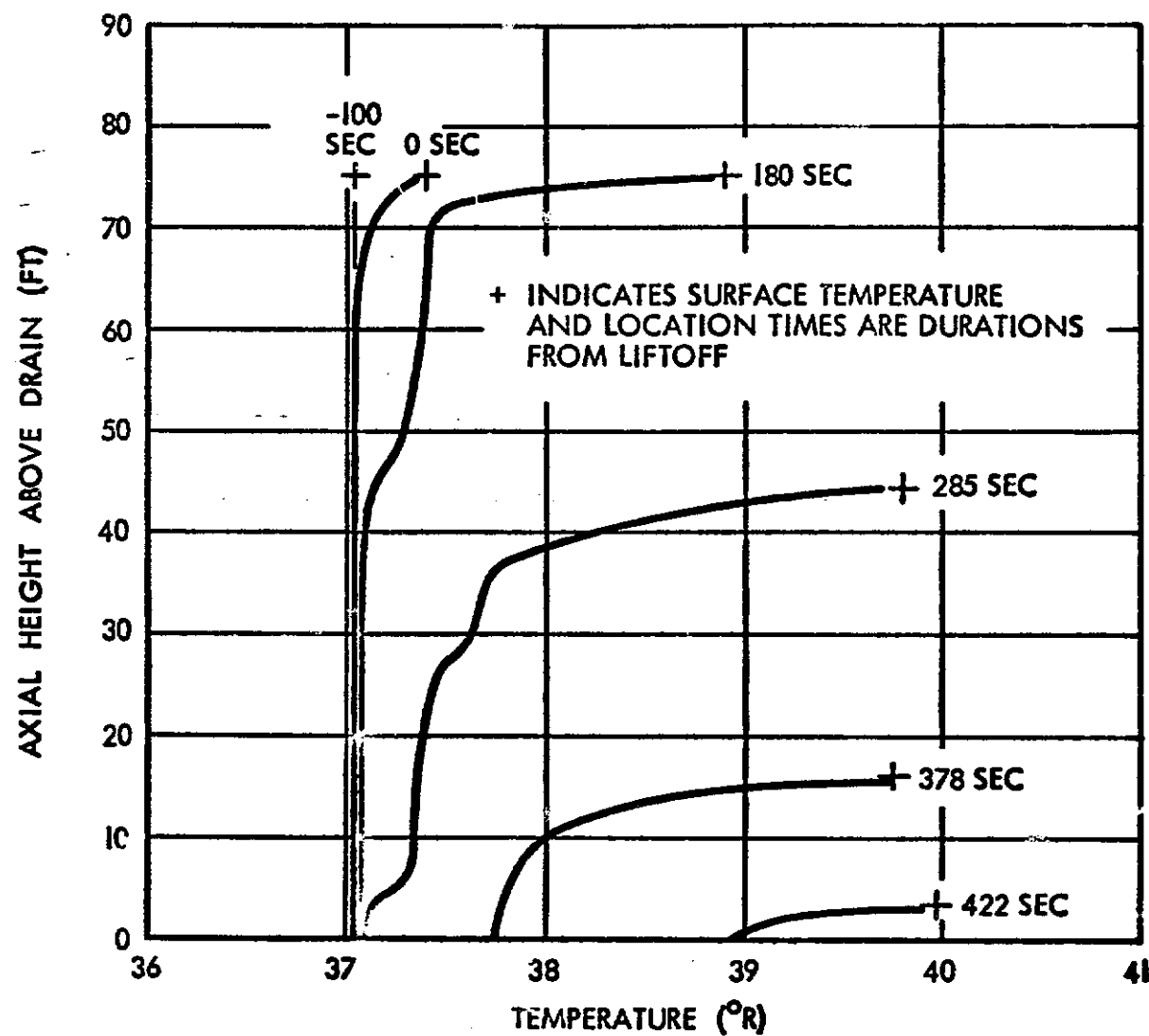


Fig. 6

DM No. 12-12-02-M-2
18 June 1971

EC3824

ENGINEERING MEMORANDUM

TITLE: ORBITER EXTERNAL LH ₂ DROPTANK FUNCTIONAL SCHEMATIC, CONTROLS AND INSTRUMENTATION	EM NO: L2-12-03-M1-1 REF: DATE: 18 June 1971
AUTHORS: R. E. Gaura <i>R. E. Gaura</i>	APPROVAL: ENGINEERING SYSTEM ENGRG <i>R. A. Byers</i>

PROBLEM STATEMENT

To show system functional schematic, indicating location and complexity of hardware required to meet operational and redundancy requirements.

To show schematically the automatic control loops of the system and the complexity inherent in providing fail safe/fail operational capability.

RESULTS AND WORK BREAKDOWN ELEMENTS

The followings figures and accompanying discussion thereof essentially constitute the results of the problem statement above.

Figure 1 - Droptank Vent and Pressurization System

Figure 2 - Droptank Feed and Circulation System

Figure 3 - Control Logic Schematic For Recirculation Pump(s) Inlet Valves

Figure 4 - Controls Schematic For Helium Prepressurization

Figure 5 - Controls Schematic For Helium Regulation

Figure 6 - Controls Schematic For Tank Venting

Figure 7 - Fail Safe/Fail Operational Control Circuit For Quad-Redundant Analog Sensors

Figure 8 - Fail Safe/Fail Operational Logic Control Circuit For Quad-Redundant Pressure Switch Assembly

Figure 9 - Timer Commanded Events

DISCUSSION

The location of system hardware was influenced strongly by the need to minimize the amount of hardware jettisoned. Therefore, as much of the hardware as possible is located on the orbiter side without compromising the operational requirements of the system. An effort was also made to minimize system weight, length of lines, and system complexity - while meeting the fail safe/fail operational requirements.

Squib-actuated valves were selected for one-shot applications, thus taking advantage of the high reliability and power/weight ratio inherent in squib actuators.

Quad-redundant sensors are used throughout except for the optical type liquid level point sensors. Single optical sensors are mounted at the following volumetric levels

in each tank; 2%, 3%, 10%, 20%, 30%, 40%, 50%, 60%, 70%, 80%, 90%, 91%, 98%, 99%, and 101% - with four sensors at the 1% and 100% levels.

Post-separation tank venting is accomplished by squib actuating valves 5VO1 and SV02 open, via a sequence timer command, so that relief valves RV01 and RV02 will maintain the tank pressures below the level required during reentry of the tanks.

All fluid lines, on the orbiter half of the droptank-orbiter interface, will be closed to minimize venting after separation.

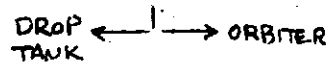
In addition to the automatic control loops, there are various control functions based on ground command, guidance computer commands, and droptank sequence timer commands.

The following Table 1 can be used in conjunction with Figures 1 thru 9 to analyze system operation.

Table 1
System Operation Analysis

Component or Subsystem	Condition
SV01 and SV02	Closed until post-separation pyro actuation.
RV01 and RV02	Inactive until SV01 and SV02 actuated.
SV03 and SV04	Normally open until pre-separation command from guidance computer.
PS01 and VV01 thru VV06	See Figure 6. Active from Start of Fill to Separation.
PS02 and VV07 thru VV12	
P1 and HV01 thru HV06	Active during Ground Pre-pressurization Operation only (Figure 4).
P2 and HV02 thru HV12	
P3 and HSV1 — HSV3	Active from Start of Fill Operation thru Separation (Figure 5).
Liquid Level Sensors	Active from Fill thru Separation.
SV06 thru SV10	Normally open - Pyro actuated closed prior to separation via orbiter guidance computer.
FV01 and FV02	Open only during Fill Operation
FV03 and FV04	Normally open - Pyro actuated close upon completion of Fill.
IV01 and IV02	Open from Start of Fill to Engine Off Command.
P ₀ and V1 — V9	Active from Start of Fill up to Engine Start Command (Figure 3).

L2-12-03-M1-1
16 June 1971



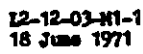
-4-

Inlet Control Valves - For Recirculation Pumps. (See Figure 3)

To insure the fail-safe/fail-operational requirement - the (9) valve configuration was selected. The purpose of these valves is to assure proper flow and shutoff of LH_2 to the recirculation pumps upon command.

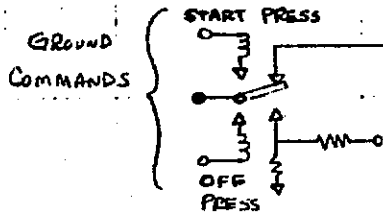
OPERATIONAL SEQUENCE

1. Start the fill operation with the first set of valves (V1, V2, V3) and the output transducer (P_o /control logic activated. The remaining (6) valves are inhibited at this time with V4, V5, V7 and V8 in the closed position.
2. Valves V1, V2 and V3 remain open until the engine start command is received and the fill command removed.
3. If a failure occurs in which V1 and V2 fail to control flow properly - the resulting low or high output from the redundant P_o circuit will disable the first set of valves by closing V3 and will activate the next set of valves (V4, V5, V6). This meets the fail operational requirement.
4. If V4 and V5 fail to control flow properly - V6 will be similarly actuated closed and the last set of valves (V7, V8 and V9) will be activated to provide the control function. This then satisfies the fail safe requirement.
5. The pump motors are ON when valves are open, and OFF when valves are closed.



**Figure 3 - Control Logic Schematic For Recirculation Pump(s)
Inlet Valves**

18 June 1971

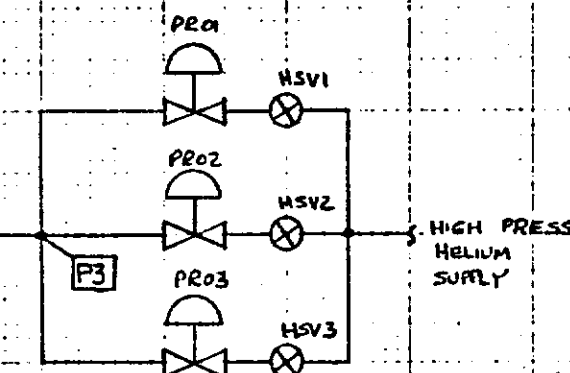
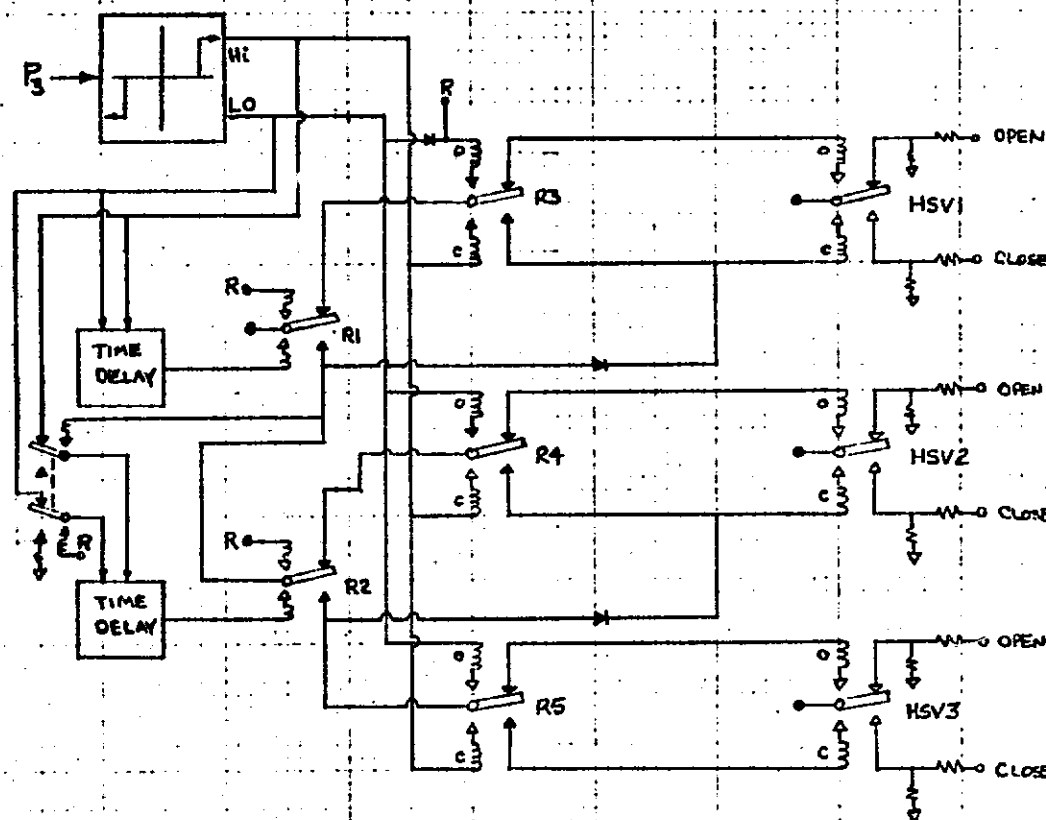


HELIUM PRE-PRESSURIZATION CONTROLS

1. Upon initiation of the start pressurization command, the control circuit for HVO1 and HVO2 is activated and the output of P1 will command HVO1 and HVO2. ON/OFF to maintain the tank helium pressure within the desired limits.
2. An out of limits (Hi or Lo) output from P1 that persists longer than the design time interval - will command HVO1 and HVO2 closed and activate HVO3 and HVO4.
3. Similarly, an out of limits (Hi-or Lo) output from P1 will command HVO3 and HVO4 closed and activate the last set of valves HVO5 and HVO6.

Figure 4 - Controls Schematic For Helium Prepressurization

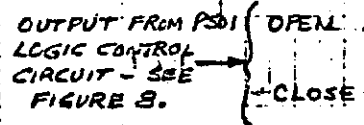
12-12-03-H1-1
18 June 1971



HELIUM REGULATION CONTROLS

1. The start of operation begins with a reset (R) command which opens HSV1, closes HSV2 and HSV3, and sets the various relays for subsequent FAIL SAFE-FAIL OPERATIONAL SEQUENCING.
2. If HSV1 and/or P301 fail in such a manner so as to cause an OUT-OF-TOLERANCE output from the P3 pressure transducer Output Circuit (HI or LO) - HSV1 will be commanded closed and HSV2 commanded open. HSV3 remains closed. This then meets the fail operational requirement.
3. If HSV3 and P302 fail to provide proper regulation - HSV2 is similarly commanded closed and HSV3 commanded open. This then provides the fail safe capability.

Figure 5 - Controls Schematic For Helium Regulation



VENT VALVE CONTROLS

1. Operation begins with application of 28vdc power to system and a reset (R) command which closes VV01, VV02, VV03 and VV04, and sets the logic control relays for subsequent operation.
2. If VV01 and VV02 fail to provide the proper pressure levels in tank after a pre-selected time interval - VV03 will be actuated closed and VV04 and VV05 activated to control the tank pressure level.
3. If VV04 and VV05 fail to provide the proper pressure levels - VV06 will be actuated closed. This then leaves the burst disc (BD01) and relief valve RV03 to provide the pressure control of the tank pressure.
4. Each LH₂ tank has separate and identical pressure control capability.

Figure 6 - Controls Schematic For Tank Venting

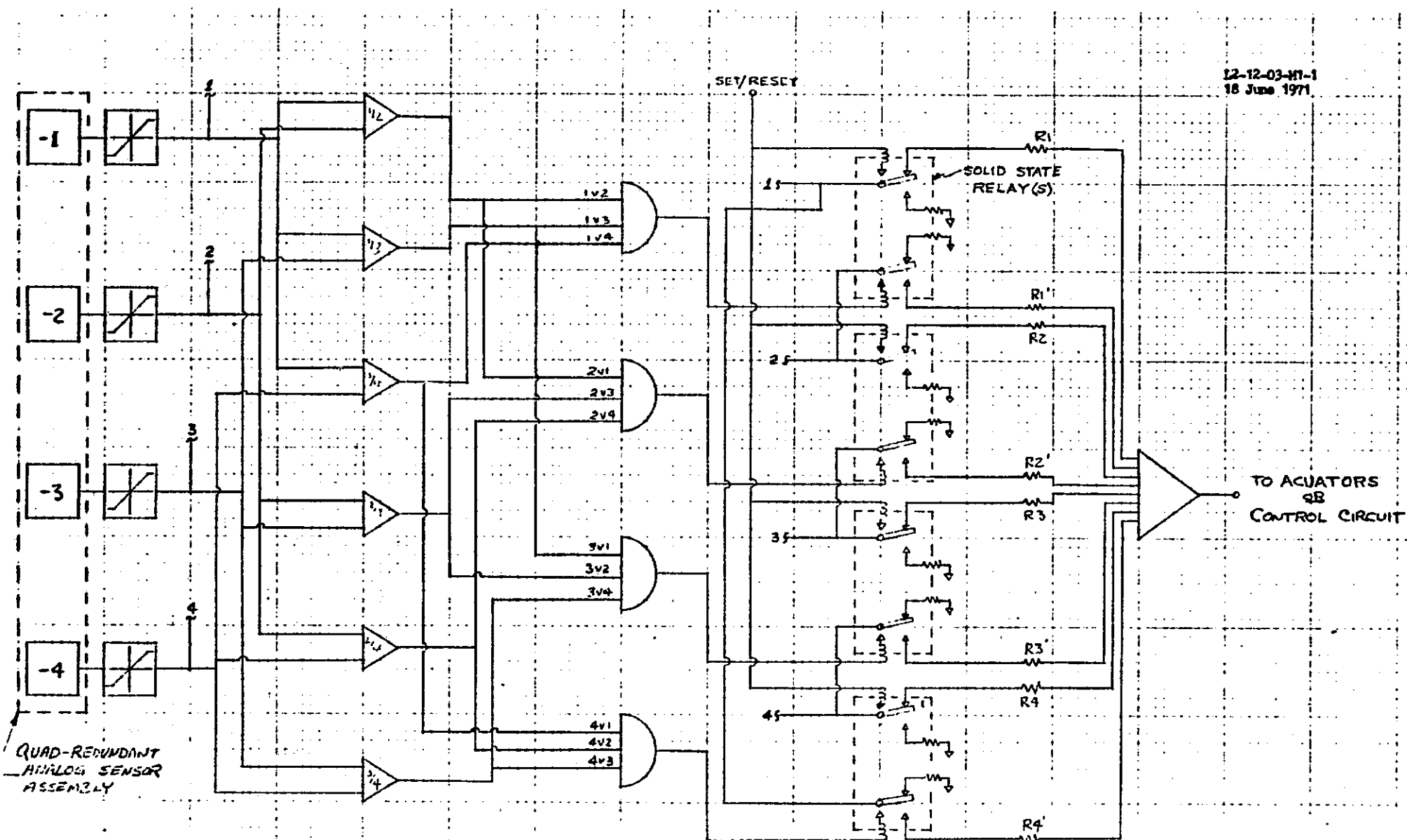


Figure 7 - Fail Safe/Fail Operational Control Circuit
For Quad-Redundant Analog Sensors

12-12-03-M1-1
18 June 1971

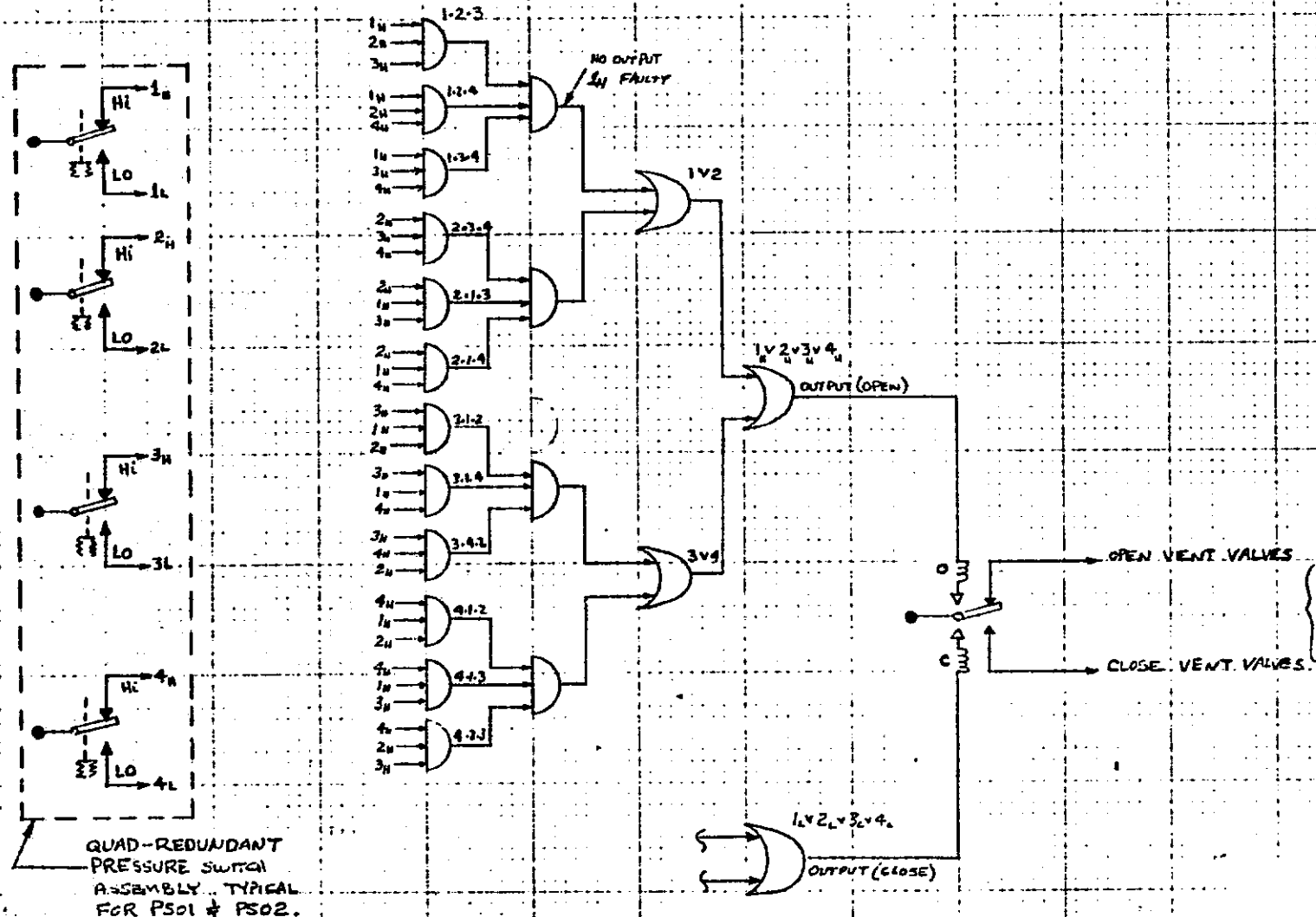


Figure 8 - Fail Safe/Fail Operational Logic Control
Circuit For Quad-Redundant Pressure Switch
Assembly

L2-12-03-M1-1
18 June 1971

GUIDANCE COMMANDS/TIMER

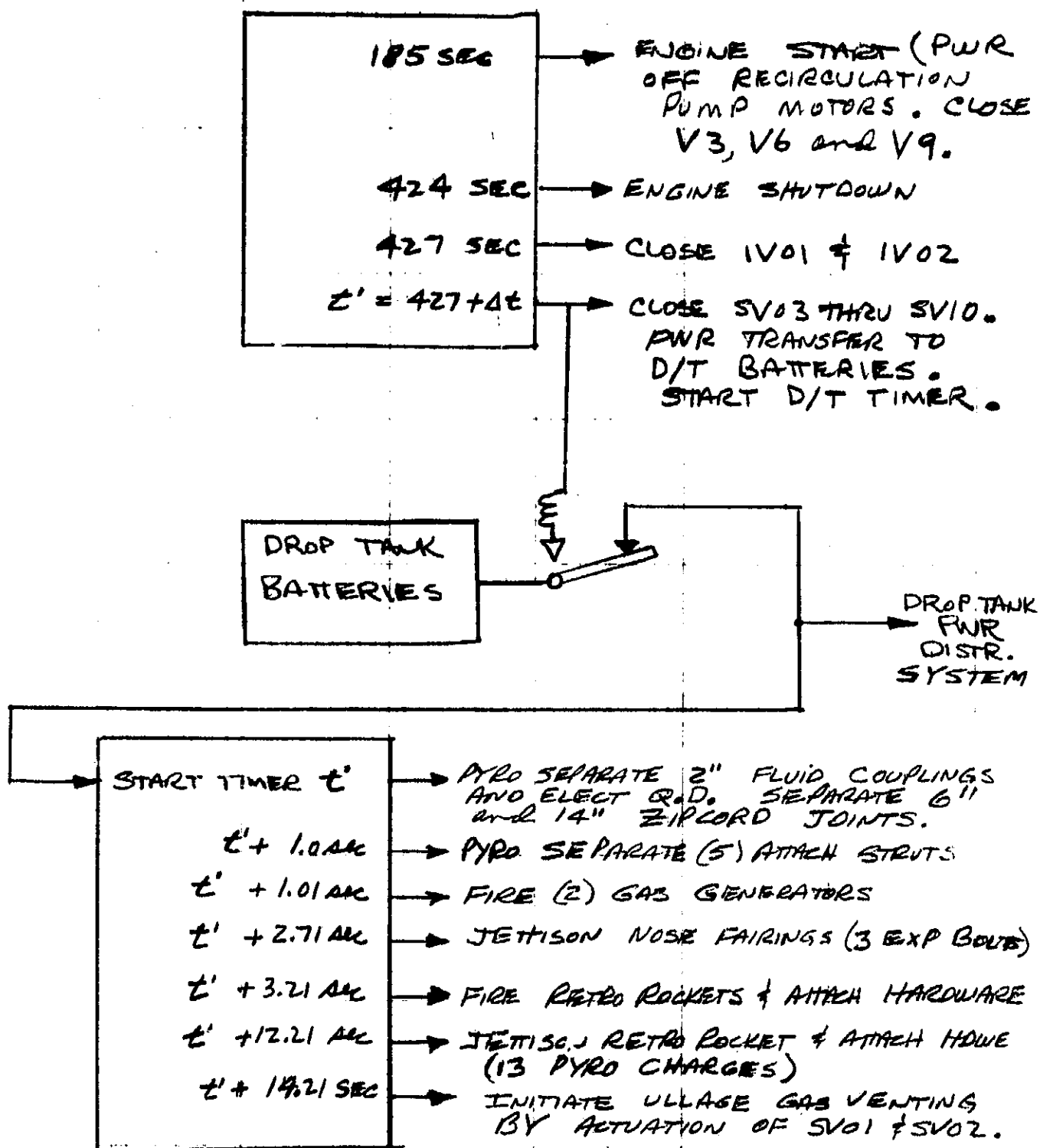


Figure 9 - Timer Commanded Events

ENGINEERING MEMORANDUM

TITLE: ORBITER EXTERNAL LH ₂ DROPTANK EVENT TIMING CONCEPT	EM NO: L2-12-03-M1-2 REF: DATE: 16 June 1971
AUTHORS: P. T. Harper <i>P.T. Harper</i>	APPROVAL: ENGINEERING SYSTEM ENGRG <i>R. A. Byers</i>

PROBLEM STATEMENT

To provide a means of firing the orbiter tank retro rocket including associated timed events for assuring tank dispersion over the chosen target area.

Affected work breakdown structure:

Orbiter
Orbiter External LH₂ Tank

RESULTS

This EM describes a method of checking droptank angular velocity and attitude prior to, and as a condition upon, firing of the retro rocket. It investigates methods of checking attitudes of the droptank and concludes that a minimal check system is required to assure safety to the orbiter.

Assumptions:

1. Tanks jettisoned between 50 and 100 nm during coast
2. Both tanks separated from orbiter simultaneously
3. Typical sequence of timed events from the initiation of separation (t_s) employed. (At t_s minus 2 sec, the droptank electrical system is transferred over to the droptank battery from orbiter power. All propellant system events have been completed (See EM L2-12-03-M-1). Actual separation initiation is done by the guidance computer:

$t_s = 0$ Pyro separate 2-in. fluid and electrical
quick disconnects. Separate zipcord joints

$t_s = 1$ sec Pyro separate (5) attachment struts

$t_s = 1.01$ sec Fire (2) gas generator charges

$t_s = 2.71$ sec Jettison nose fairing (3 explosive bolts)

- $t_g = 3.21$ sec Fire retrorocket and separate attach hardware
- $t_g = 12.21$ sec Jettison retrorocket and attach hardware (13 pyrocharges)
- $t_g = 14.21$ sec Initiate ullage gas vent
4. Tanks attached to orbiter at two points: near tank nose and tail. Separation thrust provided by two gas generators at these points
 5. Tanks should be a minimum of one tank length away from orbiter at retrorocket firing, if possible.
 6. High acceleration ejection (order of 5 g) preferred over low g ejection
 7. Tanks ejected with impact of 56,000 lb for 0.2 sec (11,320 ft-sec) provided by gas generators
 8. To hit target area, the total error in attitude of the tank longitudinal axis from desired trajectory should be within ± 3 deg at retro ignition. Present angular velocity in ejection plan to attain this is assumed to be 3 deg/sec maximum
 9. Desirability of a minimum system aboard the tank that has high probability of the tank reaching the dispersion area while satisfying minimum safety constraints
 10. As further investigation reveals safety enhancement to be desirable, further sophistication can be added.

Discussion

Probable approaches to solving the problem:

- 1.0 A basic approach to the problem is to start a timer aboard each tank at the time of initiating the separation sequence. The timer runs through its timing sequence, and the retrorocket motor fires at $t_g = 3.21$ sec.

This approach assumes the attitude of the tank never exceeds the maximum error angle described in Assumption 8.

- 2.0 A second approach is to ascertain error in the rotation of the tank from alignment in one-degree-of-freedom. That is, rotation in the plane-of-ejection due to unequal forces of ejection at the two ends of the tank would be the most probable source of alignment error. Using accelerometers or other means to check that rotation in this plane is within limits as a constraint upon the timer firing the retrorocket is a further refinement over 1.0 above. If limits were exceeded, a further refinement of the system would be necessary to determine the time of ignition.

EM NO: L2-12-03-M1-2
DATE: 16 June 1971

- 3.0 An additional refinement is to use another set of two accelerometers to check the longitudinal axis rotation at 90 deg from the rotation error mentioned in 2.0. Again, in conjunction with the timer, firing of the retrorocket is inhibited if either set of accelerometers indicates that acceptable rotation error has been exceeded. (See Par. 2.0)
- 4.0 Going to a stable platform with a gyro aligned prior to separation and with accelerometers checking all degrees of rotational freedom is an additional step in refinement. If alignment error is exceeded, again the timer firing of the retrorocket is inhibited. (See Par. 2.0)
- 5.0 A further refinement in 2.0, 3.0 and 4.0 is to allow the retrorocket to fire early - that is, before droptanks are one-tank length away from the orbiter but not less than some timed interval that assures a minimum distance from the orbiter, of say, 2/3-tank length, if the rotational errors that puts the tank in the dispersion area reaches its limit. Thus, timing limits exist, limiting nearness to the orbiter at which firing could take place, if angular velocity limits are reached. However, normal firing takes place at one-tank length from the orbiter if angular velocity limits are not exceeded.
- 6.0 As a backup to these methods, a UHF (or S-band) radio link can be used to manually over-ride firing of the retrorocket. Providing a manual inhibit mode controlled by the astronaut appears impractical if the time from actual separation to retrorocket firing is 2.2 sec as assumed. However, if a lower g separation with a velocity of say 10 feet per second were used, the astronaut could supply an additional safety factor by manually inhibiting firing in cases where it was obvious to the respective astronauts observing each tank that the safety of the orbiter was endangered by the attitude of the tank as it approaches retrorocket firing distance. Regardless of the inhibit possibilities, a UHF (or S-band) radio link can be used as a backup for firing of the retrorocket if it becomes obvious to the astronaut that the tank is continuing to deploy from the orbiter in normal fashion but the automatic firing of the retrorocket has failed. In connection with this aspect, some method of illumination along the length of the tank is required should the tank disposal occur in darkness. Lighting must be such that the astronaut will be able to ascertain attitude of the droptank by visual observation.

EM NO: 12-12-03-M1-2
DATE: 16 June 1971

Solution Considerations

Method 1.0 has the deficiency that no check is made on the actual angular velocity or attitude of the droptank before firing the retrorocket leading to the possibility of the tank becoming an impacting projectile. It would be highly desirable to go to some more sophisticated checks, as described in approaches 2.0 through 4.0, to assure that the attitude of tanks is within limits, from the standpoints of hitting the target area and safety to the orbiter itself. However, the increasing complexity of items 2.0 through 4.0 also represents increasing costs of a throwaway system. It is felt that using Method 2.0 for the present is adequate, because rotation in the ejection plane has the highest probability of error. Reference 1 shows that errors from roll in the proposed solution scheme, where angular velocity is checked at approximately 0.3 seconds after separation, would be minimal. If further study shows greater sophistication to be desirable as discussed in 5.0, (i.e., early firing of the retrorocket), it may be added to the proposed system by the addition of minimal hardware. In addition, if further study indicates a backup firing method is required, a UHF (or S-band) radio frequency link can be added with appropriate encoders and decoders.

Solution

The solution described here checks the angular velocity rate, based on translation time measurements, in the ejection plane, (i.e., a plane through the longitudinal axis of the two ejection chambers). The measurement is made at fixed distances from the orbiter after completion of the separation impulse. In addition, a check is made on the attitude of the droptank, assuming angular velocity = 0, and only translation is occurring.

The system to accomplish this is shown in block diagram form in Fig. 1. Main components of the system are two light-emitting diodes (LED) for light sources, the two phototransistor pickup sensors, the two 10-ft tapes onboard the tank (lead ends anchored on the orbiter), and the timer with arithmetic logic.

The metallic tapes are initially rolled up within a cylindrical container of large diameter or may simply be contained in straight tubular enclosures. As the tank deploys, the tapes are pulled out of their containers. Sensing holes are located just after the initial position of the sensors, say 1 in. away. At precisely 8 and 10 ft further down the tapes are precision holes that are sensed by the phototransistors causing the timer to read out into registers as the timer continues to count, (see Fig. 2). Precision of the measurements depends primarily upon the precision of the time base and mechanical precision of the sensing holes. Logic is used to calculate angular velocity and tank attitude in the ejection plane. The resulting values are compared against limits that allow the timer to fire the retro-rocket when both limit conditions are satisfied.

When the droptank is deployed, the timer will read out into register 1 when either one of the tapes causes the first hole to be sensed.

In addition, times t_2 and t_3 are read out at 8 ft and 10 ft on tape 1, and t'_2 and t'_3 for tape 2.

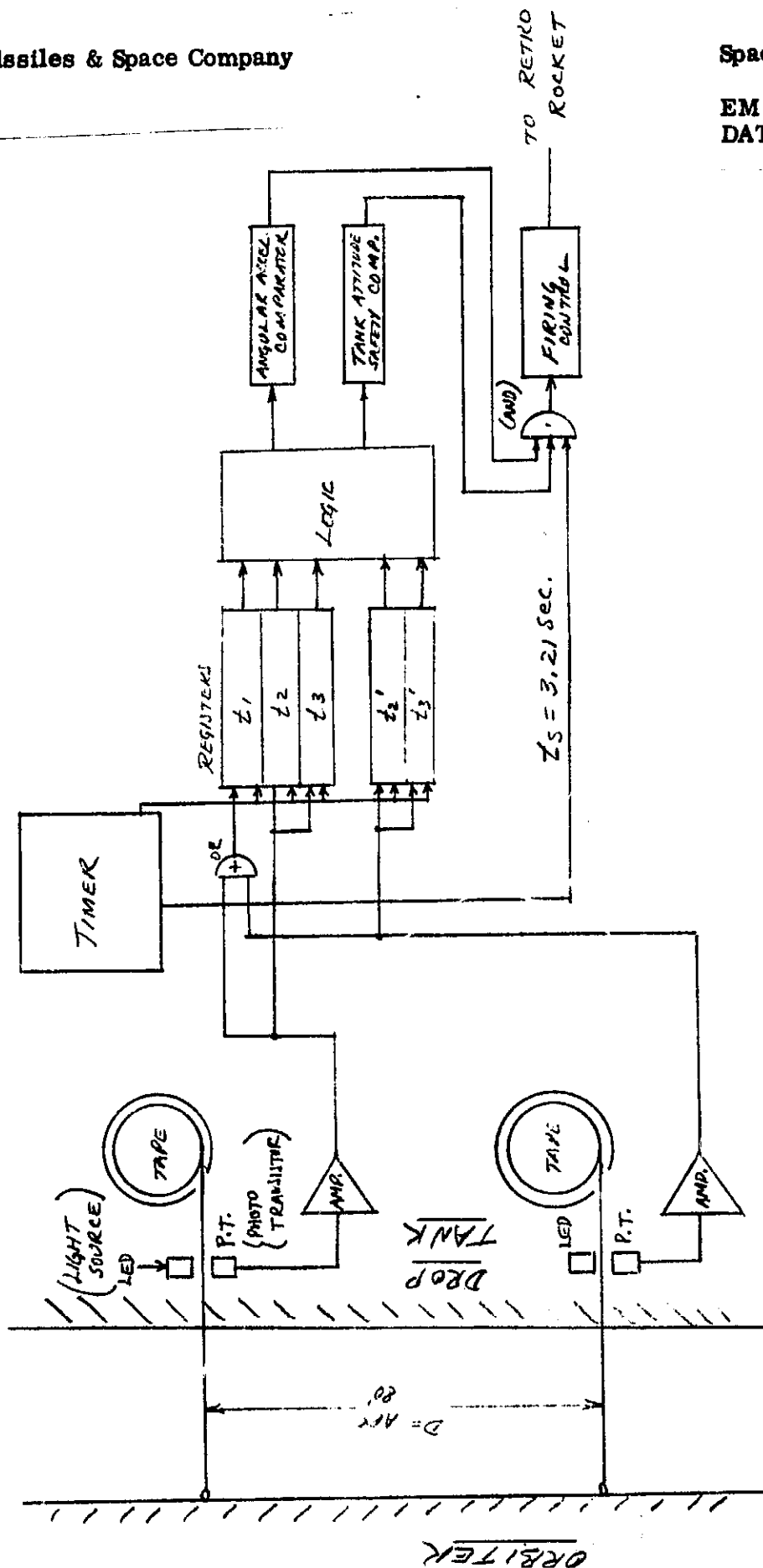


Figure 1

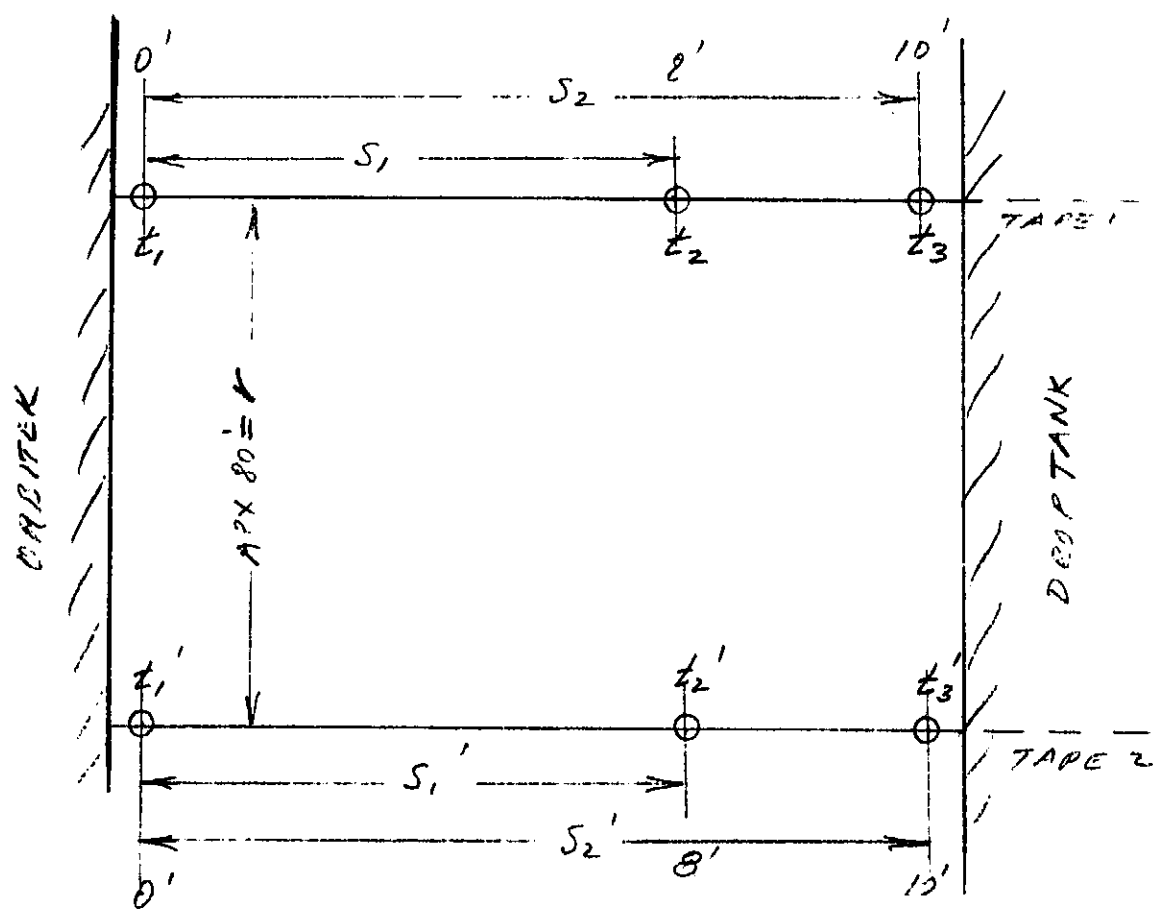


Figure 2

Lockheed Missiles & Space Company

Space Shuttle Project

EM NO: L2-12-03-M1-2

DATE: 16 June 1971

$$v_1 = \frac{s_2 - s_1}{t_3 - t_2} \quad \text{and} \quad v_2 = \frac{s'_2 - s'_1}{t'_3 - t'_2}$$

For $s_2 - s_1 = s'_2 - s'_1 = 2 \text{ ft}$,

$$r = 80 \text{ ft}$$

and where ω = tank angular velocity.

$$|v_2 - v_1| = \left| \frac{2}{t'_3 - t'_2} - \frac{2}{t_3 - t_2} \right| = r\omega$$

Assuming $\omega_{\max} = 2 \text{ deg/sec}$, then

$$2 \left[\frac{1}{t'_3 - t'_2} - \frac{1}{t_3 - t_2} \right] \leq \frac{80 \times 2}{57.3}, \left| \frac{1}{t'_3 - t'_2} - \frac{1}{t_3 - t_2} \right| \leq 1.4$$

A further check is made to ensure that, although the angular velocity is within limits, translation has not occurred that would exceed safety limits. This calculation assumes that angular velocity = 0 and only translation has occurred. See Fig. 3.

$$s_2 = s'_2 = 10 \text{ ft}, \quad v_2 = \frac{10}{t'_3 - t'_2} \quad \text{and} \quad v_1 = \frac{10}{t_3 - t_2}$$

Logic determines if $v_2 > v_1$ or $v_1 > v_2$.

Assume $v_1 > v_2$.

Then

$$\begin{aligned} ds &= v dt \\ ds &= v_1 (t'_3 - t'_2) \\ \theta &= \frac{ds}{r} \end{aligned}$$

REFERENCES:

1. Engineering Memo No. EM L2-05-02-M1-2
2. LMSC Report, "Study of Alternate Space Shuttle Concepts," Ninth Letter of Progress and Status Report, 1 Mar 1971 to 1 Apr 1971
3. Singer, F. L., "Engineering Mechanics," Harper and Brothers, 1943

Lockheed Missiles & Space Company

Space Shuttle Project

EM NO: 12-12-03-M1-2
DATE: 16 June 1971

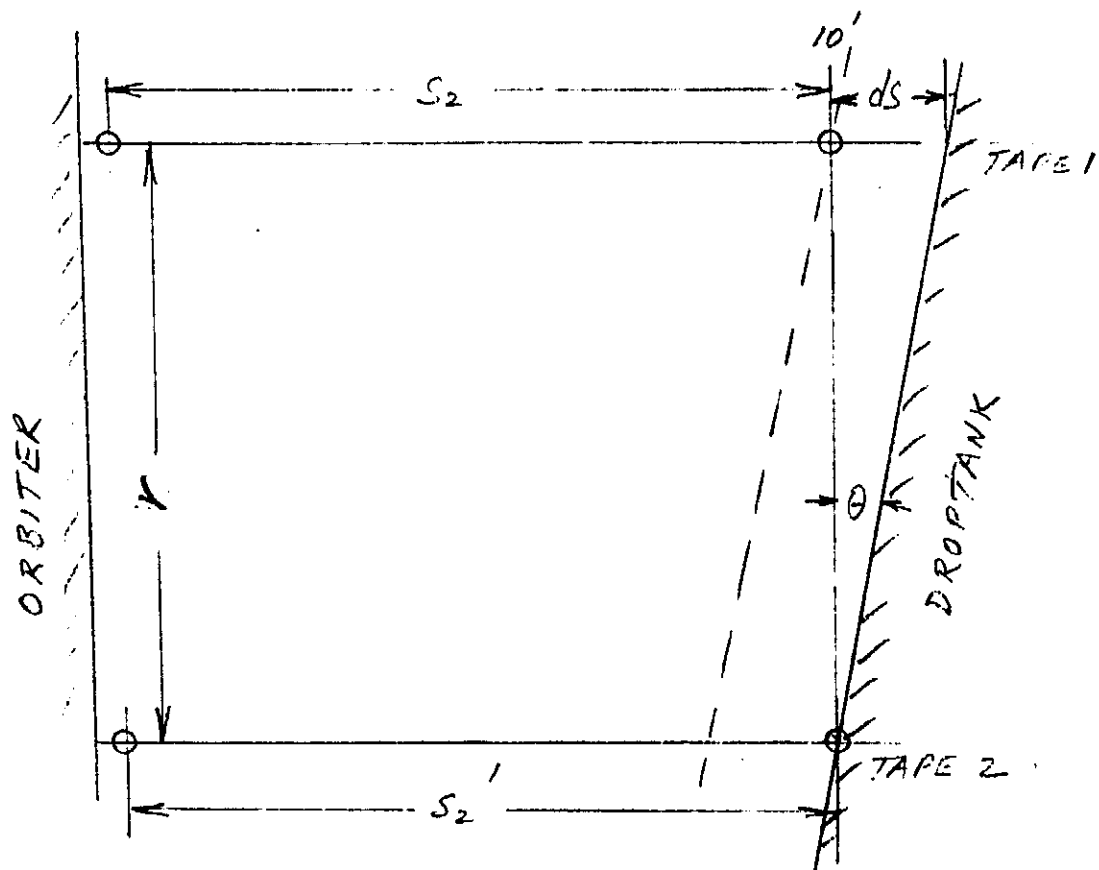


Figure 3

ENGINEERING MEMORANDUM

TITLE: THERMODYNAMIC ANALYSIS OF DROPTANK SURFACE IRREGULARITIES	EM NO: L2-12-01-M1-8 REF: DATE: 3 June 1971
AUTHORS: K.W. McGee <i>K.W. McGee</i>	APPROVAL: ENGINEERING SYSTEM ENGRG <i>R.A. Byers</i>

PROBLEM

Surface irregularities and manufacturing defects on the surface of the foam insulation on the GAC external droptanks will cause localized increases in heating. The allowable magnitude of the surface defects to prevent excessive heating must be determined.

RESULTS

For a 10 percent increase in surface heat rates over smooth surface values, the maximum allowable surface defect height was 0.12 inch on the forward portion of the droptank and 0.20 inch on the aft portion. A 20 percent heat rate increase would allow a 0.25-inch defect height on the forward part of the droptank and 0.40 inch on the aft portion. Examination of a piece of sprayed polyurethane foam showed that surface irregularities were within the 20 percent heat rate increase boundaries.

ANALYSIS

The GAC external droptank orbiter is shown in Fig. 1 (Ref. 1). All required ascent LH₂ is carried in the external droptanks, which are jettisoned in orbit. The orbiter has a 157-ft overall length with a 106-ft wingspan and 55-deg leading-edge sweep. Droptanks are 14-ft in diameter and 85-ft in length with an LH₂ capacity of 10,433 ft³ per tank. Droptanks are sprayed with 0.75 in. of 2 pcf polyurethane foam over their entire outer surface for cryogenic protection. Ablator was assumed to cover the foam insulation over the entire nose cone and interference heating regions of the droptanks.

The GAC design ascent trajectory is shown in Fig. 2 (Ref. 2). Booster burnout is 185 sec after liftoff with orbiter injection into a 28.5-deg inclination orbit at 50-nm altitude 422 seconds after liftoff. The droptanks are jettisoned in orbit where retrorockets on the droptanks are fired to deorbit the tanks.

Based on the ascent trajectory shown in Fig. 2, the boundary layer momentum thickness (θ) was calculated by the method of Reshotko and Tucker for a real gas (Ref. 3) for two tank locations, 30 and 60 ft aft of the nose. The displacement layer thickness (δ^*) was derived from the momentum layer thickness, (Ref. 4, pp 281-2). The results are shown in Fig. 3 for the portion of the flight during which the boundary layer is turbulent. The laminar boundary layer displacement thickness increases rapidly to several feet after transition, and was deemed not to be of importance in determining allowable roughness. The minimum displacement thickness is approximately 1.2 in and 2.0 in. at the 30 ft and 60 ft locations, respectively, 70 seconds after liftoff. These thicknesses increase to a maximum of 14 in. and 25 in. 190 seconds after liftoff.

As shown in Ref. 5, the increase in local heating due to surface roughness is a function of the local Mach number (M_L), the ratio of the roughness height to boundary layer displacement thickness (R/δ^*), and the roughness width to height ratio (W/R).

Typical results (from Ref. 5) are plotted in Fig. 4 for a two-dimensional protrusion which is representative of the anticipated foam roughness. For the present study, permissible roughness height corresponding to 10- and 20-percent heating increases were determined. Boundary layer displacement thicknesses at 95 sec after liftoff were used, since these are the minimum anticipated values during the period of significant heating. The results of these calculations are shown in Fig. 5 which plots the permissible roughness height versus width for the two heating increases studied, 10- and 20-percent.

Also shown are the observed roughness dimensions from a typical piece of foam insulation. The observed roughness will cause heating increases of less than 20 percent over almost all of the droptank, and less than 10 percent over the portion aft of the 60-ft location. If the surface roughness on the droptanks is controlled to the tolerances shown in Fig. 5, no additional surface preparation, other than application of a moisture barrier should be required.

REFERENCES

1. Grumman Aircraft Company Brochure MSC-03804, SS-884.
2. GAC Data Package, 19 April 1971, SS-900.
3. Reshotko, E. and Tucker, M., "Approximate Calculation of the Compressible Turbulent Boundary Layer with Heat Transfer and Arbitrary Pressure Gradient," NASA-TN-4154, Dec 1957.
4. Truitt, R. W., "Hypersonic Aerodynamics," Ronald Press Company, 1959.
5. Jue, J., "Surface Roughness Heating Effects - A Survey of Prediction Methods Including Design Curves," LMSC-A970123, 6 May 1970.

Lockheed Missiles & Space Company

Space Shuttle Project

EM NO: L2-12-01-M1-8

DATE: 3 June 1971

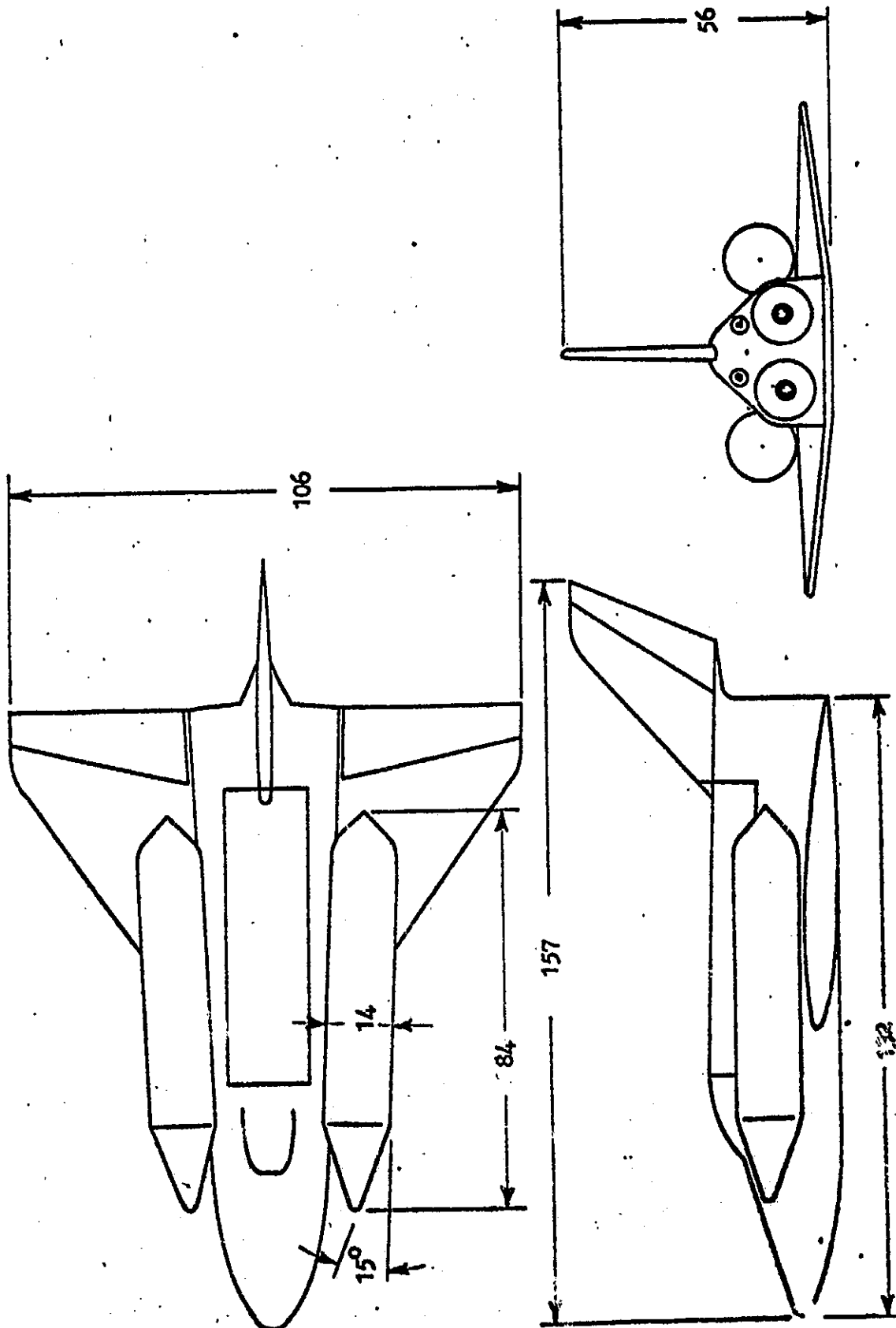


Figure 1 GAC External Tank Orbiter

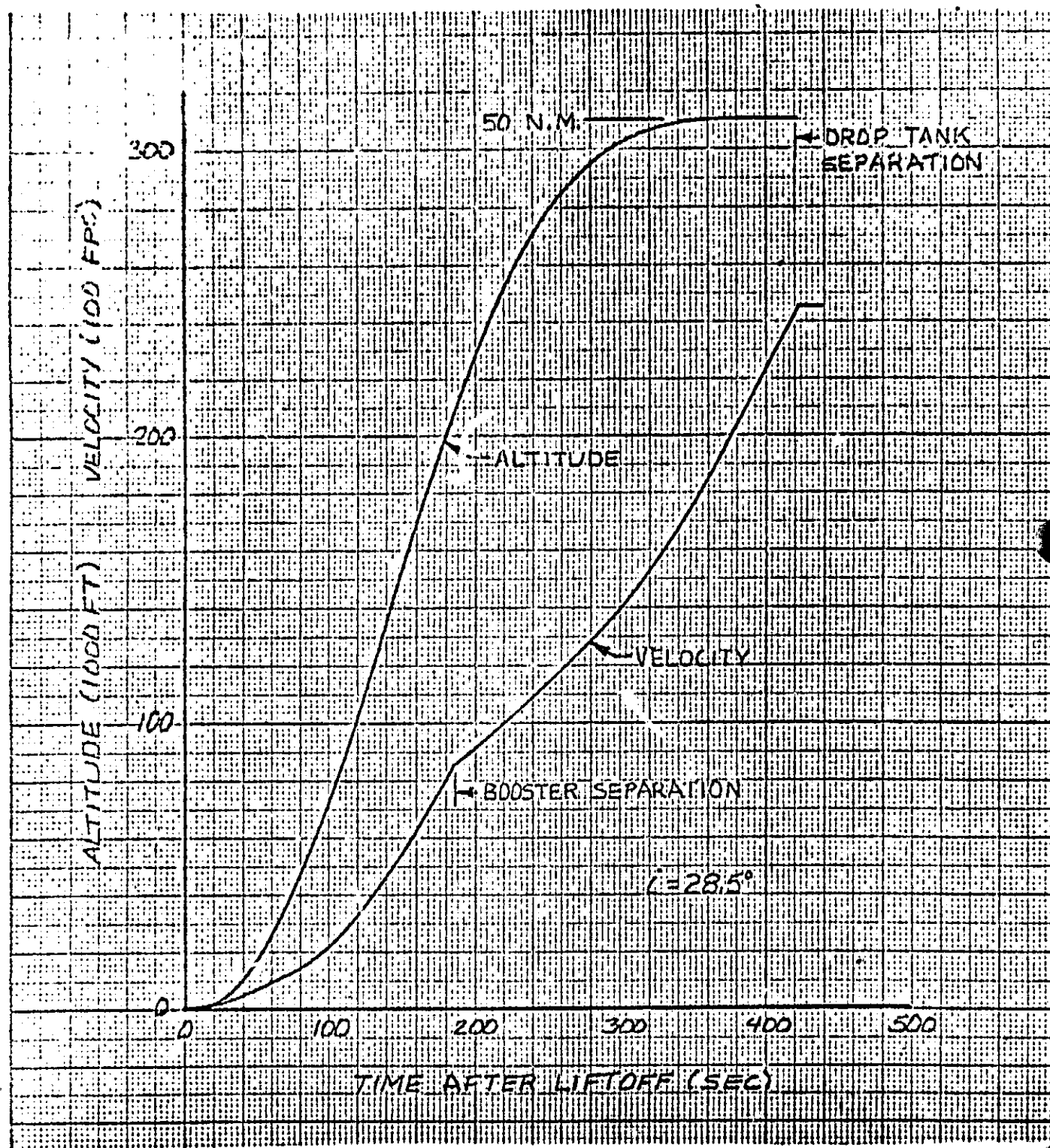


Figure 2 GAC 2-1/2 Stage Ascent Trajectory

EM NO. L2-012-01-M1-8

DATE 3 June 1971

PAGE OF

PREPARED BY

BOUNDARY LAYER DISPLACEMENT THICKNESS (IN)

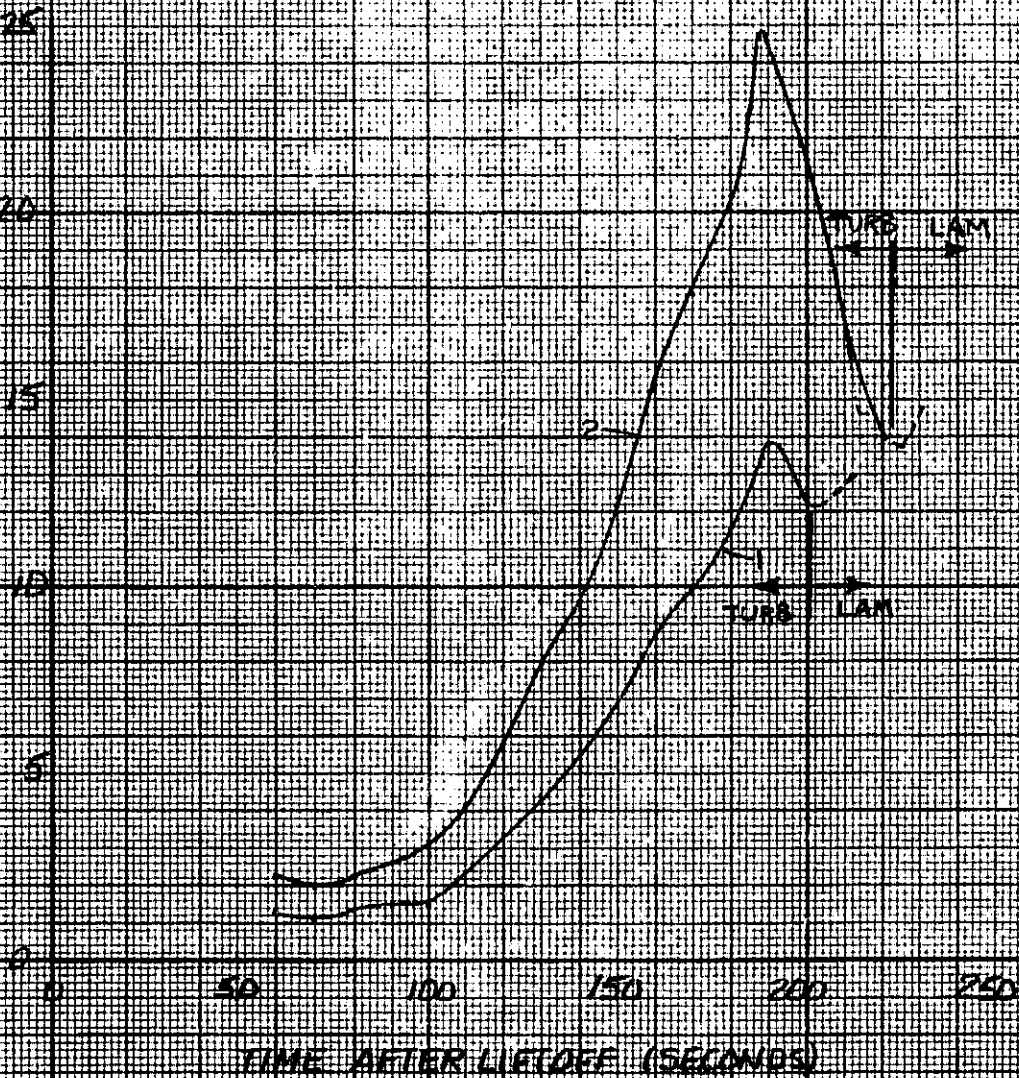
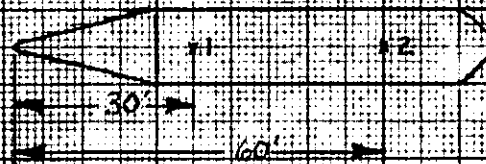


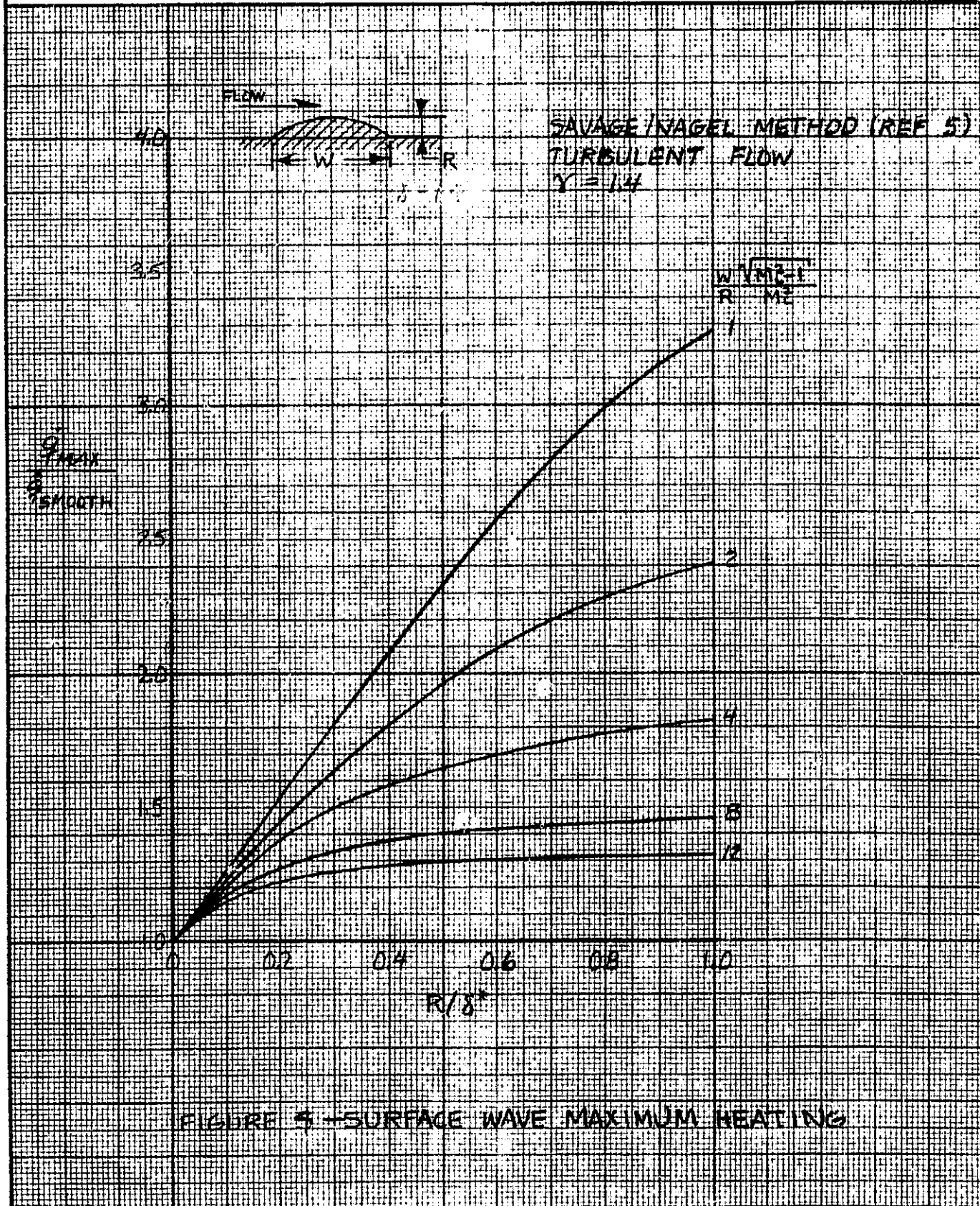
FIGURE 3- ASCENT BOUNDARY LAYER THICKNESS

EM NO. 12-12-01-M1-8

DATE 3 June 1971

PAGE OF

PREPARED BY K.W. McGee



EM NO. L2-12-01-M1-8

DATE 3 June 1971

PAGE OF

PREPARED BY

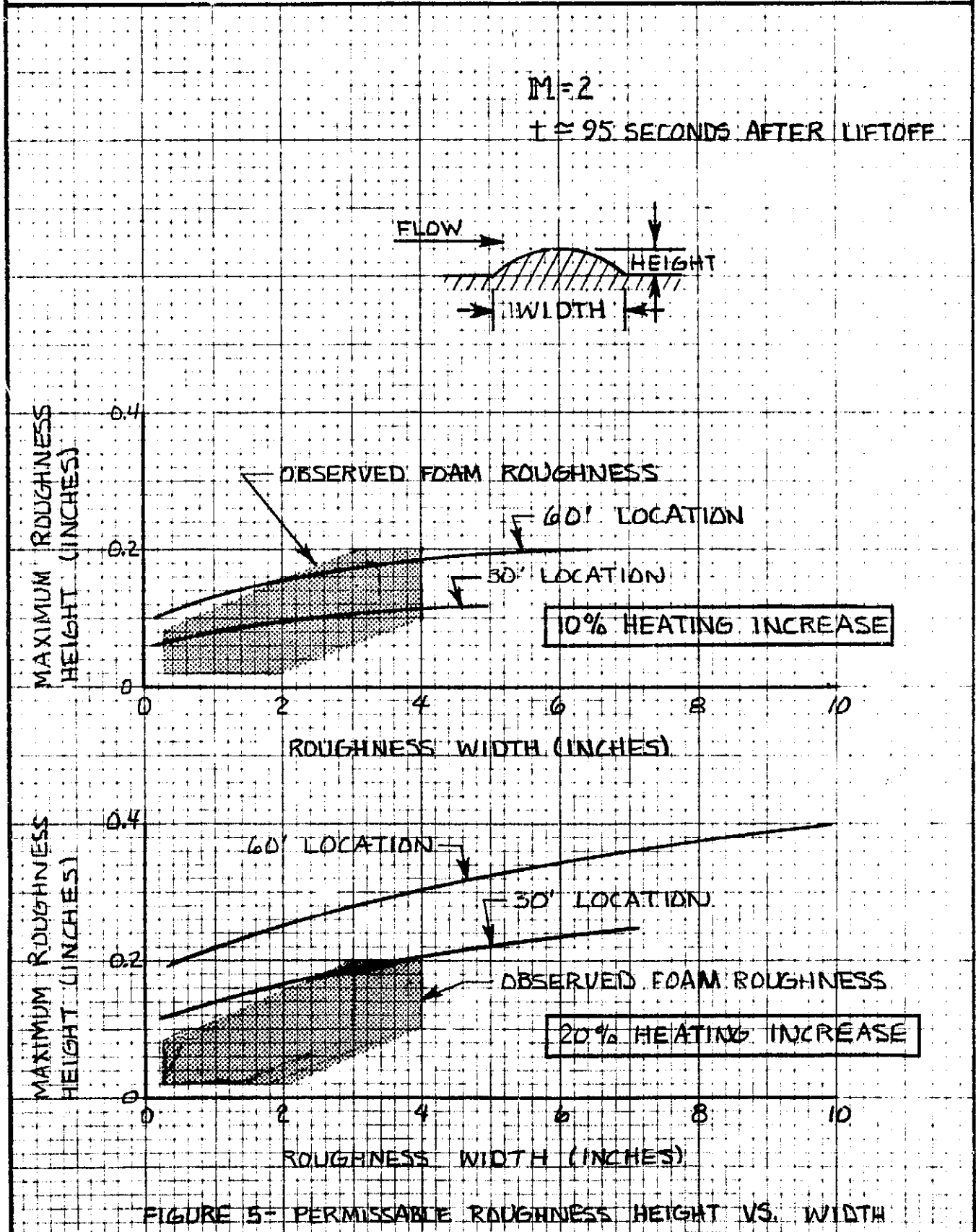


FIGURE 5- PERMISSABLE ROUGHNESS HEIGHT VS. WIDTH